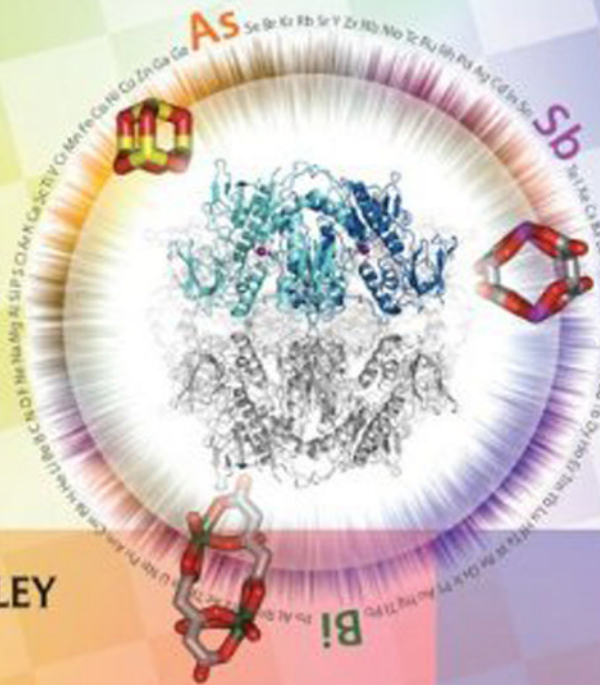



Editor
HONGZHE SUN

Biological Chemistry

*of Arsenic, Antimony
and Bismuth*



 WILEY

**Biological Chemistry of Arsenic,
Antimony and Bismuth**

Biological Chemistry of Arsenic, Antimony and Bismuth

Editor

HONGZHE SUN

*Department of Chemistry, University of Hong Kong,
P. R. China*



A John Wiley and Sons, Ltd, Publication

This edition first published 2011

© 2011 John Wiley & Sons Ltd

Registered office

John Wiley & Sons Ltd, The Atrium, Southern Gate, Chichester, West Sussex, PO19 8SQ, United Kingdom

For details of our global editorial offices, for customer services and for information about how to apply for permission to reuse the copyright material in this book please see our website at www.wiley.com.

The right of the author to be identified as the author of this work has been asserted in accordance with the Copyright, Designs and Patents Act 1988.

All rights reserved. No part of this publication may be reproduced, stored in a retrieval system, or transmitted, in any form or by any means, electronic, mechanical, photocopying, recording or otherwise, except as permitted by the UK Copyright, Designs and Patents Act 1988, without the prior permission of the publisher.

Wiley also publishes its books in a variety of electronic formats. Some content that appears in print may not be available in electronic books.

Designations used by companies to distinguish their products are often claimed as trademarks. All brand names and product names used in this book are trade names, service marks, trademarks or registered trademarks of their respective owners. The publisher is not associated with any product or vendor mentioned in this book. This publication is designed to provide accurate and authoritative information in regard to the subject matter covered. It is sold on the understanding that the publisher is not engaged in rendering professional services. If professional advice or other expert assistance is required, the services of a competent professional should be sought.

The publisher and the author make no representations or warranties with respect to the accuracy or completeness of the contents of this work and specifically disclaim all warranties, including without limitation any implied warranties of fitness for a particular purpose. This work is sold with the understanding that the publisher is not engaged in rendering professional services. The advice and strategies contained herein may not be suitable for every situation. In view of ongoing research, equipment modifications, changes in governmental regulations, and the constant flow of information relating to the use of experimental reagents, equipment, and devices, the reader is urged to review and evaluate the information provided in the package insert or instructions for each chemical, piece of equipment, reagent, or device for, among other things, any changes in the instructions or indication of usage and for added warnings and precautions. The fact that an organization or Website is referred to in this work as a citation and/or a potential source of further information does not mean that the author or the publisher endorses the information the organization or Website may provide or recommendations it may make. Further, readers should be aware that Internet Websites listed in this work may have changed or disappeared between when this work was written and when it is read. No warranty may be created or extended by any promotional statements for this work. Neither the publisher nor the author shall be liable for any damages arising herefrom.

Library of Congress Cataloging-in-Publication Data

Biological chemistry of arsenic, antimony and bismuth / editor, Hongzhe Sun.

p. cm.

Includes bibliographical references and index.

ISBN 978-0-470-71390-7 (cloth)

1. Arsenic—Physiological effect. 2. Antimony—Physiological effect. 3. Bismuth—Physiological effect.
4. Group 15 elements—Physiological effect. I. Sun, Hongzhe.

QP535.A7B56 2011

615.9'25715—dc22

2010032741

A catalogue record for this book is available from the British Library.

ISBN 9780470713907

ePDF: 9780470975497

oBook: 9780470975503

ePub: 9780470976227

Set in 10/12pt, Times by Thomson Digital, Noida, India

Printed in Singapore by Markono Print Media Pte Ltd

Contents

<i>List of Contributors</i>	<i>xiii</i>
<i>Preface</i>	<i>xv</i>
1 The Chemistry of Arsenic, Antimony and Bismuth	1
<i>Neil Burford, Yuen-ying Carpenter, Eamonn Conrad and Cheryl D.L. Saunders</i>	
1.1 Properties of the Elements	1
1.2 Allotropes	3
1.3 Bond Energies	4
1.4 Oxidation States	4
1.5 Relativistic Effects and Orbital Contraction	5
1.6 Structure and Bonding	6
1.7 Clusters and Extended Structures	9
1.8 Hybridization and Inversion	11
1.9 Coordination Chemistry	12
1.10 Geological Occurrence	14
1.11 Aqueous Chemistry and Speciation	14
1.12 Analytical Methods and Characterization	15
1.13 Conclusions	15
References	15
2 Arsenic's Interactions with Macromolecules and its Relationship to Carcinogenesis	19
<i>Kirk T. Kitchin</i>	
2.1 Introduction	19
2.2 Arsenic's Interactions with DNA and Proteins	20
2.2.1 Release of Zinc from Zinc Finger Proteins has been Chemically Demonstrated	26
2.2.2 Binding of Trivalent Arsenic to Zinc Finger Proteins	26
2.2.3 Reduced Function of Zinc Finger Proteins	27
2.2.4 Restoration of Zinc Finger Protein Function	27
2.3 Cancer – MOA	30
2.3.1 Binding to RSH Groups	30
2.3.2 Cancer – MOA – Oxidative Stress	31
2.3.3 Cancer – MOA – DNA Methylation	33

2.4	Arsenic's Many Connections to Carcinogenesis	34
2.4.1	Human Carcinogenicity	34
2.4.2	Animal Studies - Promotion of Carcinogenesis	38
2.4.3	Animal Studies - Complete Carcinogenesis	38
2.4.4	Arsenicals in the Treatment of Leukaemia - APL	40
2.5	Sources of Information on Arsenic's Mode of Action, Biochemical Effects, Carcinogenesis in Animals and Man, Metabolism and Analytical Chemistry	40
2.6	Conclusion	46
	Acknowledgements	46
	Disclaimer	46
	Abbreviations	47
	References	48
3	Biological Chemistry of Antimony and Bismuth	53
	<i>Nan Yang and Hongzhe Sun</i>	
3.1	Introduction	53
3.2	Biorelevant Coordination Chemistry of Antimony and Bismuth	53
3.3	Antimony and Bismuth Compounds in Medicine	54
3.3.1	Antimony in Medicine	54
3.3.2	Bismuth in Medicine	55
3.4	Interaction with Nucleic Acids	56
3.4.1	Interaction of Antimony with Nucleosides and Nucleotides	56
3.4.2	Interaction of Bismuth with Nucleosides and Nucleotides	58
3.5	Interaction with Amino Acids and Peptides	58
3.5.1	Interaction of Antimony with Amino Acids and Peptides	58
3.5.2	Interaction of Bismuth with Amino Acids and Peptides	61
3.6	Interaction with Proteins and Enzymes	62
3.6.1	Interaction of Antimony with Proteins and Enzymes	62
3.6.2	Interaction of Bismuth with Proteins and Enzymes	68
3.7	Conclusion and Perspectives	77
	Acknowledgements	77
	References	77
4	Metallomics Research Related to Arsenic	83
	<i>Hiroki Haraguchi</i>	
4.1	Metallomics – Integrated Biometal Science	83
4.2	Analytical Feasibility of ICP-AES and ICP-MS	85
4.3	Chemical Speciation of Trace Elements in Biological Samples	87
4.3.1	Speciation of Arsenic in Salmon Egg Cells	89
4.3.2	Speciation of Arsenic Species in Human Urine	93
4.3.3	Speciation of Arsenic Species in Human Blood Serum	96
4.3.4	Arsenic Metabolism in Hamsters and Rats after an Oral Dose of Arsenite	98

4.3.5	Animal Species Difference in the Uptake of Dimethylated Arsenic by Red Blood Cells	103
4.3.6	Speciation and Excretion Patterns of Arsenic Metabolites in Human Urine after Ingestion of Edible Seaweed, Hijiki	105
4.4	Summary	109
	Acknowledgements	110
	References	110
5	Arsenic in Traditional Chinese Medicine	113
	<i>Kui Wang, Siwang Yu and Tianlan Zhang</i>	
5.1	Arsenic Bearing Minerals and their Clinical Applications	113
5.1.1	Introduction	113
5.1.2	Arsenolite and its Clinical Applications in Traditional Chinese Medicine (TCM)	115
5.1.3	Realgar and Orpiment and their Clinical Applications in TCM	116
5.1.4	Processing of Arsenic Bearing Minerals	117
5.2	Metabolism and Pharmacokinetics of Arsenic Bearing Minerals	119
5.2.1	Arsenolite and Arsenic Trioxide	119
5.2.2	Metabolism and Pharmacokinetics of Realgar and Orpiment	121
5.2.3	Nanoparticles of Realgar	122
5.3	Pharmacological Activities and Mechanisms of Actions of ABMs	122
5.3.1	Mechanisms of Anticancer Action of Arsenolite and ATO	122
5.3.2	Mechanisms of Anticancer Actions of Realgar	125
5.3.3	Arsenolite on Asthma Prevention	127
5.3.4	Realgar on Brain Protection	128
5.4	Perspectives	128
	References	130
6	Microbial Transformations of Arsenic in Aquifers	135
	<i>Jonathan R. Lloyd</i>	
6.1	An Introduction to the Microbial Cycling of Arsenic	135
6.2	The Biochemistry of Microbial Arsenic Transformations	137
6.2.1	Microbial Resistance to As(V) via the Arsenic Operon	137
6.2.2	Gaining Energy from Arsenic: the Dissimilatory Reduction of As(V) under Anaerobic Conditions	137
6.2.3	Closing the Arsenic Cycle: the Oxidation of As(III)	138
6.3	Microbially Driven Mobilization of Arsenic in Aquifers: a Humanitarian Disaster	139
6.3.1	Microbial Ecology of Arsenic Impacted Aquifers: Hunting for the Organisms that Mobilize Arsenic	140
6.4	Conclusions and Future Directions	141
	Acknowledgements	142
	References	142

7	Biomethylation of Arsenic, Antimony and Bismuth	145
	<i>Richard O. Jenkins</i>	
7.1	Introduction	145
7.2	Biomethylation of Arsenic	147
7.2.1	Microbial Biomethylation of Arsenic	147
7.2.2	Mammalian Biomethylation of Arsenic	150
7.2.3	Arsenic Biomethylation/Demethylation and Organoarsenic Compounds in the Environment	156
7.3	Biomethylation of Antimony	159
7.3.1	Organoantimony Compounds in the Environment	159
7.3.2	Antimony Biomethylation in Mammals	161
7.3.3	Antimony Biomethylation and its Relation to SIDS	161
7.3.4	Microbial Biomethylation of Antimony	162
7.3.5	Biological Mechanism of Antimony Biomethylation	168
7.3.6	Abiotic Reactions of Particular Relevance to Antimony Biomethylation Studies	169
7.4	Biomethylation of Bismuth	169
7.4.1	Organobismuth Compounds in the Environment	171
7.4.2	Microbial Biomethylation of Bismuth	171
7.4.3	Biological Mechanism of Bismuth Biomethylation	173
	Abbreviations	174
	References	175
8	Metalloid Transport Systems	181
	<i>Hsueh-Liang Fu, Xuan Jiang and Barry P. Rosen</i>	
8.1	Introduction	181
8.2	Metalloid Uptake Systems	183
8.2.1	Arsenate Uptake Systems	183
8.2.2	Uptake Systems for Arsenite and Antimonite	184
8.2.3	Boron Uptake Systems	191
8.2.4	Uptake Systems for Silicon and Germanium	193
8.3	Metalloid Efflux Systems	195
8.3.1	Eukaryotic MRP Efflux Pumps	195
8.3.2	ArsB	196
8.3.3	ArsA	197
8.3.4	Acr3	200
8.3.5	Efflux Systems for Silicon	201
8.3.6	Efflux Systems for Boron	202
8.4	Summary and Conclusions	202
	Acknowledgements	202
	References	203

9	Bismuth Complexes of Porphyrins and their Potential in Medical Applications	209
	<i>Bernard Boitrel</i>	
9.1	Introduction	209
9.2	Early Work (1969-1994)	210
9.3	Bismuth Complexes of Unfunctionalized Porphyrins	211
9.3.1	The First X-ray Structure of (OEP)Bi(SO ₃ CF ₃)	211
9.3.2	Other X-ray Structures with Tetra-Mesoaryl Porphyrin: Bi(tpClpp)NO ₃ and Bi(tpClpp)Br	211
9.4	Bismuth Complexes of Functionalized Porphyrins	212
9.4.1	Picket Porphyrins	213
9.4.2	Bis-Strapped Porphyrins	223
9.4.3	Single-Strapped Porphyrins	236
9.5	Future Strategies Towards Bifunctional Chelates (BFC) – Conclusions	237
	References	239
10	<i>Helicobacter pylori</i> and Bismuth	241
	<i>Aruni H.W. Mendis and Barry J. Marshall</i>	
10.1	Introduction	241
10.2	<i>Helicobacter pylori</i>	243
10.2.1	Disease Associations and Clinical Manifestations	245
10.3	Bismuth as an Antimicrobial Agent	246
10.3.1	Bismuth Subsalicylate (BSS)	246
10.3.2	Colloidal Bismuth Subcitrate (CBS)	249
10.4	Mechanism of Action of Bismuth Citrate and CBS on <i>H. pylori</i> and Ulcer Healing	250
10.4.1	Bismuth Toxicity	253
10.5	<i>In Vitro</i> Susceptibility of <i>H. pylori</i> and other Bacteria to Bismuth Compounds and Antibiotics	253
10.6	The Effect of pH on Bactericidal Activity of Bismuth Compounds	254
10.7	Novel Preparations of Bismuth Compounds	255
10.8	Novel Delivery Systems for Bismuth Compounds and Other Antibiotics	255
10.9	The Biochemical Targets of Bismuth	256
10.9.1	Enzymes with Zn(II) and Fe(III) Sites	256
10.9.2	Heat Shock Proteins	256
10.9.3	Other Metabolic Enzymes	257
10.9.4	Fumarase and Translational Factor Ef-Tu	257
10.9.5	Phospholipases	257
10.9.6	Pepsin	257
10.9.7	Alcohol Dehydrogenase	258
10.9.8	Urease	258
10.10	Binding of Bismuth Compounds to Plasma Proteins	258
	References	259

11	Application of Arsenic Trioxide Therapy for Patients with Leukaemia	263
	<i>Bo Yuan, Yuta Yoshino, Toshikazu Kaise and Hiroo Toyoda</i>	
11.1	Introduction	263
11.2	Cellular and Molecular Mechanisms of ATO Actions	264
11.2.1	History of Arsenic as a Drug	264
11.2.2	Uptake of Arsenic	265
11.2.3	Efflux of Arsenic	266
11.2.4	Apoptosis Induction	267
11.2.5	Differentiation Induction	273
11.2.6	Degradation of PML-RAR α	274
11.2.7	Proliferation Inhibition and Angiogenesis Inhibition	275
11.3	Pharmacokinetics of ATO in APL Patients	276
11.3.1	Administration Route and Distribution	276
11.3.2	Metabolism and Pharmacokinetics	277
11.3.3	Adverse Effects and Biological Monitoring	280
11.4	Potential Combination Therapies with ATO	281
11.4.1	Natural Product Derived Substances	281
11.4.2	Cytokine	282
11.4.3	Other Reagents	283
11.5	Potential ATO Application to Other Leukaemias	284
11.6	Conclusion	285
	Acknowledgements	286
	References	286
12	Anticancer Activity of Molecular Compounds of Arsenic, Antimony and Bismuth	293
	<i>Edward R.T. Tiekink</i>	
12.1	Introduction	293
12.2	Arsenic Compounds	295
12.3	Antimony Compounds	298
12.4	Bismuth Compounds	303
12.5	Conclusions	307
	References	307
13	Radiobismuth for Therapy	311
	<i>Martin W. Brechbiel and Ekaterina Dadachova</i>	
13.1	Introduction	311
13.2	Targeting Vectors	312
13.3	α -Emitters versus β^- -Emitters	313
13.4	Radionuclides	313
13.4.1	^{212}Bi	314
13.4.2	^{213}Bi	315

13.5	Radiolabeling – Chemistry	315
13.6	Preclinical Studies	317
13.6.1	^{212}Bi	317
13.6.2	^{213}Bi	317
13.7	Targeted α -Therapy versus Targeted β -Therapy	321
13.8	Clinical Studies	322
13.8.1	^{213}Bi	322
13.9	Alternate Delivery Methods and Uses	323
13.10	Prospects and Conclusions	324
	Abbreviations	326
	Acknowledgements	326
	References	326
14	Genetic Toxicology of Arsenic and Antimony	331
	<i>Toby G. Rossman and Catherine B. Klein</i>	
14.1	Introduction	331
14.2	DNA Damage in Cells Treated with Arsenicals	332
14.3	Mutagenesis in Cells Treated with Arsenicals	333
14.4	Other Genotoxic Events in Cells Treated with Arsenicals	335
14.5	Effects of Arsenicals on DNA Repair	337
14.6	Indirect Mechanisms of Mutagenicity and Comutagenicity by Arsenicals	339
14.7	Mutagenesis and Transformation as Secondary Effects of Genomic Instability	340
14.8	Antimony	344
	References	345
15	Metalloproteomics of Arsenic, Antimony and Bismuth Based Drugs	353
	<i>Cheuk-Nam Tsang, Ruiguang Ge and Hongzhe Sun</i>	
15.1	Introduction	353
15.2	Chemical Speciation of Arsenic Based Drugs and their Metallometabolism	355
15.2.1	Metallometabolism in Biological Matrices	355
15.2.2	Arsenic Metabolism	355
15.3	Metalloproteomics and its Applications to As-, Sb- and Bi-Based Metallo drugs	356
15.3.1	From Proteomics to Metalloproteomics	356
15.3.2	Metal Specific Selection, Detection and Prediction Methods in Metalloproteomics	357
15.3.3	Identification of Potential Targets of As-, Sb-, and Bi-Based Drugs by Metalloproteomics	364

15.4	Biological Regulation of Arsenic and Antimony	366
15.4.1	Arsenic and Antimony Uptake Systems	366
15.4.2	Arsenic and Antimony Extrusion Systems	369
15.5	Conclusions	370
	Acknowledgements	371
	References	371

<i>Index</i>	377
---------------------	------------

List of Contributors

Bernard Boitrel UMR CNRS 6226, Sciences Chimiques de Rennes, (I.C.M.V.), Université de Rennes 1, Campus de Beaulieu 263, F-5042 RENNES Cedex, France

Martin W. Brechbiel Radioimmune & Inorganic Chemistry Section, Radiation Oncology Branch, National Cancer Institute, Building 10, Center Drive, Bethesda, MD 20892, USA

Neil Burford Department of Chemistry, Dalhousie University, Halifax, Nova Scotia, B3H 4J3, Canada

Yuen-ying Carpenter Department of Chemistry, Dalhousie University, Halifax, Nova Scotia, B3H 4J3, Canada

Eamonn Conrad Department of Chemistry, Dalhousie University, Halifax, Nova Scotia, B3H 4J3, Canada

Ekaterina Dadachova Albert Einstein College of Medicine of Yeshiva University, Bronx, New York, NY 10461, USA

Hsueh-Liang Fu Department of Biochemistry and Molecular Biology, Wayne State University School of Medicine, Detroit, MI 48201, USA

Ruiguang Ge The Laboratory of Integrative Biology, College of Life Sciences, Sun Yat-Sen University, Guangzhou 510006, P. R. China

Hiroki Haraguchi Association of International Research Initiatives for Environmental Studies, Taito-ku, Tokyo 110-0005, Japan

Richard O. Jenkins Faculty of Health & Life Sciences, De Montfort University, The Gateway, Leicester, LE1 9BH, UK

Xuan Jiang Department of Biochemistry and Molecular Biology, Wayne State University School of Medicine, Detroit, MI 48201, USA

Toshikazu Kaise Laboratory of Environmental Chemodynamics, School of Life Sciences, Tokyo University of Pharmacy & Life Sciences, 1432-1 Horinouchi, Hachioji, Tokyo 192-0392, Japan

Kirk T. Kitchin Integrated Systems Toxicology Division, National Health and Environmental Effects Research Laboratory, Office of Research and Development, U.S. Environmental Protection Agency, Research Triangle Park, NC 27711, USA

Catherine B. Klein The Nelson Institute of Environmental Medicine, New York University Langone School of Medicine, Tuxedo, NY 10987, USA

Jonathan R. Lloyd School of Earth, Atmospheric and Environmental Sciences, and Williamson Research Centre for Molecular Environmental Science, University of Manchester, Manchester, M13 9PL, UK

Barry J. Marshall Discipline of Microbiology and Immunology, School of Biomedical, Biomolecular and Chemical Sciences, Faculty of Life and Physical Sciences, The University of Western Australia, Crawley WA 6009, Australia

Aruni H.W. Mendis Manager Scientific & Regulatory Affairs, Tri-Med Australia, Subiaco, Western Australia

Barry P. Rosen Department of Cellular Biology and Pharmacology, Florida International University College of Medicine, Miami, FL 33199, USA, and Department of Biochemistry and Molecular Biology, Wayne State University School of Medicine, Detroit, MI 48201, USA

Toby G. Rossman The Nelson Institute of Environmental Medicine, New York University Langone School of Medicine, Tuxedo, NY 10987, USA

Cheryl D. L. Saunders Department of Chemistry, Dalhousie University, Halifax, Nova Scotia, B3H 4J3, Canada

Hongzhe Sun Department of Chemistry, The University of Hong Kong, Hong Kong, P.R. China

Edward R. T. Tiekink Department of Chemistry, University of Malaya, Kuala Lumpur 50603, Malaysia

Hiroo Toyoda Department of Clinical Molecular Genetics, School of Pharmacy, Tokyo University of Pharmacy & Life Sciences, 1432-1 Horinouchi, Hachioji, Tokyo 192-0392, Japan

Cheuk-Nam Tsang Department of Chemistry and Open Laboratory of Chemical Biology, The University of Hong Kong, Hong Kong SAR, P. R. China

Kui Wang Department of Chemical Biology, School of Pharmaceutical Sciences, Peking University, Beijing 100191, P.R. China

Nan Yang Department of Chemistry, The University of Hong Kong, Hong Kong, P.R. China

Yuta Yoshino Department of Clinical Molecular Genetics, School of Pharmacy, Tokyo University of Pharmacy & Life Sciences, 1432-1 Horinouchi, Hachioji, Tokyo 192-0392, Japan

Siwang Yu Department of Chemical Biology, School of Pharmaceutical Sciences, Peking University, Beijing 100191, P.R. China

Bo Yuan Department of Clinical Molecular Genetics, School of Pharmacy, Tokyo University of Pharmacy & Life Sciences, 1432-1 Horinouchi, Hachioji, Tokyo 192-0392, Japan

Tianlan Zhang Department of Chemical Biology, School of Pharmaceutical Sciences, Peking University, Beijing 100191, P.R. China

Preface

Arsenic (As), antimony (Sb) and bismuth (Bi) are in Group 15 in the periodic table together with nitrogen and phosphorus. All of them are directly and indirectly related to human life. Both nitrogen and phosphorus are essential to life whereas arsenic (and antimony) is double-edged. The therapeutic effect of arsenic has been recognized even in ancient China and arsenic minerals have often been used in traditional Chinese medicine (e.g., realgar and orpiment). Partially based on this application, arsenic trioxide (Trisenox) was tested and subsequently approved to be used as an anticancer drug against leukaemia. In fact the first modern pharmaceutical is an organoarsenic compound, arsphenamine (Salvarsan or Ehrlich 606). Ironically, the structure of the drug in solution was not clear until recently. Both antimony and bismuth have been used in clinics for decades. The toxicity of arsenic (and antimony) is also well-known and indeed the contamination of groundwater by arsenic is becoming a major health problem in Asian countries such as India and Bangladesh. In spite of their importance to our lives and the environment, there is no book that reports the latest progress of biological chemistry of arsenic, antimony and bismuth.

This book gives readers a comprehensive update of the progress, particularly in the past decade. The 15 chapters which constitute the book have been written by leading scientists who are experts in their relevant field. Chapter 1 is an overview of the current knowledge of the chemistry of arsenic, antimony and bismuth. Chapters 2 and 3 are devoted to the biological chemistry of arsenic, antimony and bismuth. The latest information on structures of clinically used antimony and bismuth drugs, and arsenic/antimony-protein complexes, is described extensively. The transport and trafficking of the metalloid (As and Sb) is summarized in Chapter 8. Chapters 6 and 7 are devoted to biotransformation and biomethylation of arsenic, antimony and bismuth, one of the most important metabolism processes in biological systems. Chapter 5 is devoted the application of arsenic minerals in traditional Chinese medicine whereas Chapter 11 summarizes the modern applications of arsenic trioxide for leukaemia. Subsequently, Chapter 12 reviews the latest progress of the development of anticancer agents based on arsenic, antimony and bismuth complexes. Chapters 9 and 13 are devoted to medical applications of (radio)bismuth especially for potential anticancer treatment. Since the discovery of the bacterium *Helicobacter pylori* and its role in gastritis and peptic ulcer disease by Warren and Marshall in the 1980s, bismuth containing drugs has been commonly recommended in clinics together with antibiotics. Chapter 10 summarizes clinical applications of bismuth for *Helicobacter pylori* infection and the potential mechanism of action. Chapter 14 is devoted to the genetic toxicology of arsenic and antimony. In view of the rapid development of modern bioanalytical techniques such as metallomics and metalloproteomics, Chapters 4 and 15 review the concept and methodology of these techniques and more importantly, the application of the ‘-omics’ towards our understanding of the biological chemistry of arsenic, antimony and bismuth.

Such topics will be of particular interest to researchers, scientists and postgraduate students working in the fields of chemistry, biochemistry, environmental chemistry, toxicology and medicine.

I would like to thank all contributors for the hard work and tremendous effort that they have put into writing this book. During the preparation of the book chapter, Professor Toshikazu Kaise (Tokyo University of Pharmacy and Life Sciences, Japan) passed away suddenly. He was an excellent scholar and he promoted the work of the younger generation of scientists in various countries. Professor Kaise will be remembered by all his colleagues and friends. This book, therefore, is dedicated to him for his outstanding contributions to biological chemistry of arsenic. I would also like to express my sincere appreciation to Dr. Nan Yang, Dr. Hongyan Li, and Cheuk-Nam Tsang and Commissioning Editor Paul Deards, and Rebecca Ralf from John Wiley & Sons, Ltd. Without their kind help and strong support, the publication of this book would be impossible. Hongyan and Frances are acknowledged for their endless support and encouragement. And last but not least, I hope that you, the reader, will enjoy reading this book and develop the interdisciplinary spirit that lives in biological inorganic chemistry.

Hongzhe Sun
Hong Kong, China

1

The Chemistry of Arsenic, Antimony and Bismuth

Neil Burford, Yuen-ying Carpenter, Eamonn Conrad and Cheryl D.L. Saunders

Department of Chemistry, Dalhousie University, Halifax, Nova Scotia, B3H 4J3, Canada

Arsenic, antimony and bismuth are the heavier pnictogen (Group 15) elements and consistent with their lighter congeners, nitrogen and phosphorus, they adopt the ground state electron configuration ns^2np^3 . Arsenic and antimony are considered to be metalloids and bismuth is metallic, while nitrogen and phosphorus are non-metals. Arsenic and antimony are renowned for their toxicity or negative bioactivity [1, 2] but bismuth is well known to provide therapeutic responses or demonstrate a positive bioactivity [3]. As a background to the biological and medicinal chemistry of these elements, the fundamental chemical properties of arsenic, antimony and bismuth are presented in this introductory chapter.

1.1 Properties of the Elements

Selected fundamental parameters that define the heavier pnictogen elements are summarized in Table 1.1 [4]. While arsenic and bismuth are monoisotopic, antimony exists as two substantially abundant naturally occurring isotopes. All isotopes of the heavy pnictogens are NMR active nuclei, indicating that the nuclear spin will interact with an applied magnetic field. However, as the nuclear spins of these isotopes are all quadrupolar, NMR spectra generally consist of broad peaks and provide limited information. The atoms As, Sb and Bi all have the same effective nuclear charge ($Z_{\text{eff}} = 6.30$, Slater), which estimates the charge

Table 1.1 Elemental parameters for arsenic, antimony and bismuth (adapted with permission from [4]). Copyright Springer Science + Business Media

Parameter	As	Sb	Bi
Atomic Number	33	51	83
Natural Isotopes (abundance)	⁷⁵ As (100) <i>Stable</i>	¹²¹ Sb (57.4) <i>Stable</i>	²⁰⁹ Bi (100) <i>α-decay</i> [5]
Radioactive Stability		¹²³ Sb (42.6) <i>Stable</i>	$t_{1/2}: (1.9 \pm 0.2) \times 10^{19} \text{yr}$
Nuclear Spin, I	-3/2	+5/2 (¹²¹ Sb) +7/2 (¹²³ Sb)	-9/2
Ionization Energies (kJ mol ⁻¹)			
M → M ⁺	947	833.7	703.2
M ⁺ → M ²⁺	1798	1794	1610
M ²⁺ → M ³⁺	2735	2443	2466
M ³⁺ → M ⁴⁺	4837	4260	4372
M ⁴⁺ → M ⁵⁺	6043	5400	5400
Electron Affinity (kJ mol ⁻¹) M(g) → M ⁻ (g)	78	101	91.3
Electronegativity, χ^{P} (Pauling scale)	2.18	2.05	2.02
Atomic Radius (Å)	1.25	1.82	1.55
Single-bond Covalent Radius (Å)	1.21	1.41	1.52
Van der Waals Radius (Å)	2.00	2.20	2.40
Ionic Radii (Å)			
M ⁵⁺	0.46	0.62	0.74
M ³⁺	0.58	0.76	0.96

experienced by a valence electron taking into account shielding by the other electrons. As a consequence, the ionization energies and electron affinities for As, Sb and Bi are very similar. The ionization energy is the energy required to remove a valence electron from an atom or an ion in the gas phase. The ionization energies are predictably greater for ions with higher positive charge and are typically lower for atoms or ions with higher principal quantum number (n). The electron affinity is the energy released when an atom gains an electron to form an anion in the gas phase. The electronegativity (χ^{P}), defining the relative ability of an atom to attract electrons to itself in a covalent bond, is sufficiently larger for arsenic than for antimony and bismuth. The atomic radii, covalent radii and ionic radii are smallest for arsenic and largest for bismuth atoms consistent with the relative atomic mass and number of electron shells.

Selected biological and toxicity data for As, Sb and Bi are summarized in Table 1.2. While some arsenic compounds are essential to certain animal species [4], most arsenic compounds display toxic biological effects even when present in only small amounts. Some compounds, such as Salvarsan 606 [6], are therapeutic, although there are reported side effects, including death in high dosages. Neither antimony nor bismuth has any known natural biological function. While antimony has toxicity comparable with that of arsenic, bismuth can be tolerated in large quantities. Bismuth compounds have been used for more than two centuries to treat many medical disorders and are now commonly available in the preparations known commercially as Peptobismol and DeNol [3].

Table 1.2 Biological and toxicity data for arsenic, antimony and bismuth

	As	Sb	Bi
Biological Role [4]	Essential to some species including humans; toxic; stimulatory; carcinogenic	Not essential; toxic; stimulatory	Not essential; nontoxic
Amount in Average (70 kg) Human Body (dry mass, mg) [7]	0.5–15 depending on diet	2	<0.5
Daily Dietary Intake (mg)	0.04–1.4 [4]	0.002–1.3 [4, 8]	0.005–0.02 [1]
Lethal Intake (mg/kg body weight)	1–3 inorganic [1] 500 dimethylarsinic acid [9]	0.75 mg/kg antimony potassium tartrate [1]	5–20 g/day for years [2]

1.2 Allotropes

Elemental antimony and bismuth are most stable in the α form, which is rhombohedral and typically grey in appearance, while the most common form of arsenic is β -arsenic (grey arsenic). The α -allotropic forms are analogous to black phosphorus, composed of layers of hexagonally connected sheets, as shown in Figure 1.1. The interatomic distances (r_1 , r_2) are predictably larger for the heavier elements due to their larger atomic radii. The difference in the interlayer distance (r_2) between each adjacent pnictogen atom decreases from P to As to Sb to Bi (Table 1.3).

Arsenic is observed to exist in two (yellow and black) [10, 11] additional allotropic forms, while antimony adopts five allotropes [11, 12] and bismuth adopts at least three allotropes [11]. Most of these alternate allotropes are only nominally stable or require high temperature or pressure conditions [11, 13].

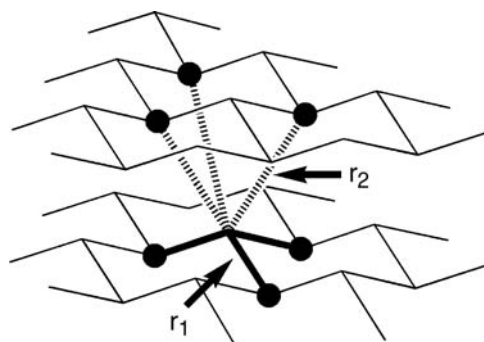


Figure 1.1 Schematic drawing of the α -rhombohedral form of elemental As, Sb or Bi, r_1 is the interatomic distance within a sheet and r_2 is the interlayer distance (Table 1.3)

Table 1.3 Comparative structural parameters for α -rhombohedral arsenic, antimony and bismuth at 298 K

	r_1 (Å)	r_2 (Å)	r_2/r_1	Angle M–M–M	References
α -As	2.517	3.120	1.240	96°73'	[14, 15]
α -Sb	2.908	3.355	1.153	95°60'	[15, 16]
α -Bi	3.072	3.529	1.149	95°45'	[15, 17]

1.3 Bond Energies

Arsenic, antimony and bismuth form stable covalent bonds with most elements. For direct comparison, Table 1.4 lists experimentally determined bond energies for the dissociation of selected pnictogen-element diatomic species in the gas phase. While these energies are not representative of pnictogen element bonds in larger molecules, the same relative trends are exhibited. Bond energies are dependent on the molecular environment in the specific compound studied. For a particular element, Pn-element bond energies generally decrease from As to Sb to Bi. For example, the Pn–H bonds in AsH₃ and SbH₃ are 319.2 kJ mol⁻¹ and 288.3 kJ mol⁻¹, respectively [18]. Moreover, bonds involving lighter elements are generally stronger. For example, the Bi–X bonds in BiF₃ and BiBr₃ are 435 kJ mol⁻¹ and 297.1 kJ mol⁻¹, respectively [18]. Similarly, in OAsPh₃ and SAsPh₃, the As=Ch bond is 429 kJ mol⁻¹ and 293 kJ mol⁻¹, for Ch=O and Ch=S respectively [18].

1.4 Oxidation States

The pnictogen elements access oxidation states ranging from –3 to +5, as summarized in Figure 1.2, which presents the relative energy of each oxidation state in volts (J C⁻¹) and in Gibbs energy. In contrast to nitrogen and phosphorus, arsenic, antimony and bismuth thermodynamically favour the elemental form. While positive oxidation states for

Table 1.4 Experimentally determined pnictogen-element bond energies of selected diatomic molecules in the gas phase, kJ mol⁻¹ (from reference [19])

[kJ mol ⁻¹]	As	Sb	Bi
H	274.0 ± 2.9	239.7 ± 4.2	≤283.3
D	270.3	—	283.7
N	489 ± 2.1	460 ± 84	—
O	484 ± 8	434 ± 42	337.2 ± 12.6
F	410	439 ± 96	366.5 ± 12.5
P	433.5 ± 12.6	356.9 ± 4.2	281.7 ± 13
S	379.5 ± 6.3	378.7	315.5 ± 4.6
Cl	448	360 ± 50	300.4 ± 4.2
As	385.8 ± 10.5	330.5 ± 5.4	—
Se	96	—	280.3 ± 5.9
Br	—	314 ± 59	240.2
Sb	330.5 ± 5.4	301.7 ± 6.3	252.7 ± 3.9
I	296.6 ± 24	—	186.1 ± 5.8
Bi	—	252.7 ± 3.9	204.4

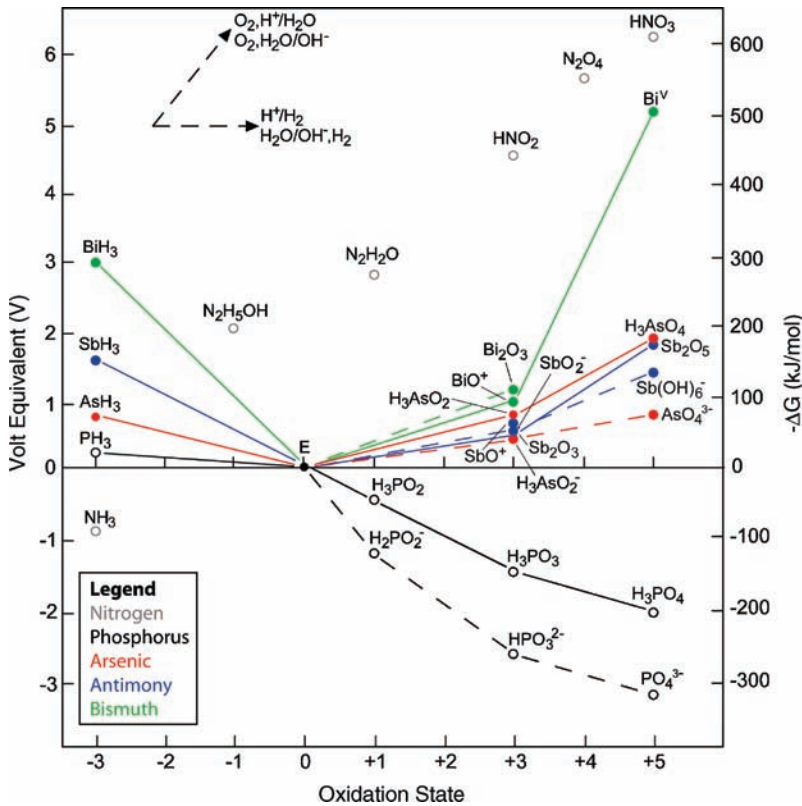


Figure 1.2 Oxidation state diagram for the pnictogen elements. Dashed lines represent basic conditions. Solid lines represent acidic conditions. Adapted with permission from [11]. Copyright Elsevier (1997)

phosphorus are stable, compounds containing arsenic, antimony or bismuth in positive oxidation states are unstable with respect to elemental forms. This phenomenon is most dramatic when comparing the relative energy differences for compounds containing pnictogens in +5 oxidation state.

1.5 Relativistic Effects and Orbital Contraction

The property trends observed for the pnictogens can be rationalized by consideration of orbital contraction (for arsenic) and relativistic effects (for bismuth). The elements at the end of the third period exhibit a contraction and a more tightly bound ns^2 ($n > 3$) electron pair, due to a relatively high effective nuclear charge (Z_{eff}) [20]. The electrons in the d -orbitals provide less effective screening of the nuclear charge than those in s - and p -orbitals due to the directionality and diffuse nature of the d -orbitals. This effect is most dramatic for arsenic, and rationalizes the relatively high fourth and fifth ionization energies of arsenic and antimony, since the ns^2 electron pair is accordingly anomalously stabilized. Consequently, the electronegativity for arsenic is comparable to that of

phosphorus (χ^{P} : As 2.18, P 2.19 [21]; χ^{AR} : As 2.20, P 2.06) [22] and is significantly greater than those of the heavier pnictogens. Bismuth is further affected by the contraction corresponding to the less effective screening provided by occupied *f*-orbitals.

When the velocity of an electron (*v*) (Equation 1.1) in an atom is a fraction of the speed of light (*c*), relativistic effects occur [20, 23–25]. As this velocity is directly proportional to atomic number (*Z*), these effects can generally be neglected for the lighter elements (*Z* < 79) but they dominate the chemical behaviour of the heavier elements.

$$v = [(2\pi e^2)/(nh)]Z \quad (1.1)$$

$$m = m_o[1-(v/c)^2]^{-1/2} \quad (1.2)$$

The strongest relativistic effects occur in the orbital that is closest to the highly positive nucleus, the 1*s* orbital. This results in an increase of mass (according to the special theory of relativity [26, 27] [Equation 1.2]) and corresponding reduction of the Bohr radius of the atom. In bismuth, the velocity of a 1*s* electron is 60% of the speed of light, leading to a mass of 1.26 times the rest mass (*m*_o) and a 26% reduction in the radius of the 1*s* orbital. In contrast, the 1*s* radial contraction of arsenic and antimony are only 3 or 8%, respectively [28]. Accordingly, the energies of all of the *ns* orbitals in bismuth are substantially lower than those of arsenic and antimony. The *p*-orbital energies are also lower but the difference is smaller than that of the *s*-orbitals [29]. The lower energy of the valence 6*s* orbital implies that the 6*s*² lone pair of electrons is less readily available for bonding, making bismuth(III) a significantly weaker Lewis base than the lighter pnictogens and disfavours the +5 oxidation state for bismuth. In addition, the *s*-orbital is less readily available [30], so that compounds of As, Sb and Bi adopt bond angles close to 90° implicating the use of pure *p*-orbitals [31] in bonding (see also Section 1.8 – *Hybridization and Inversion*).

1.6 Structure and Bonding

The chemistry of a molecule is defined by the structure of the molecule and the bonding therein. Furthermore, the local structure and bonding of the feature element(s) within a molecule are particularly influential in governing reactivity. The heavy pnictogen elements are observed to adopt a wide variety of coordination numbers and geometries depending on the substituents involved. Representations of possible bonding environments for the pnictogen centre, up to a coordination number of six, are illustrated in Figure 1.3.

The low coordination numbers in bonding arrangements A and B require that the pnictogen centre engage in π -bonding with neighbouring atom of the substituent(s). As π -bonding involving elements beyond the second period of the Periodic Table is thermodynamically disfavoured with respect to σ -bonding [30] the presence of sterically bulky substituents is required to enable the isolation of compounds containing such bonding arrangements, as in the case of AsCMes* (Mes* = 2,4,6-tri-*t*-butylphenyl) [32]. Structure C represents the σ -bonded framework of a pnictide anion. Structure D is perhaps the most common geometry known for these elements, possessing three covalent bonds and one lone pair of electrons. Reluctance for the heavy elements to engage in hybridization (*sp* mixing)

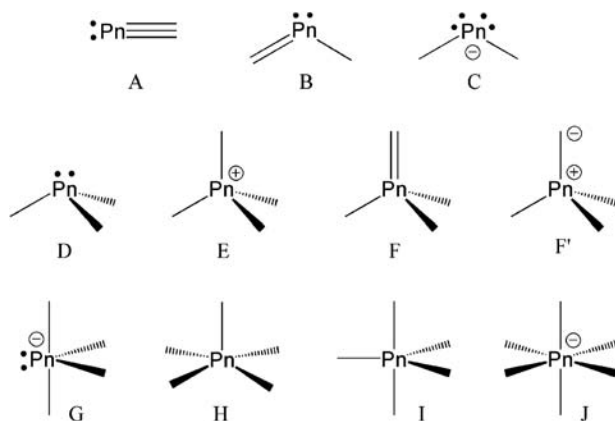


Figure 1.3 Bonding models for possible geometries (arrangements of substituents) at the pnictogen centre for coordination numbers from 1–6

results in typical bond angles in such species approximating 90° (see also Section 1.8 *Hybridization and Inversion*). Nevertheless, substituent steric interactions or chelated structures can enforce other geometries. The tetracoordinate tetrahedral geometry E is common for arsenic but less evident for antimony and rare for bismuth.

Computational studies of potential bonding arrangement F suggest that d-orbital participation is minimal for the heavy elements (As, Sb, Bi), therefore, this traditional double bond arrangement is better described as a singly bonded zwitterion F' (analogous to environment E with localized negative charge at one substituent) [33]. Moreover, many derivatives adopt bridged or extended structures (see also Section 1.7 *Clusters and Extended Structures*) [34].

Structures G, H, I and J are typically associated with the +5 oxidation state. Geometries that can be described as distorted versions of H (square based pyramid) or I (trigonal bipyramid) are common due to Berry pseudo rotation between these two extremes. In geometry I and other pseudo trigonal bipyramidal arrangements, the more electronegative atoms are typically located in axial positions, barring steric constraints. In addition to the indicated geometries, bismuth can readily adopt geometries with coordination numbers even greater than six, usually with interactions to more distant ligands that are within the sum of the van der Waals radii [35, 36]. For example, nonahydratobismuth(III) triflate contains nine relatively short Bi–O bond distances at 2.45 Å (equatorial) or 2.58 Å (trigonal prism), Figure 1.4.

Common geometries for arsenic, antimony and bismuth are summarized in blue in Table 1.5, with examples of known geometries for comparison.

Pnictogen-oxygen compounds are of particular interest in a biological context and their potential structural diversity is depicted in Figure 1.5. Derivatives containing a pnictogen centre that bears a lone pair and therefore representing pnictines (arsines, stibines or bismuthines), are represented by **1** and show diversity by virtue of one, two or three alkoxide substituents. Pnictine oxides, **2**, show similar alkoxide substituent variability. Further diversity is possible for alkoxides of pentacoordinate pnictogen centers, shown in **3**, although few derivatives have been reported in the absence of chelating oxygen donors. For antimony and bismuth, the pnictine oxides and pentacoordinate alkoxides form associated arrangements

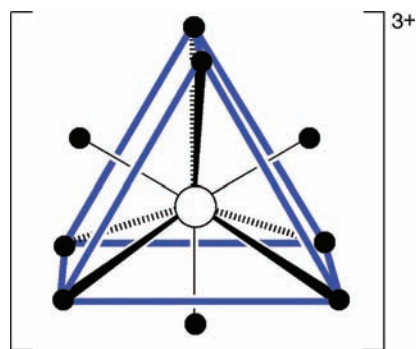


Figure 1.4 Cation of the nonahydratobismuth(III) triflate salt, with bismuth depicted as a white circle, water molecules as black circles and the trigonal prism geometry in blue

Table 1.5 Coordination numbers and approximate geometries for the pnictogen (Pn) centre in representative compounds

Coordination No.	Approximate geometry	Formula of representative compound	Refs
1	A	AsCMes*	[32]
2	B	[As(NMe) ₂ C ₃ H ₆] ⁺	[37]
	C	[SbPh ₂] [−]	[38]
	C	[As(PR ₃) ₂][BPh ₄]	[39]
	C	Li[AsPh ₂]	[41]
3	D	AsPh ₃	[40]
	D	SbR₃, R=organic substituent	[41]
	D	BiMe₃	[35]
		Bi(L-cysteine) ₃ ·H ₂ O	[42]
		PhSb[Mn(CO) ₂ C _p] ₂	[43]
4	E	[AsO₄]^{3−}	[44]
	E	[Me ₆ As ₂][OTf] ₂	[45]
	T-shaped	[(BIAN)As][SnCl ₅ (THF)]	[46]
	G	PhSb[(SCH ₂ CH ₂) ₂ O]	[41]
	G	[Ph ₂ SbCl ₂] [−]	[41]
	G	[Ph₂Bi(OCOFCF₃)₂][−]	[35]
	I	(Me₂C(O)CO₂)₂AsPh	[47]
5	H	Ph ₅ Sb	[41]
	H	Ph ₅ Bi	[35]
	I	Bi(C ₆ H ₄ CH ₃ -4) ₃ (C ₆ H ₄ F-2) ₂	[35]
	H	Bi(C ₆ H ₄ F-4) ₃ (C ₆ F ₅) ₂	[35]
6	J	[AsF₆][−]	[35]
	J	[Bi(Me) ₆] [−]	[35]
7	Distorted pentagonal bipyramid	(κ ² -O ₂ CCF ₃) ₂ Ph ₃ Bi	[35]
9	Tricapped trigonal prism	[Bi(OH ₂) ₉] ³⁺	[35]
12	Icosahedral	SbRh ₁₂ (CO) ₂₇ ^{3−}	[48]

Approximate geometries refer to the legend in Figure 1.3 where possible and the most common coordination geometries (and associated representative compounds) for each element are highlighted in blue. aryl-BIAN = 1,2-bis(arylimino)acenaphthene.

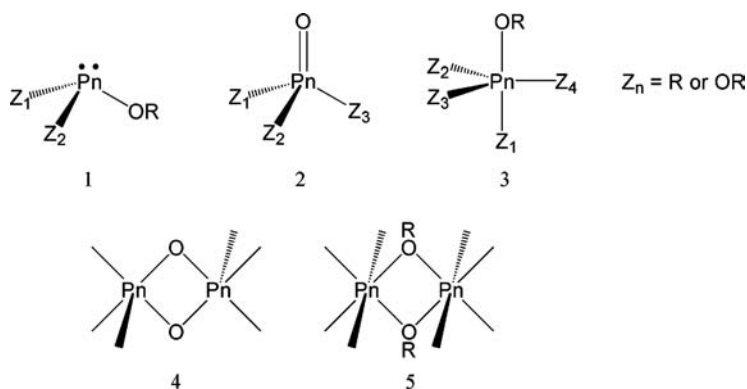


Figure 1.5 Molecular structures for oxygen-pnictogen compounds

such as those shown in **4** and **5**, respectively. Analogous structures are extremely rare for arsenic, with only few characterized examples [49]. Occurrences of single bridging oxides between antimony and bismuth centres are also known, forming oligomers or polymers. Bismuth oxyhalides of the general formula $BiOX$ are well known and typically adopt ionic structures containing $[Bi=O]^+$ [50, 51]. Other chalcogen-containing species (sulfides, selenides) show similar structural features. For example, $Bi(L\text{-cysteine})_3 \cdot H_2O$ has a trigonal pyramidal structure and contains only Bi–S metal-ligand interactions [42].

1.7 Clusters and Extended Structures

Pnictogen mineral oxides contain anions of the type PnO_4^{3-} (e.g., arsenate) and PnO_3^{3-} (e.g., arsenite) and adopt extended structures similar to phosphate (PO_4^{3-}) and phosphite (PO_3^{3-}). The common oxide of bismuth (Bi_2O_3 , bismite) does not contain a molecular unit but some of the common mineral forms of arsenic (realgar and orpiment) display molecular cage structures [11], shown in Figure 1.6. Cage structures such as these recur regularly in pnictogen cluster chemistry and are analogous to the elemental cluster anions, for example Pn_7^{3-} . Bismuth is observed to form a variety of cationic element clusters of the type Bi_m^{n+} , examples of which are illustrated in Figure 1.7 [52].

The Lewis acceptor properties of antimony and bismuth are responsible for extended structures involving halogen centers in bridging positions that are analogous to the

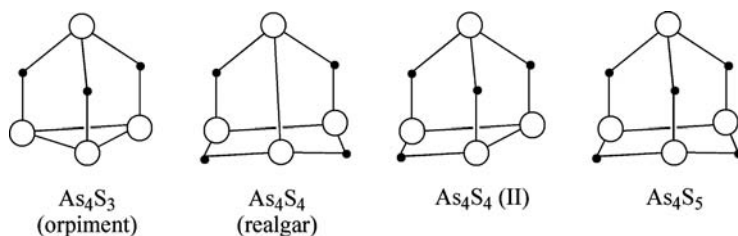


Figure 1.6 Selected structures of $As_m S_n$ clusters (As = white circles; S = black dots)

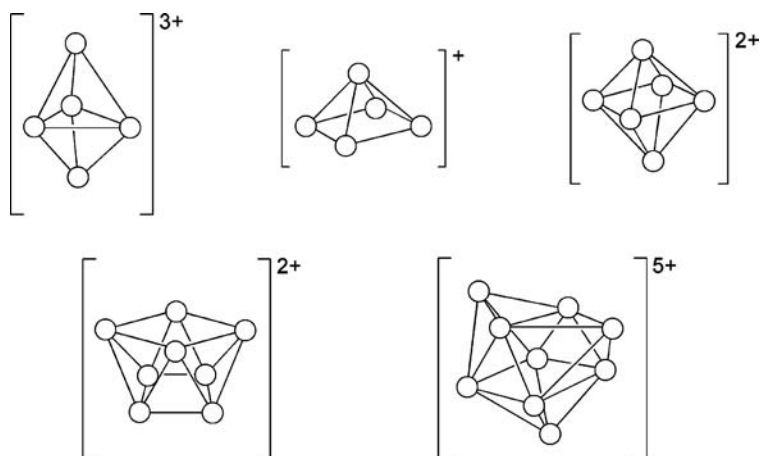


Figure 1.7 Examples of bismuth (white circles) cluster cations, including trigonal bipyramid, square based pyramid, distorted octahedron, square antiprism, and tricapped trigonal prism

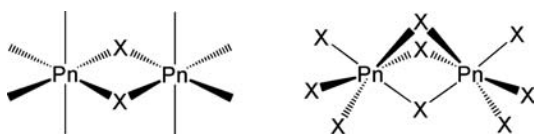


Figure 1.8 Edge sharing and confacial bi-octahedral structures observed for antimony and bismuth (Pn) halides (X)

associated structures described above for oxides and alkoxides [12]. The two bi-octahedral frameworks (edge sharing and confacial) are shown in Figure 1.8.

Larger cage structures with multiple bridging ligands are commonly observed for bismuth [11, 41]. For example, solid state structures of medically relevant bismuth compounds with chelating ligands (citrate, subsalicylate) have recently been reported [53]. The structures of many bismuth-oxygen compounds derive from the $[\text{Bi}_6(\text{OH})_{12}]^{6+}$ unit shown in Figure 1.9, which contains one bridging hydroxide (black dots) along each of the

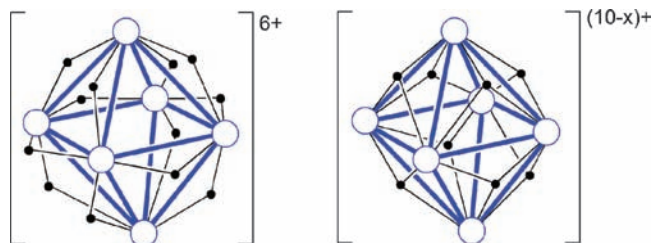


Figure 1.9 $[\text{Bi}_6(\text{OH})_{12}]^{6+}$ and $[\text{Bi}_6\text{O}_x(\text{OH})_{8-x}]^{(10-x)+}$: representative examples of bismuth (white circles) clusters, containing bridging oxygen atoms or hydroxides (black dots), with bismuth octahedra depicted in blue

12 edges of a bismuth octahedron (white circles) [11, 54]. An alternative structure [55, 56] involves bridging oxygen atoms or hydroxides on each of the eight faces of the bismuth octahedron giving formulae of the type $[\text{Bi}_6\text{O}_x(\text{OH})_{8-x}]^{(10-x)+}$.

The crystal structures of compounds containing a bismuth(III) atom (bearing a lone pair of 6s electrons) often reveal an empty coordination site at the bismuth centre. This structural feature has been defined as a hemidirected geometry and implicates the stereochemical activity of the lone pair at the bismuth site. This observed geometry may alternately be rationalized in terms of a *pseudotrans*-influence of ligand coordination on the bismuth centre. In the case of oxygen donors, mixing of the filled oxygen 2p and empty bismuth 6p orbitals leads to weaker ligand interactions at the coordination site opposite the oxygen atom(s); in turn, this may result in a vacant coordination site [36].

1.8 Hybridization and Inversion

Hybridization (or the Valence Bond Model) [30] is used extensively to rationalize the observed geometry of an atomic centre in a covalent molecule and the model is very effectively applied to most compounds containing the elements of the second period. However, the elements after neon in the Periodic Table adopt geometries that are inconsistent with the hybridization model due to the diffuse nature of *np*-orbitals relative to the *ns*-orbitals ($n > 2$) and the spatial incompatibility of these orbitals relative to 2s and 2p orbitals [30]. Consequently, the heavier pnictines (Pn=P, As, Sb, and Bi) adopt bond angles close to 90° representing the pure *p*-orbital overlap that is responsible for the bonds to the pnictogen centre [57].

Effective hybridization by nitrogen in amines and ammonia allows vertex inversion (Figure 1.10a) to take place with a minimal energy barrier ($5\text{--}6\text{ kcal mol}^{-1}$), while

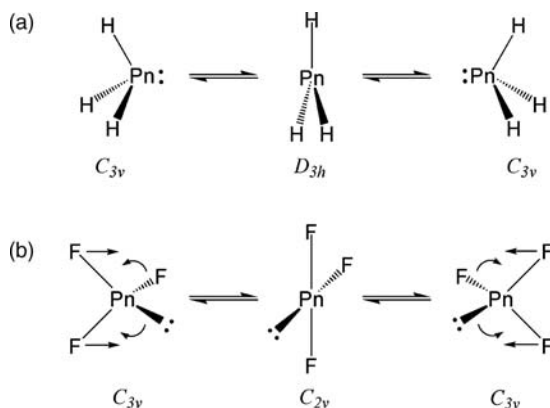


Figure 1.10 Inversion mechanism for (a) PnH_3 , vertex inversion via a trigonal planar (D_{3h}) transition state and (b) PnF_3 , edge inversion via a T-shaped (C_{2v}) transition state. Reprinted with permission from [58]. Copyright John Wiley & Sons, Ltd

Table 1.6 Inversion barriers for PnH_3 and PnF_3 ($Pn = N, P, As, Sb, Bi$). Adapted with permission from [58]. Copyright John Wiley & Sons, Ltd

Inversion Barrier (kcal mol ⁻¹)	Calculated	Experimental
<i>Hydrides (PnH₃): vertex inversion via D_{3h} transition state</i>		
NH ₃	5–6	5.8
PH ₃	35–38	31.5
AsH ₃	39–42	—
SbH ₃	43–48	—
BiH ₃	61–65	—
<i>Fluorides (PnF₃): edge inversion via C_{2v} transition state</i>		
PF ₃	53–68	
AsF ₃	46–58	
SbF ₃	38–47	
BiF ₃	34–39	

phosphines, arsines, stibines and bismuthines have a substantial barrier to vertex inversion (Table 1.6). The D_{3h} transition state for inversion of a pnictine requires ammonia to adopt trigonal planar sp^2 hybridization and promotion of the non-bonding (lone pair) electrons in the sp^3 orbital to a $p\pi$ orbital [58]. The energy associated with this bonding adjustment is small for nitrogen, while for the heavier pnictines the s to p promotional energy for nonhybridized orbitals is substantial. In contrast, the halopnictines undergo edge-inversion via a C_{2v} transition state as illustrated in Figure 1.10b, which exhibits an opposite trend in terms of the inversion energy barrier (Table 1.6).

1.9 Coordination Chemistry

The lone pair of electrons at the pnictogen centre in derivatives of PnR_3 is available for bonding with a Lewis acid. The electron donating ability decreases according to $PR_3 > AsR_3 > SbR_3 \gg BiR_3$ [28, 59]. The presence of electron donating substituents increases the basicity of the pnictogen centre and bulky substituents impose a steric shield resulting in a kinetic barrier to bond formation and a decreased basicity relative to pnictines bearing less bulky substituents. Nevertheless, heavy pnictines adopt smaller cone angles than amines, which affects their relative steric restrictions [60, 61]. According to Pearson's hard-soft acid-base theory [62], relatively soft donors favour interactions with relatively soft acceptors. For instance, coordination of an arsine to a soft metal centre is favoured over the coordination of a phosphine despite the weaker donor ability of the arsine [28].

Lewis acid behaviour is most common for compounds involving higher oxidation states and higher coordination numbers. For example, the fluoride anion forms a strong complex with PF_5 and SbF_5 to give PF_6^- and SbF_6^- , respectively. Although pnictines are more traditionally described as Lewis bases with reference to their available lone pair, complexes of pnictines as Lewis acids are known. Introduction of both a formal positive charge and an open coordination site in pnictogenium cations, PnR_2^+ , results in their extensive chemistry as Lewis acids [45, 63].

Table 1.7 Geological Data (adapted with permission from [4]. Copyright Springer Science + Business Media)

Abundance	As	Sb	Bi
Earth: Crust	1.5 ppm [7] 3.4 ppm [1]	0.2–0.5 mg/kg [1]	0.048 ppm [7]
Soil (mg/kg dry wt.)	*Average range 4.8–13.6 [9] 0.1–10 [1] Up to 90 nmol/g bound to humic acids	1×10^{-3} [1] Up to 10 nmol/g bound to humic acids	
Chief ores and sources	realgar [As ₄ S ₄] orpiment [As ₂ S ₃] loellingite [FeAs ₂]	stibnite [Sb ₂ S ₃] ullmanite [NiSbS]	bismite [α -Bi ₂ O ₃] bismuthinite [Bi ₂ S ₃] bismutite [(BiO) ₂ CO ₃] main source is by-product from Pb and Cu smelters
Seawater (ppm)			
Atlantic surface	1.45×10^{-3}	c. 0.3×10^{-3}	5.1×10^{-8}
Atlantic deep	1.53×10^{-3}	—	n.a.
Pacific surface	1.47×10^{-3}	—	4×10^{-8}
Pacific deep	1.75×10^{-3}	—	0.4×10^{-8}
Residence time in ocean (years) (oxidation state in parentheses)	90 000 (V)	c. 3.5×10^5 (III)	n.a. (III)
*Freshwater [8, 9]			
Surface water	Average 1.6 µg/l; ranges from 0.1–25.0 µg/l	<10 µg/l; ranges from 0.001–9.1 mg/l	—
Ground water and deep lake sediments	Average 1.5 µg/l; ranges from 0.1–60 µg/l	<5 µg/l	—
*Air (ng/m ³)	Average 1; ranges from 0.5–17 (urban) [9]	0.11–0.23 (urban) [1]	1–66 (urban) [1] 0.1–0.6 (rural) [1]

Values marked with * indicate geological data from Canada, while remaining values are nonspecific global data.

1.10 Geological Occurrence

The natural abundance in land and water sources of arsenic is significantly greater than that of antimony or bismuth (where bismuth has the lowest natural abundance). The most common ores of arsenic are realgar (As_4S_4), orpiment (As_2S_3), arsenolite (As_2O_3), arsenopyrite (FeAsS) and enargite (Cu_3AsS_4) [4, 64]. Arsenic is typically introduced into the biosphere in bioavailable non-mineral forms through the industrial processing of ores, improper handling of wastes, as well as use in herbicides and pesticides that are now banned in North America [9].

The common ores of antimony are stibnite (Sb_2S_3), ulmanite (NiSbS), livingstonite (HgSb_4S_8), tetrahedrite (Cu_3SbS_3) and jamesonite ($\text{FePb}_4\text{Sb}_6\text{S}_{14}$) [64]. Antimony is most commonly introduced to the biosphere via natural biological and geochemical cycling processes [65]. The low aqueous solubility of antimony relative to arsenic [1] hinders its transport and bioaccumulation does not occur [8]. Only tartar emetic (antimony potassium tartrate, $\text{C}_8\text{H}_4\text{K}_2\text{O}_{12}\text{Sb}_2\cdot 3\text{H}_2\text{O}$) has high water solubility (83 g/l) [1]. Dissolved antimony discharged into the natural aquifer typically precipitates as Sb_2O_3 or Sb_2O_5 [8].

Bismuth occurs in the ore bismite ($\alpha\text{-Bi}_2\text{O}_3$), bismuthinite (Bi_2S_3) and bismuthite ($\text{BiO})_2\text{CO}_3$ [64]. Most bioavailable bismuth has been introduced via human activity; however, small amounts may be released due to volcanic activity or aqueous action [64]. Table 1.7 provides geological and environmental abundance data for these heavier pnictogens.

1.11 Aqueous Chemistry and Speciation

The dominant forms of arsenic in dilute aqueous solutions are $\text{As}(\text{OH})_3$, $[\text{As}(\text{OH})_4]^-$, $[\text{AsO}_2(\text{OH})]^{2-}$ and $[\text{AsO}_3]^{3-}$, where $\text{As}(\text{OH})_3$ behaves as a Lewis acid and can form adducts in aqueous media. Oxygen exchange between water molecules and arsenite anions is catalysed by trace amounts of $[\text{H}_2\text{AsO}_3]^-$ [65]. In both acidic and basic environments, arsenic is commonly methylated [64] as $[\text{MeAsO}_4]^{2-}$, $[\text{Me}_2\text{AsO}_2]^-$ and Me_3AsO [9]. Arsenobetaine and arsenocholine (Figure 1.11) are the common forms of arsenic in marine organisms and are found to be nontoxic in mice and hamsters [66]. In general, inorganic forms of arsenic have higher toxicity in humans than organoarsines [64], which are readily excreted [1, 9].

Antimony occurs most commonly as $[\text{Sb}(\text{OH})_6]^-$, although it has also been postulated as $\text{Sb}(\text{OH})_5\cdot\text{H}_2\text{O}$ in aqueous environments at $\text{pH} > 4$ [65]. Under acidic conditions ($\text{pH} 2$), $[\text{SbO}]^+$ or $[\text{Sb}(\text{OH})_2]^+$ are found [12, 65], while at $\text{pH} > 11$, $[\text{Sb}(\text{OH})_4]^-$ is the dominant form [65]. Bismuth has a diverse aqueous chemistry analogous to arsenic. The dominant species observed in natural waters is $\text{Bi}(\text{OH})_3$ [67].



Figure 1.11 *Molecular structures of the nontoxic forms of arsenic in marine organisms*

1.12 Analytical Methods and Characterization

Due to the quadrupolar nuclear spins (Table 1.1) of the heavy pnictogen elements, they are not readily analysed by NMR spectroscopy, one of the most versatile methods of characterization. X-ray diffraction can provide the most definitive characterization data for compounds of these elements, if crystalline samples [68] are available, although powder diffraction data [69] also yields useful information. Infrared [70] and Raman [71] vibrational spectroscopy of solids and solutions, as well as UV-visible absorbance [72] spectroscopy of solutions, have been employed to elucidate structural information. Mass spectrometry [73] has also been employed to determine the formula of ions in the gas phase. Antimony-121 (^{121}Sb) can be analysed by Mössbauer spectroscopy [74, 75] giving both structural (e.g., molecular symmetry and lone pair orientation) and electronic information (e.g., oxidation state, electronic configuration, bond ionicity and orbital population analysis with respect to calculated orbitals).

1.13 Conclusions

Arsenic, antimony and bismuth display a diverse chemistry that is distinct from that of their lighter congeners in Group 15. Furthermore, the relative instability of the +5 oxidation state for arsenic and bismuth and the tendency of antimony and bismuth to form extended molecular structures distinguish these elements from one another. The resulting coordination environments preferred by these elements leads to structural features that may prove significant in biological and medicinal contexts.

References

1. Nordberg, G.F., Fowler, B.A., Nordberg, M. and Friberg, L. (eds) (2007) *Handbook on the Toxicology of Metals*, Elsevier, Burlington.
2. Seiler, H.G., Sigel, A. and Sigel, H. (eds) (1994) *Handbook on Metals in Clinical and Analytical Chemistry*, Marcel Dekker, New York.
3. Briand, G.G. and Burford, N. (1999) *Chemical Reviews*, **99**, 2601–2657.
4. Norman, N.C. (ed.) (1998) *Chemistry of Arsenic, Antimony and Bismuth*, Blackie Academic and Professional, London.
5. de Marcillac, P., Coron, N., Dambier, G. *et al.* (2003) *Nature*, **422**, 876–878.
6. Lloyd, N.C., Morgan, H.W., Nicholson, B.K. and Ronimus, R.S. (2005) *Angewandte Chemie-International Edition*, **44**, 941–944.
7. Emsley, J. (1998) *The Elements*, Oxford University Press, Inc., New York.
8. Health Canada (1999) *Guidelines for Canadian Drinking Water Quality - Supporting Documentation - Antimony*, Water Quality and Health Bureau, Healthy Environments, and Consumer Safety Branch, Health Canada, Ottawa.
9. Health Canada (2006) *Guidelines for Canadian Drinking Water Quality: Technical Document - Arsenic*, Water Quality and Health Bureau, Healthy Environments, and Consumer Safety Branch, Health Canada, Ottawa.
10. Smith, P.M., Leadbetter, A.J. and Apling, A.J. (1975) *Philosophical Magazine*, **31**, 57–64.
11. Greenwood, N.N. and Earnshaw, A. (1997) *Chemistry of the Elements*, Butterworth-Heinemann, Oxford.

12. King, R.B. (1994) in: *The Encyclopedia of Inorganic Chemistry* (ed. R.B. King), John Wiley & Sons, Canada Ltd Toronto, pp. 170–176.
13. Sisler, H.H. (1988) in: *Inorganic Reactions & Methods* (eds J.J. Zuckermann and A.P. Hagen), Wiley-VCH Verlag GmbH Weinheim, pp. 30–31.
14. Schiferl, D. and Barrett, C.S. (1969) *Journal of Applied Crystallography*, **2**, 30–36.
15. Group V. (1982) in: *The Structure of the Elements* (ed. J. Donohue), John Wiley & Sons, Inc., New York, pp. 280–316.
16. Barrett, C.S., Cucka, P. and Haefner, K. (1963) *Acta Crystallographica*, **16**, 451–453.
17. Cucka, P. and Barrett, C.S. (1962) *Acta Crystallographica*, **15**, 865–872.
18. Luo, Y.-R. (2007) *Comprehensive Handbook of Chemical Bond Energies*, CRC Press, Boca Raton.
19. Lide, D.R. (ed.) (2008) *CRC Handbook of Chemistry and Physics*, CRC Press, Boca Raton.
20. Baerends, E.J., Schwarz, W.H.E., Schwerdtfeger, P. and Snijders, J.G. (1990) *Journal of Physics B-Atomic Molecular and Optical Physics*, **23**, 3225–3240.
21. Pauling, L. (1932) *Journal of the American Chemical Society*, **54**, 3570–3582.
22. Allred, A.L. and Rochow, E.G. (1958) *Journal of Inorganic & Nuclear Chemistry*, **5**, 264–268.
23. Schwarz, W.H.E., Chu, S.Y. and Mark, F. (1983) *Molecular Physics*, **50**, 603–623.
24. Christiansen, P.A. and Ermler, W.C. (1985) *Molecular Physics*, **55**, 1109–1110.
25. Najafpour, M.M. (2007) *Chemical Education*, **12**, 142–149.
26. Einstein, A. (1918) *Annals of Physics*, **55**, 241–244.
27. Wereide, T. (1923) *Physical Review*, **21**, 391–396.
28. Lange, K.C.H. and Klapötke, T. (1994) in: *The Chemistry of Organic Arsenic, Antimony and Bismuth* (ed. S. Patai), John Wiley & Sons, Ltd, Chichester, pp. 315–366.
29. Thayer, J.S. (2005) *Journal of Chemical Education*, **82**, 1721–1727.
30. Kutzelnigg, W. (1984) *Angewandte Chemie-International Edition*, **23**, 272–295.
31. Pyykko, P. (1988) *Chemical Reviews*, **88**, 563–594.
32. Märkl, G. and Sejpka, H. (1986) *Angewandte Chemie-International Edition*, **25**, 264–265.
33. Ferguson, G., Glidewell, C., Kaitner, B. *et al.* (1987) *Acta Crystallographica*, **C43**, 824–826.
34. Pebler, J., Weller, F. and Dehnicke, K. (1982) *Zeitschrift für Anorganische und Allgemeine Chemie*, **492**, 139–147.
35. Suzuki, H. and Matano, Y. (2001) *Organobismuth Chemistry*, Elsevier, Netherlands.
36. Payne, D.J., Egdell, R.G., Walsh, A. *et al.* (2006) *Physical Review Letters*, **96**, 157403(-1)–157403(-4).
37. Burford, N., Macdonald, C.L.B., Parks, T.M. *et al.* (1996) *Canadian Journal of Chemistry*, **74**, 2209–2216.
38. Bartlett, R.A., Dias, H.V.R., Hope, H. *et al.* (1986) *Journal of the American Chemical Society*, **108**, 6921–6926.
39. Barnham, R.J., Deng, R.M.K., Dillon, K.B. *et al.* (2001) *Heteroatom Chemistry*, **12**, 501.
40. Mazhar-Ul-Harque, Tayim, H.A. and Horne, W. (1985) *Journal of Crystallographic and Spectroscopy: Resolution*, **15**, 561–571.
41. Sowerby, D.B. (1994) in: *The Chemistry of Organic Arsenic, Antimony and Bismuth* (ed. S. Patai), John Wiley & Sons, Ltd, Chichester, pp. 25–88.
42. Wang, Y.-J. and Xu, L. (2008) *Journal of Inorganic Biochemistry*, **102**, 988–991.
43. Cotton, F.A., Wilkinson, G., Murillo, C.A. and Bochmann, M. (1999) *Advanced Inorganic Chemistry*, John Wiley & Sons, Inc., New York.
44. Sorribas, V. and Villa-Bellosta, R. (2008) *Toxicology and Applied Pharmacology*, **232**, 125–134.
45. Conrad, E.D., Burford, N., McDonald, R. and Ferguson, M.J. (2008) *Inorganic Chemistry*, **47**, 2952–2954.
46. Reeske, G., Hoberg, C.R., Hill, N.J. and Cowley, A.H. (2006) *Journal of the American Chemical Society*, **128**, 2800–2801.
47. Holmes, R.R., Day, R.O. and Sau, A.C. (1985) *Organometallics*, **4**, 714–720.
48. Vidal, J.L. and Troup, J.M. (1981) *Journal of Organometallic Chemistry*, **213**, 351–363.
49. Haase, W. (1974) *Chemische Berichte*, **107**, 1009–1018.
50. Whitmire, K.H. (1998) in: *The Encyclopedia of Inorganic Chemistry* (ed. R.B. King), John Wiley & Sons, Canada Ltd, Toronto, pp. 280–291.

51. Whitmire, K.H. (1998) in: *The Encyclopedia of Inorganic Chemistry* (ed. R.B. King), John Wiley & Sons, Canada Ltd, Toronto, pp. 292–300.
52. Ruck, M. and Hampel, S. (2002) *Polyhedron*, **21**, 651–656.
53. Ge, R. and Sun, H. (2007) *Accounts of Chemical Research*, **40**, 267–274.
54. Maroni, V.A. and Spiro, T.G. (2009) *Inorganic Chemistry*, **7**, 183–188.
55. Henry, N., Mentre, O., Abraham, F. et al. (2006) *Journal of Solid State Chemistry*, **179**, 3087–3094.
56. Sundvall, B. (1983) *Inorganic Chemistry*, **22**, 1906–1912.
57. Glausinger, W.S., Chung, Y.S. and Balasubramanian, K.J. (1993) *Chemical Physics*, **98**, 8859–8869.
58. Nagase, S. (1994) in: *The Chemistry of Organic Arsenic, Antimony and Bismuth Compounds* (ed. S. Patai), John Wiley & Sons, Ltd, Chichester, pp. 1–24.
59. Carmalt, C.J. and Norman, N.C. (1998) in: *Chemistry of Arsenic, Antimony and Bismuth* (ed. N.C. Norman), Blackie Academic and Professional, London, pp. 1–38.
60. Imyanitov, N.S. (1985) *Koordinatsionnaya Khimiya*, **11**, 1041–1045.
61. Imyanitov, N.S. (1985) *Koordinatsionnaya Khimiya*, **11**, 1171–1178.
62. Pearson, R.G. (1968) *Journal of Chemical Education*, **45**, 581–587.
63. Ellis, B.D. and Macdonald, C.L.B. (2007) *Coordination Chemistry Reviews*, **251**, 936–973.
64. Reglinski, J. (1998) in: *Chemistry of Arsenic, Antimony and Bismuth* (ed. N.C. Norman), Blackie Academic and Professional, London, pp. 403–440.
65. Richens, D.T. (1997) *The Chemistry of Aqua Ions*, John Wiley & Sons, Ltd, Chichester.
66. Maeda, S. (1994) in: *The Chemistry of Organic Arsenic, Antimony and Bismuth Compounds* (ed. S. Patai), John Wiley & Sons, Ltd, Chichester, pp. 725–759.
67. Stumm, W. and Morgan, J.J. (1996) *Aquatic Chemistry: Chemical Equilibria and Rates in Natural Waters*, John Wiley & Sons, Inc., New York.
68. Massa, W. (2004) *Crystal Structure Determination*, Springer, New York.
69. David, W.I.F., Shankland, K., McCusker, L.B. and Baerlocher, Ch. (eds) (2002) *Structure Determination from Powder Diffraction Data*, Oxford University Press, Oxford.
70. Griffiths, P.R. and de Haseth, J.A. (2007) *Fourier Transform Infrared Spectroscopy*, John Wiley & Sons, Inc., Hoboken.
71. Smith, E. and Dent, G. (2005) *Modern Raman Spectroscopy, A Practical Approach*, John Wiley & Sons, Inc., Hoboken.
72. Perkampus, H.-H. (1992) *UV-Vis Spectroscopy and its Applications*, Springer-Verlag, Berlin.
73. Becker, J.S. (2007) *Inorganic Mass Spectrometry, Principles and Applications*, John Wiley & Sons, Inc., Hoboken.
74. Bowen, L.H. (1973) in: *Mössbauer Effect Data Index, Covering the 1972 Literature* (eds J.G. Stevens and V.E. Stevens), Plenum, New York, pp. 71–110.
75. Stevens, J.G. (1984) in: *Chemical Mössbauer Spectroscopy* (ed. R.H. Herber), Plenum, New York, pp. 319–342.

2

Arsenic's Interactions with Macromolecules and its Relationship to Carcinogenesis

Kirk T. Kitchin

*Integrated Systems Toxicology Division, National Health and Environmental Effects
Research Laboratory, Office of Research and Development, U.S. Environmental
Protection Agency, Research Triangle Park, NC 27711, USA*

2.1 Introduction

This book chapter presents selected aspects of arsenic biochemistry, some of the effects of arsenicals on biochemical endpoints, three possible modes of action (MOA) (binding, oxidative stress and DNA methylation) for arsenic causing human cancer, several of the connections between arsenic and carcinogenicity (epidemiological studies, animal studies and the use of arsenic in the treatment of leukaemia) and finally some sources of information for newcomers to this large and complex research area. This chapter focuses more on individual speciated arsenicals and the individual proteins or other cellular targets of arsenicals rather than more descriptive studies of adverse animal health effects or pathological endpoints. The general order of the chapter is from smaller to larger biological systems. Entire books [1–3] and comprehensive review articles [4–9] have been published on the subject of arsenic. Therefore, in many cases this material is deliberately not included in this chapter if the material is well presented elsewhere.

2.2 Arsenic's Interactions with DNA and Proteins

The charge state of common arsenicals can be deduced from their pK_a values arsenite (9.23), arsenate (2.25, 6.77, 11.6), monomethylarsonic acid (4.1, 8.7) and dimethylarsinic acid (6.9) [9–11]. Thus at physiological pH, arsenite, monomethylarsonous acid, dimethylarsinous acid, trimethylarsine oxide and all four arsines should be uncharged. Because carcinogenesis is the development of heritable changes in cells, alterations in DNA are normally the first place to look for causes of cancer. Studies looking for the formation of covalent bonds between arsenic atoms and the DNA backbone have generally come back negative. Formation of reversible coordination complexes between arsenic and DNA have been looked for but not found by one experimental group [12]. At concentrations up to about 1 mM, no specific binding was observed between ^{73}As labeled arsenite and calf thymus DNA. Similarly in one study radioactive pentavalent arsenate did not specifically bind to DNA. The inorganic arsenicals might have interacted with any number of functional groups present in DNA such as amines, keto groups, phosphates or ring nitrogen atoms. Apparently arsenic does not form any appreciable coordination complexes with any of the atoms or functional groups contained in DNA [12].

Histones are positively charged proteins that contain large numbers of lysine and arginine moieties. However, in the sequences of major cow histones there are only two cysteines and 10 histidines in a total of 595 amino acids. Neither arsenite nor arsenate showed specific binding to purified calf thymus histones type II-A or to purified cow histone H3/H4, at concentrations up to about 1 mM [12].

Although positively charged metals such as Ni^{II} and Cu^{II} bind well to histidine, arsenite binds well only to the cysteine containing peptides and proteins [10]. There have been observations of arsenic interacting with the hetero atoms of Se [13, 14], Mo [15] and rarely the hydroxyl group of two tyrosine moieties [16].

Although it is an indirect interaction, arsenical exposures are well known for increasing the concentration of 8-hydroxydeoxyguanosine (8-OHdG), an oxidized DNA base [6]. An attractive biochemical hypothesis is that the changes in arsenic's valence state between +3 and +5 produce reactive oxygen species (ROS) such as superoxide anion. The arsenical induced increased concentrations of superoxide anion, hydrogen peroxide and hydroxyl radical can then lead to increased 8-OHdG by attack of the hydroxyl radical on dG of DNA. Hydroxyl radical is also expected to be a good hydrogen atom abstractor from DNA leading to single strand breaks which have been frequently observed as an arsenical induced biological effect in both *in vitro* [4] and animal studies [17–19].

A good review of the mutational, DNA damage and cytogenetic effects of arsenicals has been written by Basu *et al.* [4]. Although it is a poor point mutagen, arsenic does interact with DNA. Arsenic cause many clastogenic and chromosomal changes. Many of arsenic's effects on DNA can be explained by (a) trivalent arsenicals acting via the proteins associated with DNA synthesis, repair and replication and (b) free radical attack on existing DNA which yields primarily single strand breaks. Kligerman *et al.* [20] used several different genetic toxicology endpoints (chromosome aberrations, sister chromatid exchanges (SCE), mutagenicity in L5178Y/Tk(+/-) mouse lymphoma cells, *Salmonella* reversion assay, prophage induction in *Escherichia coli*) and found that generally dimethylarsinous acid (DMA(III)) and monomethylarsonous acid (MMA(III)) were the most potent genotoxic arsenicals. None of the six tested arsenicals (arsenate (As(V)), arsenite (As(III)),

monomethylarsonic acid (MMA(V)), MMA(III), dimethylarsinic acid (DMA(V)) and DMA(III)) caused SCE, *Salmonella* mutations or prophage induction [20].

Andrewes *et al.* [21] studied all 11 arsenicals shown in Figure 2.1 including the four arsine forms of arsenic. Arsines have hydrogen and methyl groups but no hydroxyl groups attached to the arsenic atom. In most mammals, dimethylated forms of arsenic are rapidly excreted in the urine. In some rare situations, arsenic methylation will proceed all the way to the addition of either three [22] or four methyl groups (e.g., the marine polychaetes *Nereis diversicolor* and *Nereis virens* [23]. In the experimental system of pBR322 supercoiled plasmid DNA, single strand breaks were caused by MMA(III), DMA(III), monomethylarsine, dimethylarsine, and trimethylarsine [21]. The two most potent arsines, trimethylarsine and dimethylarsine, were about 100 times more potent than DMA(III) [21]. Previously, DMA(III) had been the most potent genotoxic arsenical known. Although these reduced methylated arsines might only be produced *in vivo* in small quantities, these highly reactive arsenicals interact rapidly with both triplet state dioxygen molecules and DNA.

In Chinese hamster ovary cells, (CHO) cells exposed to seven arsenicals (As(V), As(III), MMA(V), MMA(III), DMA(V), DMA(III) and TMAO) and the ability of these arsenicals to enter cells and cause micronucleus (MN) induction, chromosome aberrations (CA), and SCE was determined [24]. Their results showed that MMA(III) and DMA(III) induce

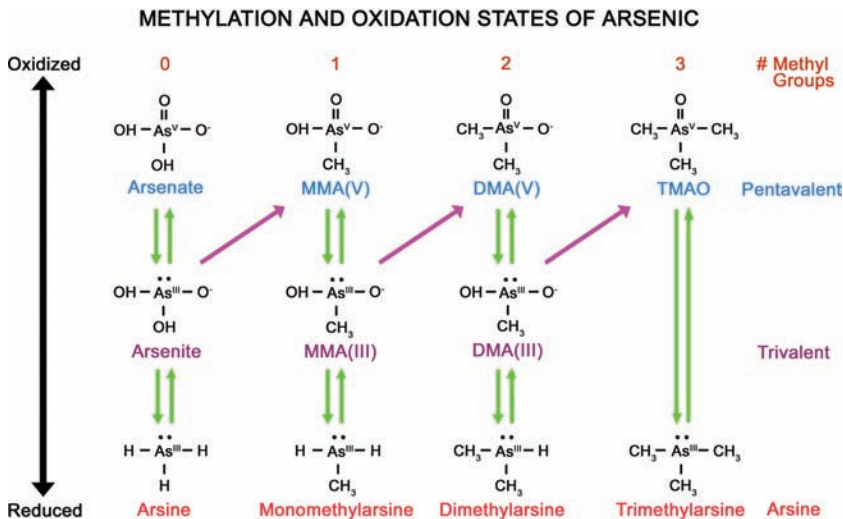


Figure 2.1 The metabolic conversions and interrelationships of the chemical forms of arsenic are shown above. The common valence states of arsenic in mammals are +5 and +3. The downward green arrows are reductions. The upward green arrows are oxidations. The diagonal purple arrows are oxidative methylations which are enzymatically performed. The most common arsenic chemical forms found in mammals are arsenate, arsenite, MMA(V), MMA(III), DMA(V) and DMA(III). MMA(III) and DMA(III) are prone to oxidation during sample collection, storage and assay and may occur in higher concentrations *in vivo* than have been chemically demonstrated so far. In most mammals, there is less positive evidence for the occurrence of substantial tissue concentrations of any of the arsines and TMAO

cytotoxic and genotoxic effects to a greater extent than MMA(V) or DMA(V). MN, CA and SCE were significantly increased by exposure to DMA(III) and MMA(III). As(III) and As(V) induced CA and SCE but no MN. At up to 5 mM, MMA(V), DMA(V) and TMAO(V) were not genotoxic to CHO cells. Overall, the potency of the DNA damage decreased in the order DMA(III) > MMA(III) > As(III), As(V) > MMA(V) > DMA(V) > TMAO(V) [24]. When the uptake of arsenicals into CHO cells was measured, it was found that only about 0.03% MMA(V) and DMA(V), 2% of the MMA(III), As(III) and As(V) and 10% of the DMA(III) was taken up. As(V), MMA(V) and DMA(V) all have one or more negative charges on them at physiological pH. Charged arsenicals should have reduced passive transport across cell membranes. Evidently, the electrical neutrality of DMA(III) and the lipophilicity of the two methyl groups assist in getting DMA(III) across cell membranes. The observed order of transport across the CHO cell membrane was DMA(III) > As(III) > MMA(III) > As(V) > DMA(V), MMA(V) and TMAO [24]. Transport processes (e.g., aquaglyceroporins [25] and the phosphate transport system [26]) are known to transport arsenicals across cell membranes. Although arsenicals do not seem to directly interact in either a covalent or coordination chemistry manner with DNA, there are excellent experimental reasons to believe in interactions between trivalent arsenicals and cysteine containing proteins. Among the amino acids, arsenite interacts well with one or more cysteine moieties and seems to completely leave methionine, histidine, arginine, lysine and hydroxyl containing amino acids alone [27]. It seems that sulfur and selenium account for almost all the coordination complexes that arsenicals are known to form in biology. Since sulfhydryls are so common in biological systems, they dominate the *in vivo* biochemical complexes of arsenic. Much of the biological effects of arsenic containing compounds, particularly those of the inorganic arsenic to either DMA(V) or trimethylarsine oxide methylation pathway, can be interpreted as downstream events of protein binding of trivalent arsenicals (e.g., arsenite, MMA(III), DMA(III) and possibly even trimethylarsine (via the fourth and fifth possible coordinations of arsenic [28]). The amino acid sequences and binding constant data of all seven synthetic peptides discussed in this chapter are summarized in Table 2.1.

With monothiol binding sites of peptides and proteins, arsenite is expected to bind with a dissociation equilibrium constant value (K_d) of approximately 100–200 μM [27]. About 99% of the arsenite is bound to tissue sulfhydryl groups at any given time point [27]. About 91% of the total arsenite binding is to the more numerous monothiol sites. The association rate constant of ligand receptor complex (k_{on}), dissociation rate

Table 2.1 Synthetic peptides and their binding constants

Peptide	#C (Cys)	Amino Acid Sequence	K_d (μM)	$B_{max}\eta_M/\text{mg}$
15	4	RYCAVCNDYASGYHYGVWSCEGCKA	2.20	89.2
24	3	RYCAVCNDYASGYHYGVWSCEGGKA	4.28	234
16	2	RYCAVCNDYASGYHYGV	2.71	36.2
20	1	RVCAVGNDYASGYHYGV	190	26.1
10	3	LECAWQGKCVEGTEHLYSMKCKNV	1.32	59.3
19	1	LEGAWQGKGVTEHLYSMKCKNV	1.24	26.4
5	3	YYGCGLVIPEHLENCWILDGLSGSGRDCYVLK	2.0	36.0

The amino acid sequences of peptides 15, 24, 16 and 20 are based on the zinc finger region of the human estrogen receptor alpha. Peptides 10 and 19 are based on the amino acids in the interior of the estrogen binding pocket of the human estrogen receptor alpha. Peptide 5 is based on human arsenic +3 methyltransferase.

constant of ligand receptor complex (k_{off}) and the half life ($T_{1/2}$) for arsenite binding to monothiol sites were too fast to be measured [29]. The overall picture that emerges is one of arsenite having a very short occupancy time on particular monothiol binding sites [29]. Thus, it is difficult to believe that trivalent arsenical binding to monothiol sites is biologically important in causing carcinogenesis or any other biological effects because (1) the occupancy time is so short and (2) the percentage of the biological monothiol sites occupied is less than 0.1%.

In contrast, dithiol binding sites have a long history of perceived importance in arsenic toxicology going back at least to the 1940s. For dithiol sites the K_d can be 1–20 μM , much lower than the value for monothiol sites. Estimates of the k_{off} rates are between 0.3–0.5 min^{-1} which leads to a measurable half life ($t_{1/2}$) of about 1.3–2.0 min for arsenite binding to dithiol sites [29]. Such dithiol sites on important proteins and peptides can easily be occupied by trivalent arsenicals long enough and the resulting complex stable enough to cause some of the adverse health effects of arsenic.

Trithiol binding sites are expected to be rarer in biology than dithiol sites. However, trithiol binding sites are known to exist. Several examples include the arsenic metallochaperone (ArsD) and extrusion (ArsA) proteins studied by Barry Rosen and colleagues (and covered in Chapter 8 of this book), C3H1 and C4 zinc finger proteins that normally coordinate to zinc and possibly the arsenite binding site of the enzyme arsenic (+3 oxidation state) methyltransferase (AS3MT) [30, 31]. Sites that are effectively trithiol sites can occur when arsenite binds to a dithiol protein site containing two cysteines from a protein and then the tridentate arsenite coordinates to either a glutathione or to the free amino acid cysteine. This would result in a tridentate coordination that would be expected to have a long $T_{1/2}$ of about 1–3 h [29].

At trithiol binding sites of peptides and proteins, arsenite is expected to bind with a K_d of about 1–20 μM (the same as dithiol sites), but the k_{off} rates are much slower (0.0045–0.007 min^{-1}) and thus the $T_{1/2}$ is much longer, 1.7–2.6 h [29]. Such stable binding sites are excellent candidates for mediating many of arsenic's toxicological and carcinogenic effects.

The monothiol peptide 20 (RVCAVGNDYASGYHYGV) and the trithiol peptide 10 (LECAWQGKCVEGTEHLYSMKCK) were used in disassociation binding studies using radioactive ^{73}As -labeled arsenite and vacuum filtration methodology [29]. Intermolecular arsenite binding to up to three different proteins or peptides is schematically shown in panel A of Figure 2.2; intramolecular arsenite binding to a peptide with a trithiol binding site is shown in panel B.

Nonlinear regression analysis of the dissociation of both arsenite-peptide complexes showed that triphasic fits gave excellent r^2 values (0.9859 for peptide 20 and 0.9890 for peptide 10). The first phase of arsenite peptide dissociation had the largest span (decrease in binding) and the rate was too fast to be measured using vacuum filtration methods. The dissociation rate constants of arsenite peptide complexes for the second phase were 0.35 and 0.54 min^{-1} and for the third phase were 0.0071 and 0.0045 min^{-1} for peptides 20 and 10, respectively [29].

For the trithiol peptide 10 there was more total binding found and more of the total binding was of a dithiol and trithiol type. For peptide 10, the three spans of triphasic decay were 59%, 16% and 25% of the total binding of 43.7 nM/mg protein (or 0.14 nM bound/nM of peptide 10).

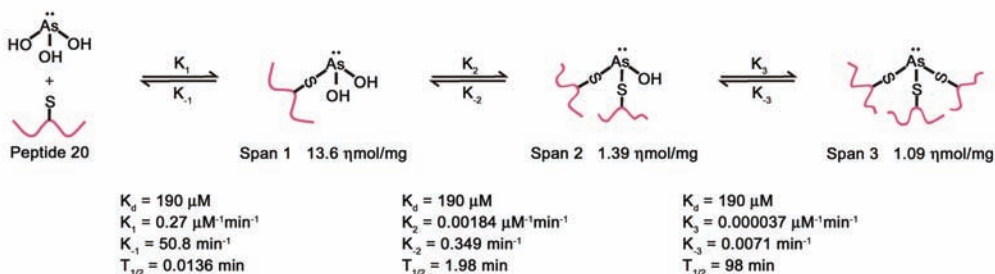
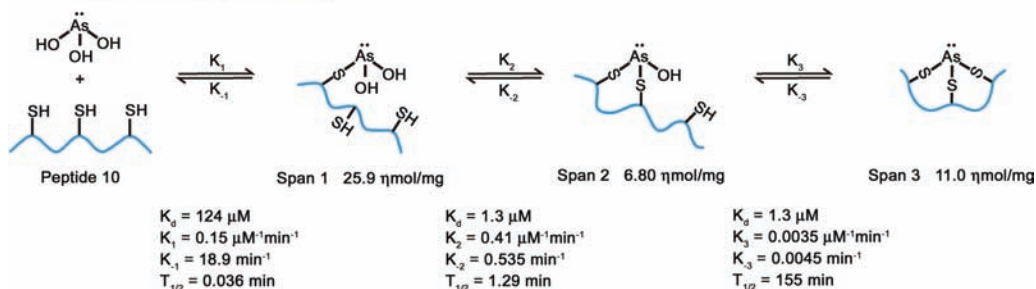
A (Inter Molecular Binding)**B (Intra Molecular Binding)**

Figure 2.2 Schematic representation of arsenite-peptide complexes associating and dissociating (a) in an intermolecular manner with peptide 20 with one cysteine as an example and (b) in an intramolecular manner with peptide 10 with three cysteines as an example. Peptide 10 can bind arsenite in both the intermolecular and intramolecular manner. The K_d values of 190, 124 and 1.32 μM are based on the saturation binding studies of peptide 20, 10 and 19 by Kitchin and Wallace [29]. Estimates of the arsenite peptide complexes dissociation rates k_{-1} , k_{-2} and k_{-3} come from Kitchin and Wallace [29]. The three respective association rates, k_1 , k_2 and k_3 are calculated by the using the equation $K_d = k_{-1}/k_1 = k_{\text{off}}/k_{\text{on}}$ while the half lives are estimated by using the equation $T_{1/2} = 0.693/k_{\text{off}}$. Reprinted with permission from [29]. Copyright John Wiley & Sons, Ltd 2006

The binding scheme presented in Figure 2.2 is consistent with (a) the known coordination chemistry of arsenic, (b) known intermolecular complexes of this type of structure with glutathione and cysteine and (c) intramolecular bidentate complexes of trivalent arsenicals and small chelator molecules such as 2,3-dimercaptopropanol (British Anti-Lewisite) [32], meso-dimercaptosuccinic acid (DMSA) and 2,3-dimercapto-1-propanesulfonic acid, sodium salt (DMPS) [33].

This dissociation study (a) demonstrated the long half lives of tridentate arsenite-peptide complexes, (b) demonstrated the large dissociation rate constant for a unidentate complex of a trivalent arsenic and a single sulfhydryl group, (c) showed that the kinetics of dissociation of intermolecular and intramolecular complexes of arsenite and one, two or three cysteines of peptides is quite similar and (d) demonstrated the great difference (almost four orders of magnitude) between the rates of dissociation of a single arsenic-sulfur coordination versus arsenic coordinated to three sulfur atoms [29].

These types of binding experiments show that arsenite can crosslink peptides and proteins and thus form long lived complexes of two and three cysteine containing peptides (Figure 2.2a). The matter of greatest importance in determining the stability of the overall arsenite peptide complex is the number of arsenic coordinations to sulfur and not if the coordinations are in a ring geometry or not.

The arsenite μM values of (a) the K_d for both dithiol and/or trithiol binding sites (about 1–20) [29], (b) the K_d for monothiol binding sites (about 100–200) [27] and (c) the observed 24 h μM inhibitory concentration 50 (IC_{50}) for rat hepatocytes (~ 10), human hepatocytes (> 20), human keratinocytes (> 20), human bronchial cells (3.2) and UROsta human urinary bladder cells (17.8) [34] can all be compared. Clearly, arsenite binding to monothiol sites cannot explain arsenite's lethality to cultured cells because substantial numbers of cells are dying at arsenite μM concentrations much lower than the K_d values for arsenite binding to monothiol binding sites. Only dithiol and trithiol arsenite binding sites have a low enough K_d values to explain arsenite's observed IC_{50} curves.

Arsenite (with up to tridentate binding), MMA(III) (with up to bidentate binding) and DMA(III) (with only unidentate binding) are expected to be very different in their peptide and protein binding affinities, dissociation rate constants and the arsenic-peptide complex half lives. The inorganic arsenicals arsenite and arsenate have water solubilities in the molar range. MMA(V) and DMA(V) are also highly water soluble. Adding methyl groups to arsenic increases the degree of lipophilicity and changes the water/octanol partition coefficient.

A scheme for the ability of thiols (RSH) to both reduce (pentavalent \rightarrow trivalent oxidation state for arsenic) and to complex to inorganic and methylated arsenicals has been presented by Cullen's group [35]:



Because the intracellular concentration of reduced glutathione (GSH) is so large, glutathione can form coordination complexes with various trivalent arsenicals *in vivo*. Complexes of arsenic triglutathione and methylarsenic diglutathione have been demonstrated *in vivo* [36]. For dimethylarsenic glutathione there is only limited indirect evidence that this species occurs *in vivo* [36]. Chromatography experiments have demonstrated that methylarsenic diglutathione and dimethylarsenic glutathione are more stable than arsenic triglutathione [37]. Arsenic triglutathione and methylarsenic diglutathione have been detected in bile from arsenite and arsenate treated rats [36] and in urine from arsenite treated mice deficient in gamma-glutamyl transpeptidase [38]. Once a glutathione moiety is coordinately complexed to arsenic, the resulting complex can be exported into the bile by the multidrug resistance associated protein 2 (MRP2/cMOAT) transport system [39]. Representative rat GSH concentrations (in $\mu\text{M}/\text{g}$ or ml) are 7.2 in liver [40], 1.0 in kidney [40], 1.59 in bile [41] and 0.011 in serum [40]. In CDF1 mice, tissue GSH concentrations were 7.4, 2.9, 1.7, 1.7, 2.4, 2.0, 0.8 and 0.5 $\mu\text{M}/\text{g}$ in liver, kidney, urinary bladder, lung, spleen, pancreas, heart and muscle, respectively [42]. As the concentration of GSH is so low in serum and urine [40], coordination complexes between arsenic and GSH tend to dissociate in these two compartments.

A very unusual type of binding is known to take place between DMA(III) and rat hemoglobin [43, 44]. The amount and strength of DMA(III) binding to rat hemoglobin is

more than can be explained on the basis of simple unidentate binding of a trivalent arsenical to one cysteine of a peptide chain. Thus, rat hemoglobin is the first known major example of a trivalent arsenical binding at unexpectedly low concentrations for very long periods of time. Other unknown binding sites may hold a major key to understanding arsenic's toxicity and carcinogenicity.

Binding of trivalent arsenicals to peptides and proteins can alter their structure and function and contribute to adverse health outcomes such as toxicity and carcinogenicity. Historically, the lipoic acid moiety of the enzyme system pyruvate dehydrogenase was considered an important site of action of trivalent arsenicals. Lipoic acid offers a typical dithiol binding site for trivalent arsenicals. Among the protein targets frequently considered as possible components of an arsenic carcinogenesis mode-of-action (MOA) are tubulin, thioredoxin reductase, *Drosophila* actin binding protein Kelch (Keap-1), metallothionein, poly(ADP-ribose) polymerase-1 protein (PARP-1), xeroderma pigmentosum group A protein (XPA) and many steroid receptor proteins. Hundreds of proteins might offer good dithiol or even trithiol binding sites. Arsenite is capable of changing peptide or protein conformation by linking several cysteines that may initially be somewhat far apart [45, 46].

In order for zinc finger proteins (i.e., C2H2, C3H1 or C4) to be an important key event of an MOA for arsenic carcinogenesis, it should be first demonstrated that (a) trivalent arsenicals can release zinc from zinc finger proteins, (b) trivalent arsenicals can bind to zinc finger sites containing two or more cysteines, (c) reduced function of arsenic treated zinc finger proteins and (d) exogenous zinc induced antagonism of arsenic's inhibition of enzyme function (e.g., DNA repair). This is because the exogenous zinc should be capable of removing arsenic from the zinc binding site and restoring the zinc finger site structure to its normal conformation.

There are now sufficient experimental data that all four of the above criteria are met. This evidence is summarized in sections 2.2.1 to 2.2.4 given below:

2.2.1 Release of Zinc from Zinc Finger Proteins has been Chemically Demonstrated

Arsenite, MMA(III) and DMA(III) have released zinc from ZnXPAzf, the zinc finger region of XPA, a crucial member of the nucleotide excision repair (NER) complex [47].

2.2.2 Binding of Trivalent Arsenic to Zinc Finger Proteins

1. When MMA(III) released Zn(II) from ZnXPAzf, it formed mono- and diarsenical derivatives of XPAzf. It also caused the oxidation of unprotected thiol groups to intramolecular disulfides. The estimated affinity of MMA(III) to XPAzf was 30-fold higher than that of arsenite [47].
2. Direct binding of radioactive arsenite to synthetic zinc free peptides having zinc finger regions of two, three or four cysteines:
peptide 16 (RYCAVCNDYASGYHYGV),
peptide 24 (RYCAVCNDYASGYHYGVWSCEGGKA) and
peptide 15 (RYCAVCNDYASGYHYGVWSCEGCKA) has been demonstrated [27].
Kd values ranged between 2.2 and 4.3 μM [27]. Binding of ^{14}C -MMA(III) to cysteine containing proteins has been demonstrated using peptide 10 (LECAWQGKCVEG-TEHLYSMKCK) (unpublished observations, Kitchin and Wallace).

2.2.3 Reduced Function of Zinc Finger Proteins

1. Arsenite, MMA(III) and DMA(III) inhibited DNA repair in human lung cells [48].
2. MMA(III) and DMA(III) inhibited the activity of the DNA repair enzyme formamido-pyrimidine-DNA glycosylase protein (Fpg) [47].
3. MMA(III) and DMA(III) inhibited PARP-1 enzyme activity in the low concentration range between 1–1000 nM [49].
4. Arsenite inhibited the repair of ultraviolet radiation induced cyclobutane pyrimidine dimers in human keratinocytes [50]. p38 MAPK and NF- κ B may mediate this nitric oxide and inducible nitric oxide synthase dependent effect [50].
5. By the criteria of the comet DNA assay, arsenite (2 μ M) alone did not cause single strand breaks in keratinocytes but this concentration of arsenite greatly enhanced the single strand breaks induced by ultraviolet radiation. This was attributed to PARP-1 inhibition [51].
6. In HeLa cells, 0.01–1 μ M arsenite reduced PARP-1 activity. Arsenite (0.5 μ M) increased DNA strand breaks as well [52].
7. In HeLa cells increased Fpg sensitive sites in DNA were observed after treatment with arsenite (0.010–1 μ M), MMA(III) (0.1–7.5 μ M), DMA(III) (0.1–7.5 μ M), MMA(V) (10–500 μ M) and DMA(V) (10–500 μ M) [48].

2.2.4 Restoration of Zinc Finger Protein Function

This has been demonstrated *in vitro* using a system in which trivalent arsenite and ultraviolet light exposure were used together to damage DNA. Then either 8-OHdG concentration in cellular DNA or DNA damage in a comet assay was measured. Exogenous zinc was an effective antagonist of arsenite and ultraviolet radiation induced DNA damage in cultured human keratinocytes [51]. In other experiments with human keratinocytes, zinc supplementation restored the PARP-1 activity inhibited by arsenite, reduced the formation of 8-OHdG but interestingly did not decrease ROS concentrations [51]. siRNA knockdown of PARP-1 greatly increased the 8-OHdG level produced by hydrogen peroxide but not by arsenite. This ineffectiveness of arsenite in the siRNA mediated PARP-1 knock down condition is an additional type of evidence that arsenite acts via the zinc finger protein PARP-1 [51].

In conclusion, the above data are consistent with arsenite replacing Zn from a zinc finger protein and lowering DNA repair enzyme activity (e.g., PARP-1, Fpg). Arsenic could act both by (a) binding to dithiol and trithiols sites such as the zinc finger proteins PARP-1 and Fpg and (b) ROS generation and oxidative stress. Inactivation or incorrect function of DNA repair proteins can be caused by either (a) conformational changes induced by binding of trivalent arsenicals to cysteine(s) containing sites of the enzyme, (b) oxidation of the DNA repair protein and/or (c) arsenic induced alterations in the amount of DNA repair protein present (translational effects on proteins).

Another prominent feature of arsenic biochemistry in many biological systems is that arsenic is methylated. Bacteria, fungi/algae/yeast, plants and animals can all methylate arsenic in addition to the related atoms of S, Se and Co [53]. Other elements that undergo methylation in fewer biological systems include Ni, Hg, Sn, Te, Sb, Bi, Tl, Pb, Po, P, I, Cl and Br [53]. Thus, at least 17 elements are methylated by various life forms. The microbial

methylation of arsenic, antimony and bismuth has been reviewed by Bentley and Chasteen [54]. The classical pathway of arsenic methylation first put forward by Challenger in 1945 [55] requires sequential reductions of arsenic to trivalency (by cellular thiols, GSH, cysteine, etc.) [35] and then oxidative methylation steps (Figure 2.1). This pathway of arsenic methylation proceeds in most animals to the addition of two or rarely three methyl groups [56]. In most mammals, dimethylated forms of arsenic are rapidly excreted in the urine. In some rare situations, arsenic methylation will proceed all the way to the addition of either three [57] or four methyl groups. The marine polychaetes *Nereis diversicolor* and *Nereis virens* both contain about 25% tetramethylarsonium ion in addition to the expected arsenobetaine [23]. These marine worms apparently methylate inorganic arsenic four times, all the way to tetramethylarsonium ion.

Because trivalent arsenicals have about 100-fold lower K_d values for bidentate binding to dithiol sites in comparison to monodentate binding to monothiol sites [27, 58], it is easy to see why arsenic methylation generally stops after two methyl groups are added. The second methyl group on arsenic makes bidentate binding impossible and the weaker monodentate binding is usually insufficient to keep the potential substrate of a dimethylated arsenical from drifting away from the enzymatic site of reduction and/or methylation. A peptide based on the human amino acid sequence of arsenic (+3 oxidation state) methyltransferase (AS3MT), YYGCGLVIPEHLENCWILDLGSGGRDCYVLK, bound arsenite with a K_d of 2.0 μM and a B_{max} of 36 $\eta\text{M}/\text{mg}$ [58]. The three cysteines in this region are conserved across man, rat, mouse, cow and chicken [30, 59]. Another cysteine rich region of AS3MT has the sequence DSMKSRCVPDAAGGCCGTKKSC. Of these four cysteines either three or four cysteines are conserved between man, rat, mouse, cow and chicken [30, 59].

The oxidative methylation steps of Figure 2.1 are catalysed by an enzyme called arsenic (+3 oxidation state) methyltransferase (EC 2.1.1.137) [60]. Both arsenic reduction and methylation capacities have been demonstrated by this single enzyme [30, 60]. The kinetic constants of rat AS3MT for methylating MMA(III) are a K_m of 0.25 μM and a V_{max} of 68 pM/mg protein/min [60]. AS3MT is 369, 376, 375 and 205 amino acids long in rat, mouse, human and chimpanzee, respectively [59]. There are 12 conserved cysteines among human, rat and mouse enzymes. Because there are 14 total cysteines (Swiss Protein entry #Q9HBK9) in the human arsenic methyltransferase enzyme, it is easy to see how the same enzyme could both oxidatively methylate and subsequently reduce trivalent arsenic substrates [30, 61]. As there is not much monomethylated arsenic excretion found in most mammals (humans are unusually high in monomethylated arsenic excretion), if MMA(V) does actually leave the AS3MT methylation site, this arsenical must be reduced and then recaptured by the enzyme for subsequent methylation with extreme efficiency.

The enzymatic or nonenzymatic methylation of arsenic can be chemically thought of as a S_N2 mechanism where there is positively charged carbocation character in the methyl group of S-adenosylmethionine (SAM) (for enzymatic methylation) or CH_3I (for the Meyer Reaction of synthetic organometallic chemistry). There is also negatively charged character on the arsenic atom due to the electron donating properties of sulfur (for enzymatic methylation) [31] or oxygen atom(s) (for the Meyer Reaction). In the Meyer Reaction, alkylation of arsenic always results in a pentavalent, never a trivalent, arsenical product.

Several animals (guinea pig, marmoset, tamarin and chimpanzee) are deficient in the capacity to methylate arsenic [62, 63]. Chimpanzees express an inactivated truncated arsenic methyltransferase enzyme [59]. The sequential view of arsenic methylation of

arsenic in mammals is well covered by several review articles from the same experimental group [30, 56, 57, 64].

Another point of view is that arsenic is not sequentially reduced and oxidatively methylated but rather reduced to trivalency, bound to a RSH site on a methyl transferase enzyme and then successively methylated without going through a pentavalent intermediate [31, 65]. This second view requires that the methylation product is trivalent rather than pentavalent arsenic [31, 65]. If this is true, it is easy to see how a second or even a third round of methylation can occur without arsenic ever leaving the enzymatic site of the methyltransferase.

Based on the known K_d values for arsenite and the known RSH concentrations inside of cells, it is easy to conclude that 99% of arsenite inside of cells is bound and not free [27]. Thus, inside a cell most arsenite (and also MMA(III) (Kitchin and Wallace, unpublished data) and DMA(III)) will be bound to cysteine, GSH, the many reduced cysteine containing proteins that are not methylation enzymes and most importantly the cysteine groups close to or at the enzymatic site(s) of arsenic methylation enzyme(s).

These two views of arsenic methylation differ on what is the true substrate for arsenic methylation (arsenic triglutathione [65] or protein bound trivalent arsenicals [31] versus free or protein bound forms of arsenite, MMA(III) or DMA(III) [60]. They also differ on whether the required reduction and methylation steps are sequential [60] or simultaneous [31, 65]. Both views of arsenic methylation completely agree that both reduction and methylation are required for inorganic arsenic to be methylated to mono- di- and tri- methylated arsenicals.

Arsenic complexes not only with oxygen but also with sulfur. Particularly in the relative anaerobic parts of the organisms such as the gastrointestinal tract, arsenic may form multiple coordination complexes with sulfur either by forming two coordination bonds (in place of oxygen) or by replacing an OH with SH. Some of the thioarsenicals compounds that have been either synthesized or found in biological matrixes are listed below in order of the increasing degree of methylation:

- a. a monomethylarsenic form $\text{CH}_3\text{As}(\text{S})(\text{OH})_2(\text{V})$ monomethylmonothioarsenic acid (MMMTA(V)),
- b. dimethylarsenic forms $(\text{CH}_3)_2\text{As}(\text{S})\text{OH}$ (dimethylmonothioarsenic acid (DMMTA(V)), $(\text{CH}_3)_2\text{AsSH}(\text{III})$ dimethylthioarsinous acid (DMTA(III)), $(\text{CH}_3)_2\text{As}(\text{S})\text{SH}$ (dimethyl-dithioarsenic acid (DMDTA(V)), $(\text{CH}_3)_2\text{As}(\text{O})\text{SH}(\text{V})$ dimethylmonothioarsenic acid (DMMTA(V)), $(\text{CH}_3)_2\text{As}(\text{S})\text{OAs}(\text{S})(\text{CH}_3)_2$ dimethylthioarsenic anhydride (an oxygen linked dimer (DMTA(V), M2)), $(\text{CH}_3)_2\text{As}(\text{S})\text{SNa}$ sodium dimethyldithioarsinate (DMDTA(V) or M3) and
- c. a trimethylarsenic form $(\text{CH}_3)_3\text{AsS}$ trimethylarsine sulfide (TMAS, M1).

In respect to occurrence of sulfur containing arsenicals, DMMTA(V) was found present in 44% of the urine of Bangladesh women exposed to inorganic arsenic [66]. After administration of 5 mg/kg of arsenite to male Syrian hamsters and Wistar rats, hamster urine contained the thioarsenicals MMMTA(V), DMDTA(V) and DMMTA(V), while rat urine contained MMMTA(V) and DMMTA(V) [67]. Both rat and hamsters urine contained the normal oxygen containing and methylated forms of arsenic (As(III), As(V), MMA(V), DMA(V)) as well.

At this point in time, we do not know a great deal about the biological properties of sulfur containing arsenicals. However, in comparison to similar pentavalent oxygen containing

arsenicals, sulfur containing arsenicals are often less charged and thus may cross cell membranes more efficiently and can subsequently be transformed back into various chemical forms that do not contain sulfur (e.g., DMA(III)) [68].

In some comparisons of the LC₅₀ of sulfur containing arsenicals in cell culture, the values are often fairly similar to related trivalent arsenicals. For example, in human hepatocarcinoma HepG2 cells, DMMTA(V) was about 10 times more cytotoxic than DMA(V) [66]. In human epidermoid carcinoma A431 cells, the μM LC₅₀ values were 2.2 for DMA(III), 5.5 for As(III), 10.7 for DMMTA(V), 571 for As(V) and 843 for DMA(V) [68]. In human bronchial epithelial BEAS-2B cells, the minimally μM cytotoxic concentrations of arsenicals were 15 for As(III), 1 for MMA(III), 1 for DMA(III) and 0.9 for DMTA(V) [69].

2.3 Cancer – MOA

2.3.1 Binding to RSH Groups

From the biochemically oriented world of individual arsenicals interacting with certain macromolecules, it is a long jump and multiple levels of biological organization to reach the adverse health consequences associated with arsenic exposure in humans such as black foot disease, increased cardiovascular risk, diabetes, cancer, toxicity and rarely death [1]. In the inorganic arsenic risk assessments presently done in the USA, it is the biological endpoint of cancer and the linearity associated with its causality that drives the arsenic risk assessment to low exposure levels.

Information at many different levels of biological organization can contribute to make a more complete picture of the overall biological processes and also of the individual components that are causally related to one another. Among the many aspects that are important are the temporal sequence of biological changes and the dose-response relationship.

Societies and governments try to protect their citizens by using tools such as toxicological data, mode of action (MOA) analysis and risk assessment to set levels of exposure to arsenicals to minimize the risk of adverse health consequences. In current and future risk assessment, MOA will receive more attention and utilization. A MOA should have enough detail to capture several of the more important causal stages of carcinogenesis, but not so much detail as to become untenably complex and too difficult to collect experimental evidence on all the key events of the process. The next sections of this chapter will present facts and theories centered on three different proposed MOA for arsenic carcinogenesis – binding, oxidative stress and DNA methylation changes. Only with such MOA based knowledge can risk assessors confidently select defensible extrapolation models to make the order of magnitude jumps required in environmental risk assessment [70]. For arsenic this can easily be two to five orders of magnitude for human and animal exposure data respectively.

With respect to trivalent arsenicals binding to protein as a cause of cancer, this subject has been reviewed recently [58] and thus will not be presented here in detail. Examples of chemical carcinogens where binding to proteins is likely to be an important causal event include estrogens and polyhalogenated dioxins and biphenyls. Some remaining problems include (1) too many possible protein targets to examine, (2) proteins or peptides of

unusually low K_d for binding trivalent arsenicals have not been discovered yet and (3) difficulty in determining which pathways are more tightly linked to carcinogenesis. For example, growth factors and transcription factors, redox related target proteins, DNA methylation enzymes, inhibited DNA repair, incorrect DNA repair or chromosomal alterations could all be involved in arsenic carcinogenesis. But which of these many possibilities is the most important? Again it is the large number of arsenic's possible dithiol and trithiol type of intracellular binding sites that make it such a difficult biological and risk assessment problem.

Thus, in arsenic research we have too many clues, not too few. In spite of this, no biological experiment has ever been able to isolate and identify the proteins of the cell that are of the highest probability (either by direct binding or by being targets or responders to oxidative stress) for being part of the causal chain of arsenic-induced carcinogenesis.

This situation of multiple possible protein targets is similar to that of arsenic exposures and genomics data. In these experiments various arsenic exposures *in vitro* and *in vivo* have led to data sets with hundreds or thousands of differentially expressed genes. In such situations it is difficult to decide what particular effect is of the highest probability to be biologically important such as a cause for a particular disease state such as cancer.

2.3.2 Cancer – MOA – Oxidative Stress

Oxidative stress has been attributed as a cause or partial cause of many different human diseases. By the strict criteria of causality such as the Hill criterion, few human disease states can be strictly linked to oxidative stress. Some of the diseases associated with oxidative stress are carcinogenesis, neural diseases and aging. A good review on the linkages between oxidative stress and carcinogenesis is available [71]. At this point, there is a lot of positive information that links oxidative stress type parameters to various arsenical exposures both *in vitro* and *in vivo*. There are many arsenical induced DNA related effects (as summarized in Table 2.2) that fit the general pattern of low or zero point mutations and a high degree of single strand breaks and chromosomal aberrations. In arsenic exposures, free radical generation has been shown by electron spin resonance (ESR), cellular fluorescent probes, malondialdehyde formation and enzyme and protein effects consistent with diminished defences against oxidative attack and response to oxidative attack. More detailed information can be obtained in a book chapter on arsenic, oxidative stress and carcinogenesis written by Hughes and Kitchin [6].

In trying to decide the degree of attribution between rival hypotheses of arsenic carcinogenesis, there are almost no data to use that have biological indicators of the several most probable MOA for arsenic carcinogenesis. Thus, claims of responsiveness at low

Table 2.2 Oxidative stress parameters known to be effected by arsenic exposures [6]

DNA RELATED: 8-OHdG, DNA fragmentation by alkaline elution or comet assays, micronucleus and genomic parameters
ESR with spin trapping
ENZYMES AND PROTEINS: Heme oxygenase, Heat shock and stress proteins, Superoxide dismutase, Catalase, Thioredoxin reductase, GSH reductase, GSH Peroxidase, GSH
Cellular fluorescent probes
Malondialdehyde (MDA)

arsenic concentrations and occurrence early in the causal chain of key carcinogenic events in a MOA are not possible to make in this field with current biological data sets.

One oxidative stress time course data set that stands out is that contributed by Santra *et al.* [72] who exposed BALB/c mice to 3.2 ppm arsenic in the drinking water. The arsenic containing water used in the study came from an Indian well that produced dermal symptoms in several human beings. Although 3.2 ppm of arsenic is a low concentration for most animal studies, the concentration is extremely high for human drinking water exposures.

Only one oxidative stress parameter changed at three months and three parameters changed after six months of arsenic exposure (Table 2.3). At 12 and 15 months of exposure, 12 and 14 out of the 15 total parameters had been changed by arsenic exposure [72]. Although human livers respond to arsenic exposure by developing carcinogenesis, mouse livers are not currently known to develop cancer following arsenic exposures. To date, liver cancer in animals has been demonstrated only in TMAO treated rats [73]. Thus, it is desirable to repeat this type of oxidative stress time course study in mouse skin, lung and either mouse or rat urinary bladder as these organs are more responsive targets of arsenic carcinogenesis, both in the appropriate rodent model and in humans.

Mouse tissue DNA 8-OHdG concentrations are increased by prior administration of DMA(V) (Figure 2.3) [74]. Six different mouse tissues were studied in two different experiments with exposures to DMA(V) at 400 ppm in the drinking water for either two or four weeks. Statistically significant elevations in 8-OHdG were observed in liver, lung and skin [74]. Mouse urinary bladder also showed an increase but the standard deviation prevented it from reaching the $p < 0.05$ level [74]. Kidney and spleen showed only slight elevations in 8-OHdG concentrations. Although this study is sometimes criticized for

Table 2.3 *Time course of arsenic-induced mouse hepatic oxidative stress*

Endpoint	Time (month)				
	3	6	9	12	15
Malondialdehyde (MDA via TBARS)			↑	↑	↑
Glutathione (GSH)		↓	↓	↓	↓
Glucose-6-phosphate dehydrogenase (G6PDH)		↓	↓	↓	↓
Glutathione reductase (GR)				↓	↓
Catalase				↓	↓
Glutathione peroxidase (GSH-Px)			↓	↓	↓
Glutathione-S-transferase (GST)		↓	↓	↓	↓
Alanine aminotransferase (ALT)	↑			↑	↑
Aspartate aminotransferase (AST)				↑	↑
Alkaline phosphatase (ALP)					↑
Na ⁺ /K ⁺ ATPase			↓	↓	↓
Albumin					↓
Liver Weight				↑	↑
Liver Histology				Fatty infiltration	Fatty infiltration, Fibrosis

The livers of mice exposed to 3.2 ppm inorganic arsenic in their drinking water developed oxidative stress over time [72]. Arrows refer to statistically significant increases (in red) or decreases (in green).

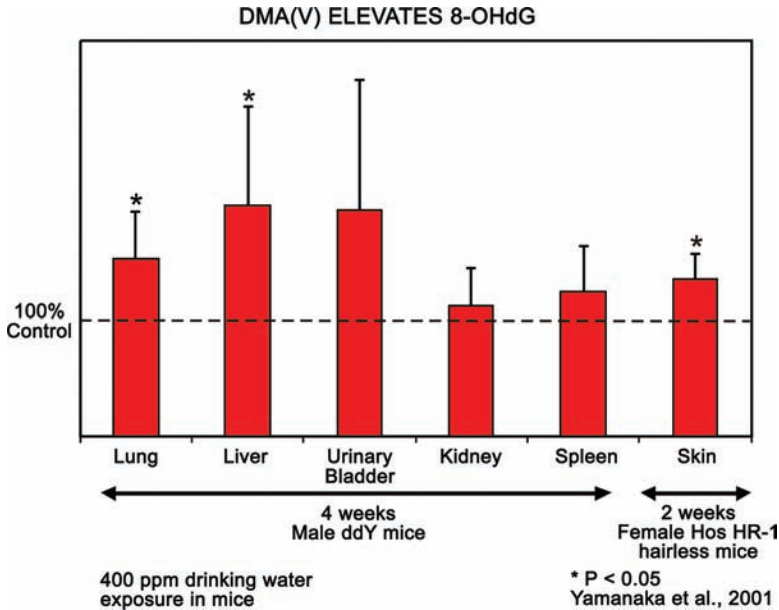


Figure 2.3 DMA(V) induced increases in tissue 8-OHdG concentration in different mouse tissues based on the studies of Yamanaka et al. [74]

employing a high DMA(V) concentration, this high concentration of DMA(V) is necessary because the negatively charged molecule DMA(V) enters cells so poorly [24], oxidative stress takes so long to demonstrate in arsenical exposed rodents [72] and the capacity for DNA repair is so high [75, 76].

Similar to the situation with trivalent arsenicals binding to cysteine containing proteins, we do not know what cellular targets are the most likely targets of arsenic induced oxidative stress. However, oxidation of DNA, particularly to 8-OHdG, certainly seems to be an effect of arsenic exposures in animals and in man.

2.3.3 Cancer – MOA – DNA Methylation

Arsenic consumes two methyl groups from SAM in its metabolism from inorganic arsenic to dimethylated arsenic forms. Thus, many people have believed that cellular SAM status might interact in some way with the methylation state of DNA and hence account for some of the carcinogenic properties of arsenic. It appears unlikely that arsenic directly causes a shortage of methyl groups by consuming too many SAM methyl groups directly. Experimentally, the dominant fact that emerges is that arsenic can cause global DNA hypomethylation and in limited regions of DNA hypermethylation as well.

As shown in Table 2.4, there are several studies that show global DNA hypomethylation in mouse liver or lung. Most of the exposures to inorganic arsenic were for long times but one exposure was for just 11 days during gestation. In liver, prostate and ovary cells, global hypomethylation has been noted as well, again usually after many weeks of exposure (Table 2.4). Cell division is required before there can be a good chance of demonstrating hypomethylation of DNA. Global hypomethylation may occur because the amount or

Table 2.4 *Global DNA hypomethylation caused by arsenic exposures*

Species/Cells	Organ	Dose/Concentration	Reference
Male mice strain A/J	Lung	0, 1, 10, 100 ppm for 18 mo	[107]
Male mice SvJ	Liver	45 ppm for 48 wk	[108]
Male mice C57BL/6J	Liver	2.6–14.6 ppm for 130 d	[109]
Mice C3H newborns	Liver	85 ppm, days 8–18 of gestation	[110]
TR 1215 Rat Cells	Liver	0.125–0.5 μ M for 8 wk	[111]
Tg.AC transgenic mice	Liver	150 ppm arsenite, 200 ppm arsenate, 1500 ppm MMA(V) and 1000 ppm DMA(V) for 17 wk	[112]
Goldfish (both sexes)	Liver	200 μ M for 1, 4 and 7 d	[113]
RWPE-1 human cells	Prostate	5 μ M for 37 wk	[114]
V79-C13 Chinese hamster cells	Ovary	10 μ M for 24 h	[115]
HaCat human cells	Skin	0.2 μ M for 10 passages	[78]

activity of DNA methylation enzymes is reduced by arsenic exposures. Two examples of this are already known (Figure 2.4). In the Ahlborn *et al.* study [77] mouse skin mRNA coding for DNA methyltransferase 3A was significantly reduced after a one month exposure to arsenite. In a study of human HaCat keratinocytes, arsenic reduced the mRNA levels coding for both DNA methyltransferase 3A and 1 enzymes [78].

So far only one scientist has put forward a complete carcinogenic MOA for DNA methylation and arsenic carcinogenesis [79] (Figure 2.5). Key events in this MOA are DNA hypomethylation of the estrogen receptor alpha promoter, increased expression of the estrogen receptor alpha protein and cyclin D1, followed by increased estrogen action in tissues and eventually cancer in several target tissues [79]. At this point, there is less supporting evidence and fewer details for this DNA hypomethylation theory of arsenic carcinogenesis as compared to either the protein binding or oxidative stress theories of carcinogenesis. However, additional positive evidence may come forward in the future to further support the DNA methylation theory. At present, the DNA methylation theory is the best explanation of the gestational arsenite exposure induced mouse tumors [79, 80]. It is quite difficult to believe that oxidative stress and short lived protein binding could account for heritable changes and tumors that appear more than one year after the maternal exposure to arsenite has stopped and > 99% of the original gestational arsenic has been excreted.

2.4 Arsenic's Many Connections to Carcinogenesis

2.4.1 Human Carcinogenicity

In the third section of this chapter, four connections of arsenic to carcinogenesis will be presented: evidence for human carcinogenicity of arsenic, animal evidence for complete carcinogenicity, animal experiments showing promotion of carcinogenesis and finally the relatively new use of arsenicals in the treatment of a particular form of leukaemia, acute promyelocytic leukaemia (APL).

Arsenic has been identified as a human carcinogen in many studies. The first positive association was discovered in 1888 by Hutchinson, a British physician. He observed that in people consuming medicinal arsenicals (Fowler's solution, a 1% solution of potassium

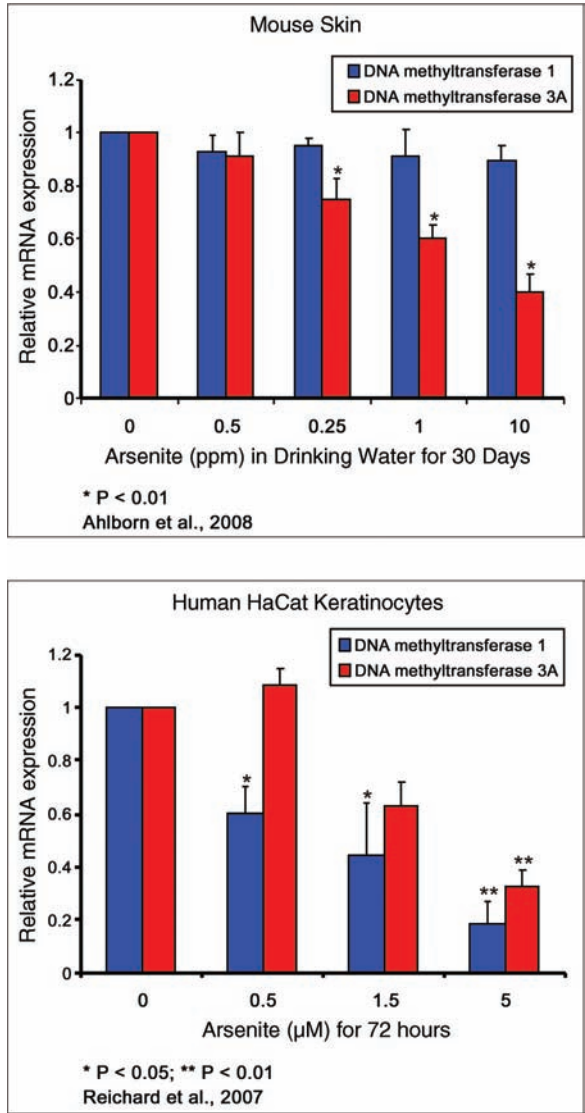


Figure 2.4 Arsenic exposures decrease the level of mRNA coding for DNA methylation enzymes [77, 78]. Reprinted with permission from [78]. Copyright Elsevier (2007)

arsenite), there was an elevated incidence of skin cancer. Subsequent studies in Taiwan showed that drinking water containing arsenic caused skin cancer (Table 2.5) [81] and then later studies showed association of arsenic and internal tumors as well (Table 2.5) [82–84]. These internal tumors are much more lethal than skin tumors. However, skin tumors have been positively associated with human death in both Chile [85] and Taiwan [82, 83]. The human organs which typically show arsenic induced increases in tumor incidences are the lung, urinary bladder and skin followed by smaller increases in liver and kidney (Table 2.6).

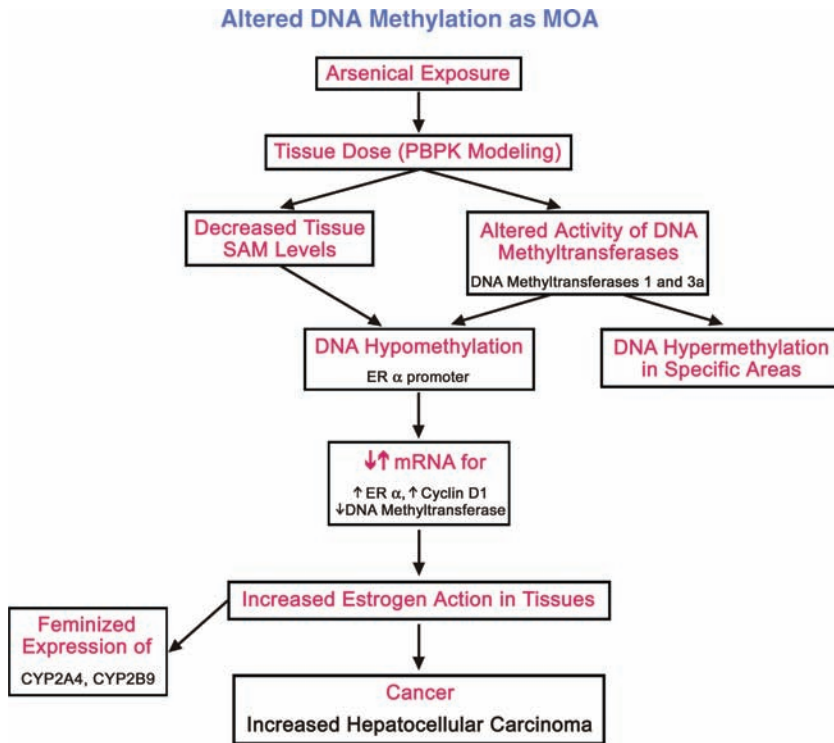


Figure 2.5 DNA methylation MOA for arsenic carcinogenesis [79]

Prostate tumors have been associated with arsenic exposures but only in the Taiwanese cohorts [82, 83]. The epidemiological data of arsenic exposures are interesting in many respects, one of which is the large size of several of the exposed populations – about 69 000 in Taiwan [81], 400 000 in Chile [85] and 1 369 000 people in Argentina [86, 87] (Table 2.6). In respect to drinking water concentrations, many of the positive epidemiological associations have had arsenic drinking water exposures in the 150–300 ppb range all the way up to as high as 1000 ppb. Demonstrating increased human tumor rates with arsenic exposures in the 10–150 ppb range has been problematic mainly because of the low incidence of cancer, the statistical power needed to detect a true positive effect, problems of arsenic exposure assessment in large populations and the limited study size available in certain arsenic concentration ranges. It has been argued that arsenic exposures even in the lower exposure ranges found in the USA pose significant cancer hazards when the risks are extrapolated out with certain models [88].

Three of the more quantitative studies from Taiwan, Argentina and Chile are presented in Table 2.6. The standardized mortality rate (SMR) numbers presented in Table 2.6 are the average of male and female rates. One sees substantial increases in standardized mortality rate (SMR) in skin, lung, kidney and bladder in Taiwan and in skin, lung and bladder in Chile. The remaining positive associations in epidemiological standardized mortality ratios were close to 2.0 (all the Argentina data and the liver and kidney data from Chile). Overall, the hazard identification of arsenic drinking water exposures and human cancer is complete.

Table 2.5 *Positive associations between ingested arsenic and human cancer*

Location authors reference #	Population studied	Arsenic concentration (ppb)	Skin	Lung	Bladder	Kidney	Liver
Taiwan Wu [83]	~69 000 individuals in the black foot endemic region	<300 300–590 >600	Yes	Yes	Yes	Yes	Yes
Taiwan Chen and Wang [82]	>20 million inhabitants of Taiwan	Many	Yes	Yes	Yes	Yes	Yes
Taiwan Guo [84]	All Taiwan	<50 50–80 90–160 170–320 330–640 >640			Yes	Yes	
Cordoba, Argentina, Hopenhayn-Rich [86, 87]	~1 369 000 exposed to arsenic versus all of Argentina	~120 ~178		Yes	Yes	Yes	
Chile Smith [85]	~400 000 exposed to arsenic versus rest of Chile	~420	Yes	Yes	Yes	Yes	

Remaining epidemiological work should focus on difficult matters such as the possible influence of diet, dose response relationship particularly at low exposures and determinants of individual susceptibility.

Table 2.7 summarizes the human mortality data from the same studies in a slightly different way. The average excess mortality from both sexes above the referent population incidence is expressed as a rate per 200 000 people (with half of the people male and half female). These numbers show that arsenic exposure in both Chile [85] and Taiwan [83] have

Table 2.6 *Standardized mortality ratios for human cancer following arsenic exposure*

Location Authors Reference #	Population studied	Arsenic Concentration (ppb)	Skin	Lung	Bladder	Kidney	Liver
Taiwan Wu [83]	~69 000 individuals in the black foot endemic region	<300 300–590 >600	2.00 12.94 26.94	2.30 3.82 6.68	8.50 18.63 47.05	4.45 12.90 28.30	1.38 1.82 3.02
Cordoba, Argentina Hopenhayn-Rich [86, 87]	~1 369 000 exposed to arsenic versus all of Argentina	~120 ~178	1.16 2.14	1.44 1.97	1.34 1.98	1.35 1.69	1.84 1.88
Chile Smith [85]	~400 000 exposed to arsenic versus rest of Chile	~420	5.45	3.45	7.10	2.15	1.10

Table 2.7 Excess cancer mortality for humans exposed to arsenic

Location	Author Reference #	Population studied	Arsenic concentration (ppb)	Skin	Lung	Bladder	Kidney	Liver
Taiwan	Wu [83]	~69 000 individuals in the black foot endemic region	<300	1.6	32.7	27.9	7.0	9.9
			300–590	19.1	76.7	68.4	23.6	24.6
			>600	41.5	142.9	176.1	52.9	63.7
Chile	Smith [85]	~400 000 exposed to arsenic versus rest of Chile	~420	22.2	505.8	134	35.6	8.2

caused the highest number of excess tumor deaths in lung and bladder followed by lower numbers of excess deaths in skin, kidney and liver.

2.4.2 Animal Studies - Promotion of Carcinogenesis

Historically, animal studies of arsenic carcinogenicity have been frustrated by a long and fairly unproductive era of time in which no really useful animal models of arsenic induced cancer were developed. After 1995 however, good models of the promotion of carcinogenesis by the methylated pentavalent arsenical dimethylarsinic acid (DMA(V)) [89] and eventually complete carcinogenesis in animal models by some arsenicals have been developed. Thus, it is no longer true to say that no animal models of arsenic carcinogenesis exist. Many animal models of arsenical induced cancer currently exist, although no single model is 100% perfect and meets the understandable human desire to demonstrate low dose complete carcinogenesis in all five human target organs in the same experimental animal.

The well known animal models of promotion of carcinogenesis are (1) DMA(V) induced promotion of carcinogenesis in a rat after multi organ initiation by several initiators of carcinogenesis [89] and (2) single organ promotion of carcinogenesis in a rat liver [90] and rat urinary bladder [91], mouse skin [92] and mouse lung [93]. In all of these positive promotion of carcinogenesis experiments, DMA(V) and not inorganic arsenic is the treatment chemical. Interestingly, at physiological pH DMA(V) is negatively charged and is poorly transported across cell membranes [24]. A good review of animal carcinogenesis and promotion experiments has been written by Wanibuchi *et al.* [94].

2.4.3 Animal Studies - Complete Carcinogenesis

Complete carcinogenicity in experimental animals has been difficult to demonstrate for arsenicals. Exposure to only DMA(V) causes cancer in rat bladder [95]. Trimethylarsine oxide (TMAO) caused increased rat hepatocellular adenomas [73]. In strain A/J mice, DMA (V) increased the multiplicity of lung tumors (papillary adenomas and adenocarcinomas) observed at 50 weeks [96]. Transgenic K6/ODC mice have been employed to study the degree of tumorigenicity of arsenicals. This transgenic mouse system has responded positively to more arsenicals than any other *in vivo* system so far. Arsenite, monomethylarsonous acid (MMA(III)) and DMA(V) are all positive to a degree in this transgenic mouse system [97, 98]. The tumors that developed were exophytic squamous cell carcinomas, a benign tumor with a

low frequency of progression to higher degrees of carcinogenicity. The increased number of arsenical induced tumors was low with few tumors in each of the individual treatment groups. The overall message from the K6/ODC mouse data is that several different administered arsenicals demonstrated a degree of complete tumorigenesis and thus possibly a degree of *in vivo* genotoxicity in this superpromoted transgenic animal model system.

Transplacental exposure to 85 ppm of arsenite has increased the incidence of mouse liver, adrenal, lung and ovary [79, 80]. Two strains of mice (CD-1 and C3H) have shown this transplacental sensitivity to arsenite induced tumors. As there is no appreciably administered arsenical compound left during the majority of the time of carcinogenesis, simple modes of action (MOA) do not seem to operate well in this situation. The current hypothesis is that estrogen receptor alpha increases and cyclin D protein elevations are causes of some of the gestational tumors that seem centered on organs that are either estrogen sensitive or endocrine organs (Figure 2.5).

Data from this transgenic mouse system are included in Figure 2.6 which compares the external drinking water concentrations of human and animal skin studies. There are several orders of magnitude differences between the incidences of human cancer in either control or arsenic exposed human populations (e.g., Table 2.7) [83, 85–87, 99] and the incidences that can be meaningfully measured in experimental animal studies (2–100%). The animal exposure concentrations are as much as three orders of magnitude higher than human arsenic concentrations that have been linked to human tumors.

Figure 2.6 displays the best control animal or referent human population incidence for human skin cancer (graphed at 1 ppb on this log scale), as well as elevated human skin disease incidences, deaths from human skin cancer and papilloma development in a

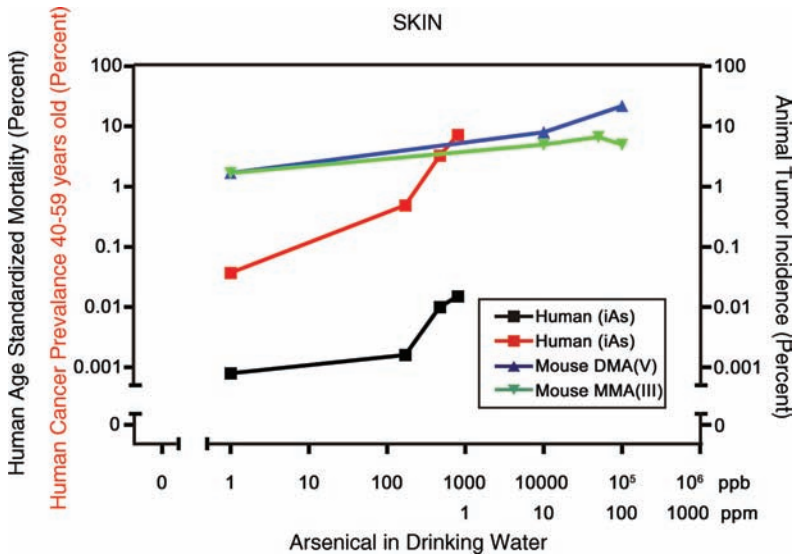


Figure 2.6 Incidences of skin lesions in humans and transgenic K6/ODC mice. The occurrence of skin cancer [81] (in red) and deaths attributed to skin cancer [99] (in black) in a Southwest Taiwan population are shown using the y axis labels on the left. The percent tumor incidence in K6/ODC mouse skin is shown for DMA(V) (in blue) [97] and for MMA(III) (in green) [98]

transgenic animal model. Relative to the x axis in this log-log plot, we observe that the common human drinking water concentrations are in the range of 1–5 ppb, highly exposed human populations that respond with skin tumors are in the range of 150–1000 ppb, while tumorigenic animal exposures for transgenic mouse skin are in the range of 10–100 ppm. Overall this is five orders of magnitude on the x axis of external drinking water concentration of arsenical. In respect to the y axis there are only about two orders of magnitude separating the incidences of skin tumors in humans and transgenic mice. It is expected that interior tissue concentrations (good information is available for experimental animals but lacking for humans) are a better dose metric than exterior drinking water arsenic concentrations.

Considering the human and animal differences in tumorigenic responses to arsenic, it seems clear that either that (1) humans are the more sensitive species, far more so than mice, transgenic mice, rats or beagle dogs [100], and/or (2) that rats and mice are superb methylators and excretors of administered arsenicals. Indeed, pharmacokinetic data from a 90 day exposure show that C57BL/6 mice on a normal rodent lab diet begin to build up appreciable tissue levels of arsenicals only above about 2 ppm arsenate in their drinking water, a concentration above almost all human exposures [101]. This has also been observed in C3H female mice given seven different concentrations (0.05–250 ppm) of arsenite in their drinking water for 1 month; only at arsenic concentrations at or higher than 10 ppm did mouse tissue arsenical levels begin to accumulate to high levels [102]. Thus, with animal models of arsenic induced adverse health effects, the animal interior tissue concentrations are a better dose metric than external arsenic drinking water concentrations.

2.4.4 Arsenicals in the Treatment of Leukaemia - APL

Arsenicals were used for the treatment of many diseases starting in Western medicine at least in the Hippocrates era (460–370 BC) and in Eastern medicine from about 263 BC [103]. The use of arsenicals in treatment of clinical diseases ended in the era of modern chemotherapy in the mid 1900s [104].

Acute promyelocytic leukaemia (APL) is a distinct subtype of acute myeloid leukaemia. In the early 1970s a group at Harbin Medical University in northeastern China, working from principles of traditional Chinese medicine, showed that arsenic trioxide was an effective agent for the treatment of APL [103]. However, arsenic is not effective against other subtypes of leukaemia. Present chemotherapy of APL includes the drugs daunorubicin, idarubicin, cytosine arabinoside, all-trans retinoic acid and arsenic trioxide (which generates arsenite in water) [103]. In APL cells a lower concentration range of 0.25–0.5 μM arsenic with longer treatment periods promotes differentiation of APL cells. However, a higher concentration of 1–2 μM arsenic induces apoptosis of APL cells [103]. Arsenic trioxide is the current clinical standard treatment for relapsed APL and is being investigated as a treatment in newly diagnosed cases of APL [105, 106].

2.5 Sources of Information on Arsenic's Mode of Action, Biochemical Effects, Carcinogenesis in Animals and Man, Metabolism and Analytical Chemistry

The data connecting arsenical exposures and carcinogenesis are vast with over 3300 hits in a 2010 PubMed search of the terms arsenic and cancer. Newcomers to the field can quickly learn important facts by reading some of the sources cited in Table 2.8, particularly in the

Table 2.8 Some information sources on arsenic's biochemistry and biomolecule interactions, MOA, metabolism and analytical chemistry, epidemiology, and carcinogenicity

Author and reference number	Title	Remarks
<i>General comprehensive sources:</i>		
IARC [3]	Some drinking water disinfectants and contaminants, including arsenic (Volume 84)	229 pages covering exposure data, studies of cancer in humans, studies of cancer in experimental animals and data relevant to evaluate cancer and its mechanisms
Mandal and Suzuki [5]	Arsenic round the world: a review	This review article touches many points but is strongest on the geographical and historical aspects of human-arsenic interactions particularly from groundwater and industrial sources in many different parts of the world (389 references)
National Research Council [1]	Arsenic in drinking water	310 pages covering chemistry, health effects, disposition, biomarkers, mechanisms of toxicity, sensitivity, essentiality, and statistical issues
National Research Council [2]	Arsenic in drinking water 2001 Update	225 pages updating the prior 1999 NRC report covering human health effects, animal studies, variability and uncertainty, modeling risks and hazard assessment
World Health Organization, 2001 (International Programme on Chemical Safety) [116]	Environmental Health Criteria 224 Arsenic and Arsenic compounds	502 pages covering sources, analytical procedures, environmental transport, kinetics and metabolism, health effects, ecotoxicology and human health risks (ISBN 9 24157 224 8)
<i>Mode of action, biochemical effects:</i>		
Andrewes et al. [21]	Dimethylarsine and trimethylarsine are potent genotoxins in vitro	This research report is a structure activity study of 11 different arsenicals including the reactive arsine series, causing DNA single strand breaks in pBr 322 plasmid DNA
Aposhian [11]	Biochemical toxicology of arsenic	This book chapter covers the biochemistry of arsenic and its interactions with tissue sulfhydryls. It also includes chelation, metabolism, seafood arsenic forms and MOA (74 references)
Basu et al. [4]	Genetic toxicology of a paradoxical human carcinogen, arsenic: a review	A long comprehensive review covering genetic toxicology and some MOA considerations (183 references)

(continued)

Table 2.8 (Continued)

Author and reference number	Title	Remarks
Bode and Dong [117]	The paradox of arsenic: molecular mechanisms of cell transformation and chemotherapeutic effects	Major elements of this review of anticancer and carcinogenic effects are apoptosis, AP-1, MAP kinases and NFκB
Carter <i>et al.</i> [118]	The metabolism of inorganic arsenic oxides, gallium arsenide, and arsine: a toxicochemical review	The compounds gallium arsenide and arsine get much attention in this review that also covers inorganic and methylated arsenic species
Dixon [119]	The biochemical action of arsenic acids especially as phosphate analogues	This review covers the biological effects of arsenate substituting for phosphate in biological systems
Dopp <i>et al.</i> [24]	Uptake of inorganic and organic derivatives of arsenic associated with induced cytotoxic and genotoxic effects in Chinese hamster ovary (CHO) cells	This research report is a structure activity study of seven arsenicals and their cellular uptake and genotoxicity in CHO cells
Hartwig <i>et al.</i> [120]	Modulation of DNA repair processes by arsenic and selenium compounds	This review centers on oxidative DNA damage, nucleotide and base excision repair, zinc finger proteins involved in DNA repair and/or DNA damage signaling such as poly(ADP-ribosyl)ation also the DNA repair enzymes Fpg and XPA
Hei and Filipic [121]	Role of oxidative damage in the genotoxicity of arsenic	This free radical centered review emphasizes cellular effects and the degree of genotoxicity that arsenic causes particularly genetic deletions
Hughes [122]	Arsenic toxicity and potential mechanisms of action	A review centered on toxicity and several different MOA
Hughes <i>et al.</i> [123]	Research approaches to address uncertainties in the risk assessment of arsenic in drinking water	A look at future research needs to better assess the true risk of arsenic induced adverse health effects.
Kenyon and Hughes [124]	A concise review of the toxicity and carcinogenicity of dimethylarsinic acid	This review summarizes the evidence that dimethylated arsenic species [either DMA(III) or DMA(V)] are important causal chemical species of arsenic's toxicity and carcinogenicity

Table 2.8 (Continued)

Author and reference number	Title	Remarks
Kitchin and Ahmad [19]	Oxidative stress as a possible mode of action for arsenic.	This short review present evidence for oxidative stress as a cause of carcinogenesis
Kitchin and Wallace [58]	The role of protein binding of trivalent arsenicals in arsenic carcinogenesis and toxicity	This minireview presents the facts arguing for ligand-receptor type binding of arsenic to biological molecules as a major cause in arsenic carcinogenesis
Kitchin <i>et al.</i> [10]	Some chemical properties underlying arsenic's biological activity	This short review emphasizes the chemical basis (hard/soft acid/base principle, nucleophilicity and formation of free radicals) that account for arsenic's biochemical properties and actions
Kligerman <i>et al.</i> [20]	Methylated trivalent arsenicals as candidate ultimate genotoxic forms of arsenic: induction of chromosomal mutations but not gene mutations	This experimental study compared 6 different arsenicals activity for many different genotoxicity parameters and shows the comparative potency for each individual parameter
Rossman [7]	Mechanism of arsenic carcinogenesis: an integrated approach	Animal models of arsenic carcinogenesis, genotoxicity, oxidative stress, cell transformation, DNA methylation, DNA repair, cell cycle control, cell proliferation are featured (299 references)
Shi <i>et al.</i> [125]	Oxidative mechanism of arsenic toxicity and carcinogenesis	This review covers arsenic, oxidative stress and its possible role in carcinogenesis with an emphasis on cellular systems
Simeonova and Luster [126]	Mechanisms of arsenic carcinogenicity: Genetic or epigenetic mechanisms?	This review article covers cancer MOA emphasizing epigenetic aspects such as cell proliferation and protein phosphorylation in normal and transgenic mice (51 references)
Snow <i>et al.</i> [127]	Arsenic, mode of action at biologically plausible low doses: What are the implications for low dose cancer risk?	Low dose exposures, mode of action, enzymatic effects and risk assessment are covered in this review
Styblo <i>et al.</i> [34]	Comparative toxicity of trivalent and pentavalent inorganic and methylated arsenicals in rat and human cells	This <i>in vitro</i> cellular study includes five different cell types and IC50 values for up to four different arsenicals

(continued)

Table 2.8 (Continued)

Author and reference number	Title	Remarks
Styblo <i>et al.</i> [64]	The role of biomethylation in toxicity and carcinogenicity of arsenic: a research update	This review focuses on metabolism to methylated trivalent arsenicals, their cellular effects, gene transcription and the control of arsenic's methylation
<i>Carcinogenesis in experimental animals:</i>		
Cohen <i>et al.</i> [128]	Methylated arsenicals: the implications of metabolism and carcinogenicity studies in rodents to human risk assessment	The view that cytotoxicity and regenerative hyperplasia is an important driver in the animal carcinogenicity of dimethylarsinic acid (DMA(V)) is presented in this review
Hughes and Kitchin [6]	Arsenic, oxidative stress and carcinogenesis	A book chapter presenting the oxidative stress theory of arsenic carcinogenesis (142 references)
Kitchin [100]	Recent advances in arsenic carcinogenesis: modes of action, animal model systems and methylated arsenic metabolites	This review covers the nine most likely modes of action in arsenic induced cancer and emphasizes the role of methylated trivalent arsenic species
Waalkes <i>et al.</i> [79]	Animal models for arsenic carcinogenesis: inorganic arsenic is a transplacental carcinogen in mice	This review discusses transplacental arsenite exposures which induce tumors in the liver (including hepatocellular carcinoma), adrenal, lung, and ovary of adult mice long after the initial gestational exposure to arsenite has stopped
Wanibuchi <i>et al.</i> [94]	Understanding arsenic carcinogenicity by the use of animal models	A review article that summarizes this groups experimental carcinogenesis and pathology studies, particularly with methylated arsenicals, over about a 10 yr period
<i>Epidemiology:</i>		
Bates <i>et al.</i> [129]	Arsenic ingestion and internal cancers: a review	A review emphasizing the available epidemiological information, dose-response aspects, possible biases and degree of evidence for causality (with 82 references)
Smith <i>et al.</i> [88]	Cancer risks from arsenic in drinking water	A review including human studies of arsenic-induced cancer, dose-response and risk characterization (with 80 references)

Table 2.8 (Continued)

Author and reference number	Title	Remarks
Smith <i>et al.</i> [85]	Marked increase in bladder and lung cancer mortality in a region of Northern Chile due to arsenic in drinking water	Epidemiological information about a cohort of about 400 000 people in Chile exposed to a single concentration of arsenic that showed elevations in human cancer mortality in bladder, lung, skin and kidney
Tapio and Grosche [8]	Arsenic in the etiology of cancer	A epidemiology review article covering exposure assessment, confounders, metabolism, MOA and carcinogenesis (352 references)
<i>Metabolism and analytical chemistry:</i>		
Adair <i>et al.</i> [57]	Commonalities in metabolism of arsenicals	This analytical chemistry and public health oriented review emphasizes arsenosugars, other marine forms of arsenic, metabolism and methylation of arsenicals (with 39 references)
Cullen and Reimer [130]	Arsenic speciation in the environment	This ecology and chemistry oriented review emphasizes different chemical forms of arsenic and its transformations (458 references)
Le <i>et al.</i> [131]	Arsenic Speciation	A review covering analytical chemistry, environmental chemistry and occurrence of arsenicals (with 50 references)
Li <i>et al.</i> [59]	Arsenic (+3 oxidation state) methyltransferase and the methylation of arsenicals	Inorganic arsenic methylation phenotypes are compared in three methylating species (human, rat and mouse) and one nonmethylating species (chimpanzee) (28 references)
Rosen [132]	Biochemistry of arsenic detoxification	This minireview covers cellular uptake, reduction of arsenate to arsenite and cellular extrusion systems mostly in prokaryotes (68 references)
Thomas <i>et al.</i> [56]	The cellular metabolism and systemic toxicity of arsenic	Methylation of arsenic and some biological effects of methylated trivalent arsenicals are included in this metabolism centered review
Thomas <i>et al.</i> [30]	Arsenic (+3 oxidation state) methyltransferase and the methylation of arsenicals	This review presents and contrasts two models of arsenic methylation. (52 references)

(continued)

Table 2.8 (Continued)

Author and reference number	Title	Remarks
Vahter [133]	Species differences in the metabolism of arsenic compounds	Comparative species differences in urinary arsenic excretion between up to seven different species (65 references)

sections covering general sources on arsenic, epidemiology and animal carcinogenesis. There are so many good sources of useful information on arsenic that any such compilation regrettably omits many good sources.

2.6 Conclusion

Research into the biochemical effects and carcinogenesis of arsenic has advanced a great deal in the past 20 years. Better methods and additional scientists have arrived to contribute a deeper look in the causal pathways of how arsenicals adversely affect various life forms including man. Advancements in better animal carcinogenesis model systems [80, 89, 94, 97] and the insight that methylated trivalent arsenicals have a great deal of biological potency [20, 21, 24] have been major developments. So far, the use of genomic and proteomic tools in arsenic's biological effects have not yielded major advances to our understanding. These comprehensive biological tools may play an important future role in arsenic research particularly in contributing to the common interpretive problem that arsenicals cause too many biological effects (Chapter 4). The dose and time dependence of what biological effects happen at the lowest doses and at the earliest times may finally emerge from future genomic and proteomic experiments. This can provide us badly needed information on where we should be looking to better understand the causal nature of arsenic's many effects on cellular macromolecules, biochemistry and the carcinogenic process.

Acknowledgements

I thank Drs. Mike Hughes and Jaya Chilakapati for reviewing this manuscript as part of EPA clearance procedures. Kathleen Wallace also reviewed the manuscript, performed all the binding studies and prepared all of the Figures.

Disclaimer

This manuscript has been reviewed in accordance with the policy of the National Health and Environmental Effects Research Laboratory, U.S. Environmental Protection Agency, and approved for publication. Approval does not signify that the contents necessarily reflect the views and policies of the Agency, nor does mention of trade names or commercial products constitute endorsement or recommendation for use.

The author has no competing financial interests.

Abbreviations

APL	acute promyelocytic leukaemia
As(III)	arsenite
As(V)	arsenate
BAL	dimercaptol (British Anti-Lewisite),
B_{\max}	maximal binding capacity
CA	chromosome aberrations
CHO	Chinese hamster ovary cells
DMA(III)	dimethylarsinous acid
DMA(V)	dimethylarsinic acid
DMDTA(V)	dimethyldithioarsinic acid
DMDTA(V)	sodium dimethyldithioarsinate
DMMTA(V)	dimethylmonothioarsinic acid
DMPS	2,3-dimercapto-1-propanesulfonic acid, sodium salt
DMSA	meso-dimercaptosuccinic acid
DMTA(III)	dimethylthioarsinous acid
DMTA(V)	dimethylthioarsinic anhydride
ESR	electron spin resonance
Fpg	formamidopyrimidine-DNA glycosylase protein
GSH	reduced glutathione
IC ₅₀	inhibitor concentration that reduces the number of cultured cells by 50%
LC ₅₀	concentration that reduces the number of cultured cells by 50%
K6/ODC	a knock in transgenic mice overexpressing ornithine decarboxylase in its skin
K_d	dissociation equilibrium constant
Keap-1	drosophila actin-binding protein Kelch
k_{off}	dissociation rate constant of ligand-receptor complex. This is often called k_{-1}
k_{on}	association rate constant of ligand-receptor complex. This is often called k_1
M1	trimethylarsine sulfide
M2	dimethylthioarsinic anhydride
M3	sodium dimethyldithioarsinate
MMA(III)	monomethylarsonous acid
MMA(V)	monomethylarsonic acid
MMMTA(V)	monomethylmonothioarsonic acid
MN	micronucleus
MOA	mode of action
8-OHdG	8-hydroxydeoxyguanosine
PARP-1	poly(ADP-ribose) polymerase-1 protein
ROS	reactive oxygen species
SAM	S-adenosylmethionine
SCE	sister chromatid exchange
SOD	superoxide dismutase
SMR	standardized mortality rate
$t_{1/2}$	half life

TBARS	thiobarbituric acid reactive substance
TMAO	trimethylarsine oxide
TMAS	trimethylarsine sulfide
XPA	xeroderma pigmentosum group A protein
ZnXPAzf	the zinc finger region of XPA

References

1. NRC (ed.) (1999) *Arsenic in Drinking Water*, National Academy Press, Washington, DC.
2. NRC (ed.) (2001) *Arsenic in Drinking Water 2001 Update*, National Academy Press, Washington, DC.
3. IARC (ed.) (2004) *Some Drinking Water Disinfectants and Contaminants, including Arsenic*, International Agency for Research on Cancer, IARC Press, Lyon, France.
4. Basu, A., Mahata, J., Gupta, S., and Giri, A.K. (2001) *Mutation Research*, **488**, 171–194.
5. Mandal, B.K. and Suzuki, K.T. (2002) *Talanta*, **58**, 201–235.
6. Hughes, M.F. and Kitchin, K.T. (2006) in *Oxidative stress, disease and cancer* (ed. K. Singh), Imperial College Press, London, pp. 825–850.
7. Rossman, T.G. (2003) *Mutation Research*, **533**, 37–65.
8. Tapio, S. and Grosche, B. (2006) *Mutation Research*, **612**, 215–246.
9. Cullen, W.J. and Reimer, J. (1989) *Chemical Reviews*, **89**, 713–764.
10. Kitchin, K.T., Wallace, K., and Andrewes, P. (2002) in *Arsenic exposure and health effects - V* (eds W.R. Chapell, C.O. Abernathy, R.L. Calderon, and D.J. Thomas), Elsevier, San Diego, pp. 345–354.
11. Aposhian, H.V. (1989) in *Reviews in Biochemical Toxicology* (eds E. Hodgson, J. Bend, and R. Philpot), Elsevier, New York, pp. 265–300.
12. Kitchin, K.T. and Wallace, K. (2008) *Toxicology and Applied Pharmacology*, **232**, 252–257.
13. Gailer, J. (2002) *Applied Organometallic Chemistry*, **16**, 701–707.
14. Gailer, J., George, G.N., Pickering, I.J. et al. (2002) *Chemical Research in Toxicology*, **15**, 1466–1471.
15. Stewart, R.C., Hille, R., and Massey, V. (1984) *The Journal of Biological Chemistry*, **259**, 14426–14436.
16. Page, J.D. and Wilson, I.B. (1985) *The Journal of Biological Chemistry*, **260**, 1475–1478.
17. Yamanaka, K., Hoshino, M., Okamoto, M. et al. (1990) *Biochemical and Biophysical Research Communications*, **168**, 58–64.
18. Yamanaka, K., Hasegawa, A., Sawamura, R., and Okada, S. (1989) *Biochemical and Biophysical Research Communications*, **165**, 43–50.
19. Kitchin, K.T. and Ahmad, S. (2003) *Toxicology Letters*, **137**, 3–13.
20. Kligerman, A.D., Doerr, C.L., Tennant, A.H. et al. (2003) *Environmental and Molecular Mutagenesis*, **42**, 192–205.
21. Andrewes, P., Kitchin, K.T., and Wallace, K. (2003) *Chemical Research in Toxicology*, **16**, 994–1003.
22. Adair, B.M., Moore, T., Conklin, S.D. et al. (2007) *Toxicology and Applied Pharmacology*, **222**, 235–242.
23. Geiszinger, A.E., Goessler, W., and Francesconi, K.A. (2002) *Environmental Science & Technology*, **36**, 2905–2910.
24. Dopp, E., Hartmann, L.M., Florea, A.M. et al. (2004) *Toxicology and Applied Pharmacology*, **201**, 156–165.
25. Liu, Z., Styblo, M., and Rosen, B.P. (2006) *Environmental Health Perspectives*, **114**, 527–531.
26. Ballatori, N. (2002) *Environmental Health Perspectives*, **110**, S689–S694.
27. Kitchin, K.T. and Wallace, K. (2005) *Toxicology and Applied Pharmacology*, **206**, 66–72.
28. Cullen, W.R., McBride, B.C., and Reglinski, J. (1984) *Journal of Inorganic Biochemistry*, **21**, 45–60.

29. Kitchin, K.T. and Wallace, K. (2006) *Journal of Biochemical and Molecular Toxicology*, **20**, 48–56.
30. Thomas, D.J., Li, J., Waters, S.B. *et al.* (2007) *Experimental Biology and Medicine*, **232**, 3–13.
31. Naranmandura, H., Suzuki, N., and Suzuki, K.T. (2006) *Chemical Research in Toxicology*, **19**, 1010–1018.
32. Aaseth, J. (1983) *Human Toxicology*, **2**, 257–272.
33. Aposhian, H.V. (1983) *Annual Review of Pharmacology and Toxicology*, **23**, 193–215.
34. Styblo, M., Del Razo, L.M., Vega, L. *et al.* (2000) *Archives of Toxicology*, **74**, 289–299.
35. Cullen, W.R., McBride, B.C., and Reglinski, J. (1984) *Journal of Inorganic Biochemistry*, **21**, 45–60.
36. Cui, X., Kobayashi, Y., Hayakawa, T., and Hirano, S. (2004) *Toxicological Sciences*, **82**, 478–487.
37. Percy, A.J. and Gailer, J. (2008) *Bioinorganic Chemistry and Applications*, **2008**, 539–582.
38. Kala, S.V., Kala, G., Prater, C.I. *et al.* (2004) *Chemical Research in Toxicology*, **17**, 243–249.
39. Kala, S.V., Neely, M.W., Kala, G. *et al.* (2000) *The Journal of Biological Chemistry*, **275**, 33404–33408.
40. Gregus, Z., Stein, A.F., and Klaassen, C.D. (1987) *The Journal of Pharmacology and Experimental Therapeutics*, **242**, 27–32.
41. Igarashi, T., Satoh, T., Ueno, K., and Kitagawa, H. (1983) *Journal of Pharmacobio-Dynamics*, **6**, 941–949.
42. Roberts, J.C. and Francetic, D.J. (1991) *Toxicology Letters*, **59**, 245–251.
43. Lu, M., Wang, H., Li, X.F. *et al.* (2007) *Chemical Research in Toxicology*, **20**, 27–37.
44. Lu, M., Wang, H., Li, X.F. *et al.* (2004) *Chemical Research in Toxicology*, **17**, 1733–1742.
45. Ramadan, D., Cline, D.J., Bai, S. *et al.* (2007) *Journal of the American Chemical Society*, **129**, 2981–2988.
46. Kitchin, K.T. and Wallace, K. (2006) *Journal of Biochemical and Molecular Toxicology*, **20**, 35–38.
47. Schwerdtle, T., Walter, I., and Hartwig, A. (2003) *DNA Repair*, **2**, 1449–1463.
48. Schwerdtle, T., Walter, I., Mackiw, I., and Hartwig, A. (2003) *Carcinogenesis*, **24**, 967–974.
49. Walter, I., Schwerdtle, T., Thuy, C. *et al.* (2007) *DNA Repair*, **6**, 61–70.
50. Ding, W., Hudson, L.G., Sun, X. *et al.* (2008) *Free Radical Biology & Medicine*, **45**, 1065–1072.
51. Qin, X., Hudson, L.G., Liu, W. *et al.* (2008) *Chemical Research in Toxicology*, **21**, 1806–1813.
52. Hartwig, A., Pelzer, A., Asmuss, M., and Burkle, A. (2003) *International Journal of Cancer*, **104**, 1–6.
53. Thayer, J.S. (2002) *Applied Organometallic Chemistry*, **16**, 677–691.
54. Bentley, R. and Chasteen, T.G. (2002) *Microbiology and Molecular Biology Reviews*, **66**, 250–271.
55. Challenger, F. (1945) *Chemical Reviews*, **36**, 315–361.
56. Thomas, D.J., Styblo, M., and Lin, S. (2001) *Toxicology and Applied Pharmacology*, **176**, 127–144.
57. Adair, B.M., Waters, S.B., Devesa, V. *et al.* (2005) *Environmental Chemistry*, **2**, 161–166.
58. Kitchin, K.T. and Wallace, K. (2008) *Journal of Inorganic Biochemistry*, **102**, 532–539.
59. Li, J., Waters, S.B., Drobna, Z. *et al.* (2005) *Toxicology and Applied Pharmacology*, **204**, 164–169.
60. Lin, S., Shi, Q., Nix, F.B. *et al.* (2002) *The Journal of Biological Chemistry*, **277**, 10795–10803.
61. Fomenko, D.E., Xing, W., Adair, B.M. *et al.* (2007) *Science*, **315**, 387–389.
62. Zakharyan, R.A., Wildfang, E., and Aposhian, H.V. (1996) *Toxicology and Applied Pharmacology*, **140**, 77–84.
63. Healy, S.M., Zakharyan, R.A., and Aposhian, H.V. (1997) *Mutation Research*, **386**, 229–239.
64. Styblo, M., Drobna, Z., Jaspers, I. *et al.* (2002) *Environmental Health Perspectives*, **110**, S767–S771.
65. Hayakawa, T., Kobayashi, Y., Cui, X., and Hirano, S. (2005) *Archives of Toxicology*, **79**, 183–191.

66. Raml, R., Rimpler, A., Goessler, W. *et al.* (2007) *Toxicology and Applied Pharmacology*, **222**, 374–380.
67. Naranmandura, H., Suzuki, N., Iwata, K. *et al.* (2007) *Chemical Research in Toxicology*, **20**, 616–624.
68. Naranmandura, H., Ibata, K., and Suzuki, K.T. (2007) *Chemical Research in Toxicology*, **20**, 1120–1125.
69. Chilakapati, J., Wallace, K., Ren, H. *et al.* (2010) *Toxicology*, **268**, 31–39.
70. Kitchin, K.T. (2008) *Genes and Environment*, **30**, 150–159.
71. Klaunig, J.E. and Kamendulis, L.M. (2004) *Annual Review of Pharmacology and Toxicology*, **44**, 239–267.
72. Santra, A., Maiti, A., Chowdhury, A., and Mazumder, D.N. (2000) *Indian Journal of Gastroenterology*, **19**, 112–115.
73. Shen, J., Wanibuchi, H., Salim, E.I. *et al.* (2003) *Carcinogenesis*, **24**, 1827–1835.
74. Yamanaka, K., Takabayashi, F., Mizoi, M. *et al.* (2001) *Biochemical and Biophysical Research Communications*, **287**, 66–70.
75. Moustacchi, E. (2000) *Mutation Research*, **464**, 35–40.
76. Hakem, R. (2008) *The EMBO Journal*, **27**, 589–605.
77. Ahlborn, G.J., Nelson, G.M., Ward, W.O. *et al.* (2008) *Toxicology and Applied Pharmacology*, **227**, 400–416.
78. Reichard, J.F., Schnekenburger, M., and Puga, A. (2007) *Biochemical and Biophysical Research Communications*, **352**, 188–192.
79. Waalkes, M.P., Liu, J., Chen, H. *et al.* (2004) *Journal of the National Cancer Institute*, **96**, 466–474.
80. Waalkes, M.P., Ward, J.M., Liu, J., and Diwan, B.A. (2003) *Toxicology and Applied Pharmacology*, **186**, 7–17.
81. Tseng, W.P., Chu, H.M., How, S.W. *et al.* (1968) *Journal of the National Cancer Institute*, **40**, 453–463.
82. Chen, C.J. and Wang, C.J. (1990) *Cancer Research*, **50**, 5470–5474.
83. Wu, M.M., Kuo, T.L., Hwang, Y.H., and Chen, C.J. (1989) *American Journal of Epidemiology*, **130**, 1123–1132.
84. Guo, H.R., Chiang, H.S., Hu, H. *et al.* (1997) *Epidemiology*, **8**, 545–550.
85. Smith, A.H., Goycolea, M., Haque, R., and Biggs, M.L. (1998) *American Journal of Epidemiology*, **147**, 660–669.
86. Hopenhayn-Rich, C., Biggs, M.L., and Smith, A.H. (1998) *International Journal of Epidemiology*, **27**, 561–569.
87. Hopenhayn-Rich, C., Biggs, M.L., Fuchs, A. *et al.* (1996) *Epidemiology*, **7**, 117–124.
88. Smith, A.H., Hopenhayn-Rich, C., Bates, M.N. *et al.* (1992) *Environmental Health Perspectives*, **97**, 259–267.
89. Yamamoto, S., Konishi, Y., Matsuda, T. *et al.* (1995) *Cancer Research*, **55**, 1271–1276.
90. Wanibuchi, H., Hori, T., Meenakshi, V. *et al.* (1997) *Japanese Journal of Cancer Research: Gann*, **88**, 1149–1154.
91. Wanibuchi, H., Yamamoto, S., Chen, H. *et al.* (1996) *Carcinogenesis*, **17**, 2435–2439.
92. Yamanaka, K., Katsumata, K., Ikuma, K. *et al.* (2000) *Cancer Letters*, **152**, 79–85.
93. Yamanaka, K., Ohtsubo, K., Hasegawa, A. *et al.* (1996) *Carcinogenesis*, **17**, 767–770.
94. Wanibuchi, H., Salim, E.I., Kinoshita, A. *et al.* (2004) *Toxicology and Applied Pharmacology*, **198**, 366–376.
95. Wei, M., Wanibuchi, H., Morimura, K. *et al.* (2002) *Carcinogenesis*, **23**, 1387–1397.
96. Hayashi, H., Kanisawa, M., Yamanaka, K. *et al.* (1998) *Cancer Letters*, **125**, 83–88.
97. Chen, Y., Megosh, L.C., Gilmour, S.K. *et al.* (2000) *Toxicology Letters*, **116**, 27–35.
98. Chen, Y., O'Brien, T., Del Razo, L.M. *et al.* (2008) *Journal of Environmental Pathology, Toxicology and Oncology*, **27**, 43–52.
99. Chen, C.J., Kuo, T.L., and Wu, M.M. (1988) *Lancet*, **1**, 414–415.
100. Kitchin, K.T. (2001) *Toxicology and Applied Pharmacology*, **172**, 249–261.

101. Kenyon, E.M., Hughes, M.F., Adair, B.M. *et al.* (2008) *Toxicology and Applied Pharmacology*, **232** (3), 448–455.
102. Kitchin, K.T. and Conolly, R. (2010) *Chemical Research in Toxicology*, **23** (2), 327–335.
103. Wang, Z.Y. and Chen, Z. (2008) *Blood*, **111**, 2505–2515.
104. Dilda, P.J. and Hogg, P.J. (2007) *Cancer Treatment Reviews*, **33** (6), 542–564.
105. Jurcic, J.G., Soignet, S.L., and Maslak, A.P. (2007) *Current Oncology Reports*, **9**, 337–344.
106. Bonati, A., Rizzoli, V., and Lunghi, P. (2006) *Current Pharmaceutical Biotechnology*, **7**, 397–405.
107. Cui, X., Wakai, T., Shirai, Y. *et al.* (2006) *Toxicological Sciences*, **91**, 372–381.
108. Chen, H., Li, S., Liu, J. *et al.* (2004) *Carcinogenesis*, **25**, 1779–1786.
109. Okoji, R.S., Yu, R.C., Maronpot, R.R., and Froines, J.R. (2002) *Carcinogenesis*, **23**, 777–785.
110. Xie, Y., Liu, J., Benbrahim-Tallaa, L. *et al.* (2007) *Toxicology*, **236**, 7–15.
111. Zhao, C.Q., Young, M.R., Diwan, B.A. *et al.* (1997) *Proceedings of the National Academy of Sciences of the United States of America*, **94**, 10907–10912.
112. Xie, Y., Trouba, K.J., Liu, J. *et al.* (2004) *Environmental Health Perspectives*, **112**, 1255–1263.
113. Bagnyukova, T.V., Luzhna, L.I., Pogribny, I.P., and Lushchak, V.I. (2007) *Environmental and Molecular Mutagenesis*, **48**, 658–665.
114. Benbrahim-Tallaa, L., Waterland, R.A., Styblo, M. *et al.* (2005) *Toxicology and Applied Pharmacology*, **206**, 288–298.
115. Sciandrello, G., Caradonna, F., Mauro, M., and Barbata, G. (2004) *Carcinogenesis*, **25**, 413–417.
116. WHO (2001) *Environmental Health Criteria*, **224**, 1–405.
117. Bode, A.M. and Dong, Z. (2002) *Critical Reviews in Oncology/Hematology*, **42**, 5–24.
118. Carter, D.E., Aposhian, H.V., and Gandolfi, A.J. (2003) *Toxicology and Applied Pharmacology*, **193**, 309–334.
119. Dixon, H.F. (1997) *Advances in Inorganic Chemistry*, **44**, 191–227.
120. Hartwig, A., Blessing, H., Schwerdtle, T., and Walter, I. (2003) *Toxicology*, **193**, 161–169.
121. Hei, T.K. and Filipic, M. (2004) *Free Radical Biology & Medicine*, **37**, 574–581.
122. Hughes, M.F. (2002) *Toxicology Letters*, **133**, 1–16.
123. Hughes, M.F., Kenyon, E.M., and Kitchin, K.T. (2007) *Toxicology and Applied Pharmacology*, **222**, 399–404.
124. Kenyon, E.M. and Hughes, M.F. (2001) *Toxicology*, **160**, 227–236.
125. Shi, H., Shi, X., and Liu, K.J. (2004) *Molecular and Cellular Biochemistry*, **255**, 67–78.
126. Simeonova, P.P. and Luster, M.I. (2000) *Journal of Environmental Pathology, Toxicology and Oncology*, **19**, 281–286.
127. Snow, E.T., Sykora, P., Durham, T.R., and Klein, C.B. (2005) *Toxicology and Applied Pharmacology*, **207**, 557–564.
128. Cohen, S.M., Arnold, L.L., Eldan, M. *et al.* (2006) *Critical Reviews in Toxicology*, **36**, 99–133.
129. Bates, M.N., Smith, A.H., and Hopenhayn-Rich, C. (1992) *American Journal of Epidemiology*, **135**, 462–476.
130. Cullen, W.J. and Reimer, J. (1989) *Chemical Reviews*, **89**, 713–764.
131. Le, X.C., Lu, X., and Li, X. (2004) *Analytical Chemistry*, **76**, 27A–33A.
132. Rosen, B.P. (2002) *FEBS Letters*, **529**, 86–92.
133. Vahter, M. (1994) *Applied Organometallic Chemistry*, **8**, 175–182.

3

Biological Chemistry of Antimony and Bismuth

Nan Yang and Hongzhe Sun

Department of Chemistry, The University of Hong Kong, Hong Kong, P.R. China

3.1 Introduction

Antimony (Sb) and bismuth (Bi) are located in the periodic table Group 15. In spite of not being essential for life, they play a therapeutic role in human healthcare via interaction with biomolecules. Antimony and bismuth compounds interact with nucleotides, amino acids, peptides, proteins and enzymes, which are closely related to their uptake, accumulation, redox, transport and excretion in human bodies and in turn account for their antimicrobial, anticancer, antiviral and antiparasite activities. Investigation of interactions of antimony or bismuth complexes with their potential biomolecular targets at a molecular level will lead to a significant improvement of our understanding of the mechanism of action of antimony and bismuth drugs in biological systems and subsequently facilitate the development of more efficient metallodrugs for human healthcare.

3.2 Biorelevant Coordination Chemistry of Antimony and Bismuth

In biological systems, the most common and stable oxidation states of antimony are antimonite (Sb^{III}) and antimonate (Sb^{V}) with a $\text{Sb}^{\text{V}}/\text{Sb}^{\text{III}}$ potential of $E^\circ = 0.59 \text{ V}$. Sb^{III} has a high affinity towards nitrogen, oxygen and thiolate containing ligands and its coordination number (CN) can vary. While the coordination conformations of Sb^{V} complexes are

normally simple or distorted octahedra due to the absence of the long pair electrons of Sb^{V} ion. The reduction process of Sb^{V} to Sb^{III} can readily proceed with the involvement of specific reductases or some low molecular mass thiolate containing biomolecules *in vitro* or *in vivo*.

Trivalent and pentavalent bismuth (Bi^{III} and Bi^{V}) are the two major oxidation states of the metal. Since Bi^{V} is a powerful oxidant in aqueous solutions with a $\text{Bi}^{\text{V}}/\text{Bi}^{\text{III}}$ potential (E°) of 2.03 V, it is unstable in biological systems. The oxidation state of biological interest is Bi^{III} that readily hydrolyses in aqueous solutions ($\text{p}K_{\text{a}} = 1.51$) and has a high affinity to oxygen, nitrogen and thiolate containing ligands. The high affinity of Bi^{III} to thiolate containing ligands in biological systems is an important feature of Bi^{III} because the thiolate ligands are simultaneously kinetically labile and can exchange with free thiol on a millisecond time scale, therefore Bi^{III} may be a highly mobile ion inside cells [1].

3.3 Antimony and Bismuth Compounds in Medicine

3.3.1 Antimony in Medicine

The medicinal applications of antimony can be traced back to the sixteenth century as an emetic drug [2]. At present, antimony compounds have commonly been used in clinic for the treatment of Leishmaniasis, caused by *Leishmania* that is injected into mammals via sand flies [2]. The first antimony antileishmanial drug, potassium Sb^{III} tartrate (Tartar emetic) was developed around 1910. Figure 3.1a shows the crystal structure of the building unit of potassium antimony(III) tartrate, where each Sb^{III} coordinates to four oxygens from two tartrates with each in a bidentate mode [3]. Currently, antimony pentavalent compounds such as sodium stibogluconate (Pentostam) and meglumine antimonite (Glucantime) (Figure 3.1b) are predominantly used in many countries as the first choice antileishmanial drugs due to their efficient therapeutic indices and low toxicity, though it has been suggested that the relatively nontoxic Sb^{V} only serves as a prodrug and is reduced into the more toxic Sb^{III} at or near the site of action in biological systems [2, 4]. This pharmacokinetics of antimony drugs is evidenced by the observation that significant amounts of Sb^{III} are detected in tissues and serum in *Leishmania garnhami* infected hamsters after the treatment with Sb^{V} drug, meglumine antimonite [5].

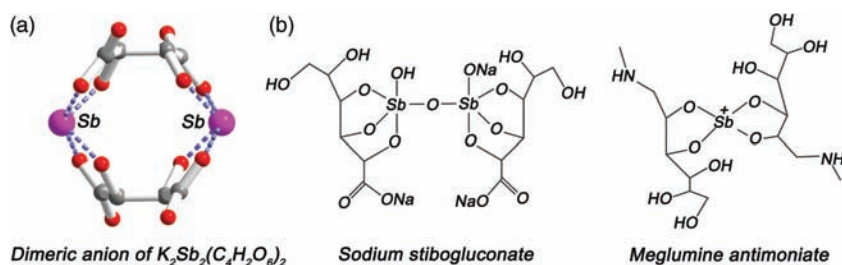


Figure 3.1 (a) Crystal structure of the dimeric anion of clinically used potassium antimony(III) tartrate (CCDC: 247426). (b) Proposed structures of Sb^{V} drugs: sodium stibogluconate and meglumine antimonite. Color code: C, gray; O, red; Sb, purple

Besides the antiparasite activity, antimony compounds have also exhibited other applications in human healthcare. For examples, potassium antimony tartrate is used to treat cough for reducing the excretion of sputum as an effective ingredient in Compound Liquorice. Antimony sodium subgallate has been used to treat schistosomiasis since 1970s whereas antimony tartrate has been found to be cytotoxic *in vitro* to various lung cancer cell lines with IC_{50} ranging from 4.2 to 322 $\mu\text{g}/\text{ml}$, as effective as cisplatin and doxorubicin [6]. Sodium stibogluconate shows complete suppression effect of Hepatitis C virus (HCV) replication in four out of six human liver slices at a concentration of 100 $\mu\text{g}/\text{ml}$, as demonstrated from HCV infected patients [7]. Antimoniotungstate ($[(\text{NH}_4)_{17}\text{Na}(\text{NaSb}_9\text{W}_{21}\text{O}_{86})_{14}\text{H}_2\text{O}]$) was reported to be active in reducing HIV levels in a patient with AIDS [8], stimulating the search for other antimony polyoxometalates which may have potentials for the treatment of HIV leishmania coinfection cases [9]. A series of aromatic Sb^{V} compounds (NSC 13778, NSC 13755 and NSC 13759) exhibits the antiHIV potent with EC_{50} values from 0.9 ~ 8.7 μM in CEM–SS cells, probably via disrupting the interactions between the viral envelope glycoprotein (gp120) and the glycoprotein expressed on the cell surface (CD4) [10].

3.3.2 Bismuth in Medicine

The use of bismuth compounds in medicine can be traced back to the Middle Ages and the first account of using bismuth as medicine was in 1786 by Louis Odier for the treatment of dyspepsia. Although bismuth compounds have been used to treat various microbial infections such as syphilis, colitis, wound infections and quartan malaria, and so on [11], the major medicinal applications of bismuth compounds are associated with gastrointestinal disorders and ulcers, and the medicinal efficacies are related to their inhibition activity to *Helicobacter pylori* (*H. pylori*, firstly discovered in 1983), a bacterium that can prevent ulcers from healing [11–13]. Bismuth subsalicylate (BSS, Pepto–Bismol) has been used for the fast relief of heartburn, nausea, indigestion, upset stomach, and diarrhea. Its structure and hydrolysis mechanism have been modeled on two bismuth oxosalicylate clusters, that is, $[\text{Bi}_{38}\text{O}_{44}(\text{Hsal})_{26}(\text{Me}_2\text{CO})_{16}(\text{H}_2\text{O})_2]$ and $[\text{Bi}_9\text{O}_7(\text{Hsal})_{13}(\text{Me}_2\text{CO})_5]$ [14]. The core of $[\text{Bi}_9\text{O}_7(\text{Hsal})_{13}(\text{Me}_2\text{CO})_5]$ lies at the heart of $[\text{Bi}_{38}\text{O}_{44}(\text{Hsal})_{26}(\text{Me}_2\text{CO})_{16}(\text{H}_2\text{O})_2]$ (Figure 3.2a). The crystal of $[\text{Bi}_9\text{O}_7(\text{Hsal})_{13}(\text{Me}_2\text{CO})_5]$ initially predominates with cocrystallization of a relatively small amount of the $[\text{Bi}_{38}\text{O}_{44}(\text{Hsal})_{26}(\text{Me}_2\text{CO})_{16}(\text{H}_2\text{O})_2]$, following the transposition of predominance when extend the crystal growth time, revealing a possible hydrolysis process for BSS [14]. Another type of bismuth drug is based on bismuth citrate complexes such as colloidal bismuth subcitrate (CBS, De–Nol; Gist Brocades and Yamanouchi), and ranitidine bismuth citrate (RBC, Tritac and Pylorid, GSK), which is used worldwide to treat various gastrointestinal diseases, caused by the *H. pylori* infection [15–18]. Both X–ray analysis and structural modeling suggest that the dimeric units of bismuth citrate ($[\text{Bi}_2(\text{cit})_2]^{2-}$, Figure 3.2b) may form the negative charged polymeric skeletons in both CBS and RBC, and aggregate to a type of ‘hybrid’ metal organic framework containing regular meshes with the ‘encapsulated’ NH_4^+ and K^+ (in CBS) or ranitidine (in RBC) [19, 20]. Ranitidine bismuth citrate is believed to be more potent in the treatment of gastrointestinal disorders since it combines the activity of ranitidine, which reduces the excretion of gastric acid and bismuth citrate, which protects the mucous membrane of the stomach and inhibits *H. pylori* colonization. Furthermore, the combination of RBC with antibodies can provide a higher efficacy in healing stomach ulcers [21]. A new

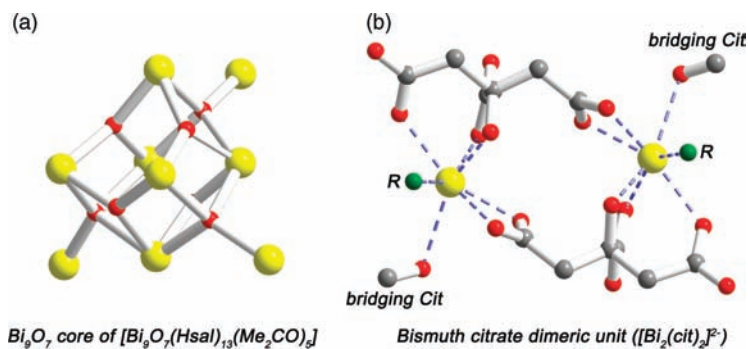


Figure 3.2 (a) Bi_9O_7 core of $[\text{Bi}_9\text{O}_7(\text{Hsal})_{13}(\text{Me}_2\text{CO})_5]$ (CCDC: 289351). (b) Bismuth citrate dimeric unit $([\text{Bi}_2(\text{cit})_2]^{2-})$, bridging Cit: citrates that connect the adjacent dimeric units in the polymer, R: coordinating H_2O or Cl^- (CCDC: 702077). Color code: C, gray; O, red; Bi, yellow; R, green

complex of bismuth with *d*-polygalacturonic acid, the so called ‘colloidal bismuth pectin’, approved in clinical use in China, shows the similar effectiveness to CBS in the treatment of *H. pylori* positive duodenal ulcer in triple and quadruple therapies [22].

Besides the anti *H. pylori* activity, bismuth compounds also show the potentials as anticancer agents. Both ^{212}Bi and ^{213}Bi were shown recently to exhibit potentials as novel therapeutic agent for the small volume tumors (Chapter 13) [23, 24]. Sequential therapy with cytarabine and ^{213}Bi labeled HuM195 has entered a phase I/II clinical trial for the treatment of advanced myeloid leukaemia [25]. The ^{213}Bi labeled monoclonal antibody C595 can target the MUC1 protein that is overexpressed in $\sim 90\%$ of tested tumor samples and effectively inhibit growth of pancreatic cell clusters and preangiogenic lesions *in vivo*, eventually killing cancer micrometastases. This suggests that ^{213}Bi treatment may have a role as adjuvant therapy immediately after resection of macroscopic tumor to prevent recurrence [26]. Bismuth compounds not only inhibit cancer cells directly but also reduce the side effects of platinum-based anticancer drugs such as cisplatin and its analogues. For example, bismuth subnitrate (BSN) was found to be able to reduce the side effects of cisplatin when use citrate as a transporter to enhance bismuth distribution in kidneys (Figure 3.3) [27, 28]. This may relate to the elevated levels of metallothionein (MT) expression in tissues stimulated by bismuth [29].

3.4 Interaction with Nucleic Acids

3.4.1 Interaction of Antimony with Nucleosides and Nucleotides

Sb^{V} , upon interaction with ribose containing biomolecules, is able to form complexes with stoichiometries of 1: 1, 1: 2 and 1: 3 (Figure 3.4a), which were confirmed by the observation of signals of $[\text{Sb} + \text{X} - \text{H} + 3\text{OH}]^+$, $[\text{Sb} + 2\text{X} - 3\text{H} + \text{OH}]^+$ and $[\text{Sb} + 3\text{X} - 4\text{H}]^+$ (X = neutral biomolecule) species in their ESI-MS spectra [30]. The collision-induced dissociation (CID) tandem mass spectrometry (MS) and multistage MS^n results suggest that the presence of vicinal *cis*-hydroxyl groups is critical for such a complexation to occur [30]. An

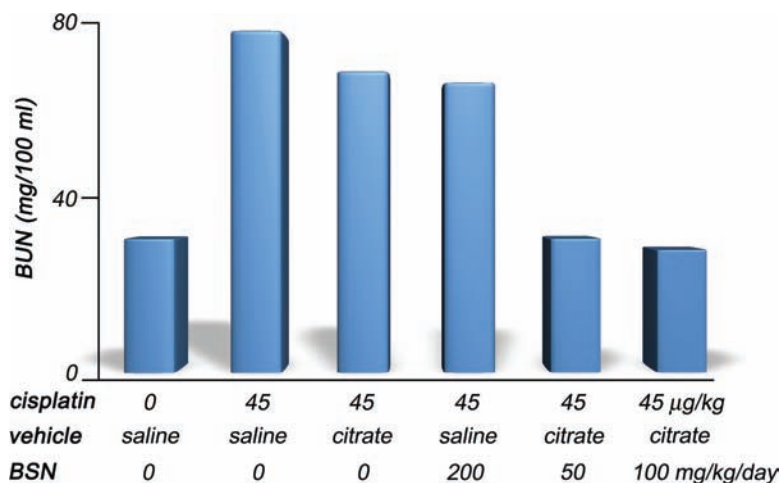


Figure 3.3 Effect of oral pretreatment of bismuth subnitrate (BSN) with a saline or citrate buffer on renal toxicity of cisplatin in mice inoculated with Meth-A fibrosarcoma. Blood urea nitrogen (BUN), an indicator of renal toxicity, is measured five days after the cisplatin injection [27]

RNA oligonucleotide 5'-AGUCCAGUUGAGUCU-3' and a DNA oligonucleotide 5'-TATAG-3' are used to test the binding ability of Sb^{V} . Both the size exclusion HPLC chromatogram and direct infusion negative ionization MS show that Sb^{V} only binds RNA oligonucleotides, indicating the importance of the vicinal *cis*-hydroxyl group on ribose. In contrast, nucleobase is not involved in Sb^{V} coordination [30].

Trivalent antimony (Sb^{III}) forms stable complexes with nucleosides in a similar way as Sb^{V} by binding to the *cis*-2',3'-diol fragments of the ribose. In a reported crystal structure of $\text{Na}[\text{Sb}^{\text{III}}(\text{adenosine})_2] \cdot \text{H}_2\text{O}$, the deprotonated *cis*-2',3'-diol fragments of two adenosines have been found to be chelating metal binding sites. The coordination of sodium to 5',3'-diol and the intermolecular hydrogen bonds between 5'- and 2'-diol groups of different adenosines result in aggregation of Sb^{III} complexes to a metal biomolecular polymer (Figure 3.5a) [31].

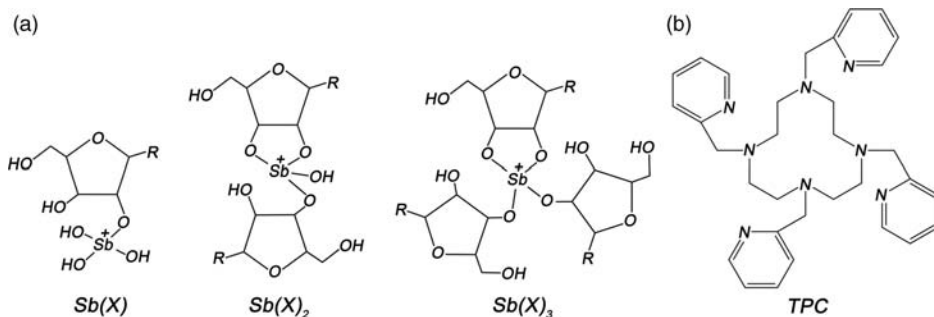


Figure 3.4 (a) Proposed complexation of Sb^{V} with ribose containing biomolecules ($X =$ neutral biomolecule). (b) Structure of TPC (1,4,7,10-tetrakis(2-pyridylmethyl)-1,4,7,10-tetraazacyclododecane)

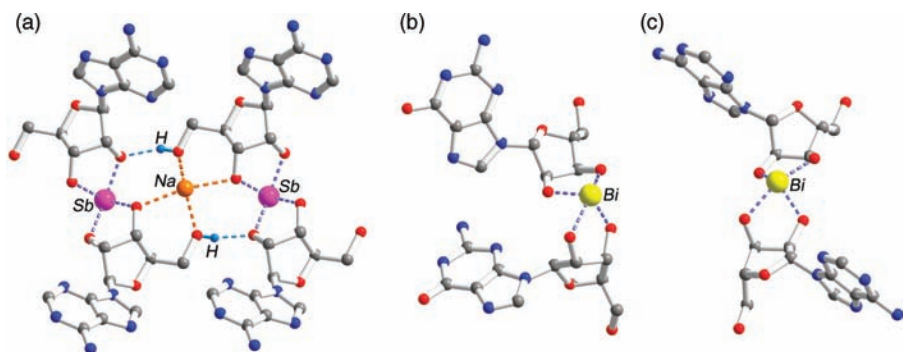


Figure 3.5 (a) Crystal structure of complex $\text{Na[Sb}^{\text{III}}(\text{adenosine})_2\cdot\text{H}_2\text{O}$ (CCDC: 634531). Sb^{III} binds to the *cis*-2',3'-diol fragment of two adenosines, and the hydrogen bonds and sodium coordination bonds lead the complex to a polymer. (b) Crystal structure of complex $\text{Bi}(\text{guanosine})_2$ (CCDC: 634530) where Bi^{III} binds to the *cis*-2',3'-diol groups of two guanosines. (c) Crystal structure of complex $\text{Bi}(\text{adenosine})_2$ (CCDC: 634532) where Bi^{III} binds to the *cis*-2',3'-diol groups of two adenosines. Color code: C, gray; N, blue; O, red; H, cyan; Na, orange; Sb, purple; Bi, yellow

3.4.2 Interaction of Bismuth with Nucleosides and Nucleotides

Bismuth can form complexes with nucleosides with a stoichiometry of 1: 2. The crystal structures of $\text{Bi}(\text{guanosine})_2$ and $\text{Bi}(\text{adenosine})_2$ complexes show that the two guanosine or adenosine bind one Bi^{III} via the deprotonated *cis*-2',3'-diol groups (Figure 3.5b and c) [31] and the nucleobases are not involved in coordination, similar to that of antimony adenosine complexes (Figure 3.5a).

Bismuth also binds to oligonucleotides. Binding of a bismuth complex, $\text{Bi}(\text{TPC})$ (TPC = 1,4,7,10-tetrakis(2-pyridylmethyl)-1,4,7,10-tetraazacyclododecane) (Figure 3.4b), to calf thymus DNA (5'-GMP, guanosine-5'-monophosphate) has been investigated by mass spectrometry, UV spectroscopy and DNA-EB (ethidium bromide) fluorescent titrations [32]. Upon addition of $\text{Bi}(\text{TPC})$ complex to the DNA-EB solution, the fluorescent emission intensity of the DNA-EB decreased gradually, indicative of the substitution of EB by $\text{Bi}(\text{TPC})$. The ESI-MS data showed two peaks corresponding to $[\text{Bi}(\text{TPC}) + 5'\text{-GMP}]^+$ (m/z 1106.2) and $[\text{Bi}(\text{TPC}) + 5'\text{-GMP}]^{2+}$ (m/z 553.6). Binding of bismuth to DNA was further confirmed by the absorbance band of $\text{Bi}(\text{TPC})$ at 334 nm exhibiting hypochromism of about 25.7% [32]. Such a binding property of Bi^{III} may contribute to the high cytotoxic activity of the complex ($\text{Bi}(\text{TPC})$) against melanoma B16-BL6 cells with an IC_{50} of 4.1×10^{-8} M, which is 100 times more potent than the clinically used antitumor drug cisplatin [32].

3.5 Interaction with Amino Acids and Peptides

3.5.1 Interaction of Antimony with Amino Acids and Peptides

Sb^{III} coordinates to the carboxylate group of valine in a bidentate mode, resulting in the formation of a linear polymer [33]. Since Sb^{III} and thiolates are substantially soft

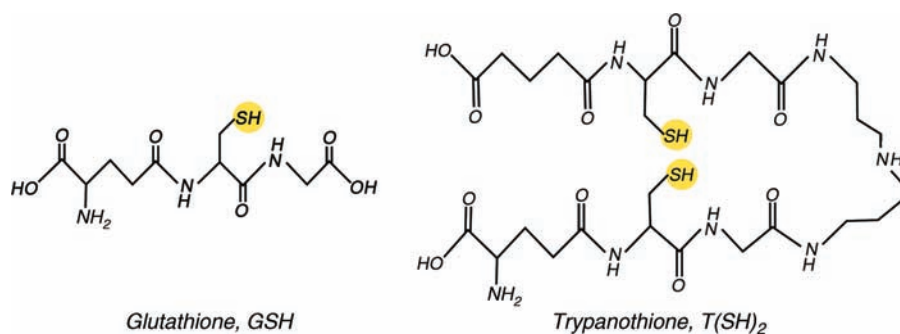


Figure 3.6 The structures of glutathione, GSH (γ -L-Glu-L-Cys-Gly) and trypanothione, T(SH)₂

electrophiles and nucleophiles respectively, the cysteine and cysteine containing peptides such as glutathione (γ -L-Glu-L-Cys-Gly, GSH) and trypanothione (N^1, N^8 -bis(glutathionyl)spermidine, T(SH)₂) (Figure 3.6), can form stable complexes with Sb^{III}. The deprotonated thiol group of cysteine residue of GSH is shown to be the only binding site for Sb^{III} and the formed complex has a stoichiometry of [Sb(GS)₃] with the stability constant ($\log K$) of 25 ($I = 0.1$ M, 298 K) [34]. As a major low molecular mass thiol inside *Leishmania*, T(SH)₂ can coordinate Sb^{III} to form a complex with a stoichiometry of [Sb(TS₂)], where Sb^{III} binds to T(SH)₂ at the two thiolates of the cysteine residues [35]. Binding of Sb^{III} to T(SH)₂ is pH dependent with a stability constant ($\log K$) of 23.6 ($I = 0.1$ M, 298 K) at the biological pH [36]. In spite of the high stability of both [Sb(GS)₃] and [Sb(TS₂)] complexes, they are kinetically labile. The exchange rate of GSH between its free and Sb^{III} bound forms is pH dependent, ranging from a slow exchange at a low pH (2 s⁻¹ at pH 3.2) to relatively rapid exchange at the biological pH (>440 s⁻¹) [34]. Notably, addition of low molecular monothiol ligands such as cysteine and GSH to [Sb(TS₂)] results in the formation of a ternary complex, as confirmed by the appearance of peaks at m/z of 1005.3/1007.1 and 1149.5/1151.2 in ESI-MS spectra, corresponding to NAC-Sb-TS₂ (NAC = *N*-acetyl-L-cysteine) and GS-Sb-TS₂, respectively. Such facile exchange of thiolate containing ligands and the formation of Sb^{III} ternary complex may allow Sb^{III} to be transported among various biofluids and tissues *in vivo* [36].

The zinc finger motif always plays the structural role in proteins and enzymes and is characterized by the coordination of Zn^{II} ions to several conserved amino acids, usually cysteine and histidine. Sb^{III} was found to bind to the zinc finger domain of nucleocapsid protein p7 (NCp7) of human immunodeficiency virus type 1 (HIV-1). NCp7 contains two conserved CX₂CX₄HX₄C (CCHC) motifs (Figure 3.7), and the substitution of Zn^{II} by Sb^{III} was approved by fluorescent spectroscopy. Upon addition of Sb^{III} (as Sb(GS)₃) to a solution of Zn-NCp7, the peptide intrinsic fluorescent emission at 360 nm, which is due to Zn^{II} binding and the proper folding of NCp7, was quenched, indicating that Sb^{III} binds the peptide and induces the conformational changes. Remarkably, the CCHC motif is highly conserved among almost all known strains of retroviruses, except human foamy viruses [37], binding of Sb^{III} to such a motif may provide a potential target for the metallodrug. Furthermore, a conjugate of Sb^{III}-GSH-NCp7 is observed in an ESI-MS spectrum at m/z of 1324.6, suggesting a transport functional role for glutathione conjugates beyond a

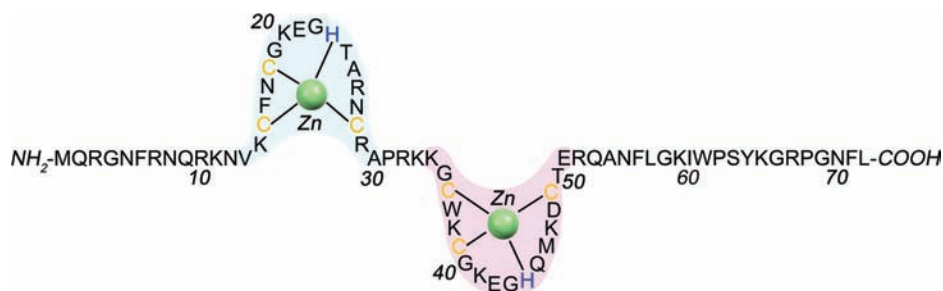


Figure 3.7 Sequence of the HIV nucleocapsid NCP7 protein which contains two conserved zinc finger domains (CX₂CX₄HX₄C) highlighted in light blue and pink, likely serving as biological targets for Sb^{III}

simple reduction [37]. Recent biochemical characterization also shows that As^{III} binds directly to cysteine residues in zinc fingers located within the RBCC (N-terminal RING finger/B-box/coiled coil) domain of promyelocytic leukaemia protein (PML) and PML-RAR α (PML retinoic acid receptor alpha). Such binding induces PML oligomerization, subsequently resulting in enhanced SUMOylation and degradation [38].

One of the most important aspects of Sb^V when interacting with amino acids and peptides is related to its reduction, from Sb^V to Sb^{III}, in biological systems, which is probably a key feature for Sb^V drugs to exhibit antiparasite activity. Low molecular mass thiols such as cysteine, cysteine-glycine, GSH and T(SH)₂ have been reported to be able to reduce Sb^V to Sb^{III} (Table 3.1) [2, 36, 39–42]. The reduction of Sb^V is favored at an acidic pH and is much faster in the presence of Cys-Gly and Cys than that of GSH. The initial reduction rates at pH 5 (mimic lysosomes) for Cys-Gly or Cys are about 26- and 17-fold more than GSH; while the reduction rates at pH 7 (mimic extracellular medium and cytosol) for Cys-Gly or Cys are three-fold lower than those at pH 5, however are still about 60- and 40-fold greater than GSH, respectively. The same tendencies are observed for meglumine antimonite (Glucantime) [41], suggesting that the reduction rate is independent of Sb^V species.

Since T(SH)₂ is the most abundant (> 80%) low molecular mass thiol inside *Leishmania* [43] and the combination of T(SH)₂ with trypanothione reductase (TR) provides an intracellular reducing environment against oxidative stress for parasite. T(SH)₂ is likely to be a reducing agent for Sb^V drugs. The reduction of Sb^V by the unique T(SH)₂ is again favored at a low pH and high temperature as shown by a larger reduction rate in amastigotes (pH ~ 6.4, 310 K) than in promastigotes (pH ~ 6.8, 298 K) of *Leishmania* [44, 45].

Table 3.1 The initial reduction rates ($\mu\text{M}\cdot\text{min}^{-1}$) of Sb^V in the presence of Cys-Gly, Cys or GSH at 310 K [41]

Thiol	Potassium hexahydroxoantimonate		Meglumine antimonate	
	pH 5	pH 7	pH 5	pH 7
Cys-Gly	5.1 ± 0.4	1.6 ± 0.3	0.6 ± 0.16	0.17 ± 0.07
Cys	3.3 ± 0.3	1.1 ± 0.1	0.44 ± 0.03	0.13 ± 0.01
GSH	0.19 ± 0.01	0.026 ± 0.007	0.042 ± 0.001	0.013 ± 0.001

Table 3.2 The reduction rates of Sb^{V} (Pentostam) by cysteine, GSH and $\text{T}(\text{SH})_2$ (as half lives) [40]

Thiol	Reduction rate ($t_{1/2}$)	
	310 K	298 K
Cysteine	> 3.5 d	No reduction
GSH	> 3.5 d	No reduction
$\text{T}(\text{SH})_2$	113 \pm 5 min (pH 6.4) 6 h (pH 7.4)	402 \pm 5 min (pH 6.4) > 20 h (pH 7.4)

In comparison with cysteine and GSH, the reduction of Sb^{V} (sodium stibogluconate, the active component of Pentostam) is faster in the presence of $\text{T}(\text{SH})_2$. Table 3.2 summarizes the reduction rates of Sb^{V} , measured by ^1H NMR, in the presence of cysteine, GSH or $\text{T}(\text{SH})_2$ at different temperatures [40]. Upon reduction, Sb^{III} can form a $\text{SbT}(\text{S})_2$ complex with trypanothione sequentially and further a ternary complex with other thiolate containing biomolecular ligands, which may play a crucial role in antimony trafficking and distribution among biomolecules in biological systems [35, 36].

3.5.2 Interaction of Bismuth with Amino Acids and Peptides

Cysteine and cysteine containing low molecular mass molecules can prevent the precipitation of colloidal bismuth subcitrate (CBS) at pH 2, indicating the strong binding of Bi^{III} to thiolate groups. The crystal structure of bismuth cysteine complex ($\text{Bi}(\text{Cys})_3$) has been resolved recently. As shown in Figure 3.8, each Bi^{III} binds three thiolate groups of cysteine residues with average Bi–S bond length of ~ 2.54 Å. A weak interaction between Bi^{III} and thiolate group from an adjacent complex unit (Bi–S bond length of 3.48 Å) and intermolecular hydrogen bonds (not shown) are observed, which connect the adjacent complex units and result in the formation of a chainlike polymer [46]. The tripeptide glutathione (GSH) is present in many cells at relatively high concentrations (0.5 \sim 10 mM) and may play a role in the transport of Bi^{III} in cells and biofluids. ESI–MS results show that Bi^{III} binds to GSH with stoichiometries of Bi: GSH = 1: 1, 1: 2 and 1: 3 [47], suggesting that thiolation of bismuth is likely to be the primary biochemical fate of bismuth drugs [48]. NMR studies show that Bi^{III} forms a complex with GSH intracellularly and passes through the membrane of red blood cells slowly [49] and the transport of each Bi^{III} ion results in the cotransport of three glutathione molecules [50]. Such an enhancement of intracellular bismuth uptake facilitated by thiolate ligands (e.g., GSH) may account for the high antimicrobial activities of bismuth thiolate complexes. Binding of Bi^{III} to other cysteine containing peptides was also studied. For example, Bi^{III} can bind to the CXC motifs (e.g., Ac–Cys–Gly–Cys– NH_2 , Cys–Gly–Cys– NH_2 and Met–Asp–Pro–Glu–Thr–Cys–Pro– NH_2) via coordination to the thiol sulfurs of cysteines with stoichiometries of 1: 1 or 1: 2, as determined by NMR and ESI–MS [51].

Human gastrin is a peptide that exhibits the dose dependent and highly specific effect on stimulating the growth of *H. pylori* [52]. Bismuth was found to be an inhibitor against the biological activity of glycine extended gastrin 17 (Ggly) in stimulating inositol phosphate production, cell proliferation and cell migration [53]. Fluorescence experiments show that both Ggly and amidated gastrin 17 (Gamide) (Figure 3.9) bind two Fe^{III} or Bi^{III} ions [54, 55].

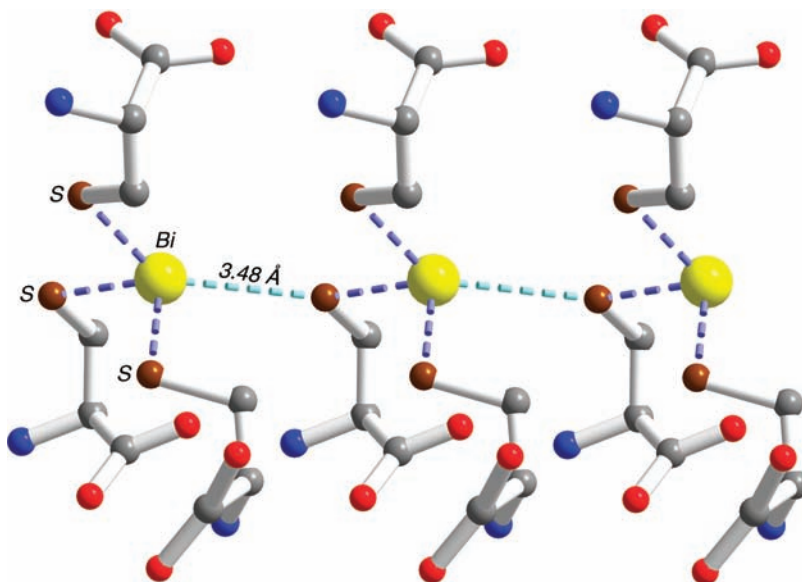


Figure 3.8 Crystal structure of $\text{Bi}(\text{Cys})_3$. In a complex unit, each Bi^{III} coordinates to three deprotonated thiolate groups of cysteine with average Bi-S bond length of $\sim 2.54 \text{ \AA}$. Color code: C, gray; O, red; N, blue; S, brown; Bi, yellow

They share the same coordination residues/motifs (Glu7, Glu8 and Glu9), evidenced by the observation that upon addition of 4M equivalent Bi^{III} to a Ggly solution, the signals of Glu7, Glu8 and Glu9 which are putative Fe^{III} binding ligands were broadened in a two dimensional ^1H NMR spectrum. Although Bi^{III} binds Gamide, it does not affect the biological activity of Gamide, indicating that the Ggly receptors are distinct from the CCK-2 receptors (essential for Gamide biological activities).

3.6 Interaction with Proteins and Enzymes

3.6.1 Interaction of Antimony with Proteins and Enzymes

Drug resistance is a major impediment to successful treatment of leishmaniasis [56, 57]. Down regulation or loss of uptake systems have been shown to lead to drug resistance. In spite of the poorly understood entry route of Sb^{V} into *Leishmania* (or into macrophages), it has been speculated that Sb^{V} enters the parasite via a protein that recognizes a sugar moiety



Figure 3.9 Sequences of Gamide and Ggly where Z represents a pyroglutamate residue. The potential Fe^{III} or Bi^{III} binding residues (Glu7, Glu8 and Glu9) are highlighted in yellow

like structure shared with gluconate, based on the competitive inhibition of gluconate to Sb^{V} uptake in axenic amastigotes [58]. The differential accumulation of Sb^{V} and Sb^{III} in both stages of the *Leishmania* suggests that two forms of antimony may use different routes [59]. The accumulation of Sb^{III} is competitively inhibited by the As^{III} , indicating that Sb^{III} and As^{III} may enter cells by the same route as those in yeasts and mammals [59].

Aquaglyceroporins (AQPs) have been identified as uptake systems for trivalent metalloids in eukaryotes and prokaryotes [60–62]. GlpF, a homologue of AQPs, was first identified as an uptake pathway for Sb^{III} in *Escherichia coli* (*E. coli*). The major form of Sb^{III} , $\text{Sb}(\text{OH})_3$, derived from antimonous acid at neutral pH, may be recognized as an inorganic equivalence of a polyol by GlpF, and was then transported into cells [60]. Mammalian AQP9 has the broadest specificity and can mediate the passage of water, glycerol, urea, carbamides, polyols, purines, and pyrimidines in a phloretin- and mercury-sensitive manner [63, 64]. Mammalian AQP9 also shows the ability to facilitate the uptake of As^{III} and Sb^{III} when expressed in either *S. cerevisiae* or oocytes [62]. The leishmanial homologue of the mammalian AQP9, aquaglyceroporins from *Leishmania major* (LmAQP1), was also identified and approved to be responsible for the uptake of Sb^{III} in *Leishmania*. As shown in Figure 3.10, many amino acids and several motifs are conserved in GlpF, AQP9 and LmAQP1, indicative of functional similarity in antimony uptake in biological systems. Figure 3.11 shows that LmAQP1 can catalyse the uptake of Sb^{III} in three species of wild type *Leishmania*, for example, *Leishmania major*, *Leishmania infantum* and *Leishmania tarentolae* [65]. All the three *LmAQP1* transfected species of *Leishmania* exhibit the rapid uptake of Sb^{III} compared with transfectants with vector alone. Furthermore, transfection of *LmAQP1* to an isolated antimony resistant *Leishmania donovani* (FDA9518), obtained from a patient who failed to respond to Sb^{V} therapy in

```

GlpF          -----MSQTST-----LKGQCIAEFLGTGLLIFFGVGCVAALKVAG-- 36
HAQP9        MQPEGAERKGSFKQRLVLKSS-----LAKETLSEFLGTFFILIVLGCQVAQAILSR-- 51
LmAQP1       MHEEEDQHESKRNFMSQNRWPLYRYRWLRREYVAEFGTFFLVTFGTGVVAATTVFHGGT 60

GlpF          ----ASFG-QWEISVIWGLGVAMAIYLTAGVSGAHLNPAVTIILWLFACFDKRKVIPFIV 91
HAQP9        ---GRFGVITINVGFSMAVAMAIYVAGGVSGGHINPAVSLMCLFGRMKWFKLPFYVG 107
LmAQP1       TAMYQSNSSYLATFGWAFGLAISLFLSMAVSGGHLNPAVTLANCVETGTFPWVWKLPGYFL 120

GlpF          SQVAGAFCAAAALVYGLYLNLFDFEQTHHIVRGSVESVDLAGTFSYFNPHINFVQAFAV 151
HAQP9        AQFLGAFVGAATVFGIYYDGLMSFAGGKLLIVG---ENATAHIFATYPPAPYLSLANAFAD 164
LmAQP1       AQFLGGEVGAANTYVLPFKSHFDEAEKRLLLNET--MASKYGGIFATYFN--VANTYAVWS 176

GlpF          EMVITAILMGLILALTDGN-GVVRGPLAPLLIGLLIAVIGASMCPLTGFAMNPARDFGF 210
HAQP9        QVVAIMILIIIVFAIFDSRNLGAFRG-LEFIAIGLLIIVTASSLGLNSGCAMNPARDLSP 223
LmAQP1       EVFNIMALMMGILAITDARM--TFAVDYKEVAIGLLLFVIGIASGINSYGLNPARDLSP 234

GlpF          KVFAWLAGWGNVAFTGGRDIPYFLVPLFGFIVGAVIVGAFAYRKLIGRHLP-CDICVVEEK 269
HAQP9        RLFTALAGWGFVFRAGN--NFWWIPVVGPLVGAIVIGGLIYVLVIEIHHPEPDSVFKEQTE 281
LmAQP1       RILSAML-WGSEPTLHS--YYFWILVVFVVGALFGMFLYVFFIIPPS----- 281

GlpF          ETTTPSEQKASL-- 281
HAQP9        SEDKPEKYELSVIM 295
LmAQP1       -----

```

Figure 3.10 Sequences alignment of GlpF (from *E. coli*), AQP9 (from mammal) and LmAQP1 (from *Leishmania major*) proteins, which are related to Sb^{III} uptake in biological systems. The conserved residues are highlighted

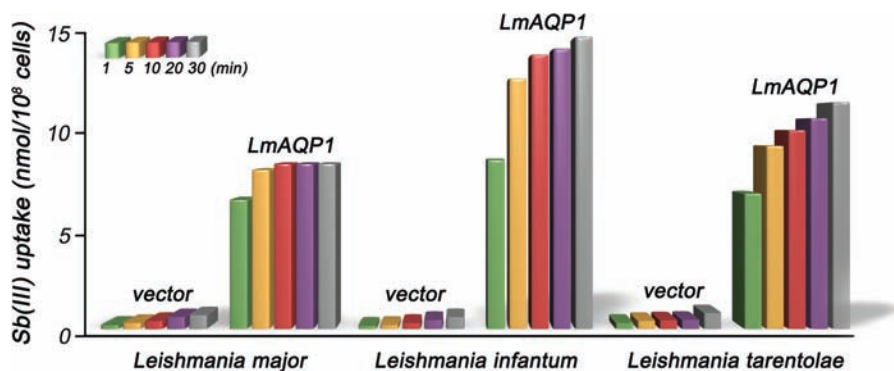


Figure 3.11 *LmAQP1* catalyses Sb^{III} transport in the wild type *Leishmania* promastigotes. Comparison with the vector alone, *LmAQP1* transfected strains *Leishmania major*, *Leishmania infantum* and *Leishmania tarentolae* show significant increase in the uptake of Sb^{III}

India, shows three-fold more sensitive to Pentostam as amastigotes inside macrophages, compared with the strain transfected with vector alone. The resistant strain transfected with *LmAQP1* is also 200-fold more sensitive to Sb^{III} as promastigotes *in vitro* [65].

Since relatively nontoxic Sb^V probably serves as a prodrug and is reduced into more toxic Sb^{III} at or near the site of action to exert antileishmanial activities, the reduction process *in vivo* is essential for antimony therapies. The conversion of Sb^V to Sb^{III} occurs both in the infecting *Leishmania* cells and in host macrophages [66]. As mentioned in Section 3.5.1, cysteine and some thiolate containing peptides (e.g., GSH and TSH) can reduce Sb^V into Sb^{III} in both stages of the parasite, however, specific enzymes involved in reduction of Sb^V may account for the high sensitivity of amastigotes to Sb^V , even though amastigotes has lower intracellular concentration of TSH and GSH than promastigotes [67, 68].

The enzymes responsible for the reduction of Sb^V in macrophages are currently not clear, but a parasite specific enzyme, namely thiol dependent reductase TDR1 has been identified recently [69]. TDR1 is a trimer composed of two-domain monomers in which each domain is similar to Omega class glutathione *S*-transferases (GSTs). The reductase is able to catalyse the enzymic reduction of pentavalent antimonials to trivalent by using GSH as the reductant [69]. The highest initial reduction activities were obtained when the substrates (sodium arsenate or sodium stibogluconate or glucantime) were preincubated with GSH for several minutes prior to the addition of TDR1. This suggests that the TDR1 may work on a spontaneously formed intermediate between metal compounds and GSH rather than on two components individually [69].

Arsenate reductases are ubiquitous in prokaryotes and eukaryotes and are essential for conferring resistance to arsenate [70]. Recently, the arsenate reductase homologue from *Leishmania major*, LmACR2, has been identified [71]. The crystal structure of LmACR2 has been resolved by X-ray crystallography [72]. LmACR2, comprising of 127 amino acids (14.5 kDa), displays sequence and functional similarity to the arsenate reductase ScACR2 from *Saccharomyces cerevisiae* (Figure 3.12a), and shows an ability to reduce both As^V and Sb^V to their trivalent forms respectively. As shown in Figure 3.13, the transfection of *leishmania infantum* with *LmACR2* can augment Pentostam sensitivity in intracellular amastigotes [71]. The crystal structure of LmACR2 exhibits a central five-stranded β sheet

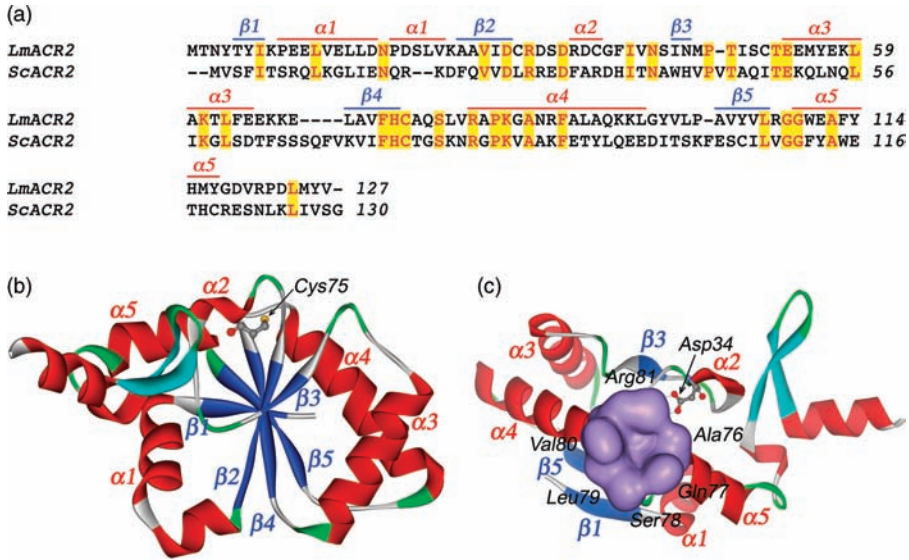


Figure 3.12 (a) Sequences of *Sb*^V reductases, LmACR2 (from *Leishmania major*) and ScACR2 (from *Saccharomyces cerevisiae*). The conserved residues are highlighted. The $\beta 1$ to $\beta 5$ represent the central five β sheets in LmACR2, and the $\alpha 1$ to $\alpha 5$ represent the five α helices that pack against each side of the central β sheet in LmACR2. (b) X-ray crystal structure of LmACR2 with α helices in red and β sheets in blue (PDB: 2J6P). Cys75 is presented in a ball and stick mode. (c) Surface conformation of the active site pocket of LmACR2. The surface modeling is made by Accelrys DS Visualizer software (version 2.0) with a probe radius of 1.40 Å. Asp34 is highlighted in a ball and stick mode

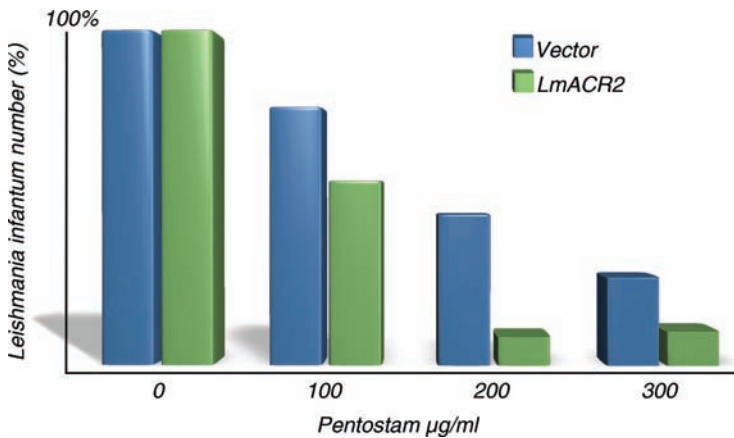


Figure 3.13 Comparison of the transfection of vector alone, the expression of LmACR2 in *Leishmania infantum* augments Pentostam sensitivity

configuration ($\beta 1$, $\beta 2$, $\beta 3$, $\beta 4$ and $\beta 5$) with three ($\alpha 1$, $\alpha 2$ and $\alpha 5$) and two ($\alpha 3$ and $\alpha 4$) α helices packed against each side of the central β sheet (Figure 3.12a and b). Seven residues (Cys75, Ala76, Gln77, Ser78, Leu79, Val80 and Arg81) compose the active site pocket in LmACR2, Figure 3.12c. The catalytic center of LmACR2 is the S atom of Cys75, which is located at the geometric center of the shallow circular depression on the protein surface formed by the amino acids of the active site loop (Figure 3.12c) [72]. The side chain of Arg81, roughly planar with the active site loop, is kept in an extended conformation by a hydrogen bonded salt bridge with the carboxyl group of Asp34 (Figure 3.12c) [72]. Compared to the structure of Cdc25 phosphatases, the main chain conformations of the active site loop are conserved in the two enzymes, indicating that LmACR2 likely share a similar physiological function to that of Cdc25 phosphatase, with a bifunctional capacity to reduce both As^V and Sb^V [72, 73].

Although antimony based drugs have been the frontline drugs for more than half a century, the mode of action of these drugs is still poorly understood. Recent studies suggest that Sb^{III} interferes with trypanothione metabolism by two inherently distinct mechanisms [68]. First, Sb^{III} decreases thiol buffering capacity by inducing rapid efflux of intracellular trypanothione and glutathione. Second, Sb^{III} inhibits trypanothione reductase in intact cells resulting in accumulation of the disulfide forms of trypanothione and glutathione. The combination of these two mechanisms profoundly compromises the thiol redox potential in both amastigote and promastigote stages of the parasite life cycle [68]. The trypanothione/trypanothione reductase system (trypanothione/TR system), which replaces the nearly ubiquitous glutathione/glutathione reductase system (glutathione/GR system), is only found in parasitic protozoa such as leishmania and trypanosomes and can protect parasites from oxidative damage and toxic heavy metals and deliver the reducing equivalents for DNA synthesis.

The inhibition of Sb^{III} to trypanothione reductase (TR) was examined *in vitro* and *in vivo* [68, 74]. When the NADPH (nicotinamide adenine dinucleotide phosphate) preincubated TR was treated with trivalent sodium antimonyl gluconate (Triostam), the residual activity of TR was sharply reduced within 10 min [74]. Determination of the ability of the cell lines for the regeneration of T(SH)₂ from T(S)₂ following oxidation with diamide can indirectly provide evidence of the inhibition of Sb^{III} to TR *in vivo* [68, 75]. The dimeric structures of oxidized TR (native form) and Sb^{III} bound TR (with NADPH) were reported recently [76]. As shown in Figure 3.14a and b, Sb^{III} coordinates two cysteine residues (Cys52 and Cys57), one threonine residue (Thr335) and a His461' from the two-fold symmetry related subunit in the TR dimer [76]. The binding of Sb^{III} not only blocks the formation of cysteine disulfide between Cys52 and Cys57 which is required in TR native state, but also induces the side chain of Tyr198 (localized in NADPH binding domain) undergoes a 120° rotation (Figure 3.14c). In this way, the π - π interactions between the parallel rings of FAD (flavin adenine dinucleotide), NADPH and Tyr198 are interrupted, and subsequently resulting in the malfunction of TR. Because TR is critical for survival and virulence of the parasite and is absent in mammalian cells, the understanding of its inhibition mechanism will promote the design of new affordable drugs against Leishmaniasis.

Not only are the uptake, reduction and action of antimony equally important for living organisms, but also the extrusion of high level antimony from cytosol is essential for survival of the organism. In *E. coli*, resistance to As^{III} and Sb^{III} at a high level is conferred by the *ars* operon of plasmid R773 [77]. The ArsAB pump provides resistance to arsenite and

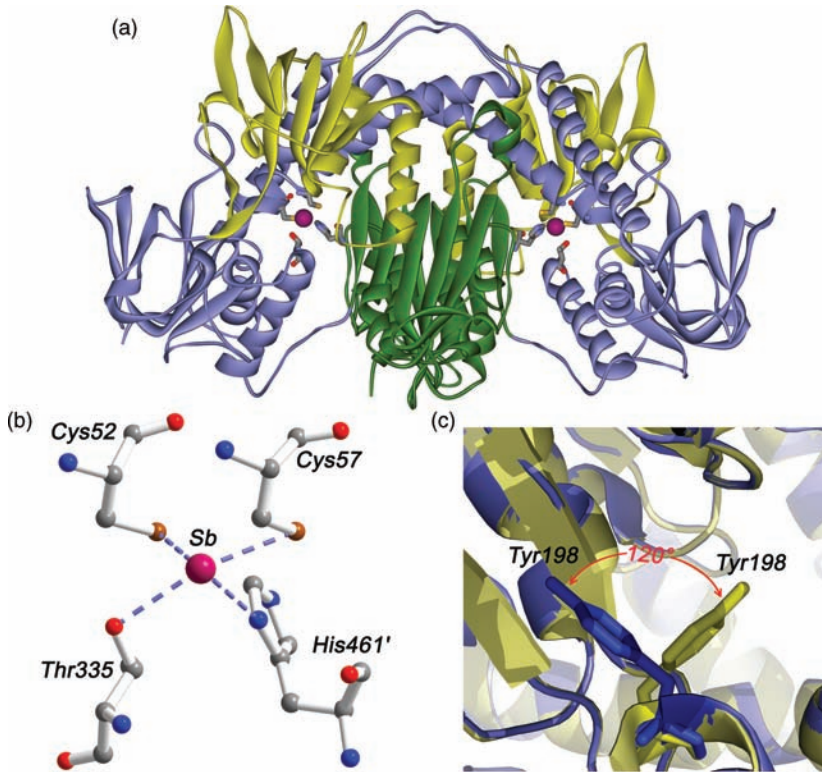


Figure 3.14 (a) X-ray crystal structure of Sb^{III} -bound trypanothione reductase (TR) with FAD binding domain (residues 1–160 and 289–360) in sky blue, the NADPH binding domain (residues 161–288) in yellow and the interface domain (residues 361–488) in green (PDB: 2W0H). (b) Coordination of Sb^{III} in TR. Sb^{III} coordinates Cys52, Cys57, Thr335 from one monomer and His461' from the two-fold symmetry related monomer. Color code: C, gray; O, red; N, blue; S, brown; Sb, purple. (c) The structure alignment of the oxidized TR (PDB: 2JK6, in yellow) and TR–NADPH– Sb^{III} (PDB: 2W0H, in blue). The side chain of Tyr198 undergoes a 120° rotation with respect to the oxidized trypanothione reductase upon the binding of Sb^{III} . The two Tyr198 residues are represented in a ball and stick mode. The picture was generated using PyMOL

antimonite. This pump consists of a soluble ATPase (ArsA) and a membrane channel (ArsB) encoded by genes *arsA* and *arsB* respectively [78]. Crystal structure of Sb^{III} bound ArsA of *E. coli* represents the first Sb^{III} (and As^{III}) bound protein structure. As shown in Figure 3.15, the protein consists of two structurally homologous domains, that is, A1 and A2, and each domain is approximately L-shaped, with a core of eight β strands accompanying by α helices on both sides of the central sheets [79]. Superposition of the structurally equivalent regions of A1 and A2 domains results in a diamond shaped molecule with a central cavity [79]. Two nucleotide binding sites, A1NBS and A2NBS, are located at the interface between the A1 and A2 domains and close to each other with $\sim 8 \text{ \AA}$ apart at their closest approach. Mg–ADP molecules are observed in both nucleotide binding sites with the

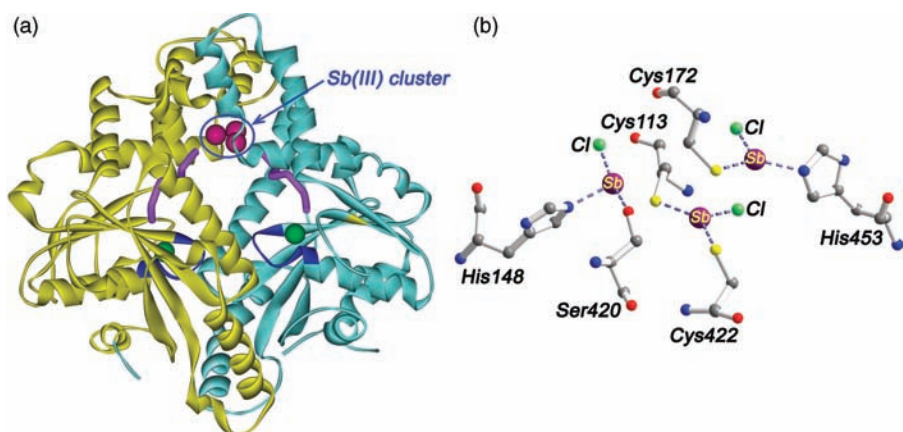


Figure 3.15 (a) X-ray crystal structure of *E. coli* ArsA ATPase (PDB: 1f48). The two domains are highlighted in different colors. The ADP binding residues (GKGGVGTK) of the P-loop in A1 and A2 domains are presented in dark blue. The signal transduction paths (DTAPTGH) that connects the Sb^{III} -binding site (via coordinating to Sb^{III} by terminal His residue) and nucleotide binding sites (via coordinating to Mg^{II} by Asp residue at another terminal) are represented as a tube model (in purple). (b) Coordination of Sb^{III} at the trinuclear cluster. Residues His148, Cys113 and Cys172 are from A1 domain whereas Ser420, Cys422 and His453 are from A2 domain. Color code: C, gray; O, red; N, blue; S, yellow; Cl, light green; Sb, purple; Mg, green

phosphate groups of ADP bound to the conserved GKGGVGTK sequence of the P loop in both A1 and A2 domains. The Sb^{III} binding site is located at the upper half of the protein and surprisingly formed a trinuclear cluster (Figure 3.15). Each Sb^{III} coordinates three donor atoms, with two of them from the protein and one from a nonprotein ligand chloride (Cl^-), that is, one Sb^{III} coordinates His148 (A1), Ser420 (A2) and a chloride; the second Sb^{III} coordinates two cysteines, Cys113 (A1), Cys422 (A2) and a chloride, and the third Sb^{III} coordinates Cys172 (A1), His453 (A2) and a chloride (Figure 3.15b). Two stretches of seven residues with the identical sequence DTAPTGH form two signal transduction pathways that connect the two nucleotide binding sites to the Sb^{III} binding site respectively, which may account for the transition of metal occupancy information to the ATP hydrolysis site (Figure 3.15a) [79].

3.6.2 Interaction of Bismuth with Proteins and Enzymes

Although it is generally believed that the bismuth compounds are almost nontoxic, in particular compared with the analogues of arsenic and antimony in the same group, the cases of bismuth poisoning still occur during some medical therapies or after extensive industrial exposure. The potential toxicity of bismuth is normally diagnosed by measuring bismuth levels in human blood [80–82]. The potential Bi^{III} target in human blood serum is hypothesized originally to be albumin (HSA), the most abundant protein in serum (~0.63 mM). *In vitro* experiments show that 70% of Bi^{III} binds to apo human serum transferrin (apo-hTF) with the rest (30%) to HSA in spite of a 13-fold higher concentration of HSA than transferrin. However, almost all Bi^{III} associates with HSA when serum

transferrin was saturated by Fe^{III} , suggesting that HSA is the second major target of Bi^{III} in blood plasma [92]. The binding constant ($\log K_a$) of Bi^{III} to HSA was measured to be 9–12 by fluorescent spectroscopy [92].

The transferrins comprise a family of large (molecular mass *about* 80 kDa) nonheme iron binding glycoproteins with biological function of Fe^{III} transporting (Figure 3.16) [83–86]. Four major types of transferrins have been characterized. Serum transferrin occurs in blood and other mammalian fluids including bile, amniotic fluid, cerebrospinal fluid, lymph, colostrom, and milk. Ovotransferrin is found in avian and reptilian oviduct secretions and in avian egg white. Lactoferrin is found in milk, tear, saliva and other secretions, and binds Fe^{III} about 100 times stronger than that of serum transferrin [87]. It has been speculated that lactoferrin has a bacteriostatic function in depriving microorganisms of essential iron required for their growth [88]. Melanotransferrin (or melanoma tumor antigen p97) has been identified as an integral membrane protein in human malignant melanoma cells and in some fetal tissues [89].

Transferrins are single chain glycoproteins containing *about* 700 amino acids. The sequence identity between different transferrins is extremely high, for example, 78%

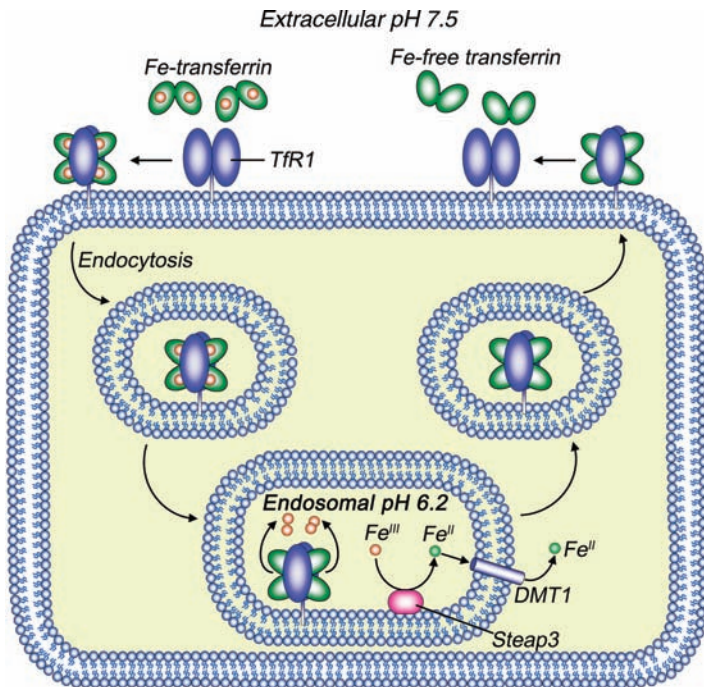


Figure 3.16 The transferrin cycle. Fe_2 -hTF has a high affinity for transferrin receptor (TfR1) at extracellular pH ($\text{pH}=7.5$) and forms the Fe_2 -transferrin-TfR complex sequentially. Fe_2 -transferrin-TfR complexes are then internalized into endosome and, at endosomal pH ($\text{pH}=6.2$), Fe^{III} is released from transferrin, further reduced by Steap family reductases before being transported across the endosomal membrane by DMT1. Once in the cytoplasm, the iron can be incorporated into a haem for erythropoiesis. The iron free hTF-TfR complex go back to the cell surface and, at extracellular pH, apotransferrin is released back into serum

identity between rabbit and human serum transferrin, 60% between serum transferrin and lactoferrin, and *about* 40% identity between melanotransferrin and other transferrins [89]. The high levels of conservation in their primary structures are also reflected in their three-dimensional structures. The protein is folded into two structurally similar but functionally different lobes, the N- and C-lobe respectively (Figure 3.17a). The two lobes are connected by a short polypeptide chain, and a deep hydrophilic cleft bearing an iron binding site is localized in each lobe. Each lobe can be further separated into two subdomains, namely N1 and N2 in the N-lobe; C1 and C2 in the C-lobe. N1- and C1-subdomains consist of two discontinuous sections, whereas N2- and C2-subdomains are composed of a single region of continuous polypeptide [90]. The subdomains in each lobe rotate around a ‘hinge’ to undergo the conformational change between ‘open’ and ‘closure’, corresponding to the iron release and uptake, respectively (Figure 3.17a). Although both ‘hinges’ between subdomains are composed by two β strands in each lobe, one of the strands in C-lobe is relatively shorter, which probably accounts for the different Fe^{III} binding and release rates in two lobes [90]. At the metal binding site, Fe^{III} coordinates with distorted octahedral geometry to two oxygens from Tyr, one nitrogen from His, one oxygen from Asp, and two oxygens from a bidentate carbonate (as a synergistic anion) (Figure 3.17b).

Since transferrin is only 30% saturated with Fe^{III} and has the capacity to bind other metal ions such as Bi^{III} , Ga^{III} , In^{III} , Al^{III} , Tl^{III} , Ru^{III} , La^{III} , Ce^{III} , Cu^{II} , Ni^{II} and Zn^{II} , the protein is therefore regarded as a ‘carrier’ for metal ions and metallodrugs [91]. Serum transferrin is the first major target of Bi^{III} in blood plasma and plays the essential roles in Bi^{III} transport. *In vitro* experiments show that the majority of Bi^{III} binds to human serum transferrin even in

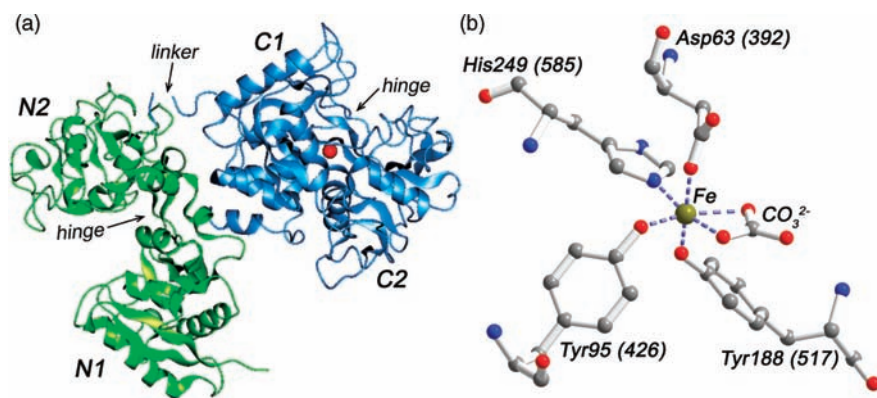


Figure 3.17 (a) X-ray crystal structure of human serum transferrin with a Fe^{III} in the C-lobe (H.J. Zoccla, Georgia Institute of Technology). The rotation of N1 (residues 1–92 and 247–331) and N2 (residues 93–246) subdomains around the ‘hinge’ confers N-lobe an ‘open’ conformation, and there is in the absence of Fe^{III} . Subdomains C1 (residues 339–425 and 573–679) and C2 (residues 426–572) form a ‘closure’ conformation in the C-lobe where with a Fe^{III} -binding to four amino acids in the cleft. (b) Coordination of Fe^{III} in the N-lobe of human serum transferrin. Four amino acids (Asp63, Tyr95, Tyr188 and His249) and a carbonate (CO_3^{2-}) coordinate to Fe^{III} ion. The corresponding amino acids involved in Fe^{III} coordination in C-lobe are shown in parentheses. Color code: C, gray; O, red; N, blue; Fe, red or olive

the presence of a large excess of albumin at pH 7.4 with 10 mM sodium bicarbonate [92]. Bi^{III} binds strongly to both the C- and N-lobe of human serum transferrin, preferentially to the C-lobe with carbonate (CO_3^{2-}) as a synergistic anion, which was approved by 2D NMR using recombinant ϵ - ^{13}C Met-hTF and ^{13}C -NMR [93–95]. The detailed kinetics of Bi^{III} translocation between $\text{Bi}(\text{NTA})$ ($\text{NTA} = 2$ -(bis(carboxymethyl)amino)acetic acid) and human serum transferrin has also been examined [96]. The uptake of Bi^{III} by transferrin is a multistep kinetic process, including the rapid metal exchange (ms) between $\text{Bi}(\text{NTA})$ and the C-lobe of apotransferrin (the first step), a proton loss ($\text{p}K_{1a}$ of 8.6) to yield a kinetic intermediate, followed by an intermediate conformational change and the uptake of Bi^{III} by the N-lobe (the final step) [96].

Cell uptake experiments showed that Bi^{III} transferrin can block both membrane binding and cellular uptake of Fe^{III} transferrin, indicative of a similar uptake mechanism to iron, that is, transferrin receptor mediated endocytosis. The binding affinity between Bi^{III} transferrin and transferrin receptor (TfR) was determined to be $4 \mu\text{M}$, around three orders of magnitude lower than that of Fe^{III} transferrin and TfR (23 nM).

Bi^{III} was also found to bind human lactoferrin strongly and reversibly at the specific iron sites together with either carbonate or oxalate as the synergistic anion [97]. Notably, the Bi_2 -hLF complex can compete with the $^{59}\text{Fe}_2$ -hLF complex for both membrane and intracellular binding, almost as effectively as the Fe_2 -hLF, Ga_2 -hLF and apo-hLF (Figure 3.18), suggesting that lactoferrin recognition by its receptor is independent of whether the lactoferrin is metal loaded or apoform. This is markedly different from human

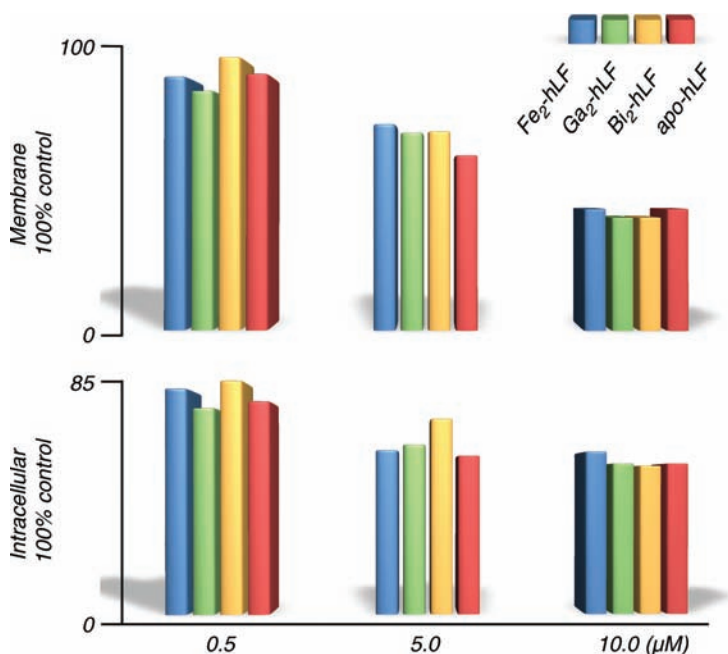


Figure 3.18 Effect of apo- and metal loaded human lactoferrin (Fe_2 -hLF, Ga_2 -hLF and Bi_2 -hLF) on the uptake of ^{59}Fe -human lactoferrin complex by rat intestinal IEC-6 cells. Top: membrane bound ^{59}Fe ; bottom: intracellular ^{59}Fe

serum transferrin, revealing that lactoferrin receptor is more promiscuous in function than human serum transferrin receptor.

Since Bi^{III} readily binds to thiolate containing ligands, cysteine rich proteins and enzymes in biological systems provide the potential binding targets for Bi^{III}. Metallothionein (MT) is a low molecular mass protein with ~30% cysteine residues out of its ~60 amino acid residues (Figure 3.19) [98, 99]. Four isoforms of MT have been identified, namely MT-I, MT-II, MT-III and MT-IV. MT-I and MT-II prevail over all tissues, primarily accounting for the protection against metal toxicity. MT-III is mainly expressed in the brain and is thought to play a role in zinc homeostasis in neurons. MT-IV is found to be specifically expressed in stratified squamous epithelia where it may play an essential but poorly defined role in regulating zinc or copper metabolism [100, 101]. All the cysteine residues are conserved in MT proteins (Figure 3.19). The cysteine rich character of MT provides a high capacity for this protein to coordinate with metal ions, such as Zn^{II}, Cu^I and Cd^{II}. Bi^{III} was found to bind strongly to MT-II via coordinating to cysteine residues, with a stoichiometry of Bi: MT = 7: 1 (Bi₇-MT). Remarkably, it was found that Bi^{III} can readily replace both Zn^{II} and Cd^{II} from MT-II by a biphasic process [102]. ¹H NMR studies demonstrate that Zn^{II} is replaced by Bi^{III} from MT faster than Cd^{II}, and that both Zn^{II} and Cd^{II} are replaced much faster in the β-domain than that in the α-domain. Upon exposure of 50 μM bismuth citrate to macrophage cells at 12 and 24 h, metallothionein genes can be increased by 18- and 10-fold respectively, representing the largest increase in gene expression. The significant increase in MT gene expression probably reflects a part of common defense and/or repair mechanisms following different stress stimuli [103].

NTPase/helicase protein of Severe Acute Respiratory Syndrome coronavirus (SCV), an enzyme capable of unwinding DNA and RNA duplexes, is a potential drug target for SARS therapy [104]. SCV NTPase/helicase contains a cysteine-rich metal binding domain (MBD), consisting of 13 cysteines out of its 102 amino acids, Figure 3.19b. MBD of helicase has been approved to be a Bi^{III} binding site, and binding of Bi^{III} in MBD induces a conformational change of the protein, which probably accounts for the inhibition of bismuth to helicase unwinding activity *in vitro* and *in vivo* (Figure 3.20) [105]. By use

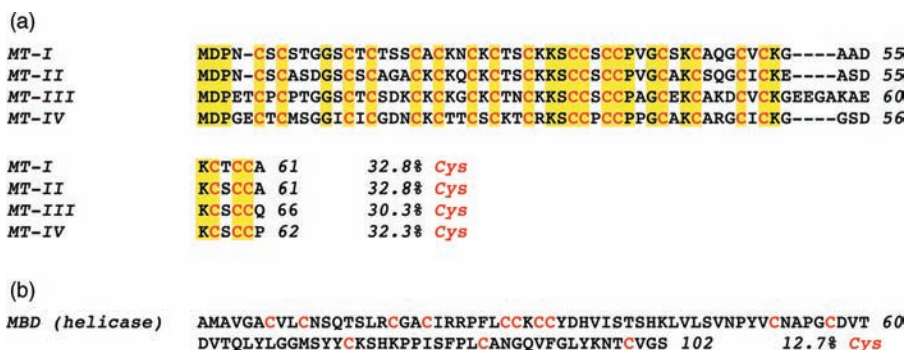


Figure 3.19 (a) Sequence alignment of mouse metallothionein isoforms (MT-I, MT-II, MT-III and MT-IV) with conserved residues highlighted. (b) Protein sequence of metal binding domain (MBD) of SARS coronavirus NTPase/helicase

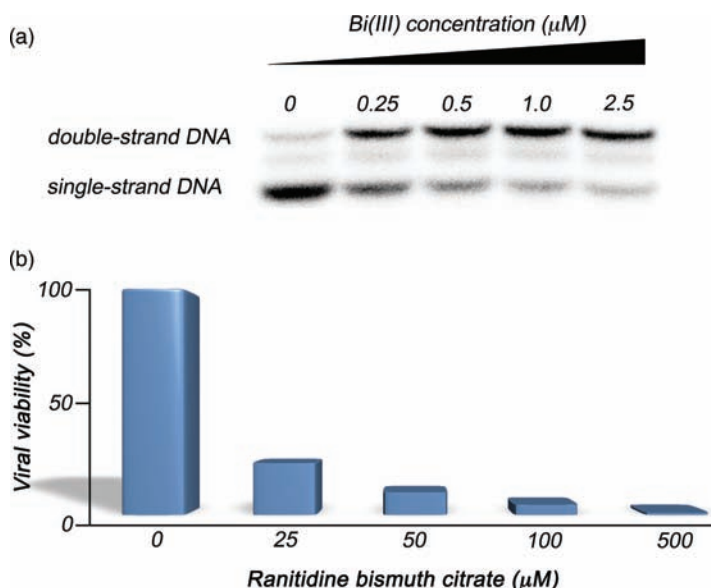


Figure 3.20 (a) Bi^{III} inhibits SARS NTPase/helicase unwinding activity to duplex DNA. Upon increasing Bi^{III} concentrations gradually from 0–2.5 μM , intensity of the lower band, released single strand DNA, decreased gradually, indicating that the unwinding activity of helicase is inhibited by Bi^{III} . (b) The effect of ranitidine bismuth citrate (RBC) on the infectivity of SARS-CoV. The viral viability is reduced dramatically upon addition of RBC

of ranitidine bismuth citrate (RBC), a clinical antiulcer drug, a IC_{50} of 0.6 μM was obtained for inhibition of helicase unwinding activity *in vitro*, and the *in vivo* experiment shows that the bismuth metallodrug significantly inhibits SCV reproduction, with the viral titer reduced by $\sim 80\%$ at a RBC concentration of 25 μM . Furthermore, the inhibition activities were examined on a series of bismuth compounds which showed that the Bi^{III} coordination environment in different compounds may affect the activities, that is, the stronger the Bi^{III} binds to the ligand, the lower inhibition activity the bismuth compound exhibits to helicase [106].

The *cad* operon encoded on plasmid PI258 of *Staphylococcus aureus* is a resistance system which responds to Cd^{II} , Pb^{II} and Zn^{II} [107]. The *cad* operon is composed of two genes: one encodes CadC, the metal-responsive transcriptional repressor or metal sensor, and another one encodes CadA, a Cd^{II} and Pb^{II} specific ATPase efflux pump. In a recent study, Bi^{III} was found to coordinate to the Cys7, Cys11, Cys58 and Cys60 residues of CadC, eventually inducing significant reduction of DNA binding affinity. Such an action enables RNA polymerase to access the promoter, leading to derepression of transcription and the expression of the gene encoding the CadA efflux pump [108].

Histidine rich proteins are prevailing over many microorganisms and play important roles in the storage and transport of metal ions. Figure 3.21 shows sequences of several histidine rich proteins. For example, Hpn has 28 histidine residues out of its 60 amino acids (46.7%) and presents as a multimer in solution playing a crucial role on intracellular nickel storage and homeostasis [109]. Mutagenesis experiments have shown that *H. pylori* with *hpn* gene

(a)	<i>Hpn</i> (<i>H. pylori</i>)	1	MAHHEEQHGGHHHHHHHTHHHHYHGGEHHHHHSSHHEE	
			GCCSTSDSHHQEEGCCGHHE	60
	<i>HpnI</i> (<i>H. pylori</i>)	1	MAHHEQQQQQANSQHHHHHAHHHHYYGGEHHHHNAQQ	
			HAEQQAEQQAQQQQQQAHHQQQQQKAQQQNQQY	72
(b)	<i>UreE</i> (<i>K. aerogenes</i>)	124	TVTFGQLPEEPEAGAYASESHGHHHAHDDHHAHSH	158
	<i>HspA</i> (<i>H. pylori</i>)	84	DVLGIVGSGSCCHTGNHDKHKAKEHEACCHDKKH	118
	<i>HypB</i> (<i>B. Japonicum</i>)	16	DAHGHHDHGDGHEHGHHHHHRGDGHDHGHHHHH	50
	<i>SlyD</i> (<i>E. coli</i>)	146	ELAHGHVHGARDHHHDHDDGCCGGHGDHGHGHEHG	180

Figure 3.21 Selected histidine rich protein sequences. (a) Full length protein sequences of *Hpn* (*H. pylori*) and *HpnI* (*H. pylori*), and (b) partial protein sequences of *UreE* (*K. aerogenes*), *HspA* (*H. pylori*), *HypB* (*B. Japonicum*) and *SlyD* (*E. coli*)

knockout are four times as susceptible to bismuth antiulcer drugs than that of the wild type [110], indicating a role of *Hpn* in *H. pylori* responses to the bismuth therapy. Apo-*hpn* was found to bind $5.1 \pm 0.2 \text{ Ni}^{\text{II}}$ reversibly with a binding constant (K_d) of $\sim 6 \mu\text{M}$ and also bind $3.81 \pm 0.23 \text{ Bi}^{\text{III}}$ per monomer with a K_d of $\sim 11 \mu\text{M}$ [111]. At Bi^{III} concentration over $30 \mu\text{M}$, *E. coli* BL21 cells with the *hpn* gene on a pET plasmid grow better upon induction by IPTG than those without, whereas *E. coli* cells without the *hpn* gene grew much slower than those with *hpn*, suggesting that *Hpn* plays a role in protecting *H. pylori* by sequestering excess intracellular bismuth ions (Figure 3.22) [111].

Using a metalloproteomic approach (Chapter 15), seven proteins including a heat shock protein A from *H. pylori* (*HspA*, also referred to as *HpGroES*) have been identified to bind Bi^{III} [112]. *H. pylori* *HspA* has a histidine and cysteine rich domain in the C-terminus. The protein binds two Ni^{II} as well as two Bi^{III} per monomer with a dissociation constants (K_d) of 1.1 and $5.9 \times 10^{-19} \mu\text{M}$ respectively [113, 114]. A

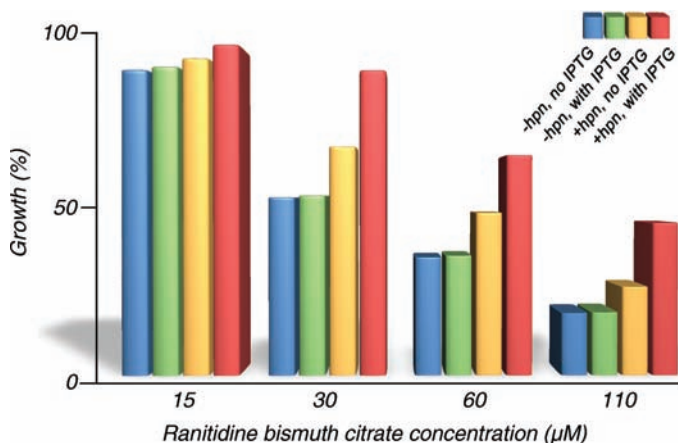


Figure 3.22 Altered *E. coli* sensitivity to Bi^{III} (as ranitidine bismuth citrate) with and without *hpn* gene at 310 K

characteristic UV–visible absorption of Bi–S bond appeared at 364 nm upon addition of Bi^{III} , indicating that the cysteine residues are involved in Bi^{III} coordination. Mutation experiments show that Bi^{III} strongly binds to residues His45, Cys51 and Cys53 at an apical domain [114]. Binding of Bi^{III} induces HspA dissociation from its native heptamer to a dimer, suggesting that bismuth may interfere with the biological functions of the protein by altering its quaternary structures [113, 114].

Urease is an enzyme that can convert urea into ammonia for neutralizing the acidic environment, and is therefore crucial for the survival of bacteria (*H. pylori*) in the acidic environment of stomach [115]. Several reports have revealed that bismuth compounds can inhibit urease activity [116–118]. The metal was found to inhibit urease activity via the binding to Cys319, a cysteine at the entrance of the active site of the enzyme. Upon Bi^{III} binding, the entrance of the active site is sealed and consequently substrates cannot reach the active site any more, therefore the urease activity is inhibited. This was confirmed by comparing the inhibition activities of the wild type *K. aerogenes* urease with its C319A mutant. Bi^{III} has almost no activity toward the mutant urease (C319A) while significantly reduces the activity of the wild type (Figure 3.23).

Alcohol dehydrogenase (ADH) is a type of zinc metalloenzyme that catalyses the oxidation of alcohols to aldehydes or ketones. The inhibition of *H. pylori* ADH by bismuth suggests that ADH is a potential target for the treatment of *H. pylori* infection. Baker's yeast alcohol dehydrogenase (YADH) was used as a model of *H. pylori* ADH due to the high sequence identity (47%) of conserved active sites [119]. Bi^{III} binds to cysteine residues of YADH, as evidenced by the appearance of a characteristic UV–visible absorbance band of Bi–S at ~ 360 nm upon addition of Bi^{III} . The interaction of Bi^{III} with the enzyme exhibits a biphasic process and only one of the two bound Zn^{II} ions can be substituted by Bi^{III} (i.e., about one Zn^{II} per monomer). Since bismuth inhibits the enzyme activity in a noncompetitive mode, the Zn^{II} at the structural site may be substituted by Bi^{III} . Surprisingly, the binding

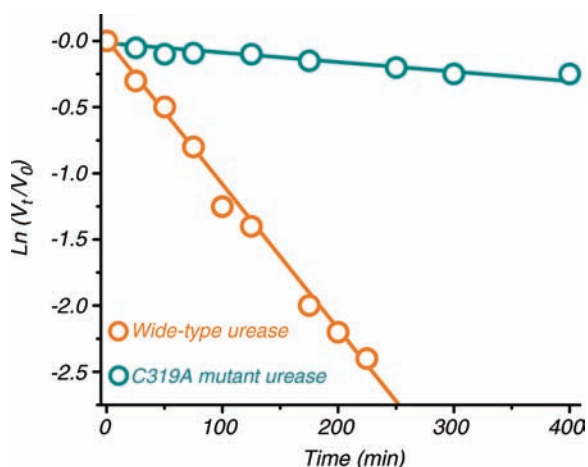


Figure 3.23 Kinetics of urease inactivation upon addition of $\text{Bi}(\text{EDTA})$. The wild type urease is represented by brown and C319A mutant urease is represented by cyan. Reprinted with permission from [118]. Copyright Springer Science + Business Media

of Bi^{III} to the enzyme interferes with the protein–protein interaction and gradually induces YADH dissociation, from its native form (a tetramer) to a dimer. Since ADH from *H. pylori* has high similarity to YADH in terms of sequence, the inhibition of bismuth on *H. pylori* ADH is probably similar.

The presence of a phospholipid monolayer adsorbed to the luminal surface of the mucus gel layer may account for the nonwettable lining of the stomach and play a protective role [120–122]. Phospholipase, a protease enzyme that is released by *H. pylori* or many other pathogenic microorganisms, may have the capacity of degrading the glycoprotein constituents of mucin, thus weakening the protective properties of the mucus gel layer of the stomach [123, 124]. Colloidal bismuth subcitrate (CBS) can induce a dose dependent inhibition of phospholipase A2 (PLA_2) and C (PLC) activity of both *H. pylori* lysates and filtrates [125]. Notably, the inhibitory effect of CBS on PLA_2 is antagonized in a dose dependent fashion by addition of CaCl_2 to the incubation mixture, that is, addition of CaCl_2 to the mixture containing either purified *N. naja* venom PLA_2 or the *H. pylori* lysate in the presence of 0.8 mM CBS can induce a recovery in PLA_2 activity, and the activity can be almost completely restored (>90% of control) when the concentration of CaCl_2 reaches 4 mM, suggesting that both Ca^{II} and Bi^{III} may compete for the same binding site of the enzyme (Figure 3.24).

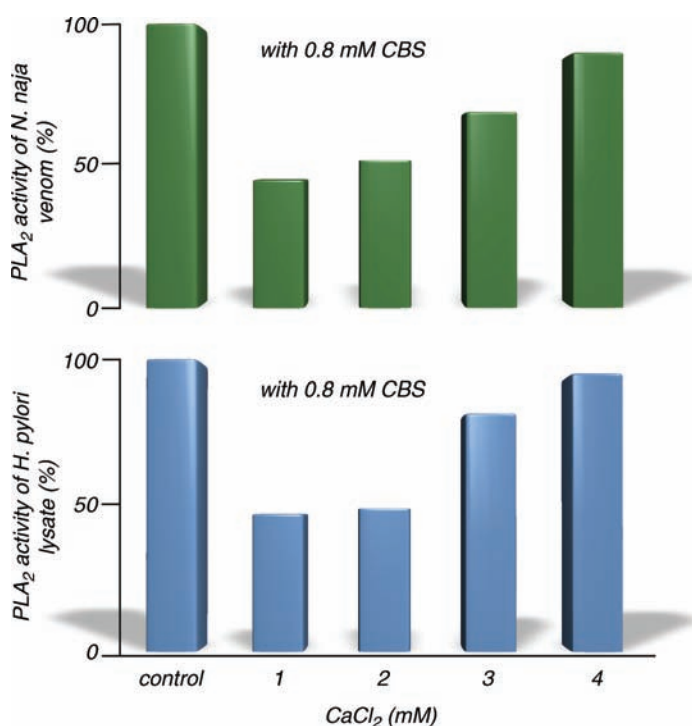


Figure 3.24 CaCl_2 antagonizes the inhibitory effect of CBS (0.8 mM) on the phospholipase A2 (PLA_2) activity of *N. naja* venom (top) and *H. pylori* (bottom)

3.7 Conclusion and Perspectives

Significant progress has been made on the biological chemistry of antimony and bismuth in the past decade. Proteins and enzymes have commonly been believed to be their targets. Possible target sites for Bi^{III} are likely to be ferric iron site(s) (e.g., oxygen and nitrogen donors in transferrin) and zinc and nickel sites (e.g., thiolate donors in metallothionein and nitrogen/thiolate donors in histidine rich proteins, Hpn and HspA). Inhibition of (metallo)enzymes by antimony (and bismuth) is probably ascribed to their binding to the key cysteine (and histidine) residues within the enzyme (e.g., trypanothione reductase). The facile exchange of Sb^{III} (and Bi^{III}) thiolate bonds may be important for their transport and could represent a common feature for metal trafficking among different molecules in biological systems (e.g., cells). Metallomics and metalloproteomics including structural biology (Chapter 4 and 15) should help to establish the molecular mechanism underlying their biological activities of antimony and bismuth in a more comprehensive way, and ultimately will help us to design better therapeutic agents as well as to control potential toxicity.

Acknowledgements

This work was supported by the Research Grants Council of Hong Kong (HKU7043/06P, HKU2/06C HKU7042/07P, HKU1/07C, HKU7038/08P, HKU7049/09P and N_HKU752/09), the Area of Excellence Scheme of the University Grants Committee of HKSAR, Croucher Foundation and the University of Hong Kong.

References

1. Sadler, P.J., Muncie, C., and Shipman, M.A. (2007) *Biological Inorganic Chemistry Structure & Reactivity* (eds I. Bertini, H.B. Gray, E.I. Stiefel, and J.S. Valentine), University Science Books, California, pp. 95–135.
2. Yan, S., Jin, L., and Sun, H. (2005) *Metallotherapeutic Drugs and Metal-Based Diagnostic Agents* (eds M. Gielen and E.R.T. Tiekink), John Wiley & Sons, Ltd., Chichester, pp. 441–461.
3. Palenik, R.C., Abboud, K.A., and Palenik, G.J. (2005) *Inorganica Chimica Acta*, **358**, 1034–1040.
4. Tiekink, E.R.T. (2002) *Critical Reviews in Oncology/Hematology*, **42**, 217–224.
5. Lugo de Yarbuh, A., Añez, N., Petit de Peña, Y. *et al.* (1994) *Annals of Tropical Medicine and Parasitology*, **88**, 37–41.
6. Duffin, J. and Campling, B.G. (2002) *Journal of the History of Medicine and Allied Sciences*, **57**, 61–78.
7. Yeh, C.T., Hwang, D.R., Lai, H.Y., and Hsu, J.T.A. (2003) *Biochemical and Biophysical Research Communications*, **310**, 537–541.
8. Rozenbaum, W., Dormont, D., Spire, B. *et al.* (1985) *Lancet*, **325**, 450–451.
9. Pintado, V. and Lopez-Velez, R. (2001) *Clinical Microbiology and Infection*, **7**, 291–300.
10. Yang, Q., Stephen, A.G., Adelsberger, J.W. *et al.* (2005) *Journal of Virology*, **79**, 6122–6133.
11. Briand, G.G. and Burford, N. (1999) *Chemical Reviews*, **99**, 2601–2657.
12. Yang, N. and Sun, H. (2007) *Coordination Chemistry Reviews*, **251**, 2354–2366.
13. Ge, R. and Sun, H. (2007) *Accounts of Chemical Research*, **40**, 267–274.
14. Andrews, P.C., Deacon, G.B., Forsyth, C.M. *et al.* (2006) *Angewandte Chemie International Edition*, **45**, 5638–5642.

15. Thompson, K.H. and Orvig, C. (2003) *Science*, **300**, 936–939.
16. Marshall, B. (2006) *ChemMedChem*, **1**, 783–802.
17. Suerbaum, S. and Michetti, P. (2002) *The New England Journal of Medicine*, **347**, 1175–1186.
18. Gisbert, J.P., Gonzalez, L., and Calvet, X. (2005) *Helicobacter*, **10**, 157–171.
19. Asato, E., Katsura, K., Mikuriya, M. *et al.* (1995) *Inorganic Chemistry*, **34**, 2447–2454.
20. Li, W., Jin, L., Zhu, N. *et al.* (2003) *Journal of the American Chemical Society*, **125**, 12408–12409.
21. Beales, I.L.P. (2001) *BMC Gastroenterology*, **1**, 7–15.
22. Nie, Y.Q., Li, Y.Y., Wu, H.S. *et al.* (1999) *Helicobacter*, **4**, 128–134.
23. McDevitt, M.R., Nikula, T.N., Finn, R.D. *et al.* (1996) *Tumor Targeting*, **2**, 182.
24. McDevitt, M.R., Finn, R.D., Ma, D. *et al.* (1999) *Journal of Nuclear Medicine*, **40**, 1722–1727.
25. Mulford, D.A. and Jurcic, J.G. (2004) *Expert Opinion on Biological Therapy*, **4**, 1–11.
26. Qu, C.F., Song, Y.J., Rizvil, S.M.A. *et al.* (2005) *Cancer Biology & Therapy*, **4**, 848–853.
27. Kondo, Y., Satoh, M., Imura, N., and Akimoto, M. (1991) *Cancer Chemotherapy and Pharmacology*, **29**, 19–23.
28. Kondo, Y., Himeno, S., Satoh, M. *et al.* (2004) *Cancer Chemotherapy and Pharmacology*, **53**, 33–38.
29. Kondo, Y., Satoh, M., Imura, N., and Akimoto, M. (1992) *Anticancer Research*, **12**, 2303–2307.
30. Hansen, H.R. and Pergantis, S.A. (2006) *Analytical and Bioanalytical Chemistry*, **385**, 821–833.
31. Klüfers, P. and Mayer, P. (2007) *Zeitschrift für Anorganische und Allgemeine Chemie*, **633**, 903–907.
32. Wang, X., Zhang, X., Lin, J. *et al.* (2003) *Journal of the Chemical Society Dalton Transactions*, 2379–2380.
33. Zemnukhova, L.A., Davidovich, R.L., Udovenko, A.A., and Kovaleva, E.V. (2005) *Russian Journal of Coordination Chemistry*, **31**, 115–120.
34. Sun, H., Yan, S., and Cheng, W.S. (2000) *European Journal of Biochemistry*, **267**, 5450–5457.
35. Yan, S., Ding, K., Zhang, L., and Sun, H. (2000) *Angewandte Chemie International Edition*, **39**, 4260–4262.
36. Yan, S., Li, F., Ding, K., and Sun, H. (2003) *Journal of Biological Inorganic Chemistry: JBIC: a Publication of the Society of Biological Inorganic Chemistry*, **8**, 689–697.
37. Demicheli, C., Frézard, F., Mangrum, J.B., and Farrell, N.P. (2008) *Chemical Communications*, 4828–4830.
38. Zhang, X.W., Yan, X.J., Zhou, Z.R. *et al.* (2010) *Science*, **328**, 240–243.
39. Frézard, F., Demicheli, C., Ferreira, C.S., and Costa, M.A.P. (2001) *Antimicrobial Agents and Chemotherapy*, **45**, 913–916.
40. Yan, S., Wong, I.L.K., Chow, L.M.C., and Sun, H. (2003) *Chemical Communications*, 266–267.
41. Ferreira, C.S., Martins, P.S., Demicheli, C. *et al.* (2003) *Biometals: An International Journal on the Role of Metal Ions in Biology, Biochemistry, and Medicine*, **16**, 441–446.
42. Oliveira, F.B., Schettini, D.A., Ferreira, C.S. *et al.* (2006) *Journal of the Brazilian Chemical Society*, **17**, 1642–1650.
43. Fairlamb, A.H. and Cerami, A. (1992) *Annual Review of Microbiology*, **46**, 695–729.
44. Marchesini, N. and Docampo, R. (2002) *Molecular and Biochemical Parasitology*, **119**, 225–236.
45. Shaked–Mishan, P., Ulrich, N., Ephros, M., and Zilberstein, D. (2001) *The Journal of Biological Chemistry*, **276**, 3971–3976.
46. Wang, Y. and Xu, L. (2008) *Journal of Inorganic Biochemistry*, **102**, 988–991.
47. Burford, N., Eelman, M.D., and Groom, K. (2005) *Journal of Inorganic Biochemistry*, **99**, 1992–1997.
48. Burford, N., Eelman, M.D., Mahony, D.E., and Morash, M. (2003) *Chemical Communications*, 146–147.
49. Sadler, P.J., Sun, H., and Li, H. (1996) *Chemistry - A European Journal*, **2**, 701–708.
50. Gyurasics, Á., Koszorus, L., Varga, F., and Gregus, Z. (1992) *Biochemical Pharmacology*, **44**, 1275–1281.

51. Rowinska-Zyrek, M., Valensin, D., Szyrwiol, L. *et al.* (2009) *Journal of the Chemical Society Dalton Transactions*, 9131–9140.
52. Chowers, M.Y., Keller, N., Meir, S.B., and Chowers, Y. (2002) *FEMS Microbiology Letters*, **217**, 231–236.
53. Pannequin, J., Kovac, S., Tantiongco, J.P. *et al.* (2004) *The Journal of Biological Chemistry*, **279**, 2453–2460.
54. Baldwin, G.S., Curtain, C.C., and Sawyer, W.H. (2001) *Biochemistry*, **40**, 10741–10746.
55. Pannequin, J., Barnham, K.J., Hollande, F. *et al.* (2002) *The Journal of Biological Chemistry*, **277**, 48602–48609.
56. Guerin, P.J., Olliaro, P., Nosten, F. *et al.* (2002) *Lancet Infectious Diseases*, **2**, 564–573.
57. Sundar, S., More, D.K., Singh, M.K. *et al.* (2000) *Clinical Infectious Diseases*, **31**, 1104–1107.
58. Brochu, C., Wang, J., Rory, G. *et al.* (2003) *Antimicrobial Agents and Chemotherapy*, **47**, 3073–3079.
59. Ashutosh, S.S. and Neena, G. (2007) *Journal of Medical Microbiology*, **56**, 143–153.
60. Sanders, O.I., Rensing, C., Kuroda, M. *et al.* (1997) *Journal of Bacteriology*, **179**, 3365–3367.
61. Wysocki, R., Chery, C.C., Wawrzycka, D. *et al.* (2001) *Molecular Microbiology*, **40**, 1391–1401.
62. Liu, Z., Shen, J., Carbrey, J.M. *et al.* (2002) *Proceedings of the National Academy of Sciences of the United States of America*, **99**, 6053–6058.
63. Tsukaguchi, H., Shayakul, C., Berger, U.V. *et al.* (1998) *The Journal of Biological Chemistry*, **273**, 24737–24743.
64. Tsukaguchi, H., Weremowicz, S., Morton, C.C., and Hediger, M.A. (1999) *The American Journal of Physiology*, **277**, F685–F696.
65. Gourbal, B., Sonuc, N., Bhattacharjee, H. *et al.* (2004) *The Journal of Biological Chemistry*, **279**, 31010–31017.
66. Sereno, D., Cavaleira, M., Zemzoumi, K. *et al.* (1998) *Antimicrobial Agents and Chemotherapy*, **42**, 3097–3102.
67. Ariyanayagam, M.R. and Fairlamb, A.H. (2001) *Molecular and Biochemical Parasitology*, **115**, 189–198.
68. Wyllie, S., Cunningham, M.L., and Fairlamb, A.H. (2004) *The Journal of Biological Chemistry*, **279**, 39925–39932.
69. Denton, H., McGregor, J.C., and Coombs, G.H. (2004) *The Biochemical Journal*, **381**, 405–412.
70. Mukhopadhyay, R. and Rosen, B.P. (2002) *Environmental Health Perspectives*, **110**, 745–748.
71. Zhou, Y., Messier, N., Oulette, M. *et al.* (2004) *The Journal of Biological Chemistry*, **279**, 37445–37451.
72. Mukhopadhyay, R., Bisacchi, D., Zhou, Y. *et al.* (2008) *Journal of Molecular Biology*, **386**, 1229–1239.
73. Zhou, Y., Bhattacharjee, H., and Mukhopadhyay, R. (2006) *Molecular and Biochemical Parasitology*, **148**, 161–168.
74. Cunningham, M.L. and Fairlamb, A.H. (1995) *European Journal of Biochemistry*, **230**, 460–468.
75. Tovar, J., Cunningham, M.L., Smith, A.C. *et al.* (1998) *Proceedings of the National Academy of Sciences of the United States of America*, **95**, 5311–5316.
76. Baiocco, P., Colotti, G., Franceschini, S., and Ilari, A. (2009) *Journal of Medicinal Chemistry*, **52**, 2603–2612.
77. Silver, S., Budd, K., Leahy, K.M. *et al.* (1981) *Journal of Bacteriology*, **146**, 983–996.
78. Chen, C.M., Misra, T.K., Silver, S., and Rosen, B.P. (1986) *The Journal of Biological Chemistry*, **261**, 15030–15038.
79. Zhou, T., Radaev, S., Rosen, B.P., and Gatti, D.L. (2000) *The EMBO Journal*, **19**, 4838–4845.
80. Slikkerveer, A. and de Wolff, F.A. (1989) *Medical Toxicology and Adverse Drug Experience*, **4**, 303–323.
81. Noach, L.A., Eekhof, J.L.A., Bour, L.J. *et al.* (1995) *Hum Toxicol*, **14**, 349–355.
82. Vanhoe, H., Versieck, J., Vanballenberghe, L., and Dams, R. (1993) *Clinica Chimica Acta; International Journal of Clinical Chemistry*, **219**, 79–91.
83. Lawrence, C.M., Ray, S., Babyonyshev, M. *et al.* (1999) *Science*, **286**, 779–782.

84. Drakesmith, H. and Prentice, A. (2008) *Nature Reviews Microbiology*, **6**, 541–552.
85. Aisen, P., Enns, C., and Wessling–Resnick, M. (2001) *The International Journal of Biochemistry & Cell Biology*, **33**, 940–959.
86. Cheng, Y., Zak, O., Aisen, P. *et al.* (2004) *Cell*, **116**, 565–576.
87. Aisen, P. and Leibman, A. (1972) *Biochimica et Biophysica Acta*, **257**, 314–323.
88. Bullen, J.J., Rogers, M.J., and Griffiths, E. (1974) *Microbial Iron Metabolism* (ed J.B. Neilands), Academic Press, New York.
89. Qian, Z.M., Li, H., Sun, H., and Ho, K. (2002) *Pharmacological Reviews*, **54**, 561–587.
90. Wally, J., Halbrooks, P.J., Vornrhein, C. *et al.* (2006) *The Journal of Biological Chemistry*, **281**, 24934–24944.
91. Sun, H., Li, H., and Sadler, P.J. (1999) *Chemical Reviews*, **99**, 2817–2842.
92. Sun, H. and Szeto, K.Y. (2003) *Journal of Inorganic Biochemistry*, **94**, 114–120.
93. Li, H., Sadler, P.J., and Sun, H. (1996) *The Journal of Biological Chemistry*, **271**, 9483–9489.
94. Sun, H., Li, H., Mason, A.B. *et al.* (1999) *The Biochemical Journal*, **337**, 105–111.
95. Sun, H., Cox, M.C., Li, H. *et al.* (1998) *FEBS Letters*, **422**, 315–320.
96. Miquel, G., Nekaa, T., Kahn, P.H. *et al.* (2004) *Biochemistry*, **43**, 14722–14731.
97. Zhang, L., Szeto, K.Y., Wong, W.B. *et al.* (2001) *Biochemistry*, **40**, 13281–13287.
98. Braun, W., Vašák, M., Robbins, A.H. *et al.* (1992) *Proceedings of the National Academy of Sciences of the United States of America*, **89**, 10124–10128.
99. Vašák, M. and Hasler, D.W. (2000) *Current Opinion in Chemical Biology*, **4**, 177–183.
100. Park, J.D., Liu, Y., and Klaassen, C.D. (2001) *Toxicology*, **163**, 93–100.
101. Meloni, G., Zovo, K., Kazantseva, J. *et al.* (2006) *The Journal of Biological Chemistry*, **281**, 14588–14595.
102. Sun, H., Li, H., Harvey, I., and Sadler, P.J. (1999) *The Journal of Biological Chemistry*, **274**, 29094–29101.
103. Magnusson, N.E., Larsen, A., Rungby, J. *et al.* (2005) *Cell and Tissue Research*, **321**, 195–210.
104. Tanner, J.A., Watt, R.M., Chai, Y.B. *et al.* (2003) *The Journal of Biological Chemistry*, **278**, 39578–39582.
105. Yang, N., Tanner, J.A., Zheng, B.J. *et al.* (2007) *Angewandte Chemie International Edition*, **46**, 6464–6468.
106. Yang, N., Julian, J.A., Wang, Z. *et al.* (2007) *Chemical Communications*, 4413–4415.
107. Yoon, K.P., Misra, T.K., and Silver, S. (1991) *Journal of Bacteriology*, **173**, 7643–7649.
108. Busenlehner, L.S., Apuy, J.L., and Giedroc, D.P. (2002) *Journal of Biological Inorganic Chemistry: JBIC: a Publication of the Society of Biological Inorganic Chemistry*, **7**, 551–559.
109. Ge, R., Watt, R.M., Sun, X. *et al.* (2006) *The Biochemical Journal*, **393**, 285–293.
110. Mobley, H.L., Garner, R.M., Chippendale, G.R. *et al.* (1999) *Helicobacter*, **4**, 162–169.
111. Ge, R., Zhang, Y., Sun, X. *et al.* (2006) *Journal of the American Chemical Society*, **128**, 11330–11331.
112. Ge, R., Sun, X., Gu, Q. *et al.* (2007) *Journal of Biological Inorganic Chemistry: JBIC: a Publication of the Society of Biological Inorganic Chemistry*, **12**, 831–842.
113. Cun, S., Li, H., Ge, R. *et al.* (2008) *The Journal of Biological Chemistry*, **283**, 15142–15151.
114. Cun, S. and Sun, H. (2010) *Proceedings of the National Academy of Sciences of the United States of America*, **107**, 4943–4948.
115. Mulrooney, S.B. and Hausinger, R.P. (2003) *FEMS Microbiology Reviews*, **27**, 239–261.
116. Asato, E., Kamamuta, K., Akamine, Y. *et al.* (1997) *Bulletin of the Chemical Society of Japan*, **70**, 639.
117. Murafuji, T., Azuma, T., Miyoshi, Y. *et al.* (2006) *Bioorganic & Medicinal Chemistry Letters*, **16**, 1510–1513.
118. Zhang, L., Mulrooney, S.B., Leung, A.F.K. *et al.* (2006) *BioMetals*, **19**, 503–511.
119. Jin, L., Szeto, K.Y., Zhang, L. *et al.* (2004) *Journal of Inorganic Biochemistry*, **98**, 1331–1337.
120. Butler, B.D., Lichtenberger, L.M., and Hills, B.A. (1983) *The American Journal of Physiology*, **7**, G645–G651.
121. Hills, B.A., Butler, B.D., and Lichtenberger, L.M. (1983) *The American Journal of Physiology*, **7**, G561–G568.

122. Kao, Y., Goddard, P.J., and Lichtenberger, L.M. (1990) *Gastroenterology*, **98**, 592–606.
123. Slomiany, B.L., Bilski, J., Sarosiek, J. *et al.* (1987) *Biochemical and Biophysical Research Communications*, **144**, 307–314.
124. Sarosiek, J. and Slomiany, B.L. (1988) *Scandinavian Journal of Gastroenterology*, **23**, 585–590.
125. Ottlecz, A., Romero, J.J., Hazell, S.L. *et al.* (1993) *Digestive Diseases and Sciences*, **38**, 2071–2080.

4

Metallomics Research Related to Arsenic

Hiroki Haraguchi

Association of International Research Initiatives for Environmental Studies, Tokyo, Japan

4.1 Metallomics – Integrated Biometal Science

In 2002, the International Symposium on Bio-Trace Elements 2002 (BITREL 2002) was held in Wako, Japan, which was organized by S. Enomoto in RIKEN (Research Institute of Physics and Chemistry). In this symposium, Haraguchi delivered the lecture entitled ‘Trace Element Speciation for Metallomics’ [1], in which he emphasized the importance of speciation analysis (species analysis) of trace elements in biological samples and biological systems. Because trace elements (metals and metalloids) contained in metalloproteins and metalloenzymes generally play essential roles as the active centers for biological and/or physiological functions, metal and metalloid elements often cause serious toxic infection to humans and living organisms in environmental pollution problems. ‘Metallomics’ was used as the scientific term for the first time in this symposium.

In 2004, Haraguchi also published the paper entitled ‘Metallomics as Integrated Biometal Science’ in the *Journal of Analytical Atomic Spectrometry* [2], which was the review paper based on the concept proposed in the lecture in BITREL 2002. After publication of the above paper, metallomics has been receiving great attention as a newly emerging scientific field [3–5]. Three years later, the International Symposium on Metallomics 2007 (ISM 2007) was held in Nagoya which was organized by Haraguchi [6]. In the scientific advisory board meeting of ISM 2007, it was agreed that this ISM meeting would be held regularly every two years. The second ISM (ISM 2009) was held in Cincinnati, USA in June, 2009 [7].

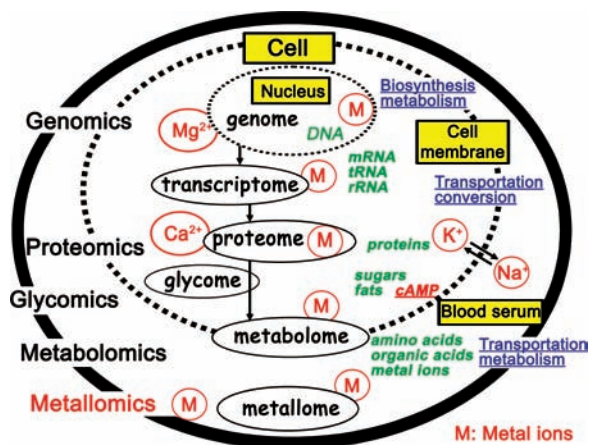


Figure 4.1 Simplified model of biological systems, showing the relationship of -omics sciences. The outer line is corresponding to organ or whole body, and the inner dotted line is to biological cells. Reproduced from [2] by permission of The Royal Society of Chemistry

Furthermore, the third ISM (ISM 2011) will be held at the University of Münster, Germany, in June 15–18, 2011. Metallomics has been the topic of original papers as well as review articles in various scientific journals [8–15]. In addition, the journal ‘*Metallomics-integrated bimetals science*’ was launched in January, 2009, by the RSC.

The abstract of the paper in *J. Anal. At. Spectrom.* [2] is introduced here because it is suggestive of the future direction of metallomics research.¹

In order to understand the relationship of metallomics with genomics, proteomics and other -omics sciences (for example, glycomics and metabolomics), a simplified model of the biological system is illustrated in Figure 4.1 [2, 15], where the dotted line (inside) and continuous line (outside) indicate a biological cell and an organ/whole body, respectively. Some biological functions in the biological system are also shown in Figure 4.1. Taking into consideration the biological functions and roles of the elements, the research subjects required for metallomics study are summarized in Table 4.1 [2]. Metallomics covers the wide range of research subjects related to biometals. Among the subjects listed in Table 4.1, the distributions of the elements [subject 1] and chemical speciation of metals and metalloids (metallome) [subject 2] in biological systems may provide the basic information for metallomics research. Although such information would constitute fundamental codes of metals (and metalloids) encoded in biological systems in analogy to base sequences in genes and amino acid sequences in proteins, no ordered distribution or sequence of metals

¹ In this Chapter, ‘*Metallomics*’ is proposed as a new scientific field in order to integrate the research field related to biometals. Metallomics should be a scientific field in symbiosis with genomics and proteomics because syntheses and metabolic functions of genes (DNA and RNA) and proteins cannot be performed without the aid of various metal ions and metalloenzymes. In metallomics, metalloproteins, metalloenzymes and other metal containing biomolecules are defined as ‘metallome’, in a similar manner to genome in genomics and proteome in proteomics. Since identification of metallome and the elucidation of their biological or physiological functions in the biological systems is the main research target of metallomics, chemical speciation for specific identification of bioactive metallome is one of the most important analytical technologies to establish metallomics as integrated biometal science. In order to rationalize the concept of metallomics, the distributions of the elements in man, human blood serum and seawater (a challenge to an all-elements analysis of one biological cell), along with some other topics are introduced with emphasis on the recent development of chemical speciation of trace metals in some biological samples.]

Table 4.1 Research subjects in metallomics [2]

1.	Distributions of the elements in the biological fluids, cells, organs, and so on.
2.	Chemical speciation of the elements in the biological samples and systems
3.	Structural analysis of metallome (metal binding molecules)
4.	Elucidation of reaction mechanisms of metallome using model metal complexes (bioinorganic chemistry)
5.	Identification of metalloproteins and metalloenzymes
6.	Metabolisms of biological molecules and metals (metabolome and metabolites)
7.	Medical diagnosis of health and disease related to trace metals on multielement basis
8.	Design of inorganic drugs for chemotherapy
9.	Chemical evolution of the living systems and organisms on the earth
10.	Other metal assisted function biosciences in medicine, environmental science, food science, agriculture, toxicology, biogeochemistry, and so on.

has been found in biological systems. Even so, metals as metallic ions bound with proteins play essential roles for the regulation of three-dimensional structures of metalloproteins and metalloenzymes as well as their biological activities.

As discussed in other chapters of the book, inorganic As^{III} (arsenite) and As^V (arsenate) cause acute and chronic toxicities to humans and animals. Most metallomics studies related to arsenic have been concerned with the elucidation of arsenic metabolites and their formation reactions in relation to toxicity and metabolism. In the following sections, the identification of metabolites from arsenic species by speciation analysis using HPLC/ICP-MS will be described.

4.2 Analytical Feasibility of ICP-AES and ICP-MS

The study of metallomics grew following recent developments in analytical atomic spectrometry, such as ICP-AES (inductively coupled plasma atomic emission spectrometry) and ICP-MS (inductively coupled plasma mass spectrometry) [2] because these analytical methods provide excellent analytical feasibilities in sensitivity. As has been noted by many [2, 6, 9, 10, 13, 14, 16–19], the distribution and speciation analyses of the elements in the biological fluids, cells, organs and organisms are generally performed by ICP-AES and ICP-MS as they are highly sensitive analytical methods. The detection limits obtained by commercially available ICP-AES and ICP-MS instruments are shown in Figure 4.2 [20], where the elements are plotted on the vertical axis (concentration unit) corresponding to the detection limits obtained by each analytical method. In the case of ICP-MS, the detection limits obtained by two types of instruments, Q-ICP-MS and HR-ICP-MS, are shown, where Q-ICP-MS and HR-ICP-MS are the ICP-MS instruments equipped with a low resolution quadrupole mass spectrometer and high resolution double focusing mass spectrometer, respectively [21, 22]. As shown in Figure 4.2, the detection limits at the ppb (ng/ml) level are obtained for almost all metallic (and metalloid) elements by ICP-AES. On the other hand, the detection limits obtained by ICP-MS are improved down to the ppt (pg/ml) level. It should be noted here that the direct detection at the sub-ppt level can be performed for many elements in the case of HR-ICP-MS.

In addition to the detection limits, ICP-AES and ICP-MS have other excellent analytical capabilities such as wide linear dynamic ranges of working calibration curves (4–6 orders

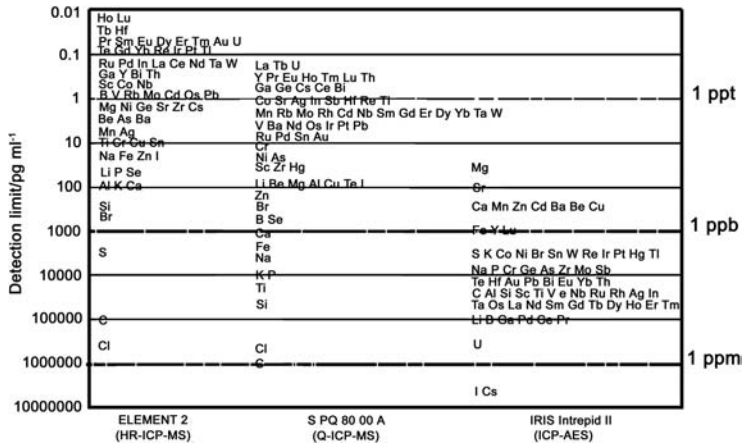


Figure 4.2 Comparison of the detection limits obtained by HR-ICP-MS, Q-ICP-MS and ICP-AES [20]. HR-ICP-MS: high resolution ICP-MS with double focusing mass spectrometer from Thermo-Fisher Scientific Co., Q-ICP-MS (SPQ 8000A): ICP-MS with quadrupole mass spectrometer from Seiko Instruments, ICP-AES: ICP-AES with a CID (Charge Injection Device) multielement detector from Thermo-Fisher Scientific

of magnitude) as well as simultaneous multielement detection, which allow the determination of many elements in the concentration range of 1 ppb – 1000 ppm in ICP-AES and of sub-ppt -1 ppm in ICP-MS. Thus, if we can use both ICP-AES and ICP-MS, analyte elements in the concentration range from sub-ppt up to 1000 ppm, that is, over 10^{10} orders of magnitude, can be simultaneously determined for any biological sample. These analytical feasibilities provide the possibility to determine almost all metallic elements including some nonmetallic elements (S, P, Cl, Br, I) [2, 16, 21]. Then, the multielement concentration data obtained by analytical plasma spectrometry may be available as the fingerprints of biological cells, organs and systems if the database of the elemental distributions in the biological samples is constructed in future.

In the early 1930s, Noddack proposed the concept of *the All-Present Theory of the Elements* [16, 23, 24], in which she suggested that all elements in the periodic table were supposed to be present in all rock and mineral samples. At present, however, owing to the progress in analytical methodology mentioned above, almost all elements can be determined or detected not only in geochemical samples but also in biological and environmental samples [2, 15]. As a consequence, Haraguchi proposed the new concept of ‘*The Extended All-Present Theory of the Elements*’ [2, 16, 19], in which he suggested that all elements in the periodic table might be contained in all materials or substances on the earth, including biological systems, such as animals, plants and microorganisms. Of course, human beings are also the subject of the *Extended All-Present Theory*. *The Extended All-Present Theory* was proposed as the extended concept of Noddack’s. It is now expected that the final goal in the study on the *Extended All-Present Theory* is to elucidate the existence of all elements in a single biological cell, which is referred to as ‘cell microcosm’ [2, 19]. That is, a single biological cell is composed of a small compartment of the Earth or the universe.

H		Mn										Element										He	
10%		512 ppb										Concentration											
Li	Be	M: Essential elements for humans										B	C	N	O	L	Ne						
247 ppm	568 ppm	M: Essential elements for animals										7.8 ppb	25%	4.20%	60%								
Na	Mg											Al	Si	P	S	Cl	Ar						
247 ppm	568 ppm											6.44 ppb	25.1 ppb	0.36%	0.30%	0.28%							
K	Ca	Sc	Ti	Y	Cr	Mn	Fe	Co	Ni	Cu	Zn	Ga	Ge	As	Se	Br	Kr						
0.19%	357 ppm	5.9 ppt	1.42 ppt	18.8 ppb	0.73 ppb	512 ppb	10.7 ppm	12.5 ppb	26.5 ppb	8.9 ppm	3.6 ppm	2.3 ppt	5.83 ppb	192 ppb	1.97 ppm	20 ppm							
Rb	Sr	Y	Zr	Nb	Mo	Tc	Ru	Rh	Pd	Ag	Cd	In	Sn	Sb	Te	I	Xe						
523 ppb	3.6 ppm	112 ppt			6.43 ppb		0.19 ppb		8.0 ppb	10.7 ppb	1.1 ppb	7.0 ppt	960 ppt	0.12 ppb		3.7 ppm							
Cs	Ba	La-Lu	Hf	Ta	W	Re	Os	Ir	Pt	Au	Hg	Tl	Pb	Bi	Po	At	Rn						
5.58 ppb	47.3 ppb				32.7 ppt		1.9 ppt		4.3 ppt	54 ppt	12 ppb	50 ppt	480 ppt										
Fr	Ra	Ac-Lr																					
		La	Ce	Pr	Nd	Pm	Sm	Eu	Gd	Tb	Dy	Ho	Er	Tm	Yb	Lu							
		75.3 ppt	14 ppt	10.4 ppt	74.3 ppt		10.2 ppt	1.1 ppt	15.6 ppt	2.1 ppt	7.4 ppt	1.7 ppt	3.4 ppt	0.37 ppt	2.7 ppt	0.78 ppt							
		Ac	Th	Pa	U	Np	Pu	Am	Cm	Bk	Cf	Es	Fm	Md	No	Lr							
			0.9 ppt		663 ppt																		

Determined
 Detected
 Not detected
 Radioactive and rare gas elements

Figure 4.3 The concentrations of the elements in a single salmon egg cell, determined by ICP-AES and ICP-MS. Reprinted with permission from [19]. Copyright 2008 IUPAC

In order to establish the concept of cell microcosm, salmon egg cells have been analysed on the multielement basis by ICP-AES and ICP-MS after acid digestion, and the analytical results are summarized in Figure 4.3 [2, 19]. In a conventional standard laboratory, 78 elements in the periodic table can be detected, excluding natural/artificial radioactive elements and rare gas elements. So far, 72 elements among the 78 have been determined or detected in salmon egg cells [19]. As shown in Figure 4.3, the concentrations of As and Sb in salmon egg cell are 192 ppb (10^{-9} g/g) and 0.12 ppb, respectively but Bi has not been determined yet. Perhaps because of too low a concentration.

4.3 Chemical Speciation of Trace Elements in Biological Samples

The biological or physiological functions of trace elements (metals and metalloids) are substantially dependent on their chemical forms. For example, inorganic arsenic (arsenite and arsenate) are toxic and carcinogenic, while methylated arsenicals are nontoxic, as will be explained later. In the case of chromium, Cr^{III} is bio-essential but Cr^{VI} is toxic. Thus, the identification of the chemical forms of trace elements including oxidation states is very important to elucidate their biological functions and activities in biological systems [2, 3, 8, 14]. The identification and quantification of trace elements is now defined as 'chemical speciation' or 'speciation' in analytical chemistry [2, 8, 13, 18, 25].

Since trace metallic elements are usually bound to large molecular proteins in biological cells and fluids, their concentrations in biological samples are generally very low. The highly sensitive analytical methods are required for detection in chemical speciation of trace metals. In addition, the chemical compositions of biological samples are very complicated. In other words, trace elements exist in very complex matrices as well as in chemical equilibrium, and thus an element selective detection is required in speciation analysis. At present, in order to fulfill such requirements of chemical speciation analysis, a hyphenated system (HPLC/ICP-MS), that is, a combined system of HPLC with ICP-MS, is most suitable

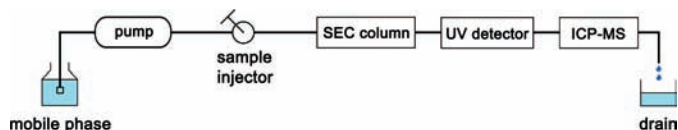


Figure 4.4 A schematic diagram of SEC/ICP-MS with a UV absorption detector for chemical speciation of metalloproteins

for chemical speciation analysis, where various types of chromatographic methods are used for efficient separation of chemical species and ICP-MS is used for the highly sensitive and element selective detection of many metallic and metalloid elements.

In Figure 4.4, a schematic diagram of SEC (size exclusion chromatography)/ICP-MS for metalloprotein analysis is shown as an example, where a UV absorption detector is also used for monitoring protein elution. In Figure 4.5, the chromatogram of standard proteins for molecular weight calibration of the SEC column with the UV absorption detection (in absorbance) is shown together with the retention times of proteins measured. The blue zone in Figure 4.5 indicates the permeation range of the SEC column and the numbers (1–7) in the chromatogram correspond to proteins (proteins and their molecular weights are indicated in the caption). These days, various methods for chemical speciation have been developed and applied to the elucidation of the chemical forms of biometals. In Figure 4.6, the present state-of-the-art methods for chemical speciation are summarized [13], although the detailed explanation is not given here, since many excellent review papers can be referred to [2, 8, 13, 14].

In the following sections, chemical speciation of arsenicals in biological samples is described mainly in terms of arsenic metabolites. In 1971, Braman and Foreback reported the methylated forms of arsenic in the environment [26], where they generated iAs^{III} (arsenite), iAs^V (arsenate) and MMA (monomethylarsonic acid)/DMA (dimethylarsinic acid) as arsines (hydrides) with stepwise chemical reduction and detected those species by

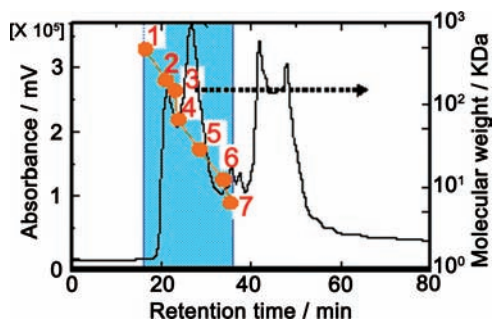


Figure 4.5 Chromatogram of standard proteins obtained by a hyphenated system of SEC/ICP-MS. Stationary phase: SuperoseTM 12 10/300 GL (Molecular permeation range 1–300 kDa), Mobile phase: 0.1 M Tris-HCl (pH 8.0), Flow rate of mobile phase: 0.5 ml/min, Sample injection volume: 100 μ l, Wavelength of UV absorption detection: 254 nm. Standard proteins: 1. ferritin (440 kDa), 2. β -amylase (200 kDa), 3. alcohol dehydrogenase (150 kDa), 4. albumin (66 kDa), 5. carbonic anhydrase (29 kDa), 6. cytochrome c (12 kDa), 7. aprotinin (7 kDa)

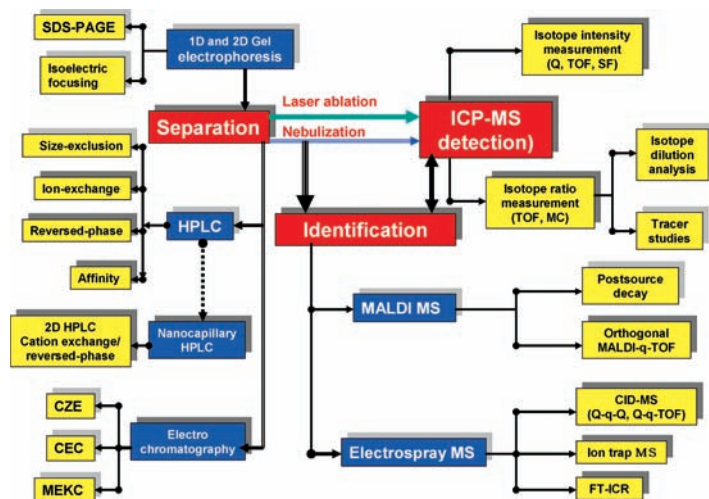


Figure 4.6 Various combined technologies for chemical speciation analysis. Reproduced from [13] by permission of The Royal Society of Chemistry

an electrical discharge emission after cold trapping. They could improve the sensitivity, but their analytical method was tedious and time consuming. In 1977, Andrae published the paper on the determination of arsenic species (iAs^V , iAs^{III} , MMA and DMA) in natural waters by hydride-generation/cold gas trapping separation with the sequential detection by AAS (atomic absorption spectrometry) using the hydrogen-air flame or by GC (gas chromatography) separation with the detection by EC (electron capture detector [27]. In 1981, Morita *et al.* developed a HPLC/ICP-AES system for the determination of arsenic species of AsB, iAs^{III} and iAs^V in biological samples (*Hijiki* extract), where they used the anion or cation exchange column [28]. In 1989, Shibata and Morita also reported the pioneer work of the use of HPLC/ICP-MS for speciation of arsenic species in biological samples [29]. Using HPLC/ICP-MS, they analysed biological samples such as marine algae [30], bivalves [31] and lobster [32] and identified various arsenic species in those biological samples including arsenobetaine and several arsenosugar derivatives. Since their pioneer works, various arsenic metabolites have been identified in human urine, human blood serum and other biological samples due to the efficient separation and highly sensitive detection methods using HPLC/ICP-MS [33]. Thus, before describing speciation studies on arsenic metabolites, arsenic compounds of interest are summarized in Table 4.2, together with their abbreviations. The abbreviations of arsenic compounds are followed after definitions from the references of Suzuki's group [34–37]. The chemical forms of arsenic compounds listed in Table 4.2 can be found in the figures in this chapter.

4.3.1 Speciation of Arsenic in Salmon Egg Cells

The elemental concentrations of salmon egg cells (whole cell) are shown in Figure 4.3, in which 72 elements have been determined or detected in a single biological cell [19]. As mentioned earlier, the salmon egg cell contains 192 ng of As/g. Then, speciation analysis of arsenic in salmon cells was performed by HPLC/ICP-MS in order to identify

Table 4.2 Arsenic compounds and their abbreviations

Compounds	Abbreviation
1. arsenate	iAs^V
2. arsenite	iAs^{III}
3. monomethylarsonic acid	MMA^V
4. dimethylarsinic acid	DMA^V
5. monomethylarsonous acid	MMA^{III}
6. dimethylarsinous acid	DMA^{III}
7. trimethylarsine oxide	$TMA^V O$
8. tetramethylarsine	$TeMA^V$
9. arsenobetaine	AsB
10. arsenocholine	AsC
11. dimethylmonothioarsenic acid	$DMMTA^V$
12. dimethyldithioarsinic acid	$DMDTA^V$
13. arsenotriglutathione	$iAs^{III} (GS)_3$
14. methylarsenic diglutathione	$CH_3As(GS)_2$
15. monomethylmonothioarsonic acid	$MMMTA^V$

arsenic species in the cell cytoplasm and cell membrane [38]. Before analyzing salmon egg cells, the separation and identification of commercially available standard compounds of arsenic (iAs^V , iAs^{III} , MMA^V , DMA^V , AsB, $TMA^V O$, $TeMA$ and AsC) were examined by HPLC/ICP-MS with ^{75}As detection. The chromatogram obtained is shown in Figure 4.7 [38]. The separation of arsenic compounds was carried out by using a CAPSELL PAK C18 column (250 mm \times 4.6 mm i.d. from Shiseido, Tokyo, Japan) with the mobile phase of 4 mM malonic acid + 4 mM TMAH (tetramethylammonium hydroxide) + 10 mM 1-butane sulfonic acid sodium salt + 0.05% methanol (pH 3.0), where TMAH and 1-butane sulfonic acid sodium salt were added as the ion pairing reagents [29]. As shown in Figure 4.7, all arsenic compounds examined are well separated from each other. Thus, the present method was applied to speciation analysis of arsenic species in the salmon egg cell.

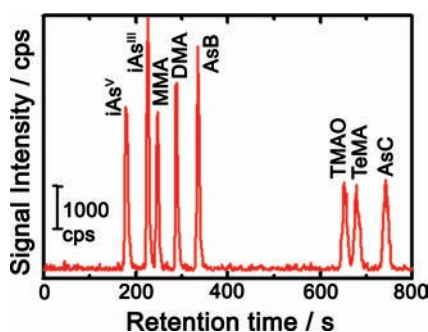


Figure 4.7 Chromatogram of standard arsenic compounds detected by ^{75}As ICP-MS. Concentration: 10 ng of As/ml each, column: CAPCELL PAK C18 (ODS column), mobile phase: 4 mM malonic acid + 4 mM TMAH + 10 mM 1-butane sulfonic acid sodium salt + 0.05% methanol (pH 3.0); flow rate: 0.75 ml/min, sample injection volume: 10 μ l. Reprinted with permission from [38] Copyright 2005 by Japan Society for Biomedical Research on Trace Elements

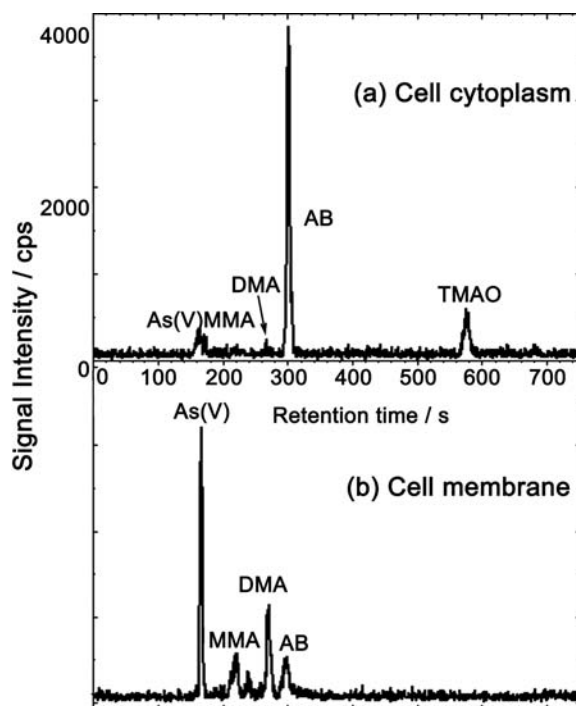


Figure 4.8 HPLC chromatogram for arsenic species in (A) egg cell cytoplasm, and (B) egg cell membrane detected by ICP-MS at m/z 75 [38]. Experimental conditions are the same as in Figure 4.7

The chromatograms for arsenic species in salmon egg cell cytoplasm and the cell membrane are shown in Figure 4.8(a) and (b), respectively. Cell cytoplasm (intracellular fluid) and cell membranes were separately collected from whole egg cells by using Teflon tweezers and a Teflon needle. Then, arsenic species were extracted from cell cytoplasm and cell membranes as follows. Approximately 1 g of cell cytoplasm or cell membrane sample was taken in a centrifugation tube, and 10 ml of 50% methanol was added. The sample was sonicated for 30 min and then centrifuged at 4000 rpm for 5 min. The supernatant was collected as the analysis sample. This extraction procedure was performed repeatedly. The supernatants collected two times were put together and evaporated almost to dryness at 40 °C using a rotary evaporator. The residue was dissolved in 1 ml of the HPLC mobile phase solution and then filtered with a membrane filter (pore size; 0.45 μm). This dissolved solution was subjected as the cell cytoplasm sample to the HPLC/ICP-MS. In the case of cell membrane, 0.5 ml of TMAH was added as an alkali reagent into the sample before the extraction procedure mentioned above, to dissolve arsenic species from lipids or proteins in cell membrane.

A large peak of AsB and three small peaks of $i\text{As}^{\text{V}}$, DMA and TMAO were observed in cell cytoplasm (Figure 4.8). The concentrations of these AsB, $i\text{As}^{\text{V}}$, DMA and TMAO were estimated to be 17.6, 1.7, 0.4 and 3.0 ng/g as As, respectively, on the wet weight basis. On the other hand, $i\text{As}^{\text{V}}$, MMA, DMA and AsB were found in the cell membranes, whose

concentrations were 15.4, 8.1, 12.3 and 8.4 ng/g as As, respectively. As a result, the total concentrations of arsenic species in the extracts from cell cytoplasm and cell membrane were 22.7 ng/g and 44.2 ng/g, respectively, which corresponded to about 12% and 35% of the total amounts of arsenic in cell cytoplasm and cell membrane, respectively. These results suggest that large molecular arsenic species such as protein binding arsenic may exist in both cell cytoplasm and the cell membrane because only small molecular arsenic species could be identified by HPLC/ICP-MS using the ODS column in ion pair mode. Inorganic arsenic (iAs^V) was the main arsenic species in the cell membrane, while AsB (arsenobetaine) was the main species in cell cytoplasm. These facts indicate that methylation of inorganic arsenic to AsB occurs on passing through the cell membrane or after entering into cell cytoplasm.

Since various metallic and metalloid elements exist in salmon egg cells, as shown in Figure 4.3, fractionation analysis of the elements in salmon egg cell cytoplasm was carried out by HPLC/ICP-MS using the surfactant-mediated CHAPS (3-[(3-cholamidopropyl)-dimethylammonio]-1-propane sulfonate; zwitterionic surfactant)-coated ODS column in order to elucidate the protein bindings of the elements [19]. The CHAPS-coated ODS column was prepared by the dynamic coating method. As reported previously [39, 40], the CHAPS-coated ODS column has unique characteristics for simultaneous separation of ions or small molecules and large molecules (e.g., proteins) and the useful information about the elements binding or non binding with proteins is easily obtained. The chromatograms for salmon egg cytoplasm obtained by HPLC/ICP-MS using the CHAPS-coated ODS column are shown in Figure 4.9. In Figure 4.9, the element selective chromatograms are illustrated

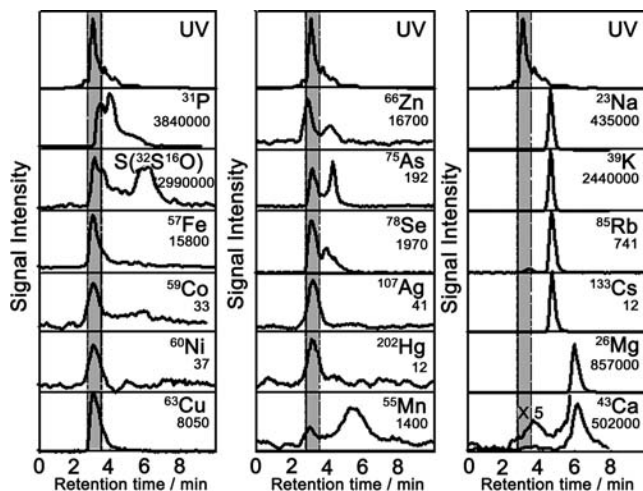


Figure 4.9 The element selective chromatograms for salmon egg cytoplasm obtained by HPLC/ICP-MS. Sample: salmon egg cell cytoplasm diluted five-fold with 0.1 M Tris buffer (pH 7.4), Column: CHAPS-coated ODS column, mobile phase: 0.1 M Tris buffer solution (pH 7.4), ICP-MS detection: at m/z shown in the figure, UV absorption detection: 254 nm. The numbers below the elements indicate the concentrations of the elements in salmon egg cell. The retention time range between 3.0–3.5 min (gray zone) corresponds to the protein elution zone. Reprinted with permission from [19]. Copyright 2008 IUPAC

together with those with the UV-absorption detection at 254 nm, where isotopes detected and elemental concentrations determined by ICP-MS are also indicated in each chromatogram. It should be noted here that the retention range of 3.0–3.5 min shown as the gray zones in Figure 4.9 indicates the elution zone of large molecules with molecular weights (MW) greater than about 10 kDa, while the retention range after 3.5 min indicates the elution zone of small ions and molecules [40]. However, the molecular weights of the eluted molecules can not be estimated from the chromatograms obtained by the CHAPS-coated ODS column, since the CHAPS-coated ODS column has no size exclusion property.

It is seen in Figure 4.9 that most heavy metals such as Fe, Co, Ni, Cu, Ag, and Hg, which are biologically essential or toxic elements, provided single broad peaks within the protein elution zone. These results indicate that such heavy metals mostly exist as protein binding complexes. On the other hand, Zn and Mn provided two main peaks inside and outside the protein elution zone, which suggests that Zn and Mn exist partly as small molecules, maybe free ions or amino acid complexes, in addition to protein binding complexes. Furthermore, in Figure 4.9, alkali and alkaline earth elements, such as Na, K, Rb, Cs and Mg, provided single peaks as the ionic forms after the protein binding zone, although a small amount of Ca was binding to proteins. As for arsenic as well as selenium, two main peaks in the small and large molecular ranges were observed in a similar manner to the cases of Zn and Mn. These suggest that arsenic exists not only as small molecules, but also as protein binding molecules in salmon egg cell cytoplasm. Although we cannot get any further information about proteins binding to arsenic from this experiment, the results in Figure 4.9 suggest that we should take into consideration protein binding molecules of arsenic as the reaction intermediates or metabolites in biological systems. These results are consistent with the conclusion drawn from the experiment for small molecular arsenic species shown in Figure 4.8; large molecular arsenic species, for example, protein binding arsenic, may exist in cell cytoplasm.

4.3.2 Speciation of Arsenic Species in Human Urine

People in South East Asian Countries such as India and Bangladesh are exposed to naturally originated arsenic because of inorganic arsenic pollution of ground water for drinking water. It is now well known that ingestion of inorganic arsenic may cause cancer of the skin, bladder, kidney, lung and liver, as well as disorders of the circulatory and nervous systems [41–43]. Thus, studies on environmental pollution due to arsenic in South East Asian areas have been conducted by several research groups [44–46]. In the case of inorganic arsenic ingestion, it has been reported that about 60–75% of the dose was excreted into urine within a few days [47, 48] and also that the distribution of arsenic species in urine was 10–15% inorganic arsenic, 10–15% MMA^V and 60–80% DMA^V [48, 49]. Thus, DMA^V is a major urinary metabolite in humans exposed to inorganic arsenic. Since pentavalent methylated metabolites are less toxic than iAs^{III} or iAs^V, methylation is considered to be the principal pathway for detoxification mechanism of inorganic arsenic. According to the metabolic scheme [50], it is considered that MMA^V is reduced to MMA^{III} and further methylated to DMA^V. Reduction of DMA^V to DMA^{III} may also be the third pathway methylation in arsenic metabolism [51].

Most investigations about arsenic species in urine have been carried out using commercially available pentavalent arsenic compounds. Thus, little is known about trivalent

methylated arsenic metabolites. Suzuki *et al.* reported identification of arsenicals in human urine of the arsenic affected areas in West Bengal, India, with special interest in trivalent methylated arsenic species, DMA^{III} and MMA^{III} [34]. They prepared DMA^{III} and MMA^{III} from standard DMA^V and MMA^V respectively, by reduction with metabisulfite and thio-sulfate reagents as followed from the description by Reay and Asher [52] and synthesized DMA^{III} and MMA^{III} were available as the standards for trivalent methylated arsenic compounds. In urine analysis they used HPLC/ICP-MS, in which a polymer based anion exchange resin column (100 mm × 7.6 mm i.d.; Shodex Asahipack ES-502N 7C from Showa Denko, Tokyo, Japan) was utilized for arsenic separation. The chromatogram of a mixture of eight authentic arsenic compounds (20 μg of As/l each) including DMA^{III} and MMA^{III} is shown in Figure 4.10. The optimized experimental conditions are described in the caption of Figure 4.8. Eight arsenic compounds examined are quite well separated from each other. The method was validated by analyzing Standard Reference Material Toxic Metals in freeze dried urine (SRM 2670; NIST, Gaithersburg, MD, USA) containing both normal (reference value of 60 μg/L) and elevated (certified value of 480 ± 100 μg/L) levels of arsenic. Since there was no certified reference material for individual arsenic species in urine, only reference or certified values of the total concentrations of arsenic were estimated as the total amount of AsB, DMA^V and MMA^V in the normal level of SRM 2670 and AsB, DMA^V, MMA^V, and As^V in the elevated level of SRM 2670, which were determined by HPLC/ICP-MS. The analytical values for those different levels of arsenic in urine were

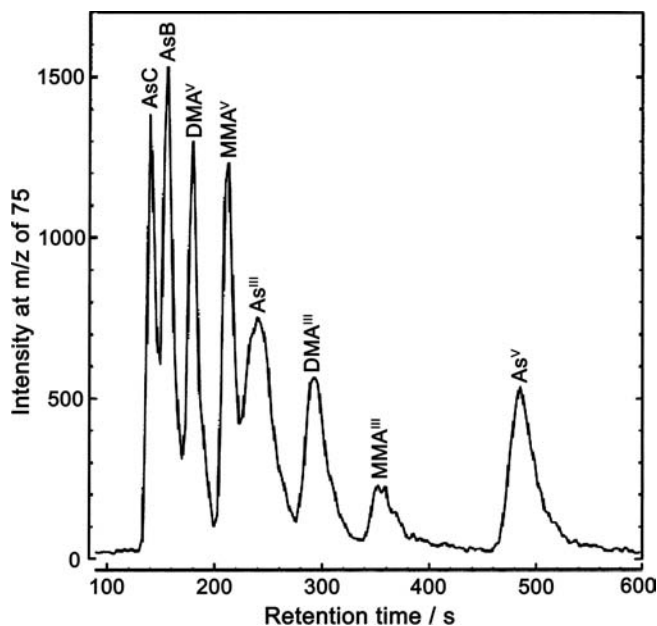


Figure 4.10 The chromatogram of a mixture (20 μg of As/l) of eight authentic arsenic compounds obtained by HPLC/ICP-MS with the detection of ⁷⁵As. Separation column: an anion exchange column (ES-502N 7C; 100 mm × 7.6 mm i.d.), mobile phase: 15 mM citric acid (pH 2.0), flow rate of the mobile phase: 1 ml/min, sample injection volume: 20 μl. Reprinted with permission from [34]. Copyright 2001 American Chemical Society

$57.82 \pm 2.5 \mu\text{g/l}$ and $495 \pm 11.7 \mu\text{g/l}$, respectively. These analytical values were quite consistent with the reference and certified values given above. It is noted here that the method developed above can be applied to speciation of arsenic not only in the urine samples but also in the natural water samples.

In the arsenic pollution experiment, 78 tube well waters and 428 human urine samples were collected from four differently arsenic affected blocks (groups A–D) in West Bengal, India [34]. Some typical chromatograms of the urine samples collected from groups A–D are shown in Figure 4.11, where the urine samples were diluted fourfold and subjected to speciation analysis by HPLC/ICP-MS. As shown in Figure 4.11, in addition to As^{V} , As^{III} , MMA^{V} and DMA^{V} , DMA^{III} and MMA^{III} were detected in human urine, which were found for the first time in this experiment. The analytical results of arsenic species in human urine collected from people in West Bengal are summarized in Table 4.3. It is seen from Table 4.3 that the concentrations of total urinary arsenic as well as DMA^{III} and MMA^{III} increased with the increase in water arsenic collected from four different areas. Although further detailed discussion about the experimental results shown in Table 4.3 is not made here, Suzuki gave some important comments based on the experimental results for the arsenic affected areas in Bengal [34], as follows; (i) MMA^{III} and DMA^{III} have large affinity for some specific cellular proteins. (ii) MMA^{III} inhibits glutathione reductase, and DMA^{III} causes a carcinogenic

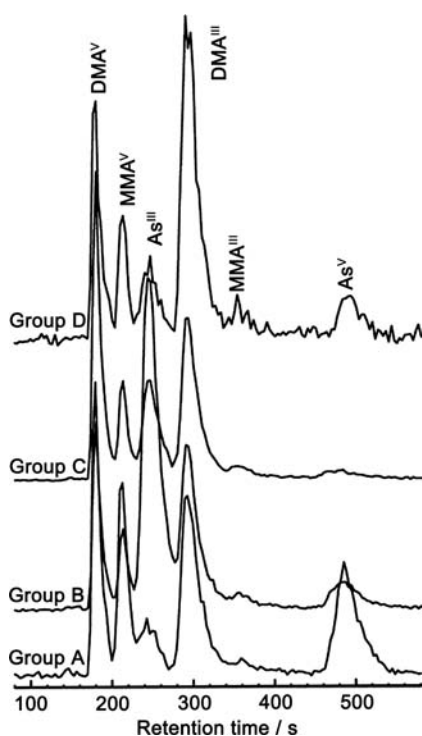


Figure 4.11 Elution profiles of arsenicals obtained by HPLC/ICP-MS with detection of ^{75}As . The urine samples collected from four different volunteer groups, groups A–D were diluted fourfold before analysis. Experimental conditions were the same as in Figure 4.10. Reprinted with permission from [34]. Copyright 2001 American Chemical Society

Table 4.3 The analytical results of arsenicals in human urine of the arsenic affected areas in West Bengal, India [34]

	Group A	Group B	Group C	Group D
Urinary arsenic				
MMA ^{III} (%)	5	4	5	2
MMA ^V (%)	8	10	10	11
DMA ^{III} (%)	19	11	21	4
DMA ^V (%)	45	46	44	74
arsenite (%)	14	13	13	8
arsenate (%)	10	13	8	2
mean concentration ($\mu\text{g/l}$)				
water arsenic	33.0 ± 7.0	148 ± 34	210 ± 2.6	248 ± 59
urinary MMA ^{III}	3.0 ± 0.4	6.0 ± 0.6	10 ± 0.8	30 ± 7
urinary DMA ^{III}	8.0 ± 1	18.6 ± 3	42 ± 5	63.8 ± 24
total urinary As	50.8 ± 3.4	195 ± 14	242 ± 19	1487 ± 172

action by generating reactive oxygen species (ROS). (iii) Moreover, there is a possibility that DMA^{III} and MMA^{III} are more toxic than inorganic arsenic. Thus, Suzuki concluded that the hypothesis that methylation is the detoxification pathway for inorganic arsenic should be re-evaluated in future.

4.3.3 Speciation of Arsenic Species in Human Blood Serum

Human blood serum contains relatively high concentration levels of proteins (albumin; 5%, α_2 -macroglobulin; 400 mg/l, transferrin 300 mg/l and ceruloplasmin; 50 mg/l) as well as those of inorganic salts (Na^+ ; 3130 mg/l, Cl^- ; 3200 mg/l), together with other components, such as amino acids, organic acids and so on. Thus, human blood serum is consisted of a variety of matrix components, while urine contains only inorganic salts and some low molecular mass organic compounds, usually not containing proteins. Furthermore, the concentration of total arsenic in human blood serum is very low at the level of 0.45 $\mu\text{g/l}$ (0.45 ppb) [2]. Thus, the direct determination of arsenic species in blood serum of healthy people has not been reported so far. This is because arsenicals accumulate in red blood cells (RBCs) of blood, as will be described in the following sections, and only a small amount of arsenic is distributed in blood serum. In recent years, however, medical treatment of leukaemia by intravenous injection of arsenic trioxide (arsenite; iAs^{III}) has been developed, and then speciation analysis of arsenicals in human blood serum or plasma is required for monitoring the kinetic behaviors of arsenicals in the chemotherapy of acute myeloid leukaemia.

Kaise's group reported speciation of arsenic metabolites in blood cells and plasma collected from the patients of acute promyelocytic leukaemia after treatment with iAs^{III} [53, 54]. After separation of blood into blood cells and plasma by centrifugation (1000 rpm for 10 min at 4 °C), they determined the total concentrations of arsenic in blood cells and plasma by ICP-MS after $\text{HNO}_3/\text{H}_2\text{O}_2$ acid digestion, in which they detected the As signal at m/z 91 ($^{75}\text{As}^{16}\text{O}^+$) to avoid the interference of $^{40}\text{Ar}^{35}\text{Cl}$ with ^{75}As . In speciation analysis, a CAPCELL PAC C18 MG II column; Shiseido) was used for separation of arsenicals with the mobile phase of 4 mM malonic acid + 4 mM TMAH + 10 mM butane sulfonic sodium salt + 0.5% methanol (adjusted to pH 2.0 with HNO_3). In their experiment,

blood plasma was filtered with an ultrafiltration filter (molecular permeation limit: 10 000 Da) to remove large molecular proteins, and the filtrate was subjected to speciation analysis of arsenic by HPLC/ICP-MS [54]. As a result, As^{V} , As^{III} , MMA, DMA, and AsB were successfully detected in blood plasma in terms of their daily change for 18 days after iAs^{III} administration.

It may be more desirable for medical diagnosis or monitoring of arsenic therapy for myeloid leukaemia with iAs^{III} , if speciation analysis of arsenic metabolites in blood serum can be performed with direct sample injection. Hasegawa *et al.* developed a phosphatidylcholine-coated ODS column (hereafter referred to as PC-coated ODS column) as a stationary phase for direct sample injection analysis of biological fluid samples [55]. The PC-coated ODS column was prepared by a dynamic coating method (coating solution; 1% phosphatidylcholine in 50% methanol) for an ODS column (Mightysil RP-18 GP Aqua packed with 5 mm C18-bonded silica, 250 mm \times 4.6 mm i.d; Kanto Chemicals, Tokyo, Japan). The chemical structure of phosphatidylcholine is shown in Figure 4.12. Phosphatidylcholine is a phospholipid with double chained zwitterionic properties, having a phosphate and a quaternary ammonium group, and thus phosphatidylcholine act as a surfactant with unique characteristics to form micelles as well as mono- and di-layer membrane structures. Hasegawa *et al.* reported that the PC-coated ODS column provided the unique separation characteristics of simultaneous separation of large and small molecules/ions, in a similar manner to the case of the CHAPS-coated ODS column, and they applied the PC-coated ODS column to speciation analysis of arsenic in urine and some medical drugs in blood serum [55].

In Figure 4.13, the chromatograms for arsenic standard compounds obtained by HPLC/ICP-MS using (a) the PC-coated ODS column and (b) the conventional ODS column are shown for comparison, where the reverse phase ion-pair mode was employed for separation with the mobile phase of 5 mM citrate buffer (pH 4.0) containing 5 mM SDS (sodium 1-dodecanesulfonate), and 5 mM THAH. In both cases, five arsenic standards (iAs^{V} , iAs^{III} , MMA, DMA, and AsB) are well separated. This PC-coated ODS column was applied to speciation analysis of arsenic in urine samples and drug analysis in blood serum [55].

The chromatograms for arsenic in (a) human blood serum reference material spiked with arsenic compounds, and (b) human blood serum from a leukaemia patient after therapeutic treatment with arsenite (iAs^{III}) are shown in Figure 4.14 [56], where human blood serum reference material 'SerormTM Human' purchased from Sero As (Billingstad, Norway) was used. When the mobile phase solution used in Figure 4.13 was employed for blood serum analysis, the PC coated ODS column deteriorated after 5–10 times of analysis because of clogging of the column, most likely due to the adsorption of serum proteins.

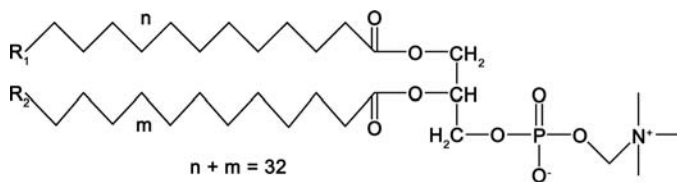


Figure 4.12 The chemical structure of phosphatidylcholine

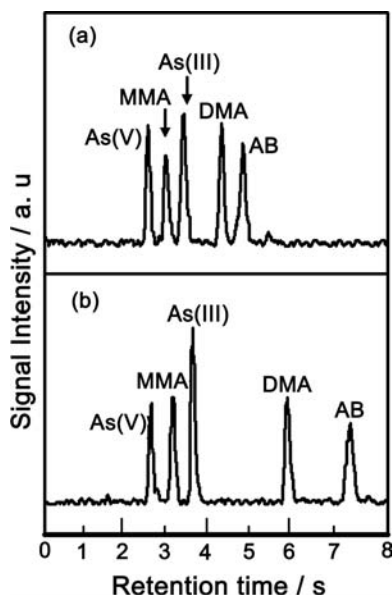


Figure 4.13 Chromatograms for standard arsenic compounds obtained by HPLC/ICP-MS using (a) PC-coated ODS column and (b) conventional ODS column. Mobile phase; 5 mM citric acid containing 5 mM SDS and 5 mM TMAH (pH 4.0), flow rate; 0.75 ml min^{-1} , sample injection volume; $20 \mu\text{l}$, concentration of standard arsenic compounds added: 10 ng of As/g each. Reprinted with permission from [55] Copyright 2007 The Chemical Society of Japan

Thus, in Figure 4.13 CHAPS was added in the mobile phase as a protein solubilizing agent to prevent adsorption of proteins on the column. Then, the column separation became very stable, and the chromatograms with clear peaks of arsenic species in human blood serum could be obtained, as is shown in Figure 4.14. It is just noted here that only MMA^{V} and DMA^{V} were detected in human blood serum collected from a leukaemia patient 10 days after therapeutic treatment with arsenite (iAs^{III}).

Since the PC-coated ODS column has the long term stability for blood serum analysis, it may be used not only for arsenic species, but also for other metabolites and drugs in human blood serum.

4.3.4 Arsenic Metabolism in Hamsters and Rats after an Oral Dose of Arsenite

Hamsters and rats have different metabolic capacity and toxicity tolerance to arsenic, so it is interesting to investigate the arsenic metabolites and pathways in these animal species after an arsenic dose. Thus, arsenic metabolism in hamsters and rats after arsenite dose was examined as follows [37]. Hamsters and rats were given a one time oral dose of arsenite (iAs^{III}) at 5.0 mg As/kg body weight. The heparinized blood was centrifuged at 3000 g for 10 min to separate it into plasma and red blood cells (RBCs). Organs were dissected after whole body perfusion, and the concentrations of arsenic in organs and body fluids were determined by ICP-MS after digesting with HNO_3 and H_2O_2 . Figure 4.15 shows the changes in the concentrations of arsenic and percentage of dose in the liver and kidney and in body fluids for plasma and RBCs (red blood cells) after administration of arsenic [37]. It is seen

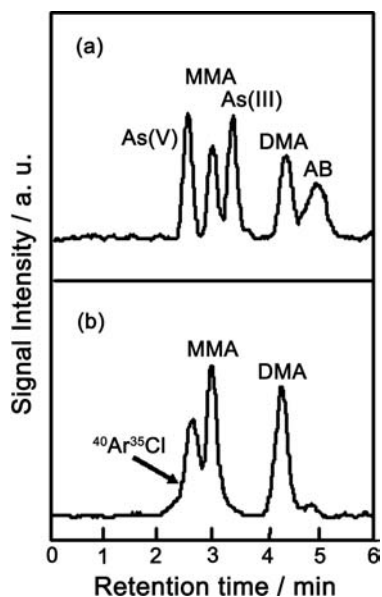


Figure 4.14 Chromatograms for (a) human blood serum reference material spiked with standard arsenic compounds, and (b) human blood serum from a leukaemia patient after therapeutic treatment with arsenite (iAs^{III}). Mobile phase; 5 mM citric acid containing 5 mM SDS, 5 mM TMAH and 0.2 mM CHAPS (pH 4.0), flow rate; 0.75 ml min^{-1} , sample injection volume; $20 \mu\text{l}$, concentration of standard arsenic compounds added: $10 \text{ ng of As g}^{-1}$ each. Reprinted with permission from [56] Copyright 2007 The Chemical Society of Japan

from Figure 4.15 that more than 75% of the dose accumulated in rat RBCs, whereas less than 0.8% of the dose accumulated in hamster RBCs. It should be noticed here that massive amounts of arsenic ($3.7\text{--}4.6 \mu\text{g}$ of As/g) were found in hamster kidneys (B) throughout seven days, compared to that in rat kidneys (b). On the other hand, arsenic was retained at the high level in rat RBCs (d), while it was at the significantly low level in hamster RBCs. In addition, it is seen from Figure 4.15 that arsenic accumulates more and is retained longer in kidneys than that in livers in both animals. The time course of the changes in the concentration of arsenic and the percentage of dose in urine after a single oral administration of iAs^{III} in hamsters and rats is also shown in Figure 4.16 [37]. As described above in hamsters, arsenic accumulated at the low level in RBCs and then more than 60% of the dose was recovered in urine within seven days, which was 7.8-fold higher than that in rat urine. These results indicate that arsenic orally dosed is rapidly excreted through urine in the case of hamsters, while it is accumulated and retained in RBCs in the case of rats.

In order to elucidate the differences in metabolism between hamsters and rats, HPLC/ICP-MS was applied to chemical speciation of arsenic in livers and kidneys. The element selective chromatograms of arsenic in livers (A and a) and kidneys (B and b) of hamsters (A and B) and rats (a and b) after the oxidation of arsenic metabolites with H_2O_2 are shown in Figure 4.17 [37]. These element selective chromatograms were obtained by HPLC/ICP-MS using an anion exchange column (Shodex Asahipak ES-502N 7C; Showa Denko). In the analysis, a 0.2 g portion of livers and kidneys (crushed organs) was heat

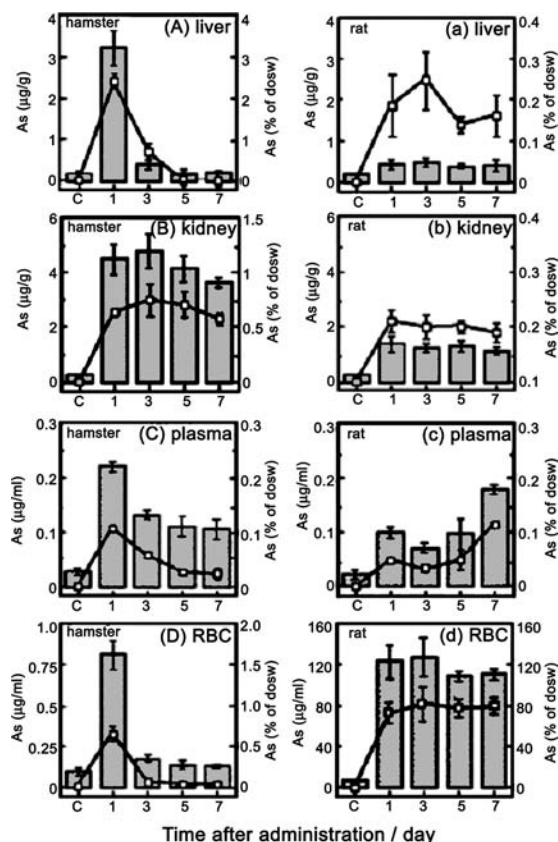


Figure 4.15 The time course of the changes in the concentration of arsenic and the percentage of dose in organs (liver/kidneys) and body fluids (plasma/RBCs) after a single oral administration of arsenite to hamsters and rats. Male hamsters (A–D) and Wistar rats (a–d) were orally administered $i\text{As}^{\text{III}}$ at a single dose of 5.0 mg of As/kg body weight and dissected one, three, five, or seven days later. The concentrations of arsenic (columns) and the percentage of dose (line graphs) are shown for livers (A and a), kidneys (B and b), plasma (C and c), and RBCs (D and d) of hamsters and rats, respectively. Control samples were prepared from hamsters and rats with the administration of the same volume of water alone. It was assumed that blood is 7% of the body weight, and hematocrit is 0.4. Data are expressed as the mean \pm SD ($n = 3$). Reprinted with permission from [37]. Copyright 2007 American Chemical Society

treated at 95°C for 10 min to denature catalase and then oxidized with 0.5 ml of H_2O_2 (5%) for 12 h. The reaction mixtures were centrifuged at 800 rpm for 5 min to obtain supernatants, which were then subjected to speciation analysis. As shown in Figure 4.17, $i\text{As}^{\text{V}}$ and MMA^{V} and DMA^{V} were detected in livers of both hamsters and rats in the first 24 h, although the concentrations of these species were much higher in hamsters than in rats. In rat kidneys, furthermore, $i\text{As}^{\text{V}}$ was not detected through seven days and the concentration of DMA^{V} was relatively higher than that of MMA^{V} .

The time course of the changes of the chromatograms of arsenic in urine after a single oral administration of arsenite to hamsters and rats is shown in Figure 4.18 [37]. Twentyfour hour

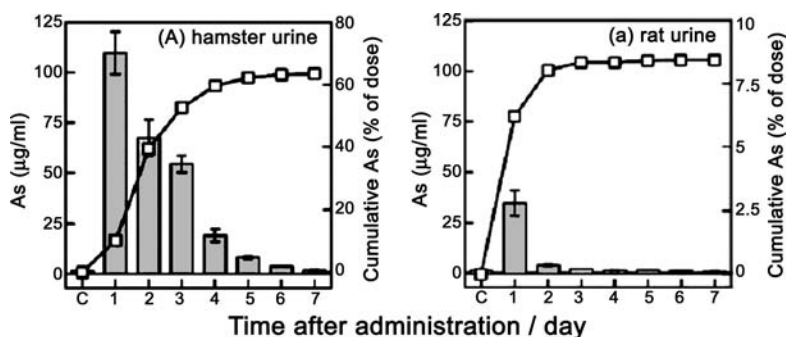


Figure 4.16 The time course of the changes in the concentration of arsenic and the percentage of dose in urine after a single oral administration of arsenite to hamsters and rats. 24 h urine was collected from hamsters and rats for seven days after an oral administration of $i\text{As}^{\text{III}}$ at a dose of 5.0 mg of As/kg body weight. The urine samples were centrifuged to remove non-soluble matter and then stored at -50°C until use. The data are shown as concentrations of arsenic (columns) and cumulative recoveries relative to the dose (line graphs). Control urine was collected from hamsters and rats administered with the same volume of water alone. Data are expressed as the mean \pm SD ($n = 3$). Reprinted with permission from [37]. Copyright 2007 American Chemical Society

urine was collected daily for seven days (1–7 D). The distributions of urinary arsenic metabolites in hamsters (A and B) and rats (a and b) were determined by HPLC/ICP-MS using the anion exchange ES-502N 7C column (A and a) and the gel filtration GS-220 HQ column (B and b). The GS-220 HQ column (300 mm \times 7.6 mm i.d.) was purchased from Showa Denko. It is seen in Figure 4.18 that in the first 24 h urine, arsenite ($i\text{As}^{\text{III}}$), MMA^{V} and

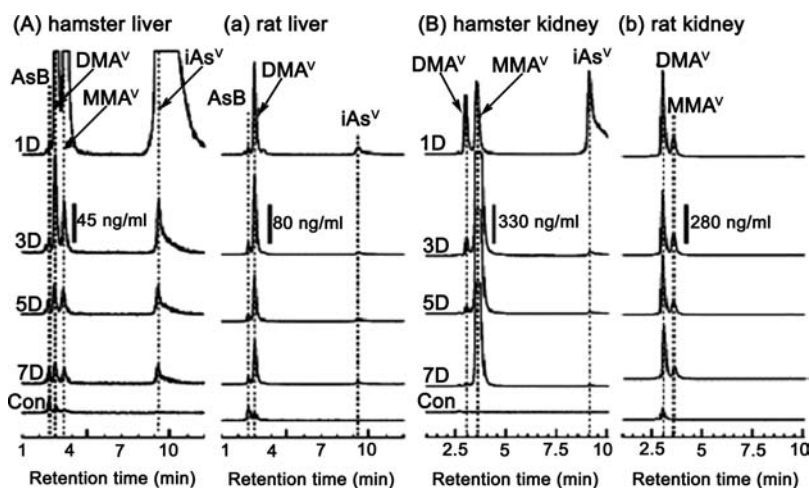


Figure 4.17 The changes of species of arsenic in livers (A and a) and kidneys (B and b) of hamsters (A and B) and rats (a and b) at different times after the oxidation of arsenic metabolites with H_2O_2 by HPLC-ICP-MS on an anion exchange column. The control livers and kidneys were obtained from hamsters and rats given water alone. Reprinted with permission from [37]. Copyright 2007 American Chemical Society

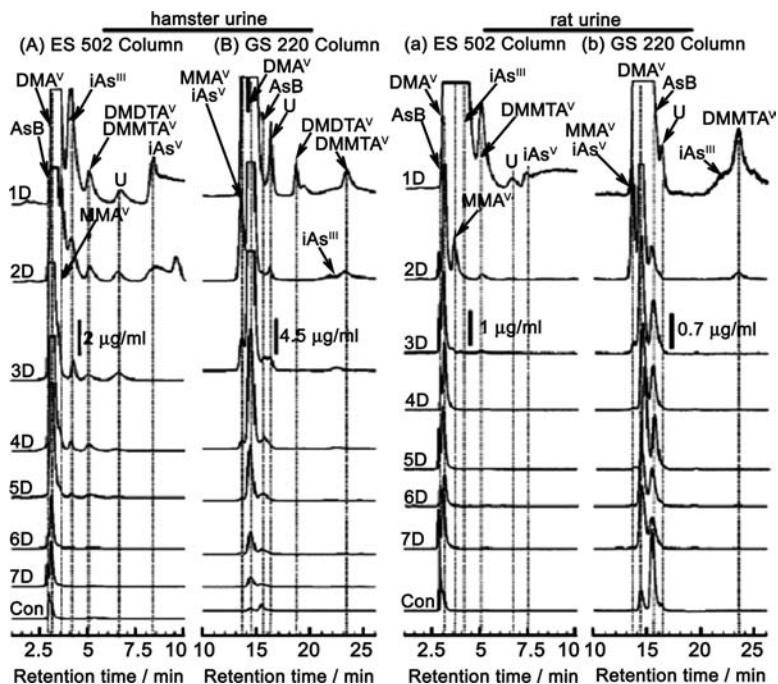


Figure 4.18 Time related changes in the arsenic distribution in urine after a single oral administration of arsenite to hamsters and rats by HPLC-ICP-MS on gel filtration and anion exchange columns. 24 h urine was collected daily for seven days (1–7 D). The distributions of urinary arsenic metabolites in hamsters (A and B) and rats (a and b) were determined on an anion exchange ES-502N7C column (A and a) and on a gel filtration GS-220 HQ column (B and b) by HPLC-ICP-MS. Control urine was collected from hamsters and rats administered water alone. Reprinted with permission from [37]. Copyright 2007 American Chemical Society

DMA^V were detected in both hamsters and rats. These results suggest that iAs^{III} was quickly oxidized and methylated to MMA^V and DMA^V in hamsters and rats. In fact, in rats iAs^{III} and iAs^V were detected only for the first 24 h, while in hamsters iAs^{III} and iAs^V were found for five days and two days, respectively. However, the distributions of these inorganic arsenicals were much lower than those of methylated species in both animals. The distribution of DMA^V was significantly larger than MMA^V and it was gradually excreted through seven days in both animals, Figure 4.18. It is also pointed out here that in rats AsB was detected through seven days and the excreted amount of AsB was increased in later days. In addition to arsenic species described above, the more interesting result found in Figure 4.18 is that in 24 h urine, thioarsenicals such as dimethylmonothioarsenic (DMMDTA^V) and dimethyldithioarsenic (DMDTA^V) acids were clearly detected in hamsters, and that only DMMDTA^V was in rats. These thioarsenicals disappeared in the first two or three days in both hamsters and rats. Furthermore, a new urinary arsenic metabolite, which is shown as U in the all the chromatograms in Figure 4.18, was found in both hamsters and rats, although it disappeared within two or three days after the arsenic dose. This new metabolite was subsequently identified to be monomethylmonothioarsonic acid

(MMMTA^V; CH₃As(=S)(OH)₃), which was artificially synthesized and examined by ESI-MS (electrospray ionization-mass spectrometry) [37].

As the conclusive remarks, it can be said that in hamsters arsenic does not accumulate in RBCs, and thus hamsters exhibit a more uniform tissue distribution and faster urinary excretion of arsenic than rats. Furthermore, arsenic is thiolated more in hamsters than in rats, resulting in excretion of mono- and dimethylated thioarsenicals in urine.

4.3.5 Animal Species Difference in the Uptake of Dimethylated Arsenic by Red Blood Cells

It is known that the rat is one of the most tolerant animal species [57] and that iAs^{III} is effectively transformed to DMA and arsenic mostly accumulates in red blood cells (RBCs) [58, 59]. On the other hand, hamster is one of the animal species most sensitive to arsenic, and methylation of iAs is less efficient in hamsters than in rats, which results in the low distribution in RBCs [60, 61]. According to the oral dose experiment of iAs^{III} [37], which was described in the previous section, it was found that in rats inorganic arsenic accumulated in RBCs and was excreted less in urine, while in hamsters arsenic did not accumulate in RBCs and was rapidly excreted, mainly as DMA^V in urine. In Figure 4.19, the possible reduction and methylation reactions in the metabolic pathway for inorganic arsenic in mammals, proposed by Suzuki *et al.* [62], is shown, which results in the major urinary metabolite DMA. In general, it is considered that the metabolic reactions illustrated in Figure 4.19 mostly occur in liver and detoxification processes in mammals. However, the metabolism after arsenic dose is not well understood in different animal species.

In order to elucidate the metabolism and metabolite formation reaction mechanisms in different animal species, therefore, Suzuki *et al.* carried out the study on the animal species

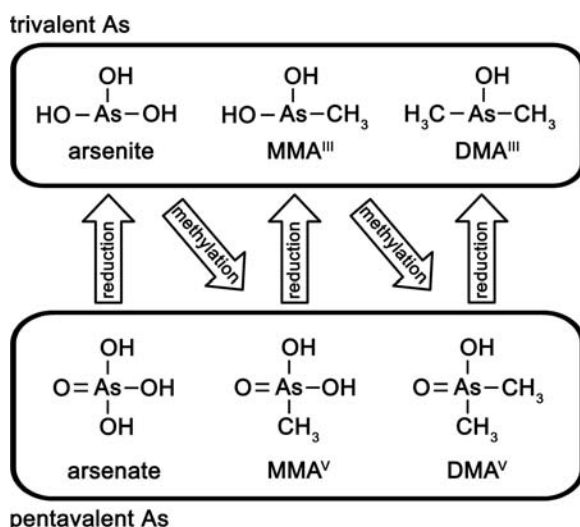


Figure 4.19 Reduction and methylation reactions in the metabolic pathway for inorganic arsenic in mammals. Reprinted with permission from [62]. Copyright 2001 American Chemical Society

difference in arsenic metabolism from the viewpoint of the mechanism underlying the distribution in the forms of arsenic in RBCs [63]. In the experiment, the uptake of dimethylarsenic species by RBCs was examined, especially in terms of DMA^{III} , which was found in human urine as well as hamster and rat urine. Since DMA^{III} is not commercially available, they prepared DMA^{III} by reduction of DMA^{V} by the method of Reay and Asher [52], as described previously. Then, DMA^{V} and DMA^{III} were incubated with rat, hamster, mouse and human RBCs and the chemical forms of arsenic were determined by HPLC/ICP-MS. The species differences in the uptake of DMA^{V} and DMA^{III} by rat (A), hamster (B), mouse (C) and human (D) RBCs *in vitro* are shown in Figure 4.20, where DMA^{V} or DMA^{III} was incubated with suspended RBCs (10% RBCs in Tris-HCl buffered saline). It is seen in Figure 4.20 that DMA^{III} is efficiently taken in RBCs in the order of rat > hamster > human > mouse but DMA^{V} was practically not or taken up slowly by RBCs of all the animal species.

The changes in the chemical forms of arsenic in the medium on incubation of DMA^{III} with rat, hamster and human RBCs were examined by HPLC/ICP-MS using an anion exchange column, which was the same as those in Figures 4.10 and 4.11. The results are shown in Figure 4.21 and it can be seen that DMA^{III} taken up by rat RBCs is effluxed as DMA^{V} very slowly, which means that DMA^{III} is retained in RBCs for long time, while DMA^{III} taken up by hamster RBCs is effluxed very quickly in the form of DMA^{V} . In addition, the uptake of DMA^{III} and efflux of DMA^{V} take place more slowly in human

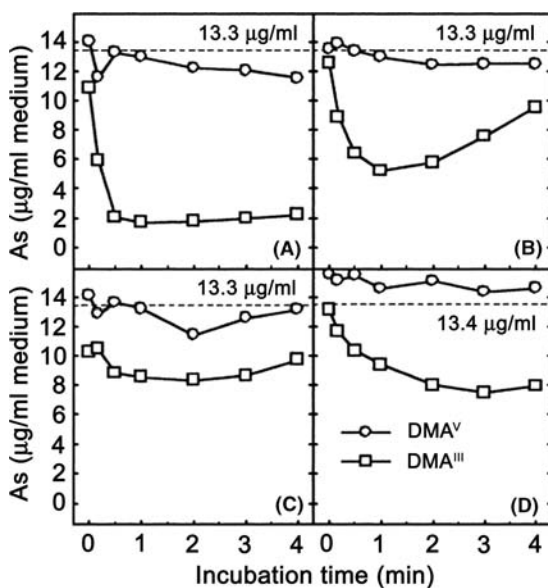


Figure 4.20 Species differences in the uptake of dimethylarsinous acid (DMA^{III}) by rat, hamster, mouse and human RBCs *in vivo*. DMA^{III} or DMA^{V} was incubated with suspended RBCs (10% RBCs in Tris-HCl buffered saline) of rat (A), hamster (B), mouse (C), and human (D) origin, and the concentration of arsenic was plotted against the incubation period. The dotted horizontal line shows the concentration of arsenic distributed evenly in the medium and RBCs. Reprinted with permission from [63]. Copyright 2001 American Chemical Society

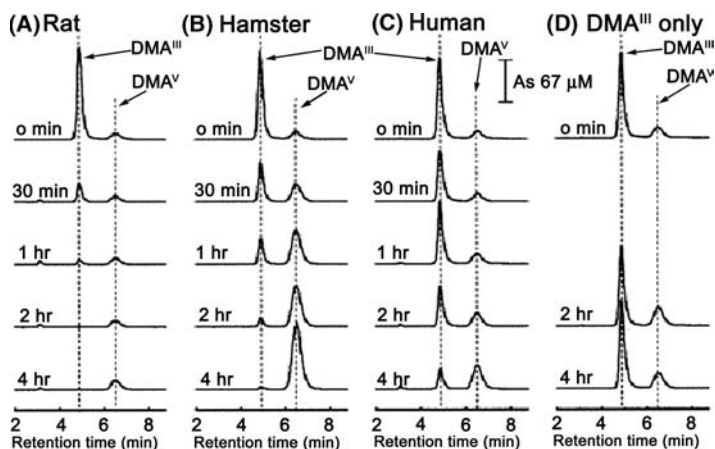


Figure 4.21 Changes in the chemical form of arsenic in the medium on incubation of DMA^{III} with rat, hamster, and human RBCs. DMA^{III} was incubated with suspended RBCs (10% RBCs in Tris-HCl buffered saline) of rat (A), hamster (B), and human (C) origin, or without RBCs in Tris-HCl buffered saline (D), at 37°C for up to 4 h, and then the distribution of arsenic in the medium was determined on a cation exchange column by the HPLC-ICP MS method. The vertical bar indicates the detection level for arsenic. Reprinted with permission from [63]. Copyright 2001 American Chemical Society

RBCs than that of rat and hamster ones. Furthermore, it should be noted here that DMA^{III} is not oxidized to DMA^{V} without RBCs (Figure 4.21D).

4.3.6 Speciation and Excretion Patterns of Arsenic Metabolites in Human Urine after Ingestion of Edible Seaweed, Hijiki

In July 28, 2004, the Food Standards Agency of UK announced the ‘Seaweed Warning’ via the internet that people should not eat one type of seaweed called *hijiki* (*Hizikia fusiformis*) because of the high levels of arsenic contained. The warning said that *hijiki* contained inorganic arsenic, a form that occurs naturally in some food and might increase the risk of developing cancer if eaten regularly. Since the Japanese daily eat a lot of *hijiki*, as it is a mineral rich health food, this warning surprised the Japanese people. So far, the possible toxicity due to arsenic in *hijiki* has been reported by several research groups [64, 65]. However, the metabolism of arsenic after ingestion of *hijiki* had not been clearly elucidated at that point. So, species distribution of seaweeds and inspection of arsenic metabolites in human urine after ingesting seaweeds were investigated by utilizing HPLC/ICP-MS [66].

In Figure 4.22, the chromatograms for the water extract samples for seaweeds (*hijiki* and *wakame*) are shown together with that for eight arsenic standard compounds. Arsenic compounds were separated with ion-pair HPLC using an ODS column (L-column, 250 mm \times 4.6 mm i.d.; Chemicals Evaluation and Research Institute, Tokyo, Japan) in a similar manner to those in Figures 4.7 and 4.8 and arsenicals were detected by ICP-MS using ^{75}As . As shown in Figure 4.22a, all 8 arsenic standard compounds of iAs^{V} (11.6 ng/ml), iAs^{III} (15.4 ng/ml), MMA^{V} (10.4 ng/ml), DMA^{V} (11.6 ng/ml), AsB (11.8 ng/ml), TMAO (9.9 ng/ml), TeMA (9.5 ng/ml), and AC (9.9 ng/ml), were detected separately (the numbers

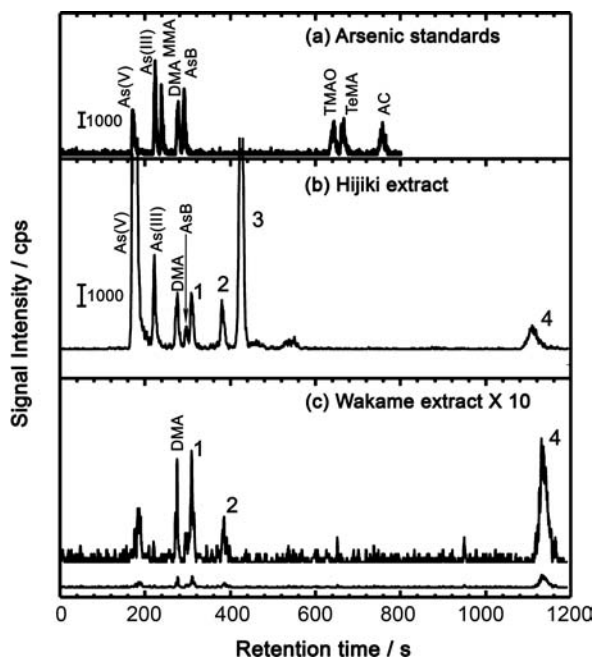


Figure 4.22 Chromatograms for the seaweed extracts obtained by HPLC/ICP-MS with the detection of ^{75}As . (a) arsenic standard compounds (10 ng of As/g each), (b) hijiki extract, (c) wakame extract. An ODS column (L-column, 250 mm \times 4.6 mm i.d.) was used in ion-pair mode with the use of the same mobile phase as described in Figure 4.7. Reprinted with permission from [66] Copyright 2005 The Chemical Society of Japan

in parentheses indicate the concentrations of arsenic species as As). From the retention times for arsenic standards observed in Figure 4.22a), As^{V} , As^{III} , DMA^{V} and AB were identified in *hijiki*, while only DMA^{V} was in *wakame*. It is also seen in Figure 4.22 that the content of arsenic in *wakame* was significantly lower than that in *hijiki*. In addition to the peaks identified above, several peaks, which are numbered as 1, 2, 3, and 4 in Figure 4.22b) and (c), were detected in the chromatograms for *hijiki* and *wakame* extracts. Since the retention times of the numbered peaks are not consistent with any of the retention times for arsenic standards, they have not been identified yet. Even so, the present authors' group speculates from the observation of ESI-MS spectra that those unidentified peaks might be due to arsenosugar compounds [28]. Further investigation is really required for identification of the numbered peaks in Figure 4.22b) and (c).

In fact, iAs^{V} was contained only in *hijiki*, as was warned by the Food Standards Agency, UK, while other seaweeds such as *wakame* and *konbu* contained only small amounts of DMA^{V} , Figure 4.22. Since Japanese people eat *hijiki* regularly and/or daily, the dietary test was carried out in order to elucidate the arsenic metabolites after ingesting seaweed by using the urine samples [65]. In the test, 15 male volunteers (most of them were university students) were divided into three groups (five in each); Group (a) ingested *hijiki*, Group (b) ingested *wakame*, and Group (c) did not ingest any seaweed. Only volunteers in Group (a) ingested 15 g (dry weight) of *hijiki* (containing about 0.9 mg of arsenic) once which was

cooked after being kept in water for about 1 h. After ingestion of *hijiki* ($t=0$ h), urine samples were collected from all volunteers at 3–5 h time intervals for the following three days. During the experimental period, all group members ate the same meals with low arsenic food for three days. The urine samples before ingestion were also collected to determine the background arsenic level. All urine samples were filtered with the membrane filters and stored at 4 °C until analysis by HPLC/ICP-MS.

The chromatograms of arsenic metabolites in human urine for three days after ingestion of *hijiki* are shown in Figure 4.23. First, it is noted that the chromatograms for the urine samples collected from the volunteers without ingestion of any seaweed were almost the same in the excretion patterns of arsenic metabolites in urine through the experimental days, although small peaks of iAs^V , MMA^V , DMA^V and AsB were always observed. In the case of Group (b), who ingested *wakame*, the peak of DMA^V significantly increased until 21 h after ingestion, but it gradually decreased down to the background level. As is seen in Figure 4.22, *wakame* contains DMA^V and thus it may be reasonable to consider that DMA^V in *wakame* was gradually excreted as the metabolite in urine. Other arsenic species did not show any change in the excretion pattern in urine from Group (b).

In the case of Group (c), the time dependent chromatograms for urine samples showed very complicated excretion patterns (Figure 4.23a). Inorganic arsenic (iAs^V) was certainly detected and it provided the highest concentration among arsenic species in the first 3 h, although the result is not shown in Figure 4.23. As shown in Figure 4.23a, however, after 7 h, iAs^{III} became at the higher level than iAs^V and the methylated arsenic species such as MMA^V and DMA^V appeared on the chromatogram. Furthermore, 27 h later, the concentration of DMA^V was significantly high, compared to other arsenic species in urine. These results suggest that the arsenic metabolite formation reactions due to reduction and

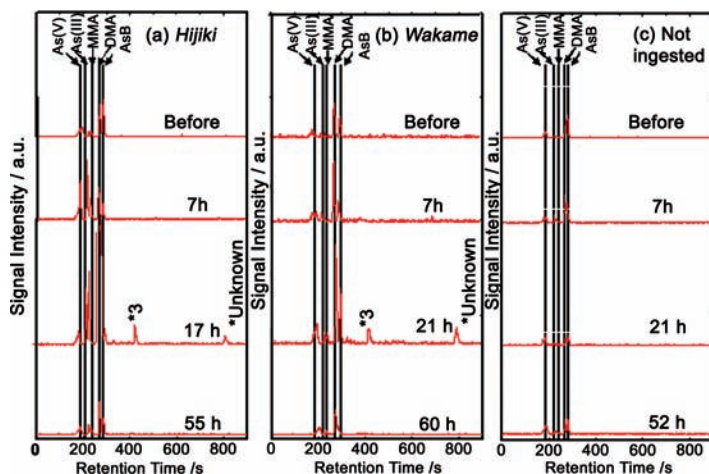


Figure 4.23 Time dependent chromatograms for urine samples from volunteers with and without ingestion of seaweeds. (a) *Hijiki* ingested, (b) *wakame* ingested, (c) seaweed not ingested. The time shown in the figures indicates the sampling time after ingestion of seaweeds. The peak of *3 is the same peak as the unknown peak of *3 in Figure 4.22, and the peak of *Unknown was a newly appeared one in this experiment. Reprinted with permission from [66] Copyright 2005 The Chemical Society of Japan

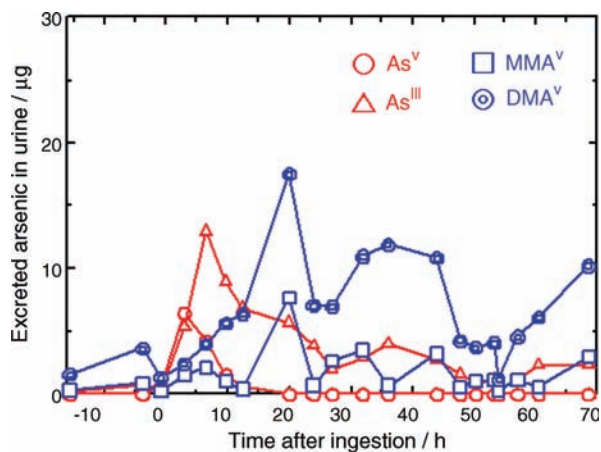


Figure 4.24 The time dependent changes of the amounts of excreted arsenic species in human urine after ingestion of hijiki. Reprinted with permission from [66] Copyright 2005 The Chemical Society of Japan

methylation in liver also occur in human body and that DMA^V is excreted as the major urinary arsenic metabolite, as described in Figure 4.19. As discussed in Sections 4.7 and 4.8, it is considered that DMA^{III} may be produced in liver and effluxed into the blood stream but DMA^{III} was not detected in the present experiment. One reason is that the lifetime of DMA^{III} is short because it is efficiently taken up by RBCs. Another reason is that the research group who conducted the experiment had no DMA^{III} and MMA^{III} standards, and so the existence of these species could not be examined. From the experimental results shown in Figure 4.23, it can be concluded that most of arsenic taken up with *hijiki* as well as other seaweeds is excreted in urine within three days after ingestion. However, if we examine the results carefully, we can find another slow excretion pathway. The longer time dependent changes of the amounts of excreted arsenic species in urine is shown in Figure 4.24. It is seen from Figure 4.24 that DMA^V is increasingly excreted again after 60 h. As discussed in Section 4.8, DMA^{III} excreted from liver is again taken up by RBCs and retained there for quite long time.

The mechanisms underlying the uptake and retention of dimethylated arsenicals (DMAs) by red blood cells (RBCs), which was proposed by Suzuki from the study on animal species difference in the uptake of dimethylated arsenical by RBCs, introduced in Section 4.8, is shown in Figure 4.25 [63]. It is understood from the pathway for the arsenic metabolism in Figure 4.24 that inorganic As is taken into liver, in which reduction and methylation of inorganic As occur, and then DMA^{III} is effluxed into blood stream and RBCs uptake it immediately. In RBCs, DMA^{III} is oxidized by reacting with glutathione (GSH) to produce DMA^V, which is again effluxed into blood stream and excreted in urine through kidney. It is also suggested as is seen in Figure 4.25 that the part of DMA^{III} binds with reduced protein in RBCs. The existences of the conjugates of methylated arsenicals with GSH and protein-binding molecules of arsenic are proved by detecting such species with HPLC/ICP-MS [36, 67, 68].

After the reactions with GSH and proteins in RBCs, as is shown in Figure 4.25, arsenic is excreted as DMA^V in urine. The processes take time and retain arsenic before excretion

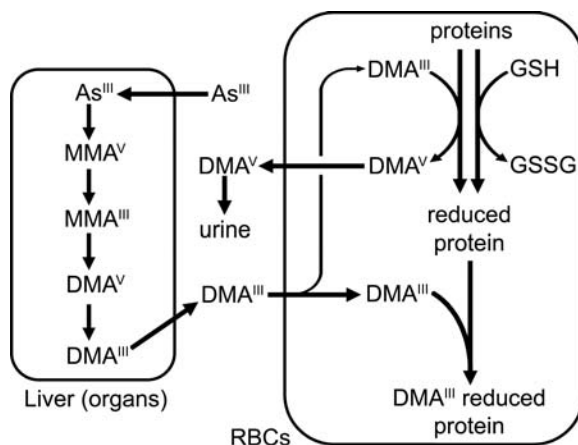


Figure 4.25 Proposed mechanisms underlying the uptake and retention of dimethylated arsenic (DMAs) by red blood cells (RBCs). Reprinted with permission from [63]. Copyright 2001 American Chemical Society

in urine. Thus, the delayed excretion of DMA^{V} , shown in Figure 4.24, may be interpreted by this pathway through RBCs. Other cells in various organs of human body may also contribute to arsenic metabolism, as is discussed in Section 4.7. The possible existence of protein binding arsenic was also suggested from the experimental results for arsenic in salmon egg cell cytoplasm in Section 4.4.

4.4 Summary

In this chapter, metallomics research, a newly emerging scientific field in life science was introduced with emphasis on the importance of chemical speciation as well as the distributions of the metal and metalloid elements in biological systems. The recent progress in the studies on the metabolism of arsenic in biological cells and systems (mammals) was introduced mainly in relation to speciation of arsenic metabolites, which were detected by HPLC/ICP-MS. The important findings in these studies are the elucidation of metabolic pathways, in which inorganic arsenic is reduced and methylated and mainly excreted in urine as DMA^{V} . Also, part of arsenic ingested by drinking water or food is converted to the conjugated forms of GSH (glutathione) bound arsenic ($\text{iAs}(\text{GS})_3$ and $\text{CH}_3\text{As}(\text{GS})_2$) [36], which are excreted in feces through bile, although such mechanisms are not interpreted in this chapter.

In general, we think that inorganic arsenic is toxic and carcinogenic and that the methylation of inorganic arsenic is the detoxification mechanism in biological systems. However, Suzuki *et al.* suggested that DMA^{III} may be more responsible for arsenic carcinogenesis because it produces reactive oxygen species (ROS) which may cause DNA damage *in vivo* [67]. Thus, it is desirable that more detailed studies on the metabolism of arsenic should be carried out to elucidate arsenic toxicity in humans as well as various animals. The HPLC/ICP-MS system will contribute as one of the most powerful tools to such studies in future.

Acknowledgements

In this chapter, the author has cited much literature published by Professor Kazuo T. Suzuki and his research group members because of their excellent and advanced works on arsenic metabolism in biological systems. I express my sincere thanks to Prof. Suzuki, who also gave me many valuable suggestions and advice in metallomics research from the beginning. Unfortunately, however, he passed away on July 25, 2008 at the age of 65. I would like to dedicate this chapter to the late Prof. Kazuo T. Suzuki with my great sorrow as well as my great respect.

References

1. Haraguchi, H. and Matsuura, H. (2003) *Proceedings of the International Symposium on Bio-trace Elements. 2002 (BITREL 2002)* (eds S. Enomoto and Y. Seko), The Institute of Physical and Chemical Research (RIKEN), Wakov, pp. 3–8.
2. Haraguchi, H. (2004) *Journal of Analytical Atomic Spectrometry*, **19**, 5–14.
3. Jakubowski, N., Lobinski, R., and Moens, L. (2004) *Journal of Analytical Atomic Spectrometry*, **18**, 1–4.
4. Koppelaar, D.W. and Hieftjie, G.M. (2007) *Journal of Analytical Atomic Spectrometry*, **22**, 855.
5. Szpunar, J. (2004) *Analytical and Bioanalytical Chemistry*, **19**, 54–56.
6. Haraguchi, H. (2008) *Pure and Applied Chemistry*, **80**, iv.
7. Caruso, J. (2010) *Metallomics*, **2**, 103.
8. Szpunar, J. (2005) *Analyst*, **130**, 442–465.
9. Haraguchi, H. (2005) *Biomedical Research on Trace Elements*, **16**, 217–232.
10. Sanz-Medel, A. (2005) *Analytical and Bioanalytical Chemistry*, **381**, 1–2.
11. Gonzalez-Fernandez, M., Garcia-Barrera, T., Jurado, J. *et al.* (2008) *Pure and Applied Chemistry*, **80**, 2609–2626.
12. Shi, W. and Chance, M.R. (2008) *Cellular and Molecular Life Sciences*, **65**, 3040–3048.
13. Mounicou, S. and Lobinski, R. (2008) *Pure and Applied Chemistry*, **80**, 2565–2575.
14. Mounicou, S., Szpunar, J., and Lobinski, R. (2009) *Chemical Society Reviews*, **38**, 1119–1138.
15. Lobinski, R., Sabine Becker, J., Haraguchi, H., and Sarkar, B. (2010) *Pure and Applied Chemistry*, **82**, 493–504.
16. Haraguchi, H. (1999) *Bulletin of the Chemical Society of Japan*, **72**, 1163–1186.
17. Szpunar, J., Lobinski, R., and Prange, A. (2003) *Pure and Applied Chemistry, Applied Spectroscopy*, **57**, 102A–112A.
18. Sanz-Medel, A., Montes-Bayon, M., and Fernandez Sanchez, M.L. (2003) *Analytical and Bio-analytical Chemistry*, **377**, 236–247.
19. Haraguchi, H., Ishii, A., Hasegawa, T. *et al.* (2008) *Pure and Applied Chemistry*, **80**, 2565–2575.
20. Hasegawa, T. (2006) Ph. D. Thesis, Nagoya University.
21. Vandecasteele, C. and Block, C.B. (1991) *Modern Methods for Trace Element Determination*, John Wiley & Sons, Ltd, Chichester.
22. Montaser, A. (ed.) (1998) *Inductively Coupled Plasma Mass Spectrometry*, John Wiley & Sons, Inc., New York.
23. Noddack, I. (1936) *Angewandte Chemie*, **47**, 835–852.
24. Kuroda, P. (1982) *The Origin of the Chemical Elements and the Okhlo Phenomenon*, Springer-Verlag, Berlin.
25. Templeton, D.M., Ariese, F., Cornelis, R. *et al.* (2000) *Pure and Applied Chemistry*, **72**, 1453–1470.
26. Braman, R.S. and Foreback, C.C. (1973) *Science*, **182**, 1247–1249.
27. Andrae, M.O. (1977) *Analytical Chemistry*, **49**, 820–823.
28. Morita, M., Uehiro, T., and Fuwa, K. (1981) *Analytical Chemistry*, **53**, 1806–1808.

29. Shibata, Y. and Morita, M. (1989) *Analytical Sciences*, **5**, 107–109.
30. Morita, M. and Shibata, Y. (1990) *Applied Organometallic Chemistry*, **4**, 181–190.
31. Shibata, Y. and Morita, M. (1992) *Applied Organometallic Chemistry*, **6**, 343–349.
32. Edmonds, J.S., Shibata, Y., Francesconi, K.A. *et al.* (1992) *The Science of the Total Environment*, **122**, 321–335.
33. Mandal, B.K., Ogra, Y., Inazai, K., and Suzuki, K.T. (2004) *Toxicology and Applied Pharmacology*, **198**, 307–318. Other references are therein.
34. Mandal, B.K., Ogra, Y., and Suzuki, K.T. (2001) *Chemical Research in Toxicology*, **14**, 371–378.
35. Suzuki, K.T. (2005) *Analytica Chimica Acta*, **540**, 71–76.
36. Naranmandura, H., Suzuki, N., and Suzuki, K.T. (2006) *Chemical Research in Toxicology*, **19**, 1010–1018.
37. Naramandura, H., Suzuki, N., Iwata, K. *et al.* (2007) *Chemical Research in Toxicology*, **20**, 616–624.
38. Matsuura, H., Kuroiwa, T., Inagaki, K. *et al.* (2004) *Biomedical Research on Trace Elements*, **15**, 37–41.
39. Inagaki, K., Umemura, T., Matsuura, H., and Haraguchi, H. (2000) *Analytical Sciences*, **16**, 787–788.
40. Hasegawa, T., Asano, M., Takatani, K. *et al.* (2005) *Talanta*, **68**, 465–469.
41. Wu, M.M., Kuo, T.L., Hwang, Y.H., and Chen, C.J. (1989) *American Journal of Epidemiology*, **130**, 1123–1132.
42. Smith, A.H., Hopenhayn-Rich, C., Bates, M.N. *et al.* (1992) *Environmental Health Perspectives*, **97**, 259–267.
43. Chen, C.J., Chen, C.W., Wu, M.M., and Kuo, T.L. (1992) *British Journal of Cancer*, **66**, 888–892.
44. Mandal, B.K. and Suzuki, K.T. (2002) *Talanta*, **58**, 201–235.
45. Chatterjee, A., Das, D., Chowdhury, T.R. *et al.* (1995) *Analyst*, **120**, 643–650.
46. Chowdhury, U.K., Biswas, B.K., Chowdhury, T.R. *et al.* (2000) *Environmental Health Perspectives*, **108**, 393–397.
47. Tam, G.K.H., Charbonneau, S.M., Bryce, F. *et al.* (1979) *Toxicology and Applied Pharmacology*, **50**, 319–322.
48. Buchet, J.P., Lauwerys, R., and Roels, H. (1981) *International Archives of Occupational and Environmental Health*, **49**, 71–79.
49. Fao, V., Colombi, A., Maroni, M. *et al.* (1984) *The Science of the Total Environment*, **34**, 241–259.
50. Cullen, W.R., McBride, B.C., and Reglinski, J. (1984) *Journal of Inorganic Biochemistry*, **21**, 179–194.
51. Cullen, W.R., McBride, B.C., manji, H. *et al.* (1989) *Applied Organometallic Chemistry*, **3**, 71–78.
52. Reay, P.F. and Asher, C.J. (1977) *Analytical Biochemistry*, **78**, 557–560.
53. Fujisawa, S., Ohno, R., Shigeno, K. *et al.* (2007) *Cancer Chemotherapy and Pharmacology*, **59**, 485–493.
54. Yoshino, Y., Yuan, B., Miyashita, S. *et al.* (2009) *Analytical and Bioanalytical Chemistry*, **393**, 689–697.
55. Hasegawa, T., Fukumoto, Y., Ishise, J. *et al.* (2007) *Bulletin of the Chemical Society of Japan*, **80**, 329–334.
56. Hasegawa, T., Ishise, J., Fukumoto, Y. *et al.* (2007) *Bulletin of the Chemical Society of Japan*, **80**, 498–502.
57. Vahter, M. (2000) *Science Progress*, **82**, 69–88.
58. Vahter, M., Marafante, E., and Dencker, L. (1984) *Archives of Environmental Contamination and Toxicology*, **13**, 259–264.
59. Lerman, S. and Clarkson, T.W. (1983) *Fundamental and Applied Toxicology*, **3**, 309–314.
60. Yamauchi, H. and Yamamura, Y. (1985) *Toxicology*, **34**, 113–121.
61. Marafante, E. and Vahter, M. (1987) *Environmental Research*, **42**, 72–82.
62. Suzuki, K.T., Tomita, T., Ogra, Y., and Ohmichi, M. (2001) *Chemical Research in Toxicology*, **14**, 1604–1611.
63. Shiobara, Y., Ogra, Y., and Suzuki, K.T. (2001) *Chemical Research in Toxicology*, **14**, 1446–1452.

64. Watanabe, T., Hirayama, T., Takahashi, T. *et al.* (1979) *Toxicology*, **14**, 1–22.
65. Yamauchi, H. and Yamamura, Y. (1979) *Japanese Journal of Industrial Health*, **21**, 47.
66. Matsuura, H., Asano, M., Hasegawa, T. *et al.* (2005) *Bulletin of the Chemical Society of Japan*, **78**, 1977–1981.
67. Naranmandura, H., Ibata, K., and Suzuki, K.T. (2007) *Chemical Research in Toxicology*, **20**, 1120–1125.
68. Naranmandura, H. and Suzuki, K.T. (2008) *Chemical Research in Toxicology*, **21**, 678–685.

Arsenic in Traditional Chinese Medicine

Kui Wang, Siwang Yu and Tianlan Zhang

*Department of Chemical Biology, School of Pharmaceutical Sciences,
Peking University, Beijing 100191, P.R. China*

5.1 Arsenic Bearing Minerals and their Clinical Applications

5.1.1 Introduction

Traditional Chinese Medicine (TCM), due to the assimilating of the concepts of Chinese alchemy during its development, has a long history in using minerals as therapeutic agents. Later on, in modern clinical trials their therapeutic as well as toxic effects were ‘rediscovered’. Based on clinical experiences accumulated for several centuries, the ancient TCM practitioners outlined a series of principles, one of which is ‘using poison to combat poison’. Poison, differing from the modern toxicological concept, includes various exogenous and endogenous pathogens in TCM, such as virus, microbes, toxins, inflammation mediators, carcinogens and so on. Thus, a classical TCM strategy, ‘elimination or removal of *poison* and its impact’ has been followed to treat infection, inflammation and endotoxin induced symptoms, even cancers. Based on such a strategy, several toxic minerals, including three arsenic based minerals (ABMs), realgar, orpiment and arsenolite, were used in TCM to target the ‘poisons’. Among the three ABMs, realgar is still frequently used in TCM today, whereas arsenolite is seldom used due to its fatal toxicity. However, since an arsenolite containing composite Ailing-1 was successfully applied clinically in the treatment of acute promyelocytic leukaemia (APL) [1], arsenic was put under the spotlight. Arsenious trioxide (ATO) became more appealing to the researchers after the disclosure of its underlying mechanism of anticancer activity [2] and its approval by FDA for the treatment of relapsed and refractory APL [3]. Its anti-asthma and anti-inflammatory activities also attracted some

researchers' interest. It should be mentioned, however, that ABMs have rarely been used alone. Instead, they were mostly combined with herbs as adjuvant in the forms of composites, which are supposed to improve the activity and to minimize the adverse effects. It is hard to know how many composites containing realgar, orpiment or arsenolite had emerged and how many had vanished in the past hundreds of years. However, several long experienced ABM containing composites are still in use (Table 5.1).

From Table 5.1, we noted that an ABM was used with a variety of herbs in different composites for the treatment of different diseases. Since the therapeutic effect of a composite is the integrated outcome of all the ingredients, the role of an ABM in certain composites is hard to define. Nevertheless, intensive studies have demonstrated the anticancer activity of arsenolite (or ATO) and the underlying mechanisms of the action have also been revealed. Realgar exhibits similar anticancer activity and probably shares the same mechanism as ATO. Besides their anticancer activities, several composites were prescribed to treat the symptoms related to inflammation, brain damage, asthma and so on. However, it is not clear why they exert such therapeutic effects and may warrant further studies.

In exploration of the medical application of ABMs, their toxicity is an unavoidable issue. In the early days, arsenic compounds had been widely used in medical practice for chemotherapy. But with increased knowledge on arsenic toxicity and the development of antibiotics, arsenicals were gradually withdrawn from the drug market and finally almost abandoned. Moreover, in the past two decades, ABMs and other heavy metal containing minerals used in TCM composites were subject to huge controversies and challenges over their potential toxicity and their applications were restricted by formally issued regulations [4]. Thus development of arsenic containing TCM fell in a dilemma. Should these minerals be removed from the composite formulations or not? It has been a controversy for a long time, although these mineral components are toxic, they have long been regarded as major active ingredients. However, numerous studies on the therapeutic effects of ABMs for the treatment of APL as well as their mechanisms of action have been driven by successful approval of ATO by FDA, which have changed people's view on ABMs tremendously. Nevertheless, the toxicity of ATO is still a serious problem. Perhaps it was ingenious to use

Table 5.1 *Several ABM containing TCM composites*

ABM Containing Composites	ABM	Pharmacological Effects
<i>Niu Huang Bao Long Wan</i>	Realgar	Inflammation, high fever, unconsciousness, convulsion
<i>Niu Huang Qing Xin Wan</i>	Realgar	Stroke, coma, apoplexy, cerebral embolism
<i>Niu Huang Jie Du Pian</i>	Realgar	Clear up 'heat' and 'poisons': inflammation, constipation
<i>Niu Huang Zhen Jing Pian</i>	Realgar	Convulsion, dysphasia, high fever
<i>An Gong Niu Huang Wan</i>	Realgar	Stroke, brain damage, encephalitis, encephalorrhagia, hemiplegia
<i>Ju Fang Zhi Bao San</i>	Realgar	Fever, convulsion
<i>Zi Jin Dan</i>	Arsenolite	Asthma, excessive phlegm
<i>Ai Ling 1</i>	Arsenolite	Cancer

the scarcely soluble realgar or orpiment as relatively safe substitutes of ATO. This is an important reason that both the applications and researches on realgar composites are still of interest.

5.1.2 Arsenolite and its Clinical Applications in Traditional Chinese Medicine (TCM)

5.1.2.1 General Description of Arsenolite

Arsenolite (by Chinese, *Pi Shi*; *Pi* = arsenic and *Shi* = stone) is the naturally occurred crystallized arsenic trioxide with a composition of As_2O_3 but its crystal structure is in a cubic form characterized by the As_4O_6 unit as showed in Figure 5.1a.

Arsenolite is stable at room temperature. It dissolves in water slowly and forms arsenious acid species, AsO_3^{3-} , $\text{As}(\text{OH})\text{O}_2^{2-}$, $\text{As}(\text{OH})_2\text{O}^-$, $\text{As}_3\text{O}_3(\text{OH})_3$ and oligomeric $\text{As}_3\text{O}_3(\text{OH})_3$ and other related species [5]. Its solubility in pure water was determined to be 2 g per 100 g water. Both the solubility and rate of dissolving increase with increasing pH. The species existed in solution are depending on pH and the reduction potential of solution. The main species in aqueous solution under physiological conditions are $\text{As}(\text{OH})_2\text{O}^-$ and $\text{As}(\text{OH})\text{O}_2^{2-}$ as well as their oligomeric species.

Natural arsenolite had been used as *Pi Shi* in TCM but due to the rare distribution of this mineral, later on, most of *Pi Shi* used in TCM was actually substituted by the combustion product of realgar (As_4S_4). The varied amounts of residual sulfides and other contaminated minerals give *Pi Shi* a variety of colors. By repeated sublimation, *Pi Shi* is purified to be *Pi Shuang* (*Shuang* = frost), pure arsenic trioxide.

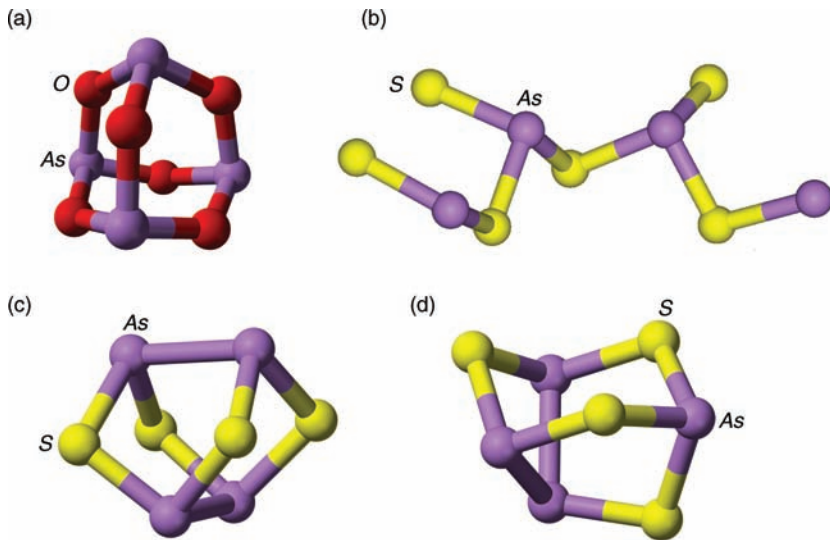


Figure 5.1 Structures of arsenicals. (a) As_2O_3 (arsenolite); (b) As_2S_3 (orpiment); (c) $\alpha\text{-As}_4\text{S}_4$ (realgar); (d) $\beta\text{-As}_4\text{S}_4$ (pararealgar). Color code: As, purple; O, red and S, yellow

5.1.2.2 Clinical Applications of Arsenolite in TCM

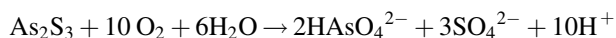
Arsenolite in TCM has experienced dramatic ups and downs. Historically, arsenolite was administered orally for the treatment of malaria, asthma and dysentery, or topically for the treatment of hemorrhoids and some dermatoses [6, 7]. In spite of the toxicity of arsenic as drugs, the TCM practitioners still kept ABMs in the traditional prescriptions but the numbers of arsenolite containing TCMs dramatically declined. The use of arsenic was revived when an arsenious acid injection was shown to be effective in the treatment of APL in 1970s and peaked by the approval of clinical use of ATO (Trisenox, pH 8 solution of ATO) by FDA in 2000 to induce remission and consolidation in APL patients who are refractory to retinoid and anthracycline chemotherapy. The effect of arsenious acid on other hematologic malignancies is also in clinical trial subsequently [8].

Another notable medical application of *Pi Shi* is to treat asthma. Arsenolite has been used in composite forms to treat asthma patients for centuries in China. Recently, *in vivo* tests have confirmed its efficacy in the treatment of asthmatic bronchial inflammation [9].

5.1.3 Realgar and Orpiment and their Clinical Applications in TCM

5.1.3.1 General Description of Realgar and Orpiment

Two naturally occurring As(III) sulfide minerals have been used in TCMs. Now realgar (*Xiong Huang*, *Xiong* = male; *Huang* = yellow) is still used in many TCMs, but orpiment (*Ci Huang*, *Ci* = female; *Huang* = yellow) is rarely used. Orpiment is a monoclinic arsenious sulfide mineral, with a chemical composition of As_2S_3 but its crystalline unit is As_4S_6 (Figure 5.1b). The realgar currently used in TCM is a monoclinic α - As_4S_4 mineral, as shown in Figure 5.1c. It is transformed to β - As_4S_4 (Figure 5.1d) upon exposure to light. Both realgar and orpiment are almost insoluble in pure water, which is the reason that they have a low toxicity. In fact a small amount of arsenic still can be leached out from realgar into water by oxidative hydrolysis:



A leaching experiment showed that as high as 1500 $\mu\text{g/g}$ of arsenic can be detected from realgar in artificial body fluids [10]. A maximum of 0.6% of the total arsenic content of realgar was found to be leached out under simulated alimentary tract conditions [11]. The dissolving of As_2S_3 can be enhanced by the presence of excess sulfide ions, giving thioarsenite species, for example, AsS_3^{3-} . Besides, As_2S_3 can be dissolved in alkaline solution by forming a mixture of thioarsenite and arsenite species, for example, AsS_3^{3-} and AsO_3^{3-} . Accordingly, a variety of arsenic species exist in the aqueous suspension of realgar.

5.1.3.2 Clinical Applications of Realgar and Orpiment in TCM

The TCM composites containing realgar can be classified into several groups according to their therapeutic actions. Realgar and realgar containing composites were used in the treatment of various tumors in ancient China and despite a lot of experiences were accumulated, the role of realgar in several anticancer TCM composites was not clear and has been overlooked until ATOs successful clinical application in the treatment of APL and

the possible mechanisms were reported [12]. Comparing with ATO, realgar, if appropriately processed to remove water soluble contaminants is almost insoluble, has low toxicity, and so is suitable for oral administration. ATO has been found to inhibit proliferation and induce apoptosis in APL cell line NB4 and HL60 [13], all-trans retinoic acid resistant acute promyelocytic leukaemia MR2 cells [14], K562 cells [15], human breast cancer cells MCF-7 [16], human lung adenocarcinoma cancer cells SPC-A-1 [17] and liver cancer cells BEL7402 [18]. Realgar was also found to induce apoptosis, to inhibit tumor growth and angiogenesis of transplanted ovarian SKOV3 carcinoma cells in nude mice [19].

Composite Huang Dai Pian (Tablet), in which realgar is incorporated with *Indigo naturalis*, *Salvia miltiorrhiza*, and *Radix psudostellariae*, exhibited a similar efficacy to APL compared with ATO injection [20, 21], but it is orally administratable. The mechanistic study of the synergic action of realgar and *indigo naturalis* significantly enhanced our understanding of not only anticancer action of realgar, but also the working principle of TCM [21]. The realgar containing formulae were known to be effective against both leukaemia and several solid tumors (*vide post*). Other than this, a number of antipyretic and anti-inflammatory composites containing realgar are still the first choices in the treatment of symptoms associated with inflammatory responses, such as Liu Shen Wan, Zhi Bao Dan, and so on. The anti-inflammatory action was preliminarily attributed to the inhibition of excess release of inflammatory factors [22]. Realgar is also used with cinnabar (mercury sulfide) and a number of herbs as composites to control inflammation and protect cells, such as An Gong Niu Huang Wan, Niu Huang Jie Du Pian, and so on. An Gong Niu Huang Wan is used to ‘wake up the brain’ of patients in coma and unconsciousness after ischemic and inflammatory brain injury. Niu Huang Jie Du Pian, according to the ‘endogenous heat and poison’ TCM theory, is used to clear up the heat and poison. In the terms of Western medicine, its effect is likely exerted on the enterotoxin induced inflammation, and so on. Zi Jin Ding, composed of realgar, cinnabar and several herbs, is a classical composite for dysentery treatment, in which realgar is thought to be employed as an anti-inflammatory and bactericidal agent.

5.1.4 Processing of Arsenic Bearing Minerals

Practically, the mineral drugs, prior to being used to prepare TCM composites should be processed by traditional methods to remove the contaminated substances, reduce toxicity and improve bioavailability. A variety of methods have been adopted depending on the properties of individual ABMs and the purposes to use.

5.1.4.1 Processing of Arsenolite

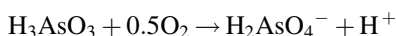
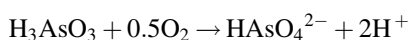
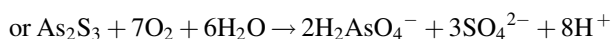
The processing of arsenolite is carried out mainly for the purpose of purification. By traditional procedures, the crude arsenolite (in TCM, raw *Pi Shi*) was heated in a sealed vessel with or without other materials and the solid residues were collected and pulverized after being cooled down. This was used as calcined *Pi Shi*. By sublimation of raw arsenolite, pure arsenious trioxide was prepared and used as ‘*Pi Shuang*’ (*Shuang* = ‘frost-like powder’). Nowadays, *Pi Shuang* was prepared from arsenic sulfide or arsenopyrite minerals by the combustion method. Further processing of *Pi Shi* or *Pi Shuang* is necessary for preparation of composites. Several special methods for preparing orally administrable *Pi Shi* have been documented in ancient manuals. According to ‘*Pu Ji Ben Shi Fang*’, a

classical manual first published during the Song Dynasty, *Pi Shi* was powdered with fermented soybeans (*Dou Chi*) to reduce toxicity, which was recently attributed to the binding of arsenic to mercapto compounds in fermented beans [23].

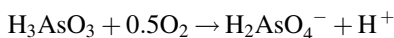
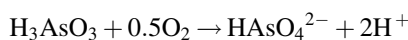
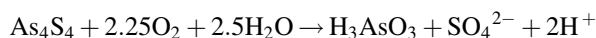
5.1.4.2 Processing of Realgar and Orpiment

The processing of realgar and orpiment is necessary in order to prepare the ultrafine particles of these ABMs and to remove the soluble toxic contaminants. The most important toxic contaminants are ATO related species, which are produced from oxidation of arsenic sulfides when exposed to air. A traditional procedure was known as ‘*Shui Fei*’ (*Shui* = water; *Fei* = float), and a grinding-in-water method has been developed for this purpose. Briefly, the shivers of the arsenic sulfides are ground under water until a certain amount of fine particles are floating on water surface. The suspension of floating particles is collected and the residues are ground underwater again. After repeated grinding and floatation, the suspensions collected are combined. The particles settled down are then collected and ready for use. Provided there is an adequate amount of water, As_2O_3 and other soluble impurities will be substantially removed. By following such a procedure, particles as small as a few hundred nanometers in diameter can be obtained. Recently, the ‘*Shui Fei*’ method has been improved by utilization of modern techniques, for example, nanoparticles of realgar have been prepared with a microfluidizing equipment [24, 25] or by grinding in a ball mill in an aqueous medium [26–28]. Alcohol, vinegar or edible oil have been used to replace water, however, most of them have been abandoned.

Even in laboratory, the method employed to process insoluble ABMs is still an inevitable and intriguing issue. Several approaches have been applied to render the insoluble ABMs ‘soluble’ in water. By whatever means, though a small fraction of the sulfide was ‘dissolved’, it has been doubtlessly transformed into a new chemical species. The Trisenox solution is prepared by dissolving solid ATO in sodium hydroxide, follow by adjusting pH to 7.9. Similarly, realgar or orpiment was dissolved in NaOH solution and the solution was then neutralized with acid [21]. Such a chemical treatment will allow realgar and orpiment to be transformed to arsenites and arsenates via oxidative hydrolysis in aqueous media. The reactions involved in orpiment dissolution were described as follows [29]:



For realgar [30], similar reactions are involved as follows:



The dissolving process is pH dependent, thus treatment with sodium hydroxide solution facilitates arsenite/arsenate formation. Once oxidized, the reaction can hardly be reversed by addition of acid. Therefore, the results obtained vary in different processing methods, which might result in different conclusions.

5.2 Metabolism and Pharmacokinetics of Arsenic Bearing Minerals

It is known that the metabolism of arsenic compounds plays important roles in both their activities and toxicities. In fact, the anticancer activity of arsenic compounds is mechanistically correlated with their carcinogenicity/toxicity, and arsenic metabolites exhibit dual effects on both sides. Thus, to understand the metabolism and pharmacokinetics of ABMs is essential for the identification of the active species and rational design of arsenic drugs. The metabolism of arsenic compounds has been studied from different starting points for various purposes, which is likely to provide an insight into the understanding of metabolism of ABMs. Indeed, the metabolism and active species of arsenolite are practically the same with that of chemical arsenic trioxide, which has been studied in depth by environmental scientists and toxicologists. But so far little is known on the metabolism of realgar and orpiment and it is ambiguously described based on the knowledge of soluble arsenic compounds.

It is notable that all the absorption-distribution-metabolism-excretion (ADME) behaviors and biological effects of arsenic compounds are determined by their three chemical properties: sulfur affinity, reversible two-electron As(III)-As(V) redox and the similarity between arsenate and phosphate anions.

5.2.1 Arsenolite and Arsenic Trioxide

5.2.1.1 Cell Uptake

In general, cell uptake of a soluble electrolyte depends on its speciation, which in turn depends on pH and other conditions. In neutral aqueous ATO solution, the dominating species is the uncharged free arsenious acid, $\text{As}(\text{OH})_3$, which can cross the plasma membrane readily and appear in cytosol [31–33]. Based on this, arsenious acid was previously hypothesized to enter eukaryotic cells by simple diffusion. However, recent studies suggested that the diffusion is facilitated by the mammalian aquaglyceroporins, aquaporin isozyme 7 and 9 (AQP7 and AQP9) [34–36]. Such a mechanism is supported theoretically by the similarity in the charge distribution of $\text{As}(\text{OH})_3$ to glycerol molecules [37]. In relation to this, the expression of AQP9 in APL cells was found higher than that in other leukemic cell types and this may account for the higher sensitivity of the APL cells to arsenious acid than the others [38]. An additional evidence is that uptake of arsenic from a TCM formula by NB4 cells was enhanced by the herbal ingredients which upregulated the AQP9 [21]. A small amount of arsenate is produced during the dissolution of ABMs by the oxidation of As(III), thus the uptake of arsenate species cannot not be overlooked. Differing from arsenious acid, the dominant forms of arsenic acid in aqueous solution at physiological pH are anionic forms, for example, $\text{AsO}_2(\text{OH})_2^-$ and $\text{AsO}_3(\text{OH})^{2-}$. These arsenate species

were presumed to enter the cells as analogs of phosphate species via phosphate transporters [32, 39, 40].

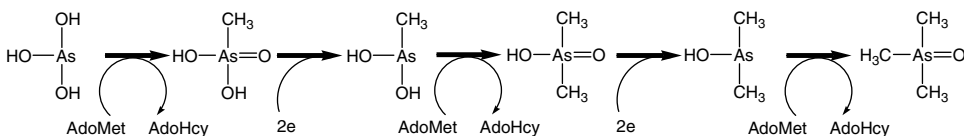
In summary, As(III) enters the cells in the form of $\text{As}(\text{OH})_3$, mainly by AQP7/9 facilitated diffusion, but As(V), in forms of anionic arsenate, enters via the phosphate transporter system. It should be mentioned, however, that these behaviors and the transport systems might be different for different cells.

5.2.1.2 Metabolism and Excretion of Arsenic

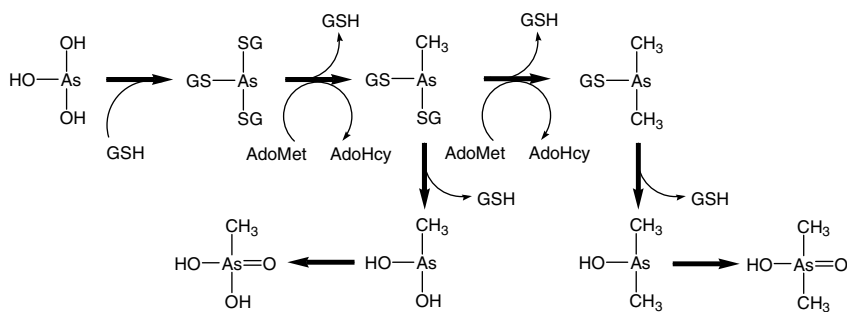
The arsenic metabolism has been studied in detail in relation to its toxicity and environmental impact. To review the results of these toxicological studies is beyond the scope of this chapter. But, in order to understand the behaviors of ABMs on the basis of these achievements, it is necessary to summarize the pathways of metabolism and excretion of arsenite and arsenate at first [41, 42]. The absorbed arsenate and arsenite are metabolized mainly in liver and converted into a series of methylated and glutathione (GSH)-conjugated species and thioarsenicals [43–45], which have recently been detected in human urine [46]. Previously, the methylation of inorganic arsenicals was thought to be a detoxification pathway, but latterly it was found that the relative toxicity of different methylated arsenicals forms exhibit rather different toxicities, methylated arsenic species in many cases are more toxic [47, 48], which might be the active species of both cytotoxicity and toxicity. In the course of metabolism in hepatocytes, inorganic arsenite is transformed into intermediate methylated As(III)/As(V) species and their GSH conjugates, $\text{As}(\text{SG})_3$, $(\text{CH}_3)\text{As}(\text{SG})_2$ and $(\text{CH}_3)_2\text{As}(\text{SG})$ [49]. This metabolic cascade comprised two types of transformation: oxidative methylation and reduction-coupled glutathione conjugation in alternation. Two models have been proposed based on accumulated evidences [50, 51]. In the first model shown in Scheme 5.1, inorganic arsenite is oxidized and simultaneously methylated by an enzyme, arsenic (+3 oxidation state) methyltransferase (As3MT), using S-adenosyl-methionine (AdoMet) as the methyl donor, and the methylated As(V) species are reduced by an enzyme glutathione S-transferase omega (GSTO) with GSH as a reducing agent [42, 52].

Recently, Hayakawa *et al.* [49] proposed a new model for arsenic metabolism, in which, with the aid of As3MT, the GSH in $\text{As}(\text{SG})_3$ is replaced sequentially by the methyl group of AdoMet (Scheme 5.2). Meanwhile the As(III) species were oxidized to the low toxic As(V) species via hydrolysis and oxidation.

By HPLC-ICP-MS, several arsenic metabolites were identified to be thioarsenicals, for example, the sulfur-substituted arsenic or arsenious acids species, $\text{As}(\text{CH}_3)_2\text{SH}$, $\text{AsS}(\text{CH}_3)_2\text{OH}$ and $\text{AsS}(\text{CH}_3)_2\text{SH}$. They were formed by the reactions of $\text{As}(\text{CH}_3)_2\text{OH}$ and $\text{AsO}(\text{CH}_3)_2\text{OH}$ with sulfur donors, for example, $\text{H}_2\text{S}/\text{S}^{2-}$, $\text{S}_2\text{O}_3^{2-}/\text{HSO}_3^-$ [53].



Scheme 5.1



Scheme 5.2

Similarly, these thioarsenicals might be formed in realgar metabolism. Moreover they may exert potent inhibitory actions on thioredoxin reductase [48]. However, the reactions of thioarsenicals with biomolecules may warrant further studies.

It was shown that As(III) can be oxidized to As(V) by hydrogen peroxide in a Tris-HCl buffer at pH 8.0 [54]. Since hydrogen peroxide is one of the ROS generated in mitochondria under arsenic induced oxidative stress, thus both As(III)- and As(V)-containing species might contribute to arsenic based biological effects but the toxicity of arsenite is higher than arsenate.

Apart from glutathione S-transferase, As(V) can also be reduced to As(III) by glyceraldehyde-3-phosphate dehydrogenase (GAPDH) [55], which has a higher level and specific activity in malignant cells than in normal cells and thus may accelerate the reduction of As(V) [56]. This feature probably accounts for the higher arsenic sensitivity of malignant cells. All these transformations mentioned above proceed in liver cells, while the arsenic GSH conjugates, either methylated or not, for example, $\text{As}(\text{SG})_3$ and $(\text{CH}_3)_2\text{As}(\text{SG})_2$, were excreted into bile via the multidrug resistance protein MRP1/ABCC1 [57]. However, the species excreted in bile and urine depends on the route, dose, and chemical forms of administration [58]. The biological effects of these metabolites are similar but not identical. Whether they act by different ways is not clear [59].

5.2.2 Metabolism and Pharmacokinetics of Realgar and Orpiment

The pharmacokinetics and metabolism of realgar and orpiment are partially attributed to the water soluble fraction but the behaviors of the insoluble portion cannot be excluded. The soluble fraction is mainly As(III) oxide, which might be leached out, absorbed, and metabolized as mentioned above. The relative amount of the soluble fraction depends on the extent of oxidative hydrolysis in the course of processing and the leaching kinetics in the body. The metabolism of insoluble arsenic sulfides remains obscure owing to lack of studies on the absorption, distribution and metabolism of insoluble ABMs. The results of five week oral administration of realgar to Wistar rats indicated that arsenic was distributed among almost all organs, but mostly found in blood [60]. The pharmacokinetic behavior and the distribution of arsenic in rats after a single dose of arsenic orally indicated that arsenic was accumulated in all organs and tissues but varied as follows: spleen, hair, lung and suprarenal gland organs > kidney, heart, liver, bladder > skin, After 15 days of continuous

administration, arsenic contents in kidney and bladder tissues increased appreciably. After two weeks of discontinuation, arsenic contents in organs and tissues decreased by 21.1–69.5%, except in the heart. Only a small amount of arsenic in realgar was absorbed in blood circulation [61].

Since realgar is mostly used in the form of TCM composites, the arsenic absorption and metabolism are varied depending on the herbs added in these composites. Therefore, the amount of arsenic leached out from different realgar containing composites and the amount of bioavailable arsenic were evaluated. The dissolution of arsenic from a compound recipe (Liu Shen Wan) was shown to be enhanced [10]. In one case, up to 39% of the arsenic in the recipe was readily extractable by artificial stomach fluid as compared < 1% in the realgar mineral itself. Contradictorily, Tang *et al.* reported that less arsenic was leached from another TCM, An Gong Niu Huang Wan in artificial stomach fluid than that from realgar [62]. Similar results were reported by Zhao *et al.* [63] and Hong *et al.* [64]. Moreover, it was observed by Koch *et al.* that after taking one pill of Niu Huang Jie Du Pian, containing about 28 mg arsenic in the form of realgar, up to 4% of arsenic (1 mg) was bioavailable for absorption into the bloodstream, and 40% of the absorbed arsenic (0.4 mg) was excreted in urine [65]. Evidently the arsenic bioavailability of realgar in different composites might be increased or reduced depending on the components.

5.2.3 Nanoparticles of Realgar

There is plausible evidence that the bioavailability of nanometer sized realgar is significantly higher than that of the conventionally pulverized one. The pharmacokinetic behaviors of realgar nanoparticles were compared with pulverized realgar and results showed that realgar nanoparticles exhibit an enhanced absorption and the reduced excretion as well as a better pharmacokinetic profile [24, 66]. The distribution of arsenic has been studied in mice with Ehrlich ascites tumors after subcutaneous injection of realgar nanoparticles [67]. After consecutive administration for 10 days, the highest arsenic level was found in kidney and spleen, followed by liver and cancer tissues, with the plasma the least. An *in vivo* study with rats revealed that, compared with the realgar powder, nanosized realgar elevated the urinary recovery of arsenic in the first 48 h of administration [68].

5.3 Pharmacological Activities and Mechanisms of Actions of ABMs

Enormous efforts have been made to understand the mechanisms of action and toxicity of arsenic compounds ever since the successful utilization of ATO in the treatment of APL and the serious threatening from environmental arsenic contamination. Although the biological effects of arsenic chemicals have been extensively studied, ABMs were seldom investigated. Nevertheless, it is usually presumed that ABMs exert their effects via mechanisms similar to that of arsenic compounds.

5.3.1 Mechanisms of Anticancer Action of Arsenolite and ATO

Although arsenic minerals such as realgar and orpiment also exhibit remarkable pharmacological activities and are frequently used in TCM, most clinical and mechanistic studies have been focused on ATO, which is reviewed in detail in the Chapter 11 of this book. In the

current section, the pharmacological activities and mechanisms of ATO will be outlined briefly as background information, and such information on ABMs in TCM will be followed in detail.

5.3.1.1 Anticancer Activities of ATO

The most notable medicinal application of arsenic in modern medicine is to treat leukaemia, especially acute promyelocytic leukaemia (APL). APL is a subtype of acute myeloid leukaemia (AML) characterized by a balanced reciprocal translocation between chromosomes 15 and 17, which leads to the fusion of the promyelocytic leukaemia (PML) gene to retinoid acid receptor α (RARA) gene [69]. All-trans retinoid acid (ATRA) alone or in combination with anthracycline and ara-C based chemotherapy is the classic treatment of APL prior to the 'revival' of ATO. Compared to conventional therapies, ATO treatment demonstrated consistently higher complete remission rates in both newly diagnosed and relapsed APL [70], lower resistance to the drug [71] and better tolerability [72]. Furthermore, combination of ATO with ATRA achieved even better therapeutic effects [73, 74].

ATO has also been tested in many other hematological malignancies, including myelodysplastic syndromes (MDS), chronic myeloid leukaemia (CML), Non-M3 AML, and lymphoid malignancies such as multiple myeloma, and even in solid tumors. Most of the tested malignancies are refractory to current therapies. Nevertheless, promising results were obtained in both preclinical studies and clinical trials, though solid tumors were much less responsive to ATO [70]. ATO alone induced hematological responses and exhibited moderate activity in MDS patients [75, 76], and induced apoptosis in BCR-Abl positive lymphoblast and CML cells [77, 78]. Non-M3 AML cells were not sensitive to the proapoptotic effects of ATO, however when combined with ascorbic acid, ATO is able to inhibit cell growth and to induce apoptosis in primary AML cell lines [79, 80]. Furthermore, ATO also exhibited growth inhibitory, proapoptotic and antiangiogenesis effects in multiple myeloma cells, and is active in 30–40% of patients with relapse/refractory myeloma either alone or in combination with other approved agents [81].

5.3.1.2 Cellular and Molecular Mechanisms of the Actions of ATO

In contrast to Western medicine which often focuses on a single target, traditional Chinese medicine considers the human body in a holistic way, and generally deals with multiple targets involved in a specific disease condition [82]. Similarly, ATO acts on multiple targets through diversified mechanisms. It is generally accepted that ATO facilitates cell differentiation at lower concentrations, while it induces cell cycle arrest and apoptosis at higher concentrations [83]. Various concentrations of ATO could exist *in vivo* under clinical settings [83], thus these mechanisms, though not totally understood yet, together account for the pharmacological activities of ATO.

Induction of Differentiation. Essentially APL is a disease in which abnormal promyelocytes (APL blasts) replaced the marrow due to blocked differentiation of granulocytic cells at this stage, in which RAR α plays a pivotal role. Without stimulations, RAR α binds to DNA as a heterodimer with retinoid X receptor (RXR) and recruits transcriptional corepressors such as silencing mediator of retinoic and thyroid receptors (SMRT) and histone deacetylases (HDACs) [84, 85]. Upon retinoid acid (RA) or cytokine treatment,

RAR α is activated and regulates the differentiation of the myeloid lineage. However, in most APL cells RAR α is fused with PML, which increases the binding of the fusion protein to transcriptional corepressors, thus potentiates the transcriptional repressor activity of RAR α and blocks RAR α -regulated differentiation [69].

Lower doses of ATO induce partial myelocyte-like differentiation and upregulate the expression of cytokines and cyclic AMP level which terminates the differentiation [86, 87]. In further mechanism studies, PML-RAR α was identified as the primary target of ATO in ATO-induced differentiation [88]. Both RA and ATO induce differentiation but target distinct domains or molecules. Compared to RA which targets RAR α , ATO acts mainly on the PML protein. It has been shown to induce sumoylation of PML and PML-RAR α proteins at multiple lysine residues, consequently directs the sumoylated proteins to proteasome dependent degradation [89]. ATO also mediates the phosphorylation of SMRT through mitogen-activated protein kinases (MAPK) pathways, leading to dissociation of SMRT from PML-RAR α [85]. The above two mechanisms are believed to allow partially differentiated cells to complete their differentiation.

Induction of Cell Cycle Arrest and Apoptosis. Induction of cell cycle arrest and/or apoptosis is a more generalized mechanism contributed to the anticancer activities of ATO. The proapoptotic activity of ATO involved a series of molecular events, including accumulation of high ROS levels, activation of MAPK cascades, perturbation of mitochondria permeability, release of cytochrome *c* and other proapoptotic proteins, downregulation of Bcl-2, upregulation of p53/MDM2 response, inhibition of NF- κ B signaling, and activation of caspases [70, 86]. On the other hand, ATO-mediated cell cycle arrest (either G1 or G2/M phase) is often accompanied by downregulation of CDK2/6, cyclin D1/E and upregulation of cell cycle inhibitors such as p21. In addition to the mechanisms mentioned above, ATO has been reported to exert its anticancer activities through inhibition of DNA repair, suppression of human telomerase reverse transcriptase (hTERT) and modification of cytoskeleton [90]. In general, most of these events are correlated with the ability of arsenic to react with vicinal sulfhydryl groups [91].

Given the universal participation of cell cycle arrest/apoptosis in therapies against almost all cancers, ATO has been proposed as a broad spectrum anticancer drug. However, clinical and preclinical studies in other tumors are much less successful than in APL [86], which is likely attributed to two factors. The first one is that PML-RAR α fusion protein, which plays an important role in APL carcinogenesis and ATO-mediated differentiation, is expressed exclusively in APL cells. The second one involves the resistance of specific cancer cells to ATO-induced ROS, which has been postulated as a key mediator of the proapoptotic activity of ATO [92]. ROS activates stress response kinases such as JNK and results in oxidative damages to DNA and proteins. Normally cells are equipped with an inducible cytoprotective system consisting of antioxidant enzymes, such as glutathione-S-transferase, heme oxygenase and catalase, and redox buffers such as glutathione (GSH) and N-acetylcysteine (NAC) [93]. The induction of such systems is an important determinant of sensitivity to cytotoxic agents; however APL cells have a low level of GSH and less inducible antioxidant enzymes, which make them more susceptible to ATO [80].

In conclusion, ATO as an ancient drug achieved amazing success in the treatment of cancer, especially APL, in modern medicine. The pharmacological activities of ATO have

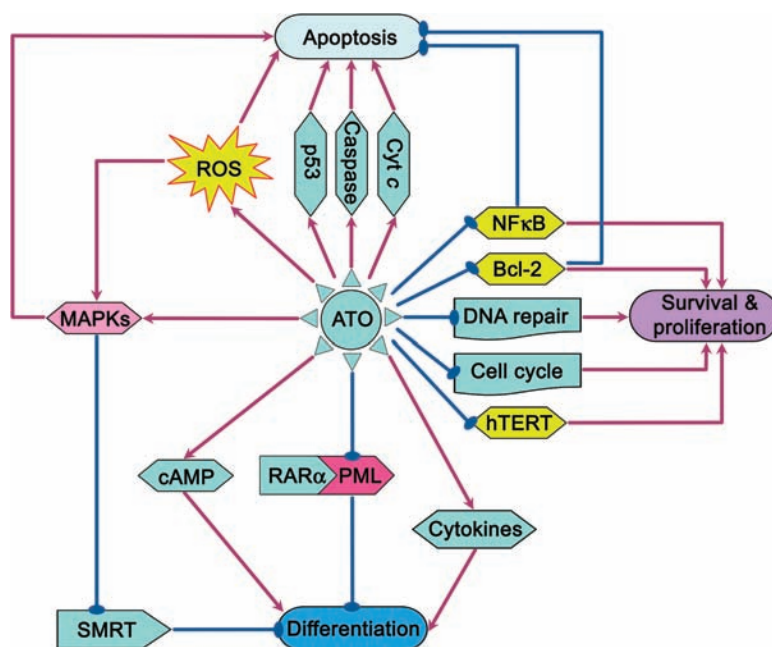


Figure 5.2 Possible mechanisms of action of arsenic trioxide (ATO)

been proved by numerous preclinical and clinical studies, while the underlying mechanisms, as summarized in Figure 5.2, are beginning to be unveiled. Some other ABMs frequently used in TCM, such as realgar and orpiment, have been shown to possess similar pharmacological activities but less toxicity [94], and could be served as better anticancer drugs.

5.3.2 Mechanisms of Anticancer Actions of Realgar

The therapeutic activity of realgar and orpiment is likely the same as that of arsenolite, despite of different route of administration. Due to very low solubility and toxicity of realgar, it was used both orally and externally. On the other hand, orpiment is now rarely used and reported.

Realgar, like ATO, inhibits proliferation and induces differentiation and apoptosis in APL cells and other hematological cancer cells. A few studies have been reported on similar effects on solid tumors but the conclusions remain uncertain.

5.3.2.1 Induction of Differentiation

Similar to ATO, realgar induced differentiation of APL derived NB4 cells by inducing degradation of PML/RAR α fusion protein [95–97]. Zhong *et al.* reported that realgar inhibited proliferation and induced apoptosis in HL60 and K562 cell lines. These effects were also associated with the degradation of PML/RAR α [98]. Nevertheless, unlike NB4, the differentiation of HL-60 induced by realgar proceeds through the monocytic pathway, in which serine/threonine-specific protein phosphatases, in particular PP1 and PP2A were

involved [99]. The differentiation was synergized, enhanced or suppressed by the inhibition of p38 MAPK, JNK and ERK pathways, respectively [28].

5.3.2.2 *Inhibition of Proliferation and Induction of Apoptosis*

It has been reported that realgar is able to inhibit proliferation and to induce apoptosis in several cell lines. The proapoptotic effect of realgar in HL-60 cells was associated with down-regulation of Bcl-2 and mutated p53 gene expression, indicating the involvement of mitochondrial pathway [100]. On the other hand, Ye *et al.* suggested that realgar nanoparticles induced apoptosis was resulted from oxidative damage to cell membrane [26].

The realgar-induced apoptosis in human cervical HeLa cancer cells has been attributed to downregulation of the expression of COX-2 and PGE2 [101]. Realgar inhibited the expression of tumor-associated antigen RCAS1 (receptor binding cancer antigen expressed on SiSo cells) [25], suggesting it may affect the defensive capability of tumor cells [102]. Inhibition of the telomerase activity in HeLa cells might be another event pertinent to realgar-induced apoptosis [103].

In addition, realgar nanoparticles were found to inhibit growth and to induce apoptosis in human leukemic monocyte lymphoma cell line (U937) in a time- and dose-dependent manner, which was attributed to cleavage of PARP, the downregulation of Bcl-2 and upregulation of Bax. Among the MAPK signaling pathways, only the JNK pathway was activated by realgar treatment. Thus the realgar-induced apoptosis was ascribed to JNK and mitochondrial pathways [27]. Recently, it was also suggested that realgar induced apoptosis is likely related to the inhibition of the PI3K/Akt signaling pathway, the inactivation of the mitochondrial pathway related protein sirtuin type 1 (SIRT1) and the activation of p53 tumor suppressor gene [28].

In contrast, only a weak proapoptotic action was found for realgar in chronic myeloid leukaemia (CML)-derived K562 cells compared to APL derived NB4 cells [104]. It is reasonable since CML cells were less sensitive to realgar than APL cells, presumably due to the higher expression of *bcl-xL* in CML cells [105].

Huang Dai Pian, is an interesting example to illustrate the role of realgar in TCM. It is a composite, consisting of realgar, *Indigo Naturalis*, *Salvia miltiorrhiza*, and *Radix Pseudostellariae* used in clinical practice for the treatment of APL successfully [106]. Based on the results obtained in NB4 cells, realgar was demonstrated to be the main active ingredient. Although the composite exhibits a higher activity than realgar alone, the contribution of one of the components, *Indigo Naturalis* was not established [107]. Recently, a reorganized composite composed of realgar, indirubin (ingredient of *Indigo Naturalis*) and tanshinone IIA (ingredient of *Salvia miltiorrhiza*) is developed and used to evaluate the efficacy of different recipes and the role of each components. The experimental results showed that the composite caused ubiquitination/degradation of PML-RAR α oncoprotein, enhanced re-programming of myeloid differentiation regulators in APL cells and arrested the cells in G1/G0 phase. These effects are similar to those of ATO, but interestingly, the composite upregulated the expression of AQP9, thus facilitating the transport of arsenite [21]. However, in their experiments the insoluble realgar was dissolved in sodium hydroxide solution, thus the consequence probably resulted from arsenite formed during dissolution. Nevertheless, these results are potentially important, especially for the understanding of the working principles in TCM prescription.

The weak proapoptotic action of realgar has also been found in a few solid tumors. Realgar nanoparticle suspension could inhibit the proliferation and induce apoptosis and G0/G1 phase arrest in SiHa human uterine cervix cancer cells, which might be associated with the reduction of human papilloma virus HPV16E6/E7 gene expression [103]. The inhibitory effect of realgar on proliferation of lung adenocarcinoma cell [17] and hepatic cancer BEL-7402 cells [18] was also reported, but no information is available on the mechanism of action.

It should be aware that the size of realgar nanoparticles as well as the method of preparation might influence their pharmacological effects. The size-dependent cytotoxicity of realgar particles in the endothelial cell line ECV-304 has been evaluated and the results showed that realgar particles with an average diameter of less than 150 nm could effectively inhibit cell proliferation [108].

5.3.3 Arsenolite on Asthma Prevention

Asthma is a complex pathological process. In brief, it is initiated from inflammation and/or allergen mediated Th2 inflammation in airway. Increased Th2 cells along with eosinophiles, mast cells, basophiles, and macrophages generate proinflammatory mediators, including cytokines (interleukin 3, 15, etc.), chemokines (eotaxin etc.), growth factors, lipid mediators (leukotrienes, etc.), and G protein coupled receptor ligands (prostanoids, leukotrienes, etc.), which consequently cause fibrosis, myocyte hyperplasia, angiogenesis, airway hyper-responsiveness and remodeling, airflow obstruction and finally lead to loss of lung function. Among these mediators, leukotriene B₄ and C₄ (LTB₄, LTC₄) play a pivotal role. They are generated from arachidonic acid by 5-lipoxygenase (5-LO), which is activated by 5-lipoxygenase activating protein (FLAP). Bronchial asthma mice express a high level of FLAP and LTC₄, whereas administration of *Pi Shi* has been shown to down-regulate FLAP, and subsequently LTC₄ [109]. Consistent to this result, *Pi Shi* was found to down regulate 5-LO activity and subsequently reduced LTB₄ levels [110].

Both prostaglandins (PG) and prostacyclins produced from arachidonic acid are also elevated under asthma condition. Among the PGs, 8-isoprostane can be easily measured and thus is used as the biomarker to evaluate this pathological condition. It was reported that a high level of 8-isoprostane was found in the asthmatic mice and was significantly reduced upon treatment with arsenolite, possibly due to regulation of redox status [111].

In summary, *Pi shi* suppresses asthmatic inflammation by downregulating the level of inflammatory cytokines.

The downstream cascades mediated by IL4 include activation of signal transducer and activator of transcription 6 (STAT6), and Th2 response. *Pi Shi* was found to down-regulate the expressions of STAT6 in asthmatic mice [112]. In the development of inflammation response, the eosinophiles infiltration is also a crucial pathologic event related to the expression of eotaxin, which acts as a chemokine to recruit eosinophiles. Arsenolite has been found to inhibit eotaxin expression [112], and to induce apoptosis of eosinophiles by downregulating antiapoptotic factor Bcl2, therefore to prevent the asthma symptoms [113].

Remodeling of airway, an event in late asthma development, is correlated to the over proliferation of airway smooth muscle cells and fibroblasts and subsequent excess deposition of extracellular matrix. In the development of airway remodeling, overexpression of protooncogenes, *c-myc*, *c-fos*, *c-jun* and *c-sis*, plays an important role. In ovalbumin induced asthmatic mice, oral administration of *Pi Shi* downregulated the overexpression of *c-myc*

and *c-sis*. These effects were ascribed to inhibition of cell proliferation and ECM deposition [114].

Taken together, arsenolite on asthma prevention is likely attributed to its ability to suppress the expression of inflammatory mediators, to inhibit inflammatory cell infiltration and the proliferation of the smooth muscle cells. However, the direct targets of arsenic are still unknown and warrant for further studies.

5.3.4 Realgar on Brain Protection

An Gong Niu Huang formulae in different forms, for example, *An Gong Niu Huang Wan* and *An Gong Niu Huang Pian* are widely used to 'wake up the brain'. It is prescribed to patients in unconsciousness or coma, usually due to brain injury. In order to meet the criteria on the arsenic concentrations in TCM composites, researchers tried to verify the necessity of addition of realgar in this composite by comparing the protective activities of the composites with or without realgar. However, the outcomes were somewhat intriguing and inconsistent. No significant difference was observed in the cerebral infarction area, water content, catalase, lipid peroxides, glutathione peroxidase (GPx) and lactic acid (LD) levels in brain of rat with middle cerebral arterial occlusion, which led to conclusion that realgar and another mineral component, cinnabar, are not necessary [115]. In contrast, Gao *et al.* demonstrated that *An Gong Niu Huang Pian* effectively activated rat neurons, such an effect was significantly impaired if realgar was removed from the composite [116]. Furthermore, the contribution of realgar to the effectiveness of *An Gong Niu Huang* composite was assessed by measuring the disturbance of consciousness in LPS induced brain injured rats using electroencephalography (EEG). The results showed that the composite without realgar was less effective in EEG activation than the composite with realgar [117]. Furthermore, the effects of the composites with or without realgar on the levels of catecholamine (CA) and their metabolites in cerebral cortex of LPS induced brain injured rats were measured, and the results are in favor of the indispensable role of realgar in the composite [118].

Nevertheless, the mechanisms of cell protection by either realgar alone or the *An Gong Niu Huang* composite still remains vague. Recently it was shown that realgar exerts anti inflammatory effect on inflammatory brain injury. Both realgar and the *An Gong Niu Huang* composite can increase the levels of heat shock protein 70 (HSP70) in brain tissue and serum and heme oxygenase-1 (HO-1) activity in brain tissue, whereas the composite exhibits a higher activity than that of realgar alone [119]. In the mean time, realgar was found to inhibit the excessive upregulation of inflammatory mediators such as IL-1 b, IL-6, TNF-a and iNOS activity. Thus the anti inflammatory activity of realgar might be attributed to both the induction of cellular protective response genes such as HSP70 and HO1, and the inhibition of inflammatory genes such as iNOS and cytokines [120]. Since realgar exhibits similar effects to the composite, it was assumed to be the active ingredient for the anti inflammatory effects of the composite [121].

5.4 Perspectives

Comprehension, though just partially, of the mechanism of the therapeutic effect of ATO on APL not only provides rationale for arsenic therapy but also expedites the reassessing of the

ABM based TCM composites. Although there are accumulative clinical experiences on the application of hundreds of ABM containing composites, their pharmacological actions and the underlying mechanisms are still far from clear. There are still many puzzles remaining to be solved.

Intensive studies have shown that arsenolite exhibits anticancer activity, which was attributed to ATO. Although two ABMs, realgar and orpiment have been used in TCM, there are few mechanism studies due to their poor solubility. Up to now, it is not clear whether realgar or/and orpiment exert their action via ATO, formed by the oxidative hydrolysis. Although the pathways leading to ATO induced differentiation and apoptosis have been largely defined, there is still a long way to go before any clear cut conclusion can be drawn on those for realgar or orpiment. It is generally accepted that practitioners of traditional Chinese medicine ingeniously used the insoluble minerals to provide the active metal ions at a therapeutic level while keeping their toxic effects at minimal levels. Cinnabar (mercuric sulfide) is another example of such mineral medicines. Similarly, realgar and orpiment are assumed to be orally administrable arsenicals, due to their low solubility, low bioavailability and thus low toxicity. However, it remains unknown whether ATO is the active species of realgar. More studies on the pharmacokinetic and ADME properties of realgar are needed before this question can be answered.

In order to clarify the mechanism of realgar's action, several studies have been carried out at the cellular level. The results are highly dependent on the method used to prepare realgar samples, by which realgar will be turned into different soluble arsenic species. Therefore, they could not be simply regarded as the actions of realgar. When the suspension of realgar fine particles were used, it is necessary to know how these particles cross the intestine-blood barrier and the cell membrane. The mechanisms of transport and absorption of arsenite and arsenate is already known, though not thoroughly, but they are very different from the realgar particles. Recent studies showed that nanoparticles might be engulfed by the cells via nonphagocytosis and the endosomes formed might activate various signaling pathways. In addition, the activity and toxicity of these fine particles are evidently dependent on particle size [108]. Thus it could not be excluded that the fine particles prepared either by the traditional *Shui Fei* method or the nanotechniques exert their action on cells by such pathways.

The low toxicity of realgar has also been ascribed to the herbal ingredients in TCM composites. However, it is hard to discriminate the influences from different herbs unless the active ingredients of certain herbs and their mechanisms are defined. It should be emphasized that herbal ingredients may enhance the cellular uptake of arsenic species [21], and may even increase the toxicity.

Nevertheless, using ABMs as therapeutic agents are like dancing on the razor's edge due to the dual effects of arsenic and its metabolites [48]. Are they carcinogens or anticancer agents? Do they kill cells or protect them? All depends on the intricate interactions and cross talk between arsenicals and the complex network controlling cell proliferation, differentiation, survival or apoptosis. The high toxicity of soluble arsenic has been well documented, but much less is known regarding the toxicity of the insoluble arsenic sulfide minerals. Environmental studies have revealed that intake of arsenic caused severe toxicity to most of organs. The high arsenic contents in water sources caused skin damage and skin cancer, as well as toxic effects on urinary bladder, liver, kidney, reproductive and development systems, lung, prostate, and so on [122]. Similar ecological survey in India and Pakistan

revealed that the ground water contains a high level of arsenic, which is leached from the arsenic sulfide minerals, mainly arsenopyrite, by oxidative hydrolysis. Moreover, toxicities of orally administered realgar, including nephrotoxicity [123] and dermatologic changes [124] have been noticed. In addition, long term administration of realgar was known to caused mutation, carcinogenesis and malformation [125]. Therefore the toxicity of realgar cannot be overlooked and should be studied in more detail.

References

1. Sun, H.D., Ma, L., Hu, X.C., and Zhang, T.D. (1992) *Chinese Journal of Integrated Traditional and Western Medicine*, **12**, 170–172.
2. Chen, G.Q. *et al.* (1997) *Blood*, **89**, 3345–3353.
3. Waxman, C.S. and Anderson, K.C. (2001) *Oncologist*, **6** (Suppl. 2), 3–10.
4. Agency for Toxic Substances and Disease Registry (2005) *Toxicological Profile for Arsenic*. CAS#7440-38-2 (<http://www.atsdr.cdc.gov/ToxProfiles/tp.asp?id=22&tid=3>). August 2007
5. Tossell, J.A. (1997) *Geochimica et Cosmochimica Acta*, **61**, 1613–1623.
6. Li, H. (ed.) (1981) *An Introduction to Mineral Drugs in Traditional Chinese Medicine*, Shandong Science and Technology Press, Jinan, China.
7. Gao, L.W. (ed.) (1993) *Handbook of Clinical Use of Toxic Drugs in TCM*, Academy Press, Beijing, China.
8. Verstovsek, S. and Estrov, Z. (2004) *Leukemia Research*, **28**, 901–903.
9. Yin, K.S., Yao, X., Chen, J.T. *et al.* (1999) *Acta Universitatis Medicinalis Nanjing*, **19**, 433.
10. Wu, X.H., Sun, D.H., Zhuang, Z.X. *et al.* (2002) *Analytica Chimica Acta*, **453**, 311–323.
11. Kwan, S.Y., Tsui, S.K., and Man, T.O. (2001) *Analytical Letters*, **34**, 1431–1436.
12. Lu, D.P., Qiu, J.Y., Jiang, B. *et al.* (2002) *Blood*, **99**, 3136–3143.
13. Bai, Y. and Huang, S. (1998) *Chinese Journal of Hematology*, **19**, 477–480.
14. Chen, S.Y., Liu, S.X., and Li, X.M. (2002) *China Journal of Chinese Materia Medica*, **27**, 211–215.
15. Zhao, X., Quan, P., Li, J., and Tian, H. (2006) *Mod Oncology*, **14**, 88–90.
16. Hu, J., Zhao, J.Y., and Yang, P.M. (2006) *Acta Anatomica Sinica*, **37**, 665–668.
17. Zhou, C.F. (2004) *Journal Practice Cancers*, **19**, 507–510.
18. Zhang, C. (2004) *China Journal of Hepatology*, **9**, 112–113.
19. Chen, W.X., Zhang, F., Yang, H.C. *et al.* (2007) *Tumor*, **27**, 787–790.
20. The Cooperation Group of Phase II Clinical Trial of Compound Huangdai Tablet (2006) *China Journal of Hematology* **27**, 801–804.
21. Wang, L., Zhou, G.B., Liu, P. *et al.* (2008) *Proceedings of the National Academy of Sciences of the United States of America*, **105**, 4826–4831.
22. Tang, Y., Wang, N.S., and Zhang, Y.Q. (2007) *Pharmacology and Clinics of Chinese Materia Medica Pract TCM*, **23**, 107–110.
23. Wang, L.F. and Liu, H.J. (2000) *Studies of Trace Elements and Health*, **17**, 3–5.
24. Zhan, X.Q., Zhao, F.M., and Guo, L.W. (2006) *Journal of Traditional Chinese Medicine Practice*, **22**, 397–399.
25. Liu, R., Pu, D.M., Cheng, Y.X. *et al.* (2008) *Chinese Journal of Hospital Pharmacy*, **28**, 459–462.
26. Ye, H.Q., Gan, L., Yang, X.L., and Xu, H.B. (2005) *Biological Trace Element Research*, **103**, 117–132.
27. Wang, X.B., Gao, H.Y., Hou, B.L. *et al.* (2007) *Archives of Pharmacal Research*, **30**, 653–658.
28. Xi, R.G., Huang, J., Li, D. *et al.* (2008) *Acta Pharmacologica Sinica*, **29**, 355–363.
29. Lengke, M.F. and Tempel, R.N. (2002) *Geochimica et Cosmochimica Acta*, **66**, 3281–3291.
30. Lengke, M.F. and Tempel, R.N. (2003) *Geochimica et Cosmochimica Acta*, **67**, 859–871.
31. Huang, R.-N. and Lee, T.-C. (1996) *Toxicology and Applied Pharmacology*, **243**, 243–249.
32. Zhang, T.L., Gao, Y.X., Lu, J.F., and Wang, K. (2000) *Journal of Inorganic Chemistry*, **79**, 195–203.

33. Delnomdedieu, M., Basti, M.M., Styblo, M. *et al.* (1994) *Chemical Research in Toxicology*, **7**, 621–627.
34. Liu, Z., Shen, J., Carbrey, J.M. *et al.* (2002) *Proceedings of the National Academy of Sciences of the United States of America*, **99**, 6053–6058.
35. Liu, Z., Carbrey, J.M., Agre, P., and Rosen, B.P. (2004) *Biochemical and Biophysical Research Communications*, **316**, 1178–1185.
36. Bienert, G.P., Schussler, M.D., and Jahn, T.P. (2008) *Trends in Biochemical Sciences*, **33**, 20–26.
37. Porquet, A. and Filella, M. (2007) *Chemical Research in Toxicology*, **20**, 1269–1276.
38. Leung, J., Pang, A., Yuen, W.H. *et al.* (2007) *Blood*, **109**, 740–746.
39. Bun-ya, M., Shikata, K., Nakade, S. *et al.* (1996) *Current Genetics*, **29**, 344–351.
40. Mukhopadhyay, R. and Rosen, B.P. (2002) *Environmental Health Perspectives*, **110**, 745–748.
41. Kumagai, Y. and Sumi, D. (2007) *Annual Review of Pharmacology and Toxicology*, **47**, 243–262.
42. Aposhian, H.V., Zakharyan, R.A., Avram, M.D. *et al.* (2004) *Toxicology and Applied Pharmacology*, **198**, 327–335.
43. Naranmandura, H., Suzuki, N., and Suzuki, K.T. (2008) *Toxicology and Applied Pharmacology*, **231**, 328–335.
44. Suzuki, K.T. (2005) *Analytica Chimica Acta*, **540**, 71–76.
45. Naranmandura, H., Suzuki, N., Iwata, K. *et al.* (2007) *Chemical Research in Toxicology*, **20**, 616–624.
46. Aposhian, H.V. *et al.* (2000) *Chemical Research in Toxicology*, **13**, 693–697.
47. Styblo, M., Drobna, Z., Jaspers, I. *et al.* (2002) *Environmental Health Perspectives*, **110** (Suppl.5), 767–771.
48. Thomas, D.J., Styblo, M., and Lin, S. (2001) *Toxicology and Applied Pharmacology*, **176**, 127–144.
49. Hayakawa, T.K.Y., Cui, X., and Hirano, S. (2005) *Archives of Toxicology*, **79**, 183–191.
50. Thomas, D.J. (2007) *Toxicology and Applied Pharmacology*, **222**, 365–373.
51. Ghosh, P., Banerjee, M., Giri, A.K., and Ray, K. (2008) *Mutation Research*, **659**, 293–301.
52. Waters, S.B., Devesa, V., Del Razo, L.M. *et al.* (2004) *Chemical Research in Toxicology*, **17**, 404–409.
53. Kazuo, T. and Suzuki, K. (2005) *Analytica Chimica Acta*, **540**, 71–76.
54. Aposhian, H.V., Zakharyan, R.A., Avram, M.D. *et al.* (2003) *Toxicology and Applied Pharmacology*, **193**, 1–8.
55. Nemeti, B., Csanaky, I., and Gregus, Z. (2006) *Toxicological Sciences*, **90**, 49–60.
56. Bagui, S., Ray, M., and Ray, S. (1999) *European Journal of Biochemistry*, **262**, 386–395.
57. Leslie, E.M., Haimeur, A., and Waalkes, M.P. (2004) *The Journal of Biological Chemistry*, **279**, 32700–32708.
58. Cui, X., Kobayashi, Y., Hayakawa, T., and Hirano, S. (2004) *Toxicological Sciences*, **82**, 478–487.
59. Eblin, K.E. (2008) *Toxicology*, **250**, 47–54.
60. Cheng, Z.J., Zhao, L., Tian, H. *et al.* (2001) *Chinese Journal of Chinese Materia Medica*, **47**, 194–197.
61. Tang, Y., Ou, W., Wang, N., and Liu, Q. (2008) *Traditional Chinese Drug Research & Clinical Pharmacology*, **19**, 372–376.
62. Tang, Y.S. and Wang, N.S. (2005) *Chinese Journal of Current Traditional Western Medicine*, **3**, 769–771.
63. Zhao, Z.J. and Jiang, P.F. (1989) *Chinese Journal of Pharmaceutical Analysis*, **9**, 34–36.
64. Hong, J.X. and Chen, T.W. (2002) *Journal of Fuzhou University (Nat SciEdn)*, **30**, 867–869.
65. Koch, I., Sylvester, S., Lai, V.W. *et al.* (2007) *Toxicology and Applied Pharmacology*, **222**, 357–364.
66. Wang, X.B. and Xi, R.G. (2002) *Pharmaceutical Journal of Chinese People's Liberation Army*, **18**, 324–326.
67. Xu, L.Y., Zeng, F.D., Ye, H.Q. *et al.* (2006) *Chinese Journal of New Drugs*, **15**, 1845–1849.
68. Wu, J.Z. and Ho, P.C. (2006) *European Journal of Pharmaceutical Sciences*, **29**, 35–44.

69. Wang, Z.Y. and Chen, Z. (2008) *Blood*, **111**, 2505–2515.
70. Dilda, P.J. and Hogg, P.J. (2007) *Cancer Treatment Reviews*, **33**, 542–564.
71. Soignet, S.L., Frankel, S.R., Douer, D. *et al.* (2001) *Journal of Clinical Oncology*, **19**, 3852–3860.
72. Shigeno, K., Naito, K., Sahara, N. *et al.* (2005) *International Journal of Hematology*, **82**, 224–229.
73. Au, W.Y., Chim, C.S., Lie, A.K. *et al.* (2002) *British Journal of Haematology*, **117**, 130–132.
74. Zhou, G.B., Zhang, J., Wang, Z.Y. *et al.* (2007) *Philosophical Transactions of the Royal Society of London. Series B, Biological Sciences*, **362**, 959–971.
75. Vey, N., Bosly, A., Guerci, A. *et al.* (2006) *Journal of Clinical Oncology*, **24**, 2465–2471.
76. Schiller, G.J., Slack, J., Hainsworth, J.D. *et al.* (2006) *Journal of Clinical Oncology*, **24**, 2456–2464.
77. Potin, S., Bertoglio, J., and Breard, J. (2007) *FEBS Letters*, **581**, 118–124.
78. Puccetti, E., Guller, S., Orleth, A. *et al.* (2000) *Cancer Research*, **60**, 3409–3413.
79. Bachleitner-Hofmann, T., Gisslinger, B., Grumbeck, E., and Gisslinger, H. (2001) *British Journal of Haematology*, **112**, 783–786.
80. Dai, J., Weinberg, R.S., Waxman, S., and Jing, Y. (1999) *Blood*, **93**, 268–277.
81. Berenson, J.R. *et al.* (2006) *British Journal of Haematology*, **135**, 174–183.
82. Konkimalla, V.B. and Efferth, T. (2008) *Journal of Ethnopharmacology*, **116**, 207–210.
83. Snow, E.T., Sykora, P., Durham, T.R., and Klein, C.B. (2005) *Toxicology and Applied Pharmacology*, **207**, 557–564.
84. Ramirez, T., Brocher, J., Stopper, H., and Hock, R. (2008) *Chromosoma*, **117**, 147–157.
85. Hong, S.H., Yang, Z., and Privalsky, M.L. (2001) *Molecular and Cellular Biology*, **21**, 7172–7182.
86. Zhu, J., Chen, Z., Lallemand-Breitenbach, V., and de The, H. (2002) *Nature Reviews. Cancer*, **2**, 705–713.
87. Zhu, Q., Zhang, J.W., Zhu, H.Q. *et al.* (2002) *Blood*, **99**, 1014–1022.
88. Zhu, J., Koken, M.H., Quignon, F. *et al.* (1997) *Proceedings of the National Academy of Sciences of the United States of America*, **94**, 3978–3983.
89. Mann, K.K. and Miller, W.H. Jr. (2004) *Cancer Cell*, **5**, 307–309.
90. Chou, W.C., Chen, H.Y., Yu, S.L. *et al.* (2005) *Blood*, **106**, 304–310.
91. Miller, W.H. Jr., Schipper, H.M., Lee, J.S. *et al.* (2002) *Cancer Research*, **62**, 3893–3903.
92. Chou, W.C. and Dang, C.V. (2005) *Current Opinion in Hematology*, **12**, 1–6.
93. Yu, S. and Kong, A.N. (2007) *Current Cancer Drug Targets*, **7**, 416–424.
94. Liu, J., Lu, Y., Wu, Q. *et al.* (2008) *The Journal of Pharmacology and Experimental Therapeutics*, **326**, 363–368.
95. Wang, H., Liu, S., Lu, X. *et al.* (2003) *Chinese Medical Journal*, **116**, 1074–1077.
96. Zhong, L., Chen, F., Han, J. *et al.* (2003) *Chinese Medical Journal*, **116**, 148–150.
97. Wang, H.Y. and Liu, S.X. (2007) *China Journal of Chinese Materia Medica*, **27**, 600–604.
98. Zhong, L., Chen, F., Han, J. *et al.* (2001) *Journal of Shanghai Second Medical University*, **13**, 6–10.
99. Luo, L.Y., Huang, J., Gou, B.D. *et al.* (2006) *Leukemia Research*, **30**, 1399–1405.
100. Peng, J., Zheng, Y.J., and Wu, Y.X. (2007) *Chinese Journal of Industrial Medicine*, **20**, 252–254.
101. Yin, L., Pu, D.M., Cheng, Y.X. *et al.* (2007) *Chinese Journal of Cancer Research*, **19**, 37–40.
102. Nakashima, M., Sonoda, K., and Watanabe, T. (1999) *Nature Medicine*, **5**, 938–942.
103. Liu, R., Pu, D., Liu, Y. *et al.* (2008) *Journal of Huazhong University of Science and Technology (Medical Sciences)*, **28**, 317–321.
104. Ye, Q.D., Gu, L.J., Zhao, J.C. *et al.* (2004) *Chinese Journal of Contemporary Pediatrics*, **6**, 15–18.
105. Zhang, J., Wang, J.C., Han, Y.H. *et al.* (2005) *Acta Haematologica*, **113**, 247–254.
106. Sun, F., Chen, N.N., and Cheng, Y.B. (2008) *Chinese Journal of Integrated Traditional and Western Medicine*, **6**, 639–642.
107. Wang, X.B., Xi, R.G., Yao, X.M. *et al.* (2007) *Chinese Journal of New Drugs*, **16**, 1869–1872.
108. Deng, Y., Xu, H., Huang, K. *et al.* (2001) *Pharmacological Research*, **44**, 513–517.

109. Song, Z.Q., Chen, H.H., Yao, W.M., and Liang, B., and Wang, H. (2005) *Chinese Journal of Clinical Pharmacology and Therapeutics*, **6**, 659–663.
110. Yao, W.M., Liang, B., and Liu, Y.Y. (2004) *Chinese Journal of Clinical Pharmacology and Therapeutics*, **2**, 193–196.
111. Li, D.M., Xie, J.X., and Liang, B. (2005) *China Journal of Chinese Materia Medica*, **30**, 1958–1960.
112. Yi, Z., Huang, R., Chen, Y., and Liang, B. (2006) *Chinese Journal of Respiratory and Critical Care Medicine*, **5**, 113–116.
113. Tan, D.Y. and Liang, B. (2004) *Chinese Journal of Tuberculosis and Respiratory Diseases*, **27**, 411–412.
114. Guo, H.R. and Liang, B. (2005) *Chinese Pharmacological Bulletin*, **21**, 895–896.
115. Zhao, Y., Cao, C.Y., Wang, X.R. *et al.* (2002) *Chinese Journal of Integrated Traditional and Western Medicine*, **22**, 684–686.
116. Gao, J.Y., Liu, S.J., and Zhang, J. (1998) *Chinese Journal of Basic Medicine in Traditional Chinese Medicine*, **4**, 30–32.
117. Zhu, K.J., Sun, J.N., Zhang, S.F., and Feng, S.Y. (2007) *Traditional Chinese Medicinal Research*, **20**, 23–25.
118. Zhu, K.J., Sun, J.N., Ma, C.H., and Geng, Y. (2007) *China Journal of Chinese Materia Medica*, **32**, 949–953.
119. Tang, Y., Wang, N., Mi, S. *et al.* (2008) *Pharmacol Clin Chin Mater Med*, **24**, 48–52.
120. Lin, P.Y., Tang, Y.S., and Wang, N.S. (2006) *Zhong Yao Cai*, **29**, 458–461.
121. Tang, Y.S., Wang, N.S., Zhang, Y.Q. *et al.* (2008) *Neural Regeneration Research*, **3**, 885–889.
122. Chen, C.J., Chuang, Y.C., Lin, T.M., and Wu, H.Y. (1985) *Cancer Research*, **45**, 5895–5899.
123. Li, G.M., Liu, S.Q., and Zhang, X.J. (2002) *Hebei Medical*, **24**, 60.
124. Dai, Y.X., Li, D.Q., and Zhang, J. (1983) *Chinese Journal of Dermatology*, **16**, 132–133.
125. Shi, G.B. (2002) *Journal of Pharmacy Practice*, **20**, 267–270.

6

Microbial Transformations of Arsenic in Aquifers

Jonathan R. Lloyd

*School of Earth, Atmospheric and Environmental Sciences, and Williamson Research Centre
for Molecular Environmental Science, University of Manchester, Manchester M13 9PL, UK*

6.1 An Introduction to the Microbial Cycling of Arsenic

Although arsenic is highly toxic to humans and indeed most other forms of life, some microorganisms have evolved to tolerate relatively high concentrations of the metalloid, while specialist examples even thrive on the element, using it as a source of energy for growth. For example, in alkali soda lakes such as Mono and Searls Lake in Eastern California the combination of alkali pH (pH 9.8), high carbonate/bicarbonate concentrations and naturally elevated concentrations of the metalloid from hydrothermal waters can result in mM (high ppm) concentrations of dissolved arsenic that sustains a diversity of specialist microorganisms adapted to using the arsenic oxyanions in energy yielding redox reactions [1, 2]. However, even at the very low concentrations of arsenic found in most other marine and freshwater environments that lack the geochemical extremes of the soda lakes, microorganisms can transform or even accumulate arsenic to concentrations many times those encountered in the environment they inhabit. Together with inorganic and physical processes, these constitute the global arsenic cycle described in [3]. For example, in the marine environment, arsenic is normally present at trace concentrations of arsenate and can be taken up by a range of organisms (including phytoplankton, algae, crustaceans and molluscs), methylated and further metabolized into organic compounds, some of which are

passed up through the marine food chain. Indeed, the major organoarsenic compound in marine animals is arsenobetaine but it can be degraded eventually by sediment microorganisms, returning arsenic to the seawater closing the marine cycle for this element (reviewed in [3]). In addition, the redox chemistry of the metalloid also makes it a useful energy source to sustain prokaryotic life and therein lies the potential for microorganisms to play a critical (and potentially lethal) role in controlling the solubility of arsenic (which is closely linked to its oxidation state) in aquifers that provide drinking and irrigation water to tens of millions of people worldwide.

There are four oxidation states of arsenic –III, 0, +III and +V. However, the predominant forms of inorganic arsenic are +V (arsenate; H_2AsO_4^- and HAsO_4^{2-}) which sorbs efficiently to a range of subsurface minerals and +III (arsenite; H_3AsO_3 and H_2AsO_3^-) which is comparatively more mobile. Under anaerobic conditions, specialist ‘dissimilatory arsenate-reducing prokaryotes’ are able to respire arsenate as the electron acceptor in place of oxygen, reducing it to As(III). Although pH and concentration dependent, the oxidation/reduction potential of As(V)/As(III) is between +60 to +135 mV [4], sufficient to support growth when organic matter or sulfide is supplied as the electron donor. As(III) is also a suitable electron donor for microbial respiratory processes, with electrons from the oxidation of As(III) to As(V) passed to a suitable electron acceptor such as oxygen or nitrate under anaerobic conditions. Finally, a wide diversity of microorganisms have also evolved an energy requiring detoxification processes catalysed by the *Ars* operon, linked to the intracellular reduction of As(V) by the *ArsC* protein and its efflux as As(III) (Chapter 8). A synopsis of these microbial processes is illustrated in Figure 6.1, with the underlying biochemistry shown and described in more detail in the next section of this review.

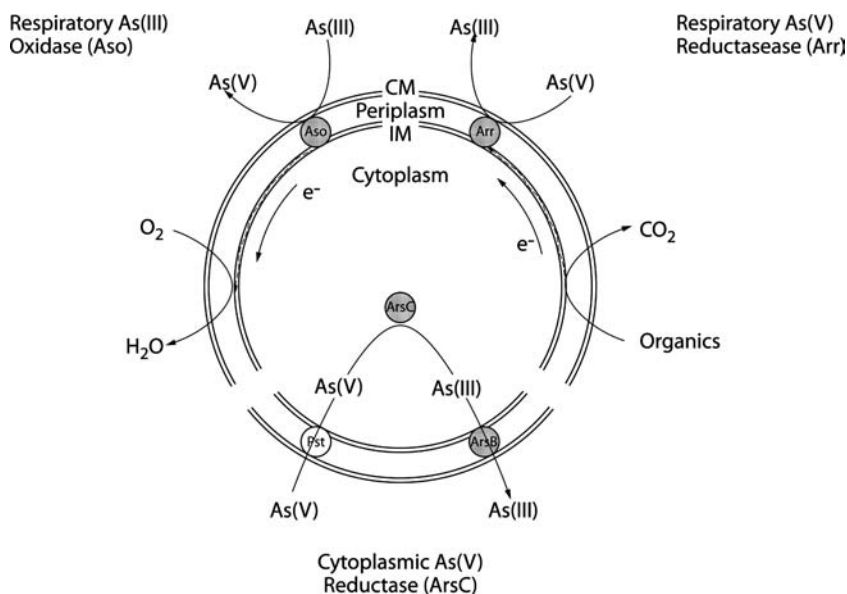


Figure 6.1 Biochemical transformations of arsenic oxyanions by microbial cells

6.2 The Biochemistry of Microbial Arsenic Transformations

6.2.1 Microbial Resistance to As(V) via the Arsenic Operon

Arsenate is a chemical surrogate for phosphate and can therefore enter the microbial cell via transporters meant for the uptake of this essential nutrient. Once within the cell it can interfere with phosphate based energy generating processes, inhibiting, for example, oxidative phosphorylation. Arsenite, on the other hand, enters via a different route (aqua glycerolporins) (Figure 8.2) and targets a broader range of cellular processes, binding to the thiol groups in important cellular proteins such as pyruvate dehydrogenase and 2-oxoglutarate dehydrogenase. Microorganisms have evolved multiple strategies to protect themselves from arsenic. For example, fungi can use methylation as a detoxification strategy, producing monomethylarsenic acid (MMA) or dimethylarsinic acid (DMA). Prokaryotes (including representatives from both the Archaeal and Bacterial Domains) can also produce volatile methylated arsines, removing arsenic from the local environment. An alternative strategy used by bacteria and yeast (e.g., *S. cerevisiae*) is based upon the 'ArsC' arsenate reductase protein. The gene for this enzyme, along with those of other proteins required for arsenic detoxification, is often encoded by plasmids, making them highly amenable to genetic study and more recently protein crystallography studies for example, for ArsC proteins [5]. This type of resistance determinant is very common in the prokaryotic world; more than 100 Ars operons had been sequenced [3] and this number is growing steadily with the increase in number of genomic sequences deposited in genetic databases. ArsC is a small (13–16 kDa) protein that is found in the cytoplasm of the microbial cell and mediates the reduction of arsenate to arsenite, with glutaredoxin, glutathione or thioredoxin supplying the reducing power for this transformation [6]. The toxic arsenite is then excreted by an energy requiring ATP-dependent efflux pump ArsB (Figure 6.1). However, despite its wide distribution throughout the prokaryotic world, there is little evidence at present linking ArsC activity directly to reduction and mobilization of arsenic in aquifers, which is the main focus of this review.

6.2.2 Gaining Energy from Arsenic: the Dissimilatory Reduction of As(V) under Anaerobic Conditions

Although the ArsC-mediated detoxification system requires energy in the form of ATP to function, some specialist bacteria are able to obtain energy for growth through the 'dissimilatory' reduction of As(V). Two closely related representatives of the ϵ -Proteobacterial phylogenetic group (*Sulfurospirillum arsenophilum* and *S. barnesii*) were the first dissimilatory arsenate-reducing bacteria identified in the mid 1990s and representatives have since been identified in other phylogenetic groupings, including the γ - and δ -Proteobacteria, the low GC 'Gram-positive' bacteria, thermophilic Eubacteria and Crenarchaea [4]. Of particular relevance to the mobilization of arsenic in aquifers, is the observation that organisms that can respire As(V) are able to reduce the pentavalent metalloid when sorbed to a range of mineral phases, resulting in significant mobilization of As(III) which sorbs less strongly to surfaces (see below). Although sharing the common ability to obtain energy for growth through the reduction of sorbed or soluble As(V), the overall metabolic diversity of these dissimilatory arsenate respiring organisms is wide. Certainly, given the low concentrations of As(V) in most environments, compared to other electron acceptors, a high level of

respiratory diversity may be crucial to the survival of these organisms. Indeed, to date only one obligate arsenate-reducing prokaryote has been identified (strain MLMS-1 isolated from Mono Lake; [7]). Other electron acceptors used by these organisms are strain specific but include selenate, nitrate, nitrite, fumarate, Fe(III), thiosulfate, elemental sulfur, dimethylsulfoxide and trimethylamine oxide. They can also use a range of electron donors, including hydrogen, sulfide, acetate, formate, pyruvate, butyrate, citrate, succinate, fumarate and glucose and aromatics such as benzoate.

Despite the environmental importance of the process, the mechanism of As(V) reduction by dissimilatory arsenate-reducing bacteria has not been studied in the same depth as the ArsC detoxification system described above. The first 'respiratory arsenate reductase' characterized was from the Gram-negative bacterium *Chrysiogenes arsenatis*, isolated from gold mine wastewater. The protein consisted of 87 and 29 kDa subunits and is related to the dimethylsulfoxide (DMSO) family of mononuclear molybdenum containing enzymes [8]. Similar proteins (and the corresponding genes designated *arrA* and *arrB*) were subsequently characterized in *Bacillus selenitireducens* [9] and *Shewanella* strain ANA-3 [10]. This does pose a considerable conundrum as all Arr proteins described to date reside in the periplasm and are unlikely to access sorbed As(V) directly. Hence, there is a need for more detailed research into the precise mechanism of reduction of sorbed arsenate in aquifers. However, recent genetic studies using *Shewanella* sp. ANA-3 have made it possible to study the interplay between the ArsC detoxification (an intracellular process) and ArrA respiratory systems in laboratory cultures, which both potentially result in As(V) reduction to As(III) [11]. Strains that were able to synthesize the ArrA protein were able to respire both soluble As(V) and also As(V) sorbed onto hydrous ferric oxide [12], confirming the earlier work discussed above by Zobrist and Oremland [13]. In contrast, *Shewanella* sp. CN-8, a detoxifying arsenate reducer carrying the *ars* operon that cannot respire arsenate as it lacks the *arrA* and *arrB* genes, reduced soluble As(V) but not arsenate sorbed onto Fe(III) oxides [14], supporting the hypothesis of ArrA-mediated (but not ArsC mediated) reduction of sorbed arsenate in sediments. Finally PCR primers have also been developed to target *arrA* genes in environmental samples for example [12, 15], making it potentially possible to retrieve *arrA* genes from species present in the environment but not currently available in culture. For example, this approach has been used successfully to investigate the diversity of arsenate respiring bacteria in Mono Lake, California [16, 17] and Cambodian sediments [18]. Such molecular tools also offer the potential to quantify active As(V)-reducing bacteria through real time quantitative polymerase chain reaction (PCR) techniques, which may give a relatively rapid indication of the rates of arsenic reduction (and potentially mobilization) in field samples.

6.2.3 Closing the Arsenic Cycle: the Oxidation of As(III)

Finally arsenite-oxidizing bacteria are also known to couple the oxidation of As(III) to the reduction of either molecular oxygen or nitrate, the latter under anaerobic conditions. As(III) oxidation is also catalysed by a wide range of microorganisms; over 30 strains from at least nine different genera have been identified so far [4], including chemolithoautotrophic examples that conserve energy for growth via arsenite oxidation, using some of this energy to fix CO₂ for the synthesis of cellular material. A comparatively well studied example is strain NT-26, which was isolated from a gold mine in the Northern Territory of

Australia and shown to be related to soil bacteria in the *Agrobacterium/Rhizobium* branch of the α -Proteobacteria [19]. A fairly recent review has also given an excellent overview of the genetic basis of arsenite oxidation by *Alcaligenes faecalis*, based on the genome sequence for this soil bacterium [6]. The first organism (*Marinobacter santoriniensis*) shown unequivocally to gain energy from either the aerobic oxidation of As(III) or the anaerobic reduction of As(V) has also been described recently [20]. It was isolated from hydrothermal sediments of the Greek island of Santorini and although it contains the genes required for the arsenite oxidase (*asoA* and *asoB*), the genes thought necessary for the dissimilatory reduction of As(V) are absent from the sequenced genome suggesting the utilisation of novel genes and corresponding proteins for As(V) respiration (Lloyd and Handley, unpublished). There are indeed surprising similarities between the respiratory arsenate reductases of dissimilatory arsenate-reducing prokaryotes and respiratory arsenite oxidases; both are molybdoproteins comprising two subunits. Thus, perhaps it is conceivable that in *Marinobacter santoriniensis* and potentially other organisms, a single biochemical system could catalyse both oxidative and reductive transformations of arsenic oxyanions. Finally, the sequence annotation of the *A. faecalis* genome is especially noteworthy, as it shows the *asoA* and *asoB* arsenite oxidase genes, encoding a large molybdopterin containing peptide and a smaller [2Fe-2S]-containing subunit, respectively, located within an 'arsenic gene island' containing more than 20 other genes potentially involved in arsenic metabolism [6].

6.3 Microbially Driven Mobilization of Arsenic in Aquifers: a Humanitarian Disaster

Contamination of groundwater from arsenic naturally occurring in aquifers poses a global public health crisis in countries including Mexico, China, Hungary, Argentina, Chile, Cambodia, India (W. Bengal) and Bangladesh [21]. For example, 28–62% of the 125 million inhabitants of Bangladesh are at risk of arsenic poisoning from water abstracted from the subsurface and used for drinking, cooking and irrigation. Long term exposure to arsenic can lead to scaling of the skin, circulatory and nervous system disorders and skin, lung and bladder cancers [22]. In W. Bengal and Bangladesh where the problem has received most attention, the aquifer sediments are derived from weathered materials from the Himalayas. Arsenic typically occurs in concentrations of 2–100 ppm in these sediments, much of it sorbed onto a variety of mineralogical hosts including hydrated ferric oxides, phyllosilicates and sulfides [22, 23]. The mechanism of arsenic release from these sediments has been a topic of intense debate and microbial processes such as those described above as well as a complementary/competing chemical processes have been invoked [4, 24–27]. The oxidation of arsenic rich pyrite has been proposed as one possible mechanism [25, 26], while other studies have suggested that the reductive dissolution of arsenic rich Fe(III) oxyhydroxides deeper in the aquifer may lead to the release of arsenic into the groundwater [22, 23, 27, 28]. Additional factors that may add further complication to potential arsenic release mechanisms from sediments include the predicted mobilization of sorbed arsenic by phosphate generated from the intensive use of fertilizers [29], by carbonate [30] produced via microbial metabolism [28] or by changes in the sorptive capacity of ferric oxyhydroxides [22].

However, microbially mediated reduction of assemblages comprising arsenic (most likely as arsenate) sorbed to ferric oxyhydroxides is gaining consensus as the dominant mechanism for the mobilization of arsenic into these groundwaters [22–24, 31, 32] and the acceptance of this mechanism of arsenic release has paralleled advances in the microbiology of organisms that can respire sorbed As(V) described above. For example, an early microcosm based study from our group in Manchester provided direct evidence for the role of indigenous metal-reducing bacteria in the formation of toxic, mobile As(III) in sediments from the Ganges Delta [31]. This study showed that the addition of acetate to anaerobic sediments, as a proxy for organic matter and a potential electron donor for metal reduction, resulted in stimulation of microbial reduction of Fe(III) followed by As(V) reduction and the subsequent release of As(III), presumably by As(V)-respiring bacteria that were previously respiring Fe(III). Microbial communities responsible for metal reduction and As(III) mobilization in the stimulated anaerobic sediment were analysed using molecular (PCR) and cultivation dependent techniques. Both approaches confirmed an increase in numbers of metal-reducing bacteria, principally *Geobacter* species. However, subsequent studies suggested that *Geobacter* strains that were available in culture at that time do not possess the *arrA* genes required to support the reduction of sorbed As(V) and the mobilization of As(III). Indeed, in strains lacking the biochemical machinery for As(V) reduction, Fe(II) minerals formed during respiration on Fe(III) have proved to be potent sorbants for arsenic, preventing mobilization of arsenic during active iron reduction [33]. However, the genomes of at least two newly isolated *Geobacter* species (*G. unraniumreducens* and *G. lovleyi*) do contain *arrA* genes and interestingly genes affiliated with the *G. unraniumreducens* and *G. lovleyi* *arrA* gene sequences have been identified recently in Cambodian sediments stimulated for Fe(III) and As(V) reduction in several studies from our group (*vide infra*) while the type strain of *G. unraniumreducens* has been shown to reduce soluble and sorbed As(V), resulting in mobilization of As(III) in the latter case (Gault *et al.* unpublished). Thus, some *Geobacter* species may play a role in arsenate reduction and release of As(III) from SE Asian sediments, perhaps alongside other well known arsenate-reducing bacteria, including *Sulfurospirillum* species that have also been detected using molecular PCR-based techniques [18, 34]. Recent advances in this area will now be described.

6.3.1 Microbial Ecology of Arsenic Impacted Aquifers: Hunting for the Organisms that Mobilize Arsenic

Although the biogeochemical conditions that promote microbial arsenic mobilization are becoming clearer, it remains a major challenge to identify the organisms that have the potential to cause the reduction and mobilization of the metalloid among the complex microbial communities that exist in the subsurface. One approach that has recently proved useful is the application of stable isotope probing (SIP) techniques, which can link the active fraction of a microbial community to a particular biogeochemical process. Using this technique, sediments are supplemented with a ^{13}C -labelled substrate, and the components of the microbial community that assimilate the substrate are identified by PCR-based analysis of the ‘heavy’ labelled DNA or RNA separated from unlabelled ‘light’ nucleic acids using an ultracentrifuge [35]. This technique has been used to identify the functional components of several microbial processes [36] and has been used recently to identify active

As(V)-respiring bacteria in Cambodian aquifer sediments [18] implicated in the reductive mobilization of arsenic [37]. ^{13}C -labelled acetate was used as a proxy for organic matter in these experiments, promoting the reduction of As(V) present naturally in the sediments, concomitant with the detection of 16S rRNA genes affiliated with the known arsenate respiring bacteria *Desulfotomaculum* sp. and *Desulfosporosinus* sp. In the presence of 10 mM added As(V), most of which was associated with the mineral phases in the microcosms, an organism closely related to the arsenate-reducing organism *Sulfurospirillum* strain NP4 [38] was identified, which was also closely related to clones identified previously in West Bengal sediments associated with high arsenic concentrations. Functional gene analysis of sediments amended with ^{13}C -labelled acetate and As(V) targeted the As(V) respiratory reductase gene (*arrA*) using highly specific primers and identified gene sequences most closely related to those found in *Sulfurospirillum barnesii* and *Geobacter uraniumreducens*. Neither *arrA* nor 16S rRNA genes affiliated with known arsenate respiring bacteria could be detected in the initial sediment, prior to incubation of the microcosms.

Although stable isotope probing experiments have proved useful in identifying anaerobic organisms that are potentially involved in the reductive mobilization of arsenic, an obvious limitation of this approach is the need to manipulate the conditions in laboratory incubations through the addition of a labelled substrate, potentially altering the geochemical matrix of the sediment. This contrasts with the approach used in a recent complementary study where sediments collected from depths of 8–30 m at an arsenic ‘hotspot’ in the Nadia district in West Bengal [39, 40] were incubated in the absence of an exogenous carbon source and added arsenate [37]. Analyses of the sediments showed the presence of indigenous organics, including petroleum compounds previously hypothesized to play a role in promoting the anaerobic metabolism of metals [34, 37]. The rates and extent of As(III) release and Fe(III) reduction were quantified alongside changes in bacterial community structure. Again, 16S rRNA analyses suggested a potential role of species from the genera *Sulfurospirillum* and *Geobacter* in the respiration of Fe(III), the reductive mobilization of arsenic and the oxidation of organic matter, including in this case petroleum compounds [34]. Thus, there are converging lines of evidence that suggest organisms affiliated *Sulfurospirillum* and *Geobacter* may play a role in the mobilization of arsenic through the activation of genes that encode respiratory arsenate-reducing enzyme systems.

6.4 Conclusions and Future Directions

Knowledge of aspects of the microbial arsenic cycle is improving in a range of environments, especially those with ‘extreme’ geochemical conditions that lead to elevated soluble concentrations of the metalloid. In aquifer sediments, which have more complex geochemical and mineralogical backgrounds and support diverse microbial communities, the role of specific microorganisms in mobilizing low (typically ppb) but significant concentrations of arsenic is less clear. However, several recent studies suggest that we are approaching a consensus that metal-reducing bacteria, especially dissimilatory As(V)-respiring bacteria may play an important role in this process. The microbiological focus of research in this area is shifting now towards the unequivocal identification of the organisms involved, which will in turn lead to studies on the underlying mechanisms at a molecular (genetic) level and the

factors that result in the activation of these physiological processes *in situ*. Given the complex interplay between arsenic metabolising microorganisms, and the arsenic bearing minerals (often Fe-phases) that they interact with, there is a need for a better understanding at the nanoscale of the microbe mineral interface. There is also an urgent need for improvements in the understanding of the mechanisms of delivery of key nutrients and electron donors that stimulate or sustain arsenate-reducing bacteria. These factors relate, in turn, to the hydrological conditions *in situ* (e.g., through pulling down of highly labile organic matter from surface waters through extensive water extractions) and/or the distribution of alternative extant electron donors in aquifer sediments. Other important research priorities include a better understanding of the *in situ* activation of alternative microbial processes that can reverse the mobilization of arsenic, e.g., sulfate reduction or Fe(II) oxidation that can lead to sulfide or Fe(III) minerals that sorb arsenic efficiently. For the latter process, the co stimulation of microbial oxidation of soluble As(III) to As(V) (which sorbs preferentially to a broad range of minerals) also requires further investigation.

Acknowledgements

Financial support from NERC (Grant NE/D013291/1) is acknowledged.

References

1. Lloyd, J.R. and Oremland, R.S. (2006) *Elements*, **2**, 85–90.
2. Oremland, R.S., Stolz, J.F. and Hollibaugh, J.T. (2004) *FEMS Microbiology Ecology*, **48**, 15–27.
3. Mukhopadhyay, R., Rosen, B., Phung, L. and Silver, S. (2002) *FEMS Microbiology Reviews*, **26**, 311.
4. Oremland, R.S. and Stolz, J.F. (2003) *Science*, **300**, 939–944.
5. Demel, S., Shi, J., Martin, P. *et al.* (2004) *Protein Science*, **13**, 2330–2340.
6. Silver, S. and Phung, L.T. (2005) *Applied and Environmental Microbiology*, **71**, 599–608.
7. Hoefft, S.E., Kulp, T.R., Stolz, J.F. *et al.* (2004) *Applied and Environmental Microbiology*, **70**, 2741–2747.
8. Krafft, T. and Macy, J.M. (1998) *European Journal of Biochemistry*, **255**, 647–653.
9. Afkar, E., Lisak, J., Saltikov, C. *et al.* (2003) *FEMS Microbiology Letters*, **226**, 107–112.
10. Saltikov, C.W. and Newman, D.K. (2003) *Proceedings of the National Academy of Sciences of the United States of America*, **100**, 10983–10988.
11. Saltikov, C.W., Cifuentes, A., Venkateswaran, K. and Newman, D.K. (2003) *Applied and Environmental Microbiology*, **69**, 2800–2809.
12. Malasarn, D., Saltikov, C.W., Campbell, K.M. *et al.* (2004) *Science*, **306**, 455.
13. Zobrist, J., Dowdle, P.R., Davis, J.A. and Oremland, R.S. (2000) *Environmental Science & Technology*, **34**, 4747–4753.
14. Langner, H.W. and Inskeep, W.P. (2000) *Environmental Science & Technology*, **34**, 3131–3136.
15. Song, B., Chyun, E., Jaffe, P.R. and Ward, B.B. (2009) *FEMS Microbiology Ecology*, **68**, 108–117.
16. Kulp, T.R., Han, S., Saltikov, C.W. *et al.* (2007) *Applied and Environmental Microbiology*, **73**, 5130–5137.
17. Kulp, T.R., Hoefft, S.E., Miller, L.G. *et al.* (2006) *Applied and Environmental Microbiology*, **72**, 6514–6526.
18. Lear, G., Song, B., Gault, A.G. *et al.* (2007) *Applied and Environmental Microbiology*, **73**, 1041–1048.
19. Santini, J.M., Skly, L.I., Schnagll, R.D. and Macy, J.M. (2000) *Applied and Environmental Microbiology*, **66**, 92–97.

20. Handley, K.M., Hery, M. and Lloyd, J.R. (2009) *Environmental Microbiology*, **11**, 1601–1611.
21. Smith, A.H., Lingas, E.O. and Rahman, M., *Bulletin WHO* (2000) **78**, 1093–1103.
22. Smedley, P.L. and Kinniburgh, D.G. (2002) *Applied Geochemistry*, **17**, 517–568.
23. Nickson, R.T., McArthur, J.M., Ravenscroft, P. *et al.* (2000) *Applied Geochemistry*, **15**, 403–413.
24. Akai, J., Izumi, K., Fukuhara, H. *et al.* (2004) *Applied Geochemistry*, **19**, 215–230.
25. Chowdhury, T.R., Kumar Basu, G.K., Mandal, B.K. *et al.* (1999) *Nature*, **401**, 545–546.
26. Das, D., Samanata, G., Mandal, B.K. *et al.* (1996) *Environmental Geochemistry and Health*, **18**, 5–15.
27. Nickson, R., McArthur, J., Burgess, W. *et al.* (1998) *Nature*, **395**, 338.
28. Harvey, C.F., Swartz, C.H., Badruzzaman, A.B.M. *et al.* (2002) *Science*, **298**, 1602–1606.
29. Acharyya, S.K., Chakraborty, P., Lahiri, S. *et al.* (1999) *Nature*, **401**, 545.
30. Appelo, C.A.J., Van der Weiden, M.J.J., Tournassat, C. and Charlet, L. (2002) *Environmental Science & Technology*, **36**, 3096–3103.
31. Islam, F., Gault, A.G., Boothman, C. *et al.* (2004) *Nature*, **430**, 68–71.
32. Van Geen, A., Rose, J., Thorai, S. *et al.* (2004) *Geochimica et Cosmochimica Acta*, **68**, 3475–3486.
33. Islam, F.S., Pederick, R.L., Gault, A.G. *et al.* (2005) *Applied and Environmental Microbiology*, **71**, 8642–8648.
34. Rowland, H.A.L., Boothman, C., Pancost, R. *et al.* (2009) *Journal of Environmental Quality*, **38**, 1598–1607.
35. Radajewski, S., Ineson, P., Parekh, N.R. and Murrell, J.C. (2000) *Nature*, **403**, 646–649.
36. Neufeld, J.D., Wagner, M. and Murrell, J.C. (2007) *ISME Journal*, **1**, 103–110.
37. Rowland, H.A.L., Pederick, R.L., Poly, D.A. *et al.* (2007) *Geobiology*, **5**, 281–292.
38. MacRae, J.D., Lavine, I.N., McCaffery, K.A. and Ricupero, K. (2007) *Journal of Environmental Engineering-Asce*, **133**, 81–88.
39. Bandyopadhyay, R.K. (2002) *Journal of the Geological Society*, **59**, 33–46.
40. Gault, A.G., Islam, F.S., Poly, D.A. *et al.* (2005) *Mineralogical Magazine*, **69**, 855–863.

7

Biomethylation of Arsenic, Antimony and Bismuth

Richard O. Jenkins

Faculty of Health & Life Sciences, De Montfort University, Leicester, LE1 9BH, UK

7.1 Introduction

Biomethylation of metals or metalloids refers to the process whereby living organisms cause direct linkage of methyl groups to the metal(loid)s through enzymatic transfer of a preformed methyl group. The attachment of a methyl group to a metal(loid) changes the chemical and physical properties of the element, which in turn influences its mobility, geological cycling and toxicity. Biomethylation of the following metal(loid)s have been definitively established, although for most very little is known about the biological mechanism involved: Cd, Hg, Tl, Ge, Sn, Pb, As, Sb, Bi, Se and Te. The biological systems responsible for metal(loid) biomethylation are almost exclusively microorganisms. Anaerobic prokaryotes, operating in anoxic environments such as sediments from environmental waters and landfill sites, are major biocatalysts of metal(loid) biomethylation in the natural environment. Methylmetal(loid)s have also been shown to occur in soils from disparate locations and some aerobic and facultatively anaerobic bacteria, fungi and lower algae have been shown to be capable of metal(loid) biomethylation. Although higher organisms have not been shown to biomethylate true metals, methyl derivatives of some metalloids (including those of Se and As) are formed in a wide range of higher animals and plants.

Over the past decade there has been a diversification of methods for the detection and measurement of organometallic compounds. Generally, this has been accompanied by improvements in reliability of detection and measurement of organometal(loid)s at low

concentration in environmental and biological samples. Volatile methylmetal(loid)s generated through biomethylation have been extracted from sample by purging with an inert gas and focused through cryotrapping (CT) on a suitable chromatographic adsorption material. Alternatively, solid-phase microextraction (SMPE) fibres have been used to directly sample the volatile methylmetal(loid)s from gaseous samples. For nonvolatile methylmetal(loid)s, hydride generation (HG) has been widely used to volatilize methylmetal(loid)s *in situ*, prior to trapping and detection. The advantage of such *in situ* derivatization of samples is that it tends to overcome matrix interferences and leads to improved sensitivity of measurement. Other approaches to pretreatment of samples include organic solvent extraction of samples (e.g., methanol extraction of plant material) prior to HG. Methods involving HG can be carried out offline using a batch mode approach followed by cryotrapping and GC separation, or online after separation of the individual species using HPLC. In a typical batch mode analysis, the sample is mixed with sodium borohydride (derivatisation agent) in an acid environment and the hydrides generated are purged onto a cold U trap. The trap is heated electrothermally and the analytes are released (separated) according to their boiling point and passed in an inert gas phase to an element specific detector, such as ICP-MS and AAS. The coupling of HG with such sensitive detectors has greatly reduced the limits of detection for many methylmetal(loid)s, including those of As, Sb and Bi. There are several recent reviews [1–4] of element speciation of particular relevance to the present chapter, covering pretreatment procedures, HG and a range of hyphenated (or coupled) techniques.

The elements under consideration in this chapter, As, Sb, Bi, have substantial differences with regards to biomethylation. Whereas biomethylation of arsenic is widespread (occurring in a wide range of microorganisms, algae, plants and animals, including humans) biomethylation of antimony seems to be limited to certain eukaryotic (fungi) and prokaryotic (bacteria and archaea) microorganisms. Bismuth biomethylation capability is even less widespread and appears to be limited to prokaryotes, especially the anaerobic archaea. Arsenic has a complex natural product chemistry, involving a diverse range of organoarsenic compounds. Biodegradation of these compounds in the natural environment leads to the formation of mono-, di- and trimethylarsenic species. It follows that the presence of such methylarsenic species in environmental or biological matrices does not necessarily reflect direct *de novo* bioconversion from inorganic arsenic, that is, biomethylation. This is not the case for antimony and bismuth since these elements do not appear to have complex natural product chemistries and there are no major anthropogenic inputs of methylated species of these elements into the environment.

Arsenic biomethylation has a long and chequered history, commencing in the early nineteenth century when cases of poisoning in Germany were linked to arsenic pigments in wallpaper. In the late nineteenth century the Italian physician Bartolomero Gosio showed that arsenic was volatilized by certain fungi. The evolved arsenical gas became known as ‘Gosio gas’. It was not until the 1930s that the volatile arsenical was identified as trimethylarsine (Me_3As) by Fredrick Challenger and his associates based at the University of Leeds. In the mid 1940s, Challenger proposed a mechanism for biomethylation of arsenic by fungi. Over the 1970s and 1980s a large number of naturally occurring arsenic compounds were identified and the range of organisms capable of biomethylation of arsenic was greatly extended. The 1989 review by Cullen and Reimer [5] was the first comprehensive review of environmental arsenic compounds and of the underlying chemical and biological processes. Since that time arsenic metabolism [6, 7] and organoarsenic

compounds in marine [8] and terrestrial [9] environments have been well served by reviews. Cullen's recent book [10] intriguingly entitled '*Is Arsenic an Aphrodisiac? The Socio-chemistry of an Element*' provides an entertaining and informative examination of the history of arsenic notoriety (and beneficial effects), and includes much in relation to biomethylation and the environmental distribution of organoarsenic compounds. Recent research on inorganic arsenic biomethylation has focused on mammalian metabolism, especially in humans. The present chapter considers the classical mechanism(s) of arsenic biomethylation as they relates to microorganisms, before dealing with the more recent developments of mammalian arsenic biomethylation. Whilst the relation between arsenic biomethylation and formation/degradation of some of the major forms of organoarsenic compounds is also considered in this chapter, it was not the intention to review the environmental distribution of organoarsenic compounds in the natural environment.

Research into antimony biomethylation has lagged behind that for arsenic, with earliest papers appearing in the mid 1990s. At around that time, microbial volatilization of antimony present in PVC covers of cot mattresses was hypothesized to be a cause of cot death and this further stimulated research into antimony biomethylation. The microbial biomethylation of antimony has been reviewed [11], as has the distribution of organoantimony compounds in the environment [12, 13]. Research into biomethylation of bismuth has lagged behind even that for antimony, with the first report [14] of microorganisms capable of bismuth biomethylation appearing as late as 2000, by Michalke and coworkers. Indeed, most of subsequent developments on bismuth biomethylation are attributed to the same group of researchers. There is little or no evidence to indicate that mammalian cells are capable of biomethylating antimony or bismuth and, as previously mentioned, the organometal (loid) chemistry of these elements is much simpler than that for arsenic. Given the relative paucity of published literature on antimony or bismuth biomethylation compared to that for arsenic, an aim of the present chapter was to comprehensively review the literature on biomethylation of antimony and bismuth, both in regards to biomethylating organisms and environmental distribution of the methylated products.

7.2 Biomethylation of Arsenic

There is a long history of research on the biomethylation of arsenic, which has involved a host of chemists, microbiologists, biochemists, toxicologists and most recently, molecular biologists.

7.2.1 Microbial Biomethylation of Arsenic

The seminal research of Fredrick Challenger and his associates commencing in the 1930s provided chemical evidence that certain fungi, including *Scopulariopsis brevicaulis*, were capable of methylating inorganic arsenic [15, 16]. A scheme for arsenic biomethylation involving a series of steps, in which the reduction of arsenate is followed by oxidative methylations, was proposed [16]. The scheme, shown as Figure 7.1, is commonly referred to as the Challenger mechanism. Subsequent research by several researchers has extended the range of fungi capable of arsenic biomethylation; see a review on arsenic speciation by Cullen and Reimer [5].

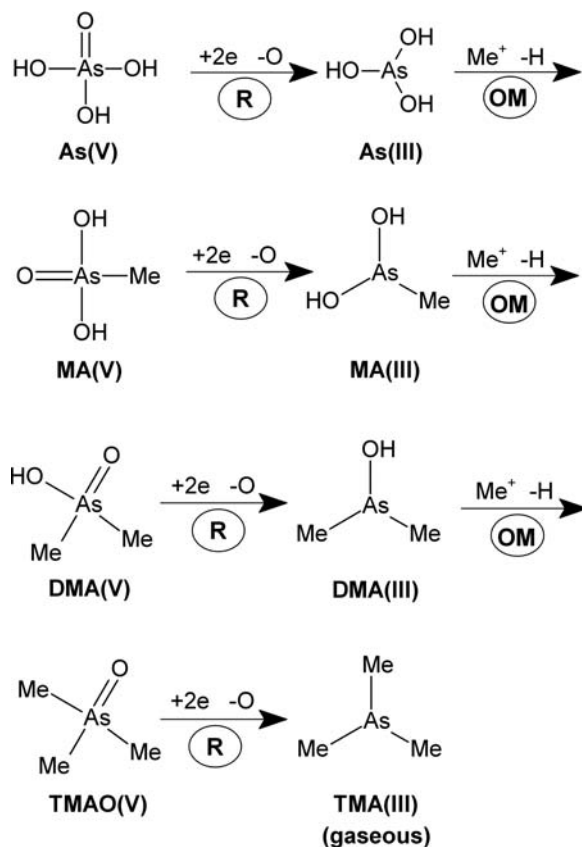


Figure 7.1 Arsenic biomethylation according to the Challenger mechanism (as proposed for fungi) involving alternate oxidative methylation (OM) and reduction (R) steps. Arsenate, As(V); arsenite, As(III); methylarsenate, MA(V); methylarsenous acid, MA(III); dimethylarsenate, DMA(V); dimethylarsinous acid, DMA(III); trimethylarsine, TMA(III)

Cullen *et al.* [17] addressed the question of what was the source of the methyl groups needed to produce methylated arsenicals by fungi. They showed that when L-methionine-methyl- d_3 was added to aerobically growing fungal cultures, the CD_3 label was incorporated intact into the evolved Me_3As to a considerable extent, which indicated that S-adenosyl-methionine (SAM) was the likely methyl donor, that is, transfer of the carbonium ion (Me^+) from SAM to arsenic. The structure of SAM is shown in Figure 7.2a. Methylated arsenic species identified during incubation of various fungi, including filamentous *Gliocladium roseum* and the yeast *Cryptococcus humicola*, with inorganic arsenic were consistent with the intermediates in the Challenger scheme. Fungal biomethylation of arsenic via the Challenger mechanism and involving SAM as methyl donor is now well established [17, 18]. Using the same CD_3 labelling approach, Cullen *et al.* [19] showed that the marine alga *Polyphysa peniculus* used SAM, or some related sulphonium compound, as the methyl donor in the bioconversion of arsenate to a dimethylarsenic derivative. The Challenger

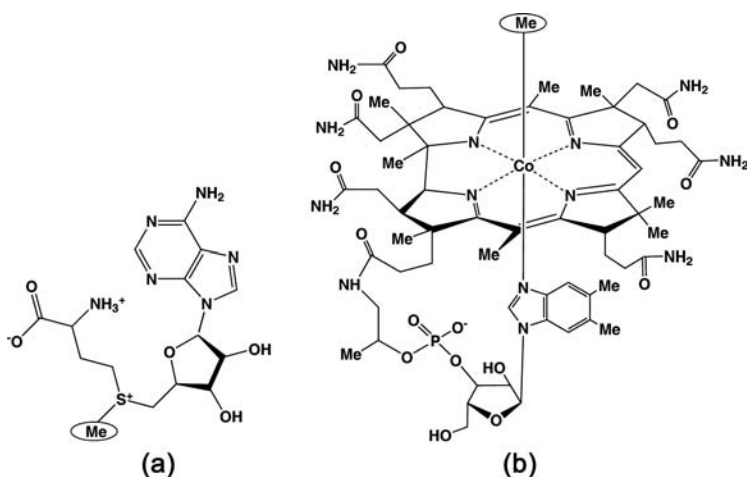
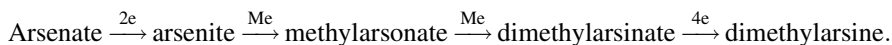


Figure 7.2 Biological methyl donors involved in metal(loid) biomethylation. (a) *S*-adenosylmethionine (SAM); (b) *N*-methylcobalamin (Me-CoB₁₂). Reprinted from [1] with permission from Elsevier

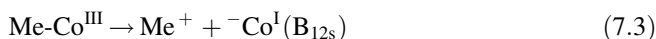
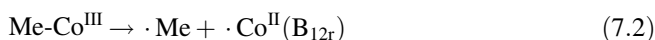
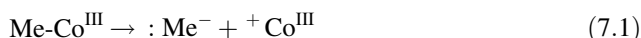
mechanism has also been suggested for prokaryotes [20], although an alternative mechanism may exist in these organisms.

Bacterial methylation of inorganic arsenic has been studied extensively in methanogenic bacteria. McBride and Wolfe [21] were the first to report on bacterial volatilization of arsenic; the formation of dimethylarsine by *Methanobacterium bryantii*. Since then several volatile methylated arsenic species have been detected in pure anaerobic cultures and in anaerobic ecosystems. Most notably, Michalke *et al.* [14] showed that *Methanobacterium formicium* was an efficient producer of mono-, di- and trimethylarsine (i.e., gaseous MeAsH₂, Me₂AsH and Me₃As) from inorganic arsenic, while three other obligate anaerobes; *Clostridium collagenovorans* and two *Desulfovibrio* spp, produced only trimethylarsine and in relatively small amounts. The original work of McBride and Wolfe [21] demonstrated that methyl transfer to arsenic by *M. bryantii* was enzymatically mediated. These authors also reported that methylcobalamin (structure shown in Figure 7.2b) was far more efficient than CO₂ as a methyl donor in the formation of dimethylarsine from arsenate by *M. bryantii*, and that neither serine nor 5-methyltetrahydrofolate was a methyl donor. Partly based on these findings, an anaerobic biomethylation pathway for dimethylarsine production by *M. bryantii* was proposed [21], involving methylcobalamin as methyl donor and a four electron reduction of dimethylarsinate as the final step:



Definitive evidence for the scheme has not been found and almost 40 years later there is still no consensus as to a mechanism for dimethylarsine formation by anaerobic bacteria. Numerous reports [5, 20, 22] have considered the possible chemistry for enzymatic and nonenzymatic methyl transfer from methylcobalamin to arsenic. In principle, methylation of arsenic by anaerobic bacteria involving methylcobalamin could occur by direct transfer

from methylcobalamine or by indirect transfer involving a carrier molecule; three possible mechanisms of methyl group transfer from methylcobalamin to arsenic have been proposed [20]:



The transfer of Me^+ (Equation 7.3) involves reduction followed by oxidative methylation and is thus mechanistically similar to the Challenger scheme involving SAM. However, in paramagnetic studies [21] the expected $\text{Co}(\text{I})^-$ species ($\text{B}_{12\text{s}}$) was not detected, rather the $\text{B}_{12\text{r}}$ with a $\text{Co}(\text{II})$ centre, which suggests operation of a free-radical mechanism involving haemolytic cleavage of the metal (Co)-carbon bond (Equation 7.2). If indirect transfer of the methyl group occurs, SAM is a candidate carrier molecules and both methionine synthetase and methionine adenosyltransferase could be involved [20]. However, methylation of SAM by methylcobalamin has not been definitively demonstrated. Other molecules hypothesized to be involved in methylcobalamin mediated biomethylation of arsenic include glutathione (GSH) and coenzyme M (CoM). The latter molecule plays a role in methane generation in methanogenic bacteria, including *M. barkeri*, with Me-CoM involved in the final step of this process.

Genome sequencing indicates that almost all bacteria and archaea have arsenic-resistance (*ars*) operons that confer resistance to arsenite and arsenate [23]. Such widespread occurrence of *ars* genes probably reflects the ubiquitous occurrence of arsenic in the environment; the molecular genetics of microbial arsenic resistance has been recently reviewed [6]. In most organisms studies, the *ars* operon encode transport proteins that exports arsenite from the cell. A methyltransferase (Cyt19) linked to thioredoxin-thioredoxin reductase has been shown to be involved in a novel SAM dependent pathway in rat liver [24]. A homologue of Cyt19, ArsM, has recently been shown to be present in 126 Bacteria and 16 Archaea [25]. ArsM has been characterized in *Rhodopseudomonas palustris* and recombinant *arsM* from *R. palustris* expressed in an arsenic hypersensitive strain of *Escherichia coli* confers the ability to generate trimethylarsine, as well as arsenic resistance [25]. The recombinant protein was purified and shown to catalyse transfer of methyl groups from SAM to As(III) forming di- and trimethylated species, with trimethylarsine as the final product. Based on these findings a mechanism of arsenite resistance through methylation and subsequent volatilization has been proposed [25]. Because ArsM homologues are known to be widespread in nature, this microbial mediated transformation could have an important impact on the global arsenic cycle.

7.2.2 Mammalian Biomethylation of Arsenic

For most mammalian species, including humans, a large proportion (50–70%) of ingested arsenate is reduced, mainly in the blood, to arsenite [26]. Reduction of arsenic can occur enzymatically via arsenate reductase, but also nonenzymatically via glutathione [27]. Since arsenite at physiological pH is mainly in an undissociated form, it is much more rapidly

taken up by hepatocytes than ionized arsenate [26]. Both forms of inorganic arsenic are actively transported into cells, arsenite via aquaglyceroporins and arsenate via phosphate transporters [28].

Cellular efflux of arsenite in eukaryotes involves glutathionylation coupled to removal of the $\text{As}(\text{GS})_2$ from the cytosol by ABC type membrane transported proteins [6]. An alternative means of extrusion of arsenite from cells is methylation, with subsequent cellular export of the methylated species and excretion via urine [29]; exposure to inorganic arsenic leads to the appearance of high concentrations of dimethylarsinic acid [DMA(V)] and to a lesser extent methylarsonic acid [MA(V)], in the urine [30]. Compared with the corresponding trivalent methylated species, these pentavalent species are much more water soluble, much less reactive and have much lower affinity for biological tissue; factors that favour preferential excretion of the pentavalent forms. Susceptibility of methylarsonous acid [MA(III)] and dimethylarsinous acid [DMA(III)] to oxidation may also contribute to the presence of MA(V) and DMA(V) in urine. Urinary arsenic profiles in humans and their relation to arsenic toxicity and to variation in genes of arsenic metabolism are discussed in Section 7.2.2.1.

In mice, the specific activity for arsenic methyltransferase in various organs has the following order: testes > kidney > liver > lung [31]. However, in most mammals including humans, the principal site of arsenic methylation is considered to be the liver [32, 33]. The two alternating steps involved in inorganic arsenic metabolism in mammals (reduction of arsenate to arsenite, followed by oxidative methylation) are thought to be catalysed by MA(V) reductase and arsenic methyltransferase respectively; both enzymes have been extensively characterized (see for example ref. [34–37]). Human MA(V) reductase is a member of the glutathione-S-transferase superfamily [34], often referred to as hGST-omega (GSTO), and catalyses the reduction of arsenate to arsenite as well the reduction of MA(V) to MA(III) and DMA(V) to DMA(III). In addition, a purine nucleoside phosphorylase (PNP) has been purified from rat and human liver and shown to catalyse inorganic arsenate to arsenite [36, 38, 39]. Figure 7.3 shows an enzyme catalysed pathway for arsenic biomethylation in mammals, which is consistent with the Challenger mechanism of alternate reduction and oxidative methylation steps. In rats, further metabolism of DMA forms trimethylarsine oxide (Me_3AsO), which can be excreted in the urine and reduced to trimethylarsine (Me_3As) [40].

An alternative arsenic methyltransferase has been described in detail by Thomas and coworkers [24, 41]; a SAM dependent methyltransferase from rat liver cytosol that catalyse, in the presence of exogenous or physiological reductant, the methylation of arsenite through to dimethylated species. This 42-kDa enzyme had sequence motifs common to many non nucleic acid methyltransferases and was closely related to methyltransferases identified by conceptual translations of *cyt19* genes of mouse and human genomes. The rat liver arsenic methyltransferase was designated as Cyt19 and a scheme linking the enzyme and thioredoxin-thioredoxin reductase in the methylation of arsenicals was proposed [24] (Figure 7.4). The scheme illustrates a possible dual enzymatic role for Cyt19: oxidative methylation of trivalent arsenicals involving SAM and reduction of MA(V) involving thioredoxin as reducing agent. In the proposed scheme, a thioredoxin reductase (TR) generates reduced thioredoxin [$\text{Trx}(\text{SH})_2$] and is coupled to MA(V) reducton through a Trx-TR-NADPH reaction. Such a reaction has been shown to provide reducing equivalents for reduction of arsenate by an arsenate reductase from *Staphylococcus aureus* [42]. Further evidence in

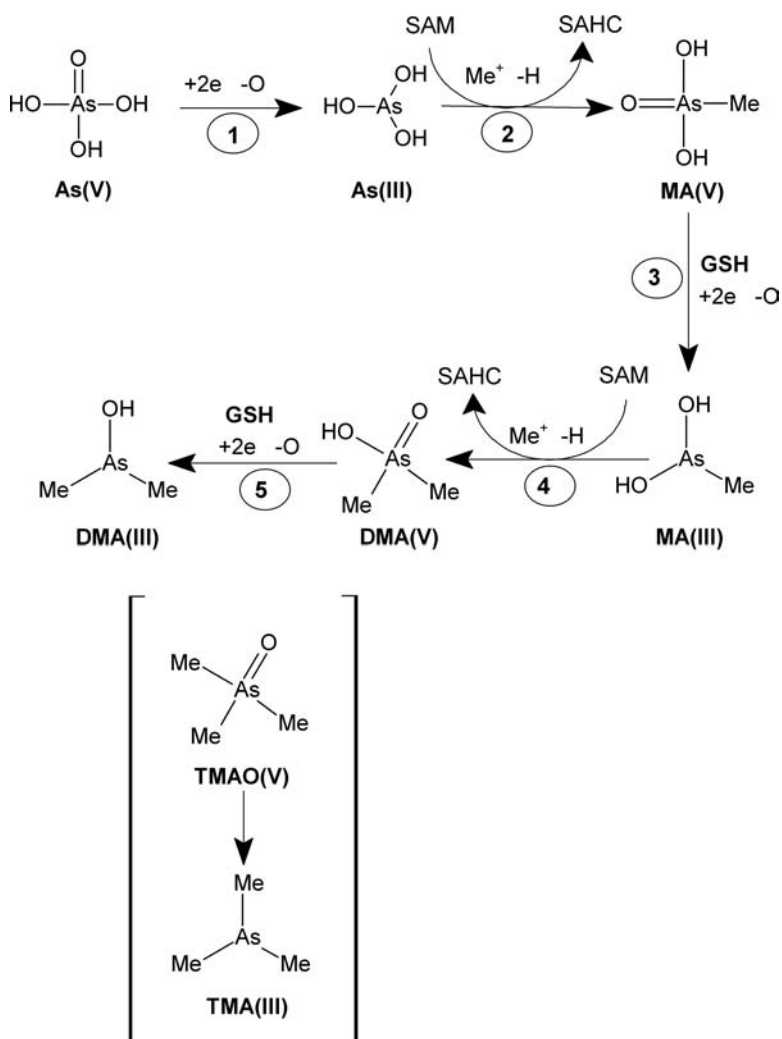


Figure 7.3 Generally accepted enzyme pathway for arsenic biomethylation in mammals based on the Challenger mechanism. *S*-adenosylmethionine, SAM; *S*-adenosylhomocysteine, SAHC; glutathione, GSH. Enzyme catalysed steps: (1) GSTO or PNP; (2) arsenite methyltransferase; (3) GSTO; (4) arsenite methyltransferase; (5) GSTO. Steps shown in parentheses apply to some rodents, with TMAO believed to be formed from DMA(V). See main text for explanation of enzymatic steps

support of the proposed scheme includes the observation that MA(III) is a very potent inhibitor of TR activity [43], which indicates a possible feedback control mechanism within the scheme involving MA(III) as effector [24]. Thomas *et al.* [24] emphasized, however, that other cellular reductants may provide reductants for Cyt19, for example, the coupled reduction system glutaredoxin–GSH reductase–GSH known to support reduction of arsenate by *Saccharomyces cerevisiae* arsenate reductase [44]. The proposed combined action of rat

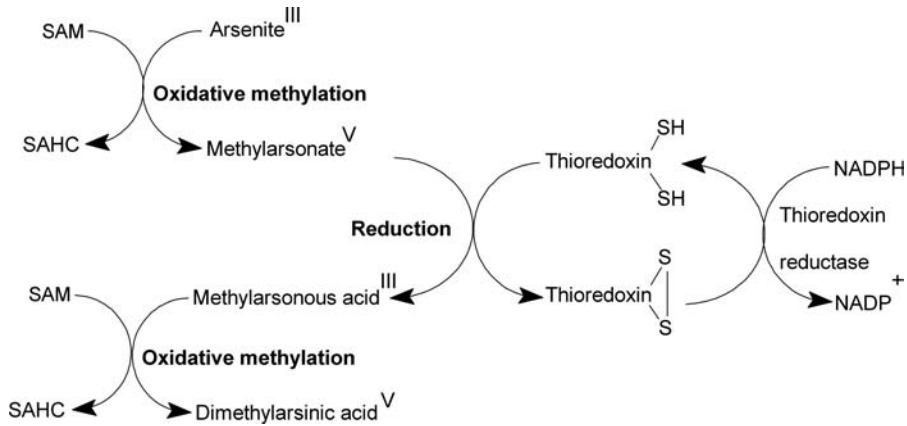


Figure 7.4 Proposed scheme for dual role, oxidative methylation and reduction, of Cyt19 in arsenic biomethylation. The redox active protein thioredoxin provides reducing equivalents for Cyt19 reduction of MA(V) to MA(III). Thioredoxin is in turn reduced by the NADPH dependent enzyme thioredoxin reductase. S-adenosylhomocysteine, SAHC. Adapted with permission from [24] with permission from Elsevier

Cyt19 as a methylase and as a reductase does not appear to apply to methyltransferases purified from tissues of other species, for which distinct reductases are involved in reduction of pentavalent forms of arsenic [6].

Kobayashi *et al.* [45] have recently reported on the expression and activity of *cyt19* in rat tissues; both mRNA and protein levels were highest in the liver, with intermediate expression of *cyt19* mRNA observed in the heart and tissue. Furthermore, the liver cytosol was identified as the site for production of methylated arsenicals [45]. Cyt19 has also recently been found as a high abundance protein in mouse neuroblastoma cells [46].

Hayakawa *et al.* [47] have proposed that human metabolism of arsenite to MA and DMA takes place through an alternative pathway to that of Challenger, not involving oxidative methylation (Figure 7.5). In the Hayakawa pathway, arsine triglutathione (ATG) is generated nonenzymatically from arsine in the presence of glutathione (GHS). Subsequently, methylation of ATG at the arsenic atom is catalysed by a methyltransferase (Cyt19) utilizing SAM as methyl donor, with the formation of monomethylarsonic diglutathione (MADG). Further methylation of MADG via Cyt19 forms dimethylarsine glutathione (DMAG). These methylated arsenic intermediates, MADG and DMAG, oxidize to MA(V) and DMA(V) respectively. The pathway has found favour [29] since the proposed final products, MA(V) and DMA(V), are the major arsenic metabolites in urine; unlike the Challenger pathway [5, 16] where these metabolites appear as intermediates. It has been noted however that the involvement of Cyt19 in human arsenic biotransformation is speculative since the enzyme has not been purified from human tissue and questions remain as to its inducibility in human liver [29]. Nevertheless, human Cyt19 has been prepared using DNA recombinant technology [48] and lack of arsenic methylation in the chimpanzee is thought to be a result of deletion of a nucleotide deletion in its *cyt19* gene [41]. The HUGO Gene Nomenclature Committee's has designated *cyt19* as *As3mt*.

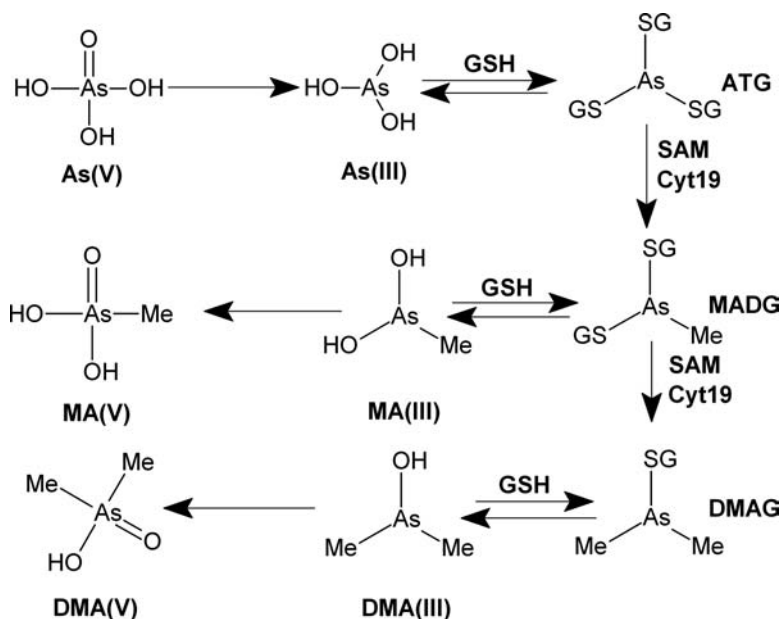


Figure 7.5 Proposed ‘alternative’ pathway for arsenic bioconversion in mammals involving glutathione arsenic compounds as substrates for a methyltransferase enzyme. In the scheme shown Cyt19 is shown as one possible methyltransferase. Unlike the scheme shown in Figure 7.3, this alternative pathway is not based on the Challenger mechanism and the ultimate products are pentavalent forms of methylarsenic compounds. Arsenic triglutathione, ATG; monomethylarsenic diglutathione, MADG; dimethylarsenic glutathione, DMAG. Adapted with permission from [47]. Copyright Springer Science + Business Media

7.2.2.1 Arsenic Biomethylation and its Relation to Arsenic Toxicity in Humans

Chronic exposure to inorganic arsenic through drinking water has been associated with hyperkeratosis, spotted melanosis, skin pigmentation and lung cancer [49]. The research of Cullen and his associates [5, 50–52] extended the concepts of Challenger’s work and explored the relationship between arsenic methylation and arsenic toxicity. Over the past decade, exploration of this relationship by researchers working with mammalian cell systems has led to significant advances in understanding of arsenic biomethylation. In a recent review, Tseng [7, 53] highlights the relation between inorganic arsenic methylation and the non cancerous health hazards associated with chronic exposure in human.

Methylation of inorganic arsenic is generally considered to be a detoxification process since it results in lowered general toxicity, with lethal doses of MA(V) and DMA(V) reported to be higher than those of their inorganic counterparts [54, 55]. Furthermore, low resistance to arsenic in some mammalian species, such marmoset monkey and chimpanzee, is often attributed to their inability to methylate inorganic arsenic [41, 56] and a greater susceptibility to serious arsenic poisoning in children is thought to be caused by a lower degree of arsenic methylation capability when compared to adults [56]. Sakurai *et al.* [54, 57] have reported on DMA(V) as an inducer of apoptosis in various mammalian

species/cells. Since apoptosis is a process by which organisms remove damaged, precancerous or redundant cells without evoking an inflammatory response, these authors proposed that biomethylation of inorganic arsenic in humans is a detoxicating event by not only reducing its acute toxicity but also by reducing its inflammatory potency.

It is well established that the arsenic species formed during biotransformation of inorganic arsenic vary markedly in their toxic potency and characteristics of interaction with biological systems, with trivalent methylated forms MA(III) and DMA(III) having greater cytotoxic and genotoxic than both arsenate and arsenite [50, 58, 59]. Some researchers have therefore questioned the involvement of arsenic methylation in detoxification [50, 51]. Trivalent methylated arsenic species have also been shown to be more potent than arsenite as inhibitors of key cellular enzymes, such as pyruvate dehydrogenase, glutathione reductase and thioredoxin reductase [52, 60, 61]. Variability in arsenic toxicity among relatively homogeneously exposed human populations has been observed [62, 63] and, although MA(V) and DMA(V) are the major urinary arsenic metabolites in humans, variations in urinary arsenic metabolic profiles in humans have also been reported [7, 64]. Increased proportions of MA(V) and decreased proportions of DMA(V) in urine are associated with increased retention of arsenic in the body and increased arsenic toxicity [7, 26, 65, 66]. Inhibition of the second methylation step of inorganic arsenic would increase the chance of cellular exposure to toxic MA(III). Conversely, individuals with an unusually lower proportion of urinary methylated arsenic as MA(V) may have a faster elimination of ingested inorganic arsenic [26]. Tseng [7] has speculated that a significant portion of measured MA(V) may be derived from MA(III), i.e. MA(III) may be excreted in the urine and rapidly oxidized to MA(V). High MA(V) in urine may therefore only be a marker of high MA(III) in blood and inside cells where the toxic effects of arsenic occur, which is a possible explanation of why individuals with a low proportion of MA(V) in urine tend to have a lower risk of developing arsenic induced diseases [7]. Tseng [7] also points out that an elevated MA(V) measured in most studies of urinary arsenic metabolites actually measures a significant proportion of MA(III), thus highlighting the need for improved speciation of arsenic metabolites in urine.

Variation in the genes of arsenic metabolism has been investigated as a possible explanation for differences in urinary arsenic profiles and in arsenic toxicity within human populations. A stronger correlation in arsenic methylation related phenotypes among siblings than among genetically unrelated individuals has been reported [67]. Genetic polymorphisms for human *cyt19* (*As3mt*) have been reported in a Mexican population [68], with some of the sites associated with differences in the ratio of urinary DMA(V) and MA(V) in children. Genetic polymorphism for hGST-omega [MA(V) reductase] has also been reported and is considered a possible explanation for differences in urine arsenic profiles and in toenail arsenic concentrations in human populations exposed to inorganic arsenic through drinking water [69–72]. Brima *et al.* [64] investigated arsenic metabolism through comparison of arsenic levels in the urine, hair and fingernails of healthy volunteers from three unexposed ethnic groups in the UK. They reported significantly different levels of total arsenic in fingernails and urine and a higher percentage of urinary DMA(V) in a Somali Black African group, which suggested a different pattern of arsenic metabolism in this ethnic group when compared with Asians and Whites. Engstrom *et al.* [73] recently investigated how polymorphisms in six genes affected the urinary metabolite pattern in a group of indigenous women in Northern Argentina exposed to arsenic in drinking water, who had low

urinary percentages on MA(V) and high percentages of DMA(V). The study found three polymorphisms in *As3mt* (i.e. *cyt19*) that were associated with lower percentage of MA(V) and higher percentage of DMA(V). The authors concluded that polymorphisms in *As3mt* were responsible for a large part of the interindividual variation in arsenic metabolism and susceptibility.

7.2.3 Arsenic Biomethylation/Demethylation and Organoarsenic Compounds in the Environment

Arsenic has an extensive organoarsenic chemistry with more than 30 naturally occurring arsenicals identified. Research on environmental organoarsenic chemistry has focused on marine systems and a summary of the literature up to 1993 is provided by Francesconi and Edmonds' 1997 review [74]. The main developments in environmental and biological aspects of organoarsenic chemistry over the 1993–2005 period have recently been summarized [1]. Developments since 1993 are large due to improved analytical techniques and includes the discovery of new classes of organoarsenic compounds, such as thioarsenicals found in sheep urine [75] and algae, and arsenolipids found in certain algae and in fish oils [76]. Figure 7.6 shows the structures of a selection of naturally occurring thioarsenicals, the oxo analogues of which been shown to be involved in the synthesis and degradation of the major classes of organoarsenic compounds (Figure 7.7). The thioarsenicals are likely to arise from sulfuration of the oxo-analogs. There are detailed reviews of the occurrence of organoarsenic compounds in both marine [8] and terrestrial [9] environments.

A scheme illustrating possible involvement of methylation/demethylation processes in the synthesis and degradation of arsenosugars and arsenobetaine is shown as Figure 7.7. Arsenosugars occur mainly in marine algae and at concentrations up to around 100 mg As kg⁻¹. They are produced *de novo* by the algae through oxidative methylation (the Challenger mechanism) of arsenate in seawater. Most of the arsenosugars identified are based on a dimethylarsinoylriboside structure with variation in arsenosugar structure arising from

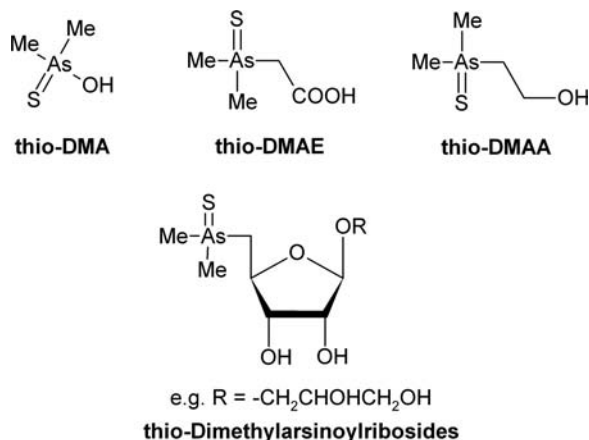


Figure 7.6 Selection of naturally occurring thioarsenicals. During storage these thioarsenicals undergo abiotic conversion to oxo-analogues (structures shown in Figure 7.7)

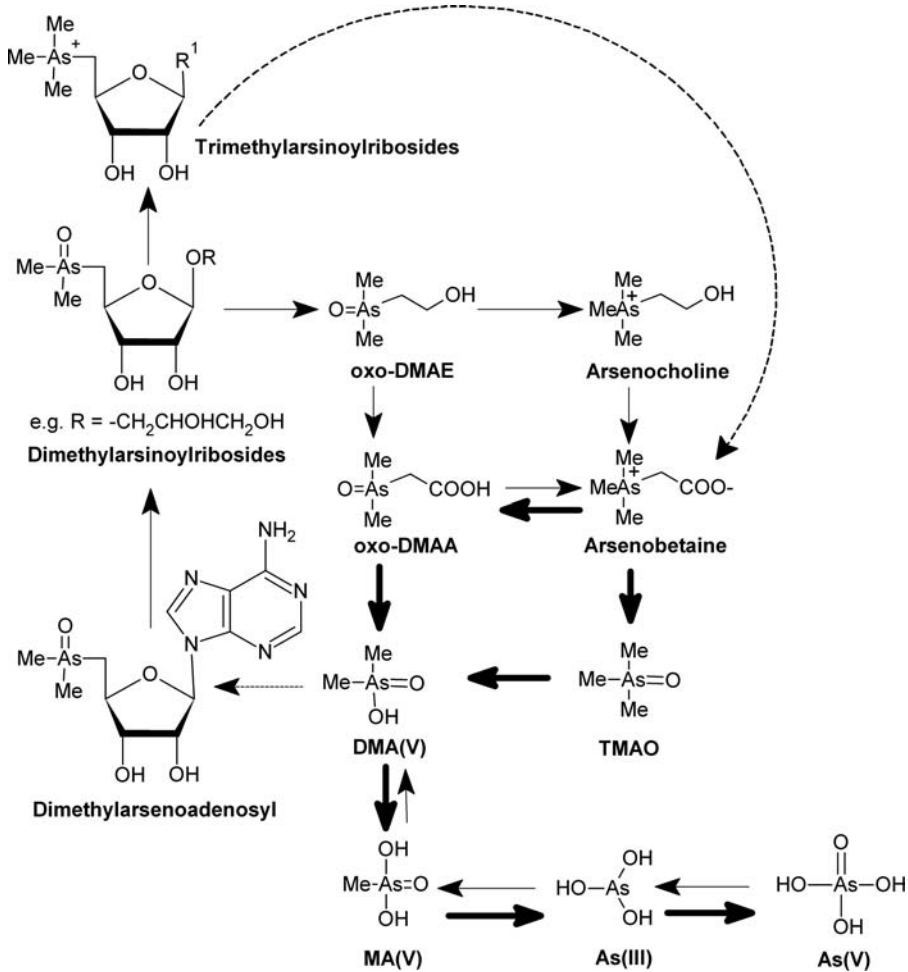


Figure 7.7 Proposed scheme illustrating the involvement of methylation/demethylation processes in the synthesis and degradation of arsenosugars and arsenobetaine. Bold arrows indicate steps in the degradation of arsenobetaine, all of which are known to be catalysed by bacteria. All steps in the degradation of arsenosugars to arsenobetaine are also known to be catalysed by bacteria. Formation of dimethylarsenoadenosyl from DMA(V) is postulated [159] to occur by transfer of the adenosyl group from SAM

different aglycone groupings comprising common algal secondary metabolites. Trimethylarsonioribosides have also been identified in trace amounts in marine algae and are thought to arise from further oxidative biomethylation of a dimethylarsinoylriboside. In marine animals, the situation is much simpler since the appreciable quantities of arsenic present are almost entirely arsenobetaine (trimethylarsonioacetate). This compound has also been found in some terrestrial biota, including mushrooms and earthworms. Although arsenobetaine was first identified as the major arsenical in marine animals some 30 years ago, the route of biosynthesis of this compound is still not clear. Central to discussion on

arsenobetaine biosynthesis are the oxo-arsenosugars, which are abundant in marine algae. Early laboratory experiments showed that anaerobic microbial activity from marine sand rapidly converts algal arsenosugars (dimethylarsinoylribosides) to the oxo-arsenosugar dimethylarsinoylethanol (oxo-DMAE), a readily seen precursor of arsenobetaine via oxo-dimethylarsinoylacetate (oxo-DMAA). More recently, Ritchie *et al.* [77] reported that a lysed cell extract of a *Pseudomonas* sp. was capable of bioconversion of pure oxo-DMAA substrate to arsenobetaine and that provision of SAM to bioconversion mixtures enhanced the enzyme catalysed reaction. This work provides further evidence for a part of the scheme illustrated as Figure 7.7 and suggests that in natural systems the oxidation of DMAE to form DMAA would precede the reduction and methylation at the arsenic atom. Since the *Pseudomonas* sp. was isolated from marine mussel, the work also highlights a possible direct involvement of bacteria in the biosynthesis of organoarsenic compounds within marine systems.

In the scheme discussed above, arsenosugars, which are formed *de novo* through biomethylation of inorganic, degrade in the natural environment to form the precursors of arsenobetaine formation through biomethylation. An alternative scheme for formation of arsenobetaine has been proposed [78] that is independent of arsenosugar biosynthesis and degradation, with DMAA being formed through a process of 'arsenylation' involving DMA(III) and glyoxylate. It has also been speculated that thioarsenicals may be involved in the formation of arsenobetaine, possibly through an abiotic methylation process; arsenobetaine is formed in a reaction of thio-DMAA in MeCN and methyl iodide [1].

Degradation of arsenosugars and arsenobetaine in the natural environment through dealkylation and demethylation processes gives rise to MA(V) and DMA(V). It follows that the presence of these methylated arsenic species in environmental samples may not reflect *de novo* synthesis of these compounds from inorganic arsenic. In the case of arsenobetaine, it is expected to be released into seawater through death and decomposition of marine animals yet this organoarsenic compound has never been detected in marine water. The ability of mixed cultures of marine microorganisms from a diversity of sources to degrade arsenobetaine is well established and two routes of arsenobetaine degradation have been established, as illustrated in Figure 7.7. Jenkins *et al.* [79] were the first to report that particular bacteria in pure culture were capable of degrading arsenobetaine, via enzymatic cleavage of both the methyl-arsenic and carboxymethyl-arsenic bonds giving rise to DMA(V). Harrington *et al.* [80] have recently reported on the biodegradation of arsenobetaine by bacteria from the human gastrointestinal tract. This research highlights the possible involvement of human gastrointestinal tract flora in the demethylation of arsenobetaine, which may contribute to increased levels of arsenic metabolites, such as MA(V) and DMA(V), excreted via the urine following consumption of seafood.

In aerobic terrestrial and aqueous environments, common bacteria such as *Alcaligenes*, *Mycobacterium* and *Pseudomonas* as known to demethylate mono- and dimethylarsenic compounds with the formation of inorganic arsenic [81, 82]. Demethylation of methylarsenic acids excreted by marine algae is considered an important part of the biogeological cycling of arsenic, although little is known about the biochemical mechanism(s) involved.

Thioarsenicals, such as the compounds shown in Figure 7.6, may be involved in the formation and degradation of arsenosugars and of arsenobetaine. Abiotic *in vitro* reactions (e.g., involving methyl iodide as methyl donor) suggests that *in vivo* methylation and reduction of thioarsenicals is likely to occur more readily than for the oxo-analogues.

However, the presence of thioarsenicals in sheep urine may be explained by degradation of dietary arsenosugars leading to formation of oxoarsenicals, which then react with H_2S (probably arising *in vivo* through desulfuration of cysteine) to form the thio analogues [75, 83].

7.3 Biomethylation of Antimony

7.3.1 Organoantimony Compounds in the Environment

Unlike arsenic, there is no evidence for an extensive organometallic chemistry for antimony in the natural environment. Methylantimony species detected in environmental samples are thought to arise *de novo* through biomethylation of inorganic antimony. The first reports on organometallic antimony compounds in the aquatic environment were in the early 1980s, using HG-GC-AAS. Later reports [84, 85], however, questioned the nature of the standard compounds used for the analysis and the experimental conditions used for the hydride generation during analysis are now known to produce artefacts [86]; demethylation of Me_3Sb species occurs during hydride generation in low pH reaction mixtures. The molecular structure of the compounds with carbon-antimony linkages detected in the environment in the early reports therefore remains unresolved.

Table 7.1 presents concentration ranges for MeSb , Me_2Sb and Me_3Sb species in various environmental compartments, based on published reports from 1991 onwards. Methylantimony species have been detected in sediment from a river in Germany using HG-GC-ICP-MS [87], with species concentration in the order $\text{MeSb} > \text{Me}_2\text{Sb} > \text{Me}_3\text{Sb}$. This order for methylantimony species in river sediments has recently been confirmed by other workers [88], who reported approximately 10-fold lower concentrations of the species in flowing water sediments compared with standing water sediments. Highest concentrations of methylantimony species in river sediment were associated with fractions containing the highest concentration humic substances and containing up to 40% clays and silt particles [88]. All three methylantimony species have also been detected, using HG-GC-ICP-MS, in geothermal waters from New Zealand, with dimethylantimony at the highest concentration (31 ng Sb kg^{-1}) [89]; the reliability of the quantification has, however, been questioned [13]. Koch *et al.* [90] detected, using HG-GC-AA, methylantimony species including Me_3Sb in water samples from two antimony rich environments in Canada. MeSb and Me_2Sb species have also been detected in various ocean and sea waters, although again the early reports [91–93] are questionable since the hydride generation methodology is known to produce artefacts [86].

Dodd *et al.* [94] have reported on organometallic antimony compounds in pondweed (*Potamogetan pectinatus*) from a polluted region in Canada. Me_3Sb , Me_2Sb and MeSb were identified in this sample, using HG-GC-MS following extraction with 0.2 mol l^{-1} acetic acid; quantification of the methylantimony species was not reported. Methylantimony compounds have also been found in plants (liverwort and moss) associated with a disused antimony mine in Scotland, using HG-GC-AAS [95]. Levels of Me_2Sb in the $100\text{--}200 \text{ } \mu\text{g (kg dry weight range)}^{-1}$ were present in the biota and MeSb was detected in some samples. In a similar study, methylated antimony species were found in a variety of plant species from antimony rich regions of Yellowstone, Canada, following extraction with methanol/water [90]. These

Table 7.1 Methylated antimony species in the environment and biota (selection of references)

Source	Concentration (range, or mean \pm SD)			Analysis	Reference
	MeSb	Me ₂ Sb	Me ₃ Sb		
Soils:					
- Arable	0.55–56.03	0.24–6.18	< 0.001–0.28 $\mu\text{g kg}^{-1}$	HG-PT-GC/ICP-MS	[103]
- Garden	< 0.007–19.98	0.05–7.59	> 0.001–0.12		
- Food plain	0.10–0.07	0.01–0.03	0.03–0.19		
- Abandoned Industrial	1.42–35.4	< 0.005–3.60	< 0.001–0.07		
Sewage gas	—	—	0.62–15 $\mu\text{g Sb m}^{-3}$	GC-ICP-MS (confirmation by GC-MS)	[100, 102]
Landfill gas	—	—	23.9–71.6		
River sediment	0.2–9.8	0.1–1.2	0.1–0.9 $\mu\text{g Sb kg}^{-1}$	HG-GC-ICP-MS	[87]
Pondweed (<i>Potamogetan</i> sp.) (polluted Canadian lakes)	0.2–18	0.02–8	0.001–0.3 $\mu\text{g kg}^{-1}$	HG-PT-GC/ICP-MS	[88]
	d-nq	d-nq	d-nq	HG-GC-MS quadrupole	[94]
Oceans/seas:	^a MeSb and/or Me ₂ Sb species detected			HG-GC-AAS (or photoionization)	[91–93, 153,154]
- Black sea (surface water)					
- Baltic sea					
- Western Atlantic ocean - North Pacific Ocean					
Plant & moss extracts: (site adjacent to Sb mine, UK)					
- Liverwort	—	181 \pm 26 $\mu\text{g kg}^{-1}$	—		[95]
- Moss	—	101 \pm 15	—		
Snail (<i>Stagnicola</i> sp)	—	d-nq	d-nq	headspace HG-GC-MS	[90]
Moss (Yellowknife, Canada)	—	d-nq	d-nq		
- various species, including <i>Drepanocladus</i> and <i>Funaria</i>				HG-GC-AAS & MS	[90]
Cot mattresses (used)	d-nq	d-nq	< 20–115 ng Sb g ⁻¹	HG-CT-GC-AAS	[115]
- inner-foam					

d-nq: detected but not quantified.

Purge and trap, PT; gas chromatography, GC; mass spectrometry, MS; hydride generation, HG; atomic absorption spectrometry, AAS; inductively coupled plasma, ICP; cryogenic trap, CT.

^aOrigin of methylated species questioned; may have arisen as artefacts of HG.

authors also reported methylantimony species in an animal, the snail *Stagnicola*, from an antimony rich region of Yellowknife, using a headspace HG-GC-MS method.

Further reports of methylantimony compounds in the environment concern volatile metalloid species in sewage and landfill fermentation gases [96–101], and in hot springs [98]. Me_3Sb was found in these emissions, with reported concentration ranges for sewage and landfill fermentation gases of 0.62–0.15 and 23.9–71.6 $\mu\text{g Sb m}^{-3}$ respectively [102]. Condensed water samples from the landfill gas collection pipeline [96] and standing water (through which landfill gases percolate) on a landfill site [86] have been reported to contain all three methylantimony species. Me_2Sb and Me_3Sb species have also been detected both above and within algal mats growing in hot springs [98].

Duester *et al.* [103] reported on concentrations of methylantimony species in a variety of different soils and on historic and present land use as factors that may have influenced such concentrations. For all soil investigated, MeSb was found to be the main organoantimony species present with highest concentrations found in arable soil. The generally higher levels of organometal(loid) (As, Sb, Sn) in agricultural and garden soils, compared with abandoned industrial sites and flood plain soil, was partly attributed to both the cultivation and the increased biological activity of the agricultural soils. Soil parameters (pH, water content or temperature) did not correlate with the degree of biomethylation observed [103]. In contrast to the lower *in vitro* biomethylation efficiency of antimony when compared with arsenic in microbial incubations (see Section 7.3.4.1), Duester *et al.* [103] detected higher proportions of methylantimony species *in situ* in soil samples and questioned the reliability of the currently accepted model of antimony biogeological cycling in the real environment.

7.3.2 Antimony Biomethylation in Mammals

Although methylantimony species have been detected in very low abundance in human urine [101], unequivocal evidence for *in vivo* antimony biomethylation by humans has not been reported. Biomethylation of arsenic by rat liver cytosol has been shown to be completely inhibited by administration of antimony trichloride to rats, but there was no evidence of antimony biomethylation *in vivo* [104]. There are recent reports of antimony biomethylation by faeces incubated anaerobically, and by methanoarchaea and bacterial isolates from human faeces [105, 106].

7.3.3 Antimony Biomethylation and its Relation to SIDS

Prior to the mid 1990s there was no definitive evidence for the biomethylation of antimony. However, the plausibility of microbial biomethylation of antimony was investigated intensively in relation to the sudden infant death syndrome (SIDS) following a claim that toxic hydride gases from chemicals in polyurethane chloride (PVC) cot mattress covers, produced by the filamentous fungus *Scopulariopsis brevicaulis*, was the primary cause of SIDS [107]. Antimony was the focus of concern and research in relation to this so called toxic gas hypothesis since Sb_2O_3 was incorporated into PVC cot mattress covers as a fire retardant and there were disputed claims that elevated antimony in postmortem serum and liver samples of SIDS infants [108]. A multifaceted enquiry by the UK Department of Health into the toxic gas hypothesis for SIDS concluded that the hypothesis was not substantiated [109]. Nonbiological leaching of antimony from PVC could explain postnatal exposure to this element leading to elevated levels in tissue and hair samples [110].

Although the generation of volatile trimethylantimony by *S. brevicaulis* from Sb_2O_3 was established during the enquiry, there was no evidence to indicate that it had a causal relationship with SIDS [109, 111]. Much of the research initiated in response to the Government enquiry into the toxic gas hypothesis focused on aerobic fungal isolates and PVC covers as the site of microbial activity. Subsequently, in response to several reports of antimony being volatilized by mixed cultures of bacteria growing under anaerobic conditions [112–114], a modified hypothesis was proposed in which anaerobic bacteria become established in the polyurethane foam of cot mattresses and volatilize the inorganic antimony arising through leaching from PVC [115]. Testing of this hypothesis demonstrated that past microbial activity had given rise to involatile methylated species of antimony in more than 60% of used cot mattress foams (see Table 7.2) [115]. Abiotic oxidation of biogenic trimethylantimony together with physical adsorption of methylantimony forms to the polyurethane foam were thought to account for an apparent absence of ‘escaped’ volatile antimony species. Furthermore, there was no evidence to suggest from comparison of SIDS and control group mattresses that levels of methylantimony forms in the foams have a causal relation to SIDS. The outcomes of this research initiated a change in focus in relation to the link between SIDS and cot mattresses, from volatile gases to the presence of harmful bacteria. There is now substantial evidence to implicate *Staphylococcus aureus* as an aetiological agent in SIDS and its variable presence in different types of cot mattresses provides a mechanistic explanation for several risk factors for SIDS [116–119].

7.3.4 Microbial Biomethylation of Antimony

A wide range of bacteria and fungi grown under aerobic and/or anaerobic conditions have been shown to biomethylate various inorganic antimony substrates, with the formation of one or more methylated species. Table 7.2 summarizes the various studies on microbial biomethylation of antimony in regards to organism, experimental incubation conditions, antimony substrate, phase analysed, methylated products, and means of product detection. The structures of antimony substrates commonly used in biomethylation studies are shown in Figure 7.8.

7.3.4.1 Microbial Biomethylation of Antimony under Aerobic Conditions

The first report [120] of antimony methylation by a characterized aerobic microorganism was in 1998, with the formation of trimethylstibine (gaseous Me_3Sb) by *S. brevicaulis*. The filamentous fungus was grown aerobically in liquid culture in the presence of inorganic antimony. The existence of biogenic Me_3Sb was established following exclusion of oxygen from cultures after growth, by remote trapping of volatile compounds and analysis by gas chromatography by mass spectrometry. No other volatile product containing antimony was detected in culture headspace gases. In a subsequent paper [111], these authors reported that the yields of volatilized antimony were around twofold higher on a solid medium [about $6\ \mu\text{g}$ antimony ($\text{g dry weight biomass}^{-1}$)], as compared to liquid culture. The order of antimony substrates in relation to ease of biovolatilization was reported as $\text{PAT} \gg \gg \text{Sb}_2\text{O}_3 \gg \gg \text{Sb}_2\text{O}_5 > \text{KSb}(\text{OH})_6$ [111]. Other fungal species (*Penicillium* spp., *Aspergillus* spp., *Alternaria* sp.) or bacteria (*Bacillus* spp.) tested under similar experimental conditions showed no evidence of volatilization of inorganic antimony [111]. Andrewes *et al.* [121] confirmed the ability of *S. brevicaulis* to methylate inorganic antimony, with the detection of

Table 7.2 Microbial biomethylation of antimony

Organisms/ enrichment	Incubation	Antimony substrate	Phase analysed	Antimony product	Detection	Ref.
<i>Scopulariopsis brevicaulis</i>	^a Biphasic	PAT	Gas	Me ₃ Sb	^c GC-AAS/GC-MS	[155, 156]
		Sb ₂ O ₃ or Sb ₂ O ₅	Gas	^b Volatile Sb	ICP-MS	[155]
		Sb ₂ O ₃	Gas	Me ₃ Sb	^c GC-MS	[156]
		Sb ₂ O ₅ or PHHA	Gas	^b Volatile Sb	ICP-MS	
	Aerobic	PAT	Gas	Me ₃ Sb	^c GC-AAS/GC-MS	[122]
		Sb ₂ O ₃	Aqueous	SbH ₃ , MeSb, Me ₂ Sb, Me ₃ Sb	^c GC-ICP-MS HG-GC-ASS	[131] [121]
<i>Phaeolus schweinitzii</i> <i>Cryptococcus humicolus</i>	Aerobic	PAT or Sb ₂ O ₃	Aqueous	Me ₂ Sb, Me ₃ Sb	HG-GC-ASS	[124]
	^a Biphasic	PAT	Gas	SbH ₃ , Me ₂ Sb, Me ₃ Sb	SPME-GC-MS	[143]
		PHHA	Gas	Me ₃ Sb	SPME-GC-MS	
	Aerobic	PAT	Aqueous	MeSb, Me ₂ Sb, Me ₃ Sb	Me ₃ Sb HG-GC- AAS	[128]
<i>Flavobacterium</i> sp.	Aerobic	Sb ₂ O ₃ or PHHA	Aqueous	Me ₂ Sb, Me ₃ Sb	HG-GC-AAS	
		PAT	Aqueous	MeSb, Me ₂ Sb, Me ₃ Sb	HG-GC-AAS	[126]
<i>Clostridium acetobutylicum</i> or <i>C. cochlearium</i>	Anaerobic	PAT	Aqueous	MeSb, Me ₂ Sb, Me ₃ Sb	HG-GC-AAS	[129]
	Anaerobic	PAT	Aqueous	MeSb, Me ₃ Sb	HG-GC-AAS	[129]
<i>C. buturicum</i> ^d <i>Clostridium</i> sp. ^d <i>Clostridium</i> sp.		PAT	Aqueous	MeSb	HG-GC-AAS	[129]
	Anaerobic	SbCl ₃	Gas	Me ₃ Sb	^c GC-ICP-MS	[14]
<i>C. collogenenovorans</i> Anaerobic or <i>Desulfovibrio vulgaris</i>	Anaerobic	SbCl ₃	Gas	SbH ₃ , MeSb, Me ₂ Sb, Me ₃ Sb	^c GC-ICP-MS	[14, 130]
<i>Methanobacterium formicicum</i>	Anaerobic	SbCl ₃	Gas	MeSb, Me ₃ Sb	^c GC-ICP-MS	[130]
<i>Methanobolus tindarius</i>	Anaerobic	SbCl ₃	Gas	Me ₃ Sb	^c GC-ICP-MS	[14, 105, 130]
<i>Methanosarcina barkeri</i>	Anaerobic	SbCl ₃	Gas	Me ₃ Sb	^c GC-ICP-MS	[14, 105, 130]

(continued)

Table 7.2 (Continued)

Organisms/ enrichment	Incubation	Antimony substrate	Phase analysed	Antimony product	Detection	Ref.
<i>Methanobrevibacter smithii</i> , <i>Methanosphaera stadtmanae</i> , <i>Methanobacterium thermoautotrophicum</i> , <i>Methanococcus vannielii</i> , <i>Methanococcus maripaludis</i> , <i>Methanolacinia paynteri</i> , <i>Methanosarcina mazei</i> , <i>Methanoplanus limicola</i> , or <i>Bacteroides vulgatus</i>						
Microbial enrichment conditions (undefined mixed cultures):						
Nitrate-reducing	Anaerobic	PAT	Gas	Me ₃ Sb	^c GC-AAS/GC-MS	[157]
		PAT or PHHA	Gas	Me ₃ Sb	GC-FIC/GC-MS	[114]
Methanogenic	Anaerobic	PAT	Gas	Me ₃ Sb	^c GC-AAS/GC-MS	[129, 157]
		Fermentative	Anaerobic	PAT	Gas	Me ₃ Sb
Faeces Sewage sludge	Anaerobic	Sb in faeces	Gas	Me ₃ Sb	^c GC-MS ^e GC-MS	[113]
		PAT	Gas	Me ₃ Sb	^c GC-ICP-MS	[106]
			Aqueous	MeSb, Me ₂ Sb, Me ₃ Sb	^c GC-ICP-MS HG-GC-ICP-MS	[135]

PAT: potassium antimony tartrate; PHHA: potassium hexahydroxyantimonate. Gas: culture headspace gases. Aqueous: spent liquid culture medium.

^aAerobic growth of fungus with trapping of headspace gases under anaerobic conditions.

^bVolatile antimony compound not identified.

^cPurge of headspace gases onto solid phase trap.

^dIsolate from fermentative enrichment culture shown to generate trimethylantimony.

^eHgCl₂ trap in culture headspace. Gas chromatography, GC; mass spectrometry, MS; hydride generation, HG; atomic absorption spectrometry, AAS; inductively coupled plasma, ICP; solid-phase micro extraction, SPME; fluorine-induced chemiluminescence, FIC.

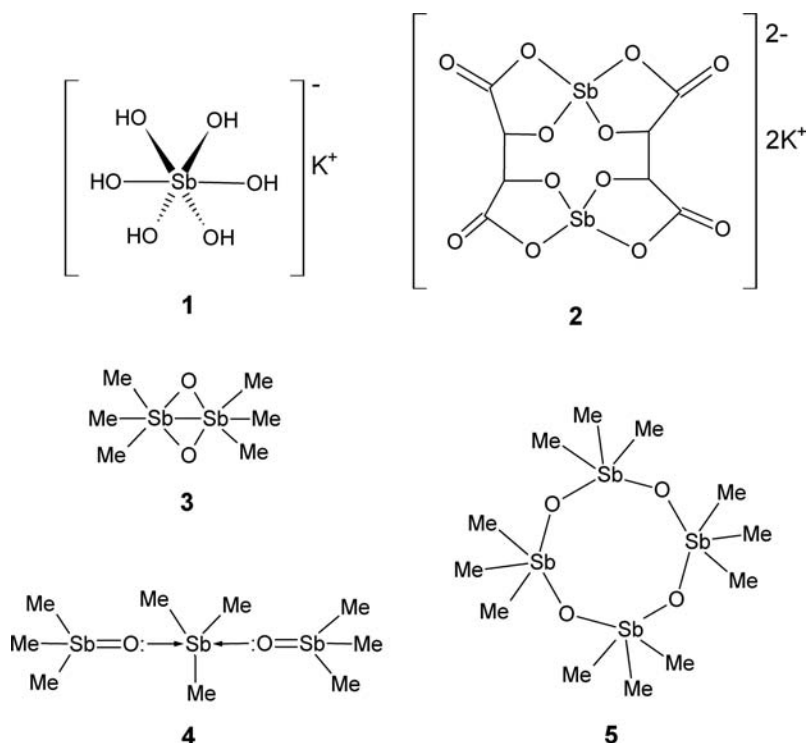


Figure 7.8 Selected structures of inorganic antimony and methylantimony. Inorganic antimony compounds commonly used as biotransformation substrates in microbial biomethylation studies: (1) potassium antimonate; (2) potassium antimony tartrate (PAT). Some possible methylantimony products (compounds 3–5) that might arise from oxidation of biogenically produced trimethylstibine (MeSb_3) [144]. Reprinted from [1] with permission from Elsevier

involatile methylantimony compounds, mostly trimethylantimonyoxide $[(\text{Me})_3\text{SbO}]$, at concentrations up to $7.1 \mu\text{g Sb } \Gamma^{-1}$ in liquid culture media containing inorganic antimony (III) compounds. The authors considered that methylantimony species in the media were the final biotransformation products of antimony (III) biomethylation by aerobic cultures but did not discount the possible abiotic oxidation of Me_3Sb to produce other methylated forms of antimony in solution. Later reports [122, 123] established that trimethylstibine could be produced under entirely aerobic cultivation condition (i.e. not requiring an anaerobic tapping stage) and that this volatile species was the final biotransformation product for inorganic antimony. Craig *et al.* [122] postulated that biogenesis of trimethylstibine in aerobic environments, with subsequent abiotic oxidation of the compound, could account for the presence of involatile methylated antimony species in natural bodies of water (Table 7.1) and in the culture media of microbial cultures (Table 7.2).

Involatile Me_2Sb and Me_3Sb species have been shown [124] to be produced by the wood rotting fungus *Phaeolus schweinitzii*, from the inorganic Sb(III) compounds potassium antimony tartrate ($\text{C}_4\text{H}_4\text{KO}_7\text{Sb}$; PAT) and antimony trioxide (Sb_2O_3); maximum yield of Me_3Sb was approximately 0.4%. Smith *et al.* [125] reported on the biomethylation of

inorganic antimony by the anamorphic basidiomycetous yeast *Cryptococcus humicolus*; SPME with polydimethylsiloxane fibres was used to trap volatile antimony species in headspace gases, with subsequent analysis by GC-MS.

Antimony biomethylation by an aerobic bacterium has been reported only relatively recently [126]. Pure cultures of an aerobically grown *Flavobacterium* sp. were shown by HG-CT-AAS to produce methylantimony species from PAT substrate. Sb(III) concentrations over the range 0–30 mg Sb Γ^{-1} were shown to influence both the extent of antimony biomethylation (up to 4.0 μg Sb Γ^{-1}) and the relative proportions of the involatile MeSb, Me₂Sb and Me₃Sb species formed. Interestingly, provision of inorganic As(III) alongside Sb(III) was shown to enhance formation of the involatile methylantimony species up to eightfold. This report [126] demonstrated that anaerobiosis was not an obligate requirement for methylantimony formation in prokaryotes, which broadened the range of habitats for potential formation of methylantimony species in nature. Based on the low yields (< 0.03%) of methylantimony species produced by a *Flavobacterium* sp., the authors proposed that antimony biomethylation by aerobic prokaryotes was fortuitous rather than a primary resistance mechanism for this element. The stimulation of antimony biomethylation through provision of inorganic arsenic alongside antimony has also been found for other aerobic microbes; the filamentous fungus *S. brevicaulis* [127] and the yeast *C. humicolus* [128].

7.3.4.2 *Microbial Biomethylation of Antimony under Anaerobic Conditions*

Trimethylstibine production by anaerobic soil/sediment enrichment culture has also been reported [112–114]. Gürleyük *et al.* [114] detected Me₃Sb in the culture headspace of soil bacteria enrichment cultures, when supplied with inorganic antimony in the (III) or (V) oxidation states. The incubation conditions were designed to promote bacterial growth through the use of nitrate as terminal electron acceptor in anaerobic respiration. This report represents the first characterisation of a volatile antimony compound thought to arise biogenically from an inorganic antimony substrate, although the identity of microorganisms in soils responsible for the biomethylation was unknown. Gates *et al.* [113] have also reported the detection of Me₃Sb in the culture headspace of undefined mixed cultures. In this work, pond sediment samples were incubated under conditions (highly proteinaceous medium) that promote growth of fermentative bacteria and supplied with PAT. Jenkins *et al.* [112] reported positive results for Me₃Sb with variable frequency for four of six soils tested and for three types of enrichment culture, each designed to encourage growth of fermentative, nitrate reducing or methane producing bacteria. These authors proposed that, as for arsenic, different metabolic categories of prokaryotic organisms are able to methylate antimony and that this capability is widely distributed in the natural environment.

Pure cultures of anaerobic bacteria have also been shown to methylate antimony. Michalke *et al.* [14] reported on biomethylation of inorganic antimony by pure cultures of three methanogenic archaea species, and by *Clostridium collagenovorans* and *Desulfovibrio vulgaris*. Me₃Sb was detected as the sole methylantimony compound in headspace gases of these cultures. The most productive species, *Methanobacterium formicicum*, had a maximum yield of methylantimony species from inorganic antimony substrate of 0.064%. Smith *et al.* [129] reported on formation of involatile methylantimony species by *Clostridium* spp. GC-MS profiles of headspace gases from soil enrichment cultures shown to generate Me₃Sb, were used to select characterized *Clostridium* spp. for assessment of

antimony biomethylation capability. Using HG-GC-AAS, these authors detected methylantimony species (up to $21 \mu\text{g Sb l}^{-1}$) in the medium of monoseptic cultures of *Clostridium acetobutylicum*, *Clostridium butyricum* and *Clostridium cochlearium*. The relative quantities of MeSb, Me₂Sb and Me₃Sb species produced over the course of a 28 day cultivation period was consistent with Me₃SbO being a final product of antimony biomethylation by these bacteria, with MeSb and Me₂Sb species appearing transiently in the cultures as intermediates of an antimony biomethylation pathway [129].

The amounts of methylantimony species produced per unit volume of culture by the end of the incubation period for *M. formicicum* and for *C. collagenovorans* [14] were 54-fold and 5325-fold lower respectively, compared to that reported for *C. acetobutylicum* at $21.3 \mu\text{g l}^{-1}$ [129]. Whereas Michalke *et al.* [14] assessed antimony biomethylation capabilities of *M. formicicum* and *C. collagenovorans* based on measurement of volatile forms of methylantimony present in culture headspace gases, that of *C. acetobutylicum* was based on measurement of involatile methylantimony species present in the culture medium [129]. It follows that accumulation of involatile forms of methylantimony, such as MeSb(OH)₂, Me₂SbOH and Me₃SbO, in the culture medium of *C. collagenovorans* [14] would have led to an underestimation of the antimony biomethylation capability of this organism. Smith *et al.* [129] proposed that this could account for the apparent lower biomethylation capability of this organism when compared to *C. acetobutylicum*. These authors [129] also proposed that the presence of involatile methylantimony species in culture supernatants might be related to the mechanism of antimony biomethylation, which has not as yet been established for methanogenic archaea or clostridia. These metabolic groups of bacteria were considered [129] likely to differ in some aspects of antimony biomethylation, such as enzymes, regulation etc. It is possible, therefore, that *Methanobacterium* spp. do not produce involatile forms of methylantimony and that *Clostridium* spp. have a higher capability for antimony biomethylation [129]. Since clostridia participate in the multi stage microbial process of methanogenesis Smith *et al.* [129] proposed they may be the principal agents of antimony biomethylation in methanogenic environments, such as municipal waste dumps [96] and environmental sediments [87]. These authors [129] also proposed that mixed community functioning was not an obligate requirement for antimony biomethylation by undefined soil/sediment enrichment conditions. They found no evidence of a correlation between antimony biomethylation by characterized clostridia cultures and low redox potential in the medium. Formation of methylantimony compounds by mixed communities of bacteria under anaerobic conditions was considered to be determined by the presence of individual prokaryotic species with specific antimony biomethylating capability, rather than by the overall environmental conditions set by mixed communities [129].

Recent reports [105, 130] have widened the range of methanoarchaea and bacterial species known to generate Me₃Sb under anaerobic conditions. Michalke *et al.* [130] also showed, that in addition to Me₃Sb, *Methanobolus tindarium* isolated from environmental sediment produced MeSbH₂, while *M. formicicum* isolated from an anaerobic sewage digester generated SbH₃, MeSbH₂ and Me₂SbH. It is interesting to note that several of the other methanoarchaea capable of producing Me₃Sb in pure culture were isolated from human faeces [105, 130], as was the case for the bacterial species *Bacteroides vulgatus* [105]. Faeces from human volunteers containing around $0.5 \mu\text{mol Sb kg}^{-1}$ (dry weight), when incubated anaerobically, has been shown to produce a range of volatile

antimony species; maximum production rates have been estimated at 0.02, 0.5 and 4.6 pmol h⁻¹ kg⁻¹ (dry weight) for SbH₃, MeSb/Me₂Sb and Me₃Sb respectively [106].

As proposed for aerobic biomethylation of antimony by *Flavobacterium* sp [126], the low yields of methylantimony species from monoseptic anaerobic bacterial cultures (<0.1%) [14, 129] are consistent with antimony being a fortuitous process rather than a primary resistance mechanism for this element.

7.3.5 Biological Mechanism of Antimony Biomethylation

Supply of ¹³CD₃-labelled L-methionine to cultures of *S. brevicaulis* incubated aerobically in the presence of PAT leads to the formation of ¹³CD₃ labelled methylantimony compounds [131, 132]. These experiments, which are analogous to Cullen's early experiments [17] with arsenic and various fungi, used hydride generation with subsequent GC-MS on collected fractions to detect the ¹³CD₃-methyl group in nonvolatile methylantimony compounds in the medium. The methyl group from ¹³CD₃-D-methionine was much less incorporated in Me₃Sb than the L-enantiomer. The high degree of stereospecificity is consistent with enzymatic (as opposed to abiotic) mediated methylation of antimony and has a similar specificity of L-enantiomer incorporation to that observed for arsenic biomethylation. The work [132] suggests that SAM is the biological methyl donor for antimony biomethylation by *S. brevicaulis* and that the mechanism of antimony biomethylation is similar to the mechanism proposed by Challenger for arsenic (Figure 7.1). Me₂Sb species have also been shown to be true intermediates of an antimony biomethylation pathway leading to trimethylantimony [132], that is, not an analytical artefact formed during the hydride generation step of the analysis. The notion that antimony and arsenic biomethylation proceeding via the same enzyme catalysed pathway is also supported by the finding that, for a variety of different microorganisms [126–128], provision of arsenic alongside antimony substrate leads to enhancement of antimony biomethylation; an effect that can be explained by enhanced induction of enzyme(s) capable of biomethylating both of these related elements [126]. The interactive influence of arsenic and antimony on microbial biomethylation is considered likely to profoundly influence the biogeochemical cycling and environmental and human toxicity of antimony [126, 128], since these two metal(loid)s coexist in a wide range of natural and manmade environments.

Determination of the isotope ratios of trimethylstibine produced by anaerobic bacteria indicates that, as for the aerobic studies on *S. brevicaulis*, isotope fractionation occurs during antimony biomethylation [133]. Wehmeier *et al.* [134] investigated the possible involvement of methylcobalamin in antimony biomethylation. They determined methylantimony products formed in both abiotic and biotic (sewage sludge/anaerobic bacteria) experiments by HG-CT-GC-ICP-MS. These experiments showed that methylcobalamin could react as a methylating agent in an abiotic methylation, forming MeSb and Me₂Sb species. However, a role for methylcobalamin in anaerobic microbial biomethylation was not unequivocally demonstrated; anaerobic sewage sludge cultures inoculated with enriched ¹²³Sb(V) produced species specific ^{123/121}Sb isotope ratio measurements of the different methylantimony species, which suggested stepwise methylation of antimony according to the Challenger mechanism [134, 135].

There are no reported studies of antimony biomethylation at the enzymatic level.

7.3.6 Abiotic Reactions of Particular Relevance to Antimony Biomethylation Studies

Trimethylantimony chloride (i.e. Me_3SbCl_2), which is commonly used as a standard for determination of methylantimony compounds involving HG hyphenated techniques, has been shown in mass spectrometry studies to hydrolyse in water (pH 7.0) most probably forming $[\text{Me}_3\text{SbOH}]^+$ [136, 137]. Upon HG, trimethylantimony chloride has been shown to undergo molecular rearrangement (or dismutation) with the formation of SbH_3 , MeSbH_2 and Me_2SbH , as well as Me_3Sb . This rearrangement has been used to good effect in culture headspace analysis, where the products of rearrangement arising from HG of trimethylantimony chloride are used as chromatographic standards for identification of biogenically produced methylantimony compounds by comparison with retention times (Figure 7.9). Several researchers [94, 138] have reported on experimental conditions for promoting or eliminating dismutation of methylantimony compounds during HG. Hansen and Pergantis [139] have recently reviewed the analytical techniques and methods used for antimony speciation analysis in biological materials, including HG and solvent extraction. They highlight problems associated with (1) quantitative extraction of methylantimony species from biological materials, (2) species instability and (3) low chromatographic recovery of species from chromatographic columns.

Studies in the mid 1970s using NMR indicated that trimethylstibine oxidizes rapidly, probably to $(\text{Me})_3\text{SbO}$ [140]. More recent studies, however, suggests that trimethylstibine has reasonable stability in the gas phases, even in the presence of some oxygen. Stability tests on volatile forms of antimony, including trimethylstibine, suggest that these compounds have an atmospheric half-life that allows them to volatilize from landfill sites and disperse in their vicinities [102, 141, 142]. These findings are consistent with detection of nonoxidized trimethylstibine produced from microbial environments that are not entirely anaerobic [122, 128, 143].

Craig *et al.* [144] used electrospray ionization and atmospheric pressure chemical ionization mass spectroscopic methods to investigate the fate of trimethylstibine when exposed to ambient oxygen. They proposed that when trimethylstibine was allowed to oxidize, species containing one to five $(\text{Me})_3\text{SbO}$ molecules chemically bonded together are produced in aqueous solution (Figure 7.8); Me_2Sb species were not detected under the experimental conditions used. There are no reports of detection of cyclic antimony species in environmental samples or in microbial incubation media. This may be a result of the limitation of current analytical methods for detection of such species at low concentration in environmental and biological matrices.

7.4 Biomethylation of Bismuth

By the mid 1990s methylated species of arsenic and antimony had been detected in various environments and, given the chemical similarities of bismuth to arsenic and antimony, it was speculated that methylated bismuth compounds also occur in the environment. However, the thermodynamic data on gaseous trimethylbismuthine (gaseous Me_3Bi) indicates that, relative to trimethylarsine and even trimethylstibine, Me_3Bi requires comparatively high levels of energy for formation and the Bi-C bonds are comparatively weak. Stability of

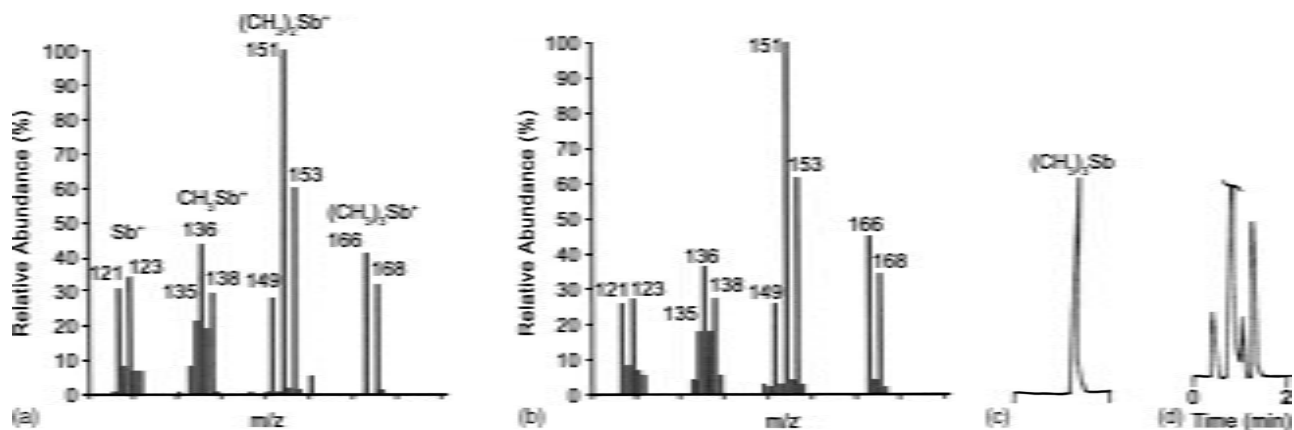


Figure 7.9 First identification of trimethylstibine (Me_3Sb) as the product of inorganic antimony biomethylation by a characterized microorganism, *S. brevicaulis*. (a) mass spectrum of biogenic Me_3Sb ; (b) simulated mass spectrum of Me_3Sb from NIST library; (c) typical GC-CT-AAS chromatogram of volatile antimony compounds from culture headspace gases; (d) typical GC-CT-AAS chromatogram of volatile antimony compounds (standards) produced by reduction of Me_3SbCl_2 . Cryogenically trapped volatile antimony species are released from the chromogenic material by electrothermal heating, according to their boiling points. The order of retention times for the standards is SbH_3 , MeSbH_2 , Me_2SbH and Me_3Sb . Reprinted with permission from [120]. Copyright 2008 American Chemical Society

Table 7.3 *Me₃Bi in the environment or generated during incubation of environmental samples*

Source	Concentration (range, or mean \pm SD)	Analysis	Reference
Landfill gas	0.0002–0.927 $\mu\text{g m}^{-3}$	CT-GC-ICP-MS	[146]
Sewage gas	0.003–24.2 $\mu\text{g m}^{-3}$	CT-GC-ICP-MS	[147]
^a Sewage sludge	46.2 \pm 6.9 $\mu\text{g m}^{-3}$	CT-GC-ICP-MS	[14]
^b River sediments	0.076–48 ng kg^{-1}	CT-GC-ICP-MS	[147]
Soil	0.1–100 ng kg^{-1}	slurry HG-GC-ICP-MS	[158]

Cryogenic trap, CT; gas chromatography, GC; mass spectrometry, MS; hydride generation, HG; inductively coupled plasma, ICP.

^aMe₃Bi detected in the headspace gases after incubation of sludge for one week at 37 °C.

^bMe₃Bi detected in the headspace gases of incubation of sediment for two weeks at 30 °C.

Me₃Bi has been reported to be lower than not only Me₃As and Me₃Sb but also Et₃Bi [145]. Nevertheless, the half life of Me₃Bi at low concentration (0.1 $\mu\text{g Bi l}^{-1}$) in moist air has been determined to be more than 7 h [142].

7.4.1 Organobismuth Compounds in the Environment

Concentrations of Me₃Bi detected in various environments, or generated during incubation of environmental samples, are presented in Table 7.3.

During the mid 1990s environmentally occurring Me₃Bi was detected in gases emitted from sewage sludge [96, 100] and volatile bismuth species were detected in gases from municipal waste deposits [146]. In later work, Feldmann *et al.* [147] used cryotrapping gas chromatography and HG coupled with an ICP-MS to detect Me₃Sb in landfill and sewage gas. Among other volatile metal compounds, Me₃Bi was found to be a major component in the gases of sludge digesters, with concentrations up to 25 mg l^{-1} measured at sewage treatment plants [147]. In fermentation experiments involving mixing of anaerobic cultures from pond sludge with contaminated soil from four different industrial areas, following incubation at 30 °C for two weeks, Me₃Bi was detected by GC-ICP-MS in the headspace of all vessels at levels of 0.076–48 $\text{ng Bi (as Me}_3\text{Bi) kg}^{-1}$ sludge. However, the volatilization rate of bismuth did not correlate with the total bismuth in the sludge nor with the available fraction of total bismuth (after acid digestion following HG). Methylated bismuth compounds and biomethylation capability have also been detected in various soils [148, 149]. Using HG, Hirner *et al.* [148] reported 110 $\text{ng Bi (as Me}_3\text{Bi) kg}^{-1}$ soil at a former gas station site, but only 0.1 and 0.3 ng kg^{-1} soil at former industrial and coal processing sites respectively. These authors also reported that Me₃Bi was present in soil from a 25 year old waste dump at a concentration of 40 $\text{ng Bi (as Me}_3\text{Bi) kg}^{-1}$, with mono- and dimethylbismuth species (as hydrides) at concentrations approximately 10-fold lower.

7.4.2 Microbial Biomethylation of Bismuth

Table 7.4 presents the volatile bismuth products generated by pure cultures of bacteria isolated from a range of sources. The capability of the bacteria to methylate inorganic arsenic and antimony is also shown.

Michalke *et al.* [14] investigated the production of volatile derivatives of bismuth by microflora involved in anaerobic digestion of sewage sludge, using a purge and trap GC

Table 7.4 *Microbial biomethylation of bismuth*

Organism	Volatile bismuth product(s)	Methylation of related elements (As and Sb)	Organism isolated from
Methanoarchaea:			
<i>Methanobacterium formicum</i>	BiH ₃ , MeBiH ₂ , Me ₂ BiH, Me ₃ Bi	As, Sb	Anaerobic sewage digester
<i>Methanosphaera stadtmanae</i>	MeBiH ₂ , Me ₂ BiH, Me ₃ Bi	As, Sb	Human faeces
<i>Methanobrevibacter smithii</i>	MeBiH ₂ , Me ₂ BiH, Me ₃ Bi	As, Sb	Human faeces
<i>Methanococcus vannielii</i>	MeBiH ₂ , Me ₃ Bi	As, Sb	Marine mud
<i>Methanococcus maripaludis</i>	Me ₂ BiH, Me ₃ Bi	Sb	Mud
<i>Methanolacinia paynteri</i>	Me ₂ BiH, Me ₃ Bi	Sb	Marine sediment
<i>Methanobolus tindarius</i>	Me ₃ Bi	Sb	Sediment
<i>Methanobacterium thermoautotrophicum</i>	Me ₃ Bi	Sb	Sewage sludge
<i>Methanosarcina mazei</i>	Me ₃ Bi	As, Sb	Anaerobic sewage digester
<i>Methanosarcina barkeri</i>	Me ₃ Bi	Sb	Anaerobic sewage digester
<i>Methanoplanus limicola</i>	Me ₃ Bi	As, Sb	Swamp mud
Bacteria:			
<i>Desulfovibrio piger</i>	Me ₃ Bi		Human faeces
<i>Eubacterium eligens</i>	Me ₃ Bi		Human faeces
<i>Lactobacillus acidophilus</i>	Me ₃ Bi		Human faeces
<i>Clostridium collagenovorans</i>	Me ₃ Bi	As, Sb	Sewage sludge digester

Table compiled from data presented in refs [14, 105, 106, 130, 150].

system coupled to an ICP-MS. The biogenic production of Me₃Bi by pure cultures was demonstrated for the first time in this study. Of several anaerobic microorganisms from different physiological groups, which are known representatives of the sewage sludge microflora, only *Methanobacterium formicum* (a methanogenic archaea) and *Clostridium collagenovorans* (a peptidolytic bacterium) produced Me₃Bi; the former organism was around 380-fold more productive than the latter with respect to generation of the volatile compound. No volatile bismuth compounds were detected in representative species of sulfate reducing bacteria. Subsequent research by these authors [150] focused on biomethylation of bismuth in anaerobic cultures of *M. formicum*. The methanogen was shown to produce Me₃Bi from bismuth nitrate [Bi(NO₃)₃] and, at far lower rates, from the bismuth containing pharmaceuticals Bismofalk (containing bismuth subgallate and Bi(NO₃)₃) and Noemin (containing bismuth aluminate). The highest production rate for Me₃Bi was reported as 1.5 ng h⁻¹ (from 1 μM bismuth nitrate) and the highest yield as 2.6 ± 1.8% (from 5 μM bismuth nitrate). Interestingly, bismuthine (BiH₃) and the partial bismuthines, mono- and dimethyl bismuth hydride (MeBiH₂ and Me₂BiH), were also detected in the late exponential growth phase of cultures spiked with relatively low concentrations of bismuth nitrate [150]. *Methanosarcina barkeri*, a representative member of the sewage sludge microflora, has been found to produce Me₃Bi only in the presence of

cyclic polydimethylsiloxanes [151]. A subsequent comparative study [152] of the effects of octamethylcyclotetrasiloxane and the ionophores monensin and lasalocid on Me_3Bi by *M. barkeri* showed that the enhancement of bismuth methylation was not specific for the siloxane and stimulation of facilitated membrane permeation of the metal ion was proposed as a mechanistic explanation for the enhanced biomethylation.

Michalke *et al.* [106] have recently reported on the biotransformation of bismuth administered to human volunteers and to mice. Their aim was to assess the capability of the microbiota of the human gut, as well as gut segments to transform bismuth and other metal(loid)s into volatile derivatives. In *ex situ* experiments under anaerobic conditions, human faeces and the gut of mice produced Me_3Bi at low concentrations of bismuth (0.2 to $1 \mu\text{mol kg}^{-1}$ [dry weight]). With increased levels of *in vivo* administration of bismuth (2 to 14mmol kg^{-1} [dry weight]), there was an upshift in Me_3Bi generation rate of around 525-fold to $2100 \text{pmol h}^{-1} \text{kg}^{-1}$ (dry weight) for human faeces and around 24-fold to $120 \text{pmol h}^{-1} \text{kg}^{-1}$ (dry weight) for gut samples. Modulation of cell metabolism in mucosal tissues by gut microbiota has been reported previously and Michalke *et al.* [106] did not exclude the possibility that epithelia cells contribute to the biotransformation of bismuth under *in vivo* conditions. Their observation, however, that gut segments of germfree mice were unable to biotransform administered bismuth supports the notion that gut microbiota play a dominant role in Me_3Bi generation by biotic animals, including humans [106]. In other recent experiments [105], growing cultures of methanoarchaea isolated from various ecological niches including the human gut were compared with bacteria from human faeces for an ability to volatilize bismuth. The 14 anaerobic bacterial strains tested showed a greatly restricted spectrum of biovolatilization and generally lower rates of production of volatile bismuth. Since the *Methanosphaera stadtmanae* and *Methanobrevibacter smithii* (methanoarchaea associated with human gut) showed higher potential for biovolatilisation of metal (loid)s compared with the anaerobic bacteria tested, the authors [105] proposed that methanoarchaea are mainly responsible for production of volatile derivatives in the human gut. Maximum production rates for Me_3Bi by *M. stadtmanae* and *M. smithii* were reported as 8.6 ± 5.7 and $18.6 \pm 3.5 \text{fmol h}^{-1} \text{mg}^{-1}$ protein respectively but was much higher at 1698 ± 1629 for the sewage sludge isolate *Methanosarcina mazei* [105].

7.4.3 Biological Mechanism of Bismuth Biomethylation

Little research has been carried out on the mechanism of bismuth biomethylation. Unlike arsenic and antimony, the +5 oxidation state of bismuth has a much lower stability than the +3 oxidation state. Methylation of bismuth by a Challenger mechanism involving repeated oxidation of Bi(III) to Bi(V) is therefore unlikely. In experiments using cell free extracts of *M. formicicum*, production of Me_3Bi was observed in assays supplemented with methylcobalamin [Me-CoB_{12}] but not in assays supplemented with SAM [150]. Some Me_3Bi was produced in the presence of methylcobalamin even in the absence of extract protein, indicating abiotic transfer of the methyl group to bismuth. However, a threefold enhancement of Me_3Bi formation in the presence of extract protein indicated involvement of enzymatic catalysed reactions in bismuth biomethylation. Based on the apparent absence of involvement of SAM in methyl transfer and the known low stability of Bi(V) compounds, the authors proposed a stepwise biomethylation of bismuth without a change in the oxidation state of bismuth [150]. Feldmann [142] has subsequently proposed a mechanism

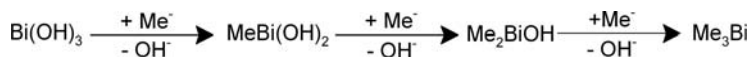


Figure 7.10 Mechanism of bismuth methylation involving successive substitution of the hydroxide ligands by carbanions, as proposed by Feldmann (2003) [142]

for bismuth biomethylation involving successive substitution of the hydroxide ligands by carbanions, i.e. transfer of the methyl group as Me^- from Me-CoB_{12} (illustrated in Figure 7.10).

Abbreviations

AAS	atomic absorption spectrometry
ArsM	methyltransferase enzyme(homologue of Cyt19, shown to be present in some prokaryotes)
As(V)	arsenate
As(III)	arsenite
As3mt	gene for methyltransferase (prokaryotes)
ATG	arsine triglutathione
BiH_3	bismuthine (gaseous)
CoB_{12}	cobalamin
CoM	coenzyme M
CT	cryotrapping/cryogenic trap
Cyt19	methyltransferase enzyme (mammals)
cyt19	gene for methyltransferase (mammals)
DMA(V)	dimethylarsinic acid/dimethylarsinate
DMA(III)	dimethylarsinous acid
DMAG	dimethylarsine glutathione
DNA	deoxyribonucleic acid
Et	ethyl group
FIC	fluorine-induced chemiluminescence
GC	gas chromatography
GSH	glutathione
GSTO	hGST-omega
HG	hydride generation
HPLC	high performance liquid chromatography
HUGO	Human Genome Organisation
ICP	inductively coupled plasma
MA(V)	methylarsonic acid/methylarsonate
MA(III)	methylarsonous acid
MADG	monomethylarsonic diglutathione
Me^+	carbonium ion
Me	methyl group
Me-CoB_{12}	methylcobalamin
Me_3As	trimethylarsine (gaseous)

Me ₃ Sb	trimethylstibine (gaseous)
MS	mass spectrometry
mRNA	messenger ribonucleic acid
NADPH	nicotinamide adenine dinucleotide phosphate (reduced form)
NIST	National Institute of Standards and Technology
NMR	nuclear magnetic resonance
oxo-DMAE	dimethylarsinoylethanol
oxo-DMAA	dimethylarsinoylacetate
PAT	potassium antimony tartrate (C ₄ H ₄ KO ₇ Sb)
PHHA	potassium hexahydroxyantimonate
PNP	purine nucleoside phosphorylase
PT	purge and trap
PVC	polyurethane chloride
SAHC	S-adenosylhomocysteine
SAM	S-adenosylmethionine
SIDS	sudden infant death syndrome
SMPE	solid-phase microextraction
thio-DMA	thiodimethylarsinate
thio-DMAA	thiodimethylarsinoylacetate
thio-DMAE	thiodimethylarsinoylethanol
TMAO(V)	trimethylarsine oxide
TMA(III)	trimethylarsine (gaseous)
TR	thioredoxin reductase
Trx-(SH) ₂	reduced thioredoxin

References

- Jenkins, R.O., Craig, P.J., Francesconi, K.A. and Harrington, C.F. (2007) *Applications III: Functional Materials, Environmental and Biological Applications*, vol. **12**, 2nd edn, (ed D. O'Hare), Elsevier, London, pp. 603–661.
- Feldmann, J. (2005) *Trends in Analytical Chemistry*, **24**, 228–242.
- Wrobel, K., Wrobel, K. and Caruso, J.A. (2005) *Analytical and Bioanalytical Chemistry*, **381**, 317–331.
- Pohl, P. (2004) *Trends in Analytical Chemistry*, **23**, 87–100.
- Cullen, W.R. and Reimer, K.J. (1989) *Chemical Reviews*, **89**, 713–764.
- Silver, S. and Phung, L.T. (2005) *Applied and Environmental Microbiology*, **71**, 599–608.
- Tseng, C.H. (2007) *Journal of Environmental Science and Health (C)*, **25**, 1–22.
- Edmonds, J.S. and Francesconi, K.A. (2003) Organoarsenic compounds in the marine environment, in *Organometallic Compounds in the Environment*, 2nd edn (ed. P.J. Craig), John Wiley & Sons, Ltd, Chichester, pp. 195–222.
- Kuehnelt, D. and Goessler, W. (2003) Organoarsenic compounds in the terrestrial environment, in *Organometallic Compounds in the Environment* (ed. P.J. Craig), John Wiley & Sons, Ltd, Chichester, pp. 223–275.
- Cullen, W.R. (2008) *Is Arsenic an Aphrodisiac? The Sociochemistry of an Element*, RSC Publishing, London, p. 428.
- Jenkins, R.O. (2002) *Trends for Organometallic Chemistry*, **4**, 109–122.
- Filella, M., Belzile, N. and Lett, M.C. (2007) *Earth-Science Reviews*, **80**, 195–217.

13. Andrewes, P. and Cullen, W.R. (2003) in: *Organometallic Compounds in the Environment*, 2nd edn (ed. P.J. Craig), John Wiley & Sons, Ltd, Chichester, pp. 277–303.
14. Michalke, K., Wickenheiser, E.B., Mehring, M. *et al.* (2000) *Applied and Environmental Microbiology*, **66**, 2791–2796.
15. Challenger, F., Higgenbottom, C. and Ellis, L. (1933) *J Chem Soc*, 95–101.
16. Challenger, F. (1945) *Chemical Reviews*, 36.
17. Cullen, W.R., Froese, C.L., Lui, A. *et al.* (1977) *Journal of Organometallic Chemistry*, **139**, 61–69.
18. Cullen, W.R., Li, H., Pergantis, S.A. *et al.* (1995) *Applied Organometallic Chemistry*, **9**, 507–515.
19. Cullen, W.R., Li, H., Pergantis, S.A. *et al.* (1994) *Chemosphere*, **28**, 1009–1019.
20. Bentley, R. and Chasteen, T.G. (2002) *Microbiology and Molecular Biology Reviews*, **66**, 250–271.
21. McBride, B.C. and Wolfe, R.S. (1971) *Biochemistry*, **10**, 4312–4317.
22. Stolz, J.E., Basu, P., Santini, J.M. and Oremland, R.S. (2006) *Annual Review of Microbiology*, **60**, 107–130.
23. Rosen, B.P. (1999) *Trends in Microbiology*, **7**, 207–212.
24. Thomas, D.J., Waters, S.B. and Styblo, M. (2004) *Toxicology and Applied Pharmacology*, **198**, 319–326.
25. Qin, J., Rosen, B.P., Zhang, Y. *et al.* (2006) *Proceedings of the National Academy of Sciences of the United States of America*, **103**, 2075–2080.
26. Vahter, M. (2002) *Toxicology*, **181**, 211–217.
27. Kitchin, K.T. (2001) *Toxicology and Applied Pharmacology*, **172**, 249–261.
28. Rosen, B.P. (2002) *FEBS Letters*, **529**, 86–92.
29. Aposhian, H.V. and Aposhian, M.M. (2006) *Chemical Research in Toxicology*, **19**, 1–15.
30. Brima, E.I., Jenkins, R.O. and Haris, P.I. (2006) *International Journal of Spectroscopy*, **20**, 125–151.
31. Healy, S.M., Casarez, E.A., Ayala-Fierro, F. and Aposhian, H.V. (1998) *Toxicology and Applied Pharmacology*, **148**, 65–70.
32. Geubel, A.P., Mairlot, M.C., Buchet, J.P. *et al.* (1988) *International Journal of Clinical Pharmacology*, **8**, 117–122.
33. Buchet, J.P., Geubel, A., Pauwels, S. *et al.* (1984) *Archives of Toxicology*, **55**, 151–154.
34. Zakharyan, R.A., Sampayo-Reyes, A., Healy, S.M. *et al.* (2001) *Chemical Research in Toxicology*, **14**, 1051–1057.
35. Wildfang, E., Zakharyan, R.A. and Aposhian, H.V. (1998) *Toxicology and Applied Pharmacology*, **152**, 366–375.
36. Radabaugh, T.R., Sampayo-Reyes, A., Zakharyan, R.A. and Aposhian, H.V. (2002) *Chemical Research in Toxicology*, **15**, 692–698.
37. Zakharyan, R.A., Ayala-Fierro, F., Cullen, W.R. *et al.* (1999) *Toxicology and Applied Pharmacology*, **158**, 9–15.
38. Nemeti, B. and Gregus, Z. (2002) *Toxicological Sciences*, **70**, 4–12.
39. Gregus, Z. and Nemeti, B. (2002) *Toxicological Sciences*, **70**, 13–19.
40. Lu, X., Arnold, L.L., Cohen, S.M. *et al.* (2003) *Analytical Chemistry*, **75**, 6463–6468.
41. Lin, S., Shi, Q., Nix, F.B. *et al.* (2002) *The Journal of Biological Chemistry*, **277**, 10795–10803.
42. Messens, J., Martins, J.C., Van Belle, K. *et al.* (2002) *Proceedings of the National Academy of Sciences of the United States of America*, **99**, 8506–8511.
43. Lin, S., Cullen, W.R. and Thomas, D.J. (1999) *Chemical Research in Toxicology*, **12**, 924–930.
44. Mukhopadhyay, R., Shi, J. and Rosen, B.P. (2000) *The Journal of Biological Chemistry*, **275**, 21149–21157.
45. Kobayashi, Y., Hayakawa, T. and Hirano, S. (2007) *Environmental Toxicology and Pharmacology*, **23**, 115–120.
46. John, J.P.P., Oh, J.E., Pollak, A. and Lubec, G. (2008) *Amino Acids*, **35**, 355–358.
47. Hayakawa, T., Kobayashi, Y., Cui, X. and Hirano, S. (2005) *Archives of Toxicology*, **79**, 183–191.

48. Li, J.X., Waters, S.B., Drobna, Z. *et al.* (2005) *Toxicology and Applied Pharmacology*, **204**, 164–169.
49. Yoshida, T., Yamauchi, H. and Sun, G.F. (2004) *Toxicology and Applied Pharmacology*, **198**, 243–252.
50. Styblo, M., Del Razo, L.M., Vega, L. *et al.* (2000) *Archives of Toxicology*, **74**, 289–299.
51. Petrick, J.S., Ayala-Fierro, F., Cullen, W.R. *et al.* (2000) *Toxicology and Applied Pharmacology*, **163**, 203–207.
52. Lin, S., Del Razo, L.M., Styblo, M. *et al.* (2001) *Chemical Research in Toxicology*, **14**, 305–311.
53. Tseng, C.H. (2007) *Journal of Environmental Monitoring*, **28**, 349–357.
54. Sukurai, T., Kaise, T. and Matsubara, C. (1989) *Chemical Research in Toxicology*, **11**, 273–283.
55. Romach, E.H., Zhao, C.Q., Del Razo, L.M. *et al.* (2000) *Toxicological Sciences*, **54**, 500–508.
56. Vahter, M. (1999) *Science Progress*, **82**, 69–88.
57. Sakurai, T., Qu, W., Sakurai, M.H. and Waalkes, M.P. (2002) *Chemical Research in Toxicology*, **15**, 629–637.
58. Styblo, M., Drobna, Z., Jaspers, I. *et al.* (2002) *Environmental Health Perspectives*, **110**, 767–771.
59. Mass, M.J., Tennant, A., Roop, B.C. *et al.* (2001) *Chemical Research in Toxicology*, **14**, 355–361.
60. Petrick, J.S., Jagadish, B., Mash, E.A. and Aposhian, H.V. (2001) *Chemical Research in Toxicology*, **14**, 651–656.
61. Chouchane, S. and Snow, E.T. (2001) *Chemical Research in Toxicology*, **14**, 517–522.
62. Rahman, M.M., Mandal, B.K., Chowdhury, T.R. *et al.* (2003) *Journal of Environmental Science and Health, Part A. Toxic/Hazardous Substances and Environmental Engineering*, **38**, 25–59.
63. Watanabe, C., Inaoka, T., Kadono, T. *et al.* (2001) *Environmental Health Perspectives*, **109**, 1265–1270.
64. Brima, E.I., Haris, P.I., Jenkins, R.O. *et al.* (2006) *Toxicology and Applied Pharmacology*, **216**, 122–130.
65. Steinmaus, C., Bates, M.N., Yuan, Y. *et al.* (2006) *Journal of Occupational and Environmental Medicine*, **48**, 478–488.
66. Tseng, C.H., Huang, Y.K., Huang, Y.L. *et al.* (2005) *Toxicology and Applied Pharmacology*, **206**, 299–308.
67. Chung, J.S., Kalman, D.A., Moore, L.E. *et al.* (2002) *Environmental Health Perspectives*, **110**, 729–733.
68. Meza, M.M., Yu, L.Z., Rodriguez, Y.Y. *et al.* (2005) *Environmental Health Perspectives*, **113**, 775–781.
69. Kile, M.L., Houseman, E.A., Rodrigues, E. *et al.* (2005) *Cancer Epidemiology, Biomarkers & Prevention: A Publication of the American Association for Cancer Research, Cosponsored by the American Society of Preventive Oncology*, **14**, 2419–2426.
70. Marnell, L.L., Garcia-Vargas, G.G., Chowdhury, U.K. *et al.* (2003) *Chemical Research in Toxicology*, **16**, 1507–1513.
71. Whitbread, A.K., Tetlow, N., Eyre, H.J. *et al.* (2003) *Pharmacogenetics*, **13**, 131–144.
72. Yu, L.Z., Kalla, K., Guthrie, E. *et al.* (2003) *Environmental Health Perspectives*, **111**, 1421–1427.
73. Engstrom, K.S., Broberg, K., Concha, G. *et al.* (2007) *Environmental Health Perspectives*, **115**, 599–605.
74. Francesconi, K.A. and Edmonds, J.S. (1997) *Advances in Inorganic Chemistry*, **44**, 147–189.
75. Hansen, H.R., Pickford, R., Thomas-Oates, J. *et al.* (2004) *Angewandte Chemie (International Edition in English)*, **43**, 337–340.
76. Schmeisser, E., Goessler, W., Kienzl, N. and Francesconi, K.A. (2005) *Analyst*, **130**, 948–955.
77. Ritchie, A.W., Edmonds, J.S., Goessler, W. and Jenkins, R.O. (2004) *FEMS Microbiology Letters*, **235**, 95–99.
78. Edmonds, J.S. (2000) *Bioorganic & Medicinal Chemistry Letters*, **10**, 1105–1108.
79. Jenkins, R.O., Ritchie, A.W., Edmonds, J.S. *et al.* (2003) *Archives of Microbiology*, **180**, 142–150.
80. Harrington, C.F., Brima, E.I. and Jenkins, R.O. (2008) *Chemical Speciation & Bioavailability*, **20**, 173–180.

81. Lehr, C.R., Polishchuk, E., Radoja, U. and Cullen, W.R. (2003) *Applied Organometallic Chemistry*, **17**, 831–834.
82. Vasapollo, G., Scarpa, A., Mele, G. *et al.* (2000) *Applied Organometallic Chemistry*, **14**, 739–743.
83. Raml, R., Goessler, W., Kienzl, N. and Francesconi, K.A. (2005) *Chemical Research in Toxicology*, **18**, 1444–1450.
84. Thayer, J.S. (1995) *Environmental Chemistry of the Heavy Elements: Hydrido and Organo Compounds*, Wiley-VCH Verlag GmbH Weinheim.
85. Dodd, M., Grundy, S.L., Reimer, K.J. and Cullen, W.R. (1992) *Applied Organometallic Chemistry*, **6**, 207–211.
86. Koch, I., Feldmann, J., Lintschinger, J. *et al.* (1998) *Applied Organometallic Chemistry*, **12**, 129–136.
87. Krupp, E.M., Grumping, R., Furchbar, U.R.R. and Hirner, A.V. (1996) *Fresenius Journal of Analytical Chemistry*, **354**, 546–549.
88. Duester, L., Hartmann, L.M., Luemers, L. and Hirner, A.V. (2007) *Applied Organometallic Chemistry*, **21**, 441–446.
89. Hirner, A.V., Feldmann, J., Krupp, E. *et al.* (1998) *Organic Geochemistry*, **29**, 1765–1778.
90. Koch, I., Wang, L.X., Feldmann, J. *et al.* (2000) *International Journal of Environmental Analytical Chemistry*, **77**, 111–131.
91. Andraea, M.O. and Froelich, P.N. (1984) *Tellus Series B-Chemical and Physical Meteorology*, **36**, 101–117.
92. Cutter, G.A., Cutter, L.S., Featherstone, A.M. and Lohrenz, S.E. (2001) *Deep-Sea Research Part II, Topical Studies in Oceanography*, **48**, 2895–2915.
93. Cutter, L.S., Cutter, G.A. and Sandiegomcglone, M.L.C. (1991) *Analytical Chemistry*, **63**, 1138–1142.
94. Dodd, M., Pergantis, S.A., Cullen, W.R. *et al.* (1996) *Analyst*, **121**, 223–228.
95. Craig, P.J., Forster, S.N., Jenkins, R.O. and Miller, D. (1999) *Analyst*, **124**, 1243–1248.
96. Feldmann, J., Grumping, R. and Hirner, A.V. (1994) *Fresenius Journal of Analytical Chemistry*, **350**, 228–234.
97. Hirner, A.V., Feldmann, J., Goguel, R. *et al.* (1994) *Applied Organometallic Chemistry*, **8**, 65–69.
98. Hirner, A.V., Feldmann, J., Krupp, E. *et al.* (1998) *Organic Geochemistry*, **29**, 1765–1778.
99. Maillefer, S., Lehr, L.R. and Cullen, W.R. (2003) *Applied Organometallic Chemistry*, **17**, 154–160.
100. Feldmann, J. and Hirner, A.V. (1995) *International Journal of Environmental Analytical Chemistry*, **60**, 339–359.
101. Kresimon, J., Gruter, U.M. and Hirner, A.V. (2001) *Fresenius Journal of Analytical Chemistry*, **371**, 586–590.
102. Feldmann, J., Koch, I. and Cullen, W.R. (1998) *Analyst*, **123**, 815–820.
103. Duester, L., Diaz-Bone, R.A., Kusters, J. and Hirner, A.V. (2005) *Journal of Environmental Monitoring*, **7**, 1186–1193.
104. Buchet, J.P. and Lauwers, R. (1985) *Archives of Toxicology*, **57**, 125–129.
105. Meyer, J., Michalke, K., Kouril, T. and Hensel, R. (2008) *Systematic and Applied Microbiology*, **31**, 81–87.
106. Michalke, K., Schmidt, A., Huber, B. *et al.* (2008) *Applied and Environmental Microbiology*, **74**, 3069–3075.
107. Richardson, B.A. (1994) *Journal of the Forensic Science Society*, **34**, 284–284.
108. Taylor, A. (1996) *Lancet*, **347**, 616.
109. Limerick (1998) Expert Group to investigate cot death theories: toxic gas hypothesis final report. UK Department of Health, London.
110. Jenkins, R.O., Craig, P.J., Goessler, W. and Irgolic, K.J. (1998) *Human & Experimental Toxicology*, **17**, 138–139.
111. Jenkins, R.O., Craig, P.J., Goessler, W. and Irgolic, K.J. (1998) *Human & Experimental Toxicology*, **17**, 231–238.

112. Jenkins, R.O., Craig, P.J., Miller, D.P. *et al.* (1998) *Applied Organometallic Chemistry*, **12**, 449–455.
113. Gates, P.N., Harrop, H.A., Pridham, J.B. and Smethurst, B. (1997) *The Science of the Total Environment*, **205**, 215–221.
114. Gürleyük, H., Van Fleet-Stalder, V. and Chasteen, T.G. (1997) *Applied Organometallic Chemistry*, **11**, 471–483.
115. Jenkins, R.O., Morris, T.-A., Craig, P.J. *et al.* (2000) *Human & Experimental Toxicology*, **19**, 693–702.
116. Jenkins, R.O. and Sherburn, R.E. (2008) *Journal of Applied Microbiology*, **104**, 526–533.
117. Jenkins, R.O. and Sherburn, R.E. (2005) *Journal of Applied Microbiology*, **99**, 573–579.
118. Sherburn, R.E. and Jenkins, R.O. (2004) *FEMS Immunology and Medical Microbiology*, **42**, 76–84.
119. Sherburn, R.E. and Jenkins, R.O. (2005) *Journal of Applied Microbiology*, **98**, 293–298.
120. Jenkins, R.O., Craig, P.J., Goessler, W. *et al.* (1998) *Environmental Science & Technology*, **32**, 882–885.
121. Andrewes, P., Cullen, W.R., Feldmann, J. *et al.* (1998) *Applied Organometallic Chemistry*, **12**, 827–842.
122. Craig, P.J., Jenkins, R.O., Dewick, R. and Miller, D.P. (1999) *The Science of the Total Environment*, **229**, 83–88.
123. Andrewes, P., Cullen, W.R. and Polishchuk, E. (1999) *Applied Organometallic Chemistry*, **13**, 659–664.
124. Andrewes, P., Cullen, W.R., Polishchuk, E. and Reimer, K.J. (2001) *Applied Organometallic Chemistry*, **15**, 473–480.
125. Smith, L.M., Maher, W.A., Craig, P.J. and Jenkins, R.O. (2002) *Applied Organometallic Chemistry*, **16**, 287–293.
126. Jenkins, R.O., Forster, S.N. and Craig, P.J. (2002) *Archives of Microbiology*, **178**, 274–278.
127. Andrewes, P., Cullen, W.R. and Polishchuk, E. (2000) *Environmental Science & Technology*, **34**, 2249–2253.
128. Hartmann, L.M., Craig, P.J. and Jenkins, R.O. (2003) *Archives of Microbiology*, **180**, 347–352.
129. Smith, L.M., Craig, P.J. and Jenkins, R.O. (2002) *Chemosphere*, **47**, 401–407.
130. Michalke, K., Meyer, J. and Hensel, R. (2007) *Archea: Evolution, Physiology, and Molecular Biology* Ed. RA Garrett and HP Klenk, Blackwell Publishing, Oxford, pp. 285–293.
131. Andrewes, P., Cullen, W.R., Feldmann, J. *et al.* (1999) *Applied Organometallic Chemistry*, **13**, 681–687.
132. Andrewes, P., Cullen, W.R. and Polishchuk, E. (2000) *Chemosphere*, **41**, 1717–1725.
133. Kim, J.P. (1995) *The Science of the Total Environment*, **164**, 209–219.
134. Wehmeier, S., Raab, A. and Feldmann, J. (2004) *Applied Organometallic Chemistry*, **18**, 631–639.
135. Wehmeier, S. and Feldmann, R. (2005) *Journal of Environmental Monitoring*, **7**, 1194–1199.
136. Zheng, J., Takeda, A. and Furuta, N. (2001) *Journal of Analytical Atomic Spectrometry*, **16**, 62–67.
137. Lintschinger, J., Scramel, O. and Kettrup, A. (1998) *Fresenius Journal of Analytical Chemistry*, **361**, 96–102.
138. Craig, P.J., Forster, S.N., Jenkins, R.O. *et al.* (2000) *Chemical Processes in the Marine Environment*, Springer-Verlag, pp. 265–280.
139. Hansen, H.R. and Pergantis, S.A. (2008) **23**, 1328–1340.
140. Parriss, G.E. and Brinckman, F.E. (1976) *Environmental Science & Technology*, **10**, 1128–1134.
141. Feldmann, J. (2003) *Biogeochemistry of Environmentally Important Trace Elements*, (ed. Y. Cai and O. C. Braids), ACS Symposium Series, American Chemical Society, Washington, pp. 128–140.
142. Feldmann, J. (2003) in *Organometallic Compounds in the Environment*, 2nd edn (ed. P.J. Craig), John Wiley & Sons, Ltd, Chichester, pp. 353–389.
143. Smith, L.M., Maher, W.A., Craig, P.J. and Jenkins, R.O. (2002) *Applied Organometallic Chemistry*, **16**, 287–293.

144. Craig, P.J., Forster, S.A., Jenkins, R.O. *et al.* (2001) *Applied Organometallic Chemistry*, **15**, 527–532.
145. Desvyatykh, G.G., Nikishin, A.S., Moiseev, A.N. and Votintsev, V.N. (1992) *Vysokochistye Veshchestva (English)*, **133**, 5–6.
146. Hirner, A.V., Feldmann, J., Goguel, R. *et al.* (1994) *Applied Organometallic Chemistry*, **8**, 65–69.
147. Feldmann, J., Krupp, E.M., Glindemann, D. *et al.* (1999) *Applied Organometallic Chemistry*, **13**, 739–748.
148. Hirner, A.V., Gruter, U.M. and Kresimon, J. (2000) *Fresenius Journal of Analytical Chemistry*, **368**, 263–267.
149. Meyer, J., Schmidt, A., Michalke, K. and Hensel, R. (2007) *Systematic and Applied Microbiology*, **30**, 229–238.
150. Michalke, K., Meyer, J., Hirner, A.V. and Hensel, R. (2002) *Applied Organometallic Chemistry*, **16**, 221–227.
151. Gruemping, R., Michalke, K., Hirner, A.V. and Hensel, R. (1999) *Applied and Environmental Microbiology*, **65**, 2276–2278.
152. Michalke, K., Meyer, J. and Hensel, R. (2006) *Applied and Environmental Microbiology*, **72**, 6819–6821.
153. Cutter, G.A. (1991) *Deep-Sea Research A*, **38**, S825–S843.
154. Cutter, G.A. and Cutter, L.S. (2006) *Geochem Geophys Geosyst*, **7**, article no. Q05M08.
155. Jenkins, R.O., Craig, P.J., Goessler, W. *et al.* (1998) *Environmental Science & Technology*, **32**, 882–885.
156. Jenkins, R.O., Craig, P.J., Goessler, W. and Irgolic, K.J. (1998) *Human & Experimental Toxicology*, **17**, 231–238.
157. Jenkins, R.O., Craig, P.J., Miller, D.P. *et al.* (1998) *Applied Organometallic Chemistry*, **12**, 449–455.
158. Gruter, U.M., Kresimon, J. and Hirner, A.V. (2000) *Fresenius Journal of Analytical Chemistry*, **368**, 67–72.
159. Edmonds, J.S. and Francesconi, K.A. (1983) *Journal of the Chemical Society-Perkin Transactions*, **1**, 2375–2392.

8

Metalloid Transport Systems

Hsueh-Liang Fu^{1,3}, Xuan Jiang^{1,3} and Barry P. Rosen^{1,2}

*¹Department of Biochemistry and Molecular Biology, Wayne State
University School of Medicine, Detroit, MI 48201, USA*

*²Department of Cellular Biology and Pharmacology, Florida International
University College of Medicine, Miami, FL 33199, USA*

³These authors contributed equally

8.1 Introduction

Arsenic is considered by the United States Environmental Agency as the most toxic environmental compound and ranks first on the Superfund List of Hazardous Substances [1]. It is introduced into the environment from both natural geochemical and anthropogenic sources. Biological transformations of arsenic create an arsenic biogeochemical cycle [2]. Its environmental ubiquity is a constant health hazard to much of the world's population. In Bangladesh and West Bengal, arsenic in the water supply is a health catastrophe [3]. Arsenic exposure in food and water causes cardiovascular and peripheral vascular diseases, neurological disorders, diabetes mellitus and various forms of cancer [4, 5]. Arsenic is introduced by man in the form of herbicides and pesticides, wood preservatives, animal feeds and semiconductors. In the United States copper-chromium-arsenic (CCA) treatment was used for many decades to protect wood against attack by fungi and insects. Although use of CCA is no longer permitted in the United States, the existing playgrounds, household decks, boardwalks, telephone poles and other places where CCA treated wood was used will ensure that arsenic will find its way into the water and food supply for many years to come. Inorganic and organic arsenicals have been and are still used for agriculture and animal husbandry. Arsenic acid (H_3AsO_4) or Desiccant L-10 by Atochem/Elf Aquitaine, which was

euphemistically called 'harvest aid for cotton' because it was used to defoliate cotton to allow planting of the next cotton crop, remains in the soil of former cotton fields throughout the southern United States even though that product has been discontinued. Many of those fields are now planted with rice, which makes grocery store rice from those states the largest non seafood source of arsenic in the American diet [6]. In addition, the sodium and calcium salts of methylarsenate (MAs(V)) and dimethylarsenate (DMAs(V)) are sold as herbicides such as one form of Weed-B-Gone Crabgrass Killer. DMAs(V) and MAs(V) are in use today as herbicides and fungicides for golf courses in Florida, and runoff from the golf courses introduce these arsenicals into the water supply of Florida municipalities. The organic arsenical roxarsone (4-hydroxy-3-nitrophenylarsonic acid) is used as a growth enhancer and feed supplement for chickens. Not only do we ingest arsenic by eating the chickens, but the chicken litter, which is very high in arsenic, is used to fertilize fields. Despite its toxicity, arsenic has a long history of usage as chemotherapeutic agents [7]. Today, arsenic and antimony containing drugs are used for treating acute promyelocytic leukaemia (the arsenical Trisenox) [8] and diseases caused by protozoan parasites (the antimonial Pentostam) [9], and their use as drugs is expanding, as is resistance to those drugs.

Inorganic arsenic has two biological important oxidation states: pentavalent arsenate (As(V)) and trivalent arsenite (As(III)). In solid form they are found as oxyacids, arsenic acid (H_3AsO_4) and arsenous acid, also called arsenic trioxide (As_2O_3), respectively. In solution at neutral pH, arsenic acid ionizes to the arsenate oxyanion, which is a substrate analogue of phosphate for many critical enzymes. The $\text{p}K_a$ of arsenic trioxide is 9.2, so that, at neutral pH, it would be protonated, and is present in solution as the neutral $\text{As}(\text{OH})_3$. The difference in $\text{p}K_a$ is important for the uptake of the pentavalent and trivalent forms of arsenic: arsenate is transported into cells as the oxyanion arsenate, while arsenite is taken up as the neutral hydroxylated species. The biogeochemical behavior of antimony is similar to arsenic based on their location in the periodic table. In the environment, antimony also has two biological important oxidation states, pentavalent antimonate (Sb(V)), and trivalent antimonite (Sb(III)). In solution at neutral pH, antimonate would be present as antimonate oxyanion, while antimonite exists as an undissociated neutral form, $\text{Sb}(\text{OH})_3$, with the $\text{p}K_a$ of 11.8.

This review will focus on two aspects of arsenic biology. First, to act as either a poison or a drug, arsenic (and antimony) needs to enter cells, which make it imperative to recognize their uptake pathways. In recent years, it has been shown that arsenic is taken up by cells adventitiously using transporters for required solutes such as phosphate or sugars [10] (Figure 8.1). Second, in response to the environmental pressure of ever present arsenic, practically all organisms, from *E. coli* to humans, have mechanisms for arsenic tolerance and detoxification, without which we would not survive. Most of these involve transport systems that catalyse extrusion from the cytosol [2] (Figure 8.1). In bacteria, the genes for arsenic detoxification are usually encoded by arsenic resistance (*ars*) operons, which provide these prokaryotes with arsenic resistance. ABC transporters in the MRP (multidrug resistance protein family) provide tolerance in fungi, plants and animals, including humans. Not only do these systems protect us, but they also protect pathogens and cancer cells from metalloid containing drugs, and resistance to these drugs is a serious challenge for chemotherapy. Thus, knowledge of the pathways and transporters for metalloid uptake and detoxification is necessary for understanding their toxicity, for rational design of metallodrugs and for treating drug resistant microorganisms and tumor cells.

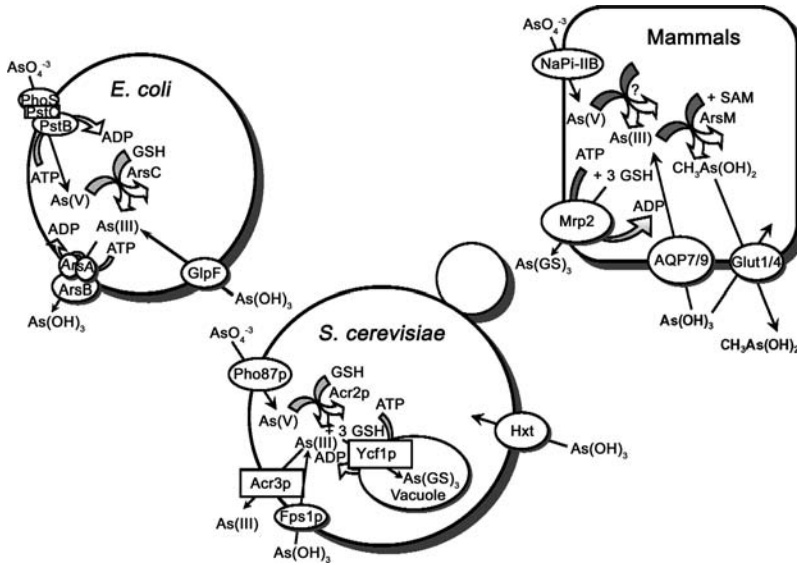


Figure 8.1 Uptake and detoxification of arsenate and arsenite in prokaryotes and eukaryotes. In most cells arsenate is taken up by phosphate transporters, while arsenite is taken up by aquaglyceroporins (GlpF in *E. coli*, Fps1p in yeast and AQPs in mammals). Fps1p is negatively regulated by Hog1p. In yeast As(III) is also taken up by a number of the hexose transporters (Hxt). In both *E. coli* and *S. cerevisiae*, arsenate is reduced to arsenite by an arsenate reductase, in *E. coli* this is ArsC, and in yeast it is Acr2p. Although these two enzymes are unrelated evolutionarily, glutathione and glutaredoxin serve as the source of reducing potential for both. Arsenite detoxification results from removal of the metalloid from the cytosol. In *E. coli*, arsenite is extruded from the cells by ArsB alone or by the ArsAB ATPase. In yeast, Acr3p is a plasma membrane arsenite efflux protein, and Ycf1p, an ABC transporter in the MRP family, pumps As(GS)₃ into the vacuole

8.2 Metalloid Uptake Systems

8.2.1 Arsenate Uptake Systems

Arsenate (As(V)) is much less toxic than arsenite (As(III)), and much of its toxicity derives from its reduction to the trivalent species. To a lesser extent, arsenate toxicity can be ascribed to its chemical similarity to phosphate [11], and hence it is a competitive inhibitor of many enzymes. For example, in human red blood cells, arsenate can replace phosphate in the sodium pump and in anion transport systems [12]. Arsenate also causes rapid hydrolysis of the high energy bonds in compounds such as ATP [13]. Subsequent generation of ADP-arsenate can uncouple oxidative phosphorylation [14].

Due to its similarity to phosphate, arsenate is recognized and taken up by phosphate transporters in most organisms (Figure 8.1). In *E. coli*, there are two phosphate transporters, Pit (Pi transport) and Pst (phosphate specific transport) [15]. Both of them have been shown to catalyse the uptake of arsenate, but the Pit system appears to be the major arsenate uptake system [16]. Similarly, in *Saccharomyces cerevisiae*, arsenate is also taken up by phosphate

transporters. The *pho84* single mutation and the *pho86-pho87* double mutation both conferred arsenate resistance in *S. cerevisiae* [17]. More recently, NaPi-IIB, the rat intestine type II Na/Pi cotransporter, has been demonstrated to play a role in arsenate uptake in several rat tissues and when expressed in *Xenopus laevis* oocytes [18]. Therefore, NaPi-IIB may be responsible for intestinal absorption following oral exposures to arsenate in rat. It is reasonable to assume that arsenate is taken up similarly in humans.

The main route for arsenate uptake in plants is also through the phosphate transporters. As the dominant form of arsenic in aerobic soil [19], arsenate has been shown to compete with phosphate for the same uptake carrier in the roots of *Holcus lanatus* [20]. In addition, arsenate resistance has been associated with constitutive suppression of phosphate transport systems by phosphate in a range of plant species, including *Holcus lanatus*, and *Cytisus striatus* [20, 21]. A recent study on an *Arabidopsis thaliana* mutant with the Pi transporter PHT1;1 disrupted, which exhibited improved arsenate resistance and reduced uptake rate for both phosphate and arsenate, further indicates the existence of an integrated phosphate/arsenate transport pathway in the plants [22].

Even though antimonite has some similar chemical properties to arsenate and phosphate, there are differences. For example, the pentavalent oxyanion AsO_4^{3-} is tetradral, while, in solution, antimonite is the octahedral Sb(OH)_6^- [23]. Antimonate is also relatively insoluble compared to the arsenate and phosphate. For these reasons the transport of antimonite has not been studied in detail in any organism. Studies on two arsenate accumulating plants, *Zea mays* (maize) and *Helianthus annuus* (sunflower), showed that phosphate did not affect uptake of antimonate, which suggests a different translocation pathway for antimonate in plants [24].

8.2.2 Uptake Systems for Arsenite and Antimonite

Trivalent arsenite is considerably more toxic than pentavalent arsenate. The toxicity of trivalent arsenic is due to its propensity to bind to thiol groups and consequently inhibit the function of the critical sulfhydryl containing proteins [25]. Trivalent arsenicals readily react with thiol containing molecules such as glutathione (GSH) and cysteine *in vitro* [13], which raises the redox potential of the cytosol, leading to the formation of damaging reactive oxygen species. Since the majority of As(III) targets are intracellular, it must be taken up to exert toxicity. To date, two pathways of As(III) uptake have been identified: aquaglyceroporin channels and glucose permeases.

8.2.2.1 Aquaglyceroporins (AQPs) and Metalloid Uptake

In *E. coli*, GlpF, the glycerol facilitator [26], was the first identified As(III) and Sb(III) uptake system [27]. A screen of random transposon mutants turned up one in which *glpF* was disrupted and conferred resistance to Sb(III). Although the mutant did not exhibit increased As(III) resistance, disruption of *glpF* greatly reduces uptake of As(III) and Sb(III) in *E. coli* [28], which clearly demonstrates GlpF is the major uptake pathway for both metalloids. GlpF is a member of the major intrinsic protein (MIP) superfamily. Members of the MIP family fall into two main evolutionary groups, the aquaporins such as AQP1 are channels for only water [29], and aquaglyceroporins such as GlpF, which transport water and uncharged organic solutes such as glycerol and urea [30]. A number of AQP structures have been solved, including bovine AQP0 [31], human AQP1 [32], *E. coli* GlpF [33],

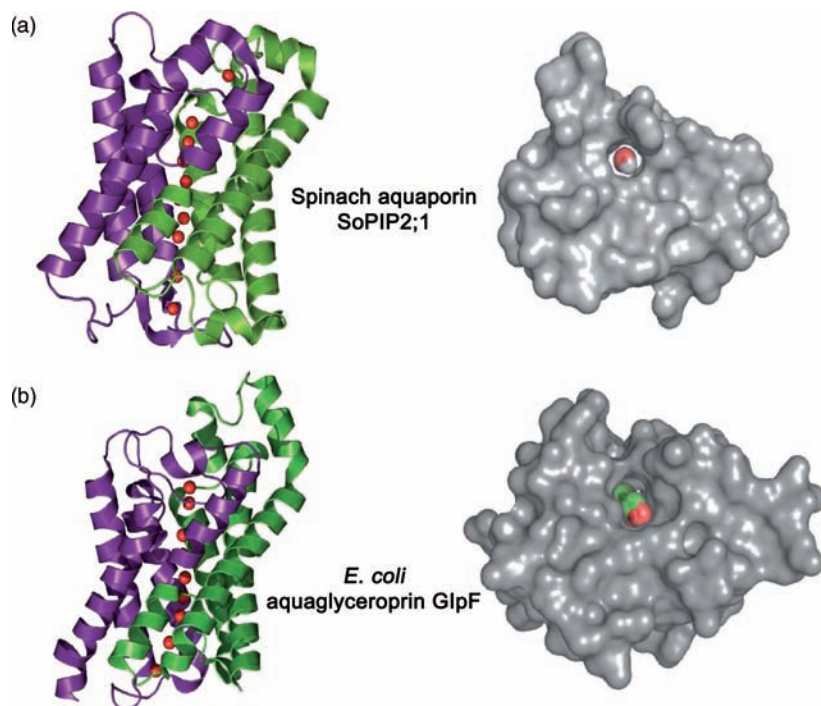


Figure 8.2 Aquaporin structures. (a) The spinach aquaporin SoPIP2;1, which is an aquaporin water channel, and (b) the *E. coli* GlpF glycerol channel (PDB 1LDI), which is aquaglyceroporin channel for glycerol and arsenite. On the left is the structure of each, with water molecules (red spheres) passing through the two channels. On the right are cross-sectional views showing the narrowest opening of the pore with a water or glycerol molecule, respectively

spinach SoPIP2 [34], and AqpM from the malarial parasite *Plasmodium falciparum* [35], and they all have a highly conserved structure with a characteristic hour glass shape [36] (Figure 8.2). The functional unit of AQP is a tetramer, with each monomer forming an independent water pore. Each monomer contains six transmembrane helices, with two membrane spanning half helices interacting with each other from opposing sides through two highly conserved Asp-Pro-Ala (NPA) motifs to form a narrow pore across the membrane. Close to the extracellular exit of the channel, a conserved aromatic/arginine (ar/R) constriction region forms the narrowest part of the channel and has been identified as playing an important role for the channel selectivity of MIPs [37, 38]. Comparison of the sizes of the constriction regions in the water channel AQP1 and the glycerol channel GlpF suggests that the almost 1 Å wider constriction region in GlpF permits larger molecules such as glycerol and arsenite compared with AQP1, whose steric limit is 2.8 Å [32, 33] and may be too small for molecules larger than water to pass through. An increase in pore diameter of human AQP1 by point mutations in the ar/R region allows the transport of urea and glycerol [37], which further indicates the importance of ar/R region in the permeation property of MIPs.

How does GlpF recognize As(III) and Sb(III) as substrates? As(OH)₃ and Sb(OH)₃, which are the major species in aqueous solution at neutral pH, exhibit similar conformation and charge distribution as glycerol [39]. A slightly smaller size of As(OH)₃ and Sb(OH)₃ can be an additional advantage for their transit through the channel. On the other hand, this advantage is counteracted by the higher rigidity of the metalloid hydroxyl groups, which prevents them from adapting their conformation to the topology of the GlpF channel such as the more flexible glycerol can do.

In *S. cerevisiae*, Fps1p, a homologue of GlpF, has been shown to be a route for As(III) and Sb(III) uptake [40]. Disruption of FPS1 increases tolerance to both As(III) and Sb(III) and greatly reduces their rate of uptake rate. Cells expressing Fps1p are highly sensitive to both As(III) and Sb(III), and uptake of both were shown to be mediated by Fps1p [41]. The Fps1p mediated pathway is osmoregulated: the channel is rapidly closed in response to hyperosmotic stress to allow glycerol accumulation, whereas hypoosmotic stress reactivates Fps1p to permit glycerol release [42]. Kinases and phosphatases may also be involved in Fps1p activity. For example, *S. cerevisiae* mitogen-activated protein kinase (MAPK) Hog1p has been demonstrated to control the basal activity of Fps1p [43]. In response to As(III) and Sb(III), Hog1p is activated by phosphorylation. The arsenite activated kinase then phosphorylates the N-terminal domain of Fps1p, which inhibits its metalloid transport activity inside the cell. Therefore, yeast cells can minimize metalloid influx and damage by regulating the channel.

In mammals, 13 AQPs (0–12) have been identified. Four have been identified as aquaglyceroporins: AQP3, AQP7, AQP9 and AQP10 [44]. The closest mammalian homologues to *E. coli* GlpF and yeast Fps1p are AQP9 and AQP7. The rat AQP9 gene was shown to complement the phenotype and function of the yeast FPS1 knockout [41]. Microinjection of rat AQP7 or AQP9 cRNA in to *Xenopus laevis* oocytes resulted in increased rates of arsenite uptake [41]. Similar results were obtained with the four known human members of the aquaglyceroporin family. Human AQP9 is found to be the most efficient human aquaglyceroporin channel for As(OH)₃ uptake in oocytes, followed by hAQP7 [45]. In oocytes neither hAQP3 nor hAQP10 catalysed significant arsenite uptake. However, overexpression of AQP3 in human embryonic kidney 293T cells increased arsenic accumulation, and the cells became more sensitive to As(III), suggesting that AQP3 may transport As(III) to some extent [46].

The finding that AQP9 is the major arsenite transport system in human is relevant to human health and disease. AQP9 is the primary liver isoform [47], and liver is the major organ of arsenic detoxification, in part by methylation to less toxic pentavalent forms (which is controversial because more toxic trivalent methylated species are also produced) [48] and in part by biliary excretion of As(GS)₃ catalysed by multidrug resistance associated protein MRP2 [49]. The trivalent monomethylated species (MAs(III)) is also a substrate of AQP9, which has led to the suggestion that As(III) enters the liver from the blood stream via AQP9 down its concentration gradient. It is then methylated to MAs(III), which flows down its concentration into the blood stream via AQP9 to other tissues or is glutathionylated and pumped into bile by MRP2 [50] (Figure 8.3). Elevated expression of AQP9 could increase arsenic uptake into liver and overwhelm its ability to detoxify arsenite. Expression of AQP9 in liver has been shown to be elevated by nutritional restriction [51]. Thus, poor nutrition in Bangladesh and West Bengal could lead to the increased individual sensitivity to arsenite, and we might predict that improved diets in

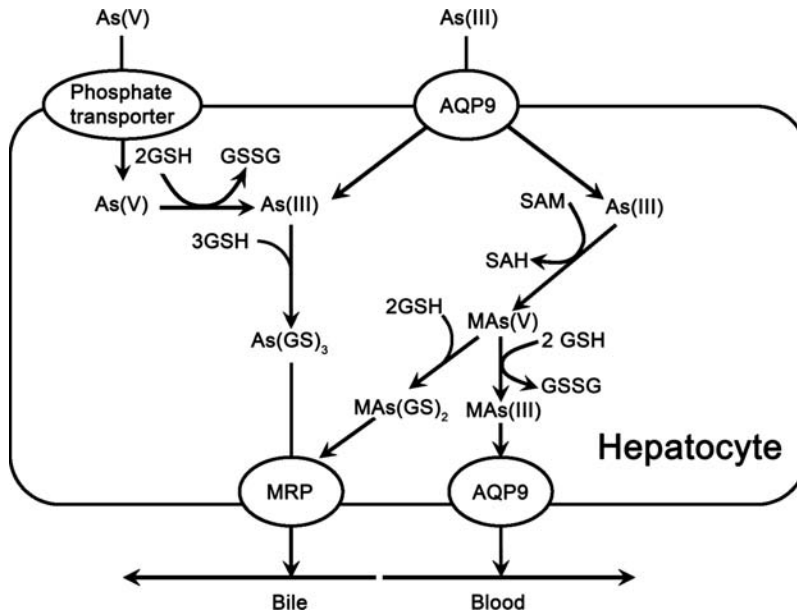


Figure 8.3 Hepatic arsenic circulation. Arsenate is actively taken into hepatocytes by phosphate transporters, where it is reduced to arsenite, most likely using GSH as the reductant. Arsenite flows into hepatocytes through the AQP9 channel in the form of $\text{As}(\text{OH})_3$. It is methylated by AS3MT, an As(III)-S-adenosylmethionine (SAM) methyltransferase to a series of species, one of which is methylarsenite ($\text{MAs}(\text{III})$ or $\text{MAs}(\text{OH})_2$). Both As(III) and $\text{MAs}(\text{III})$ can be glutathionylated and pumped into bile by MRP2. $\text{MAs}(\text{OH})_2$ flows downhill into the bloodstream via AQP9 to other tissues. Methylated arsenicals are eventually eliminated in urine

these areas could alleviate the toxicity of arsenite in arsenic contaminated regions of the world.

In addition, Trisenox, the active ingredient of which is $\text{As}(\text{OH})_3$ in solution [52], is used clinically as a chemotherapeutic agent for the treatment of acute promyelocytic leukaemia [53, 54]. Since AQP9 is expressed in human leukocytes [47], it may be responsible for the chemotherapeutic effects of arsenite by facilitating diffusion of the drug into the leukaemia cells. If AQP9 expression can be pharmacologically increased in leukaemia patients, then lowering the concentration of drug and/or reducing the duration of treatment can not only maintain drug efficiency but also diminish the cardiotoxicity and neurotoxicity of Trisenox.

To explore whether the two neutral polyhydroxylated substrates, glycerol and $\text{As}(\text{OH})_3$, use the same translocation pathway in mammalian AQPs, the role of specific residues along the channel was studied [45]. Based on the crystal structure of two homologues, bovine AQP1 and *E. coli* GlpF, two residues in the ar/R selectivity filter are likely to be involved in selectivity. Mutations of these two residues in human AQP9 affected permeation of $\text{As}(\text{OH})_3$ and glycerol equally, supporting the proposal that $\text{As}(\text{OH})_3$ and glycerol share a common channel [45].

MIPs are also expressed in high concentrations in roots of rice and other plant species [55]. The competition studies for the uptake of As(III) with glycerol in rice led to the suggestion that As(III) is transported by members of the MIP family in plants [56]. Plant MIPs form a large and divergent family, with more than 30 identified members in the genomes of *Oryza sativa* [57], *Arabidopsis thaliana* [58], and *Zea mays* [59]. Based on the sequence similarity and localization, plant MIPs have been classified into four subfamilies [60, 61]: plasma membrane intrinsic proteins (PIPs), tonoplast intrinsic proteins (TIPs), nodulin 26-like intrinsic proteins (NIPs), small and basic intrinsic proteins (SIPs). The existence of the diverse subfamilies of MIPs represents wide differences in substrate specificity, subcellular localization, and regulation. Not all plant MIPs are selective for water; some of them are also permeable to other neutral molecules [62]. For examples, TIPs have been reported to transport glycerol and ammonia [63, 64]; NIPs facilitate the transport of glycerol [65], ammonium [66], lactic acid [67] and metalloids such as boron [68] and silicon [69]; the SIP1 subgroup of SIPs has been reported to take up water [70]; and TIPs have been shown to be CO₂ channels [71]. These differences in selectivity may have derived from the properties of residues in the narrow aromatic/arginine (ar/R) selectivity filter, as has been suggested from the homology modeling of MIPs in *A. thaliana*, *Z. mays* and *O. sativa* with crystal structures of bovine AQP1, *E. coli* GlpF and AqpZ [72].

Since members of the NIP subfamily are considered to be the functional equivalents of aquaglyceroporins, it was postulated that NIPs might also serve as arsenite transporters in plants [73]. Recently, several NIP isoforms from *A. thaliana*, *Lotus japonicus*, and *O. sativa* were cloned and expressed in a yeast FPS1 knockout strain that is resistant to As(III) and Sb(III) [73]. Cells expressing AtNIP5;1, AtNIP6;1, and AtNIP7;1 from *A. thaliana*, OsNIP2;1, OsNIP2;2, and OsNIP3;2 from *O. sativa*, and LjNIP5;1 and LjNIP6;1 from *L. japonicas* regained wild type sensitivity to As(III), and direct transport assays confirmed their ability to facilitate As(III) transport across cell membranes. Yeast cells expressing AtNIP7;1 were strongly Sb(III)-sensitive [73].

Physiological studies of metalloid transport in *O. sativa* are consistent with those studies [74]. OsNIP2;1, a silicic acid transporter [69], is expressed at high levels in rice roots whether or not the plants were exposed to As(III) [74]. Disruption of OsNIP2;1 significantly decreased As(III) accumulation in the roots and shoots of rice compared with wild type. Furthermore, addition of silicic acid in the nutrient medium reduced arsenite concentration in both roots and shoots of wild type rice, but not in the mutant, which indicates that silicic acid and arsenite may use the same transporter in the rice [74]. Thus OsNIP2;1 appears to be responsible for much of the uptake of arsenic (and silicon) into rice roots (Figure 8.4a).

Similar results are also obtained from in *Arabidopsis thaliana* [75]. A loss-of-function mutation in AtNIP7;1 improved plant tolerance to As(III) and greatly reduced the uptake rate of As(III). Yeast cells expressing AtNIP7;1 were highly sensitive to As(III), and uptake assays indicated that As(III) uptake is mediated by AtNIP7;1.

Based on the diameter of their ar/R regions, the NIP family can be subdivided into three subgroups NIP I, NIP II, and NIP III [76]. NIP I channels, which are characterized by the consensus motif W I/V A/G R in its ar/R region, conduct water, glycerol and lactic acid [77, 78]. Substitution of alanine for tryptophan in that region of the NIP II channel results in a larger pore diameter that allows larger solutes, such as urea [77] and boric acid to pass through [68]. In contrast to the ar/R region of the other two, the ar/R region of NIP III

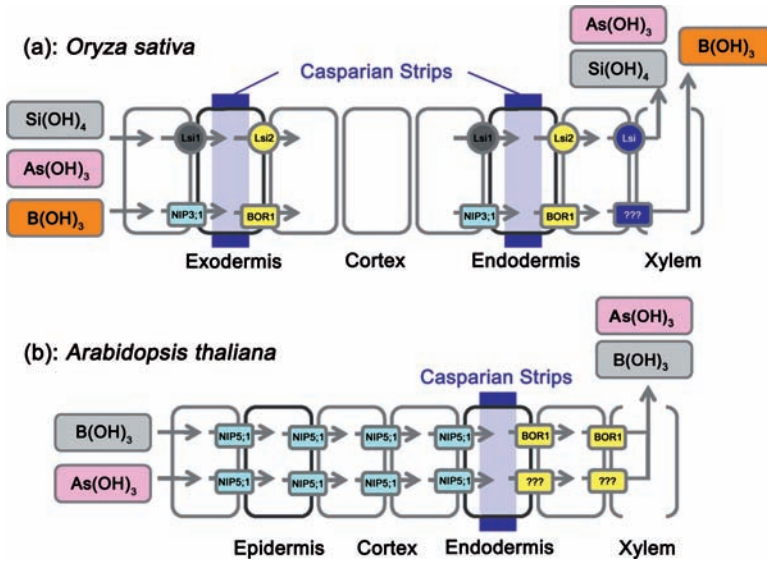


Figure 8.4 Metalloid distribution in plants. Metalloids are taken up by plant roots and distributed to above ground tissues by a series of membrane transporters. In *O. sativa* (rice) and *A. thaliana* initial uptake into roots is mediated by aquaglyceroporins in the NIP subfamily. (a) In rice, *Lsi1* facilitates influx of silicon and arsenite at both the exodermis and endodermis for transport across the casparian bands into the stele. *NIP3;1*, a close homologue of *Lsi1*, accounts for the uptake of boron into the xylem. *Lsi2*, which is an *ArsB* homologue unrelated to NIPS, catalyses efflux of silicon and arsenite into the xylem. (b) In *A. thaliana*, *AtNIP5;1* conducts arsenite and boron through root endodermis cells for further translocation from the roots to the shoot. *AtBOR1* is an efflux transporter that accounts for the xylem loading of boron. It is not clear whether *BOR1* or another efflux system exports arsenite into the xylem

has the motif GSGR. These small residues in the NIP III result in the largest pore diameter, allowing conduction of silicic acid [76]. $\text{As}(\text{OH})_3$, which is more similar in cross-section to glycerol [79], has been reported to be transported by each subgroup of NIPs.

Understanding the pathways of arsenic uptake in plant will be useful in developing strategies for reducing the arsenic content in food crops such as rice. The ar/R selectivity filter and other structural features of these channels allow aquaglyceroporins to discriminate between different solutes. For example, rice *OsNIP2;1* is permeable to $\text{As}(\text{III})$ but not glycerol [69, 74]. *AtNIP5;1* and *AtNIP6;1* are more permeable to $\text{As}(\text{III})$ than $\text{Sb}(\text{III})$, but the opposite is true for *AtNIP7;1*, which shows selectivity for $\text{Sb}(\text{III})$ [73]. Thus, engineering NIPs to reduce $\text{As}(\text{III})$ permeability is a plausible approach to creation of low arsenic crops. A recent report demonstrates the feasibility of that approach: a mutation of a single residue (Glu152) at extracellular entry point of the pore of the *Leishmania* aquaglyceroporin *LmAQP1* reduced the rate of $\text{As}(\text{III})$ movement without affecting glycerol conduction [80]. This shows that in at least one AQP metalloid and glycerol transport can be separated by a single mutation. Finally, growing crops in soil containing high levels of silicic acid might reduce their arsenic content, since it has been observed that rice seedlings grown in the presence of silicic acid show comparatively lower levels of arsenic accumulation [74]. In

summary, a detailed understanding of the mechanisms of arsenic transport by plants will lead to strategies for preventing arsenic entry in the food chain, and improving human health [81].

8.2.2.2 *Glucose Permeases and Arsenic Uptake*

The second family of membrane transporters that catalyses arsenite uptake includes glucose permeases [82], which belong to the major facilitator superfamily (MFS) [83]. In *S. cerevisiae*, most arsenite is taken up by the aquaglyceroporin Fps1p in the presence of glucose. However, in the absence of glucose, the *fps1*-deleted strain exhibits only a 25% reduction in arsenite uptake, suggesting that the majority of arsenite accumulation in yeast is via hexose permeases [82]. The family of hexose permeases in *S. cerevisiae* includes 18 members, Hxt1p to Hxt17p and Gal2p [84]. A yeast strain lacking FPS1 and the genes for all 18 hexose permeases exhibited only residual uptake of arsenic trioxide, and expression of HXT1, HXT3, HXT4, HXT5, HXT7, or HXT9 restored arsenite transport ability [82]. These data clearly demonstrate that yeast hexose permeases catalyse the transport of arsenite.

Mammalian glucose transporter isoform 1, or GLUT1, which is a homologue of the yeast hexose permeases, has also been shown to mediate a low rate of As(III) uptake and a higher rate of MAS(III) uptake in both yeast and *Xenopus* oocyte expression systems [85]. GLUT1, which is found in the epithelial cells that form the blood-brain barrier and mediates the majority uptake of glucose into brain through the blood-brain barrier [86], may represent the major pathway for entry of arsenite into brain [85].

However, it is still not clear how trivalent arsenic and glucose can be recognized and transported by the same transporter. Are these substrates transported in the same pathway or two different translocation channels? There are two possibilities: first, trivalent arsenic might occupy the same binding site as glucose in GLUT1, forming a cyclic trimer that resembles the glucose molecule [82]. This hypothesis gains some supports from the search of the Cambridge Structural Data Base, where 109 oxo-bridged As-O-As compounds, including 10 with six-membered (As-O)₃ rings, have been identified. The crystal structure of arsenious oxide, As₄O₆, is also a six-membered (As-O)₃ ring with the fourth As(III) coordinated to the three axial oxygens. So it is reasonable to consider the possibility that arsenic trioxide forms a similar six-membered cyclic oxo-bridged ring, an inorganic molecular mimic of the chair form of glucose molecule. Second, trivalent arsenic might go through a different channel through GLUT1 than glucose. Instead of forming a glucose like trimer, trivalent arsenic may be recognized in the monomeric form as As(OH)₃. Rather than filling the glucose binding site, they may interact with other hydrophilic residues in GLUT1 to form hydroxyl bonds. The results of extended X-ray absorption fine structure spectroscopy (EXAFS) indicate that As(OH)₃, the most stable structure existing in solution at neutral pH, can be considered an inorganic molecular mimic of glycerol [52], which is the form most likely to be recognized by AQP9 [41]. Similarities in structural properties between As(III) and glycerol are also indicated by quantum mechanical calculations [39]. Reminiscent of uptake of As(OH)₃ by aquaglyceroporins, arsenicals may also move through a water channel in hexose transporters. GLUT1 has been predicted to have a water channel [87]. From the results of transport studies with a GLUT1 T310I mutation, which causes a GLUT1-deficiency syndrome, it has been proposed that the water channel is

different from the translocation pathway for glucose [88]. This mutant has selectively lost glucose transport but not water transport, indicating that GLUT1 has two independent channels [88]. This assumption is supported by two lines of evidence. First, inhibition of glucose by MAs(III) is noncompetitive, which would be expected if the two substrates do not bind at the same site [85]. Second, the classic glucose transport inhibitors cytochalasin B and forskolin do not inhibit uptake of MAs(III) by GLUT1. The translocation properties of GLUT1 for trivalent methylarsenite and glucose were investigated in more detail [89]. Substitution of Ser⁶⁶, Arg¹²⁶ and Thr³¹⁰, residues critical for glucose uptake, led to decreased uptake of glucose but increased uptake of CH₃As(OH)₂. The *K_m* for uptake of CH₃As(OH)₂ of three identified mutants, S66F, R126K and T310I, were decreased 4–10 fold compared to native GLUT1. The osmotic water permeability coefficient (*P_f*) of GLUT1 and the three clinical isolates increased in parallel with the rate of CH₃As(OH)₂ uptake. GLUT1 inhibitors Hg(II), cytochalasin B and forskolin reduced uptake of glucose but not CH₃As(OH)₂. These results clearly demonstrate that CH₃As(OH)₂ and water use a common translocation pathway in GLUT1 that is different from the pathway for glucose.

8.2.3 Boron Uptake Systems

Boron (B) is much less prevalent in the Earth's crust than arsenic but, even so, is widely distributed in nature and released into the environment mainly through both geochemical sources and, to a lesser extent, anthropogenic sources. The major usage of boron in industry includes as an insulator, in the production of glass fibers and as a fire preventative material [90].

8.2.3.1 Uptake of Boron in Plants

Although apparently not required by mammals, boron is an essential element for plants [91]. In agriculture, boron deficiency is a major problem that impedes crop growth and generally leads to the rapid cessation of root elongation, reduced leaf expansion and reduced fertility in plants [92]. Most of these properties are associated with the role of boron in the structure and function of the plant cell wall, where boron crosslinks pectic polysaccharide through bonding of two rhamnogalacturonan II (RG-II), which is necessary for intercellular attachment and the maintenance of cell structure in plants [93, 94]. To maintain cell wall biosynthesis and optimal plant growth, boron is required to be continuously delivered to growing plants from soil through roots and vascular tissues. However, there is a narrow range of boron concentrations below which there is deficiency and above which is toxicity [92]. Reduced crop quality and yield in soils containing toxic levels of boron is a worldwide problem in the food production [95]. Thus, an understanding of the physiology of boron absorption and homeostasis in plants is important for alleviating boron deficiency and toxicity in agriculture.

In solution at physiological pH, boron exists mainly as uncharged boric acid B(OH)₃, a weak Lewis acid with a *pK_a* of 9.24. Boric acid is a small molecule with a molecule volume similar to urea and other small nonelectrocytes. At higher pH, this weak acid dissociates to the borate anion B(OH)₄⁻, which is chemically similar to bicarbonate. Boron is taken up by plant roots as B(OH)₃, and the uptake of boron by plant roots has been described as a combination of passive transport through the lipid bilayer and channel mediated transport [96]. The evidence for the channel mediated transport comes from the partial

inhibition of boron permeation across plasma membrane vesicles isolated from squash roots by mercuric chloride [96], which indicates the binding of mercury with the cysteine residues of the membrane boron channel and results in occlusion of the channel pore [97]. Recovery of boric acid permeability by 2-mercaptoethanol further indicates that Hg sensitive channels are involved in the boric acid transport [96]. Furthermore, small solutes such as urea and glycerol have been shown to inhibit 35–54% of boron uptake by squash roots [98], which indicates a common channel for these solutes. Several MIPs have been suggested as promising candidates to mediate the membrane transport of boron into plants. Expression of *Zea mays* PIP1, a member of MIP family, results in a 30% increase in boron uptake into oocytes [96]. Other MIPS, PIPib, PIP2a, and PIP2b from *Arabidopsis thaliana* have also been suggested to facilitate uptake of boric acid in oocytes [99].

However, the molecular identity of boric acid importers and their physiological significance has not been clear until the AtNIP5;1 gene, which encodes a member of MIP family, was identified as the boric acid channel required for both boric acid uptake and normal growth of *Arabidopsis thaliana* under boron limitation [68]. Transcriptome analysis showed that AtNIP5;1 was upregulated in boron deficient roots, and the transcript accumulation may result from the high NIP5;1 promoter activity observed in root epidermal, cortical, and endodermal cells, particularly in the elongation zone under boron limitation. The expression of AtNIP5;1 in oocytes produced a high rate of transport of boric acid and a lesser rate of water. Since AtNIP5;1 is localized in the plasma membrane of *Arabidopsis* protoplasts, it is reasonable that this transporter functions as a major boric acid channel *in planta*. Importantly, disruption of AtNIP5;1 inhibited the plant growth and greatly reduced the boron concentration in roots and shoots under boron limitation but not under adequate boron supply [68]. These results strongly suggest that AtNIP5;1, which is regulated by transcriptional mechanism, is required for boron uptake into roots, and crucial for the normal plant growth under boron limitation (Figure 8.4b) [68]. Similarly, OsNIP3;1, the closest homologue to AtNIP5;1, has also been identified as a boric acid channel required for efficient growth under boron limitation in rice (Figure 8.4a) [90].

8.2.3.2 Uptake Systems for Boron in Other Eukaryotes

It is not clear whether or how boron is involved in the normal physiology of other eukaryotes, including mammals. In mammals, boron deprivation has been associated with slower growth, abnormal bone development, impaired metabolic function and reduced activity of steroid hormones [100, 101]. Maintaining *Xenopus laevis* and Zebrafish on a low boron diet impaired reproductive and embryonic development [102, 103]. However, boron is also toxic to vertebrates: the effect of boron on *Xenopus laevis* and zebrafish growth followed a bell shaped curve [102, 103].

Boron appears to be involved in proliferation of *S. cerevisiae* [104], which is a boron tolerant eukaryotic organism that can grow under the 90 mM boron conditions [105]. Yeast has been suggested to have a specific uptake system for boric acid. Several MIPs and DUR3, a urea transporter [106], were chosen as possible candidates for boron transport. Among them, deletion of DUR3 or FPS1 was shown to decrease accumulation of boron and to confer tolerance to toxic levels of boron [105]. However, no significant increase in boron accumulation was observed in yeast cells expressing either DUR3 or FPS1 [105]. These results suggest that DUR3 and FPS1 can transport boric acid; however, other factors may

also be required for the maintenance of intracellular boron concentrations. The physiological roles of boron uptake via DUR3 or FPS1 in yeast are still uncertain, although it has been proposed to play a role in cell wall structure, as in plants.

These studies in plants and yeast clearly demonstrate the importance of MIP family in boron uptake and suggest that mammals might also have boron uptake pathways. AQP9 is a reasonable candidate for a boric acid transporter in mammals, including humans since it is the closest homologue of AtNIP7;1 and has the broadest substrate specificity [47].

Although no boric acid transporter has been identified in humans so far, a Na^+ -coupled borate cotransporter (NaBC1), which is also a bicarbonate transporter [107], has been demonstrated to catalyse uptake of borate [108]. NaBC1 is ubiquitously expressed in the basolateral membrane of salivary gland acinar cells and kidney tubules. Cloned NaBC1 was expressed in HEK 293 cells, which are derived from human embryonic kidney cells. In the absence of borate, NaBC1 increased permeability Na^+ and OH^- ; whereas in the presence of borate, NaBC1 acts as a selective, voltage regulated electrogenic Na^+ - $\text{B}(\text{OH})_4$ cotransporter. Borate activated the MAPK pathway, stimulating cell growth and proliferation at low concentrations; at high concentrations borate inhibited this growth related signaling pathway. Consistent with this observation, overexpression of NaBC1 shifted the entire borate concentration response curve to higher concentrations, whereas a knockdown of NaBC1 prevented the effect of borate on cell growth and proliferation. These results may suggest both a physiological role for borate and a mechanism of toxicity in humans.

8.2.4 Uptake Systems for Silicon and Germanium

Silicon (Si) is the second most abundant element after oxygen in the earth's crust. It is essential for animals [109] and has been implicated in optimal development of bones and connective tissue in humans [110]. It is also an essential element for diatoms [111]. Uptake and processing of silicon is required for the formation of species specific, porous and silicified structures of the diatom cell wall [112]. However, silicon is not considered essential in plants; instead, it is a beneficial or 'quasi-essential' element for the growth of plants [69, 113, 114]. Silicon helps plants to overcome both biotic and abiotic stresses [114, 115]. For examples, Si enhances resistance of plants to pathogens such as blast on rice [116], and powdery mildew on cucumber [117]. Silicon is also effective in decreasing abiotic stresses, including salt stresses, nutrient imbalance, high or low temperature, and radiation damage [118]. Most of these beneficial effects of silicon have been ascribed to the silicon deposition in the cell walls of the epidermal surfaces of leaves and roots.

Silicon is taken up by plant roots in the form of silicic acid, $\text{Si}(\text{OH})_4$, a monomeric, uncharged molecule in solution below pH 9 [119]. After it is taken up, silicic acid is translocated to the shoot via xylem in the same form [120], and finally deposited in the cell wall as a polymer of hydrated amorphous silica, $\text{SiO}_2 \cdot n\text{H}_2\text{O}$, forming silica-cuticle double layers and silica-cellulose double layers [121]. Therefore, silicon accumulation in the plants enhances the strength of cell walls, which protects the plants from various stresses.

Although all plants contain silicon, plants differ considerably in the amount of silicon accumulated in the shoots, ranging from 0.1% to 10% silicon, dry weight [114]. In the plant kingdom, Si is highly accumulated in *Gramineae* and *Cyperaceae* (> 4% Si), followed by the *Cucurbitales*, *Urticales* and *Commelinaceae*, with intermediate Si accumulation of 2–4%. Most other species show low Si level [76, 121]. This difference in Si accumulation

of different plant species has been ascribed to the different ability of the roots to take up silicon [120]. Rice, which is a typical silicon accumulating plant, with up to 10% of the shoot dry weight, has been reported to have the greatest ability to uptake silicon by roots among all the gramineous species, including wheat, maize and barley [122]. Therefore, rice roots are likely to have a specific uptake system for Si.

A gene family encoding silicon transporters, SITs, has been identified in the diatom *Cylindrotheca fusiformis* [123]. Oocytes expressing *CfSIT1* showed a significant increase in uptake of germanium, another metalloid closely related to silicon in chemical properties, in a sodium dependent pattern [124]. Inhibition of germanium uptake by silicon in oocytes expressing *CfSIT1* suggests that the two metalloids compete for uptake via SIT1. However, no SIT homologue has been identified in plants so far. Furthermore, silicon uptake was not increased by expression any one of the *CfSIT* genes in tobacco [125], indicating that the silicon uptake system in plants is different from that in diatoms.

Recently, a gene encoding a Si transporter, *Lsi1* (*OsNIP2;1*), was identified from a rice mutant defective in Si accumulation (Figure 8.4a) [69]. This *Lsi1* mutant has been shown to accumulate less silicon in the shoot and is more susceptible to pests and diseases compared with wild type rice. *Lsi1* is constitutively expressed in rice roots, but its expression level is regulated by silicon [69]. In the roots, *Lsi1* has been shown to localize at the plasma membrane of distal side of both exodermis and endodermis, where casparian strips exist [126]. Because solutes are unable to freely pass through casparian bands [69], it is likely that *Lsi1* is a transporter required at both exodermis and endodermis for transport of silicon into the stele for further translocation from the roots to the shoot. Importantly, when *Lsi1* expression was suppressed, Si accumulation in rice was also correspondingly reduced [69]. *Lsi1* shows both influx and efflux transport activity for Si in oocytes, although it only functions as an influx silicon transporter in rice roots [69]. These results suggest that *Lsi1* is a major transporter of Si into rice roots and is required for efficient uptake of silicon in rice. In addition, *OsLsi1* appears to be specific for silicon and arsenite over glycerol and boric acid [76, 127], although the basis for this selectivity is unclear.

Lsi6 (*OsNIP2;2*), a close homologue of *Lsi1* in rice (77% sequence identity) has also been isolated from cDNA of rice roots [76]. *Lsi6* is expressed in both the roots and the shoots of rice. However, knockdown of *Lsi6* in rice did not affect uptake of silicon by roots, which suggests that *Lsi6* has only a small contribution to root silicon uptake. In the shoot, *Lsi6* is expressed only in the plasma membrane of xylem parenchyma cells that are adjacent to vessels in both leaf blades and leaf sheaths. The abnormal excretion of silicon from guttation fluid excreted from xylem sap of rice with *Lsi6* disrupted suggests that *Lsi6* is a transporter that may be responsible for the transport of Si out of the xylem and subsequently affects the distribution of Si in the shoots (Figure 8.4a).

Maize (*Zea mays*) is also able to accumulate high amounts of silicon in the shoot, although the levels are lower than in rice [121]. Recently, two homologues of *OsLsi1* and *OsLsi6*, *ZmLsi1* (*ZmNIP2;1*) and *ZmLsi6* (*ZmNIP2;2*), have been identified as silicon transporter in maize [76]. Heterologous expression in oocytes showed that both *ZmLsi1* and *ZmLsi6* have the influx transport activity for Si similar to *OsLsi1*. However, the expression pattern and cellular localization of *ZmLsi1* is different from its rice homologue. The expression of *ZmLsi1* in the roots was constitutive, but its expression was not affected by continuous silicon supplementation, which may indicate a different regulatory mechanism from that of *OsLsi1*. Furthermore, *ZmLsi1* has been localized at the plasma membrane of

epidermis and hypodermis cells but not endodermis cells. This difference may be attributed to the differences in root structure of maize and rice: There is only one casparian band, which is located at the endodermis of maize roots, under normal growth conditions [128]. Silicon may be taken up by ZmLsi1 at epidermis and hypodermis and then transported to stele by the symplastic pathway in maize root. From its cellular localization and transport activity, ZmLsi1 may be responsible for uptake of Si from the soil to the root. In contrast to ZmLsi1, ZmLsi6 is localized at the xylem parenchyma cells in the leaf sheaths and blades, similar to that of OsLsi6. It is likely that ZmLsi6 has a similar function to OsLsi6 and acts mainly as a silicon transporter for xylem unloading.

OsLsi1, OsLsi6, ZmLsi1 and ZmLsi6 all belong to plant unique nodulin 26-like intrinsic protein (NIP) of the major intrinsic proteins (MIP). Lsi1 and Lsi6 have been classified as members of NIP III group due to their distinct ar/R regions. Unlike other groups of NIPs, the highly conserved ar/R constriction filter in the NIP III group consists of a GSGR motif [129]. The smaller size of the four residues in the ar/R region yields a larger pore diameter compared with other NIP groups, which allows silicic acid, with a larger diameter than other metalloids, to pass through the channel. Other members of NIP III group have been found in zucchini, which is also able to accumulate high levels of silicon [130]. Therefore, it is likely that NIP III is unique to Si-accumulated plants and functions as a silicon transporter [76].

Germanium, with a pK_a of 9.4, would be expected to be taken up in the form of $\text{Ge}(\text{OH})_4$. Although Ge has similar chemical property to Si, it is toxic to plants, causing brown spots in leaves and stems. Ge is taken up by plant roots similarly to Si. For example, plants with high Si uptake also take up high levels of Ge [131]. More specifically, plants with markedly different capacities for Si accumulation in their shoots are able to take up Ge without discriminating between these two elements [132]. A direct competition between Si and Ge has been observed in wheat (*Triticum aestivum*) [133], suggesting the antagonism between Ge and Si exists. The rice with *Lsi1* disrupted showed higher resistance to Ge toxicity [121]. This feature has been applied in the selection of rice mutants defective in Si uptake [121]. All these facts indicate that silicon transporters also take up $\text{Ge}(\text{OH})_4$.

8.3 Metalloid Efflux Systems

8.3.1 Eukaryotic MRP Efflux Pumps

In eukaryotes arsenite resistance is conferred by members of the MRP (multidrug resistance associated protein) group of the ABC superfamily of transport ATPases [134], which catalyse export of GS-conjugates such as leukotriene C4 (LTC4) [135]. MRP1 catalysed export of glutathione from cells was increased by arsenite, suggesting that MRP1 functions as a $\text{As}(\text{GS})_3$ carrier [136]. In liver MRP2 extrudes arsenic–glutathione complexes into bile and may be a major route of arsenic detoxification in humans [49].

MRP homologues have been shown to confer arsenic resistance in eukaryotic microbes. Metalloid containing drugs are still the first line therapy for trypanosomiasis and leishmaniasis, and clinical resistance is a serious problem in treatment. In arsenite resistant strains selected *in vitro* there is increased expression of *pgpA*, which encodes an MRP homologue [137]. Legare *et al.* have demonstrated that PgpA transports $\text{As}(\text{GS})_3$ [138]. In *S. cerevisiae*, an MRP homologue, Ycf1p, confers Cd(II) resistance by pumping $\text{Cd}(\text{GS})_2$

into the vacuole [139, 140]. Ycf1p also transports $\text{As}(\text{GS})_3$ into the vacuole and confers arsenite resistance in yeast [141]. In addition to Ycf1p, *S. cerevisiae* has a gene cluster of three ACR genes that also confer arsenic resistance [142]. Acr1p is a transcription factor, and Acr2p is an arsenate reductase. Acr3p is a membrane protein that is homologous to an arsenite carrier protein in *B. subtilis* and mediates efflux of arsenite [141, 143]. While Ycf1p is located in the vacuolar membrane and catalyses sequestration of $\text{As}(\text{GS})_3$ in the vacuole, Acr3p is a plasma membrane carrier protein that catalyses extrusion of arsenite from cytosol. Bacterial Acr3 family members are discussed below.

8.3.2 ArsB

Bacterial operons encoding resistance to arsenicals and antimonials (*ars* operons) can be found on transmissible plasmids and in chromosomes. These operons usually have either three (*arsRBC*) or five (*arsRDABC*) genes (Figure 8.5). The *arsB* encodes a secondary transporter that catalyses efflux of the arsenite anion from cells [144]. Nearly all *ars* operons have these three genes, but some operons have two additional genes, *arsDA*. *ArsD* is an arsenic metallochaperone that delivers $\text{As}(\text{III})$ to *ArsA* [145]. *ArsA* is an $\text{As}(\text{III})/\text{Sb}(\text{III})$ -stimulated ATPase [146] that associates with *ArsB* to form an extrusion pump that is more efficient than *ArsB* alone [147]. Interaction with *ArsD* increases the affinity of *ArsA* for arsenite, thus increasing its ATPase activity at lower concentrations of arsenite and enhancing the rate of arsenite extrusion. Cells are consequently resistant to environmental concentrations of arsenic.

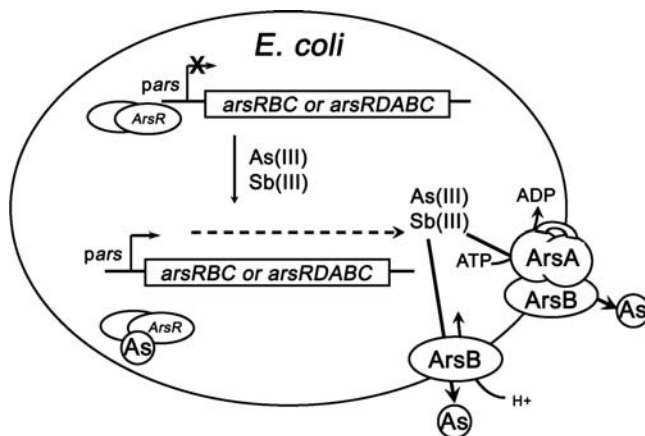


Figure 8.5 Arsenic resistance operons. There are many arsenic resistance operons in bacteria and archaea. Two *E. coli* operons illustrate the diversity. The chromosomally encoded *arsRBC* operon has three genes that encode *ArsR*, a negative regulatory protein that represses in the absence of $\text{As}(\text{III})$ and dissociates from the DNA when $\text{As}(\text{III})$ is bound; *ArsB*, a proton coupled arsenic efflux antiporter, and *ArsC*, an arsenate reductase that reduces arsenate to arsenite. The *arsRDABC* operon found on plasmid R773 has two additional genes, *arsD*, which encodes an $\text{As}(\text{III})$ metallochaperone, and *arsA*, which encodes the *ArsA* ATPase that forms a complex with *ArsB* to create an ATP-coupled $\text{As}(\text{III})$ efflux pump

ArsB is one of the most widespread determinants of arsenic resistance in bacteria and archaea. It is a member of the ion transporter superfamily [148], with 12 membrane spanning segments and a membrane topology that is similar to many carrier proteins [149]. ArsB transports trivalent metalloids in *E. coli* coupled to the proton motive force [28]. Since As(III) is the undissociated oxyacid $\text{As}(\text{OH})_3$ in solution at neutral pH [52], ArsB is most likely an $\text{As}(\text{OH})_3/\text{H}^+$ antiporter.

8.3.3 ArsA

The *arsRDABC* operon of *Escherichia coli* plasmid R773 encodes the ArsAB ATPase, a metalloid pump that confers resistance by actively extruding As(III) or Sb(III) from cells [150]. The 583-residue ArsA is a metalloid-stimulated ATPase that comprises the catalytic subunit of the pump [146, 151]. It is normally bound to ArsB [152], but, in the absence of ArsB, ArsA is found in the cytosol and can be purified as a soluble protein. ArsA has two homologous halves, the N-terminal A1 domain (residues 1~288) and the C-terminal A2 domain (residues 314~583), which are connected by a flexible 25-residue linker peptide (residues 289~313) (Figure 3.15). Each half has a consensus nucleotide-binding domain (NBD). At the interface of the two domains is a binding site for As(III) or Sb(III), the metalloid binding site (MBD) involved in activation of ATPase activity. Connecting the MBD to the two NBDs are signal transductions domains (STDs) in each half of ArsA.

8.3.3.1 The Nucleotide Binding Domain (NBD)

Although ArsA has two very similar NBDs, they are not identical in either sequence or, as discussed below, function. Mutations in either NBD1 or NBD2 resulted in a loss of resistance, transport and ATPase activity [153, 154]. Both structural information and the results of genetic suppression show that the two NBDs in ArsA interact with each other [155, 156]. Both NBDs are required for activity, and considerable effort has been expended to elucidate the role of the individual sites in arsenite transport in the presence or absence of the pump substrate, Sb(III) or As(III).

Mg^{2+} is required for ArsA ATPase activity [157]. Conformational changes at the nucleotide binding site as evidenced by the increase in intrinsic tryptophan fluorescence were observed only on the addition of MgATP, suggesting that Mg^{2+} binds to ArsA as a complex with ATP [158]. It has been shown that the aspartic residue in ATP- and GTP-binding proteins serve as Mg^{2+} ligand. Sequence alignment of ArsA with other ATPase such as nitrogenase iron protein (NifH) [159], RecA [160] and Ras p21 [161] suggested that Asp45 might be a putative Mg^{2+} ligand. Mutation studies showed that cells expressing D45 mutated *arsA* genes lost arsenite resistance. Purified D45A and D45N ArsAs were inactive, whereas the D45E enzyme exhibited 5% of wild type activity with a fivefold decrease in affinity for Mg^{2+} , demonstrating that D45 is part of the Mg^{2+} binding site.

Both NBD1 and NBD2 hydrolyse ATP, with steady state hydrolysis dominated by the activity of NBD1. The overall rate of ATP hydrolysis is slow in the absence of metalloid and is accelerated by metalloid binding. Previous results suggested that the active sites, NBD1 and NBD2, in the two halves of ArsA play different roles in catalysis. ATP binding and hydrolysis at the individual NBDs was examined binding by photolabeling with the ATP analogue 8-azido-5'-[α - ^{32}P]-ATP at 4 °C [162]. Metalloid stimulation correlated

with a >10-fold increase in affinity for nucleotide. To investigate the relative contributions of the two NBDs to catalysis, a thrombin site was introduced in the linker between A1 and A2. This allowed discrimination between incorporation of labeled nucleotides into the two halves of ArsA. The results indicate that both the NBD1 and NBD2 bind and hydrolyse ATP, even in the absence of metalloid. Sb(III) increases the affinity of NBD1 to a greater extent than NBD2. 8-Azido-5'-[γ -(³²P)]-ATP was used to measure ATP hydrolysis at 37 °C. Under these catalytic conditions, both nucleotide binding domains hydrolyse ATP, but hydrolysis in A1 is stimulated to a greater degree by Sb(III) than A2. These results are strong support for the hypothesis that the two homologous halves of the ArsA are functionally nonequivalent. Perhaps they are both catalytic, or perhaps one is regulatory. Future experiments will be required to elucidate their individual roles in ArsA function.

8.3.3.2 *The Metalloid Binding Domain (MBD)*

The two NBDs are located at the interface between A1 and A2, in close proximity to each other [156]. Over 20 Å distant from the NBDs is a metalloid-binding domain (MBS), where three Sb(III) or As(III) are bound at the A1-A2 interface (Figure 3.15). Antimonite or arsenite allosterically activates ArsA ATPase activity. In absence of the metalloids, ArsA has a low level of ATPase activity. Arsenite stimulates ATP hydrolysis by three- to five-fold, whereas a 10- to 20-fold stimulation is observed with antimonite as the activator. All other oxyanions tested had no effect on ATPase activity [157]. In the crystal structure, one Sb(III) is coordinated to Cys113 from A1 and Cys422 from the A2 (Site 1), a second to Cys172 from A1 and His-453 from A2 (Site 2), and the third to His-148 from A1 and Ser-420 from A2 (Site 3). Thus, the three metalloid atoms act as molecular glue to bring the A1 and A2 halves of ArsA together, an event that is linked to activation of ATP hydrolysis [151, 163]. Ruan *et al.* showed that ArsA binds a single Sb(III) with high affinity only in the presence of Mg²⁺-ATP γ S. Mutation of the codons for Cys113 and Cys422 eliminated Sb(III) binding to purified ArsA. C113A/C422A ArsA has basal ATPase activity similar to that of the wild type but lacks metalloid stimulated activity. Cells expressing the *arsA*_{C113A/C422A}B genes had an intermediate level of metalloid resistance and accumulation between those expressing only *arsB* alone and those expressing wild type *arsAB* genes, indicate that, whereas metalloid stimulation of ArsA activity enhances the ability of the pump to reduce the intracellular concentration of metalloid, high affinity binding of metalloid by ArsA is not obligatory for transport or resistance. However, cells bearing wild type *arsAB* replaced cells with mutant *arsA*_{C113A/C422A}B in mixed populations of cells in the sublethal concentration of arsenite, suggesting that the metalloid binding site confers an evolutionary advantage. What is the role of the other metalloids observed in the crystal structure of ArsA, which shows one liganded to Cys172 and His453, and the other liganded to His148 and Ser420? The contribution of those putative metalloid sites was examined [164]. There was little effect of mutagenesis of residues His148 and Ser420 on Sb(III) binding. A C172A ArsA mutant and C172A/H453A double mutant exhibited decreased affinity for Sb(III). Thus, while there appears to only a single high affinity metalloid binding site in ArsA, the results suggest that Cys172 controls the affinity of this site for metalloid and hence the efficiency of metalloactivation of the ArsAB efflux pump.

8.3.3.3 The Signal Transduction Domain (STD)

Connecting the single MBD to the two NBDs are the STDs, one in each half of the protein [165]. The STDs each have a 12-residue signature sequence D¹⁴²TAPTGH¹⁴⁸TIRLL (STD1) and D⁴⁴⁷TAPTGH⁴⁵³TLLLL (STD2), which correspond to the Switch II region of many other nucleotide binding proteins and have been proposed to be involved in transmission of the energy of ATP hydrolysis to metalloid transport. ArsA homologues have been found in every sequenced genome of eubacteria, archaea, fungi, plants and animals. This sequence is highly conserved in ArsA homologues from every kingdom, indicating that this common motif has a conserved function. In the crystal structure, the two DTAPTGH sequences clearly spans the spaces between the MgADP-filled NBSs and the metalated allosteric site [165]. During ATP hydrolysis the carboxy-terminal end of the A1 sequence becomes exposed to a less polar environment, whereas the amino-terminal end becomes exposed to a more hydrophilic environment as the product, ADP, is formed, indicating that this sequence exhibits considerable conformational mobility during the catalytic cycle. From these results the DTAPTGH sequences have been proposed to be signal transduction domains that are involved in cross talk between the NBSs and the allosteric domain [165, 166].

8.3.3.4 The Linker Region

Connecting A1 and A2 is a linker region of 25 residues. In the absence of ATP and metalloid, ArsA is hypersensitive to trypsin [157], with the initial attack within the linker at residue Arg-290 [167]. Binding of both nucleotide and metalloid provides substantial synergistic protection from protease. The requirement for this linker sequence was examined by the mutagenic insertion of five glycine residues or by the deletion of five, 10, 15 or 23 residues [168]. Cells expressing arsA with the five residue insertion had wild type arsenite resistance. Resistance of cells expressing modified arsA genes with deletions was dependent on the length of the linker but independent of the actual sequence. Cells with five or 10 residues deleted exhibited slightly reduced resistance. Further deletions decreased resistance significantly. The purified mutant with the five residue insertion had the same affinity for ATP and Sb(III) as the wild type enzyme. Mutants with 10-, 15- or 23-residue deletions exhibited decreased affinity for both Sb(III) and ATP. The enzyme with a 23-residue deletion exhibited only basal ATPase activity and was unable to be activated by Sb(III). These results suggest that the linker brings the two halves of the protein into proper contact with each other, facilitating catalysis.

8.3.3.5 Function of Smaller ArsA Homologues

Genomic sequencing indicates that homologues of ArsA are widely distributed in nature and are found in members of all three domains: prokarya, archaea, and eucarya [169]. Eukaryotic homologues are half the size of the bacterial ArsA. A human homologue of ArsA, hARSA-I, has been purified and shown to have ATPase activity [170]. Disruption of ARR4, a *S. cerevisiae* homologue, was not lethal, but the disrupted strain displayed increased sensitivity to metal salts and temperature [171]. The purified wild type ARR4 protein exhibited a low level of ATPase activity but was not arsenic stimulated. A mouse homologue, Asna1, had been identified that Exhibits 27% identity to the bacterial ArsA ATPase. To identify the physiological role of the protein, heterozygous Asna1 knockout mice (Asna1^{+/-})

were generated by homologous recombination. The *Asna1*^{+/-} mice displayed similar phenotype as the wild type mice. However, early embryonic lethality was observed in homozygous *Asna1* knockout embryos between the E3.5 and E8.5 stages. These findings indicate that *Asna1* plays a crucial role during early embryonic development [172].

Recently novel role involved in the insertion of proteins into biological membranes was identified for the yeast *ARR4* homologue [173]. While most membrane proteins are inserted in membranes through their N-termini, there are some that are anchored in intracellular membranes by a single transmembrane domain close to the C-terminus. A cytosolic recognition complex termed TRC40 that targets this type of membrane protein for insertion into the endoplasmic reticulum was recently identified. The putative catalytic subunit of TRC40 was identified as *Asna1*. *Asna1* interacts posttranslationally with membrane proteins for delivery to a receptor at the endoplasmic reticulum. Subsequent release from TRC40 and insertion into the membrane required ATP hydrolysis by *Asna1*. Thus this group of *ArsA* homologues appears to have evolved a function quite different from the arsenite detoxification function of the bacterial *ArsAB* pump.

8.3.4 *Acr3*

In addition to the MRP and *ArsAB* families, a third arsenic resistance transporter is *Acr3*, which is a member of the BART (bile/arsenite/riboflavin transporter) superfamily. The *Acr3* subfamily includes members found in bacteria, archaea and fungi and is at least as widespread and perhaps more than members of the *ArsB* family [174, 175]. Unfortunately, the literature is confused by the fact that many members of the *Acr3* family are annotated as *ArsB* even though they exhibit no significant sequence similarity to *ArsB*. The first identified member of this family is encoded by the *ars* operon of the skin (*sigK* intervening) element in the chromosome of *B. subtilis* [176]. The membrane topology of the *B. subtilis* *Acr3* was recently investigated using translational fusions, but the results could not distinguish between eight and 10 transmembrane segments [177]. The properties of a more distant homologue from *Shewanella oneidensis* was examined recently [178]. The *S. oneidensis* homologue confers resistance to arsenate but not arsenite. Similarly, the purified protein binds arsenate, not arsenite, indicating that this protein is not an *Acr3* orthologue. Fungal members of this family include the *S. cerevisiae* *Acr3p* metalloid efflux protein [141, 142]. Interestingly, yeast *Acr3p* appears to be selective for As(III) over Sb(III), which is surprising considering the similarity in chemical properties between the two metalloids. As discussed above, both *ArsA* and *ArsB* have higher affinity for Sb(III) than As(III). Perhaps this difference in selectivity relates to the fact that, in solution, arsenite is As(OH)₃ while antimonite is the octahedral [Sb(OH)₆]³⁻ [23].

To gain the basic structural information of a *Acr3*, Aaltonena and Silow [177] analysed the transmembrane topology of *B. subtilis* *Acr3* by constructing a total of 42 translational fusions, which create chimeric proteins of truncated forms of *Acr3* and two reporter proteins, alkaline phosphatase and Green Fluorescent Protein at 22 different positions in the amino acid sequence of Bs*Acr3*. Their results suggest that Bs*Acr3* has an even number of transmembrane (TM) segments. However, the results could not distinguish between eight and 10 transmembrane segments [177]. Moreover, this approach produces inactive proteins that may have altered topology as a result of fusion to a large protein like alkaline phosphatase. Recently Fu *et al.* [179] used cysteine scanning mutagenesis and accessibility

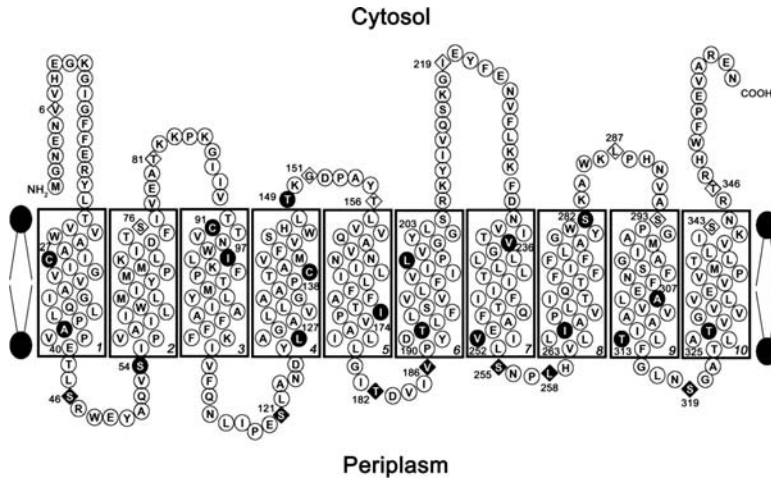


Figure 8.6 Membrane topology of the Acr3 As(III) efflux permease. Cysteine scanning mutagenesis and accessibility to thiolreactive probes was used to identify 10 transmembrane segments in the *C. glutamicum* Acr3. (◆) periplasmic residues accessible to both BM and AMS; (◇), cytosolic residues located accessible to BM but not AMS; (●), residues not labeled by BM [179]

to thiol-reactive probes to determine the transmembrane topology of Acr3 from *Corynebacterium glutamicum*. This method is more likely to yield an accurate topology since it utilizes active membrane proteins. Their results clearly demonstrate that CgAcr3 has 10 transmembrane spanning segments, with the N- and C-termini localized in the cytosol (Figure 8.6).

8.3.5 Efflux Systems for Silicon

As mentioned in Section 8.2.4, silicon enhances plant growth, and several genes involved in silicon uptake have been identified. However, there is little known about silicon efflux. To identify genes involved in the efflux transport of silicon, Ma *et al.* [130] isolated rice mutants defective in silicon uptake by selecting for tolerance to germanium they isolated an Lsi2 mutant (Lsi2) defective in silicon efflux.

Lsi2 is located on chromosome 3 and consists of two exons and one intron. The ORF of this gene is 1416 bp long, and the deduced protein consists of 472 amino acids, with a prediction of 11 transmembrane domains. When expressed in oocytes, interestingly, Lsi2 did not show influx transport activity for silicic acid but did show efflux transport activity [130], indicating that, unlike Lsi1, the silicon uptake transporter, Lsi2 is a Si efflux transporter capable of transporting Si out of cells (Figure 8.4a). Interestingly, efflux of Si was inhibited at low temperatures and by three protonophores; 2,4-dinitrophenol (DNP), carbonylcyanide 3-chlorophenylhydrazone (CCCP) and carbonylcyanide p-(trifluoromethoxy)phenylhydrazone (FCCP). Furthermore, the efflux activity of Lsi2 was increased at lower external pH values. These results suggest that transport of Si by Lsi2 is an energy dependent active process, which is driven by the proton gradient. Lsi2 is unrelated to the Lsi1 uptake system and is, in fact, a very distant relative of the bacterial ArsB As(OH)₃/H⁺ antiporter. Consistent with its

lineage, Lsi2 is possibly an efflux pump for arsenic [74]. Lsi2 mutants of rice defective in silicon efflux also had lower levels of arsenite in shoots and xylem.

8.3.6 Efflux Systems for Boron

Arabidopsis thaliana AtBOR1 is an efflux system for xylem loading of boron and is essential for preventing boron deficiency in shoots [180]. Six BOR1-like genes are present in *Arabidopsis*. BOR1-like genes have also been found in a number of other plant species, including rice, suggesting the importance of BOR1 and similar genes in plants. A homologous *S. cerevisiae* ORF, YNL275w (BOR1) is responsible for the ability of yeast to maintain a low cellular boron content following incubation for 1 h in medium containing 0.5 mM boric acid [105]. BOR1 deleted strains were more susceptible than wild type strains to growth inhibition by boric acid, and overexpression of BOR1 produced further protection against boric acid toxicity. Recently, Takano *et al.* [181] showed that efflux is slower in the BOR1-deleted yeast strain than in the wild type strain. Bor1p mediates a saturable boron efflux against a concentration gradient, with characteristics consistent with a bicarbonate independent exchange of extracellular H⁺ for intracellular H₃BO₃ [182]. BOR1 mRNA and Bor1p protein are both constitutively expressed in cells grown in rich medium without boron and are increased only slightly during growth in boron concentrations that significantly inhibit growth. Figure 8.4 summarizes current knowledge of the pathways of metalloid uptake into roots, transcellular movement and efflux into xylem.

8.4 Summary and Conclusions

Arsenic is a toxic metalloid that has no known physiological role in any organism. It is ubiquitous in the environment, and, even though cells do not take it up purposefully, arsenic gets into cells adventitiously through transporters for physiological solutes, including phosphate permeases, sugar transporters and aquaglyceroporins. This poses a serious challenge for survival, which is why nearly every organism, from *E. coli* to humans, has evolved mechanisms for arsenic tolerance, in particular efflux pathways that remove arsenic from the cytosol of cells. Members of every kingdom have such systems, although they appear to have arisen at least three times by convergent evolution.

Understanding the types and mechanisms of these uptake and efflux pathways will allow mankind to either restrict or enhance the accumulation of arsenic in cells. Engineering cells with lower uptake or higher rates of efflux can lead to lessened toxicity in individuals exposed to arsenic in the food or water supply. It can produce safer food supplies with lower levels of arsenic. Altering the selectivity of transporters could lead to plants that take up boron or silicon without accumulating arsenic. Increased uptake or decreased efflux can result in more effective chemotherapy with metalloid containing drugs. It will be interesting to see how this knowledge is applied over the next decade.

Acknowledgements

Studies described in this review from the authors' laboratory were supported by National Institutes of Health Grants R37 GM55425 and R01 AI043428.

References

1. Agency for Toxic Substances and Disease Registry (2007) 2007 CERCLA Priority List of Hazardous Substances, <http://www.atsdr.cdc.gov/cercla/07list.html> (accessed 4 August 2010).
2. Bhattacharjee, H. and Rosen, B.P. (2007) *Molecular Microbiology of Heavy Metals* (eds D.H.S. Nies and S. Silver) Springer-Verlag, Heidelberg/New York, pp. 371–406.
3. British Geological Survey and Mott MacDonald (2002) Phase I, Groundwater Studies of Arsenic Contamination in Bangladesh, <http://bicon.com/acic/resources/infobank/bgs-mmi/risumm.htm> (accessed 4 August 2010).
4. Abernathy, C.O., Thomas, D.J., and Calderon, R.L. (2003) *The Journal of Nutrition*, **133**, 1536S–1538S.
5. Beane Freeman, L.E., Dennis, L.K., Lynch, C.F. *et al.* (2004) *American Journal of Epidemiology*, **160**, 679–687.
6. Williams, P.N., Raab, A., Feldmann, J., and Meharg, A.A. (2007) *Environmental Science & Technology*, **41**, 2178–2183.
7. Kwong, Y.L. and Todd, D. (1997) *Blood*, **89**, 3487–3488.
8. Stull, D.M. (2002) *Journal of Pharmacy Practice*, **15**, 62–74.
9. Carter, N.S. and Fairlamb, A.H. (1993) *Nature*, **361**, 173–176.
10. Rosen, B.P. and Liu, Z. (2009) *Environment International*, **35**, 512–515.
11. Dixon, H.B.F. (1997) *Advances in Inorganic Chemistry*, **44**, 191–227.
12. Kenney, L.J. and Kaplan, J.H. (1988) *The Journal of Biological Chemistry*, **263**, 7954–7960.
13. Delnomdedieu, M., Basti, M.M., Otvos, J.D., and Thomas, D.J. (1994) *Chemico-Biological Interactions*, **90**, 139–155.
14. Gebel, T. (1997) *Chemico-Biological Interactions*, **107**, 131–144.
15. Rosenberg, H., Gerdes, R.G., and Chegwidien, K. (1977) *Journal of Bacteriology*, **131**, 505–511.
16. Willsky, G.R. and Malamy, M.H. (1980) *Journal of Bacteriology*, **144**, 356–365.
17. Bun-ya, M., Shikata, K., Nakade, S. *et al.* (1996) *Current Genetics*, **29**, 344–351.
18. Villa-Bellostá, R. and Sorribas, V. (2008) *Toxicology and Applied Pharmacology*, **232**, 125–134.
19. Tamaki, S. and Frankenberger, W.J. (1992) *Reviews of Environmental Contamination & Toxicology*, **124**, 79–110.
20. Meharg, A. and Macnair, M. (1992) *Journal of Experimental Botany*, **43**, 519–524.
21. Bleeker, P.M., Schat, H., Vooijs, R. *et al.* (2003) *The New Phytologist*, **157**, 33–38.
22. Catarecha, P., Segura, M.D., Franco-Zorrilla, J.M. *et al.* (2007) *The Plant Cell*, **19**, 1123–1133.
23. Baes, C.F. and Mesmer, R.E. (1976) *The Hydrolysis of Cations*, John Wiley & Sons, Inc., New York, pp. 370–375.
24. Tschan, M., Robinson, B., and Schulin, R. (2008) *Environmental Geochemistry and Health*, **30**, 187–191.
25. Scott, N., Hatlelid, K.M., MacKenzie, N.E., and Carter, D.E. (1993) *Chemical Research in Toxicology*, **6**, 102–106.
26. Sweet, G., Gandor, C., Voegelé, R. *et al.* (1990) *Journal of Bacteriology*, **172**, 424–430.
27. Sanders, O.I., Rensing, C., Kuroda, M. *et al.* (1997) *Journal of Bacteriology*, **179**, 3365–3367.
28. Meng, Y.L., Liu, Z., and Rosen, B.P. (2004) *The Journal of Biological Chemistry*, **279**, 18334–18341.
29. Agre, P., King, L.S., Yasui, M. *et al.* (2002) *The Journal of Physiology*, **542**, 3–16.
30. Borgnia, M., Nielsen, S., Engel, A., and Agre, P. (1999) *Annual Review of Biochemistry*, **68**, 425–458.
31. Gonen, T., Sliz, P., Kistler, J. *et al.* (2004) *Nature*, **429**, 193–197.
32. Sui, H., Han, B.G., Lee, J.K. *et al.* (2001) *Nature*, **414**, 872–878.
33. Fu, D., Libson, A., Miercke, L.J. *et al.* (2000) *Science*, **290**, 481–486.
34. Törnroth-Horsefield, S., Wang, Y., Hedfalk, K. *et al.* (2006) *Nature*, **439**, 688–694.
35. Lee, J.K., Kozono, D., Remis, J. *et al.* (2005) *Proceedings of the National Academy of Sciences of the United States of America*, **102**, 18932–18937.

36. Jung, J.S., Preston, G.M., Smith, B.L. *et al.* (1994) *The Journal of Biological Chemistry*, **269**, 14648–14654.
37. Beitz, E., Wu, B., Holm, L.M. *et al.* (2006) *Proceedings of the National Academy of Sciences of the United States of America*, **103**, 269–274.
38. Wang, Y., Schulten, K., and Tajkhorshid, E. (2005) *Structure (London, England: 1993)*, **13**, 1107–1118.
39. Porquet, A. and Filella, M. (2007) *Chemical Research in Toxicology*, **20**, 1269–1276.
40. Wysocki, R., Chery, C.C., Wawrzycka, D. *et al.* (2001) *Molecular Microbiology*, **40**, 1391–1401.
41. Liu, Z., Shen, J., Carbrey, J.M. *et al.* (2002) *Proceedings of the National Academy of Sciences of the United States of America*, **99**, 6053–6058.
42. Luyten, K., Albertyn, J., Skibbe, W.F. *et al.* (1995) *The EMBO Journal*, **14**, 1360–1371.
43. Thorsen, M., Di, Y., Tangemo, C. *et al.* (2006) *Molecular Biology of the Cell*, **17**, 4400–4410.
44. Hara-Chikuma, M. and Verkman, A.S. (2006) *Cellular and Molecular Life Sciences*, **63**, 1386–1392.
45. Liu, Z., Carbrey, J.M., Agre, P., and Rosen, B.P. (2004) *Biochemical and Biophysical Research Communications*, **316**, 1178–1185.
46. Lee, T.C., Ho, I.C., Lu, W.J., and Huang, J.D. (2006) *The Journal of Biological Chemistry*, **281**, 18401–18407.
47. Tsukaguchi, H., Shayakul, C., Berger, U.V. *et al.* (1998) *The Journal of Biological Chemistry*, **273**, 24737–24743.
48. Styblo, M., Drobna, Z., Jaspers, I. *et al.* (2002) *Environmental Health Perspectives*, **110** (Suppl 5), 767–771.
49. Kala, S.V., Neely, M.W., Kala, G. *et al.* (2000) *The Journal of Biological Chemistry*, **275**, 33404–33408.
50. Liu, Z., Styblo, M., and Rosen, B.P. (2006) *Environmental Health Perspectives*, **114**, 527–531.
51. Carbrey, J.M., Gorelick-Feldman, D.A., Kozono, D. *et al.* (2003) *Proceedings of the National Academy of Sciences of the United States of America*, **100**, 2945–2950.
52. Ramírez-Solis, A., Mukopadhyay, R., Rosen, B.P., and Stemmler, T.L. (2004) *Inorganic Chemistry*, **43**, 2954–2959.
53. Mushak, P. and Crocetti, A.F. (1995) *Environmental Health Perspectives*, **103**, 684–689.
54. Chappell, W.R., Beck, B.D., Brown, K.G. *et al.* (1997) *Environmental Health Perspectives*, **105**, 1060–1067.
55. Li, L., Li, S., Tao, Y., and Kitagawa, Y. (2000) *Plant Science (Shannon, Ireland)*, **154**, 43–51.
56. Meharg, A.A. and Rahman, M.M. (2003) *Environmental Science & Technology*, **37**, 229–234.
57. Sakurai, J., Ishikawa, F., Yamaguchi, T. *et al.* (2005) *Plant & Cell Physiology*, **46**, 1568–1577.
58. Quigley, F., Rosenberg, J.M., Shachar-Hill, Y., and Bohnert, H.J. (2002) *Genome Biology*, **3**, research0001.1-17.
59. Chaumont, F., Barrieu, F., Wojcik, E. *et al.* (2001) *Plant Physiology*, **125**, 1206–1215.
60. Zardoya, R. (2005) *Biology of the Cell/Under the Auspices of the European Cell Biology Organization*, **97**, 397–414.
61. Gustavsson, S., Lebrun, A.S., Norden, K. *et al.* (2005) *Plant Physiology*, **139**, 287–295.
62. Danielson, J.Å. and Johanson, U. (2008) *BMC Plant Biology*, **8**, 45.
63. Jahn, T.P., Moller, A.L., Zeuthen, T. *et al.* (2004) *FEBS Letters*, **574**, 31–36.
64. Loque, D., Ludewig, U., Yuan, L., and von Wiren, N. (2005) *Plant Physiology*, **137**, 671–680.
65. Wallace, I.S. and Roberts, D.M. (2005) *Biochemistry*, **44**, 16826–16834.
66. Uehlein, N., Fileschi, K., Eckert, M. *et al.* (2007) *Phytochemistry*, **68**, 122–129.
67. Choi, W.G. and Roberts, D.M. (2007) *The Journal of Biological Chemistry*, **282**, 24209–24218.
68. Takano, J., Wada, M., Ludewig, U. *et al.* (2006) *The Plant Cell*, **18**, 1498–1509.
69. Ma, J.F., Tamai, K., Yamaji, N. *et al.* (2006) *Nature*, **440**, 688–691.
70. Ishikawa, F., Suga, S., Uemura, T. *et al.* (2005) *FEBS Letters*, **579**, 5814–5820.
71. Uehlein, N., Lovisolò, C., Siefritz, F., and Kaldenhoff, R. (2003) *Nature*, **425**, 734–737.
72. Bansal, A. and Sankaramakrishnan, R. (2007) *BMC Structural Biology*, **7**, 27–43.
73. Bienert, G.P., Thorsen, M., Schussler, M.D. *et al.* (2008) *BMC Biology*, **6**, 26.

74. Ma, J.F., Yamaji, N., Mitani, N. *et al.* (2008) *Proceedings of the National Academy of Sciences of the United States of America*, **105**, 9931–9935.
75. Isayenkov, S.V. and Maathuis, F.J. (2008) *FEBS Letters*, **582**, 1625–1628.
76. Mitani, N., Yamaji, N., and Ma, J.F. (2008) *The Plant Cell*, **20**, 1381–1389.
77. Wallace, I.S., Choi, W.G., and Roberts, D.M. (2006) *Biochimica et Biophysica Acta*, **1758**, 1165–1175.
78. Wallace, I.S. and Roberts, D.M. (2004) *Plant Physiology*, **135**, 1059–1068.
79. Bhattacharjee, H., Mukhopadhyay, R., Thiyagarajan, S., and Rosen, B.P. (2008) *Journal of Biology*, **7**, 33–38.
80. Uzcategui, N.L., Zhou, Y., Figarella, K. *et al.* (2008) *Molecular Microbiology*, **70**, 1477–1486.
81. Zhu, Y.G. and Rosen, B.P. (2009) *Current Opinion in Biotechnology*, **20**, 220–224.
82. Liu, Z., Boles, E., and Rosen, B.P. (2004) *The Journal of Biological Chemistry*, **279**, 17312–17318.
83. Marger, M.D. and Saier, M.H. Jr. (1993) *Trends in Biochemical Sciences*, **18**, 13–20.
84. Boles, E. and Hollenberg, C.P. (1997) *FEMS Microbiology Reviews*, **21**, 85–111.
85. Liu, Z., Sanchez, M.A., Jiang, X. *et al.* (2006) *Biochemical and Biophysical Research Communications*, **351**, 424–430.
86. Vannucci, S.J., Maher, F., and Simpson, I.A. (1997) *Glia*, **21**, 2–21.
87. Fischbarg, J., Kuang, K.Y., Vera, J.C. *et al.* (1990) *Proceedings of the National Academy of Sciences of the United States of America*, **87**, 3244–3247.
88. Iserovich, P., Wang, D., Ma, L. *et al.* (2002) *The Journal of Biological Chemistry*, **277**, 30991–30997.
89. Jiang, X., McDermott, J.R., Abdul Ajees, A. *et al.* (2010) *Metallomics*, **2**, 211–219.
90. Tanaka, M. and Fujiwara, T. (2008) *Pflugers Archiv: European Journal of Physiology*, **456**, 671–677.
91. Marschner, H. (1995) *Mineral Nutrition of Higher Plants*, 2nd edn, Academic Press, San Diego, CA.
92. Takano, J., Miwa, K., and Fujiwara, T. (2008) *Trends in Plant Science*, **13**, 451–457.
93. O'Neill, M.A., Ishii, T., Albersheim, P., and Darvill, A.G. (2004) *Annual Review of Plant Biology*, **55**, 109–139.
94. O'Neill, M.A., Eberhard, S., Albersheim, P., and Darvill, A.G. (2001) *Science*, **294**, 846–849.
95. Nable, R.O., Banuelos, G.S., and Paull, J.G. (1997) *Plant and Soil*, **193**, 181–198.
96. Dordas, C., Chrispeels, M.J., and Brown, P.H. (2000) *Plant Physiology*, **124**, 1349–1362.
97. Barone, L.M., Shih, C., and Wasserman, B.P. (1997) *The Journal of Biological Chemistry*, **272**, 30672–30677.
98. Dordas, C. and Brown, P.H. (2001) *Biological Trace Element Research*, **81**, 127–139.
99. Nuttall, C. (2000) *PhD Thesis, University of Cambridge, Cambridge, UK*.
100. Hunt, C.D. (1994) *Environmental Health Perspectives*, **102** (Suppl 7), 35–43.
101. Nielsen, F.H. (2000) *Nutrition*, **16**, 512–514.
102. Fort, D.J., Rogers, R.L., McLaughlin, D.W. *et al.* (2002) *Biological Trace Element Research*, **90**, 117–142.
103. Rowe, R.I., Bouzan, C., Nabili, S., and Eckhert, C.D. (1998) *Biological Trace Element Research*, **66**, 261–270.
104. Bennett, A., Rowe, R.I., Soch, N., and Eckhert, C.D. (1999) *The Journal of Nutrition*, **129**, 2236–2238.
105. Nozawa, A., Takano, J., Kobayashi, M. *et al.* (2006) *FEMS Microbiology Letters*, **262**, 216–222.
106. ElBerry, H.M., Majumdar, M.L., Cunningham, T.S. *et al.* (1993) *Journal of Bacteriology*, **175**, 4688–4698.
107. Parker, M.D., Ourmozdi, E.P., and Tanner, M.J. (2001) *Biochemical and Biophysical Research Communications*, **282**, 1103–1109.
108. Park, M., Li, Q., Shcheynikov, N. *et al.* (2004) *Molecular Cell*, **16**, 331–341.
109. Carlisle, E. (1986) *Ciba Foundation Symposium*, **121**, 123–139.
110. Sripanyakorn, S., Jugdaohsingh, R., Thompson, R.P.H., and Powell, J.J. (2005) *Nutrition Bulletin*, **30**, 222–230.

111. Treguer, P., Nelson, D.M., Van Bennekom, A.J. *et al.* (1995) *Science*, **268**, 375–379.
112. Lopez, P.J., Descles, J., Allen, A.E., and Bowler, C. (2005) *Current Opinion in Biotechnology*, **16**, 180–186.
113. Ma, J.F. and Yamaji, N. (2008) *Cellular and Molecular Life Sciences*, **65**, 3049–3057.
114. Epstein, E. (1999) *Annual Review of Plant Physiology and Plant Molecular Biology*, **50**, 641–664.
115. Ma, J.F. (2004) *Soil Science and Plant Nutrition*, **50**, 11–18.
116. Datnoff, L., Deren, C., and Snyder, G. (1997) *Crop Protection (Guildford, Surrey)*, **16**, 525–531.
117. Fauteux, F., Remus-Borel, W., Menzies, J.G., and Belanger, R.R. (2005) *FEMS Microbiology Letters*, **249**, 1–6.
118. Liang, Y., Sun, W., Zhu, Y.G., and Christie, P. (2007) *Environmental Pollution (Barking, Essex: 1987)*, **147**, 422–428.
119. Takahashi, E. and Hino, K. (1978) *Journal of the Science of Soil and Manure, Japan*, **49**, 357–360.
120. Mitani, N. and Ma, J.F. (2005) *Journal of Experimental Botany*, **56**, 1255–1261.
121. Ma, J.F., Tamai, K., Ichii, M., and Wu, G.F. (2002) *Plant Physiology*, **130**, 2111–2117.
122. Ma, J.F., Mitani, N., Nagao, S. *et al.* (2004) *Plant Physiology*, **136**, 3284–3289.
123. Hildebrand, M., Dahlin, K., and Volcani, B.E. (1998) *Molecular & General Genetics*, **260**, 480–486.
124. Hildebrand, M., Volcani, B.E., Gassmann, W., and Schroeder, J.I. (1997) *Nature*, **385**, 688–689.
125. Ma, J.F. (2003) *Fertilizer*, **94**, 26–32.
126. Yamaji, N. and Ma, J.F. (2007) *Plant Physiology*, **143**, 1306–1313.
127. Bienert, G.P., Schussler, M.D., and Jahn, T.P. (2008) *Trends in Biochemical Sciences*, **33**, 20–26.
128. Hose, E., Clarkson, D.T., Steudle, E. *et al.* (2001) *Journal of Experimental Botany*, **52**, 2245–2264.
129. Mitani, N., Yamaji, N., and Ma, J.F. (2008) *Pflügers Archiv: European Journal of Physiology*, **456**, 679–686.
130. Ma, J.F., Yamaji, N., Mitani, N. *et al.* (2007) *Nature*, **448**, 209–212.
131. Takahashi, E., Syo, S., and Miyake, Y. (1976) *Journal of the Science of Soil and Manure, Japan*, **47**, 183–197.
132. Nikolic, M., Nikolic, N., Liang, Y. *et al.* (2007) *Plant Physiology*, **143**, 495–503.
133. Rains, D.W., Epstein, E., Zasoski, R.J., and Aslam, M. (2006) *Plant and Soil*, **280**, 223–228.
134. Cole, S.P., Sparks, K.E., Fraser, K. *et al.* (1994) *Cancer Research*, **54**, 5902–5910.
135. Leier, I., Jedlitschky, G., Buchholz, U. *et al.* (1994) *The Journal of Biological Chemistry*, **269**, 27807–27810.
136. Zaman, G.J., Lankelma, J., van Tellingen, O. *et al.* (1995) *Proceedings of the National Academy of Sciences of the United States of America*, **92**, 7690–7694.
137. Ouellette, M., Fase-Fowler, F., and Borst, P. (1990) *The EMBO Journal*, **9**, 1027–1033.
138. Legare, D., Richard, D., Mukhopadhyay, R. *et al.* (2001) *The Journal of Biological Chemistry*, **276**, 26301–26307.
139. Li, Z.S., Szczyпка, M., Lu, Y.P. *et al.* (1996) *The Journal of Biological Chemistry*, **271**, 6509–6517.
140. Szczyпка, M.S., Wemmie, J.A., Moye-Rowley, W.S., and Thiele, D.J. (1994) *The Journal of Biological Chemistry*, **269**, 22853–22857.
141. Ghosh, M., Shen, J., and Rosen, B.P. (1999) *Proceedings of the National Academy of Sciences of the United States of America*, **96**, 5001–5006.
142. Bobrowicz, P., Wysocki, R., Owsianik, G. *et al.* (1997) *Yeast (Chichester, England)*, **13**, 819–828.
143. Wysocki, R., Bobrowicz, P., and Ulaszewski, S. (1997) *The Journal of Biological Chemistry*, **272**, 30061–30066.
144. Dey, S. and Rosen, B.P. (1995) *Journal of Bacteriology*, **177**, 385–389.
145. Lin, Y.F., Walmsley, A.R., and Rosen, B.P. (2006) *Proceedings of the National Academy of Sciences of the United States of America*, **103**, 15617–15622.

146. Rosen, B.P., Weigel, U., Karkaria, C., and Gangola, P. (1988) *The Journal of Biological Chemistry*, **263**, 3067–3070.
147. Carlin, A., Shi, W., Dey, S., and Rosen, B.P. (1995) *Journal of Bacteriology*, **177**, 981–986.
148. Driessen, A.J., Rosen, B.P., and Konings, W.N. (2000) *Trends in Biochemical Sciences*, **25**, 397–401.
149. Wu, J., Tisa, L.S., and Rosen, B.P. (1992) *The Journal of Biological Chemistry*, **267**, 12570–12576.
150. Rosen, B.P. (2002) *FEBS Letters*, **529**, 86–92.
151. Bhattacharjee, H., Li, J., Ksenzenko, M.Y., and Rosen, B.P. (1995) *The Journal of Biological Chemistry*, **270**, 11245–11250.
152. Dey, S., Dou, D., Tisa, L.S., and Rosen, B.P. (1994) *Archives of Biochemistry and Biophysics*, **311**, 418–424.
153. Kaur, P. and Rosen, B.P. (1992) *The Journal of Biological Chemistry*, **267**, 19272–19277.
154. Karkaria, C.E., Chen, C.M., and Rosen, B.P. (1990) *The Journal of Biological Chemistry*, **265**, 7832–7836.
155. Li, J., Liu, S., and Rosen, B.P. (1996) *The Journal of Biological Chemistry*, **271**, 25247–25252.
156. Zhou, T., Radaev, S., Rosen, B.P., and Gatti, D.L. (2000) *The EMBO Journal*, **19**, 1–8.
157. Hsu, C.M. and Rosen, B.P. (1989) *The Journal of Biological Chemistry*, **264**, 17349–17354.
158. Zhou, T., Liu, S., and Rosen, B.P. (1995) *Biochemistry*, **34**, 13622–13626.
159. Joerger, R.D. and Bishop, P.E. (1988) *Journal of Bacteriology*, **170**, 1475–1487.
160. Story, R.M. and Steitz, T.A. (1992) *Nature*, **355**, 374–376.
161. Pai, E.F., Krengel, U., Petsko, G.A. *et al.* (1990) *The EMBO Journal*, **9**, 2351–2359.
162. Jiang, Y., Bhattacharjee, H., Zhou, T. *et al.* (2005) *The Journal of Biological Chemistry*, **280**, 9921–9926.
163. Bhattacharjee, H. and Rosen, B.P. (1996) *The Journal of Biological Chemistry*, **271**, 24465–24470.
164. Ruan, X., Bhattacharjee, H., and Rosen, B.P. (2008) *Molecular Microbiology*, **67**, 392–402.
165. Zhou, T. and Rosen, B.P. (1997) *The Journal of Biological Chemistry*, **272**, 19731–19737.
166. Bhattacharjee, H. and Rosen, B.P. (2000) *Biomaterials: An International Journal on the Role of Metal Ions in Biology, Biochemistry, and Medicine*, **13**, 281–288.
167. Ramaswamy, S. and Kaur, P. (1998) *The Journal of Biological Chemistry*, **273**, 9243–9248.
168. Li, J. and Rosen, B.P. (2000) *Molecular Microbiology*, **35**, 361–367.
169. Bhattacharjee, H., Ghosh, M., Mukhopadhyay, R., and Rosen, B.P. (1999) *Transport of Molecules Across Microbial Membranes* (eds J.K. Broome-Smith, S. Baumberg, C.J. Sterling, and F.B. Ward) Society for General Microbiology, Leeds, pp. 58–79.
170. Kurdi-Haidar, B., Aebi, S., Heath, D. *et al.* (1996) *Genomics*, **36**, 486–491.
171. Shen, J., Hsu, C.M., Kang, B.K. *et al.* (2003) *Biomaterials: An International Journal on the Role of Metal Ions in Biology, Biochemistry, and Medicine*, **16**, 369–378.
172. Mukhopadhyay, R., Ho, Y.S., Swiatek, P.J. *et al.* (2006) *FEBS Letters*, **580**, 3889–3894.
173. Stefanovic, S. and Hegde, R.S. (2007) *Cell*, **128**, 1147–1159.
174. Achour, A.R., Bauda, P., and Billard, P. (2007) *Research in Microbiology*, **158**, 128–137.
175. Mansour, N.M., Sawhney, M., Tamang, D.G. *et al.* (2007) *FEBS Journal*, **274**, 612–629.
176. Sato, T. and Kobayashi, Y. (1998) *Journal of Bacteriology*, **180**, 1655–1661.
177. Aaltonen, E.K. and Silow, M. (2008) *Biochimica et Biophysica Acta*, **1778**, 963–973.
178. Xia, X., Postis, V.L., Rahman, M. *et al.* (2008) *Molecular Membrane Biology*, **25**, 691–705.
179. Fu, H.L., Meng, Y., Ordenez, E. *et al.* (2009) *The Journal of Biological Chemistry*, **284**, 19887–19895.
180. Takano, J., Miwa, K., Yuan, L. *et al.* (2005) *Proceedings of the National Academy of Sciences of the United States of America*, **102**, 12276–12281.
181. Takano, J., Kobayashi, M., Noda, Y., and Fujiwara, T. (2007) *FEMS Microbiology Letters*, **267**, 230–235.
182. Jennings, M.L., Howren, T.R., Cui, J. *et al.* (2007) *American Journal of Physiology. Cell Physiology*, **293**, C468–C476.

9

Bismuth Complexes of Porphyrins and their Potential in Medical Applications

Bernard Boitrel

*UMR CNRS 6226, Sciences Chimiques de Rennes, (I.C.M.V.), Université de Rennes 1,
35042 Rennes Cedex, France*

9.1 Introduction

In the past, the major medical application of bismuth consisted of the treatment of gastric ulcers by ingestion of large quantities of bismuth citrate. More recently, the resurgence of interest for bismuth medical applications has been more oriented towards possible applications in radiotherapy, and particularly in alpha-radioimmunotherapy (Figure 9.1) [1]. As this specific application will be reviewed exhaustively in Chapter 13 of this book, we will only discuss the design, synthesis and coordination properties of bismuth porphyrin complexes in this chapter, assuming that the goals and limits of this peculiar application are known. However, we should keep in mind that both alpha-emitter isotopes of bismuth-212 and 213 exhibit a very short half life of 60 and 45 min respectively, as this radiochemical property directly implies fast kinetics formation of complexes. Even if this potential application is far from being achieved, this very basic requirement will guide the research for new bismuth porphyrins.

From the coordination point of view, porphyrins are known to coordinate most of the metallic and pseudometallic elements, and metalloporphyrins with over 80 different central

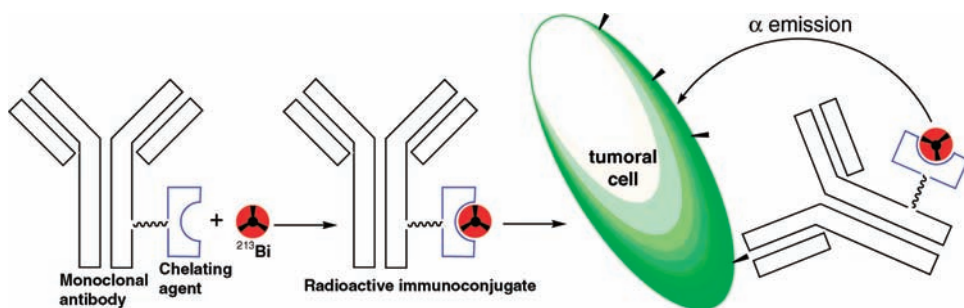


Figure 9.1 Schematic representation of α -radioimmunotherapy via targeting with a monoclonal antibody.

metals have been isolated and characterized [2]. However, despite the large number of isolated metalloporphyrin derivatives, few solid state structures of bismuth porphyrins have been published so far and the coordination chemistry and reactivity of bismuth porphyrins remain a relatively unexplored area. Also, considering practical applications of such molecules, medical implications arise if porphyrins – or macrocycles in general – can be localized in specific areas of the body. This particular field is in permanent progress with the use of specific monoclonal antibodies for which both the immunochemistry and the specificity can be tuned [3]. Thus, for our purpose, we will consider that in the future, specific and efficient targeting of metalloid chelates will be available.

9.2 Early Work (1969–1994)

The very first instances of group 15 (As, Sb, Bi) porphyrin complexes were published as recently as 1969 and 1974 by Treibs *et al.* [4] and Buchler *et al.* [5] respectively. In these works, bismuth was inserted in octaethylporphyrin (OEPH₂) by refluxing the macrocycle in pyridine at 120 °C for 30 min. Although the resulting complexes were fully characterized by proton NMR and electronic spectroscopies as well as mass spectrometry, the intimate structure of the complex remained unknown although an out-of-plane coordination of the metal was suspected. Actually, this structural feature is expected for a large cation such as bismuth which exhibits a covalent radius of 1.5 Å where the radius of the porphyrin cavity is close to 2 Å.

UV visible spectroscopy is a powerful tool in porphyrin chemistry and this is particularly true for bismuth porphyrins. Whereas usual porphyrin spectra exhibit a Soret band around 420 nm and four Q bands ranging chiefly from 500–700 nm, bismuth porphyrins show a hyper spectrum with the Soret band at 470 nm. This hyper p type of spectrum has been discussed by Gouterman *et al.* [6]. It is characterized by two Soret bands around 350 and 470 nm and two weaker bands further to the red around 600 and 650 nm. The extra Soret band at 350 nm was attributed to the presence of an allowed $6p_z$ (bismuth) $\rightarrow \pi^*$ (porphyrin) charge transfer transition in the visible near UV region.

Ten years later, in 1992, a definitive proof of the out-of-plane coordination was reported with the study of a bismuth complex of meso-tetra-tolylporphyrin (TTP). Using the same

procedure as previous research, the nitrate-bismuth porphyrin was characterized by elemental analysis and studied by variable temperature ^1H NMR spectroscopy. When the spectrum was recorded at 255 K, the four *p*-tolyl protons appeared as four doublets instead of two doublets in the free base ligand, indicating that the plane of the porphyrin was no longer a plane of symmetry and hence that the bismuth cation was out of the macrocycle plane.

Interestingly enough, the first water soluble adduct, bismuth(III) tetrakis-(*N*-methyl-3-pyridyl)porphyrin was synthesized in 1994 [7]. It was demonstrated that whereas the removal of bismuth from the macrocycle is, as expected, catalysed by protons, major anion and hydroxide contributions are also present. It is important to note that this property of base solvolysis can have important consequences in terms of stability of the complex during therapeutic applications or even during the metalation process.

9.3 Bismuth Complexes of Unfunctionalized Porphyrins

In this paragraph, the word ‘unfunctionalized’ is intended to describe porphyrins that are substituted only by inert alkyl or aryl groups in the eight β -pyrrolic or four meso positions, respectively.

9.3.1 The First X-ray Structure of $(\text{OEP})\text{Bi}(\text{SO}_3\text{CF}_3)$

The first solid state structure of a bismuth porphyrin was reported by Guilard, Kadisk *et al.* in 2000 [8]. In this work, either bismuth nitrate or bismuth triflate was used. The bismuth salt was refluxed in DMF with the free base porphyrin for 75 min. In the solid state, $(\text{OEP})\text{Bi}(\text{SO}_3\text{CF}_3)$ is a dimer (Figure 9.2) with the two entities symmetrically related by an inversion center. The two triflate molecules act as bridging counter anions between the two bismuth atoms, either as a monodentate ligand or as a bidentate ligand.

Bismuth is a seven coordinate and located 1.07(1) Å above the four-nitrogen plane towards the triflate anions. Finally, taking into account the coordination sphere of bismuth in this complex, the bismuth lone pair position should be parallel to the N(1)-N(3) axis in order to minimize electrostatic repulsion with the triflate anions. Unlike the other Group 15 elements, the Bi(III) in a porphyrin cannot be electrochemically oxidized at the metal center.

9.3.2 Other X-ray Structures with Tetra-Mesoaryl Porphyrin: $\text{Bi}(\text{tpClpp})\text{NO}_3$ and $\text{Bi}(\text{tpClpp})\text{Br}$

Two interesting structures were solved by Brothers *et al.* in 2003 by crystallizing two bismuth complexes of meso-tetrakis-*p*-chlorophenyl-porphyrin (*tpClpp*) [9]. These two structures are important as they point out the important influence of the counter anion on the structure itself. For instance, using bismuth nitrate, the first noncentrosymmetric dimer was obtained with two nitrate residues as the counter anions of both bismuth cations (Figure 9.3a). But where one of them (N(9)) coordinates Bi(1) in the usual bidentate fashion through O(1) and O(2), the second nitrate group (N(10)) bridges between the two bismuth atoms through two oxygen atoms O(6) and O(5). Additionally, the third oxygen atom of the second nitrate group, O(4) interacts with both bismuth atoms with longer Bi-distances.

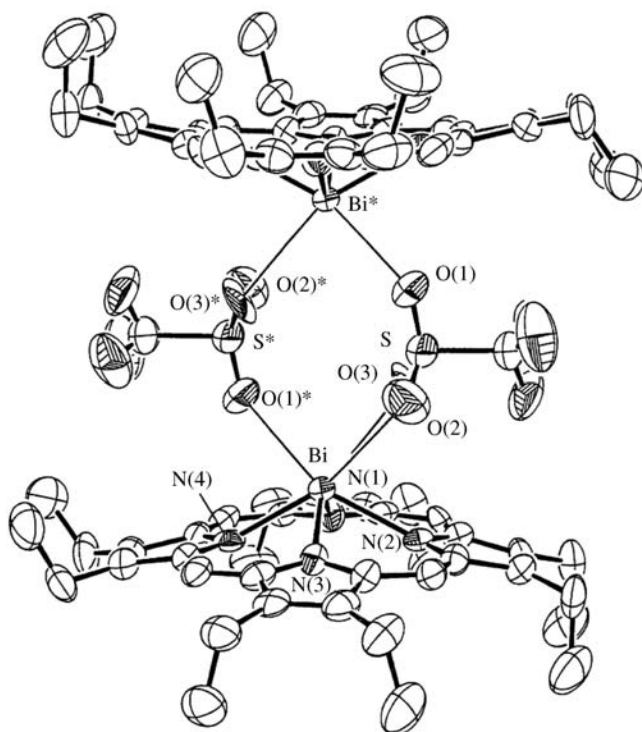


Figure 9.2 X-ray structure of $(\text{OEP})\text{Bi}(\text{SO}_3\text{CF}_3)$. Reprinted with permission from [8]. Copyright (2000) Society of Porphyrins & Phthalocyanines

These Bi-O distances are all very long when compared to other bismuth complexes containing nitrate ligands, as we will see.

At the opposite, the halide complexes (Cl, Br and I) of this bismuth complex all crystallize as centrosymmetric dimers with two μ -bridging halides (Figure 9.3b). The bridging halide groups are staggered with respect to the porphyrin nitrogen atoms, giving distorted trigonal prismatic geometry around each bismuth atom.

These data indicate that the dinuclear arrangement observed for all the above mentioned structures is the result of first, the out-of-plane bismuth coordination leading to electrostatic effects and second, its tendency to increase its coordination number (up to eight in a porphyrin).

9.4 Bismuth Complexes of Functionalized Porphyrins

In coordination chemistry, an important ligand property that increases metal complex stability is preorganization, the tendency of the free ligand to assume the conformation necessary for metal ion complexation. Additionally, bismuth is both azophylic and oxophylic, with a coordination number (CN) that ranges from three to 10. It was thus reasonable to investigate the coordination property of pendant arms porphyrins bearing

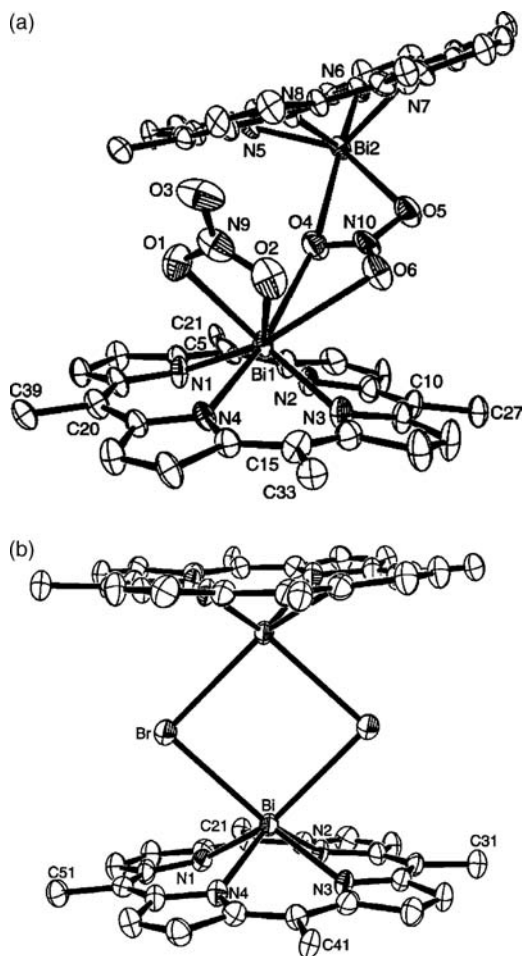
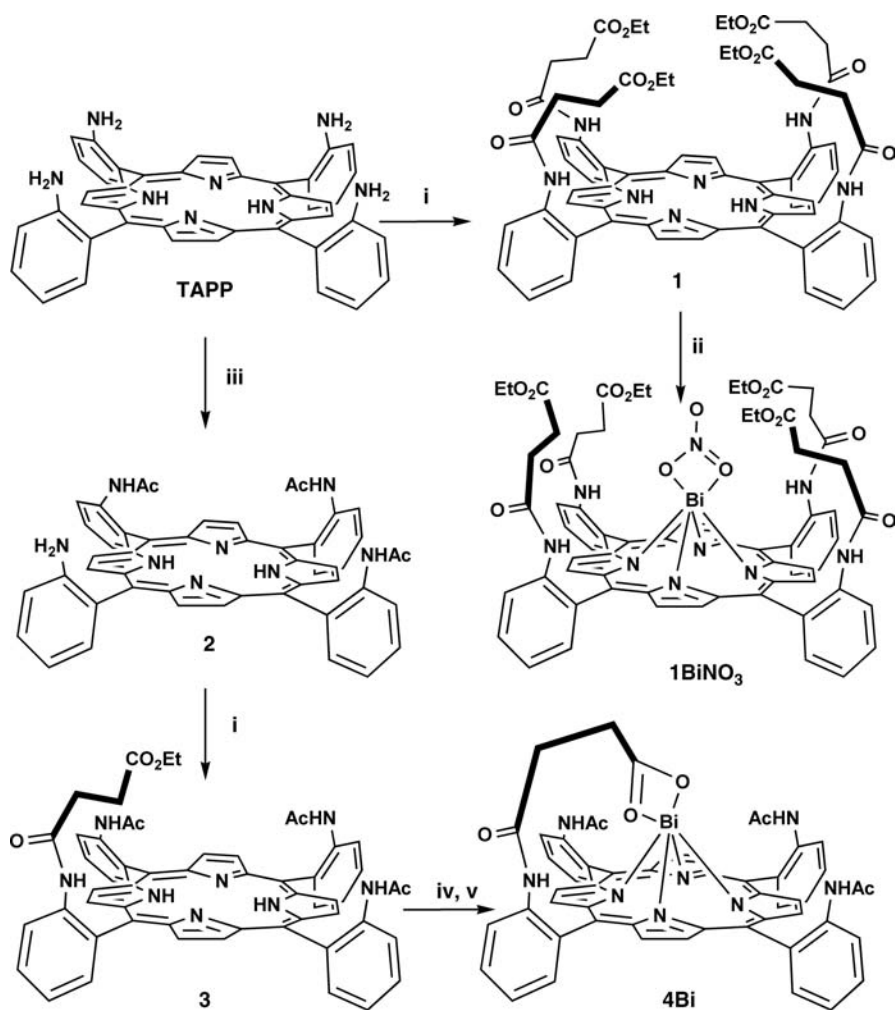


Figure 9.3 X-ray structures of (a) $\text{Bi}(\text{tpClpp})\text{NO}_3$ and (b) $\text{Bi}(\text{tpClpp})\text{Br}$. Aryl rings are omitted for clarity. Reproduced from [9] by permission of The Royal Society of Chemistry

potential oxygen atom donors, analogous of DOTA like compounds. But a major difference with the latter consists of the possible preorganization of the picket(s) if attached on the ortho position of the meso aromatic rings.

9.4.1 Picket Porphyrins

For instance, an easy raw material porphyrin is meso-tetrakis-2-aminophenyl porphyrin (TAPP), which can be acylated by any acyl chloride, leading to four picket porphyrin (Scheme 9.1). Actually, TAPP exists as a mixture of four atropisomers at room temperature and up to 50°C , and so do most of picket porphyrins synthesized from TAPP. Scheme 9.1 indicates the reaction of ethyl succinyl acyl chloride (i) on



Scheme 9.1 Synthetic pathway for the preparation of succinylamido pickets porphyrins. Reagents and conditions: (i) $\text{ClCO}(\text{CH}_2)_2\text{CO}_2\text{Et}$ (5 MM equivalent for **1** or 1.1 MM equivalent for **3**), NEt_3 , THF; (ii) $\text{Bi}(\text{NO}_3)_3 \cdot 5\text{H}_2\text{O}$ (10 M equivalent), 55°C , pyridine, 2 h; (iii) CH_3COCl (3 MM equivalent), NEt_3 , THF; (iv) KOH , EtOH, 55°C f **4**; (v) $\text{Bi}(\text{NO}_3)_3 \cdot 5\text{H}_2\text{O}$ (1.2 M equivalent), rt, pyridine, 10 min. (Reproduced with permission from The American Chemical Society. Copyright © 2004 The American Chemical Society)

TAPP $\alpha\alpha\alpha\alpha$ atropisomer – with the four anilino groups oriented towards the same side – followed by bismuth insertion (ii) with bismuth nitrate.

Thus, with porphyrin **1**, bismuth insertion was achieved under mild conditions by heating a solution of the ligand in pyridine at 50°C over two hours with the bismuth salt and led to **1BiNO₃**. Completion of the reaction was easily monitored by UV visible spectroscopy with the absorption of the bismuth porphyrin at 470 nm (Figure 9.4) [10]. Indeed, in opposition

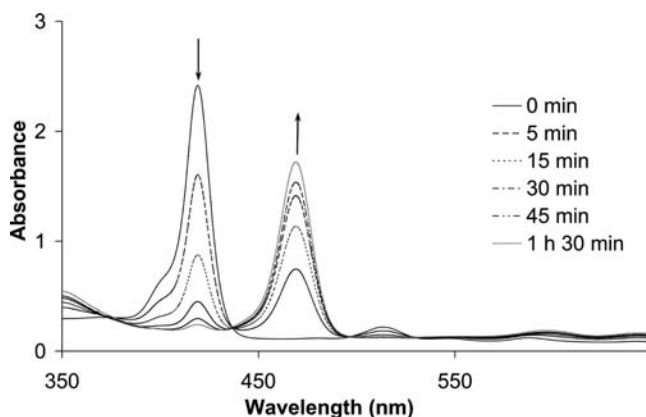


Figure 9.4 UV visible spectra of porphyrin **1** upon addition of bismuth at different time. Note that the appearance of the absorption at 479 nm is characteristic for bismuth insertion in porphyrin **1**. Reproduced from [11] by permission of The Royal Society of Chemistry

to unfunctionalized porphyrins as $(\text{OEP})\text{BiSO}_3\text{CF}_3$, the chromatography process of compound **1BiNO₃** does not afford any free base analogue.

Crystals suitable for X-ray study were obtained by a slow diffusion of a $\text{H}_2\text{O}/\text{MeOH}$ mixture onto a saturated THF solution of **1BiNO₃**. The ORTEP [11] plot of the X-ray structure is shown in Figure 9.5. The Bi(III) is eight coordinate with an approximate square

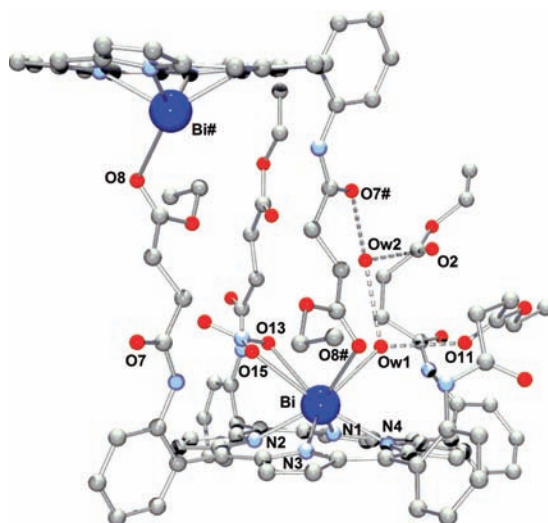


Figure 9.5 Ball and stick representation of the crystal structure of **1BiNO₃**. Reprinted with permission from [17]. Copyright 2004 American Chemical Society

antiprismatic geometry. The four nitrogen atoms of the macrocycle form a square, the distorted other square being formed by four oxygen atoms described as follows: two oxygen atoms of the nitrate anion, the oxygen atom of a water molecule and a carbonyl oxygen atom of the terminal ester group belonging to an arm attached to a symmetrically related macrocycle, forming in this way, a centrosymmetric dimer in the solid state. The Bi atom lies 1.125 Å above the four nitrogen plane and the mean Bi-N bond length is 2.34(2) Å, these values are similar to those observed in (OEP)Bi(SO₃CF₃) which also adopts a centrosymmetric dimeric form ($\Delta 4N = 1.07$ Å and $\langle \text{Bi-N} \rangle = 2.31(1)$ Å).

The Bi-O bond lengths are larger than the sum of their ionic radii ($1.13 + 1.40 = 2.53$ Å) [12] 2.706(5) and 2.789(4) Å for the bonds with the nitrate anion (respectively with O13 and O15), 2.816(5) Å with the oxygen of the water molecule (Ow1) and 3.018(5) Å with the oxygen atom of the carbonyl group (O8#). This later value is large but, to the best of our knowledge, this type of bond between a Bi atom and an ethoxycarbonyl group is unprecedented, however such a large distance is observed in the (OEP)Bi(SO₃CF₃) dimer where a Bi-O distance of 2.98(2) Å was found between the Bi atom and a triflate oxygen atom. A second water molecule (Ow2) is present in the cage and as shown in Figure 9.5, both water molecules are engaged in an intra- and intermolecular hydrogen bond net, contributing to the stability of the dimer, in which the counter anion is not bridging the two porphyrin units as in the previously reported complexes of unfunctionalized porphyrins. One arm of the molecule does not participate in any interaction and thus exhibits a regular conformation. As reported above, one arm participates to the coordination sphere of the Bi atom - belonging to the second molecule of the dimer - and the two remaining arms involved in the hydrogen bond net with Ow1 and Ow2, adopt folded conformations. Even if this ester picket porphyrin cannot be applied in therapy due to the too long time required for the metalation, the positive effect of the four pickets should be noted.

Thus, a rational evolution of this ester picket porphyrin consists of the synthesis of acidic picket porphyrins which are obviously obtained by saponification of the former ligand. The synthesis of such a porphyrin is also depicted in Scheme 9.1 for porphyrin **4Bi** bearing only one acidic picket but actually, all the possible porphyrins bearing either one, two, three or four acidic pickets were also studied. In the case of **4Bi** for which an X-ray structure was resolved, it turned out that the metalation was achieved at room temperature in only 10 minutes, and therefore, these conditions become plausible with an eventual use in alpha-radioimmunotherapy. However, the most striking difference with all bismuth porphyrins reported to date, for which X-ray data were obtained, is the mononuclear structure with the counter anion delivered by the unique arm of **4Bi** (Figure 9.6) [13]. Indeed, the two oxygen atoms of the carboxylate group (O4 and O5) bound to the metal center are stabilized by two hydrogen bonds with the neighboring nitrogen from the amide linkage, N7 and N8 respectively. The two other coordination sites are occupied by two water molecules (O7 and O8), the bismuth being eight-coordinate and lying 1.145 Å above the N4 plane.

The mean Bi-N bond length is 2.343(2) Å, the same value as 2.340(2) Å in **1BiNO₃**. The two coordinated water molecules are also included in a hydrogen bonding net. The first one, O7 is hydrogen bonded to O5 from the carboxylate group and to N5 from an acetamide residue. The second one, O8 is hydrogen bonded to N10 of a solvated pyridine molecule and to another water molecule (O9) itself hydrogen bonded to N6, also from an acetamide residue. The bismuth atom is coordinated in a distorted antiprismatic geometry as shown in Figure 9.7b. This distortion is particularly appreciable with the O7-Bi-O8 and O4-Bi-O8

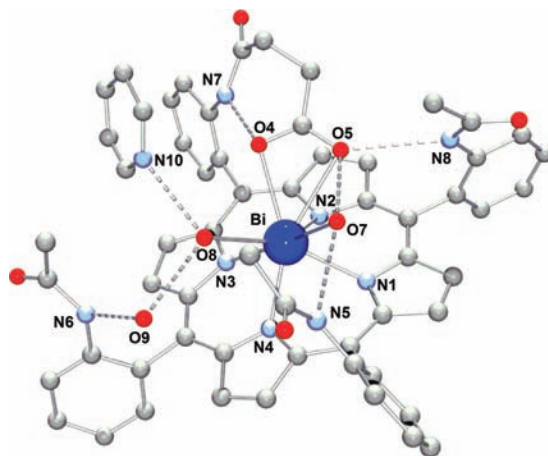


Figure 9.6 Ball and stick representation of the crystal structure of **4Bi**. Reprinted with permission from [17]. Copyright 2004 American Chemical Society

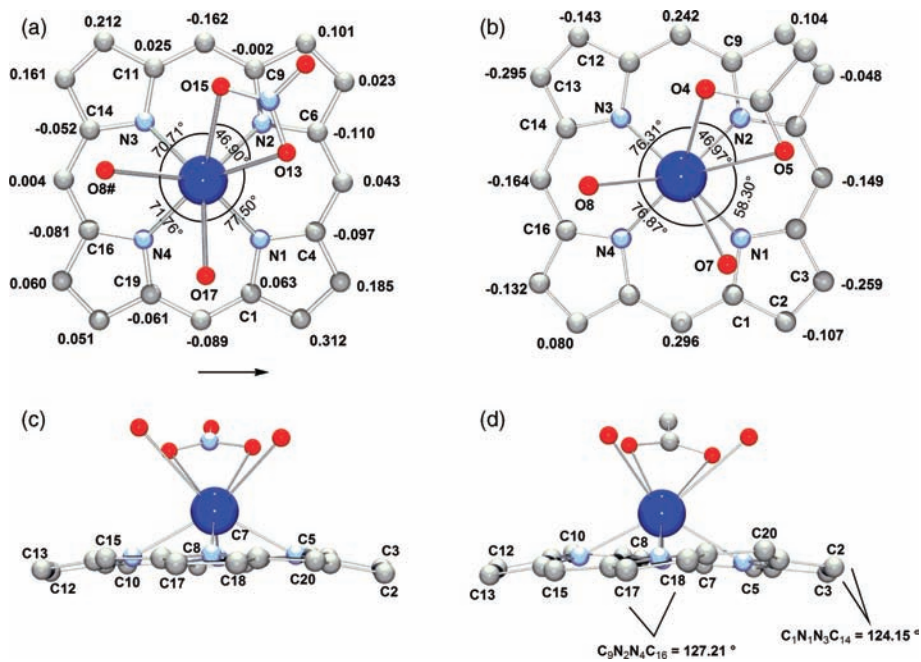


Figure 9.7 Ball and stick polyhedron coordination top views of (a) **1BiNO₃** and (b) **4Bi** and side views of (c) **1BiNO₃** and (d) **4Bi**. All the deviations refer to the mean porphyrin plane. Reprinted with permission from [17]. Copyright 2004 American Chemical Society

angles which are 76.87° and 76.31° respectively, where the O4–Bi–O5 and O5–Bi–O7 are 46.97° and 58.30° . It is reasonable to correlate this distortion to the deformation of the porphyrin plane which adopts a ‘saddle shaped’ and ruffled conformation (Figure 9.7d). To the best of our knowledge, this type of deformation of the macrocycle has never been reported for bismuth porphyrins. Indeed, the carbon atoms in the opposite meso positions (C5, C15 and C10, C20) are not located in the 24-atom least-squares plane but above or below. More precisely, the deviations (Cm) from the mean porphyrin plane of the four meso carbons are 0.297, -0.150 , 0.243 and -0.164 Å, leading to an average value of 0.213 Å, smaller than that observed for highly distorted nickel porphyrins. Furthermore, the dihedral angles between the two opposite pyrrole planes, e.g. C7–C8 and C17–C18 or C2–C3 and C12–C13 are 15.5° and 12.8° respectively. These two major distortions seem to be the result of a too short length of the coordinating arm as the latter has to pull the meso carbon on which it is tethered to be able to coordinate the metal.

For comparison purposes from the coordination point of view, Figure 9.7 summarizes both the coordination polyhedron of bismuth and the distortion of the porphyrin core in **1BiNO₃** (Figure 9.7a and c) and **4Bi** (Figure 9.7b and d). In both structures, the bismuth cation is largely displaced out of the N₄ plane of the porphyrin, 1.125 and 1.145 Å in **1BiNO₃** and **4Bi** respectively. In the binuclear structure of **1BiNO₃**, the intermetallic distance is 10.61 Å. In terms of therapeutic applications, and so in aqueous medium, if this binuclear edifice was maintained, it would be possible to deliver not one but two radioactive nuclei per complex. This would represent a simple and efficient method to directly increase the amount of alpha particles around the targeted cells.

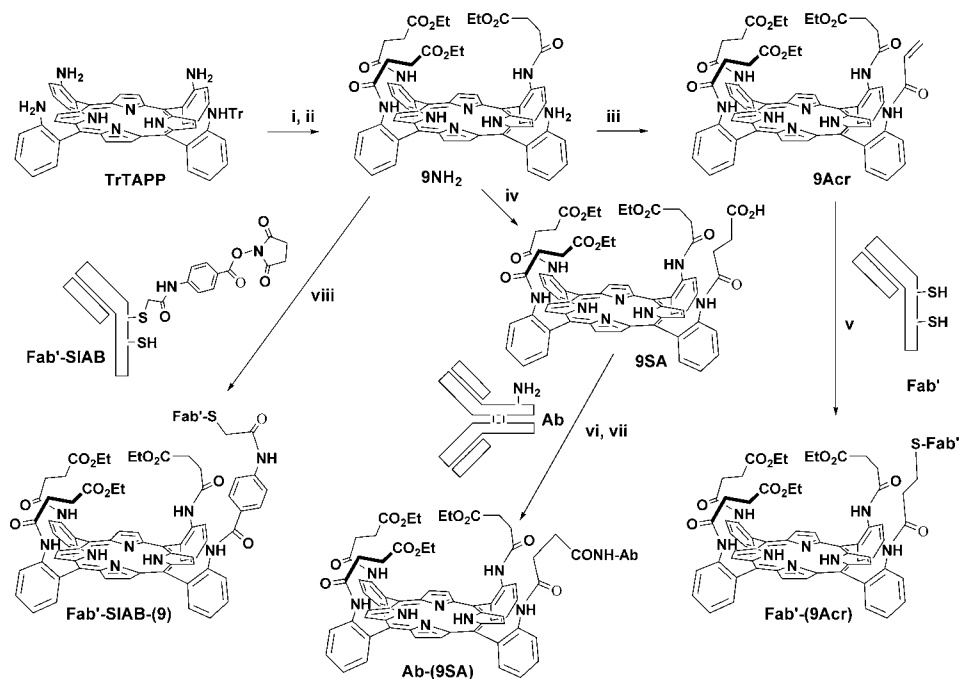
Two other significant differences between these two complexes are also exhibited in Figure 9.7. The first one concerns the antiprismatic coordination sphere which is almost regular in **1BiNO₃** but severely distorted in **4Bi**. For example, the angle in the dimer between O13–Bi and Bi–O17 is 77.5° but is only 58.3° in the monomer between O5–Bi and Bi–O7. A possible explanation for this distortion in which a labile water molecule occurs could be that O7, to be stabilized, needs to be equidistant from O5 and N5 but the length of the hydrogen bonds O5–O7 (2.821 Å) and O7–N5 (3.053 Å) are not very consistent with this explanation. In fact, the angle between the oxygen atom–Bi bonds of the bidentate ligand is the only one to be identical in the two complexes.

The second main distortion to be observed concerns the porphyrin core itself. Indeed, porphyrins are known to adopt various conformations according to the bound metal and the steric hindrance or the electronic properties of its substituents. Chiefly, to identify this distortion, the displacement of the four meso carbon atoms as well as the eight β -pyrrolic carbon atoms in respect to the 24 atom mean porphyrin plane is calculated. The mean porphyrin plane refers to the least square mean plane calculated for the 24 atom macrocycle, and not for the four coordinating nitrogen atoms, the metal being not included in the calculations. The C α –N–N–C α torsion angle is also taken into account to quantify the degree of ruffling. According to these displacements, it appears that the porphyrin in the dimer is domed whereas it is both ruffled and saddled in the monomer. The former distortion is quite usual in most of the previously reported X-ray structures of bismuth porphyrins and can be attributed to the out-of-plane coordination of the metal itself. Typically, the domed conformation is only observed when the porphyrin is coordinated to a large central metal ion, usually with one or more axial ligands. Indeed, it is clear that all the β pyrrolic carbons are on one side (below with a positive displacement) of the porphyrin mean plane where the

meso carbons are in or near the plane, Figure 9.7a. All the α carbons but two, C1 and C11, and the nitrogens are located above the mean porphyrin plane with negative displacements, on the same side than the metal [15].

In light of both X-ray structures, it has been verified that this type of porphyrin could be further functionalized without interfering with the key features of the coordination sphere. This is the reason why, as a test reaction, ligand **1** was transformed in a bifunctional linker [14] ready to react with immunoglobulins (IgG) [15]. Indeed, for potential applications with the radioactive isotope in which bismuth must be coordinated in the very last step, the free carrier, and not the metaled complex, will have to be attached to the IgG. The general synthetic pathway for such a transformation is described on Scheme 9.2.

As mentioned earlier, in **1BiNO₃**, only one picket does not seem to be decisive in the stability of the complex. Thus, it was reasoned that this ethylsuccinyl picket could be replaced by a linker properly designed without perturbing considerably the coordination properties of the ligand. The synthesis consists of sparing one amino function of TAPP by employing the single trityl TAPP (TrTAPP), as previously described [16]. The further steps



Scheme 9.2 Synthesis of various bifunctional ligands related to porphyrin **1**, starting from porphyrin **9NH₂**, and their coupling with an antibody (Ab) or reduced antibody (Fab'). Reagents and conditions: (i) $\text{ClCO}(\text{CH}_2)_2\text{CO}_2\text{Et}$ (4 M equivalent), NEt_3 , THF; (ii) TFA, CH_2Cl_2 ; (iii) $\text{ClCOCH}=\text{CH}_2$ (1.5 M equivalent), NEt_3 , THF; (iv) succinic anhydride (2 equiv), EtOH, 50°C , 48 h; (v) reduced antibody **Fab'**; (vi) NHS/DCC; (vii) antibody; (viii) SIAB-activated reduced antibody. (Reproduced with permission from The American Chemical Society. Copyright © 2004 The American Chemical Society)

then introduce a reactive function for either primary amines of the lysine residues or thiols groups from the cysteine, and particularly those obtained after reduction of the disulfide bridges of immunoglobulins which leads to the Fab' fragments (Scheme 9.2) [17]. The reaction targeting coupling with thiol groups of the Fab' was performed from the reduced fragment of the IgG obtained according to the usual methodology with 2-mercaptoethanolamine. In the first case, the sulfhydryl groups of the reduced IgG are known to react with the acrylamide function according to a 1,4-addition creating a stable thioether bond. In the second case, the resulting porphyrin **9SA** bearing a four carbon spacer was activated by the N-hydroxysuccinimide (NHS) method and then coupled with the complete IgG via formation of amide bonds. Because of the lack of precise methods as gamma emission counting, only a rough evaluation of the porphyrin/IgG ratios was possible. Indeed, as the porphyrin exhibit an absorption at around 420 nm with an average molecular coefficient (ϵ) of $350\,000\text{ M}^{-1}\text{ cm}^{-1}$ whereas the protein (IgG) at 280 nm with the molecular coefficient (ϵ) of $195\,000\text{ M}^{-1}\text{ cm}^{-1}$, this evaluation was performed by UV visible spectroscopy. Additionally, in our case, it is also expected to be convenient for future *in vivo* studies with the bismuth complex which adsorbs at 470 nm.

First, the coupling of porphyrin **9Acr** to Fab' fragments was investigated. With an excess of 50 M equivalents of this porphyrin (ϵ of $350\,800\text{ M}^{-1}\text{ cm}^{-1}$), only 40% of the Fab' was found to be conjugated to the porphyrin. When decreasing the excess of porphyrin down to 25 equivalents, only 15% of Fab' was labeled. The same type of measurement was performed to evaluate the coupling between IgG and porphyrin **9SA** according to the activated ester method but the result was as disappointing as for the previous one. Indeed, only 20% of the protein was linked to the porphyrin. In fact, although the two reactions cannot be compared, these two results are consistent one with another and could be explained by a too short length of the spacers (three - four atom lengths). Indeed, it has been reported that the approach of the reactive functions from the antibodies can be sensitive to the steric hindrance of the chelate [18].

These results prompted the authors to reinvestigate the conjugation by using a commercially available spacer. N-succinimidyl(4-iodoacetyl)aminobenzoic acid (SIAB) was chosen for two reasons. First, the length of this spacer is more important than for the two previous one with a value of 10.6 \AA . Second, the activate ester function of the spacer allows the direct coupling of the Fab' on porphyrin **9NH₂** without any other reaction or purification step on it. The iodoacetyl function of this heterobifunctional cross linker will react with the thiol groups of the reduced IgG (Fab'). According to the same method, the ratio of porphyrin over the antibody (C_p over C_{ab}) is found equal to 1.5. If one considers that the Fab' is completely labeled, 50% is attached to one porphyrin where the other 50% are doubly marked. This third coupling reaction clearly indicates that with a chelate such as picket porphyrins, the length of the linker becomes critical in comparison with other ligands such as non aromatic tetraazamacrocycles.

Another critical issue to address for therapeutic applications is the stability of the resulting complexes in physiological medium. However, as these porphyrins are not water soluble, a simple way to evaluate their relative stability at a first glance consists of dissolving the bismuth complex in an acidic solution and to monitor the release of bismuth as a function of time. As this reaction leads to the free base porphyrin that exhibits a different absorption ($\sim 420\text{ nm}$), this first evaluation is really easy to perform. For instance, we found that in the case of ester and acidic pickets porphyrins, exposing the bismuth complexes to 2500

equivalents of trifluoroacetic acid in methylene chloride gave a good evaluation scale over a 3 h period of time [19].

To experimentally verify the actual influence of the length of the arm on the distortion of the macrocycle, porphyrin **5** was also studied for its ability to complex bismuth rapidly. In the latter, the succinate motif was substituted by the glutarate motif which possesses one more carbon, but actually, no significant difference was observed about the kinetics of metalation of **4** or **5** by bismuth nitrate. On the other hand, **5Bi** proved to be much less stable than **4Bi** in acidic medium. To further address this question, a study of the decomplexation of bismuth from these two chelates bearing acid pickets differing only by one carbon atom was undertaken. The characteristic absorption at 470 nm of the metallated porphyrin [6] was monitored while the complex was exposed to 2500 equivalents of trifluoroacetic acid (TFA). A typical result is illustrated in Figure 9.8 for the bismuth complex **4Bi**. In this particular example, even after three hours only 37% of the complex (Soret at 470 nm) was transformed to the free base porphyrin (Soret at 420 nm) via bismuth decomplexation.

Thus, this methodology was also applied to the other complexes with a direct comparison with their precursors bearing ester pendant arms as it represents a simple way to compare the stability of metal complexes which are not water soluble (Figure 9.9). Clearly, the various complexes can be classified into two main groups. The first group of complexes, for which the decomplexation of the bismuth cation is evaluated to be around 80–90% after three hours in acidic medium, is composed of the following molecules in order of decreasing stability: **7Bi** (79%), **9Bi** (84%), **8aBi** (88%), **8bBi** (90%), **1Bi** (92%), **3Bi** (92%) and **5Bi** (98%). The second group is composed of the five porphyrins bearing 4-1 succinic acid picket(s) for which the percentage of demetalation remains below 40%, in order of decreasing stability:

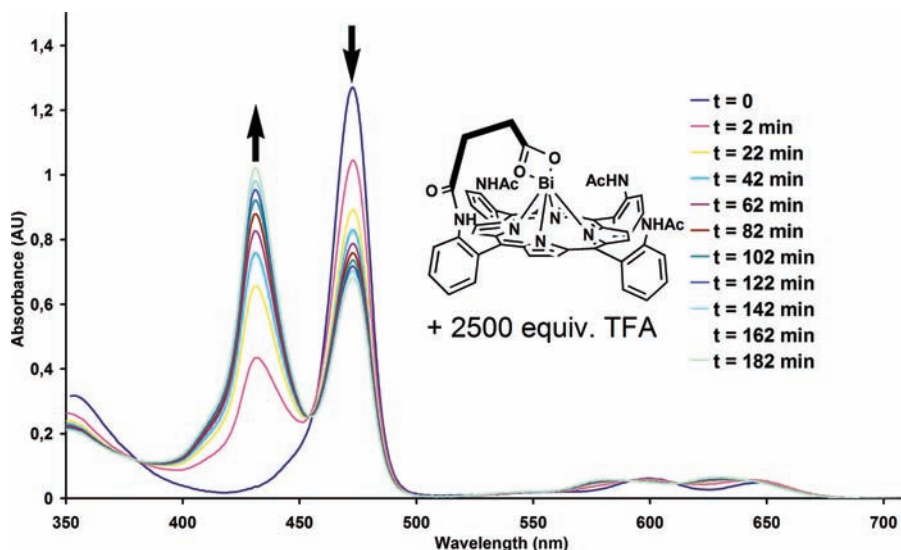


Figure 9.8 Demetalation of **4Bi** in methylene chloride in the presence of 2500 M equivalent of TFA monitored by UV visible spectroscopy. Reprinted with permission from [21]. Copyright 2006 American Chemical Society

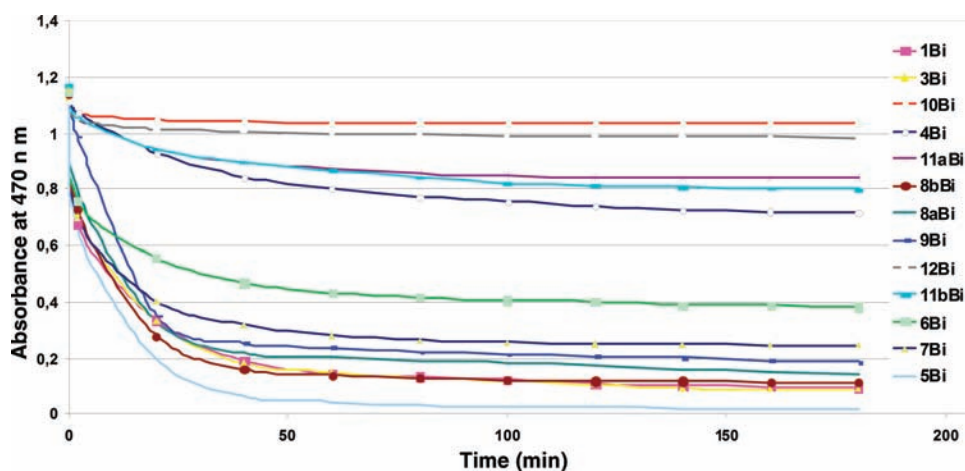


Figure 9.9 Relative stability of 12 bismuth complexes in methylene chloride in the presence of 2500 M equivalent of TFA. Reprinted with permission from [21]. Copyright 2006 American Chemical Society

10Bi (7%), **12Bi** (14%), **11aBi** (23%), **11bBi** (32%), **4Bi** (37%). Midway between these two groups is located bismuth complex **6Bi** (67%). Actually, the first group which represents the least stable complexes is mainly composed of all the pendant ester picket complexes (from **9Bi** to **3Bi**).

However, a striking result comes from complex **5Bi** which is the direct analogue of **4Bi**, with the glutaryl motif instead of the succinyl motif. Indeed, from the distortion of the macrocycle observed in the X-ray structure of **4Bi** and independently of the theoretical calculations, it was reasonable to think that an analogous complex able to release this distortion would be more stable than **4Bi**. Although no structural evidence was collected for **5Bi**, it was hypothesized that elongating the pendant arm of one atom of carbon should release this distortion. But it turns out that this change in length does not induce the expected effect as it leads to the least stable bismuth complex of this series. The stability of **5Bi** is even lower than that of the complex with one ethyl ester picket, namely **3Bi**. A plausible explanation could be that the glutaryl motif with three methylene groups would not readily allow the coordination of the intramolecular carboxylic acid to function due to the arrangement of dihedral angles along the propyl skeleton. This observation is also consistent with the conclusions from the theoretical calculations, that is, the distortion of the macrocycle is mainly due to the presence of water molecules in the bismuth surroundings rather than the length of the carboxylate picket [19].

A second approach consisted of investigating the influence of the pre-organization with the two methylene motif of the succinyl picket while increasing the rigidity of the picket. This increase in rigidity is a priori satisfied in compounds **6** and **7**. However, it was disappointing to observe that none of the resulting bismuth complexes gain stability in comparison with **4Bi**. Actually, **6Bi** and **7Bi** are just slightly more stable than the ester picket porphyrins. In these two examples, it is clear that too much pre-organization can disfavor the stability of the bismuth complex. In the case of **6Bi**, the dihedral angles between the two

methylene groups joining the amide and the carboxylic acid are dictated by the cyclohexyl ring and the *trans* configuration. If the ‘coordinating carboxylate’ is not properly located, the possibilities of movement to adjust its position are smaller than in **4Bi**.

For its aromatic analogue **7Bi**, the pre-organization is even stronger for two reasons. First, the ‘coordinating carboxylate’ is expected to be conjugated with the aromatic cycle of the picket: such an orientation does not favor the coordination in the η^2 -acetato mode. Second, in most of the known X-ray structures reported in which a phthalic acid is conjugated with an aniline just as in porphyrin **7** [20], the two aromatic cycles are almost orthogonal but not coplanar. This conformation is supposed to locate the ‘coordinating carboxylate’ away from the center of the porphyrin.

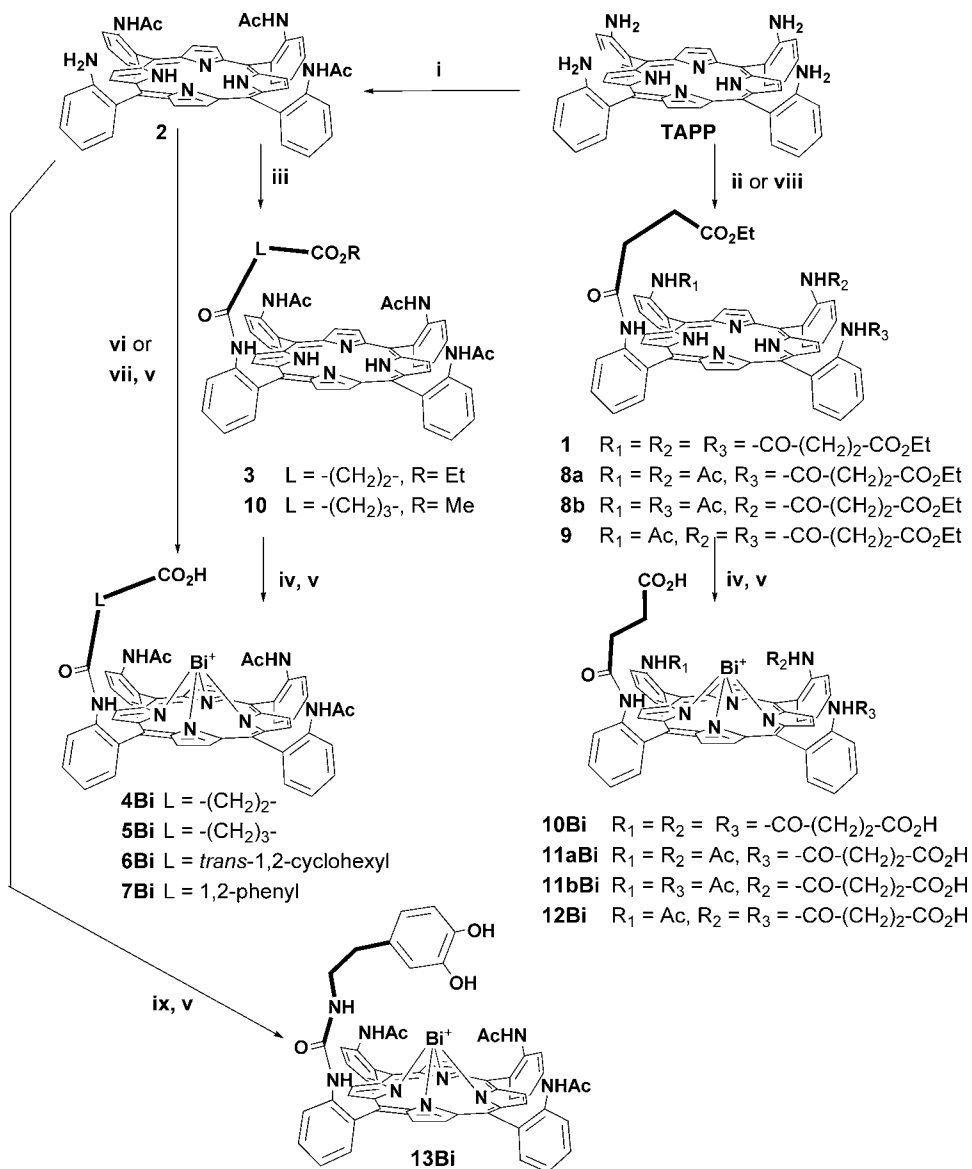
In the second group composed of all the succinic acid picket porphyrins, from **10Bi** to **4Bi**, the percentage of decomplexation of the bismuth increases from 7% for **10Bi** up to 37% for **4Bi**. In the series, it appears that the stability of the bismuth porphyrin is almost proportional to the number of succinic acid pickets of the ligand. As in the precursor series concerning the ethyl succinic ester picket porphyrins **8a** and **8b**, the 5,10-isomer is more stable than the 5,15-one but the difference between them is even more pronounced in the acid series, **11a** and **11b**. These observations indicate that porphyrins bearing succinic acid pickets as chelators for bismuth(III) cation are efficient both in terms of the kinetics of complexation and thermodynamical stability. Indeed, in comparison with their ester pickets precursors, they complex bismuth at room temperature in 10 minutes, leading to fairly stable complexes. Serendipitously, the succinyl motif led to the most efficient ligands in comparison with either the longer glutaric acid or pre-organized diacids such as *trans*-1,2-cyclohexyl dicarboxylic acid or phthalic acid, these three leading to less stable bismuth complexes.

It should also be mentioned that a picket porphyrin **13** (Scheme 9.3) bearing a dopamine picket has been successfully metalated with bismuth with a quantitative yield in 15 minutes at room temperature with only one equivalent of bismuth nitrate [21]. It is worth noting that the resulting complex **13Bi** does not demetalate at all during the purification process on silica gel column chromatography. This result seems to indicate that a synergy does exist between the two hydroxy groups of the catechol unit in the particular case of bismuth complexation. It also verifies that any coordinating group must be attached to the macrocycle via a flexible and long enough link. Unfortunately, no X-ray structure of **13Bi** that could confirm the effective coordination of the catechol to the bismuth cation was reported. However, the chemical shifts of the two methylene groups from the arm in both the free base (2.88/2.21 ppm) and the bismuth porphyrin (1.37/1.42 ppm), indicate that the arm is clearly downfield shifted upon the metalation. This observation is consistent with an interaction of the catechol group with bismuth inside the porphyrin.

However, as pre-organized structures are expected to lead to more efficient chelators in general, a balanced structure between pre-organization and flexibility to deliver a catechol or an acidic group in close proximity of the coordinated bismuth cation inside the macrocycle had to be found and this came with particular strapped porphyrins.

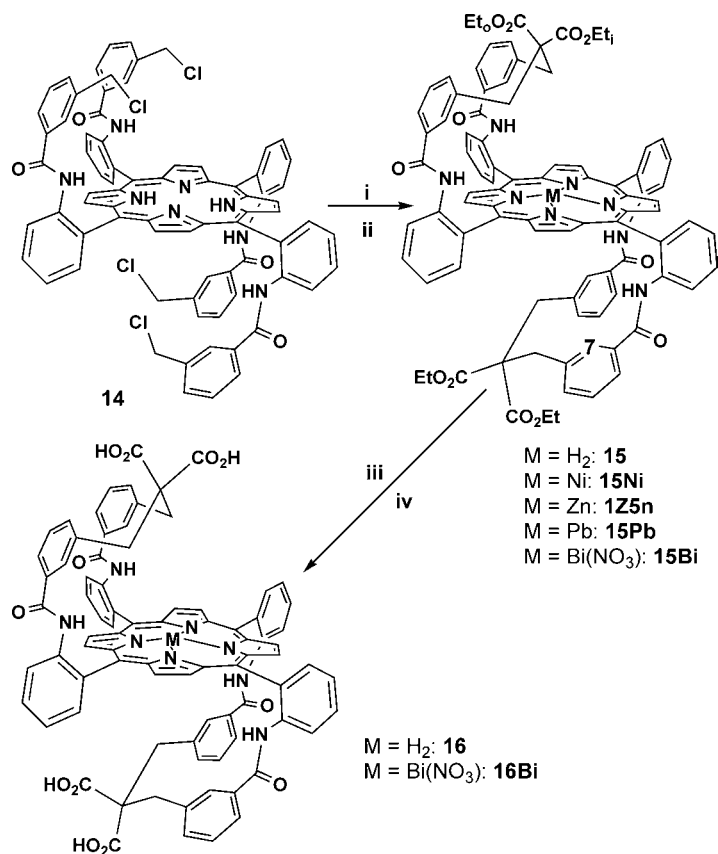
9.4.2 Bis-Strapped Porphyrins

This second approach is based on a general and easy preparation of several types of strapped porphyrins in only two steps, starting from different ‘U-shaped’ acceptors, by acylation of



Scheme 9.3 Synthetic route leading to various acid picket bismuth porphyrins. (i) 3 eq. CH_3COCl , THF, NEt_3 ; (ii) \rightarrow **1**, 5 eq. $\text{EtO}_2\text{C-(CH}_2\text{)}_2\text{-COCl}$, THF, NEt_3 ; (iii) 1.2 eq. $\text{MeO}_2\text{C-(CH}_2\text{)}_3\text{-COCl}$, THF, NEt_3 ; (iv) KOH , MeOH , 55°C ; (v) $\text{Bi(NO}_3\text{)}_3$, pyridine, rt; (vi) *trans*-1,2-cyclohexyl anhydride, AcOH ; (vii) phthalic anhydride, CH_2Cl_2 , aluminum oxide; (viii) 2 steps: 1.8 M equivalent of CH_3COCl , THF, NEt_3 , chromatography then $\text{EtO}_2\text{C-(CH}_2\text{)}_2\text{-COCl}$, THF, NEt_3 ; (ix) diphosgene (1 h) the dopamine (1.1 M equivalent), NEt_3 , THF; (as the bismuth counter anion was unambiguously shown to be the carboxylate group only for **4Bi**, the various complexes are noted as Bi^+ complexes). (Reproduced with permission from The American Chemical Society. Copyright © 2006 The American Chemical Society)

three isomers of TAPP [22]. This methodology was shown particularly adapted to the preparation of various cation binding superstructures and can be regarded as a generalization of Chang's ligand appended reaction [23]. Briefly, it consists of linking to the porphyrin an ethylmalonyl motif by the means of two benzylic chloride pickets on each side of the porphyrin. Unlike the $\alpha\alpha\alpha\alpha$ atropisomer, when achieved on the $\alpha\alpha\beta\beta$ and $\alpha\beta\alpha\beta$ atropisomers, this synthesis is unambiguous and leads to a single compound [24]. A further ester cleavage step provides a novel interesting ligand **16** possessing four carboxylic acid functions (Scheme 9.4, $\alpha\alpha\beta\beta$ atropisomer). To avoid the decarboxylation reaction expected in β -ketoesters such as in **15**, we have used a method described by Hirsch *et al.* to obtain **16**



Scheme 9.4 Synthesis of 'pearl oyster like' bis-strapped porphyrins. (i) CH₂(CO₂Et)₂ (20 M equivalent), THF/EtONa, rt, 2 h (the subscripted letters i and o of the ethyl groups stand for 'in' and 'out'); (ii) **15Ni**: Ni(OAc)₂, pyridine, reflux, 48 h; **15Zn**: Zn(OAc)₂, AcONa, CHCl₃, reflux, 1 h; **15Pb**: 10 M equivalent of Pb(OAc)₂·3H₂O, pyridine, 50 °C, overnight; **15Bi**: 10 M equivalent of Bi(NO₃)₃·5H₂O, pyridine, 100 °C 2 h; (iii) NaH/toluene then MeOH, 80 °C, 10 h; (iv) 1–10 M equivalent Bi(NO₃)₃·5H₂O, pyridine at room temperature. (Reproduced with permission from The American Chemical Society. Copyright © 2007 The American Chemical Society)

in quantitative yield [25]. The basic and simple concept of this family of ligands is the possible flexibility of the straps on which hangs either ester or acid groups. The various X-ray structures of several complexes synthesized from these ligands actually show that a bis-strapped porphyrin such as **15** can adopt several conformations.

To probe the effective flexibility of the particular strap encountered in **15**, nickel(II) and zinc(II) were inserted in **15** in the usual method [26]. Indeed, in a porphyrin, nickel(II) is known to be square planar four-coordinate and to induce a ruffled distortion of the macrocycle. Accordingly, no interaction between an ester carbonyl from a strap and nickel is expected in **15Ni**. In contrast, in the case of **15Zn**, in which zinc is expected to be square pyramidal five-coordinate with a weakly bound fifth axial ligand, usually a water, THF or methanol molecule, it would be plausible to observe an intramolecular interaction with a carbonyl ester from a strap. Incidentally, this type of intramolecular interaction has already been reported, both in solution and in the solid state, as a bond stable enough to avoid the exchange between several carbonyl functions at room temperature (length Zn-O = 2.132 Å) [27].

Luckily, **15Ni** and **15Zn** were characterized by X-ray structural analysis. The resulting structures are represented in Figure 9.10 [28]. A simple visual analysis of these structures confirms the fact that this type of strap is particularly flexible. For instance, it is striking to compare the conformation of the straps in both nickel (left) and zinc (right) porphyrins.

As expected, in the four-coordinate nickel complex, the straps exhibit a relaxed conformation, bent over the metal with an angle of 57° between the mean porphyrin

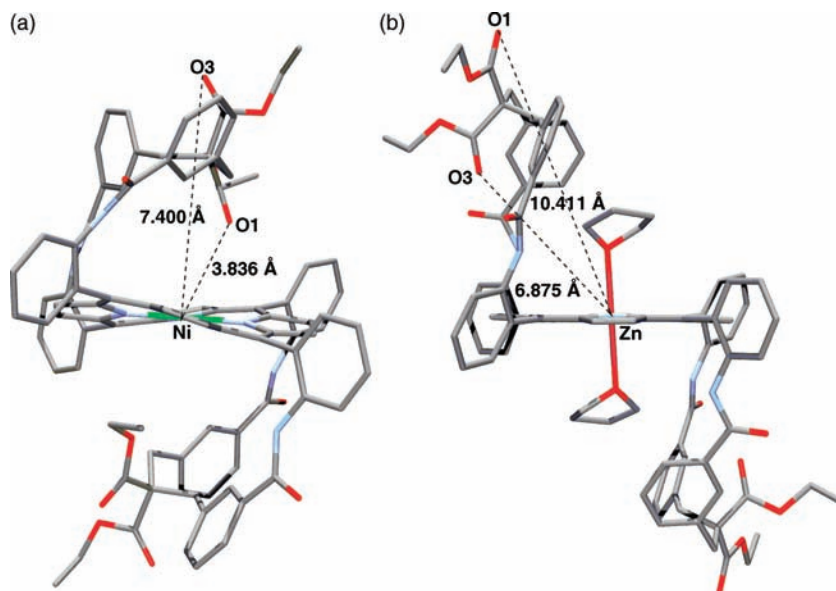


Figure 9.10 Lateral stick models of the solid state structures of (a) **15Ni** and (b) **15Zn**. Reprinted with permission from [30]. Copyright 2007 American Chemical Society

plane and the mean plane of the strap. At the opposite, in the case of the zinc complex which was synthesized to probe whether a carbonyl oxygen atom could complex the zinc atom, the straps appear almost in vertical position with an angle to the mean porphyrinic plane of 88° . This conformation is certainly a consequence of the coordination of two axial THF molecules on the metal and obviously, the intramolecular coordination of the carbonyl is not possible anymore. Another consequence of the six-coordination of the zinc [29] is the fact that the ethylmalonyl residue is rejected outside of the pocket of the porphyrin. In **15Ni**, it should be noted that the porphyrin is significantly ruffled and that the shortest distance between a carbonyl oxygen and the metal is 3.836 Å. Thus, these X-ray data demonstrate that this particular 5,10-strap is indeed flexible at two different levels. First, the strap bearing the malonyl motif can be either vertical or bent over the center of the porphyrin, like the shell of a pearl oyster in opened or closed position. Second, the malonyl unit can be oriented inside or outside the pocket of the porphyrin by a simple rotation around the benzylic carbon atoms C1 and C3. As these two structural features should allow porphyrin **15** to complex various metals of different sizes and valences as lead(II) and bismuth(III), the coordination of these two elements by **15** was also investigated. Indeed, in addition with the fact that lead(II) is isoelectronic with bismuth(III), it should be specified that for radioimmunotherapy applications, the generation of isotope 212 of bismuth starting from isotope 212 of lead via a β -decay has already been studied with DOTA [30] and fully justifies that potential chelates of bismuth(III) should also be evaluated for their aptitude to complex lead(II).

Therefore, lead insertion was performed by heating the porphyrin **15** at 50°C overnight in pyridine with 10 M equivalent of $\text{Pb}(\text{OAc})_2 \cdot 3\text{H}_2\text{O}$. The metal insertion was monitored by UV visible spectroscopy and resulted in a 'hyper' absorption spectrum with typical split Soret bands at 355 nm and 471 nm. The compound was purified by silica gel column chromatography without any demetalation. The ^1H NMR spectrum was recorded at 298 K and proved to be well resolved with sharp signals, in which the two sides of the porphyrin are slightly different (Figure 9.11a and c). These NMR data are in full agreement with an out-of-plane coordination of lead, as reported in three X-ray structures [31, 32]. Indeed, in these solid state structures of lead(II) porphyrins, the metal lies at ~ 1.2 Å above the mean porphyrinic plane without any axial ligand and therefore remains four-coordinate. This type of polyhedron of coordination is fully consistent with the ^1H NMR data observed in **15Pb** and in agreement with a lack of coordination of a carbonyl oxygen on a strap with lead. Definitely, if such a coordination occurred, it would be detected on the NMR spectrum by a shift of the ethyl groups, of the proton H_7 and, of the benzylic protons of the considered strap. However, none of these protons are significantly different from a strap to the other one in **15Pb** and all the chemical shifts in **15Pb** are very similar to those of the free base porphyrin **15**.

Thereafter, single crystals suitable for X-ray analysis were obtained by slow evaporation of a mixture of **15Pb** in CH_2Cl_2 , MeOH and water. The resulting solid state structure is represented (Figure 9.12). Lead is located 1.368 Å out of the plane of the porphyrin with no axial coordination and with an average N-Pb length of 2.389 Å. It is particularly striking that lead remains four-coordinate in spite of the possible close location of the oxygen atom from the ester carbonyl group as seen in the lower strap (Figure 9.5b). The two straps adopt a 'W-shaped' conformation with the 'out' ethoxy group closest to the metal than the 'in' ethoxy group. In this case, the shortest distance between lead and an ester carbonyl atom is

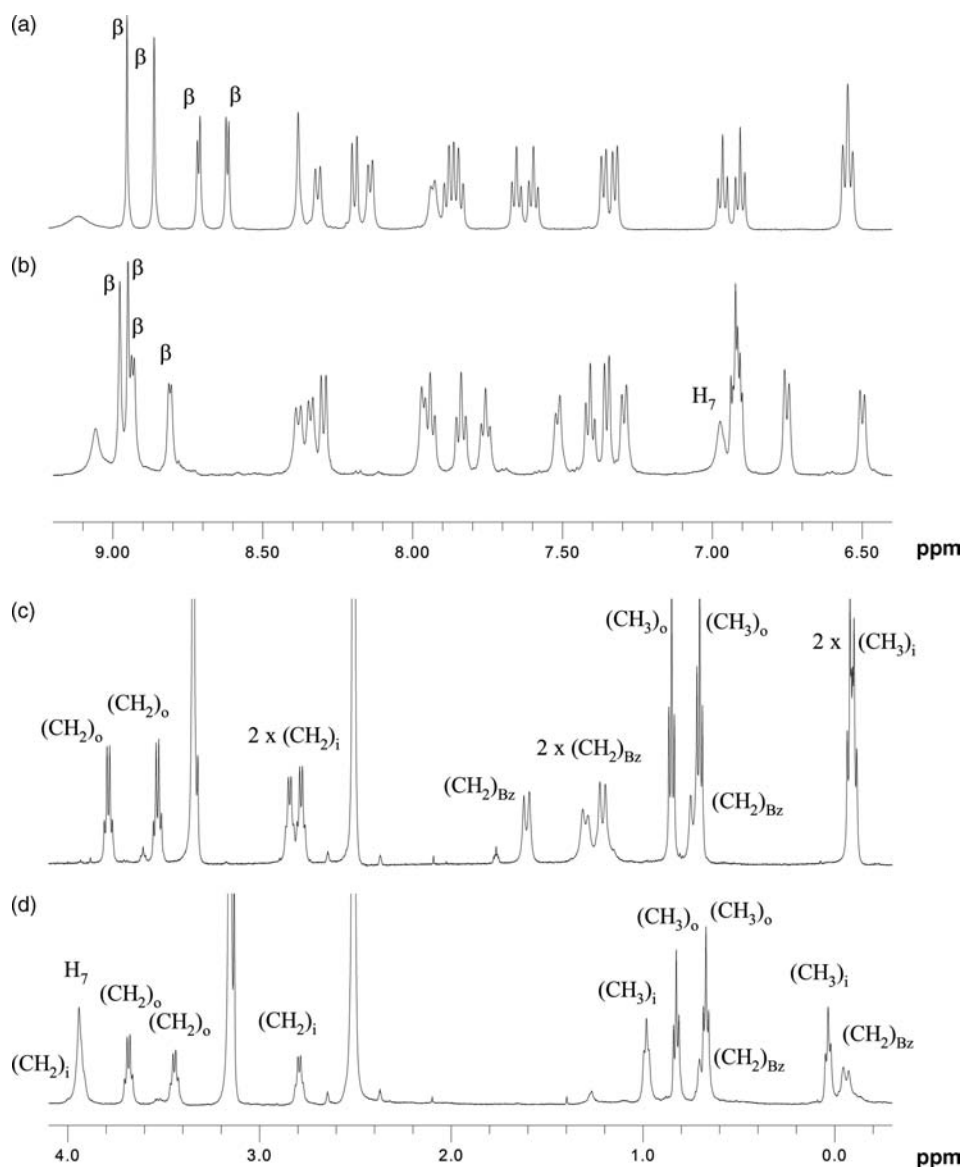


Figure 9.11 500 MHz ^1H NMR spectra of **15Pb** and **15Bi** at aromatic region (11a and 11b) and aliphatic region (11c and 11d) in $\text{DMSO}-d_6$. Reprinted with permission from [30]. Copyright 2007 American Chemical Society

6.875 Å where the longest (within the ‘in’ group) is 7.034 Å. No comparison can be performed with the other strap as the metal is out-of-plane coordinated.

Conversely to what was observed in solution where the two straps are slightly different because the two sides of the macrocycle are not equivalent, in the solid state, the two straps

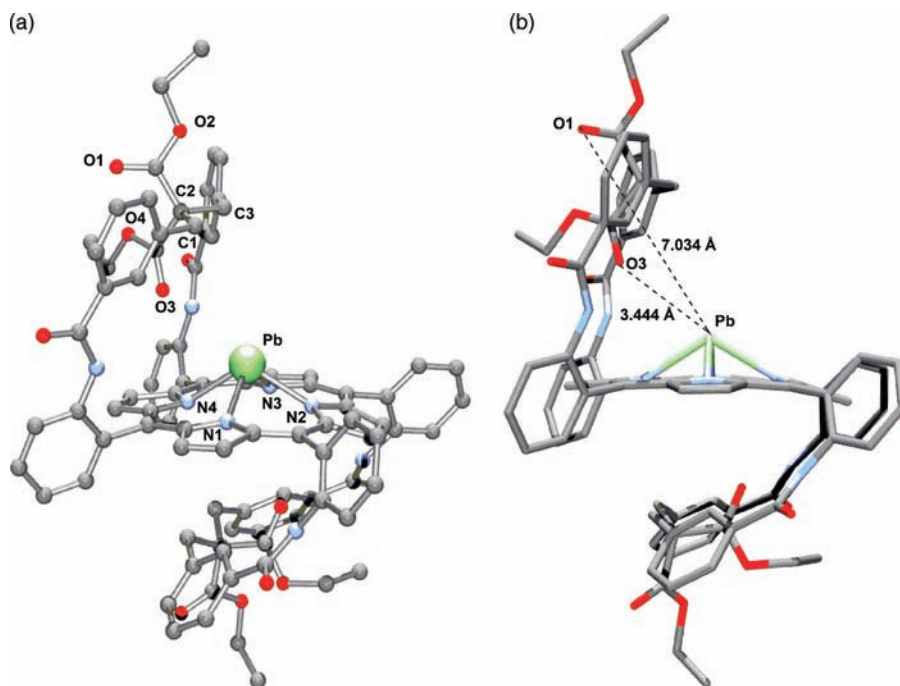


Figure 9.12 Ball and Stick (a), and lateral stick (b) views of the X-ray structure of **15Pb**. Reprinted with permission from [30]. Copyright 2007 American Chemical Society

of the complex are really in two extreme positions. Indeed, the strap on the opposite side to lead, exhibits the same relaxed ‘bent-over’ conformation as in **15Ni** with neither any coordination driving force nor any electrostatic repulsion. The angle between the mean porphyrin plane and the mean plane of this strap is 34° , a value even smaller than the angle of 57° found in **15Ni**. This smaller angle is certainly due to the domed distortion of the porphyrin as the two adjacent *meso* carbon atoms to which is attached the strap are displaced (0.20 and 0.08 Å) on the same side of the porphyrin. On the other side of the macrocycle, the strap adopts a vertical conformation as it does in **15Zn** although no axial ligand exists on lead, with an angle to the mean porphyrin plane equal to 70° . This value compares well with the analogous angle of 84° found in **15Zn**. It clearly appears that in the absence of an axial ligand on lead, this vertical position of the strap is mainly due to the electrostatic repulsion of the strap with the lone pair of lead, which is expected to be in axial position. In fact, in **15Pb**, the position of the strap can be regarded as a probe of a ‘stereochemically active lone pair’.

The same study was performed towards bismuth insertion in **15**, which was achieved in a mixture of pyridine/MeOH at 100°C overnight, using 10 M equivalent of $\text{Bi}(\text{NO}_3)_3$. Completion of the reaction was also monitored by UV visible spectroscopy (split Soret band at 355 nm and 476 nm). **15Bi** was purified on a silica gel column chromatography as a mixture of several green bands. However, each band led to the same MALDI-TOF mass

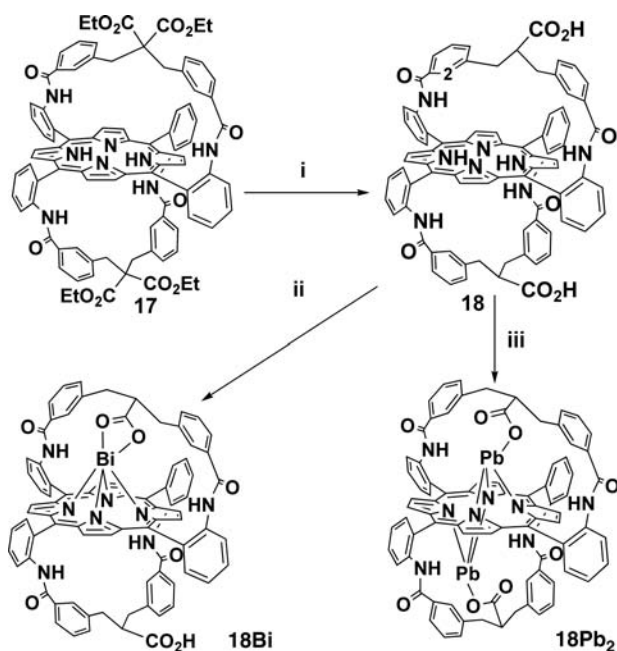
spectrum and therefore all were collected together. The proton NMR spectrum was studied but appeared at room temperature, in DMSO- d_6 not exploitable because of broad signals for most of the peaks. However, at higher temperatures, the spectrum becomes simpler with well resolved signals and is characteristic of a porphyrin in which the two sides are magnetically different, an observation consistent with bismuth insertion on one side of the porphyrin. The resolution of the spectrum was optimal at 333 K and by comparing the NMR data of **15Pb** at 298 K and those of **15Bi** at 333 K, both in DMSO- d_6 , three main differences were observed in **1Bi** (Figure 9.11b and d). First, the two signals of H₇ are really different, one of them being strongly downfield-shifted to 6.97 ppm. This value compares well with the chemical shift of the same proton of the analogous free base porphyrin in the $\alpha\alpha\alpha\alpha$ geometry for which the X-ray structure clearly showed that the two straps, located on the same side of the porphyrin and because of a reciprocal steric repulsion, were almost in vertical position [22]. Second, one doublet of the AB system corresponding to the benzylic protons is shielded down to -0.06 ppm, just like in **15Zn** (Figure 9.11d). Third, one quadruplet (3.90 ppm) and one triplet (0.97 ppm) of an 'in' ester group are down field shifted and resonate in the same region that the 'out' ester groups. These observations are consistent with one strap in vertical position as in the solid state structure of **15Zn**. As the coordinated Bi(III) cation needs a counter anion which is presumably a nitrate residue, the strap of the same side of the bismuth has to 'stand-up' to accommodate the counter anion. Actually, in terms of geometry of the straps, the structure in solution of **15Bi** seems to be close to the solid state structure of **15Zn**. There is no clear spectroscopic evidence in favor of an intramolecular interaction between a carbonyl oxygen atom and the coordinated bismuth in **15Bi**.

In a last step, we reasoned that the situation could be different in porphyrin **16**, resulting from the cleavage of the ester groups of **15**. Indeed, in **16**, the carboxylic acid functions should induce less steric hindrance for bismuth than the ester groups and moreover, the metal could have an intramolecular counter anion delivered by the strap. At this step, it is worth mentioning that no ¹H NMR spectrum of **16** suitable for conformational analysis was possibly recorded. Although the high resolution MS data of **16** were fully consistent with the proposed structure, the ¹H NMR spectrum was representative of an equilibrium of the compounds and exchanged on the 1H NMR time scale. Nevertheless, bismuth insertion in **16** was performed at room temperature in pyridine. The complexation was rapid as proved by the appearance of the typical Soret at ~470 nm in the UV-visible spectrum of the reaction mixture but never went to completion. Additionally, when pyridine was evaporated to purify the resulting mixture of the free base and the metalloporphyrin, demetalation occurred instantaneously. These two last observations concerning both **16** and **16Bi** are consistent with a possible interaction between the carboxylic acid groups and the macrocyclic core. As a result of the coexistence of both the pre-organization and the flexibility of the considered strap, this interaction could result in a partial intramolecular protonation of the internal pyrrolic NH functions. Moreover, this protonation can occur from both sides of the porphyrin with the straps in various conformations as depicted in Figure 9.10, hence the exchange phenomenon observed in the proton NMR spectrum of the free base porphyrin **16**. In the case of **16Bi**, where one carboxylic acid from one side of the porphyrin can complex bismuth inside the macrocycle, the carboxylic groups from the other side of the porphyrin can protonate the macrocycle. This protonation reaction results

obviously in the decomplexation of bismuth and explains why the metalation step cannot be quantitative.

Thus, in this first conformation with bis-strapped porphyrins, this type of 5,10-strap appears to be too flexible for delivering a carboxylate group to bismuth in the porphyrin while avoiding the possible protonation of the macrocyclic core. It has been shown that a correct balance was possible between these two possibilities with exactly the same synthetic pathway applied to the $\alpha\beta\alpha\beta$ conformation, in which the carboxylate group really hangs to the strap (Scheme 9.5) [33].

In **17**, the $\alpha\beta\alpha\beta$ analogue of porphyrin **15**, the distance between the centroid of the four nitrogen atoms of the porphyrin and the carbonyl oxygen atom from the closest ester group was measured to be 3.111 Å. However, considering the single crystal structure of a mononuclear bismuth porphyrin reported so far, in which the carboxylate was bound to the bismuth in a η^2 -carboxylato complex, the distances between the centroid of the four nitrogen atoms of the porphyrin and the two oxygen atoms from the carboxylate were found to be 3.591 Å and 3.658 Å. This means that without any coordination driving force, at least one of the two oxygen atoms of the future carboxylic group in **18** (the $\alpha\beta\alpha\beta$ analogue of **16**) is close enough to form a bond with a metal such as bismuth known to coordinate approximately 1.2 Å out of the plane of the macrocycle. Thus, bismuth insertion was



Scheme 9.5 Synthesis of hanging carboxylate porphyrins. (i) KOH, EtOH, 48 h, reflux; (ii) $\text{Bi}(\text{NO}_3)_3 \cdot 5\text{H}_2\text{O}$, 30% MeOH/pyridine, room temp.; (iii) $\text{Pb}(\text{OAc})_2 \cdot 3\text{H}_2\text{O}$, pyridine at room temperature. (Reproduced with permission from Wiley-VCH Verlag GmbH. Copyright © 2007 Wiley-VCH)

achieved at room temperature by stirring 1MM equivalent of $\text{Bi}(\text{NO}_3)_3 \cdot 5\text{H}_2\text{O}$ with a solution of **18** in MeOH and pyridine for 5 min. These mild conditions of metalation must be opposed to the fact that, even at reflux of pyridine, bismuth insertion was not observed in the precursor porphyrin **17**, and therefore are consistent with an internal coordination of the hanging carboxylate group. This argument is reinforced by the comparison of the ^1H NMR spectra of both **18** and **18Bi** and particularly proton H2 (Scheme 9.5 for atom labeling in porphyrin **18**). In the case of the free base porphyrin **18** these four protons appear as two singlets (5.05 and 5.01 ppm) since the two protons of each strap are not magnetically equivalent, whereas in **18Bi**, these four protons give rise to four singlets (5.59, 5.41, 4.96, and 4.87 ppm). This observation indicates that the two straps are not equivalent anymore in **18Bi** and is consistent with a coordinating strap via its carboxylate group. This potential coordination was also investigated by IR spectroscopy, but no conclusion could be drawn due to other CO bands from the amide groups of the compound. Incidentally, this intramolecular coordination was confirmed by the resolution of the crystal structure of **18Bi** (Figure 9.13a). Indeed, in a mixture of acetone/water/DMSO, **18Bi** crystallizes as green cubic crystals in the triclinic space group *P*-1.

This complex represents the second example of a mononuclear bismuth porphyrin with an intramolecular counter anion. The main structural feature of all known bismuth porphyrins is the large displacement of the metal from the 24 atoms mean porphyrinic plane (average value of 1.255 Å based on known structures), in **18Bi**, the metal lies 1.309 Å above from the mean plane, the largest distance reported so far for such a displacement.

Such a large displacement is presumably due to the linkage of the carboxylate group to the strap. However, this strap exhibits some flexibility as shown by the two different conformations found in **18Bi**, i.e. the carboxylic group of the non coordinating strap (Figure 9.14) is oriented outside the cavity of the porphyrin where the coordinating carboxylate of the other strap is locked inside the cavity by a 'W-shape' of the strap. The bismuth atom is seven-coordinate with the four Bi-N bonds of the macrocycle, two bonds with the oxygen atoms from the carboxylate group (2.925 Å and 2.367 Å) and a bond with a DMSO molecule (2.587 Å) from the solvent of crystallization. As a result of the coordination of the carboxylate group, the bismuth atom is slightly displaced from its apical position towards the carboxylate function as indicated by the length of two bonds Bi-N1 (2.279 Å) and Bi-N2 (2.323 Å) shorter than Bi-N3 (2.490 Å) and Bi-N4 (2.460 Å). The delocalization over the carboxylate group is not symmetrical with the two C-O bond lengths of 1.206 Å and 1.295 Å and the two Bi-O3 and Bi-O4 bond lengths of 2.925 Å and 2.367 Å, respectively. It is worth noting that the Bi-O3 bond is located close to the apical position to the bismuth and therefore, the lone pair of bismuth ($6s^2$) is expected to occupy the vacant coordination site of the polyhedron as it cannot be in apical position due to electronic repulsion. In summary, the crystal structure of **18Bi** clearly indicates that the type of strap existing in **18** is adequate for the coordination of bismuth owing to the ability of the carboxylate group to switch from the 'out' (not coordinated) to the 'in' (coordinated) position.

Consequently, lead has been inserted in **18**, to obtain a complex in which the bivalent metal is out-of-plane as shown in all reported crystal structures of lead(II) porphyrins with an average distance of metal-to-mean porphyrinic plane 1.272 Å, leaving the intramolecular carboxylic group in the 'out' position. At the opposite of the metalation conditions reported in the literature (refluxing DMF for 2 h), it was intriguing to find that **18** was metalated

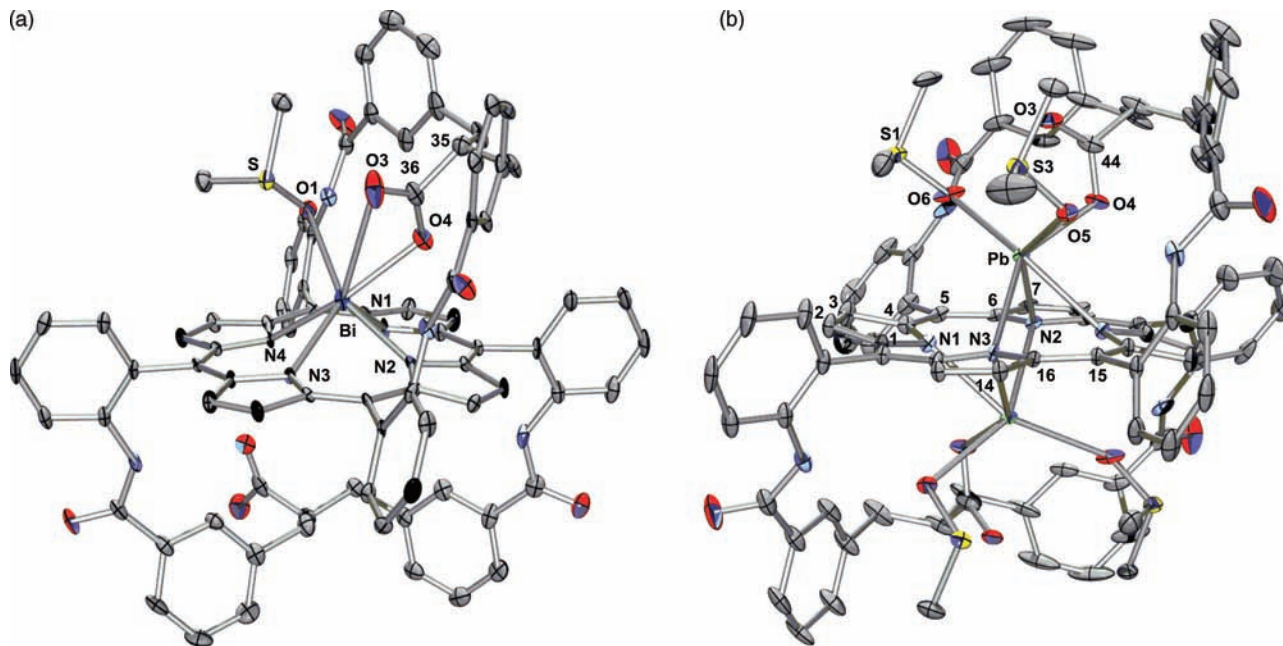


Figure 9.13 ORTEP views of **2Bi(DMSO)** (a) and **2Pb₂(DMSO)₄** (b) drawn with the thermal ellipsoids at the 30% probability level. Hydrogen atoms are omitted for clarity. Selected bond lengths [Å] and angles [°]: **2Bi(DMSO)**: N1-Bi 2.279(4), N2-Bi 2.323(4), N3-Bi 2.490(4), N4-Bi 2.460(4), O1-Bi 2.587(4), O3-Bi 2.925(4), O4-Bi 2.367(4), Bi-24 mean-plane 1.309, plane(O3-O4-C36-C35)-24 mean-plane 73.24; **2Pb₂(DMSO)₄**: Pb-Pb' 3.598(3), N1-Pb 2.480(3), N2-Pb 2.787(3), N3-Pb 2.648(3), O4-Pb 2.320(3), O5-Pb 2.651(3), O6-Pb 2.832(3), Pb-24 mean-plane 1.795, plane (O3-O4-C36-C34)-24 mean-plane 88.55, plane(N1-C1-C2-C3-C4)-24 mean-plane 11.03; plane (N2-Pb-N3-Pb')-24 mean-plane 86.04. Reprinted with permission from [35]. Copyright 2007 Wiley-VCH Verlag GmbH & Co. KGaA

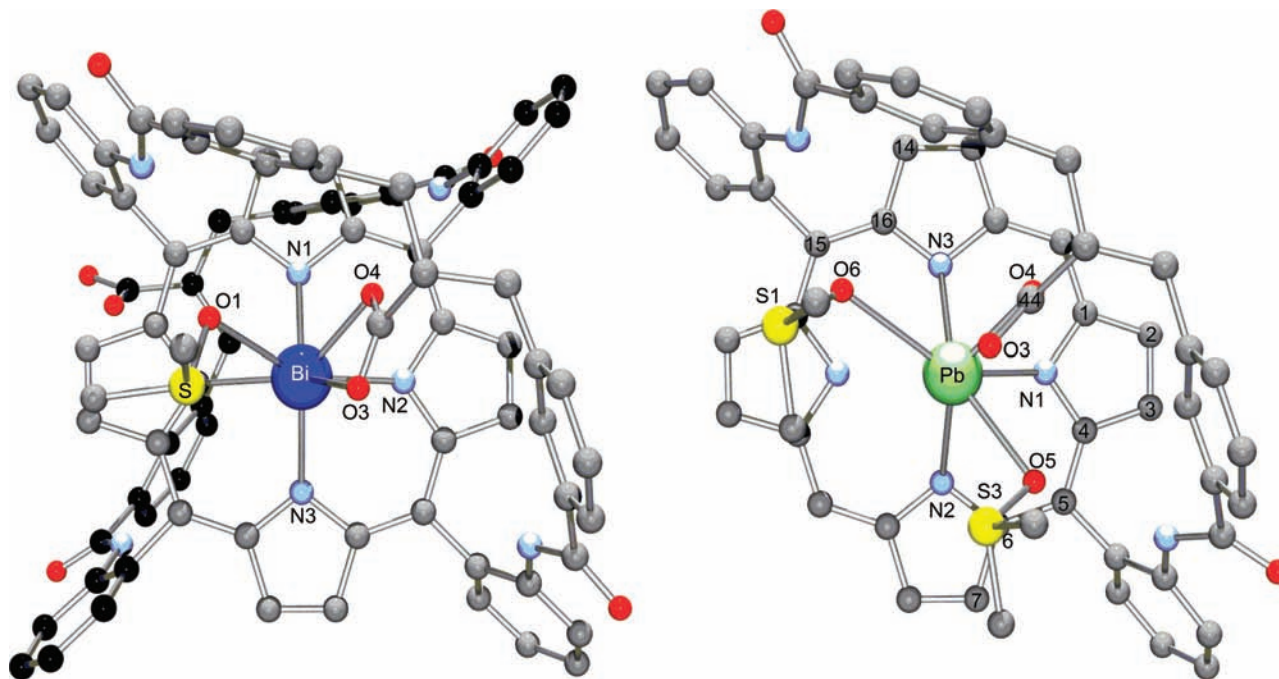


Figure 9.14 Apical ball and stick views of $2\text{Bi}(\text{DMSO})$ (Left, non coordinating strap in black) and $2\text{Pb}_2(\text{DMSO})_4$ (Right, owing to the axial symmetry, only one strap is not represented). Reprinted with permission from [35]. Copyright 2007 Wiley-VCH Verlag GmbH & Co. KGaA

by lead acetate in pyridine, after 10 min at room temperature. Surprisingly, the ^1H NMR spectrum of the lead metalloporphyrin indicates that the two sides of the macrocycle are identical to the ligand, **18**. Indeed, the protons H2 appear as two singlets at 5.90 and 5.48 ppm in **18Pb₂** instead of four singlets in **18Bi**. This could be in favor of a metal atom disordered over two positions on each side of the porphyrin as described by Plater *et al.* [32]. However, the high resolution MS spectrum of **18Pb₂** revealed a 2:1 ratio of lead for porphyrin. Additionally, the lead metalloporphyrin crystallizes in the monoclinic space group *C2/c* in a mixture of acetone/water/DMSO. The crystal structure exhibits a mononuclear bimetallic structure (Figure 9.13b) which belongs to the class III/type M in Buchler's classification of metalloporphyrins [34]. In this class, the complex is mononuclear in regards to the porphyrin which acts as a bridging ligand between the two metal atoms. The type M, also named *trans*-(MZ₃)₂(P), implies two metal atoms (one above and one below the plane of the porphyrin) bonded to three adjacent nitrogen atoms from the porphyrin and three other bonds with three neutral or negatively charged axial ligands. So far, this specific configuration has only been reported for monovalent metals such as Re, Tc [35] and Tl [36]. The crystal structure of **18Pb₂** represents the first example of such an arrangement for a bivalent metal. The coordination sphere of each six-coordinate lead atom represents an unsymmetrical trigonal antiprism as shown in Figure 9.14 (right). It is composed of three nitrogen atoms from the porphyrin N1, N2, N3, one mono-hapto carboxylate group O4 and two DMSO molecules O5 and O6 from the solvent. The plane of the carboxylate is almost perpendicular (88.55°) to the mean plane of the porphyrin. N2 and N3 atoms are bound to both lead ions with a distance of 2.787(3) and 2.648(3) Å, respectively while the N1-Bi bond as expected, is shorter (2.480 Å). The distance from the metal ion to the uncoordinated fourth nitrogen atom is rather long, 2.995(3) Å. On each side, the metal lays 1.795 Å away from the mean porphyrinic plane. The two metal ions, with distance of 3.598(3) Å, are almost positioned over the center of the porphyrin oppositely to what was reported either for bis-tricarbonyl-rhenium-tetraphenylporphyrin (TPP)[Re(CO)₃]₂ or bis-tetrahydrofuran-thallium-octaethylporphyrin (OEP)[Tl(THF)]₂ in which the metal atoms are more centered above the three adjacent nitrogens. This almost apical position of the two lead atoms is illustrated by the angle of 86.04° between the plane (Pb-N2-N3-Pb') and the mean porphyrinic plane, the C₂ axis being located along the N2-N3 axis.

Interestingly, the trigonal antiprismatic environment around the Pb atoms in **18Pb₂** is rather strongly distorted and some void can be identified in the distribution of bonds. The coordination geometry of lead is somewhat 'hemidirected' according to the terminology of Glusker *et al.*, with lead-to-ligand bonds directed throughout only part of the encompassing space. Such a distortion is not uncommon for six-coordinated Pb(II) complexes, which might reflect some evidence of a 'stereochemically active lone pair of electrons'. This phenomenon is often associated with some ionic bonding character between lead and the surrounding ligands. In agreement with this, two Pb-O and three Pb-N bonds are rather long (*vide supra*). This stereochemically active lone pair of electrons is also consistent with the examination of the deformation electron density map (Figure 9.15) [33].

Examination of the electron density supports this conclusion with a density hole clearly identified between the two Pb atoms. Obviously, they are forced by the metal-nitrogen bonds to be close to each other, and their repulsion might induce the observed porphyrin distortion. Examination of the deformation electron density map [27] shows some pockets in the vicinity of the lead atoms pointing away from the O- and N-ligands (Figure 9.15). We

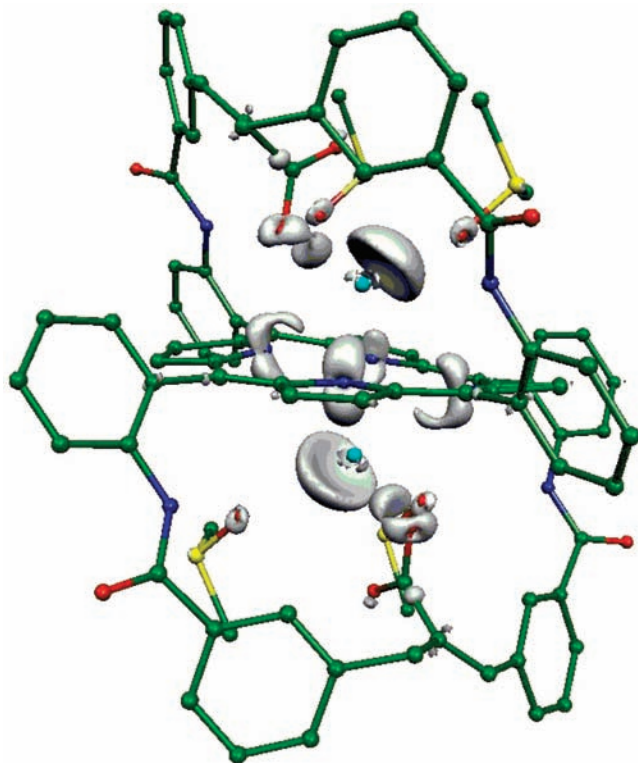


Figure 9.15 Deformation density iso-surface (contour value: $+0.01 \text{ e/bohr}^3$) of the DFT optimized molecular structure of **2Pb₂**. Color code: Pb, light blue; S, yellow; O, red; N, dark blue; and C, green. Hydrogen atoms are omitted for clarity. Reprinted with permission from [35]. Copyright 2007 Wiley-VCH Verlag GmbH & Co. KGaA

speculate that this can be associated with the presence of a lone pair of electrons which might favor an hemidirected geometry in **18Pb₂**.

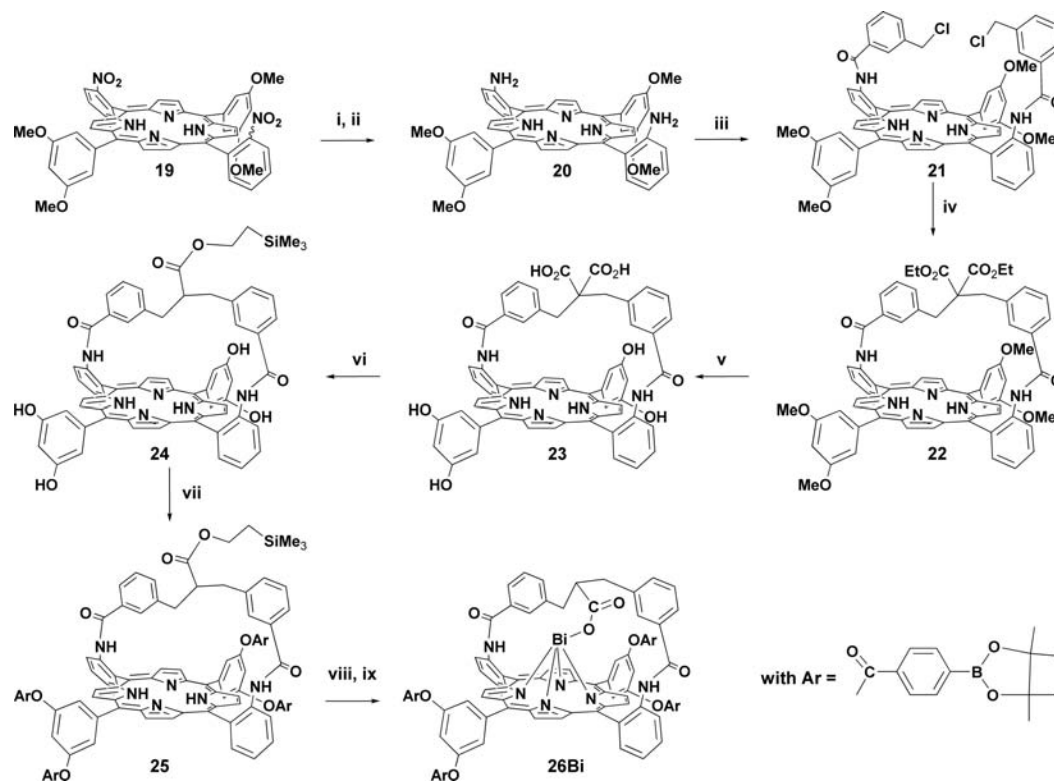
9.4.3 Single-Strapped Porphyrins

This series of porphyrins has been designed as bifunctional α -emitters, that is, these molecules were synthesized to be able to emit α -particles by two different ways that can be qualified of spontaneous as in the case of ^{212}Bi or ^{213}Bi isotopes or triggered as in the case of boron, in boron neutron captured therapy [37]. Indeed, upon irradiation of boron with a low energy thermal neutron beam, a nuclear fission reaction generates the formation of $^7\text{Li}^{3+}$ and $^4\text{He}^{2+}$ particles, accompanied by about 2.4 MeV of energy [38]. This strategy implies the synthesis of compounds bearing both boron atoms and a coordination site for an alpha emitting nuclide. A number of investigators have incorporated stable boron clusters into various carriers [39]. Boronic acid derivatives, which are usually less toxic than the corresponding carborane derivatives, are also attractive species for BNCT.

Thus, according to previous results concerning hanging carboxylate porphyrins such as **18**, porphyrin **26** was synthesized as a bismuth chelator and a boron carrier [40]. Hence, after reduction of the nitro functions of **19**, the atropisomer $\alpha\alpha$ **20** was separated by a silica gel column (Scheme 9.6). Acylation with 3-chloromethylbenzoyl chloride led to bis-picket porphyrin **21**, which was strapped by the reaction of diethylmalonate in the presence of sodium in THF. Deprotection of the hydroxy groups of **22** was performed with BBR_3 in methylene chloride with a concomitant hydrolysis of the ester functions, resulting in **23**. The acid functions of the latter had to be protected by reaction of 2-trimethylsilyl-ethanol in the presence of dicyclohexyl carbodiimide (DCC) and *N,N*-dimethylpyridin-4-amine (DMAP) in pyridine before further acylation of the hydroxy groups. Unexpectedly, this synthetic step resulted in a partial decarboxylation of the malonic system, leading to porphyrin **24**. Finally, acylation of **24** with boron substituted benzoyl chloride **ArCl** led to **25**, whose carboxylic ester was deprotected by reaction with TBAF in THF to afford the targeted molecule **26** bearing four Bpin groups and a hanging carboxylic strap to coordinate bismuth(III). The complexation of bismuth was achieved quantitatively in pyridine at room temperature with bismuth nitrate and monitored as usual by the appearance of the absorption at 479 nm, characteristic of the hyper type spectrum of bismuth porphyrins. As the solid state structure of **18Bi** (Figure 9.13a) indicated an η^2 -carboxylato coordination of the intramolecular hanging carboxylate group, and considering the identical structure of the strap in **26Bi**, it was assumed that such an intramolecular coordination also occurs in **26Bi**. Both the fast kinetics of bismuth insertion and the relative stability of the resulting complex in organic solvents of **26Bi** are comparable with those of succinic acid picket porphyrins, and are consistent with a bismuth coordination assisted by the strap of porphyrin **26Bi**. Although the number of boron atoms in **26** is not sufficient to obtain a therapeutic effect, the possibility of having the two functionalities on one porphyrinic chelate has been demonstrated.

9.5 Future Strategies Towards Bifunctional Chelates (BFC) - Conclusions

The above mentioned results about the coordination chemistry of porphyrin **18** directly imply two different orientations in the design of future bifunctional chelates based on the porphyrin macrocycle. First, based on the structure of **18Bi**, it is obvious that only one strap is sufficient to stabilize bismuth(III), and therefore, a synthetic strategy that spares one side of the porphyrin for other purposes as a linker for a biological vector will be adequate. Second, on the track to design an in-situ lead/bismuth generator, the X-ray structure of **18Pb₂** rules out the use of a symmetrical bis-strapped porphyrin. Indeed, in this strategy, the lead atom is expected to disintegrate in bismuth via a β emission and therefore, the chelate has to complex only one lead cation and only one bismuth cation. On the other hand, the bis-strapped porphyrins could be adequate structures to resist the β -emission resulting from the transformation of lead into bismuth. Therefore, a very fine tuning of the ligand will be needed but a porphyrin macrocycle, properly functionalized, may exhibit the correct conformation to stabilize both elements, for which the influence of the lone pair is crucial with structures detailed here above.



Scheme 9.6 Synthesis of porphyrins bearing four Bpin residues. Reagents and conditions: (i), SnCl_2 , HCl , 80%; (ii), silica gel chromatography, CH_2Cl_2 , 40%; (iii), 3-(chloromethyl)benzoyl chloride (3 eq), NEt_3 , THF , 85%; (iv), $\text{CH}_2(\text{CO}_2\text{Et})_2$ (10 M equivalent), THF , EtONa , room temp., 12 h, 53%; (v), BBr_3 , CH_2Cl_2 , room temp., 12 h, 97%; (vi), DCC (20 equiv.), DMAP (20 M equivalent), 2-(trimethylsilyl)ethanol (100 M equivalent), pyridine, 0°C , 18%; (vii), ArCl (20 M equivalent), NEt_3 , THF , 2 h, 38%; (viii), TBAF , THF , room temp., 12 h, 70%, \rightarrow **26**; (ix), $\text{Bi}(\text{NO}_3)_3$ (1.25 M equivalent), pyridine at room temperature for 30 min, quantitative yield. (Reproduced with permission from the Society of Porphyrins & Phthalocyanines. Copyright © 2007 Society of Porphyrins & Phthalocyanines)

Various developments including the water solubility of porphyrins have to be further studied but the chemistry of meso-tetraaryl porphyrins should allow correct functionalizations to synthesize water soluble chelates, simultaneously preserving the different spheres of coordination described in this chapter.

References

- Hassfjell, S. and Brechbiel, M.W. (2001) *Chemical Reviews*, **101**, 2019–2036.
- Barbe, J.-M. and Guillard, R. (2000) *The Porphyrin Handbook*, vol. **3** (eds K.M. Kadish, K.M. Smith, and R. Guillard) Academic Press, Boston, pp. 211–244, Coordination Chemistry.
- Karacay, H., McBride, W.J., Griffiths, G.L. *et al.* (2000) *Bioconjugate Chemistry*, **11**, 842–854.
- Treibs, A. (1969) *Justus Liebigs Annalen der Chemie*, **728**, 115–148.
- Buchler, J.W. and Lay, K.L. (1974) *Inorganic & Nuclear Chemistry Letters*, **10**, 297–300.
- Sayer, P., Gouterman, M., and Connell, C.R. (1982) *Accounts of Chemical Research*, **15**, 73–79.
- Chacko, G.-P. and Hambright, P. (1994) *Inorganic Chemistry*, **33**, 5595–5597.
- Michaudet, L., Fasseur, D., Guillard, R. *et al.* (2000) *Journal of Porphyrins and Phthalocyanines*, **4**, 261–270.
- Boitrel, B., Breede, M., Brothers, P.J. *et al.* (2003) *Dalton Transactions*, 1803–1807.
- Halime, Z., Michaudet, L., Razavet, M. *et al.* (2003) *Dalton Transactions*, 4250–4254.
- Farrugia, L.J. (1997) *Journal of Applied Crystallography*, **30**, 565.
- Shannon, R.D. (1976) *Acta Crystallographica*, **A32**, 751–767.
- Boitrel, B., Halime, Z., Michaudet, L. *et al.* (2003) *Chemical Communications*, 2670–2671.
- Liu, S. and Edwards, D.S. (2001) *Bioconjugate Chemistry*, **12**, 7–34.
- Halime, Z., Michaudet, L., Lachkar, M. *et al.* (2004) *Bioconjugate Chemistry*, **15**, 1193–1200.
- Collman, J.P., Bröring, M., Fu, L. *et al.* (1998) *The Journal of Organic Chemistry*, **63**, 8082–8083.
- Hermanson, G.T. (1996) *Bioconjugate Techniques*, Academic Press, New York.
- Bedel-Cloutour, C.H., Maneta-Peyret, L., Pereyre, M., and Beziau, J.H. (1991) *Journal of Immunological Methods*, **144**, 35–41.
- Halime, Z., Lachkar, M., Furet, E. *et al.* (2006) *Inorganic Chemistry*, **45**, 10661–10669.
- Smith, G., Kennard, C.H.L., and Katekar, G.F. (1983) *Australian Journal of Chemistry*, **36**, 2455–2463; Cauvin, C., Le Bourdonnec, B., Norberg, B. *et al.* (2001) *Acta Crystallographica*, **C57**, 1330–1332.
- Michaudet, L., Halime, Z., Lachkar, M., and Boitrel, B. (2006) *Letters in Organic Chemistry*, **3**, 753–758.
- Didier, A., Michaudet, L., Ricard, D. *et al.* (2001) *European Journal of Organic Chemistry*, **10**, 1917–1926.
- Young, R. and Chang, C.K. (1985) *Journal of the American Chemical Society*, **107**, 898–909.
- Halime, Z., Balieu, S., Lachkar, M. *et al.* (2006) *European Journal of Organic Chemistry*, **5**, 1207–1215.
- Lamparth, I. and Hirsch, A. (1994) *Journal of the Chemical Society. Chemical Communications*, 1727–1728.
- Smith, K.M. (1975) *Porphyrins and Metalloporphyrins*, Elsevier, Amsterdam.
- Boitrel, B., Baveux Chambenoit, V., and Richard, P. (2001) *European Journal of Organic Chemistry*, **22**, 4213–4221.
- Halime, Z., Lachkar, M., Roisnel, T. *et al.* (2007) *Inorganic Chemistry*, **46**, 6338–6346.
- Ehlinger, N. and Scheidt, W.R. (1999) *Inorganic Chemistry*, **38**, 1316–1321.
- Mirzadeh, S., Kumar, K., and Gansow, O.A. (1993) *Radiochim Acta*, **60**, 1–10.
- Barkigia, K.M., Fajer, J., Adler, A., and Williams, G.J.B. (1980) *Inorganic Chemistry*, **19**, 2057–2061.
- Plater, M.J., Aiken, S., Gelbrich, T. *et al.* (2001) *Polyhedron*, **20**, 3219–3224.
- Halime, Z., Lachkar, M., Roisnel, T. *et al.* (2007) *Angewandte Chemie-International Edition*, **46**, 5120–5124.

34. Buchler, J.W. (1975) *Porphyryns and Metalloporphyryns* (ed. K.M. Smith) Elsevier, Amsterdam, p. 157.
35. Tsutsui, M. and Taylor, G.A. (1975) *Porphyryns and Metalloporphyryns* (ed. K.M. Smith) Elsevier, Amsterdam, pp. 279–313.
36. Lai, J.-J., Khademi, S., Meyer, Edgar F. Jr *et al.* (2001) *Journal of Porphyryns and Phthalocyanines*, **5**, 621–627.
37. Barth, R.F., Coderre, J.A.H., Vicente, M.G., and Blue, T.E. (2005) *Clinical Cancer Research*, **11**, 3987–4002.
38. Hawthorne, M.F. (1998) *Molecular Medicine Today*, **4**, 174–181.
39. Renner, M.W., Miura, M., Easson, M.W., and Vicente, M.G.H. (2006) *Anti-Cancer Agents in Medicinal Chemistry*, **6**, 145–146.
40. Balieu, S., Bouraiou, A.M., Carboni, B., and Boitrel, B. (2008) *Journal of Porphyryns and Phthalocyanines*, **12**, 11–18.

10

Helicobacter pylori and Bismuth

Aruni H.W. Mendis¹ and Barry J. Marshall²

¹Manager Scientific & Regulatory Affairs, Tri-Med Australia, Subiaco,
Western Australia

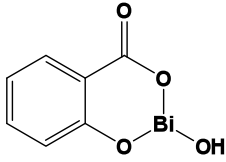
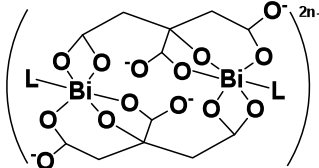
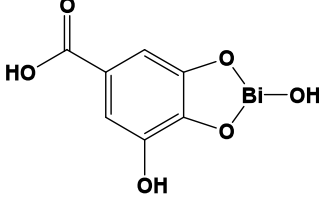
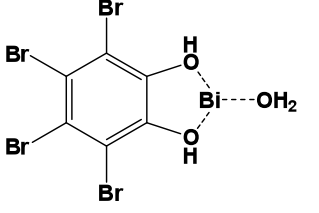
²Discipline of Microbiology and Immunology, School of Biomedical, Biomolecular and Chemical
Sciences, Faculty of Life and Physical Sciences, The University of Western Australia,
Crawley WA 6009, Australia

10.1 Introduction

Bismuth was confused in early times with tin and lead because of its resemblance to those elements [1]. The element was discovered by the Muslim alchemist, Jabir ibn Hayyan (also known as *Geber*), in the eighth-century [2, 3]. ‘Artificial bismuth’ was commonly used in place of the genuine metal. It was made by hammering tin into thin plates, and cementing them with a mixture of white tartar, saltpeter, and arsenic, stratified in a crucible over an open fire. Bismuth was also known to the Incas and used (along with the usual copper and tin) in a special bronze alloy for knives [1].

The use of bismuth compounds in medicine can be traced back to the Middle Ages. The first account of the use of bismuth as a therapeutic agent dates back to 1786 as reported by Louis Odier for the treatment of dyspepsia [4]. Presently, with the accumulation of knowledge of the properties and characteristics of elemental bismuth, many bismuth compounds have been synthesized and some have been found to have significant clinical and healthcare applications. Currently, the major medicinal use of bismuth compounds is focused in two broad areas, namely antimicrobial chemotherapy and anticancer chemotherapy [5].

Table 10.1 *Bismuth compounds used in medicine*

Name	Formula
Bismuth oxychloride	BiOCl
Bismuth subnitrate	$\text{Bi}_5\text{O}(\text{OH})_9(\text{NO}_3)_4$
Bismuth subcarbonate	$(\text{BiO})_2\text{CO}_3$
Bismuth subsalicylate	
Colloidal bismuth subcitrate (For 3D-Structure of Polymeric-form; see Figure 10.1)	
Bismuth subgallate	
Bibrocathol	

Bismuth oxychloride (BiOCl) is sometimes used in cosmetics (Table 10.1) [6]. Bismuth subnitrate ($\text{Bi}_5\text{O}(\text{OH})_9(\text{NO}_3)_4$) and bismuth subcarbonate ($\text{Bi}_2\text{O}_2(\text{CO}_3)$) are used in medicine. Bismuth subcarbonate sometimes designated as $(\text{BiO})_2\text{CO}_3$ is a chemical compound of bismuth containing both oxide and carbonate anions: in this case bismuth is in the +3 oxidation state. Bismuth subcarbonate occurs naturally as the mineral bismutite [6]. Its structure consists of Bi-O layers and BiCO_3 layers and is related to kettnerite (formula: $\text{CaBi}(\text{CO}_3)\text{OF}$). It is highly radiopaque and for example is used as a ‘filler’ in radiopaque catheters which can be seen by X-ray [7]. In modern medicine, bismuth subcarbonate has been made into nanotube arrays that exhibit antibacterial properties [8]. It was also a constituent of ‘milk of bismuth’ which was a popular ‘snake oil’ in the 1930s [9]. Bismuth subsalicylate (Table 10.1), the active ingredient in Pepto-Bismol and Kaopectate, is used as an antidiarrheal and to treat some other gastrointestinal diseases. Also, the product

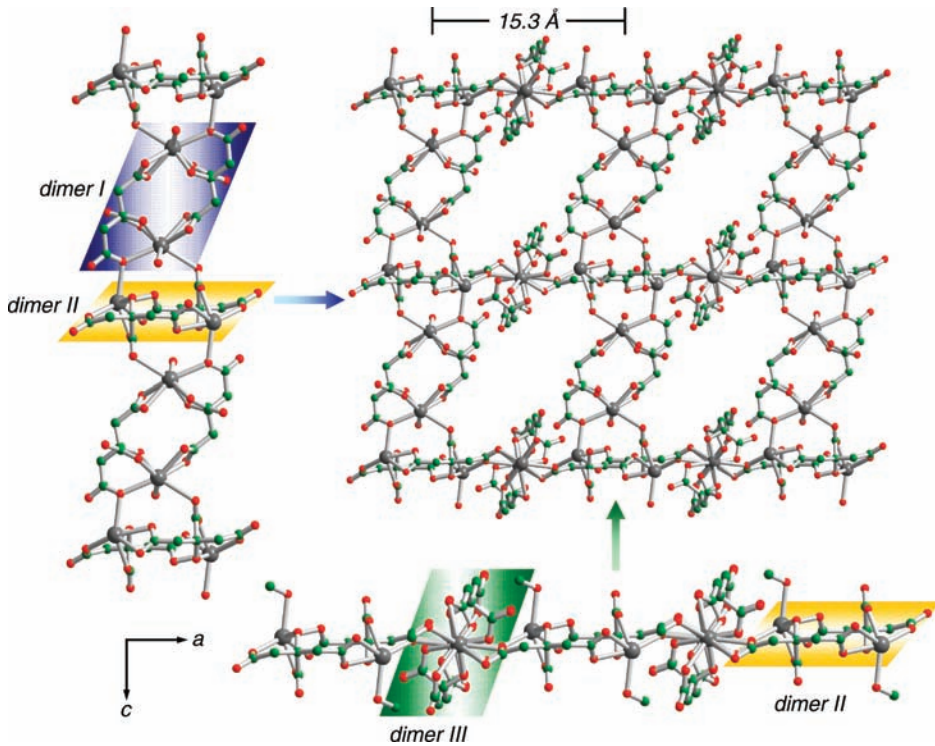


Figure 10.1 Projection of the X-ray structure of complex 1 down the *b* axis. The polyanionic chain of $[\text{Bi}(\text{cit})_2\text{Bi}]^{2-}$ was formed by the aggregation of dimers I and II along the *c* axis, and the aggregation of dimers II and III along the *a* axis. All potassium and ammonium ions, hydrogen atoms, and free lattice water molecules are omitted for clarity (courtesy of H Sun, University of Hong Kong, P.R. China)

Bibrocathol (INN, trade names Noviform and Posiformin; chemical name: 4,5,6,7-tetra-brom-1,3,2-benzodioxabismol-2-ol) is an organic molecule containing bismuth and is used to treat eye infections. Bismuth subgallate (the active ingredient in Devrom) is used as an internal deodorant to treat malodor from flatulence (or gas) and feces [6]. The X-ray structure of the aggregation complex formed *in vivo* on administration of colloidal bismuth subcitrate is shown in Figure 10.1.

10.2 *Helicobacter pylori*

Helicobacter pylori (*H. pylori*) is the type species of the new genus helicobacter [10]. As shown in Figure 10.2, *Helicobacters* are curved or spiral, Gram-negative and flagellated [11]. These are the general characteristics of most mucus associated intestinal bacteria. Figure 10.3 shows an electron micrograph of *H. pylori* on the mucosal surface of the stomach.

H. pylori grow best in an atmosphere of reduced oxygen (5–15%) with added carbon dioxide (CO_2). These conditions are easily obtained in the laboratory by use of

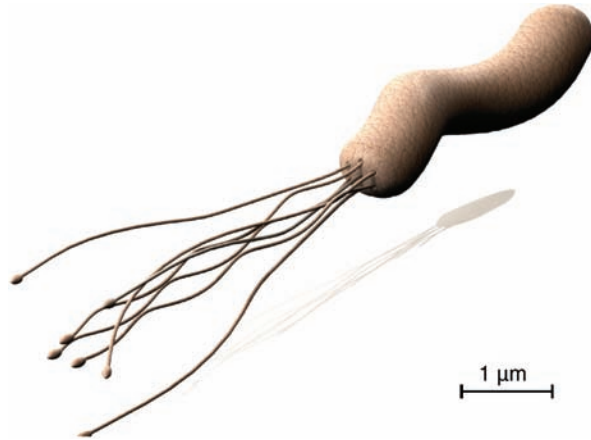


Figure 10.2 A digital construct of *H. pylori* to scale. Note the presence of seven flagella. The bacterium is $3.6\ \mu\text{m}$ long and $0.6\ \mu\text{m}$ thick with 1.5 wavelengths

Campylobacter atmosphere generation kits, or carbon dioxide incubators [12]. Ideal temperature is 37°C rather than the higher temperature (42°C) required by the campylobacters. *Helicobacters* have been separated from *Campylobacters* based on their sheathed flagella, unique fatty acid profiles, different respiratory quinones and very different 16SRNA sequences. *H. pylori* is therefore more related to the genus *Wollinella*, commensals of the cow rumen [13].

Although no ideal animal model exists for *H. pylori* and peptic ulcers, Koch's postulates have been fulfilled for *H. pylori* and gastritis in gnotobiotic pigs [14], mice [15] and monkeys [16]. Importantly, *Helicobacter felis*, the organism initially cultured from cats, can colonize the stomach of mice where it causes chronic gastritis, atrophic gastritis and

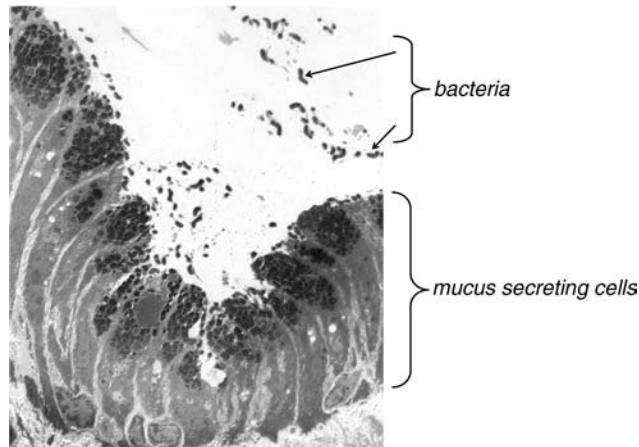


Figure 10.3 Photomicrograph of *H. pylori* on mucosa (courtesy of J.R. Warren and John Armstrong, Royal Perth Hospital, Western Australia)

possibly even premalignant changes. *H. pylori* is usually acquired in childhood, probably from infected parents and siblings, but perhaps also via fecal contamination of drinking water or the environment. When ingested, the bacterium is able to survive in gastric acid because its urease enzyme hydrolyses urea in gastric secretions and generates ammonia and bicarbonate [17], which provide an alkaline microenvironment in which the organism thrives. Detection of this urease allows simple and accurate diagnosis of HP via rapid urease biopsy tests (CLOtest) and the urea breath tests [18, 19].

The acute infection causes gastric inflammation of the whole stomach, a condition which is associated with parietal cell failure and acute achlorhydria [20]. In most cases, a mild vomiting illness which lasts a few days occurs. After the acute episode, patients return to an asymptomatic state. Acid secretion may remain low or absent for many months until the patient is able to clear most of the organisms from the body of the stomach. The mature stage of the illness is when HP causes a chronic inflammation localized to the lower part of the stomach (antral gastritis) and in the duodenal bulb (duodenitis). The upper half of the stomach is less severely involved and acid secretion returns to normal or even to high levels. This is the stage at which the patient is susceptible to peptic ulceration. Lifelong inflammation may eventually cause replacement of normal gastric mucosa with intestinal mucosa and, as a result, acid secretion fails. These changes may be precursors to gastric adenocarcinoma [21].

10.2.1 Disease Associations and Clinical Manifestations

10.2.1.1 Duodenal and Gastric Ulcer

The most obvious disease associated with HP is peptic ulceration. More than 90% of duodenal ulcers (DU) are associated with HP. When a patient with a DU does not have HP, etiologic factors such as Zollinger Ellisson syndrome or non steroidal inflammatory drug (NSAID) use are likely [22]. In gastric ulcer, two causes prevail, and many patients will exhibit both. Most gastric ulcers have HP which can be identified by presence of the bacterium and/or chronic gastritis. The stomach is also directly exposed to ingested agents such as NSAID and is more likely than the duodenum to ulcerate in response to these agents. Therefore, in the United States, about 50% of gastric ulcers are not associated with histological chronic gastritis or HP but are caused by NSAID. Other etiologies can also be suspected or proven by the histological appearance of the mucosa; Zollinger Ellisson syndrome and gastric cancer being two less common causes of gastric ulcer.

10.2.1.2 Adenocarcinoma

The incidence of this lesion has declined in the United States since 1930. At that time it was the most common cancer but now it ranks about ninth. The current incidence is only six per 100 000 persons per annum, a decline from 50 in 1930 [23]. Worldwide, gastric cancer is the second most common cancer, with high prevalence areas being Brazil, Colombia, Korea, China and Japan. HP infection affects more than half the population in all these countries. In an extensive review of gastric cancer and HP [24], the Eurogast Study Group determined that presence of HP confers an approximately six-fold risk of gastric cancer, accounting for at least half of all gastric cancers.

10.2.1.3 Lymphoma

In the initial report of the association, Wotherspoon *et al.* found that 92% of 110 mucosa associated lymphoid tissue (MALT) lymphomas were associated with HP compared with 50% of control cases [25]. Subsequent reports suggest that these tumors are sometimes driven by continuing HP antigenic stimulus and regress when HP is treated [26, 27]. In a recent study the German MALT-Lymphoma Study Group reported that apparent cure of MALT lymphoma occurred in half of the patients in whom HP was eradicated [28]. HP therapy is the initial step in the treatment of proven or suspected gastric lymphoma.

10.3 Bismuth as an Antimicrobial Agent

Bismuth compounds have been successfully utilized in the treatment of a spectrum of prokaryotic infections such as syphilis (sodium/potassium bismuth tartrate, bismuth quinone iodide, iodobismutol, bismuth chloride, etc.), colitis (bismuth subnitrate, bismuth citrate), skin-wound infections (bismuth oxide), quartan malaria (sodium bismuth thioglycolate), dyspepsia (bismuth subsalicylate, bismuth subnitrate, etc.), diarrhea (bismuth subsalicylate, bismuth nitrate, etc.) and peptic ulcers (colloidal bismuth subcitrate, bismuth citrate, bismuth subnitrate) [29, 30]. Three bismuth compounds, bismuth subsalicylate (BSS, Pepto-Bismol; the Procter & Gamble Company, Cincinnati, Ohio, USA), colloidal bismuth subcitrate (CBS, De-Nol; Gist Brocades and Yamanouchi), and ranitidine bismuth citrate (RBC, Tritec and Pylorid, GSK) are used worldwide to treat various gastrointestinal diseases which, we now recognize to be related to the infection of *Helicobacter pylori* (*H. pylori*, first discovered in 1983). A new complex of bismuth with *d*-polygalacturonic acid, the so called ‘colloidal bismuth pectin’, was approved for clinical use in China for the treatment of peptic ulcers [31].

10.3.1 Bismuth Subsalsicylate (BSS)

Marshall *et al.* were the first to note the antibacterial effects of bismuth citrate [32], CBS and other bismuth compounds on *Helicobacters* specifically *H. pylori*. Figure 10.4 shows the effect of bismuth on a culture of *H. pylori*. This leads to a clear understanding on the efficacy of bismuth compounds in the treatment of peptic ulcer disease reported in earlier studies [33, 34]. Prior to the study of Marshall *et al.* in 1985, extensive animal and clinical studies suggested that BSS was also effective in the treatment of a wide variety of diarrheal disorders [35–38]. BSS has been demonstrated to exhibit *in vitro* bactericidal activity against enterotoxigenic *E. coli* [39], and its effectiveness both in the prevention and treatment of travelers’ diarrhea is well documented [38].

Graham *et al.* reported that 600 mg BSS (equivalent to about 35 ml of Pepto-Bismol) administered eight and two hours prior to the challenge and two and four hours after the challenge, afforded prophylactic efficacy in 75% ($P < 0.03$) of the subjects [39]. Steffen has compared the efficacy of BSS in the treatment of travelers’ diarrhea with other antidiarrheal agents including loperamide, cotrimoxazole, doxycycline, mecillinam, and *Streptococcus faecium* SF 68 in a total of 2520 individuals involving four randomized studies [40]. Subjects took medication only if diarrhea occurred, and a total of 530 individuals were evaluated in the study. Around half of the subjects (47%) have symptoms relieved within

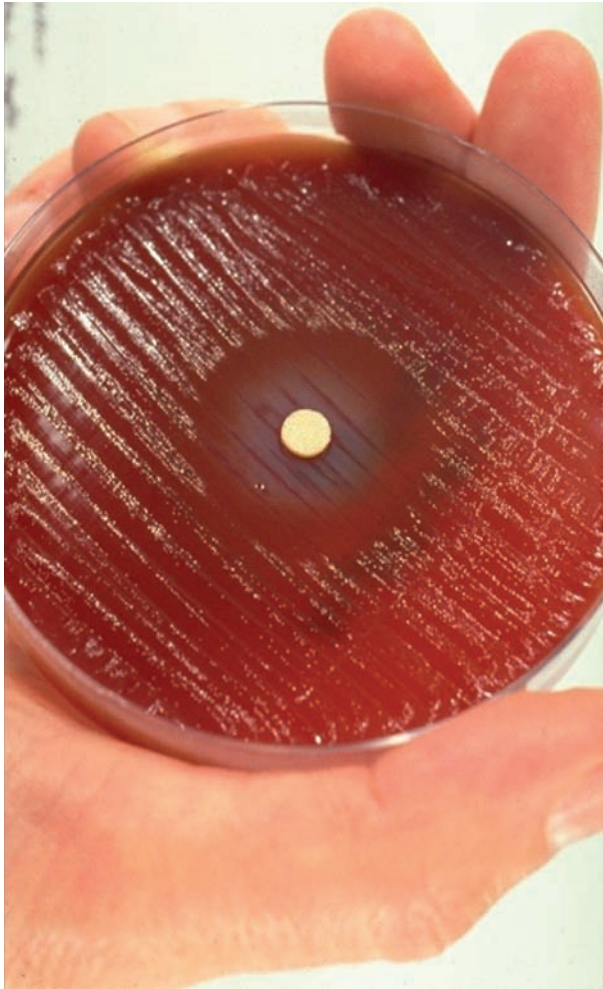


Figure 10.4 The *in vitro* effect of bismuth on an *H. pylori* culture

eight hours of BSS being administrated, while 25% to 49% of other antidiarrheal agents administrated for eight hours, in particular placebo exhibits effectiveness only in 18% of the subjects.

Prior to recognition of the etiological role of *Helicobacter* (formerly *Campylobacter*) *pylori* in gastric and peptic ulcer disease, there were only limited studies on utilizing bismuth subsalicylate (BSS) to treat disorders of the upper gastrointestinal tract in humans. In 1976, in a placebo controlled study, Goldenberg *et al.* demonstrated that BSS had antiemetic properties in dogs, and was an antinauseant and antiemetic in humans [41]. Previously, they had also demonstrated that Pepto-Bismol prevented alcohol, aspirin and cold restraint stress related gastric erosions in rats [42].

In 1984, Halley and Newsom compared the efficacy of BSS with placebo in the treatment of patients with chronic dyspepsia with BSS and the dosage used was 30 ml of BSS or



Figure 10.5 Electron micrograph of *H. pylori* obtained from stomach biopsy 30 min after oral treatment of patient with bismuth medication. Note the dark dots around the bacterium, indicative of bismuth precipitation in these regions

placebo at the onset of symptoms, followed by 30 ml every 30 min up to a maximum of eight doses. The results showed that BSS was more effective than placebo in relieving symptoms of nausea, heartburn, flatulence, sense of illness and abdominal distension [43]. Gryboski *et al.* reported that BSS was also effective in the therapy of infants and children with chronic diarrhea of diverse etiologies [44]. In their study, 29 children at age of 2–70 months were treated in double-blind fashion with BSS or placebo. The BSS treated group had significantly fewer stools with less water content, and had significant improvement in clinical status compared with the placebo treated group. BSS has also been reported to be effective in the treatment of acute diarrhea caused either by rotavirus or bacteria in children [45].

Several mechanisms apparently contribute to the effectiveness of bismuth subsalicylate in the treatment of diarrhea. Ericsson and colleagues reported that BSS significantly reduced the toxin secretory activity of *E. coli* and *Vibrio cholera* [36]. They demonstrated that Pepto-Bismol binds cholera toxin *in vitro* and reduces accumulation of fluid in secretory, and inflammatory diarrhea.

In vitro bactericidal activity of BSS against enterotoxigenic *E. coli* and other enteropathogens has been demonstrated by several investigators [36, 42]. The beneficial effect of BSS in childhood diarrhea of diverse etiologies has been demonstrated, and BSS was found to effectively eradicate enterotoxigenic *E. coli* and other enteropathogens from the stools of the infected children [42]. Moreover, the beneficial effect of BSS in a hamster model of *C. difficile* colitis has also been reported recently [46], and BSS has marked *in*

vitro antibacterial action against *C. difficile* with a very low inhibitory concentration (MIC_{90} – minimum inhibitory concentration to kill 90%, of organisms) of 128 $\mu\text{g/l}$ [47], and a low MIC_{90} values against *B. fragilis*.

Marshall *et al.* have reported relatively low MIC values of colloidal bismuth subcitrate against *C. difficile* [48]. Sox and Olson demonstrated that BSS was able to bind bacteria of diverse species based on *in vitro* studies, and such bound bacteria were subsequently killed [49]. Moreover, the intracellular ATP concentration decreased rapidly upon exposure of *E. coli* to 10 mM BSS, and the ATP content was only 1% of its original level after 30 min exposure to the metalloidrug. However, the extracellular ATP content increased after exposure to BSS, but the increase in extracellular ATP was not sufficient to account for the loss of intracellular ATP. They postulated that the bactericidal activity of BSS is likely attributed to cessation of ATP synthesis or to a loss of membrane integrity.

The salicylate component of BSS may contribute to its effectiveness in the treatment of diarrhea. Burke and Gracey *et al.* demonstrated that salicylates are capable of antagonizing or abrogating toxin induced intestinal secretion produced by a wide range of organisms including *E. coli*, *Shigella* and *Salmonella* [50]. Additionally, Manhart demonstrated that sodium salicylate, a hydrolysis product of BSS that is formed in the gut, had demonstrable antibacterial activity [51].

10.3.2 Colloidal Bismuth Subcitrate (CBS)

A colloidal suspension of bismuth subcitrate (CBS) is available as De-Nol in many countries (except in the United States) for the treatment of peptic ulcer. Its efficacy and safety in ulcer healing have been well demonstrated in a number of studies. The introduction of swallowable/chewable tablets has improved patient compliance since these preparations successfully mask the unpleasant ammonia like taste of the liquid formulation [52].

CBS shares with other bismuth preparations an antibacterial action against *H. pylori*. In addition, there is *in vitro* evidence that CBS contributes to inhibition of hydrogen ion passage through the gastric mucus [53]. CBS has also been shown to increase the prostaglandin content of rat gastric mucosa and to increase mucosal bicarbonate secretion [54, 55]. These cytoprotective mechanisms are thought to assist the ability of CBS to heal peptic ulcers and to protect against mucosal damage from aspirin, alcohol, acetic acid, and cold immobilization [56].

10.3.2.1 CBS, H_2 -Receptor Antagonists (H_2RA 's) and their Efficacy Against *H. pylori*

The important role of *H. pylori* in the etiology of gastritis and peptic ulcer disease has resulted in an important application of bismuth in the therapy of these disorders. Since the discovery of the role of *H. pylori* in the etiology of peptic ulcer disease and the antibacterial action of bismuth compounds by Marshall *et al.*, a number of studies appeared to demonstrate the healing equivalence of CBS and the histamine H_2 -receptor antagonists (H_2RA) [32]. It was reported that CBS is superior to cimetidine in six out of seven studies and equivalent to cimetidine in one study [57].

Although the difference was not statistically significant for each individual study, CBS had a significantly better healing rate when combining all the experimental data. When

ranitidine was compared with CBS, there was no difference in healing rate between the two groups [58]. Healing rates of CBS and cimetidine were found to be 93% and 86% respectively in an eight week therapy [57].

10.3.2.2 Relapse Rates of *H. pylori* Observed with CBS and H₂RAs

Although ulcer healing rates are similar for CBS and the H₂RAs, a difference in relapse rates has been observed after administration of the two agents. This was demonstrated with cimetidine by Martin *et al.* [58] and with ranitidine by Lee and Samloff [59]. Whether or not *H. pylori* was eradicated or suppressed appears to be significant in determining the relapse rate. When *H. pylori* persists, the relapse rate with any acute therapy is about 85%, whereas is less than 20% when *H. pylori* has been cleared [60, 61].

In a clinical and histologic study in 50 evaluable patients with *H. pylori* and non ulcer dyspepsia, McNulty *et al.* employed regimens of placebo, erythromycin ethylsuccinate syrup, or BSS (Pepto-Bismol) for 21 days [62]. At the end of therapy, clearance of *H. pylori* was achieved in 78% (14/18), 7% (11/15) and 0% (0/17) of patients taking BSS, erythromycin and placebo respectively. There was histological improvement of the gastritis in 81% (13/16) of patients taking BSS, 23% (3/13) of patients on erythromycin and in none of the placebo treated patients. All differences amongst BSS, erythromycin and placebo were highly significant. Symptomatically, 92% and 66% of the patients on BSS and placebo showed improvement respectively, indicating statistically non significant difference between the two drugs.

Follow up studies on some of these patients revealed that at four weeks, virtually all of the patients who had been initially cleared of *H. pylori* showed evidence of persistence of the organism and a return of the histology to baseline levels [63]. Twelve to 18 months after treatment, McNulty performed a follow up examination on 10 of the 15 patients cleared of *H. pylori* [62]. Eight patients had evidence of *H. pylori* infection with six of them having histologically proven gastritis. Only two patients were still clear of *H. pylori*; neither had histologically confirmed gastritis. When recrudescence of colonization with *H. pylori* occurs, the original *H. pylori* strain has been shown to be responsible for the recurrence. This has been demonstrated by restriction endonuclease analysis of the bacterial DNA [64]. McNulty *et al.* stated that the site and mechanism of the dormancy of the organism remains undetermined [62]. Whereas symptom improvement is dramatic for ulcer sufferers when *H. pylori* is eradicated, treatment of 'non ulcer' dyspepsia (gastritis) only cures about 20% of symptomatic patients.

10.4 Mechanism of Action of Bismuth Citrate and CBS on *H. pylori* and Ulcer Healing

In the pioneering study where Marshall *et al.* tested the *in vitro* effects of several antibiotics and bismuth citrate on pyloric campylobacter isolates, penicillin, erythromycin, and tetracycline were found to be 100% effective (53/53) against all isolates tested [32]. Tinidazole and metronidazole were 70% (28/39) and 90% (1/12) effective while rifampicin was only 50% effective (15/30). In contrast, gentamicin (13/13), cephalothin (13/13) and bismuth citrate (30/30) were 100% effective against the tested isolates.

Later in 1987, Marshall *et al.* conducted a study based on the analysis of sequential endoscopic biopsies resected from patients after treatment [48]. At the outset, cimetidine and CBS were compared for their effects on CP and gastric histopathology. It was known that colloidal bismuth subcitrate (CBS, De-Nol) heals duodenal ulcers but with a lower relapse rate than cimetidine, perhaps due to inhibition of *Campylobacter pyloridis* (CP) organisms.

In the same study Marshall *et al.* evaluated the outcome of patients receiving different forms of combination therapy aimed at achieving long term, or permanent, eradication of the gastric organism. In parallel with the clinical studies, they observed the *in vitro* effect of bismuth compounds on cultures of CP and other bacteria, and evidence was sought for direct effects of bismuth on CP organisms *in vivo* and on affected epithelial cells using electron microscopy of biopsy specimens obtained shortly after the administration of oral bismuth medications.

Cimetidine had no effect on CP or gastric mucosal histology, but with CBS therapy there was a significant reduction in the number of bacteria ($p < 0.0001$). However, relapse of both CP infection and gastritis usually occurred once CBS was withdrawn. The fecal bismuth concentration found in patients taking regular doses of CBS indicates that any gut organism with an MIC less than 4000 mg/l would be vulnerable to the drug. When CBS was combined with amoxicillin or tinidazole, long term disappearance of both CP bacteria and gastritis was achieved ($p < 0.0001$).

In ultrastructural studies for 30–90 min after single oral doses of CBS or bismuth subsalicylate, CP had detached from the gastric epithelial cells and exhibited structural degradation associated with the selective deposition of a micro-particulate bismuth complex within and on the surface of the organisms (Figure 10.5). The ‘bismuth mirrors’ observed in their Petri dishes led them to suspect that bismuth may similarly be subject to precipitation in the human stomach colonized by CP organisms.

In vitro, CP and other campylobacters were inhibited by bismuth compounds at 25 mg/l but they were resistant to cimetidine and ranitidine. CBS has a powerful antibacterial effect against CP but relapse of infection is common after treatment using CBS alone. In combination with antibiotics however, eradication of CP and long term healing of gastritis occurs. In such cases the gastroduodenal mucosa is intact, and less likely to ulcerate.

Reviewing the subject, Wagstaff *et al.* stated that although the precise mechanism by which CBS heals ulcers has not been fully elucidated, several actions might be involved [53]. They pointed out that CBS and mucus form a glycoprotein-bismuth complex *in vitro*, which provides a diffusion barrier to hydrochloric acid (HCl) and may, therefore, provide a ‘protective coating’ in the ulcer crater, which allows healing of the lesion to occur. Prostaglandin E2 production is also stimulated by CBS with subsequent secretion of alkali into the mucus layer. In addition, CBS has a direct inhibitory effect on *C. pylori*. Administration of CBS results in low levels of bismuth absorption. Most of the ingested bismuth is excreted as bismuth sulfide, causing (harmless) blackening of the faeces, and the small amount absorbed is excreted in the urine.

Stiel *et al.* also states that although the mode of action of CBS is incompletely understood, there is evidence that it acts topically as a diffusion barrier to hydrochloric acid at the ulcer base and impedes proton back diffusion into gastric mucosa [65, 66]. Its efficacy requires an acidic pH, at which it forms an insoluble precipitate [67]. It has been widely assumed that

the bismuth is not absorbed from the gastrointestinal tract after administration of colloidal bismuth subcitrate [68]. Studies in laboratory animals, however, reveal detectable concentrations of bismuth in several organs after long term high dose colloidal bismuth subcitrate administration. Low (subtoxic) bismuth concentrations have also been reported in the blood and urine of human volunteers and patients with peptic ulcers after colloidal bismuth subcitrate therapy for several weeks [69]. It is clear, therefore, that some gastrointestinal absorption of bismuth occurs after administration of colloidal bismuth subcitrate.

The results of Stiel *et al.* show uptake of bismuth by both gastric and small intestinal mucosa within 24 h of administration of colloidal bismuth subcitrate [65]. This represents intramucosal uptake and not simply adherence of bismuth to the surface mucus, as the tissue was meticulously rinsed and no measurable amounts of the non absorbable tracer could be detected in the homogenates. It should be pointed out, however, that the doses of colloidal bismuth subcitrate used in this study were high, and that gastrointestinal luminal concentrations of bismuth in this study almost certainly exceeded those achieved therapeutically in ulcer patients.

The relatively lower bismuth concentrations, in gastric compared with small intestinal mucosa, may have resulted from different yields of mucosa and submucosa during tissue harvesting. A more likely explanation, however, is that precipitation of colloidal bismuth subcitrate occurred within the acidic gastric lumen. In contrast, the pH within the intestinal lumen is generally above 4.5 (the pH below which precipitation of colloidal bismuth subcitrate occurs).

Wieriks found bismuth to be present in the stomach, duodenum, and cecum of rats and dogs after several months of daily dosing with colloidal bismuth subcitrate [70]. In this study, however, bismuth content of the entire wall of the intestine (including adherent mucus) was measured and no comment was made about mucosal bismuth concentration. Steil *et al.* also reported that the bismuth content of antral and duodenal mucosa fell progressively over 72 h after cessation of colloidal bismuth subcitrate administration, which could be explained either by gradual systemic absorption of bismuth from the mucosa, or by shedding of bismuth containing cells or their constituents into the lumen during crypt-to-villus maturation [71].

Although blood bismuth concentrations were not measured in their study, the results of the subcellular fractionation experiments clearly show the presence of bismuth within duodenal enterocytes from which it could be absorbed into the circulation. An electron microscopic study by Coghill suggests that bismuth is phagocytosed by duodenal epithelial cells and accumulates in multivesicular bodies (possibly lysosomes) [72]. Stiel *et al.* suggested that this was more indicative of localization to the brush border membrane and cytosol of the enterocyte. Accumulation in the brush border membrane could be in line with the claims that colloidal bismuth subcitrate stimulates mucus glycoprotein secretion and increases the thickness of the glycocalyx, though these findings have been disputed [73]. Moreover, accumulation of bismuth within gastrointestinal mucosal cells may exert as yet unknown influences on cellular functions. Heavy metals are well known modifiers of enzymes, and for example, bismuth has been shown to inhibit human intestinal alkaline phosphatase activity [74]. The anti ulcer effects of colloidal bismuth subcitrate may in fact be more complex than simple precipitation within the ulcer crater and further studies are needed to clarify the effect of this drug and of bismuth in particular, on brush border structure and function.

10.4.1 Bismuth Toxicity

Bismuth intoxication (encephalopathy) has been reported with prolonged administration of bismuth salts, and there has been one report of similar intoxication in a patient receiving unusually high doses of CBS for a prolonged period [52]. Concerns of bismuth toxicity arose due to experiences in France and Australia. In France, bismuth became a widely used gastrointestinal panacea during the 1970s. Bismuth subcarbonate, subgallate and subnitrate were commonly consumed in doses up to 20 g of elemental bismuth per day [75], which led to an epidemic of 'bismuth encephalopathy' between 1973 and 1977, resulting in fatalities.

In Australia, where high doses (3–20 g/day) of bismuth subgallate were widely used by patients with colostomies, 29 cases of encephalopathy were reported in patients who had taken the drug for between six months and three years [76]. Assessment of the French and Australian data revealed that prolonged use of high doses (> 1.5 g of bismuth/day) yielded bismuth toxicity. Serum levels of bismuth in toxic patients often reached 150–4000 µg/l (150–4000 ppb of whole blood), while the usual therapeutic dose of bismuth (< 1.5 g/day) in normal subjects exhibited levels of 15–35 µg/l after two months of use.

Restrictions on the use of bismuth in France and the banning of the use of bismuth subgallate in Australia have virtually eliminated further cases of bismuth toxicity. There have been no documented cases of bismuth toxicity with the recommended acute dosages of either bismuth subsalicylate or colloidal bismuth subcitrate. A single case of encephalopathy associated with BSS has been reported in Australia [77]. The diabetic patient had been taking BSS continuously for over a year, much longer than the customary short duration of BSS therapy, and for a period of time for which there is little experience with BSS.

However, no such intoxication has been reported with CBS used at its recommended dosage in the acute treatment of peptic ulcer disease, and no other serious adverse effects have been associated with CBS. Tissue accumulation during prolonged therapy seems likely, and the safety of CBS during long term maintenance therapy has not been established. The lack of effect on gastric acid secretion is observed as an additional advantage for CBS, since prolonged drug induced hypochlorhydria has been postulated to have potentially detrimental effects. Thus, while the role of *C. pylori* in peptic ulceration requires further clarification, CBS would appear to play an important role in the treatment of peptic ulcer disease with the advantage of relatively slow relapse rates after initial healing and treatment discontinuation [53].

10.5 *In Vitro* Susceptibility of *H. pylori* and other Bacteria to Bismuth Compounds and Antibiotics

Bismuth subsalicylate (BSS) is a compound with almost no solubility in aqueous media but has been widely used for the treatment of gastrointestinal disorders. BSS is able to bind bacteria of diverse species, and these bound bacteria were subsequently killed [46]. A 4-log₁₀ reduction of viable bacteria occurred within 4 h after a 10 mM aqueous suspension of BSS was inoculated with 2×10^6 *E. coli* cells per ml.

Such binding and killing were dependent on the inoculum density of the bacteria, and significant binding but little killing of the exposed bacteria occurred at an inoculum level of 2×10^9 *E. coli* per ml. Intracellular ATP decreased rapidly after exposure of *E. coli* to 10 mM BSS and, after 30 min, and was only 1% of the original level. Extracellular ATP increased

after exposure to BSS, but the accumulation of extracellular ATP was not sufficient to account for the loss of intracellular ATP. The killing of bacteria exposed to BSS may have been due to cessation of ATP synthesis or a loss of membrane integrity.

In 1987 the *in vitro* susceptibility of several Danish human clinical isolates of *Campylobacter pyloridis* to cimetidine, sucralfate, bismuth subsalicylate and 16 antimicrobial agents was studied by Andreasen and Anderson [78]. The sensitivities were determined by an agar dilution technique. Benzylpenicillin was found to be the most active drug ($MIC_{90} = 0.1 \mu\text{g/ml}$); whereas ampicillin, erythromycin, gentamicin and ciprofloxacin were slightly less active. All strains were resistant to $100 \mu\text{g}$ sulfamethizole, and nalidixic acid also had exhibited little activity on weight basis. Of the three antipeptic ulcer drugs, bismuth subsalicylate was the most active one ($MIC_{90} = 25 \mu\text{g/ml}$), but sucralfate and cimetidine also had moderate (or low) antibacterial activity with MIC_{90} of $3200 \mu\text{g/ml}$.

More recently, Li *et al.* examined the mechanism of action of CBS which possibly involves the formation of bismuth citrate 'polymeric matrix' (Figures 10.1 and 10.2) by forming a coating on ulcer craters thereby protecting the ulcer from further erosion by the gastric acid and gastric proteases [79]. In fact, minute crystalline species have been observed in ulcer craters of animal models and patients after administration with colloidal bismuth subcitrate [80, 81].

10.6 The Effect of pH on Bactericidal Activity of Bismuth Compounds

Bactericidal activity of BSS was also investigated in a simulated gastric juice at pH 3. Killing of *E. coli* at this pH was much more rapid than at pH 7 and was apparently due to salicylate released by the conversion of BSS to bismuth oxychloride. It is proposed that both the binding and killing observed for BSS contribute to the efficacy of this compound against gastrointestinal infections such as traveler's diarrhea. Insoluble salts of bismuth have been extensively used as antimicrobial agents. The product containing bismuth subsalicylate (BSS) as the active ingredient has been shown to be clinically effective in the prevention and treatment of a number of gastrointestinal infections, including traveler's diarrhea [37, 39, 82] and *Campylobacter pylori* gastritis [83].

Despite a long history of therapeutic use of BSS and other bismuth compounds, relatively little is known about their antimicrobial mode of action. The bacteriostatic [45] and bactericidal [39, 84] activities of these compounds have been reported previously. Furthermore, electron microscopy of *C. pylori* present in gastric biopsies taken after oral administration of bismuth compounds indicated both intracellular and extracellular association of bismuth with *C. pylori* [48, 85]. In the meantime, bacteria lost adherence to the gastric epithelium, and structural degradation of the bacteria was evident. Although the antimicrobial mode of action of bismuth compounds has received relatively little attention, the actions of other metals have been examined extensively. For example, mercury exerts antimicrobial activity as a result of binding to sulfhydryl groups, that is, cysteine residue, on essential macromolecules [86]. Several other metals such as uranium [87] and nickel [88] are taken up in large quantities by microorganisms; these metals do not covalently bind to the cells, and viable cells are not needed for this uptake to occur. *Micrococcus luteus* and an *Azotobacter sp.* were reported to bind large amounts of lead [89] with no effect on their growth rate or viability.

In addition to antimicrobial properties of Bi^{3+} , BSS also contains salicylate, an effective antimicrobial agent under acidic conditions [90]. Sox and Olson's work has focused on determining the events that occur during the killing of bacteria by BSS [49]. Their work demonstrated the bactericidal activity of BSS at both neutral and acidic pH. The effects of BSS described including its ability to bind several species of bacteria and the subsequent killing of the bound organisms, may contribute to the observed *in vivo* efficacy of this compound. The bacteria they used were in stationary growth phase, and the responses of bacteria in other growth phases were not examined. There appear extensive reports on the binding of microorganisms to other surfaces. Binding may occur as a result of specific (lectin like interactions) or nonspecific processes such as electrostatic and hydrophobic interactions, hydrogen bonds, and van der Waals interactions [91]. It has been suggested that BSS binds to a range of organisms via nonspecific binding. Pretreatment of BSS with a protein (albumin) decreased the rate of binding and killing, but complete killing of the exposed *E. coli* was still observed. This suggests that albumin and bacteria compete to some extent for the same binding sites.

10.7 Novel Preparations of Bismuth Compounds

Synthesis of inorganic nanotubes has attracted considerable attention since the discovery of carbon nanotubes by Iijima [92]. The general synthetic strategies involve arc discharge, laser ablations, hydrothermal process, and surfactant assisted synthesis [93]. The synthesis of metallic bismuth and antimony nanotubes using a low temperature hydrothermal reduction method has been reported [94].

Fabrication of $(\text{BiO})_2\text{CO}_3$ nanotubes from bismuth citrate has been reported and these nanotubes have uniform diameters of about 3–5 nm. Importantly, these nanotubes exhibited antibacterial properties against *H. pylori* (50% inhibition at 10 $\mu\text{g}/\text{ml}$). Sun *et al.* are currently studying the feasibility of filling other drugs into the nanotubes to form 'nanodrugs' for treating *H. pylori* infections and other diseases [8]. The synthesis of $(\text{BiO})_2\text{CO}_3$ nanotubes under moderate conditions could be useful for its potential medical applications. Furthermore, these nanotubes can also be used as carriers for other drugs. A new complex of bismuth with *D*-polygalacturonic acid, the so called 'colloidal bismuth pectin', was approved for clinical use in China for the treatment of peptic ulcers [31].

10.8 Novel Delivery Systems for Bismuth Compounds and Other Antibiotics

Among the relatively modern bismuth containing pharmaceuticals, colloidal bismuth subcitrate (CBS, De-Nol and Lizhudele) and ranitidine bismuth citrate (RBC, Pylorid) are the most widely used drugs in many countries for the treatment of gastric disorders. In combination with antibiotics, bismuth therapy has been used as one of the standard salvage treatments for *H. pylori* infections, which is refractory to first line therapies such as combinations of clarithromycin/amoxicillin/PPI (such as Losec-Hp7 and Nexium Hp7). Based on this, a single bismuth based triple therapy moncapsule (Helicid) containing colloidal bismuth subcitrate, tetracycline and metronidazole was developed and approved

for marketing in North America for the eradication of *H. pylori*. This drug is not a simple mechanical mixture but a smaller capsule inside a bigger capsule (a bismuth compound), to prevent possible reactions between these drugs. $(\text{BiO})_2\text{CO}_3$ nanotubes may be efficacious as a 'capsule' due to their unique nanostructure (e.g., size), antimicrobial activity and dissolution characteristics under acidic conditions. Moreover, these nanotubes can also be used as potential carriers for other drugs [93, 95].

10.9 The Biochemical Targets of Bismuth

Although the acquisition of antibiotic resistance by *H. pylori* is the main reason for treatment failure with standard first line therapies [96], there are no reports of *H. pylori* developing resistance to bismuth compounds, which have the potential to reduce resistance levels when co-administered with antibiotics [97]. The molecular mechanisms underlying treatment with bismuth are currently not fully understood. The major biological targets for bismuth appear to be proteins and enzymes.

10.9.1 Enzymes with Zn(II) and Fe(III) Sites

Bismuth can bind to both zinc(II) and iron(III) sites in proteins and enzymes, and the biochemical mechanisms of bismuth's bactericidal effects on *H. pylori* may reside in its ability to interfere with zinc and iron(III) cofactors in significant enzymes and iron (III) metabolism itself. In an elegant study, Ge and Sun conducted a detailed comparative proteomic analysis of *H. pylori* cells both before and after treatment with colloidal bismuth subcitrate (CBS) [98]. Eight proteins were found to be significantly upregulated or downregulated in the presence of 20 mg/ml of CBS. Bismuth induced oxidative stress was confirmed by detecting greater levels of lipid hydroperoxide (1.8-fold greater) and hemin (3.4-fold greater), in whole cell extracts of bismuth treated *H. pylori* cells, comparing with those from untreated cells. The presence of bismuth also led to an approximately eightfold decrease in the bacterium's cellular protease activities. The data of Ge *et al.*, suggest that the inhibition of a spectrum of proteases, modulation/interference with the bacterium's cellular oxidative stress regulatory mechanisms and interference with nickel homeostasis may be key processes underlying the molecular mechanism of bismuth's bactericidal actions against *H. pylori* [98].

10.9.2 Heat Shock Proteins

Using immobilized bismuth affinity chromatography, seven bismuth binding proteins from *H. pylori* cell extracts were isolated and subsequently identified [98]. The intracellular levels of four of these proteins (HspA, HspB, NapA and TsaA) were influenced by the addition of CBS, which strongly suggests that they interact directly with bismuth. Hsp's are a group of highly conserved, abundantly expressed heat shock proteins which confer protective advantage through their functions as molecular chaperones, assisting proper folding of a number of substrate proteins that are otherwise destined to aggregation [99, 100]. HspA and HspB are also involved in urease activation and protection. Urease activity was increased four-fold in *E. coli* when coexpressed with HspA, suggesting that HspA possibly plays an important role in the activation of urease, probably by means of its Ni-binding domain in the C-terminus [101].

The *H. pylori* GroEL homologue HspB belongs to the HSP60 family [102], and has been shown to increase the risk of gastric carcinoma, possibly by directly inducing the hyperproliferation of gastric cells [102, 103]. HspB has been suggested to be responsible for the protection and regulation of urease activity. Many identified Ni-interacting proteins in *H. pylori* have a functional role as antioxidant, antitoxic, and antiinflammation agents. *H. pylori* TsaA is a major component of the thioredoxin dependent thiol specific antioxidant (TSA) system that catalyses the reduction of hydroperoxides [104] and peroxynitrite [105]. The cleavage or degradation of TsaA suppresses the ability of *H. pylori* cells to protect themselves against oxidative stress. NapA is also directly involved in cell defense with reference to oxidative stress. It was so named because of NapA's ability to mediate neutrophil adhesion to endothelial cells [106], and to bind to mucin and neutrophil glycosphingolipids [107]. NapA has been identified as a 150 kDa DNA binding dodecamer that protects cells from DNA damage caused by free radicals generated under oxidative stress [108, 109]. NapA is apparently positively regulated by iron, repressed by ferric uptake regulator (Fur) [109], and unaffected by copper, nickel, or zinc [110]. An excess of iron can be potentially harmful as it catalytically mediates the generation of toxic reactive oxygen species (ROS) via the Fenton reactions.

10.9.3 Other Metabolic Enzymes

Pathogenic microorganisms such as *H. pylori* produce a range of enzymes, which serve their metabolic needs and allow them to express virulent characteristics. Inhibition of such enzymes by bismuth containing drugs is therefore thought to be central in the mechanism of action of bismuth based therapeutics. The mode of action of CBS in the treatment of gastroduodenal disorders may involve in the prevention of adhesion of *H. pylori* to epithelial cells and inhibition of hydrolase enzymes secreted by *H. pylori*, such as proteases, lipases, glycosidases, and phospholipases [111]. Some of the hydrolases incapacitated by bismuth are briefly discussed below.

10.9.4 Fumarase and Translational Factor Ef-Tu

The most notable bismuth interacting proteins identified were two enzymes (fumarase and the urease subunit UreB), and a translational factor (Ef-Tu). Fumarase is likely associated with energy metabolism and bioenergetics of the bacterium.

10.9.5 Phospholipases

It has also been found that CBS can induce a dose dependent inhibition of phospholipases A (PLA2) and C in both *H. pylori* lysates and filtrates, and it has been suggested that bismuth binds to the calcium site of PLA2 [112]. CBS was also found to be able to inhibit the F1-F0 ATPase, an enzyme involved in bacterial energy metabolism, in a dose dependent manner.

10.9.6 Pepsin

Bi(III) can also inhibit the enzyme pepsin at pH 1.0 to 2.0, and such inhibition is probably due to negatively charged bismuth salts derived from CBS via ionic interactions with positively charged groups of pepsin, thereby inactivating the enzyme [113].

10.9.7 Alcohol Dehydrogenase

Alcohol dehydrogenase (ADH) is a common denominator found in most bacterial species. ADH enables those species which possess it to carry out anaerobic energy generation by fermenting a spectrum of monosaccharides and disaccharides via acetaldehyde to alcohol. ADH from *H. pylori* is able to modulate this reversible enzyme via redox reaction (where NAD^+/NADH is the coenzyme for the dehydrogenase) to generate acetaldehyde from an excess of alcohol *in vitro*. Since acetaldehyde is a toxic and chemically reactive compound it can irreversibly bind to the host's phospholipids and proteins, and mediate mucosal damage. It has been shown that various bismuth complexes do inhibit the *H. pylori* ADH and thereby suppress acetaldehyde production by the bacterium from endogenous or exogenous ethanol and thereby indirectly prevent mucosal damage [114, 115].

10.9.8 Urease

The native urease of *H. pylori* is composed of two different subunits (with molecular weights of 61.7 and 26.5 kDa encoded by the genes *ureA* and *ureB*). These differ from other microbial ureases containing three different subunits, and also from the jack bean urease, a single polypeptide [116]. At least four accessory genes (*ureD*, *ureE*, *ureF* and *ureG*) are required for the synthesis of the biologically active enzyme. Bismuth complexes inhibit *H. pylori*-produced urease, and bismuth complexation with bimercaptoethanol shows about 1000 times higher activity than the ligand alone against urease [117]. Mercaptoethanol inhibits the enzyme by targeting the enzyme both directly by bridging the two Ni(II) ions in the active site through the sulfur atom and indirectly by forming a disulfide bond with Cys322, hence sealing the entrance to the active site cavity [118].

10.10 Binding of Bismuth Compounds to Plasma Proteins

Although bismuth complexes have been widely used in clinic as antiulcer drugs, some rather varied adverse effects have been observed and the linkage to bismuth complexes has been diagnosed and generally confirmed by the detection of bismuth in blood or blood plasma. Sun and Szeto studied the binding of bismuth to human serum albumin using fluorescence spectroscopy [119]. The binding of bismuth to human albumin and transferrin was carried out at pH 7.4 by FPLC and ICP-MS. It was found that over 70% of bismuth binds to transferrin even in the presence of a large excess of albumin. The ratio of binding albumin: transferrin was observed to be 30 : 70 at pH 7.4, 10 mM bicarbonate [120]. The distribution of bismuth between the two proteins was almost unchanged when cysteine units of albumin were blocked. Transferrin is probably the major target of bismuth in blood plasma, and may play a role in the pharmacology of bismuth. It may act as either an active sequestering site or 'bio sink' for bismuth and possibly other heavy metals entering circulatory system: thus preventing these deleterious species from further interacting with other more vulnerable biomolecules. In this regard, the binding of bismuth to transferrin is probably a neutralizing detoxification process. However, if the bismuth level in blood or serum increases beyond a certain point (i.e., beyond a saturation point afforded by transferrin), bismuth, transported by transferrin, may permeate through to the more sensitive targets including the brain, causing adverse effects. The reported neurotoxicity of bismuth drugs is probably related to

transferrin transportation and transferrin receptor recognition in the brain which is also known to cause dialysis encephalopathy [121].

References

1. Gordon, R.B. and Rutledge, J.W. (1984) *Science*, **223**, 585–586.
2. Derewenda, Z.S. and Zygumt, S. (2007) *Acta Crystallographica. Section A, Crystal Physics, Diffraction, Theoretical and General Crystallography*, **64**, 246–258.
3. Grice, J.D. (2002) *Canadian Mineralogist*, **40**, 693–698.
4. Odier, L. (1886) *Journal of Medical Chiral Pharmacology*, **68**, 49–56.
5. Sun, H., Zhang, L., and Szeto, K.Y. (2004) *Metal Ions in Biological Systems*, **41**, 333–378.
6. <http://en.wikipedia.org/wiki/Bismuth>.
7. Flexible, highly radiopaque plastic material catheter – Patent 5300048 Inventors: Drewes Jr., David A. (Bloomington, IN) Parker, Fred T. (Unionville, IN) (1991).
8. Chen, R., So, M.H., Yang, J. *et al.* (2006) *Chemical Communications*, 2265–2267.
9. Parke, Davis & Company. (1894) *Descriptive Catalogue of the Laboratory Products of Parke, Davis & Company*, Detroit, Michigan.
10. Marshall, B.J. (1994) *The American Journal of Gastroenterology*, **89** (Suppl. 8), S116–S128.
11. Lee, A. and ORourke, J. (1993) *Gastroenterology Clinics of North America*, **22**, 21–42.
12. Buck, G.E. and Smith, J.S. (1987) *Journal of Clinical Microbiology*, **25**, 597–599.
13. Sly, L.I., Bronsdon, M.A., Bowman, J.P. *et al.* (1993) *International Journal of Systematic Bacteriology*, **43**, 386–387.
14. Eaton, K.A., Morgan, D.R., and Krakowka, S. (1989) *Infection and Immunity*, **57**, 1119–1125.
15. Fox, J.G., Blanco, M., Murphy, J.C. *et al.* (1993) *Infection and Immunity*, **61**, 2309–2315.
16. Baskerville, A. and Newell, D.G. (1988) *Gut*, **29**, 465–472.
17. Marshall, B.J., Barrett, L., Prakash, C. *et al.* (1990) *Gastroenterology*, **99**, 697–702.
18. Marshall, B.J., Warren, J.R., Francis, G.J. *et al.* (1987) *The American Journal of Gastroenterology*, **82**, 200–210.
19. Marshall, B.J. and Surveyor, I. (1988) *Journal of Nuclear Medicine*, **29**, 11–16.
20. Morris, A. and Nicholson, G. (1987) *The American Journal of Gastroenterology*, **82**, 192–199.
21. Parsonnet, J., Friedman, G.D., Vandersteen, D.P. *et al.* (1991) *The New England Journal of Medicine*, **325**, 1127–1131.
22. Sonnenberg, A. and Townsend, W.F. (1991) *The American Journal of Gastroenterology*, **86**, 606–608.
23. Megraud, F., Brassens Rabbe, M.P., Denis, F. *et al.* (1989) *Journal of Clinical Microbiology*, **27**, 1870–1873.
24. Eurogast Study, Group (1993) *Lancet*, **341**, 1359–1362.
25. Wotherspoon, A.C., Ortiz Hidalgo, C., Falzon, M.R., and Isaacson, P.G. (1991) *Lancet*, **338**, 1175–1176.
26. Hussell, T., Isaacson, P.G., Crabtree, J.E., and Spencer, J. (1993) *Lancet*, **342**, 571–574.
27. Stolte, M. and Eidt, S. (1993) *Lancet*, **342**, 568.
28. Bayerdörffer, E., Neubauer, A., Eidt, S. *et al.* and Malt-Lymphoma Study Group, Germany (1994) *Gastroenterology*, **106**, 370.
29. Baxter, G.F. (1992) *Chemistry in Britain*, **28**, 445–448.
30. Briand, G.G. and Burford, N. (1999) *Chemical Reviews*, **99**, 2601–2657.
31. Me, Y.Q., Li, Y.Y., Wu, H.S. *et al.* (1999) *Helicobacter*, **4**, 128–134.
32. Marshall, B.J., McGeachie, D.B., Rogers, P.A., and Glancy, R.J. (1985) *The Medical Journal of Australia*, **142**, 439–444.
33. Gregory, M.A., Moshal, M.G., and Spitaels, J.M. (1982) *South African Medical Journal*, **62**, 52–55.
34. Wilson, P. and Alp, M.H. (1982) *The Medical Journal of Australia*, **1**, 222–223.

35. Goldenberg, M.M., Honkomp, L.J., and Castellion, A.W. (1975) *The American Journal of Digestive Diseases*, **20**, 955–960.
36. Erisson, C.D., Tannenbaum, C., and Charles, T.T. (1990) *Reviews of Infectious Diseases*, **12** (Suppl.), 16–20.
37. DuPont, H.L., Sullivan, P., Pickering, L.K. *et al.* (1977) *Gastroenterology*, **73**, 715–718.
38. DuPont, H.L., Ericsson, C.D., Johnson, P.C. *et al.* (1987) *The Journal of the American Medical Association*, **257**, 1347–1350.
39. Graham, D.Y., Estes, M.K., and Gentry, L.O. (1983) *Gastroenterology*, **85**, 1017–1022.
40. Steffen, R. (1990) *Reviews of Infectious Diseases*, **12** (Suppl. 1), 80–86.
41. Goldenberg, N.U.M., Honkomp, U., and Davis, C.J. (1976) *Journal of Pharmaceutical Sciences*, **65**, 1398–1400.
42. Goldenberg, M., Honkomp, L., Burrows, S., and Castellion, A. (1975) *Gastroenterology*, **69**, 636–640.
43. Halley, F.J. and Newsom, J.H. (1984) *Archives of Internal Medicine*, **144**, 269–272.
44. Gryboski, J.D., Hillemeier, A.C., Grill, B., and Kocoshis, S. (1985) *The American Journal of Gastroenterology*, **80**, 871–876.
45. Soriano-Brücher, H.E., Avendaño, P., O’Ryan, M., and Soriano, H.A. (1990) *Reviews of Infectious Diseases*, **12** (Suppl. 1), 51–56.
46. Chang, T.W., Dong, M.Y., and Gorbach, S.L. (1990) *Reviews of Infectious Diseases*, **12** (Suppl. 1), 57–58.
47. Cornick, N.A., Silva, M., and Gorbach, S.L. (1990) *Reviews of Infectious Diseases*, **12** (Suppl. 1), 9–10.
48. Marshall, B.J., Armstrong, J.A., Francis, G.J. *et al.* (1987) *Digestion*, **37** (Suppl. 2), 16–30.
49. Sox, T.E. and Olson, C.A. (1989) *Antimicrobial Agents and Chemotherapy*, **33**, 2075–2082.
50. Burke, V., Gravy, M., and Suharyono, S. (1980) *Lancet*, **1**, 1329–1330.
51. Manhart, M.D. (1990) *Reviews of Infectious Diseases*, **12** (Suppl. 1), 11–15.
52. Marshall, B.J. (1991) *The American Journal of Gastroenterology*, **86**, 16–25.
53. Wagstaff, A.J., Benfield, P., and Monk, J.P. (1988) *Drugs*, **36**, 132–157.
54. Hall, D.W.R. and van den Hoven, W.E. (1987) *Archives Internationales de Pharmacodynamie et de Therapie*, **286**, 308–319.
55. Konturek, S.J., Bileski, J., Kwiecien, N. *et al.* (1987) *Gut*, **28**, 1557–1563.
56. Konturek, S.J., Brzozowski, T., and Drozdowicz, D. (1988) *Campylobacter Pylori* (eds H. Menge, M. Gregor, G.N.J. Tytgat, and B.J. Marshall), Springer-Verlag, Berlin, pp. 184–194.
57. Martin, D.F., May, S.J., Tweedle, D.E.F. *et al.* (1981) *Lancet*, **317**, 7–10.
58. Tytgat, G.N.J., Nio, C., and Van Den Berg, B.T.J. (1988) *Campylobacter Pylori* (eds H. Menge, M. Gregor, G.N.J. Tytgat, and B.J. Marshall), Springer-Verlag, Berlin, pp. 195–205.
59. Lee, F., Samloff, I.M., and Hardman, M. (1985) *Lancet*, **325**, 1299–1302.
60. Rauws, E.A.J. and Tytgat, G.N.J. (1990) *Lancet*, **335**, 1233–1235.
61. Rauws, E.A.J., Langenberg, W., Houthoff, H.J. *et al.* (1988) *Gastroenterology*, **94**, 33–40.
62. McNulty, C.A.M. (1990) *Reviews of Infectious Diseases*, **12** (Suppl. 1), 94–98.
63. Marshall, B.J., Valenzuela, J.E., McCallum, R.W. *et al.* (1990) *Gastroenterology*, **98** (Part 2), A83.
64. Langenberg, W., Rauws, E.A., Widjojokusumo, A. *et al.* (1986) *Journal of Clinical Microbiology*, **24**, 414–417.
65. Stiel, D., Murray, D.J., and Peters, T.J. (1985) *Gut*, **26**, 364–368.
66. Mehta, J.G. and Morrissey, S.M. (1983) *Proceedings of the International Union Physiological Sciences*, **15**, 423.
67. Lee, S.P. (1982) *Scandinavian Journal of Gastroenterology*, **17**, 17–21.
68. Wilson, T.R. (1975) *Postgraduate Medical Journal*, **51**, 18–21.
69. Lee, S.P. (1981) *Research Communications in Chemical Pathology and Pharmacology*, **34**, 359–364.
70. Wieriks, J., Hespé, W., Jaitly, K.D. *et al.* (1982) *Scandinavian Journal of Gastroenterology*, **17**, 11–16.

71. Alpers, D.H. (1977) *Biochemical and Biophysical Research Communications*, **75**, 130–135.
72. Coghill, S.B., Hopwood, D., McPherson, S., and Hislop, S. (1983) *The Journal of Pathology*, **139**, 105–114.
73. Kang, J.Y. and Piper, D.W. (1982) *Digestion*, **23**, 73–79.
74. Komoda, T., Sonoda, M., Ikeda, M. *et al.* (1981) *Clinica Chimica Acta; International Journal of Clinical Chemistry*, **116**, 161–169.
75. Lechat, P. and Kisch, R. (1986) *Gastroenterologie Clinique et Biologique*, **10**, 562–569.
76. Lowe, D.J. (1974) *The Medical Journal of Australia*, **2**, 664–666.
77. Hasking, G.J. and Duggan, J.M. (1982) *The Medical Journal of Australia*, **2**, 167.
78. Andreasen, J.J. and Andersen, L.P. (1987) *Acta Pathologica Microbiologica Scandinavica Series B: Microbiology*, **95B**, 147–149.
79. Li, W., Jin, L., Zhu, N. *et al.* (2003) *Journal of the American Chemical Society*, **125**, 12408–12409.
80. Koo, J., Ho, J., Lam, S.K. *et al.* (1982) *Gastroenterology*, **82**, 864–870.
81. Coghill, S.B. and Axon, A.T.R.(eds) (1985) Proceedings of International Symposium, Cairo, 7.
82. DuPont, H.L., Ericsson, C.D., Johnson, P.G. *et al.* (1987) *Journal of the American Medical Association*, **257**, 1347–1350.
83. McNulty, C.A., Gearty, J.C., Crump, B. *et al.* (1986) *British Medical Journal*, **293**, 645–649.
84. Kappsteh, I. and Engels, I. (1987) *European Journal of Clinical Microbiology & Infectious Diseases*, **6**, 216–217.
85. Rauws, E.A.J., Langenberg, W., Houthoff, H.J., and Tytgat, G.N. (1987) *Zeitschrift für Gastroenterologie*, **25** (Suppl. 4), 24–28.
86. Foster, T.J. (1983) *Microbiological Reviews*, **47**, 361–409.
87. Strandberg, G.W., Shumate, S.E., and Parrott, J.R. Jr. (1981) *Applied and Environmental Microbiology*, **41**, 237–245.
88. Bordens, A. and Jofre, J. (1987) *Enzyme and Microbial Technology*, **9**, 709–713.
89. Tornabene, T.G. and Edwards, H.W. (1972) *Science*, **176**, 133–135.
90. Hugo, W.B. and Russell, A.D. (1982) *Principles and Practice of Disinfection, Presterilisation and Sterilization* (eds A.D. Russell, W.B. Hugo, and G.A.F. Ayliffe), Blackwell Scientific Publications, Boston, pp. 29–32.
91. Lentner, C.(ed.) (1981) *Geigy Scientific Tables*, 8th edn, **1**, Ciba-Geigy Corp., West Caldwell, N.J., pp. 123–133.
92. Iijima, S. (1991) *Nature*, **354**, 56–58.
93. Rao, C.N.R., Muller, A., and Cheetham, A.K.(eds) (2004) *The Chemistry of Nanomaterials: Synthesis, Properties and Applications*, **1**, Wiley-VCH Verlag GmbH, Weinheim, pp. 244–246.
94. Li, Y.D., Wang, J.W., Deng, Z.X. *et al.* (2001) *Journal of the American Chemical Society*, **123**, 9904–9905.
95. Rao, C.N.R. and Nath, M. (2003) *Journal of The Chemical Society-Dalton Transactions*, 1–24.
96. Megraud, F. (2004) *Drugs*, **64**, 1893–1904.
97. Midolo, P.D., Lambert, J.R., Kerr, T.G., and Tee, W. (1999) *European Journal of Clinical Microbiology & Infectious Diseases*, **18**, 832–834.
98. Ge, R., Sun, X., Gu, Q. *et al.* (2007) *Journal of Biological Inorganic Chemistry: JBIC: a Publication of the Society of Biological Inorganic Chemistry*, **12**, 831–842.
99. Lund, P.A., Large, A.T., and Kapatay, G. (2003) *Biochemical Society Transactions*, **31**, 681–685.
100. Lund, P.A. (1995) *Essays in Biochemistry*, **29**, 113–123.
101. Kansau, I., Guillain, F., Thiberge, J.-M., and Labigne, A. (1996) *Molecular Microbiology*, **22**, 1013–1023.
102. Suerbaum, S., Thiberge, J.M., Kansau, I. *et al.* (1994) *Molecular Microbiology*, **14**, 959–974.
103. De Luca, A., Baldi, A., Russo, P. *et al.* (2003) *Cancer Research*, **63**, 6350–6356.
104. Baker, L.M.S., Raudonikiene, A., Hoffman, P.S., and Poole, L.B. (2001) *Journal of Bacteriology*, **183**, 1961–1973.
105. Bryk, R., Griffin, P., and Nathan, C. (2000) *Nature*, **407**, 211–215.
106. Yoshida, N., Granger, D.N., Evans, D.J. Jr. *et al.* (1993) *Gastroenterology*, **105**, 1431–1440.

107. Teneberg, S., Miller-Podraza, H., Lampert, H.C. *et al.* (1997) *The Journal of Biological Chemistry*, **272**, 19067–19071.
108. Evans, D.J. Jr., Evans, D.G., Takemura, T. *et al.* (1995) *Infection and Immunity*, **63**, 2213–2220.
109. Cooksley, C., Jenks, P.J., Green, A. *et al.* (2003) *Journal of Medical Microbiology*, **52**, 461–469.
110. Dundon, W.G., Polenghi, A., Del Giudice, G. *et al.* (2001) *FEMS Microbiology Letters*, **199**, 143–149.
111. Lee, S.P. (1991) *Scandinavian Journal of Gastroenterology*, **26**, 1–6.
112. Ottlecz, A., Romero, J.J., Hazell, S.L. *et al.* (1993) *Digestive Diseases and Sciences*, **38**, 2071–2080.
113. Beil, W., Bierbaum, S., and Sewing, K.F. (1993) *Pharmacology*, **47**, 141–144.
114. Roine, R.P., Salmela, K.S., Hooknikanne, J. *et al.* (1992) *Life Sciences*, **51**, 195–200.
115. Salmela, K.S., Roine, R.P., Hooknikanne, J. *et al.* (1994) *Scandinavian Journal of Gastroenterology*, **29**, 528–531.
116. Hu, L.T. and Mobley, H.L. (1990) *Infection and Immunity*, **58**, 992–998.
117. Asato, E., Kamamuta, K., Akamine, Y. *et al.* (1997) *Bulletin of the Chemical Society of Japan*, **70**, 639–648.
118. Benini, S., Rypniewski, W.R., Wilson, K.S. *et al.* (1998) *Journal of Biological Inorganic Chemistry: JBIC: a Publication of the Society of Biological Inorganic Chemistry*, **3**, 268–273.
119. Sun, H. and Szeto, K.Y. (2003) *Journal of Inorganic Biochemistry*, **94**, 114–120.
120. Sun, H., Li, H., Harvey, I., and Sadler, P.J. (1999) *The Journal of Biological Chemistry*, **274**, 29094–29101.
121. Sun, H., Li, H., and Sadler, P.J. (1999) *Chemical Reviews*, **99**, 2817–2842.

11

Application of Arsenic Trioxide Therapy for Patients with Leukaemia¹

Bo Yuan¹, Yuta Yoshino¹, Toshikazu Kaise² and Hiroo Toyoda¹

¹Department of Clinical Molecular Genetics, School of Pharmacy

²Laboratory of Environmental Chemodynamics, School of Life Sciences,

Tokyo University of Pharmacy & Life Sciences,

1432-1 Horinouchi, Hachioji, Tokyo 192-0392, Japan

11.1 Introduction

Acute promyelocytic leukaemia (APL) is a distinct subtype of acute myeloid leukaemia (AML). Morphologically, it is identified as AML-M3 by the French-American-British classification. Cytogenetically, APL is characterized by a balanced reciprocal translocation between chromosome 15 and 17, which results in the fusion between the promyelocytic leukaemia (PML) gene and retinoic acid receptors (RAR α) [1–3]. In 90% of *de novo* APL patients, administration of all-*trans* retinoic acid (ATRA) induces differentiation of leukemic blasts and clinical remission, and 70% of them have been cured by ATRA administration in combination with chemotherapy [4]. Thus, ATRA has become a first-line administration for *de novo* APL patients [4, 5]. Nevertheless, the remaining 30% of patients relapse and often become resistant to this conventional combination treatment protocol [4]. A new breakthrough therapy has been introduced into the treatment for relapsed as well as newly diagnosed patients. Investigators from China and the USA have demonstrated that treatment with arsenic trioxide (ATO) results in complete remission in 90% of relapsed

¹This chapter was dedicated to the memory of late Prof. Toshikazu Kaise.

patients [6–8]. From then on, a dramatic clinical efficacy of ATO-based regimens against APL has been reported around the world. An impressive drug efficacy against APL led to its approval in the USA and in Europe under the brand name of Trisenox for ‘the induction of remission and consolidation in patients with APL whose conditions are refractory to, or who have relapsed from retinoid and anthracycline chemotherapy, and whose APL is characterized by the presence of the t(15;17) translocation or PML-RAR α gene expression’ [8]. These available clinical data inspire investigators to unravel the detailed mechanisms of action of ATO through biochemical and molecular biological studies. All of these achievements make us confident that APL status can evolve from highly fatal to highly curable. Furthermore, in addition to APL, it has recently been discussed that ATO exhibits a potential therapeutic benefit in the treatment of other types of leukaemia and even the nonhematologic malignancies [9]. This chapter reviews (1) cellular and molecular mechanisms of ATO actions; (2) pharmacokinetics of ATO in APL patients; (3) potential combination therapies with ATO, and (4) Potential ATO application for the treatment of other leukaemias.

11.2 Cellular and Molecular Mechanisms of ATO Actions

11.2.1 History of Arsenic as a Drug

Arsenic and its compounds are widely distributed in the environment and exist in organic and inorganic forms. There are three inorganic forms of arsenic: yellow arsenic (As_2S_3 , also known as orpiment); red arsenic (As_4S_4 , also known as realgar); and white arsenic or ATO (As_2O_3), which is made by burning realgar or orpiment (Figure 11.1) [10]. Although a

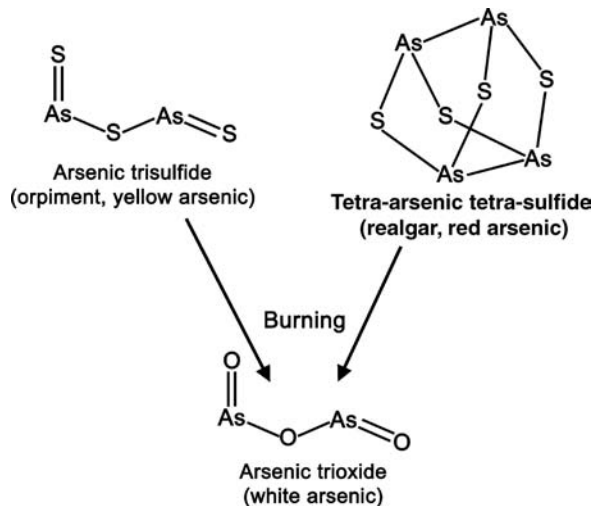


Figure 11.1 Structural formulae of three inorganic forms of arsenic. Three inorganic forms of arsenic are shown here. Arsenic trisulfide (As_2S_3 , also known as orpiment or yellow arsenic); tetra-arsenic tetra-sulfide (As_4S_4 , also known as realgar or red arsenic); and arsenic trioxide (As_2O_3 , also known as white arsenic). Arsenic trioxide (ATO) can be made by burning realgar or orpiment

well-known poison, arsenic has been used medicinally for over 2000 years. In the eighteenth-century, arsenic, in the form of Fowler solution (potassium bicarbonate-based solution of arsenic), was introduced clinically for the treatment of various types of infectious and malignant diseases [11]. However, due to its toxicity, arsenic was superseded by application of radiation and cytotoxic chemotherapy in the early twentieth-century. In the mid-1990s, there was a resurgence of interest in such a therapy when it was found to induce apoptosis and differentiation in APL cells [6, 12, 13].

11.2.2 Uptake of Arsenic

Since drug action usually requires uptake of the drug, it was considered that intracellular arsenic content might determine ATO sensitivity. Therefore, understanding the cellular mechanisms responsible for arsenic transport has both toxicological and pharmacological relevance. Pentavalent arsenate (As^{V}) is a predominant form of arsenic in nature. It has been postulated that As^{V} can be taken up by cells through phosphate transporters, since it is a phosphate analogue [14, 15]. Moreover, toxicity of As^{V} may partially result from its reduction to trivalent arsenic (As^{III}) [14, 16, 17]. Recently, Lu *et al.* have reported that organic anion transporting polypeptide-C may support to uptake inorganic arsenic (As^{III} and As^{V}) in a glutathione (GSH)-dependent manner based on a study using a human embryonic kidney cell line (HEK cells) [18]. It has been demonstrated that aquaglyceroporins (AQPs) play a pivotal role in the uptake of arsenic based on a series of studies in various leukaemia cell lines [9–21] including an APL cell line, NB4 [22]. AQPs are members of the aquaporin superfamily and transport a variety of small neutral solutes such as glycerol and urea (Chapter 8, Figure 8.2) [23, 24]. At physiological pH, As^{III} exists primarily as an aqueous form of As^{III} , $\text{As}(\text{OH})_3$, and is taken into cells via AQP pathways [25]. By expressing various AQP genes in yeast or *Xenopus* oocytes, $\text{As}(\text{OH})_3$ was transported into cells efficiently by AQP9 and AQP7 [26, 27], whereas there was little or no transport by AQP3 or AQP10 [27]. However, a possible contribution of AQP3 and AQP10 for $\text{As}(\text{OH})_3$ transport could not be excluded, since a previous study has demonstrated that AQP3 is closely associated with arsenic uptake in human lung adenocarcinoma cell line (CL3) and human embryonic kidney cell line (HEK cells) [28]. The sensitivities to ATO have been shown to be proportional to the expression of AQP9 in leukaemia cells. Intracellular arsenic concentrations in chronic myeloid leukaemia line K562 transfected with the AQP9 gene were significantly higher than those in untransfected K562, resulting in an increased ATO-induced cytotoxicity [20]. Furthermore, the study on the expression levels of AQP9 in leukaemia samples from 80 patients showed that APL expressed significantly higher AQP9 levels than all the other subtypes of acute myeloid leukaemia [20]. Moreover, methylarsonous acid (MAs^{III}), one of the initial products of As^{III} methylation, is thought to be incorporated by AQP9 [29]. Since AQP9 is expressed primarily in human leukocytes [30], it is possible that AQP9 is responsible for ATO uptake into leukaemia cells, suggesting that monitoring AQP9 expression levels in APL patients before or during ATO treatment may provide an index of their responses to ATO therapy. Therefore, AQP9 may become a novel target in the development of treatment strategies against APL. Intriguingly, pretreatment of a myeloid leukaemia line HL-60 with ATRA upregulated AQP9 expression, leading to a significant increase in arsenic uptake and ATO-induced cytotoxicity in the presence of ATO, which might explain a synergism of ARTA with ATO [20]. More recently, it should be noted that

AQP9 mediates the therapeutic effects of Realgar-Indigo naturalis formula, which has been proven to be very effective in treating human APL as a model [21] in China.

Recently, the study by Rosen and colleagues demonstrated that human glucose transporters (GLUT), such as GLUT1 and GLUT4, also catalyse uptake of both arsenite and MAs^{III} [15]. GLUT1 is the major glucose permease in erythrocytes and epithelial cells that form blood-brain barrier. These observations suggest that GLUT1 may be a major pathway responsible for the uptake of both inorganic and methylated arsenic in those tissues and may contribute to their accumulation, leading to undesirable arsenic-related cardiovascular complications and neurotoxicity [15]. Indeed, we have demonstrated that total arsenic concentrations in the blood cells, prepared from an APL patient undergoing ATO treatment, increased with time during the consolidation therapy [31]. Moreover, it has also been indicated that arsenic can pass through the blood-brain barrier with general intravenous infusion, although its content is below the therapeutic concentrations [32, 33]. A recent report has demonstrated that GLUT4, the insulin-responsive isoforms, also catalyses transportation of arsenite and MAs^{III} [15]. Since neither AQP9 nor GLUT1 can be detected in adult cardiomyocytes by Western blot, uptake of inorganic and methylated arsenicals into cardiac cells via GLUT4 may be a contributing factor to arsenic-related cardiovascular disorders [15], such as electrocardiogram abnormalities which is the most frequent adverse events in APL patients undergoing ATO treatment [8, 9, 34].

11.2.3 Efflux of Arsenic

It has been established that multidrug resistance-associated proteins (MRP1/MRP2) and P-glycoprotein (P-gp), which belong to the ATP-binding cassette transporter superfamily, are involved in the efflux of arsenic [16, 28, 35–40]. MRP1/MRP2 and P-gp are plasma membrane glycoproteins that can confer multidrug resistance (MDR) by lowering intracellular drug concentrations [28, 35–39]. A previous report has demonstrated that MRP1 is capable of transporting As^{III} , but not As^{V} , only when in the presence of GSH, based on the results using membrane vesicles from the MRP1-overexpressing lung cancer cell line, H69AR [36]. Whereas, the cytotoxicity of As^{III} and As^{V} has been abolished in HeLa and human small cell lung cancer cell line (GLC4) when these cells are transfected with MRP1 gene [39, 40]. Collectively, these results suggest that in intact cells As^{V} is reduced to As^{III} before the efflux from these cells. In fact, the reduction of As^{V} to As^{III} in mammalian cells has been considered to occur spontaneously in the presence of GSH [41]. The reduction by GSH has been shown to be linked to the formation of arsenic triglutathione, a complex in which As^{III} is bound to the thiol moieties of the cysteinyl residues of three GSH molecules [16, 41]. Indeed, it has been proposed that arsenic triglutathione are transported out from cells by MRP1/2 [16, 36]. Therefore, it is concluded that in mammalian cell models, MRP1 is shown to confer resistance to both As^{III} and As^{V} in a GSH-dependent manner. Furthermore, it has been demonstrated that glutathione S-transferase (GST) play a pivotal role in the arsenic reduction and efflux, resulting in acquiring tolerance to arsenic cytotoxicity [16, 35, 36, 38, 42, 43]. It is well known that the transport of arsenic from the liver to bile is dependent on GSH in rat model [44]. The study supported *in vivo* evidence where the conjugation of arsenic with GSH is important for its biliary excretion via the MRP2 transporter [45, 46]. Furthermore, a previous report demonstrated that a dose of 15 mg arsenite/kg caused 50% lethality in MRP1-null mice but only 17% of that in

the wild-type mice [47]. All these findings support an idea that upregulation of MRP proteins plays an important role in acquired tolerance to arsenic.

P-gp is encoded by multidrug resistant gene (MDR1). It has been demonstrated that MDR1a/1b double-knockout mice, which lack the expression of MDR1-encoded P-gp, are more sensitive to acute arsenic toxicity and accumulated more arsenic than wild-type mice, suggesting that P-gp are involved, at least partially, in arsenic efflux in mammals [48]. On the other hand, using APL cells including NB4 and blast cells from APL patients, Takeshita *et al.* demonstrated that the expression levels of P-gp were not inversely proportional to the intracellular accumulation of ATO in APL cells, and that ATO was also effective in cells that expressed considerable amounts of P-gp, suggesting that P-gp may not represent a major cause of arsenic resistance at the concentrations of ATO achievable in patients [49]. As mentioned above, although the roles of P-gp in arsenic efflux remain controversial, monitoring of P-gp expression levels should attract considerable attention in order to provide an effective treatment protocol for APL patients.

In addition, the expression of MRP and P-gp is also involved in cross-resistance to chemotherapeutic agents including anthracyclines, which have been used commonly in APL treatment [50, 51]. Therefore, efforts to increase intracellular concentrations of ATO as well as other chemotherapeutic agents by modifying these MDR transporters will benefit for APL treatment. Indeed, several MDR-reversing agents, such as MK571, VX-710, PSC833, GF120918, and LY335879, are in various stages of clinical development [35, 50]. Pathways of uptake and efflux of arsenic in mammalian systems are summarized in Figure 11.2.

11.2.4 Apoptosis Induction

11.2.4.1 Apoptosis Pathway Involved in ATO-Induced Apoptosis

The clinical results achieved with ATO in relapsed as well as newly diagnosed APL patients have prompted investigations to determine the mechanisms mediating its activity. ATO is believed to function primarily by promoting apoptosis at its concentrations ranging from 1 to 2 μM *in vivo* and *in vitro* [12, 13, 52–54]. Apoptosis is characterized by a rapid cell shrinkage and loss of normal cellular architecture. Subsequently, cells undergoing apoptosis exhibit dense chromatin condensation, nuclear fragmentation, cytoplasmic blebbing, and cellular fragmentation into apoptotic bodies [55]. Generally, apoptosis induction occurs through multiple pathways, and thus various stimuli activate different pathways [56]. So far, two principal signal pathways of apoptosis have been identified (Figure 11.3) [56]. The intrinsic mechanism of apoptosis involves a mitochondrial pathway. Apoptosis stimuli destruct mitochondrial membrane structure under the control of Bcl-2 (B-cell leukaemia/lymphoma) family, resulting in the release of mitochondrial proteins including cytochrome *c*. Once cytochrome *c* is released it activates caspase-9 (initiator caspase) through interaction with Apaf-1 (apoptotic protease activating factor-1) and dATP [57, 58], and ultimately leads to caspase-3 and -7 (effector caspases) activation [59]. On the other hand, the extrinsic pathway induced by death receptors, such as tumor necrosis factor receptor (TNFR) and Fas, is responsible for the activation of caspase-8 and caspase-10 (initiator caspase) accompanied by the activation of caspase-3 and -7 [59]. The effector caspases are the final mediators in the intrinsic and extrinsic pathways that cleave substrates and lead to cell death. Moreover, a third

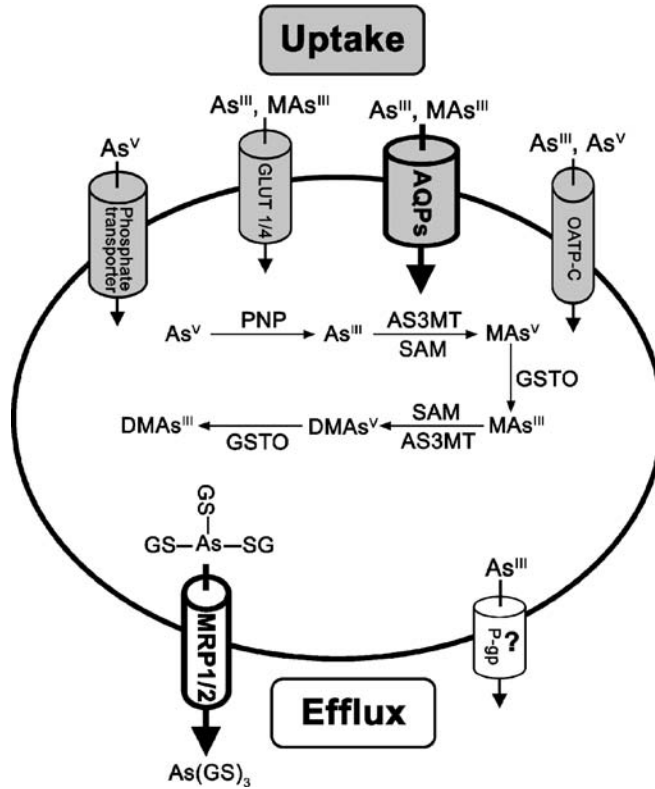


Figure 11.2 Pathways of uptake and efflux, and biotransformation of arsenic in mammalian systems. Pentavalent arsenate (As^V) is a phosphate analogue, and phosphate transporters are believed to act to incorporate As^V with phosphate. Organic anion transporting polypeptide-C (OATP-C) is thought to have an auxiliary role in arsenic uptake, since it can transport inorganic arsenic (trivalent arsenic (As^{III}) and As^V) in a glutathione-dependent manner. It has been indicated that aquaglyceroporins (AQPs) and glucose transporter GLUT1/4 can transport As^{III} and/or methylarsinous acid (MAs^{III}). In particular, the pivotal role of AQP9 on the arsenic accumulation in leukaemia cells has been identified. On the other hand, it has been demonstrated that multidrug resistance associated proteins (MRP1/2) are involved in the efflux of arsenic (arsenic triglutathione ($As(GS)_3$), whereas the roles of P-glycoprotein (P-gp) in arsenic efflux remain controversial. Biomethylation is a major metabolic pathway for inorganic arsenic in human and many animal species, and the liver apparently is the major site of biomethylation. In human, dimethylarsinous acid ($DMAs^{III}$) and dimethylarsinic acid ($DMAs^V$) appear to be the end products of this pathway [41]. In the pathway, arsenate reductases, such as the omega isoform of glutathione S-transferase (GSTO), and purine nucleoside phosphorylase (PNP), catalyse the reduction of arsenate species [16]. Human arsenic (+3 oxidation state) methyltransferase (AS3MT) catalyse the methylation of arsenite [16,43,158–161]. S-adenosylmethionine (SAM) is the methyl donor [16]

pathway involving endoplasmic reticulum and caspase-12 has been reported to associate with apoptosis [60]. A number of markers have been utilized to reveal apoptosis including cell viability, cytochrome *c* release, caspase-3 activation, poly (ADP-ribose) polymerase (PARP) cleavage, and DNA fragmentation [61].

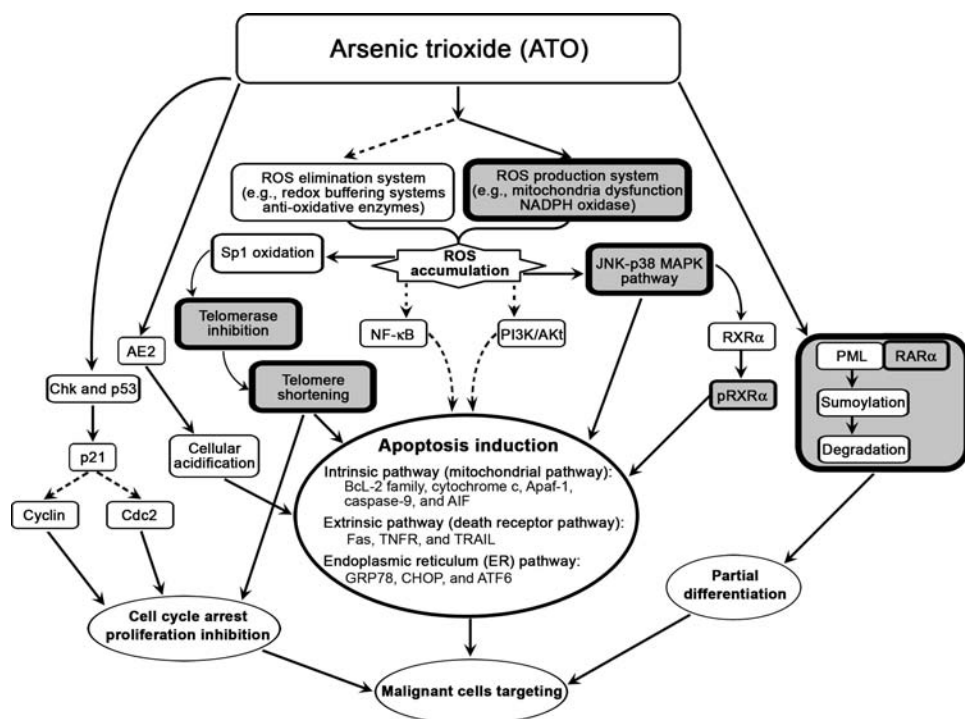


Figure 11.3 Molecular mechanisms of arsenic trioxide (ATO) in malignant cells targeting. ATO exhibits therapeutic effects against malignant cells through apoptosis induction, cell cycle arrest and proliferation inhibition, and differentiation. The detailed information can be referred to Section 11.2. ATRA synergizes with ATO to provide a superior efficacy of combination therapy in patients through promoting the effects of ATO on several genes indicated in the shaded box. NADPH, reduced nicotinamide adenine dinucleotide phosphate; MAPK, mitogen activated protein kinase; JNK, c-Jun NH₂-terminal kinase; RXR α , retinoid X receptor α ; pRXR α , phosphorylation of retinoid X receptor α ; PI3K, phosphoinositide 3-kinase; Apaf-1, apoptotic protease activating factor-1; AIF, apoptosis inducing factor; TNFR, tumor necrosis factor receptor; TRAIL, tumor necrosis factor related apoptosis inducing ligand; GRP78, glucose regulated protein of 78 kDa; CHOP, CCAAT/enhancer binding protein homologous protein; ATF-6, activating transcription factor 6; AE, Anion exchanger; Chk, checkpoint kinase; Cdc2, cell division cycle 2

It is well known that Bcl-2, localizing in the outer membranes of the mitochondria, has drawn particular attention to its potential role in the regulation of apoptosis induction pathway because of its importance in stabilizing mitochondrial transmembrane potentials [56]. It has been clarified that treatment with 1 μ M ATO potently downregulates Bcl-2 gene expression at the mRNA and protein levels in NB4 cell line, accompanying induction of mitochondrial transmembrane potentials collapse due to the opening of permeability transition pore, which triggers the release of cytochrome *c* from mitochondria to cytosol, followed by caspase activation and degradation of specific substrates [12, 52, 53]. Moreover, arsenic also causes the release of apoptosis-inducing factor from the mitochondrial intermembrane space, resulting in the induction of a caspase-independent cell death [62, 63].

Taken together, these observations suggest that mitochondria-mediated intrinsic apoptotic pathway is involved in ATO-induced apoptosis. On the other hand, the extrinsic pathway via death receptors, such as TNFR and Fas, has been reported to be implicated in ATO-induced apoptosis in HL-60 and RL, a B-cell lymphoma cell line [64]. Moreover, Szegezdi *et al.* reported that the ATO enhanced tumor necrosis factor related-apoptosis-inducing ligand (TRAIL)-mediated apoptosis in leukemic cells [65]. The same study also showed that ATO-sensitized TRAIL-induced leukemic cell apoptosis was associated with Akt-inhibition, downregulation of the short isoform of FLIP (FLICE-inhibitory protein, FLIPs), and increased cell surface expression of Death Receptor 5 (DR5) [65]. Recently, Kim *et al.* also reported that ATO treatment of human glioma cells induced DR5 upregulation, which in turn enhanced TRAIL-induced apoptosis in the cells, suggesting that DR5 upregulation is critical for ATO-induced sensitization of the cells in TRAIL-mediated apoptosis [66]. Furthermore, they also clarified that CCAAT/enhancer binding protein homologous protein (CHOP) was closely associated with DR5 upregulation, since they found siRNA-mediated CHOP suppression not only attenuated ATO-induced DR5 upregulation but also inhibited the ATO-stimulated TRAIL-induced apoptosis [66]. However, Kitamura *et al.* demonstrated that Fas-independent, but GSH concentration-dependent caspase-8 activation, was involved in ATO-induced apoptosis in NB4 cell line [67]. Meanwhile, a previous study has demonstrated that ATO induces apoptosis in NB4 cell line by promoting caspase-10 activation. [68]. Therefore, further studies are needed to verify or clarify the molecular details of whether extrinsic apoptotic pathway is implicated in ATO-induced apoptosis in APL cells. Recently, it has been demonstrated that ATO induces the endoplasmic reticulum stress-mediated apoptosis in the chronic myeloid leukaemia cell line K562, and that an apoptosis level was synergistically enhanced by combination of tyrosine kinase inhibitor imatinib mesylate (STI571) [69]. Taken together, these observations suggest that coordination of intrinsic, extrinsic and endoplasmic reticulum-mediated apoptosis is involved in the mechanisms underlying the therapeutic efficacy of ATO.

11.2.4.2 *The ROS Production System to ATO-Induced Apoptosis*

Reactive oxygen species (ROS) are oxygen containing chemical species with reactive chemical properties. They include free radicals such as superoxide and hydroxyl radicals which contain an unpaired electron and non-radical molecules such as hydrogen peroxide (H_2O_2) [56]. ROS can initiate lipid peroxidation, convert proteins to be oxidized, inactive states, and cause DNA strand breaks and mutations, leading to apoptosis induction [56]. In fact, the mechanisms underlying the apoptosis induction by ATO include generation of ROS [41, 53, 70–74]. This idea is supported by clinical data that the levels of 8-hydroxy-2'-deoxyguanosine, one of the most abundant oxidative products of DNA, are increased in plasma from APL patients after remission induction and consolidation therapy [72].

Mitochondria has been thought to be a potential source of ROS production induced by ATO, because mitochondrial respiration consumes about 90% of the oxygen used by cells [75]. It has been discussed that through blockading of electron flow at complex III and IV, ATO disrupts mitochondrial respiration to elevate the generation of oxygen free radicals, which is thought to result from leakage of electrons from the respiratory complexes [76]. This leads to an increase in the intracellular H_2O_2 concentrations which enhance the permeability of the mitochondrial membrane [53]. In addition to mitochondria, the reduced

nicotinamide adenine dinucleotide phosphate (NADPH) oxidase, which is described for the first time in professional phagocytes responsible for generating a large burst of superoxide to kill the ingested pathogens, is also associated with ATO-induced ROS generation [73, 77]. Through analyses of gene expression profiles by oligonucleotide microarrays, Chou *et al.* found that NADPH oxidase components were dramatically upregulated within days in myeloid cells treated with 0.75 μM ATO [77]. They also demonstrated that the clinically used phorbol myristate acetate analogue, bryostatin 1, synergistically enhanced arsenic-induced ROS production by stimulating NADPH oxidase enzyme activity, and that this synergism between very low doses of both arsenic and bryostatin-1 can effectively kill leukemic cells [77]. Recently, Wang *et al.* demonstrated all the components of NADPH oxidase (its membrane components gp91^{phox} and p22^{phox}, and the major cytoplasmic subunits p67^{phox} and p47^{phox}) in NB4 cells, which could be effectively activated by various stimulants, including ATO and ATRA [73, 77]. Thus, these findings suggested that NADPH oxidase-derived ROS are responsible for the high susceptibility to arsenic cytotoxicity in the cells. Taken together, these observations uncover a major role of NADPH oxidase in arsenic-induced ROS production and cytotoxicity, and also provide a conceptual basis for the development of clinical protocols for the treatment of leukaemias, in particular APL, through regulation of NADPH oxidase activity.

11.2.4.3 The ROS Elimination System to ATO-Induced Apoptosis

Normally, cells are protected from the effects of excess ROS by reductive-oxidative (redox) buffering systems, such as thioredoxin and GSH, and anti-oxidative enzymes including superoxide dismutase (SOD), catalase and glutathione peroxidase (GPx). SOD metabolizes superoxide whereas catalase and GPx metabolize H_2O_2 [78]. GST is another family of enzymes that use GSH as a cofactor to modify substrates, such as oxidized proteins and lipids [78]. Therefore, one can easily expect that insufficient ROS elimination as a result of reduced antioxidant enzyme activities, leads to the accumulation of intracellular ROS. Indeed, it is well known that NB4 cell line, which is the most sensitive to ATO, has relatively low levels of reduced GSH, GPx, catalase, and GST π , and has a constitutively higher H_2O_2 content than other non-APL leukemic cell lines, such as HL-60, U937, and KG1 [53, 70, 71]. Furthermore, apoptosis can be induced in NB4 cells at concentrations of ATO, at which no apoptosis was occurred, in the presence of the GPx inhibitor [79], such as mercaptosuccinic acid; or catalase inhibitor [79], such as 3-amino-1,2,4-triazole [53]. More importantly, from a therapeutic point of view, HL-60 and U937 cells, which require high concentrations of ATO to undergo apoptosis, become sensitive to clinically acceptable low concentrations of ATO in combination with these GPx and catalase inhibitors [53]. Recently, in addition to GPx, the other selenoenzyme thioredoxin reductase (TrxR) has emerged as an important molecular target for cancer therapy by ATO [80]. A previous report has demonstrated that ATO irreversibly inhibits mammalian TrxR with an IC_{50} value of 0.25 μM , and that both the N-terminal redox-active dithiol and the C-terminal selenothiol-active sites of reduced TrxR may participate in the reaction with ATO [80]. Arsenite and MAs^{III} have also been shown to be potent inhibitors of TrxR both *in vitro* and *in vivo* [81–83]. Furthermore, ATO decreases selenium incorporation into selenoproteins, which are essential components for selenoenzyme activities such as TrxR and GPx [84], possibly through forming a complex seleno-bis (S-glutathionyl) arsinium ions [85]. Besides participation in cellular efflux of ATO, it has

been indicated that monomeric GST π forms a complex with c-Jun NH₂-terminal kinase (JNK), resulting in the inhibition of JNK activity [86, 87]. Such inhibition is reversed by oxidative stress that causes an oligomerization of GST-GST dimers and multimers involving the Cys-47 and Cys-101 residues of the GST π , consequently JNK can exert its kinase activity, leading to apoptosis induction [88]. It is interesting to note that a similar phenomenon has been recently reported in NB4 cell line treated with ATO [89]. These observations are consistent with the concept that sulfhydryl groups of the protein could be the main targets of ATO [71, 90, 91]. Furthermore, proof-of-principle experiments have shown that SOD inhibitor, 2-methoxyestradiol, is shown to enhance the superoxide levels and apoptosis induced by ATO in primary leukaemia cells from patients with chronic lymphocytic leukaemia [76, 92]. Collectively, these observations suggest that modification of a protective network, comprising GPx, GST, TrxR, catalase, SOD, GSH, and thioredoxin, might represent a nonspecific mechanism underlying the response to antineoplastic drugs (e.g., ATO) acting on cell-redox status.

As described above, ATO can induce intracellular ROS accumulation through not only enhancing the ROS production system but also impairing the ROS elimination system. An increased intracellular ROS levels result in the opening of the permeability transition pore, which leads to activation of intrinsic apoptotic pathways in hematological cell lines including APL cell line [12, 52, 53, 70, 93, 94].

11.2.4.4 *ATO-Induced Apoptosis Mediated Through Other Molecules*

Several lines of evidence have indicated that arsenic affects several signal transduction cascades, and thus inhibits or activates transcription factors through elevating ROS production [16, 86, 87, 90, 95, 96]. The transcription factor nuclear factor-kappa B (NF- κ B) promotes cell survival and plays an important role in many malignant diseases [16, 95]. Arsenite has been shown to inhibit degradation of I κ B, NF- κ B specific inhibitory protein localizing in cytoplasm by binding to the cysteine residue (Cys-179) in the activation loop of the I κ B kinase catalytic subunit and consequently, to suppress NF- κ B activation [16, 96]. On the other hand, ATRA has been reported to induce NF- κ B activation, resulting in prolongation of the life span of mature leukocytes associated with the development of retinoic acid syndrome [97]. Intriguingly, it has been established that ATO can overcome the antiapoptotic effect of ATRA-induced NF- κ B activity, which help to reduce incidence of side effects linked to retinoic acid syndrome [97]. Furthermore, ATO has a potential to activate the mitogen-activated protein kinase (MAPK), particularly JNK and p38 that are involved in ATO-induced apoptosis [90, 94, 97–102]. Recently, Tarrade *et al.* demonstrated that retinoic acid potentially enhanced ATO-induced JNK activation, and promoted ATO-induced phosphorylation of retinoid X receptor α , resulting in the amplification of ATO-induced apoptosis in APL or non-APL cells [99]. They also indicated that retinoid X receptor α appears to be a key molecule in the cross-talk between retinoic acid and ATO for apoptosis induction through the phosphorylation of its N-terminal domain [99]. In addition, the inhibition of phosphoinositide 3-kinase/Akt [16] and activation of checkpoint kinase 2, a proapoptotic kinase associated with DNA damage [103], are also involved in ATO-induced apoptosis.

Human telomerase, a cellular reverse transcriptase (hTERT), is a nuclear ribonucleo-protein enzyme complex that catalyses the synthesis and extension of telomeric DNA, and

plays an important role in cellular immortalization and tumorigenesis. Previous reports have demonstrated that arsenic at clinically achievable concentrations is able to inhibit transcription of the human telomerase, resulting in the formation of chromosomal end lesions and consequently in apoptosis induction [74, 104–106]. This effect may be explained that arsenic triggers the oxidation of the Sp1 transcription factor and attenuates its binding to the promoter of hTERT, which contributes to its diminished expression [74, 104]. It has also been demonstrated that in NB4 cells retinoid downregulates telomerase activity and telomere length through a pathway distinct from leukaemia cell differentiation [107]. Thus, a success of ATO/ATRA treatment in APL pathology may be attributed partially to a synergistic effect of these two drugs in triggering sufficient downregulation of telomerase efficient to cause telomere shortening and subsequently, cell death [105].

Moreover, the cytoskeleton including tubulin, which contains sulfhydryl-containing proteins, is another cellular target for arsenic [91]. ATO cross-links two vicinal cysteine residues (Cys-12 and Cys-213) that are close to the guanosine triphosphate binding site in tubulin and results in the blockage of guanosine triphosphate, ultimately leads to apoptosis induction [91]. In addition, ATO-mediated upregulation of prostate apoptosis response gene-4 and downregulation of Wilms' tumor gene, which is upregulated in various subtypes of AML, are also involved in the apoptosis induction of ATO [104].

Anion exchanger 2 (AE2) mediates the exchange of chloride/bicarbonate across the plasma membrane and plays a role in the regulation of intracellular pH. Besides relieving intracellular alkaline and carbon dioxide loads, it also has an important role during development and cell death [108]. It has been demonstrated that ATO enhances directly the activity of AE2, resulting in cellular acidification and interrupting cell homeostasis, and consequently to cell death [109]. Moreover, previous results indicate that arsenite sensitizes human tumor cells to apoptosis via the TNF α -mediated apoptotic pathway [110], and that the death receptor-associated ATP induces the activation of AE [111]. These observations suggest that in addition to the direct activation described above, ATO also indirectly activate the AE2 protein.

JWA, a novel signaling molecule, has been reported to be associated with cell differentiation, growth inhibition, and apoptosis induction mediated by ATO, ATRA, and 12-O-tetradecanoylphorbol 13-acetate in human malignant cells including myeloid leukaemia cell lines and primary cultured APL blasts [112–114]. Recently, Zhou *et al.* reported that JWA is required for ATO induced apoptosis in HeLa and MCF-7 cells via ROS and mitochondria linked signal pathways [115]. Taken together, these data may be helpful to develop new strategies in using JWA as a potential target for the therapeutic use of ATO in certain types of tumors, including APL. In summary, the molecular details of ATO-induced apoptosis are proposed and shown in Figure 11.3.

11.2.5 Differentiation Induction

In vitro and *in vivo* experiments have demonstrated that a low dose of ATO (0.1–0.5 μ M) induces differentiation of NB4 cells as well as fresh APL cells [7, 13, 52]. The differentiation is characterized by several factors such as maturation of morphology, decreased nuclear-cytoplasm ratios, condensation of chromatin, decreased cytoplasmic granules, increased neutrophilic granules, increased expression of CD11b and adhesion molecules,

and decreased expression of CD33 [7, 13, 52]. Although these changes are in line with those observed in granulocyte differentiation triggered by ATRA, the extent of modulation is lower than that induced by ATRA [13, 116]. In contrast to the ATRA-induced differentiation, the nitroblue tetrazolium reduction test is negative, indicating a partial differentiation [12, 13, 52, 117, 118]. On the other hand, Cai *et al.* have demonstrated that the concentrations ranging from 0.1 to 0.5 μM of ATO do not induce differentiation in ATRA-resistant NB4-derived sublines [52], instead they induce differentiation-related changes in ATRA-sensitive HL-60 cells, but not in ATRA-resistant HL-60 sublines with RAR α mutation [52], suggesting that ATO induces APL cell differentiation partially through the activation of retinoic acid receptor-related signaling pathways.

Zhao and colleagues have provided experimental evidences that in both NB4 cells and the fresh APL cells, the ATRA-induced differentiation process is associated with a rapid increase in the intracellular cyclic adenosine monophosphate (cAMP) level as well as protein kinase A activity [119]. They showed that a strong synergy exists between a low concentration of ATO and the cAMP analogue, 8-CPT-cAMP, in inducing terminal differentiation of NB4 and fresh APL cells, suggesting that cAMP facilitates the degradation of ATO-mediated fusion protein PML-RAR α [120]. These observations suggest that ATO-mediated differentiation of APL cells is enhanced by ATRA through a cross-talk with protein kinase A-cAMP signaling pathway and RAR signaling pathway.

In addition, ATO enhances the activity of AE2 in several human leukemic cells including NB4, resulting in cellular acidification, which in turn drives the ATO-induced degradation of PML-RAR α , and promotes cell differentiation [109]. Thus interruption of intracellular pH homeostasis via ATO-induced AE2 elevation is also involved in ATO-induced cell differentiation.

11.2.6 Degradation of PML-RAR α

Although there is evidence to suggest that PML-RAR α expression is not the sole genetic event required for the development of APL, it is no doubt that the fusion protein plays a central role in the initiation of leukemogenesis [10, 117, 121]. Moreover, the fact that ATO selectively exerts therapeutic effects against APL suggests a crucial link between its mechanisms of action and PML-RAR α [8, 122]. Indeed, it is postulated that the PML is a target moiety of ATO-mediated PML-RAR α degradation [12, 13, 117, 118, 123]. Dissection of the mechanisms underlying the role of ATO-induced PML-RAR α degradation in disease remission shows that arsenic modulates the microspeckled pattern of PML distribution within the nucleus of APL cells and induces the rapid reformation of PML-nuclear bodies [121]. Furthermore, arsenic induced covalent modifications of the PML protein by the ubiquitin-related peptides, small ubiquitin-related modifier (SUMO) [121]. Sumoylation is required for the targeting of nuclear body-associated protein onto PML-nuclear bodies. It is shown that sumoylation of PML and PML-RAR α might take place at the amino acid residues, Lys65, Lys160, and Lys490, but only Lys160 is important for the effect of ATO, since Lys160 mediates not only sumoylation but also subsequent recruitment of 11S proteasome, a process which is essential for the degradation of PML and PML-RAR α proteins [122, 124]. Recently, Tatham and colleagues demonstrated that the RING-domain containing ubiquitin E3 ligase, RNF4, targets poly-SUMO-modified proteins for degradation mediated by ubiquitin [125]. RNF4 depletion or proteasome inhibition led to accumulation of

mixed, polyubiquitinated, poly-SUMO chains [125]. They also demonstrated that the PML protein accumulates in RNF4-depleted cells and is ubiquitinated by RNF4 in a SUMO-dependent fashion *in vitro* [125]. Furthermore, in the absence of RNF4, arsenic failed to induce degradation of PML and SUMO-modified PML accumulated in the nucleus [125]. Therefore, they concluded that poly-sumoylation can be a prerequisite step to initiate ubiquitin-mediated proteolysis [125]. Degradation of PML-RAR α as well as PML release their repressive effects on retinoic acid pathways and enhances the acetylation of histone, a process which is important for the transcriptional activation of retinoic acid targeted genes [10, 42]. In addition, it has been reported that arsenic, like ATRA, can activate a common caspase-dependent cleavage in the PML part of the fusion protein [121, 126]. These findings suggest that PML may be a target molecule of caspase during the executor phase of apoptosis [121, 123]. It has been well characterized that ATRA activates the RAR α through activation function 2 (AF-2) transactivation domain and induces the polyubiquitination-19S proteasome-dependent catabolism of PML-RAR α [10, 121, 122, 127]. Therefore, these studies might provide a plausible explanation for superior efficacy of the combination drug (ATO and ATRA) therapy. Collectively, the antileukemic effects of ATO have been proposed to be directly mediated by its ability to induce the relocalization and degradation of PML as well as PML-RAR α in APL cells. Contrary to expectation, Wang *et al.* have reported that ATO induced apoptosis in myeloid leukaemia cell lines and functioned in a PML and PML-RAR α independent manner, and suggesting that these agents may be more broadly used for treatment of leukaemias other than APL [128].

11.2.7 Proliferation Inhibition and Angiogenesis Inhibition

In addition to inducing apoptosis, promoting differentiation, and degradation of PML-RAR α as well as PML, ATO also acts through the intracellular environment to influence growth arrest and angiogenesis [90, 95]. It has been demonstrated that therapeutic concentrations of ATO induce growth inhibition through ATP depletion and prolongation of cell cycle time in malignant lymphocytic cells [129]. A previous report also demonstrated that treatment of U937 with ATO led to G2/M arrest which is associated with the activation of cyclin B-dependent kinase and accumulation of cyclin B, and correlates with the onset of apoptosis [130]. Whereas, treatment of an adult T-cell leukaemia cell line, MT-1, with ATO arrests the cells in the G1 phase [131]. Zhang *et al.* also demonstrated that ATO induced G1 phase arrest in HL-60, Raji, and Daudi, contributing to ATO-mediated proliferation inhibition [132]. Furthermore, in several human myeloma cells, ATO-induced G1 and/or G2/M phase arrest, which is associated with induction of p21 cyclin-dependent kinase inhibitor, has been implicated in growth inhibition [133]. These findings suggest that the cell cycle arrest induced by ATO contributes to its antitumor effects.

It is well established that angiogenesis and expansion of existing endothelium play a critical role in the growth of solid tumors [134] as well as in the proliferation of hematological tumors, such as leukaemia [135–137]. It has been shown that activated endothelial cells release cytokines responsible for stimulating leukemic cell growth [138]. Leukemic cells, in turn, can release endothelial growth factors, such as vascular endothelial growth factor [138]. To study the antiangiogenic effects of ATO, human umbilical vein endothelial cells have been used as a model [139]. In the model system, ATO induced upregulation of endothelial cell adhesion molecules, prevention of capillary tubule growth

and vessel branching, apoptosis of endothelial cells and inhibited vascular endothelial growth factor production from HL-60 [139]. Furthermore, ATO inhibited vascular endothelial growth factor production in the human erythroleukaemia cell line, HEL [139]. Therefore, it is speculated that ATO may interrupt a reciprocal stimulatory loop between leukemic cells and endothelium by acting directly on both cell types, which exerts an antileukemic effect via inhibition of angiogenesis.

11.3 Pharmacokinetics of ATO in APL Patients

11.3.1 Administration Route and Distribution

In 1970s, oral administration of ATO was found to be associated with severe gastrointestinal and liver side effects, and thus intravenous (i.v.) administration of ATO has been widely used for APL patients [140]. In fact, ATO has usually been infused either in the dose of 0.16 mg/kg (or 10 mg/day) in 250–500 ml of normal glucose saline solution over 2–3 h once a day in Chinese studies [6, 10, 141], or in the FDA-approved dose of 0.15 mg/kg in 100–250 ml of 5% dextrose in either water or 0.9% sodium chloride solution over 1–2 h daily [8, 9, 142]. In addition, a reduced dose of 0.08 mg/kg/day (low dosage) corresponding to a 50% of the conventional dosage (0.16 mg/kg/day), has also been applied in the treatment of APL patients [143, 144]. It should be noted that in two clinical trials, treating APL patients with a low dose of ATO yielded a similar complete remission rate (80%) compared to that (85.1%) attained with a conventional dosage [143, 145]. In the low dosage group, a follow-up study for over 7–33 months after complete remission in 14 relapsed patients demonstrated that the estimated disease-free survival rates and overall two year survival rates were $49.11 \pm 15.09\%$ and $61.55 \pm 15.79\%$, respectively, which were similar to the results obtained in another follow-up study for over 7–48 months in 33 relapsed patients in the conventional dosage group ($41.62 \pm 9.95\%$ and $50.24 \pm 10.25\%$, respectively) [143, 145]. Furthermore, APL patients treated with low dosage arsenic demonstrated a reduced toxicity and a similar efficacy compared with that observed with the conventional dosage, although a larger scale randomized study must be launched in order to draw a solid conclusion [143].

On the other hand, in order to overcome attendant inconvenience of intravenous administration including high-cost hospitalization, Kwong and his colleagues have recently developed an oral ATO formulation for patients in order to improve quality of life [146–148]. The treatment protocol includes 10 mg ATO administration by i.v. infusion over 1 h on Day 1, followed by taking 10 mg ATO in 10 ml solution 24 h post i.v. (Day 2) and thereafter [147]. Pharmacodynamic studies demonstrated that the mean plasma and blood AUCs (areas under the arsenic levels versus time curves) determined by oral administration are almost the same as those by i.v. dosing [147]. More importantly, all five patients in this study went into remission [147]. In spite of the satisfactory clinical outcomes, further observations and studies will be needed to define its efficacy of the oral ATO formulation.

After entrance into human body, an accumulation of arsenic mainly occurs in tissues rich in sulfhydryl group containing proteins such as hair, toenail, skin, blood, and bone marrow [6, 31, 141, 149]. Furthermore, distribution of arsenic can be observed in other internal organs, such as the brain, liver, heart, pancreas, kidney, lung, and gastrointestinal tract [141, 149–151]. Recent studies have also demonstrated that arsenic exists in the cerebrospinal fluid of patients receiving ATO administration [32, 33, 146, 148]. It is well

known that the accumulation of arsenic causes a variety of disorders, including skin lesions, respiratory system problems, nervous system effects, and cardiovascular disease, which are also observed in APL patients undergoing ATO treatment [8, 141, 150]. Therefore, a better understanding of the distribution of arsenic in human body will be valuable to lessen the side effects of arsenic through appropriate biomonitoring of arsenic.

11.3.2 Metabolism and Pharmacokinetics

It has been established that biomethylation, which occurred primarily in the liver [149, 152], is a major metabolic pathway for inorganic arsenic in human and many animal species [153], by which arsenic undergoes metabolic conversion by the reduction of As^{V} to As^{III} with subsequent methylation, yielding monomethylated and dimethylated metabolites [154, 155]. A postulated scheme is as follows: $\text{As}^{\text{V}} \rightarrow \text{As}^{\text{III}} \rightarrow$ methylarsonic acid (MAs^{V}) \rightarrow methylarsonous acid (MAs^{III}) \rightarrow dimethylarsinic acid (DMAs^{V}) \rightarrow dimethylarsinous acid (DMAs^{III}). It has been reported that following arsenic exposure, 40–60% of arsenic intake is eliminated through urine. The standard profile of urinary arsenic in human is comprised of 10–30% inorganic arsenic, 10–20% monomethylated arsenic (MAs : $\text{MAs}^{\text{III}} + \text{MAs}^{\text{V}}$), and 60–80% dimethylated arsenic (DMAs : $\text{DMAs}^{\text{III}} + \text{DMAs}^{\text{V}}$) [156, 157].

A recent study has demonstrated that among exonic single nucleotide polymorphisms (SNPs) of human arsenic (+3 oxidation state) methyltransferase (AS3MT) gene, the M287T polymorphism is considered to be related to interindividual variation in the arsenic metabolism [158]. The M287T (T \rightarrow C) polymorphism has been shown to be related to an increased percentage of urinary MAs in a central European male population [43] and a Chilean male group [159, 160]. Moreover, Fujihara *et al.* have postulated that ethnic differences in five intronic polymorphisms are associated with arsenic metabolism within the AS3MT gene [161]. It is worthy to note that a novel PCR-based genotyping method to detect exonic and intronic SNPs in the AS3MT gene has been developed [162]. Thus, future studies will be attempted to elucidate the relationship between these SNPs and arsenic metabolism in APL patients.

The toxicity of arsenic compounds varies and depends on the valency, in general, the trivalent forms are more toxic than pentavalent forms [152, 163]. Because DMAs^{V} is a major urinary metabolite in human exposed to arsenic and displays less acute toxicity than either As^{III} or As^{V} [149, 164], biomethylation has generally been considered as a major detoxification pathway for inorganic arsenicals [163]. However, intermediary metabolites of arsenic, such as MAs^{III} and DMAs^{III} , also possess cytotoxic activity against various cell types including leukaemia and lymphoma cells [152, 165, 166]. Especially, MAs^{III} was more cytotoxic than As^{III} [152]. Furthermore, a previous report indicated that methylated trivalent metabolites of As^{III} are more potent growth inhibitors and apoptotic inducers than ATO in lymphoma and leukaemia cells including NB4 cells, although they do not induce PML-RAR α degradation, restore PML-nuclear bodies or differentiation in NB4 cells [165]. These observations together with our recent study [31] suggest that biomethylation may in fact generate potentially cytotoxic metabolites that may significantly contribute to the therapeutic effect as well as side effects of ATO in APL patients. Indeed, MAs^{III} and DMAs^{III} have been detected in the urine of APL patients undergoing ATO treatment [167] and healthy individuals who have drunk water containing inorganic arsenic [155, 168], and in human hepatoma (HepG2) cells exposed to As^{III} [155]. Therefore, elucidation of arsenic

metabolism is very important for achieving better therapeutic effects, and is critical in reducing side effects of ATO.

An initial pharmacokinetic study showed that arsenic concentrations in plasma rapidly reached the peak level after about 4 h of infusion, and thereafter its plasma concentrations were maintained between 3–0.5 $\mu\text{M/l}$ in eight relapsed APL patients when 0.16 mg/kg/day (or 10 mg/day) ATO was infused [6]. The study also showed that the mean C_{pmax} , $t_{1/2\alpha}$ and $t_{1/2\beta}$ were 6.85 $\mu\text{M/l}$ (ranging from 5.54–7.30 $\mu\text{M/l}$), 0.89 h and 12.13 h, respectively [6]. Moreover, in patients given 0.08 mg/kg/day ATO plasma arsenic concentrations reached peak levels after 2 h of infusion with the mean C_{pmax} of 2.63 $\mu\text{M/l}$ (ranging from 1.54–3.42 $\mu\text{M/l}$), and thereafter its plasma concentrations were maintained between 0.5–0.1 $\mu\text{M/l}$ [143]. In the study, the $t_{1/2\alpha}$ and $t_{1/2\beta}$ were 1.41 h and 9.4 h, respectively [143]. Based on *in vitro* studies, we expect that the major effects of ATO in the conventional and low dosage lie in apoptosis and differentiation induction, respectively. On the other hand, our study utilizing a dose of 0.15 mg/kg demonstrated that plasma concentrations of As^{III} and As^{V} on Day 1 reached similar C_{pmax} values of 12.4 and 10.2 ng/ml, respectively, immediately after the completion of administration followed by a biphasic elimination [169]. The peak arsenic concentrations in plasma varied from 200 to 600 nM/after 10 mg/kg of oral ATO [146, 147]. These results suggest that plasma arsenic concentrations vary largely depending on administration dosage and route, and that monitoring of its concentrations will provide detailed information for optimizing efficacy of ATO.

Central nervous system relapse of APL occurs in 1–5% of patients [170, 171], the optimal therapy for this case remains unclear. Fortunately, clinical data have demonstrated that ATO seems to be capable of crossing the blood-brain-barrier in humans [32, 33, 146, 148, 172]. In these patients treated with ATO, ATO concentrations in the cerebrospinal fluid were in the range of 12–30% compared with those in whole blood or plasma [33, 146, 172]. Furthermore, Meng *et al.* have developed a non-invasive method via concomitant with 20% mannitol intravenous bolus injection to help ATO entering into central nervous system [173]. Their regimens include 125 ml of 20% mannitol bolus through medial cubital vein at the rate of 12 ± 30 ml/min, and followed with 250 ml of mixed solution (including 20% mannitol and ATO 0.08 mg/kg/day) through intravenous infusion at the rate of 6 ml/min, followed by ATO 0.08 mg/kg/day + 5% glucose 250 ml infusion at the rate of 0.5 ml/min in the total dosage of ATO (0.16 mg/kg/day) [32]. Results demonstrated that more dynamic changes of arsenic in cerebrospinal fluid were observed with the help of mannitol than general intravenous infusion, indicating that a significant amount of arsenic can penetrate through blood-brain barrier [32], and the arsenic in cerebrospinal fluid reached to the concentrations that is needed for APL cell differentiation [13, 52, 174, 175].

The pharmacokinetic studies in APL patients have been well discussed by using urine samples [6, 144, 169, 176]. It has been demonstrated that urinary arsenic contents slightly increased during drug administration, and the total amounts of arsenic excreted daily into the urine accounting for approximately 1–8% of the daily dose [6]. On the other hand, our previous report revealed that the mean total arsenic excretion rate including inorganic arsenic and methylated arsenic was about 20% of daily dose on Day 1 and remained at about 60% of daily dose during subsequent weeks [169]. Moreover, a clinical pharmacokinetic study performed in an APL patient showed that in the urine sample collected for 24 h after administration of ATO, the total amount of inorganic arsenic and the methylated metabolites was almost 30% more of the daily dose [144]. As described above, there are large variations

among individual patients with regard to the arsenic metabolic profiles and excretion patterns. Indeed, Wang *et al.* [176] have demonstrated that there is an interindividual difference in excretion profiles and the relative concentrations of major arsenic species in the urine among four Chinese APL patients undergoing ATO treatment. Furthermore, other pathways of excretion, such as through the bile, have been also suggested to play a partial role in the elimination of arsenic [6, 176].

Recently, to clarify the speciation of arsenic, we collected blood samples at various time points from a patient with APL after remission induction therapy and during consolidation therapy [31]. Our results demonstrated that during the drug-withdrawal period, As^V in plasma was more readily eliminated among all arsenic metabolites as reported by other groups [144, 177]. As^{III} concentrations in plasma initially declined more quickly than those of MAs and DMAs, suggesting that methylated metabolites (MAs and DMAs) are major metabolites in plasma, again in agreement with other reports [153–155]. Furthermore, we also demonstrated that the concentrations of methylated metabolites (MAs and DMAs) as well as inorganic arsenic (As^{III} and As^V) in plasma increase with multiple administration during the consolidation therapy period [31]. In contrast, Fujisawa *et al.* [169] demonstrated no increase in the maximum concentrations of inorganic arsenic (As^{III} and As^V) regardless of multiple administrations, suggesting that inorganic arsenic in plasma may reach a steady state after multiple administrations, but the concentrations of methylated metabolites (MAs and DMAs) increased. The exact cause for this apparent difference is not known, but we noted that there are many differences in patient characteristics in the two studies. For example, only one out of 14 patients who participated in the study of Fujisawa *et al.* was in the first relapse whereas the other 13 patients were in the second to fifth relapses [169]. But the patient in our study was in the first relapse [31]. Therefore, the differences in the patient characteristics may explain the discrepancy in the concentrations of inorganic arsenic. These results also suggest that understanding the differences in metabolism among patients is very useful for providing an effective treatment protocol for individual APL patients.

Most of the pharmacokinetic studies in APL patients have been conducted using plasma or urine [6, 144, 169, 176], and rarely using blood samples. It has been demonstrated that 90% of arsenic in blood is bound to hemoglobin [178], suggesting that pharmacokinetic studies including red blood cells could provide better treatment protocol for APL patients. Our recent report demonstrated that in all blood samples collected either after the remission induction therapy or during consolidation therapy, approximately 80–90% of the total arsenic in the blood samples was observed in the blood cells, suggesting that careful attentions should be paid to profiles of arsenic species in blood cells [31]. Previous *in vitro* studies demonstrated that DMAs and dimethylmonothioarsinic acid are taken up and metabolized by human red blood cells [179]. Furthermore, our results clearly demonstrated that not only inorganic arsenic, but also methylated metabolites (MAs and DMAs) could accumulate in the blood during the consecutive administration of ATO to APL patients [31]. As described above, trivalent methylated metabolites also possess cytotoxic activity against various cell types including leukaemia and lymphoma cells [152, 165, 166]. Taken together, these observations raise a possibility of application of methylated arsenic metabolites to APL patients.

Because of the different toxicities of the various arsenic metabolites, understanding of arsenic metabolism in APL patients is necessary in order to implement proper doses and duration of arsenic treatment and to optimize the treatment outcome. Actually, recently

not only total arsenic analysis but also speciations of arsenic metabolites have generally been conducted in clinical samples from APL patients undergoing ATO treatment [31, 144, 169, 176, 180]. However, an issue associated with speciation of trivalent methyl arsenic metabolites (MAs^{III} and DMAs^{III}) arose from their higher reactivity. It has been reported that preservatives, such as diethyldithiocarbamate [176] and 2,3-dimercaptopropanesulphonate [180], are added to the urine samples to stabilize these trivalent arsenic species, yet, to our knowledge, the use of these preservatives into the blood samples has not been mentioned. Furthermore, it is easily expected that considerable amounts of arsenic species exist in clinical samples as a protein-bound complex. Although analysis of these protein-bound arsenic complexes has been conducted, the losses of these complexes from the sampling to the detection stage are not resolved [180]. Therefore, the development of more applicable contemporary analytical protocols for these unstable arsenic species shall be explored.

Except for administration of arsenic to APL patients in clinical practice, arsenic usually enters the body through food chains. The most common exposure to high levels of arsenic in food is via marine products in the form of arsenobetaine or plant products in the form of various arsenosugars [163, 181]. Arsenobetaine, a trimethylarsenic compound, is one of the major organic arsenic in seafood, and is not produced by the metabolism of As^{III} in human [182–184]. Once arsenobetaine is ingested, it will be excreted from the body in the same form. Although arsenobetaine is almost nontoxic [184, 185], seafood intake during the periods of remission induction therapy and consolidation therapy will result in interruption of accurate arsenic speciation. Therefore, to evaluate the pharmacokinetics of arsenic species accurately, it is necessary to take daily diet, in particular seafood, into consideration [31, 144, 169].

11.3.3 Adverse Effects and Biological Monitoring

An immediate side effect of ATO therapy in APL is an increase in the white blood cell count [122, 186], which was observed in more than 50% of cases in most studies, but hyperleukocytosis with signs similar to retinoic acid syndrome was relatively infrequent and most cases responded to corticosteroids treatment, such as dexamethasone [122].

QT prolongation is another feared complication in ATO therapy [8, 9, 31, 34, 187]. The extent of prolongation was higher in men than in women, and in patients with hypokalemia [9]. A recent report demonstrated that in three in four African Americans given ATO developed arrhythmias versus only one in 73 non-African American patients [188]. These observations suggest that ethnic group is the primary predictor of arrhythmias, and thus more attention should be paid to African American patients. Generally, prior to commencing ATO treatment, electrolyte measurements and electrocardiogram should be performed and any preexisting electrolyte abnormalities should be corrected. Moreover, during the periods of remission induction therapy and consolidation, electrocardiogram should be performed every 1–2 weeks [9]. In general, ATO administration should be discontinued when the electrocardiogram showed QT interval prolongation (greater than 500 ms) [31, 189]. So far, the other reported main side effects of ATO administration include gastrointestinal disorders, respiratory complaints, neuropathy, liver dysfunction [6, 143, 190, 191], although these side effects are negligible compared to its clinical efficacy.

In order to achieve better therapeutic effects for individual APL patients and reduce side effects of ATO, detailed arsenic biomonitoring should be diligently performed. Clinical samples (such as blood and urine) from APL patients undergoing ATO treatment should be used for not only the study of pharmacokinetics of ATO, but also arsenic biomonitoring. Blood and/or urine samples are able to evaluate accurately the arsenic burden in individual APL patients. However, there are several attendant drawbacks, such as inconvenience and hospitalization. More convenient methods for the biological monitoring of arsenic in the body are to measure the accumulation of arsenic in hair or toenails [150]. Hair samples are used as a biosamples for arsenic because inorganic arsenic and DMAs are stored in the hair root and thus reflect past exposure [150]. Nails of fingers or toes are used as they reflect arsenic storage three months ago in fingers and six months ago in toes. Indeed, hair and nails are used as biomarkers to estimate average arsenic exposure in chronic arsenic poisoning [192]. These biomarkers should be useful for predicting occurrence of serious adverse event during long-term administration of ATO.

11.4 Potential Combination Therapies with ATO

An extensive body of literature has clearly demonstrated superiority in treating APL simultaneously with ATO and ATRA [10, 117]. In the following content, we will discuss the other potential candidate agents, which are expected to potentiate the efficacy of ATO, except for ATRA.

11.4.1 Natural Product Derived Substances

Flavonoids, including anthocyanins and isoflavone, have been shown to exhibit anticarcinogenic activity against multiple cancer cells types *in vitro* and tumor types *in vivo* [102, 193–198]. Potential cancer chemopreventive activities of anthocyanins revealed from *in vitro* studies include anti-cell proliferation, induction of apoptosis and differentiation, anti-inflammatory, antiangiogenesis and invasiveness effects [102, 193, 197]. Recently, it has been demonstrated that the most common type of anthocyanins, cyanidin-3-rutinoside, induced apoptosis in HL-60 cells in a dose- and time-dependent manner [194]. Cyanidin-3-rutinoside treatment resulted in ROS-dependent activation of p38 MAPK and JNK, which contributed to cell death by activating the mitochondrial pathway mediated by Bim, one of proapoptotic gene of Bcl-2 family [194]. More importantly, cyanidin-3-rutinoside treatment did not lead to increased ROS accumulation in normal human peripheral blood mononuclear cells (PBMNC) and had no cytotoxic effects on these cells [194] as indicated by our preliminary data concerning treatment of HL-60 and PBMNC with anthocyanidin (unpublished data). Genistein is a soy-derived isoflavone with multiple biochemical effects, including estrogen receptor binding and activation [199], DNA topoisomerase II inhibition [200], downregulation of phosphoinositide 3-kinase/Akt signaling pathway and NF- κ B transcription factor activity [201], alteration of cell cycle-regulatory kinase activities [202]. Recently, Sánchez *et al.* have reported that genistein selectively potentiates ATO-induced apoptosis in human leukaemia cells (HL-60, THP-1, and Jurkat) via ROS generation and activation of ROS-inducible protein kinases (p38-MAPK, AMP-activated kinase) [102]. However, the same phenomena were not observed in

phytohemagglutinin stimulated non-tumor peripheral blood lymphocytes [102]. Furthermore, a recent report has indicated that quercetin, a plant-derived flavonoid, specifically a flavonol which has been used as a nutritional supplement, cooperates with ATO in apoptosis induction against human myeloid leukaemia cell, although the efficacy depends very much on the used cell line [198]. The potentiation of ATO toxicity by quercetin correlates and may be explained at least partially by the capacity of the flavonoid to downregulate Akt phosphorylation and to decrease the intracellular GSH contents in the leukaemia cell model [198]. We also demonstrated recently that *Vitex agnus-castus* fruit extract, composed mainly of flavonoids, exhibits cytotoxic effects against various cancer cells, including leukaemia cell lines (Kikuchi *et al.* manuscript in preparation, [203–205]). Intriguingly, it has recently been revealed that flavonoids inhibit the function of ATP-binding cassette transporters such as MRPs as well as P-gp [195, 206], which are suggested to selectively potentiate the efficacy of ATO in APL patients.

In addition, a previous report has demonstrated that isothiocyanates, which are rich in cruciferous vegetables including broccoli, may provide protection against many different cancers, making them excellent candidates for cancer prevention [197]. The chemopreventive properties of isothiocyanates are mainly referable to modulation of carcinogen metabolism, inhibition of cell proliferation, and induction of apoptosis [197]. In fact, cell proliferation inhibition and apoptosis induction mediated by isothiocyanates have been reported in both animal and human cancer cells including leukaemia cells [207, 208].

Taken together, these observations suggest flavonoids and isothiocyanates, as potential candidate agents, can potentiate the efficacy of ATO for effective treatment of APL. On the other hand, poor absorption of flavonoids into the bloodstream of humans is an outstanding problem for their ultimate use for chemoprevention of human cancer [193]. Indeed, pharmacokinetic data indicate that the absorption of anthocyanins into the bloodstream of rodents and humans is minimal, suggesting that they may have little efficacy in tissues other than the gastrointestinal tract and skin, where they can be absorbed locally [193]. Therefore, future studies on enhancing the absorption of anthocyanins and/or their metabolites may be necessary for their optimal application in the chemoprevention of human cancer.

11.4.2 Cytokine

Recently, Matsui *et al.* have demonstrated that the granulocyte colony-stimulating factor (G-CSF) and granulocyte-macrophage colony-stimulating factor (GM-CSF) markedly increased the differentiation of NB4 cells or APL blasts from clinical samples treated with ATRA, ATO, or bryostatatin-1 as evidenced by the enhanced expression of CD 11b and the inhibition of clonogenic growth [209]. Therefore, the combined use of ATO, ATRA and these cytokines may improve the clinical efficacy of differentiation therapy in APL. Phase III clinical trials in the treatment of patients with previously untreated AML have been conducted in Japan [210]. In the clinical trials, a large randomized study selectively focused on the G-CSF priming was performed [210]. Among patients attaining complete remission in this study, the probability of relapse was reduced when receiving G-CSF along with induction chemotherapy. The benefit of chemotherapy-sensitization by G-CSF was particularly evident among the intermediate-risk group [210].

Interferons (IFNs) are a large family of multifunctional secretory proteins that regulate cellular antiviral, antitumor and immunological responses by activating the expression of IFN-stimulated genes [211]. It has been reported that IFN α and 1 μ M ATO act synergistically to induce apoptosis in non-APL cells [212, 213]. Moreover, Mounira and colleagues have demonstrated that 0.1 μ M ATO acts cooperatively with IFNs (α or γ) to induce differentiation in NB4 and in retinoic acid-resistant NB4 cells [211]. They also demonstrated that pretreatment with IFNs, particularly IFN γ , enhanced 1 μ M ATO induced apoptosis in NB4 and retinoic acid-resistant NB4 cells [211]. Therefore, it would be interesting to examine whether treatment of APL patients with ATO plus IFN γ could increase the proportion of cells undergoing differentiation or apoptosis and thereby enhance chemotherapeutic response.

11.4.3 Other Reagents

The pivotal role of GSH in ATO actions has been well discussed in the previous sections. It is easily expected that compounds that lower the GSH content potentiate the antitumor effect of ATO. Buthionine sulfoxide, a specific inhibitor for glutathione synthesis [35, 95, 129], has been demonstrated to lower the GSH content of NB4 cells and potentiate the apoptotic effect of ATO [71]. Furthermore, ATO-resistant subline, NB4/As, has been reported to have a higher concentration of intracellular GSH than NB4 [67]. However, reduction of the GSH level by buthionine sulfoxide completely restored the sensitivity to ATO [67]. Therefore, these data suggest that a favorable clinical outcome of ATO in combination with buthionine sulfoxide can be achieved in leukaemia patients who are insensitive to the clinically acceptable ATO concentrations.

It has been previously demonstrated that in HL-60 and su-DHL-4 (B-cell lymphoma) cells, ascorbic acid acts as an oxidizing agent by decreasing the GSH content of the cells, which in turn synergizes the growth-inhibitory as well as apoptotic effect of ATO [71]. The synergistic growth-inhibitory effect of ATO and ascorbic acid was observed not only in cell lines, but also in primary culture of chronic lymphocytic leukaemia cells [71]. Moreover, the study by a lymphoma mouse model revealed that ascorbic acid enhances anti-lymphoma effect of ATO *in vivo* without additive toxicity as compared with ATO or ascorbic acid treatment alone [71]. Thus, co-administration of ascorbic acid may potentiate therapeutic effects of ATO in APL.

Chou *et al.* have reported that phorbol myristate acetate and its clinically used analogue, bryostatin 1, stimulate NADPH oxidase activity and synergize with ATO to enhance ROS production and cytotoxicity in NB4 cells [77]. They have also exploited the synergistic induction of NADPH oxidase activity and ROS production by arsenic and phorbol myristate acetate to provide proof-of-concept that this synergy may be clinically applicable [77]. Moreover, Emodin, a natural anthraquinone derivative, has been revealed to enhance the cytotoxicity of ATO via the generation of ROS in HeLa cells and U937 cells, but not in nonmalignant human fibroblasts [214]. Recently, Brown *et al.* have also reported a potent synergistic effect of the combination of ATO and IFN α with emodin and docosahexaenoic acid on cell-cycle arrest and cell death of human leukaemia cells [215]. The study demonstrated that combination of emodin and docosahexaenoic acid with ATO allows the arsenic concentration to be decreased by 100-fold while preserving its antitumor activity [215], suggesting a broad application in the treatment of leukaemias and lymphomas.

Moreover, it has been revealed that combination treatment with phytosphingosine, one of sphingolipid metabolites, and ATO induces synergistic apoptosis in ATO-resistant leukaemia cells through the p38 MAPK-mediated mitochondrial translocation of Bax and the PARP activation, and that p38 MAPK and PARP activations are ROS dependent [94]. The molecular mechanism may provide an insight into the design of future combination cancer therapies to cells intrinsically less sensitive to ATO treatment. Furthermore, previously it has been demonstrated that nitric oxide induces apoptosis in human leukemic lines through mitochondria-dependent mechanisms [216], in agreement with our previous reports [79, 217, 218], suggesting that nitric oxide donor may potentiate the clinical efficacy of ATO in APL.

Recently, we have established a good model system, comprising the primary cultured cells prepared from human fetal membranes, to study the responses of these cells to various external stimuli including oxidative stress [79, 217–219]. Because the effects of ATO on normal cells have not yet been well discussed, we hypothesize that the model system can be used to study the toxicological as well as pharmacological relevance, and have obtained preliminary data associated with uptake and efflux as well as cytotoxic effect of ATO in these cells (Yoshino *et al.* manuscript in preparation). We expect these data will provide detailed information regarding to arsenic metabolisms in fetal membranes, and a new insight into reducing the side effects of arsenic in future.

11.5 Potential ATO Application to Other Leukaemias

The application of ATO to APL has been well discussed in many studies [6–8, 12, 13, 191], and it has been recognized that ATO is able to induce a high complete remission rate among relapse APL patients and can reach a relatively high relapse-free survival rate after complete remission when used with chemotherapy [6–8, 117]. Especially, the success of ATRA and ATO in APL treatment provides the first model of molecular target-based induction of differentiation and apoptosis. Recently, besides APL, the application of ATO to other leukaemias has also been discussed.

It has been reviewed that the mechanisms of action of ATO and their relevance to the treatment of myelodysplastic syndrome, a disease for which no standard treatment currently exists [34]. Recently, a phase II multicenter study has been performed and concluded that ATO treatment consisting of an initial loading dose (0.3 mg/kg per day of ATO for five days) followed by maintenance therapy (0.25 mg/kg ATO twice weekly for 15 weeks) has moderate activity in myelodysplastic syndrome, inducing hematological responses in both lower- and higher-risk patients [220].

It has been reported that the BCR/ABL tyrosine kinase inhibitor imatinib markedly improves the prognosis of chronic myeloid leukaemia patients [221], however, imatinib preferentially targets dividing cells, whereas nondividing leukemic cells are resistant to imatinib-mediated apoptosis [222]. Namely, surviving leukaemia stem and progenitor cells are a potential source for relapse. Therefore, the leukaemia-initiating cells (LIC) cannot be eradicated by the current therapy, leading to disease relapse on drug discontinuation [222]. Recently, an exciting study performed by Ito *et al.* [223] has demonstrated that PML is indispensable for LIC maintenance, and that inhibition of PML by ATO disrupts LIC maintenance and increases the efficacy of antileukemic therapy by sensitizing LIC to

proapoptotic stimuli, such as cytosine arabinoside treatment. Therefore, a new therapeutic approach, based on treatment with ATO, has been presented for targeting quiescent LIC and possibly cancer-initiating cells by pharmacological inhibition of PML [223].

Moreover, the cytotoxic effect of ATO on primary leukaemia cells from patients with chronic lymphocytic leukaemia was enhanced by a SOD inhibitor, 2-methoxyestradiol, suggesting that it is possible to use the combination of ATO and 2-methoxyestradiol to enhance the antileukaemic activity and to overcome drug resistance [76, 92, 95]. Such a combination strategy may have potential clinical applications.

The efficacy of ATO to lymphoma was initially explored by Zhu *et al.* [129] in their study on a panel of malignant lymphocytes. They demonstrated that the therapeutic concentrations of ATO (1–2 μM) induced a substantial growth inhibition and apoptosis of most malignant lymphocytes, including SKW-3, Molt-4, BJAB, su-DHL-4, Namalwa, Raji and Nalm-6 [129]. Thus, ATO may be proved to be useful in the treatment of malignant lymphoproliferative disorders.

Human T-cell lymphotropic virus type I (HTLV-I) is the causative agent of adult T-cell leukaemia/lymphoma (ATL). ATL is an aggressive proliferation of mature activated T-cells associated with a poor prognosis due to its intrinsic resistance to chemotherapy [42, 224, 225]. Although zidovudine and $\text{IFN}\alpha$ yield some responses in ATL patients and improve the prognosis, alternative therapies are required. It has been reported that arsenic and $\text{IFN}\alpha$ synergize to induce cell cycle arrest and apoptosis in HTLV-I transformed cells through mechanisms associated with Tax (known as the viral transactivator protein and a powerful activator of the $\text{NF-}\kappa\text{B}$ pathway) downregulation and reversal of $\text{NF-}\kappa\text{B}$ activation [224, 225]. Such studies provide strong rationale for combined arsenic- IFN therapy in ATL patients.

Although a previous report demonstrated that single ATO treatment did not induce a clinical response in 11 adult patients with relapsed and refractory acute lymphoblastic leukaemia (ALL) [226], a further study has showed that subtoxic doses (0.25 μM) of ATO can restore the sensitivity to dexamethasone in glucocorticoid resistant T and precursor B ALL cells, which provides evidence for the Akt/XIAP pathway as a candidate target for combinatorial therapy in glucocorticoid resistance [227]. Therefore the combination of ATO with glucocorticoid could be advantageous in glucocorticoid-resistant ALL and reveals additional targets for the evaluation of new antileukemic agents [227].

In addition, previous studies showed that ATO induced growth inhibition and apoptosis in a number of tumor cell lines, such as non-Hodgkin's lymphoma cells [132], megakaryocytic leukaemia [228], multiple myeloma [133] and non-M3 acute myeloid leukaemia [229]. Therefore, the clinical use of ATO for the treatment of diseases associated with the dysfunction of these cells should be considered.

11.6 Conclusion

A striking global arsenic research is being explored to understand the mechanisms of action of ATO in leukaemia therapy. So far, *in vitro* and *in vivo* studies have demonstrated that ATO exerts a dose-dependent dual effect on APL cells, triggering apoptosis at relatively high concentrations and inducing differentiation at lower concentrations. Both *in vitro* and *in vivo* studies have also demonstrated the effectiveness of arsenic in various hematological

malignancies besides APL. Indeed, multiple phase I and II clinical trials are also underway to evaluate its feasibility, safety and potential effects. Furthermore, ROS induction by arsenic is intimately associated with the apoptosis induction, and it has been demonstrated that the basal levels of ROS could determine the apoptotic sensitivity of cells to ATO. Therefore, a synergistic effect can be expected when combining ROS producing agents, apoptosis inducing agents and/or differentiation agents with ATO, to potentiate the ATO effect. For example, ATO-ATRA combination has been applied to treat newly diagnosed and refractory APL, and has achieved satisfactory outcomes. All these achievements show the power of integrating Western and Eastern wisdoms and make us confident that APL status has evolved from highly fatal to highly curable. In order to further optimize ATO-based regimens for a better complete remission rate and survival time, the efforts to exploit potential combination therapies with ATO are ongoing. Meanwhile, the effectiveness of ATO-induced apoptosis on some solid tumor cells has also been investigated, and the results suggest that apoptotic effects of ATO are not restricted to leukaemia cells but also in selected types of tumor cells, such as esophageal, prostate, and ovarian carcinomas and neuroblastoma cells. Thus, the experiences acquired in the treatment of leukaemia patients, especially APL, are valuable in that they mirror the way to conquer the nonhematologic malignancies.

Acknowledgements

This work was supported in part by grants from the Ministry of Education, Culture, Sports, Science and Technology and by the Promotion and Mutual Aid Corporation for Private Schools of Japan. We also acknowledge Nippon Shinyaku Co. Ltd. for kind assistance. Finally, the study could not be completed without constant encouragement from late Prof. Kaise, and his passion of the development of new therapies for APL patients will be remembered.

References

1. Goddard, A.D., Borrow, J., Freemont, P.S., and Solomon, E. (1991) *Science*, **254**, 1371–1374.
2. Tong, J.H., Dong, S., Geng, J.P. *et al.* (1992) *Oncogene*, **7**, 311–316.
3. de Thé, H., Chomienne, C., Lanotte, M. *et al.* (1990) *Nature*, **347**, 558–561.
4. Melnick, A. and Licht, J.D. (1999) *Blood*, **93**, 3167–3215.
5. Burnett, A.K., Grimwade, D., Solomon, E. *et al.* (1999) *Blood*, **93**, 4131–4143.
6. Shen, Z.X. *et al.* (1997) *Blood*, **89**, 3354–3360.
7. Soignet, S.L., Maslak, P., Wang, Z.G. *et al.* (1998) *The New England Journal of Medicine*, **339**, 1341–1348.
8. Cohen, M.H., Hirschfeld, S., Flamm Honig, S. *et al.* (2001) *Oncologist*, **6**, 4–11.
9. Litzow, M.R. (2008) *Expert Opinion on Pharmacotherapy*, **9**, 1773–1785.
10. Wang, Z.Y. and Chen, Z. (2008) *Blood*, **111**, 2505–2515.
11. Duncan, A. (1794) *The Edinburgh New Dispensatory*, 4th edn T. Dobson, Philadelphia, PA.
12. Chen, G.Q. *et al.* (1996) *Blood*, **88**, 1052–1061.
13. Chen, G.Q. *et al.* (1997) *Blood*, **89**, 3345–3353.
14. Bienert, G.P., Schüssler, M.D., and Jahn, T.P. (2008) *Trends in Biochemical Sciences*, **33**, 20–26.
15. Rosen, B.P. and Liu, Z. (2009) *Environment International*, **35**, 512–515.
16. Kumagai, Y. and Sumi, D. (2007) *Annual Review of Pharmacology and Toxicology*, **47**, 243–262.

17. Huang, R.N. and Lee, T.C. (1996) *Toxicology and Applied Pharmacology*, **136**, 243–249.
18. Lu, W.J., Tamai, I., Nezu, J. *et al.* (2006) *Journal of Biomedical Science*, **13**, 525–533.
19. Bhattacharjee, H., Carbrey, J., Rosen, B.P., and Mukhopadhyay, R. (2004) *Biochemical and Biophysical Research Communications*, **322**, 836–841.
20. Leung, J., Pang, A., Yuen, W.H. *et al.* (2007) *Blood*, **109**, 740–746.
21. Wang, L., Zhou, G.B., Liu, P. *et al.* (2008) *Proceedings of the National Academy of Sciences of the United States of America*, **105**, 4826–4831.
22. Lanotte, M., Martin-Thouvenin, V., Najman, S. *et al.* (1991) *Blood*, **77**, 1080–1086.
23. Agre, P., King, L.S., Yasui, M. *et al.* (2002) *The Journal of Physiology*, **542**, 3–16.
24. Agre, P. and Kozono, D. (2003) *FEBS Letters*, **555**, 72–78.
25. Ramírez-Solís, A., Mukopadhyay, R., Rosen, B.P., and Stemmler, T.L. (2004) *Inorganic Chemistry*, **43**, 2954–2959.
26. Liu, Z., Shen, J., Carbrey, J.M. *et al.* (2002) *Proceedings of the National Academy of Sciences of the United States of America*, **99**, 6053–6058.
27. Liu, Z., Carbrey, J.M., Agre, P., and Rosen, B.P. (2004) *Biochemical and Biophysical Research Communications*, **316**, 1178–1185.
28. Lee, T.C., Ho, I.C., Lu, W.J., and Huang, J.D. (2006) *The Journal of Biological Chemistry*, **281**, 18401–18407.
29. Liu, Z., Styblo, M., and Rosen, B.P. (2006) *Environmental Health Perspectives*, **114**, 527–531.
30. Ishibashi, K., Kuwahara, M., Gu, Y. *et al.* (1998) *Biochemical and Biophysical Research Communications*, **244**, 268–274.
31. Yoshino, Y., Yuan, B., Miyashita, S.I. *et al.* (2009) *Analytical and Bioanalytical Chemistry*, **393**, 689–697.
32. Jin, Z., Ran, M., and Man, Z. (2007) *Haematologica*, **92**, e82–e84.
33. Knipp, S., Gattermann, N., Schapira, M. *et al.* (2007) *Leukemia Research*, **31**, 1585–1587.
34. Vey, N. (2004) *Expert Opinion on Pharmacotherapy*, **5**, 613–621.
35. Liu, J., Chen, H., Miller, D.S. *et al.* (2001) *Molecular Pharmacology*, **60**, 302–309.
36. Leslie, E.M., Haimeur, A., and Waalkes, M.P. (2004) *The Journal of Biological Chemistry*, **279**, 32700–32708.
37. Zaman, G.J., Lankelma, J., van Tellingen, O. *et al.* (1995) *Proceedings of the National Academy of Sciences of the United States of America*, **92**, 7690–7694.
38. Huang, R.N. and Lee, T.C. (1996) *Toxicology and Applied Pharmacology*, **141**, 17–22.
39. Vernhet, L., Allain, N., Bardiau, C. *et al.* (2000) *Toxicology*, **142**, 127–134.
40. Cole, S.P., Sparks, K.E., Fraser, K. *et al.* (1994) *Cancer Research*, **54**, 5902–5910.
41. Thomas, D.J., Styblo, M., and Lin, S. (2001) *Toxicology and Applied Pharmacology*, **176**, 127–144.
42. Hu, J., Fang, J., Dong, Y. *et al.* (2005) *Anti-Cancer Drugs*, **16**, 119–127.
43. Lindberg, A.L., Kumar, R., Goessler, W. *et al.* (2007) *Environmental Health Perspectives*, **115**, 1081–1086.
44. Gyurasics, A., Varga, F., and Gregus, Z. (1991) *Biochemical Pharmacology*, **42**, 465–468.
45. Gregus, Z. and Gyurasics, A. (2000) *Biochemical Pharmacology*, **59**, 1375–1385.
46. Kala, S.V., Neely, M.W., Kala, G. *et al.* (2000) *The Journal of Biological Chemistry*, **275**, 33404–33408.
47. Lorico, A., Rappa, G., Finch, R.A. *et al.* (1997) *Cancer Research*, **57**, 5238–5242.
48. Liu, J., Liu, Y., Powell, D.A. *et al.* (2002) *Toxicology*, **170**, 55–62.
49. Takeshita, A., Shinjo, K., Naito, K. *et al.* (2003) *Leukemia*, **17**, 648–650.
50. Tan, B., Piwnica-Worms, D., and Ratner, L. (2000) *Current Opinion in Oncology*, **12**, 450–458.
51. Michieli, M., Damiani, D., Ermacora, A. *et al.* (2000) *British Journal of Haematology*, **108**, 703–709.
52. Cai, X., Shen, Y.L., Zhu, Q. *et al.* (2000) *Leukemia*, **14**, 262–270.
53. Jing, Y., Dai, J., Chalmers-Redman, R.M. *et al.* (1999) *Blood*, **94**, 2102–2111.
54. Zhang, T.D., Chen, G.Q., Wang, Z.G. *et al.* (2001) *Oncogene*, **20**, 7146–7153.
55. Kerr, J.F., Wyllie, A.H., and Currie, A.R. (1972) *British Journal of Cancer*, **26**, 239–257.
56. Ryter, S.W., Kim, H.P., Hoetzel, A. *et al.* (2007) *Antioxidants & Redox Signaling*, **9**, 49–89.

57. Shimizu, S., Narita, M., and Tsujimoto, Y. (1999) *Nature*, **399**, 483–487.
58. Wei, M.C., Zong, W.X., Cheng, E.H. *et al.* (2001) *Science*, **292**, 727–730.
59. Earnshaw, W.C., Martins, L.M., and Kaufmann, S.H. (1999) *Annual Review of Biochemistry*, **68**, 383–424.
60. Nakagawa, T., Zhu, H., Morishima, N. *et al.* (2000) *Nature*, **403**, 98–103.
61. McCarthy, N.J. and Evan, G.I. (1998) *Current Topics in Developmental Biology*, **36**, 259–278.
62. Kang, Y.H., Yi, M.J., Kim, M.J. *et al.* (2004) *Cancer Research*, **64**, 8960–8967.
63. Larochette, N., Decaudin, D., Jacotot, E. *et al.* (1999) *Experimental Cell Research*, **249**, 413–421.
64. Zhu, J., Okumura, H., Ohtake, S. *et al.* (2003) *Oncology Reports*, **10**, 705–709.
65. Szegezdi, E., Cahill, S., Meyer, M. *et al.* (2006) *British Journal of Cancer*, **94**, 398–406.
66. Kim, E.H., Yoon, M.J., Kim, S.U. *et al.* (2008) *Cancer Research*, **68**, 266–275.
67. Kitamura, K., Minami, Y., Yamamoto, K. *et al.* (2000) *Leukemia*, **14**, 1743–1750.
68. Li, J., Chen, P., Sinogeeva, N. *et al.* (2002) *The Journal of Biological Chemistry*, **277**, 49504–49510.
69. Du, Y. *et al.* (2006) *Blood*, **107**, 1582–1590.
70. Yi, J., Gao, F., Shi, G. *et al.* (2002) *Apoptosis: An International Journal on Programmed Cell Death*, **7**, 209–215.
71. Dai, J., Weinberg, R.S., Waxman, S., and Jing, Y. (1999) *Blood*, **93**, 268–277.
72. Ninomiya, M., Kajiguchi, T., Yamamoto, K. *et al.* (2006) *Haematologica*, **91**, 1571–1572.
73. Wang, J., Li, L., Cang, H. *et al.* (2008) *Leukemia Research*, **32**, 429–436.
74. Chou, W.C., Chen, H.Y., Yu, S.L. *et al.* (2005) *Blood*, **106**, 304–310.
75. Chen, Q., Vazquez, E.J., Moghaddas, S. *et al.* (2003) *The Journal of Biological Chemistry*, **278**, 36027–36031.
76. Pelicano, H., Feng, L., Zhou, Y. *et al.* (2003) *The Journal of Biological Chemistry*, **278**, 37832–37839.
77. Chou, W.C., Jie, C., Kenedy, A.A. *et al.* (2004) *Proceedings of the National Academy of Sciences of the United States of America*, **101**, 4578–4583.
78. Margaret, M.B. and Amanda, F.B. (1996) *Cell Death and Differentiation*, **3**, 63–70.
79. Yuan, B., Ohyama, K., Bessho, T. *et al.* (2008) *Life Sciences*, **82**, 623–630.
80. Lu, J., Chew, E.H., and Holmgren, A. (2007) *Proceedings of the National Academy of Sciences of the United States of America*, **104**, 12288–12293.
81. Lin, S., Cullen, W.R., and Thomas, D.J. (1999) *Chemical Research in Toxicology*, **12**, 924–930.
82. Lin, S., Del Razo, L.M., Styblo, M. *et al.* (2001) *Chemical Research in Toxicology*, **14**, 305–311.
83. Chouchane, S. and Snow, E.T. (2001) *Chemical Research in Toxicology*, **14**, 517–522.
84. Talbot, S., Nelson, R., and Self, W.T. (2008) *British Journal of Pharmacology*, **154**, 940–948.
85. Gailer, J., George, G.N., Pickering, I.J. *et al.* (2002) *Chemical Research in Toxicology*, **15**, 1466–1471.
86. Adler, V., Yin, Z., Fuchs, S.Y. *et al.* (1999) *The EMBO Journal*, **18**, 1321–1334.
87. Bernardini, S., Bellincampi, L., Ballerini, S. *et al.* (2002) *Journal of Cellular Biochemistry*, **86**, 340–347.
88. Shen, H., Tsuchida, S., Tamai, K., and Sato, K. (1993) *Archives of Biochemistry and Biophysics*, **300**, 137–141.
89. Bernardini, S., Nuccetelli, M., Noguera, N.I. *et al.* (2006) *Annals of Hematology*, **85**, 681–687.
90. Davison, K., Mann, K.K., and Miller, W.H. Jr. (2002) *Seminars in Hematology*, **39** (2 Suppl 1), 3–7.
91. Li, Y.M. and Broome, J.D. (1999) *Cancer Research*, **59**, 776–780.
92. Zhou, Y., Hileman, E.O., Plunkett, W. *et al.* (2003) *Blood*, **101**, 4098–4104.
93. Gao, F., Yi, J., Shi, G.Y. *et al.* (2002) *World Journal of Gastroenterology*, **8**, 36–39.
94. Park, M.T., Kang, Y.H., Park, I.C. *et al.* (2007) *Molecular Cancer Therapeutics*, **6**, 82–92.
95. Carney, D.A. (2008) *Leukemia & Lymphoma*, **49**, 1846–1851.
96. Kapahi, P., Takahashi, T., Natoli, G. *et al.* (2000) *The Journal of Biological Chemistry*, **275**, 36062–36066.

97. Mathieu, J. and Besançon, F. (2006) *Annals of the New York Academy of Sciences*, **1090**, 203–208.
98. Davison, K., Mann, K.K., Waxman, S., and Miller, W.H. Jr. (2004) *Blood*, **103**, 3496–3502.
99. Tarrade, A., Bastien, J., Bruck, N. *et al.* (2005) *Oncogene*, **24**, 2277–2288.
100. Yoda, A., Toyoshima, K., Watanabe, Y. *et al.* (2008) *The Journal of Biological Chemistry*, **283**, 18969–18979.
101. Chowdhury, R., Chowdhury, S., Roychoudhury, P. *et al.* (2009) *Apoptosis: An International Journal on Programmed Cell Death*, **14**, 108–123.
102. Sánchez, Y., Amrán, D., Fernández, C. *et al.* (2008) *International Journal of Cancer*, **123**, 1205–1214.
103. Joe, Y., Jeong, J.H., Yang, S. *et al.* (2006) *The Journal of Biological Chemistry*, **281**, 28764–28771.
104. Glienke, W., Chow, K.U., Bauer, N., and Bergmann, L. (2006) *Leukemia & Lymphoma*, **47**, 1629–1638.
105. Tarkanyi, I., Dudognon, C., Hillion, J. *et al.* (2005) *Leukemia*, **19**, 1806–1811.
106. Chou, W.C., Hawkins, A.L., Barrett, J.F. *et al.* (2001) *The Journal of Clinical Investigation*, **108**, 1541–1547.
107. Pendino, F., Flexor, M., Delhommeau, F. *et al.* (2001) *Proceedings of the National Academy of Sciences of the United States of America*, **98**, 6662–6667.
108. Reynolds, J.E., Li, J., and Eastman, A. (1996) *Cytometry*, **25**, 349–357.
109. Pan, X.Y., Chen, G.Q., Cai, L. *et al.* (2006) *British Journal of Haematology*, **134**, 491–499, Erratum in: *British Journal of Haematology*, 2006, **135**, 747.
110. Ivanov, V.N. and Hei, T.K. (2004) *The Journal of Biological Chemistry*, **279**, 22747–22758.
111. Pucéat, M., Roche, S., and Vassort, G. (1998) *The Journal of Cell Biology*, **141**, 1637–1646.
112. Huang, S., Shen, Q., Mao, W.G. *et al.* (2006) *Biochemical and Biophysical Research Communications*, **341**, 440–450.
113. Cao, H.X., Xia, W., Shen, Q. *et al.* (2002) *Chinese Science Bulletin*, **47**, 834–838.
114. Mao, W.G., Liu, Z.L., Chen, R. *et al.* (2006) *Clinical and Experimental Pharmacology & Physiology*, **33**, 816–824.
115. Zhou, J., Ye, J., Zhao, X. *et al.* (2008) *Toxicology and Applied Pharmacology*, **230**, 33–40.
116. Huang, M.E., Ye, Y.C., Chen, S.R. *et al.* (1988) *Blood*, **72**, 567–572.
117. Fang, J., Chen, S.J., Tong, J.H. *et al.* (2002) *Cancer Biology & Therapy*, **1**, 614–620.
118. Chen, Z., Chen, G.Q., Shen, Z.X. *et al.* (2001) *Seminars in Hematology*, **38**, 26–36.
119. Zhao, Q., Tao, J., Zhu, Q. *et al.* (2004) *Leukemia*, **18**, 285–292.
120. Zhu, Q., Zhang, J.W., Zhu, H.Q. *et al.* (2002) *Blood*, **99**, 1014–1022.
121. Zhu, J., Lallemand-Breitenbach, V., and de Thé, H. (2001) *Oncogene*, **20**, 7257–7265.
122. Chen, Z., Zhao, W.L., Shen, Z.X. *et al.* (2007) *Current Topics in Microbiology and Immunology*, **313**, 129–144.
123. Zhu, J., Koken, M.H., Quignon, F. *et al.* (1997) *Proceedings of the National Academy of Sciences of the United States of America*, **94**, 3978–3983.
124. Zhu, J., Zhou, J., Peres, L. *et al.* (2005) *Cancer Cell*, **7**, 143–153.
125. Tatham, M.H., Geoffroy, M.C., Shen, L. *et al.* (2008) *Nature Cell Biology*, **10**, 538–546.
126. Nervi, C., Ferrara, F.F., Fanelli, M. *et al.* (1998) *Blood*, **92**, 2244–2251.
127. vom Baur, E., Zechel, C., Heery, D. *et al.* (1996) *The EMBO Journal*, **15**, 110–124.
128. Wang, Z.G., Rivi, R., Delva, L. *et al.* (1998) *Blood*, **92**, 1497–1504.
129. Zhu, X.H. (1999) *et al. Journal of the National Cancer Institute*, **91**, 772–778.
130. Park, J.W., Choi, Y.J., Jang, M.A. *et al.* (2001) *Biochemical and Biophysical Research Communications*, **286**, 726–734.
131. Ishitsuka, K., Ikeda, R., Suzuki, S. *et al.* (1999) *Blood*, **94**, 263 (abstract).
132. Zhang, W., Ohnishi, K., Shigeno, K. *et al.* (1998) *Leukemia*, **12**, 1383–1391.
133. Park, W.H., Seol, J.G., Kim, E.S. *et al.* (2000) *Cancer Research*, **60**, 3065–3071.
134. Folkman, J. (1995) *The New England Journal of Medicine*, **333**, 1757–1763.
135. Perez-Atayde, A.R., Sallan, S.E., Tedrow, U. *et al.* (1997) *The American Journal of Pathology*, **150**, 815–821.

136. Aguayo, A., Kantarjian, H., Talpaz, M. *et al.* (1998) *Blood*, **92**, 607 (abstract).
137. Pruneri, G., Soligo, D., Carboni, N. *et al.* (1998) *Blood*, **92**, 715 (abstract).
138. Fiedler, W., Graeven, U., Ergün, S. *et al.* (1997) *Blood*, **89**, 1870–1875.
139. Roboz, G.J., Dias, S., Lam, G. *et al.* (2000) *Blood*, **96**, 1525–1530.
140. Sun, H.D., Ma, L., Hu, X.C., and Zhang, T.D. (1992) *Chinese Journal of Integrated Traditional and Western Medicine*, **12**, 170–171.
141. Huang, S.Y., Chang, C.S., Tang, J.L. *et al.* (1998) *British Journal of Haematology*, **103**, 1092–1095.
142. Soignet, S.L. *et al.* (2001) *Journal of Clinical Oncology*, **19**, 3852–3860.
143. Shen, Y. *et al.* (2001) *Leukemia*, **15**, 735–741.
144. Fukai, Y., Hirata, M., Ueno, M. *et al.* (2006) *Biological & Pharmaceutical Bulletin*, **29**, 1022–1027.
145. Niu, C. *et al.* (1999) *Blood*, **94**, 3315–3324.
146. Au, W.Y., Tam, S., Fong, B.M., and Kwong, Y.L. (2008) *Blood*, **112**, 3587–3590.
147. Kumana, C.R., Au, W.Y., Lee, N.S. *et al.* (2002) *European Journal of Clinical Pharmacology*, **58**, 521–526.
148. Au, W.Y., Tam, S., Fong, B.M., and Kwong, Y.L. (2006) *Blood*, **107**, 3012–3013.
149. Nielsen, F.H. and Uthus, E.O. (1981) *Biochemistry of the Essential Ultratrace Elements* (ed. F. Frieden) Plenum, New York, pp. 319–340.
150. Kapaj, S., Peterson, H., Liber, K., and Bhattacharya, P. (2006) *Journal of Environmental Science and Health Part A-Toxic/Hazardous Substances & Environmental Engineering*, **41**, 2399–2428.
151. Iyengar, G.V., Kollmer, W.E., and Bowen, H.J.M. (eds) (1978) *The Elemental Composition of Human Tissues and Body Fluids*, Wiley-VCH Verlag GmbH Weinheim,.
152. Styblo, M., Del Razo, L.M., Vega, L. *et al.* (2000) *Archives of Toxicology*, **74**, 289–299.
153. Aposhian, H.V. (1997) *Annual Review of Pharmacology and Toxicology*, **37**, 397–419.
154. Kitchin, K.T. (2001) *Toxicology and Applied Pharmacology*, **172**, 249–261.
155. Del Razo, L.M., Styblo, M., Cullen, W.R., and Thomas, D.J. (2001) *Toxicology and Applied Pharmacology*, **174**, 282–293.
156. Rossman, T.G. (2003) *Mutation Research*, **533**, 37–65.
157. Vahter, M. (2000) *Toxicology Letters*, **112–113**, 209–217.
158. Drobná, Z., Waters, S.B., Walton, F.S. *et al.* (2004) *Toxicology and Applied Pharmacology*, **201**, 166–177.
159. Hernández, A., Xamena, N., Surrallés, J. *et al.* (2008) *Mutation Research*, **637**, 80–92.
160. Hernández, A., Xamena, N., Sekaran, C. *et al.* (2008) *Pharmacogenet Genomics*, **18**, 349–355.
161. Fujihara, J., Fujii, Y., Agusa, T. *et al.* (2009) *Toxicology and Applied Pharmacology*, **234**, 41–46.
162. Fujihara, J., Kunito, T., Agusa, T. *et al.* (2007) *Toxicology and Applied Pharmacology*, **225**, 251–254.
163. Yamauchi, H. and Fowler, B.A. (1994) *Arsenic in the Environment, Part II: Human Health and Ecosystem Effects* (ed. J.O. Nriagu) John Wiley & Sons, Inc., New York, pp. 35–43.
164. Hopenhayn-Rich, C., Biggs, M.L., Smith, A.H. *et al.* (1996) *Environmental Health Perspectives*, **104**, 620–628.
165. Chen, G.Q., Zhou, L., Styblo, M. *et al.* (2003) *Cancer Research*, **63**, 1853–1859.
166. Aposhian, H.V., Zakharyan, R.A., Avram, M.D. *et al.* (2004) *Toxicology and Applied Pharmacology*, **198**, 327–335.
167. Wang, Z., Zhou, J., Lu, X. *et al.* (2004) *Chemical Research in Toxicology*, **17**, 95–103.
168. Aposhian, H.V. *et al.* (2000) *Chemical Research in Toxicology*, **13**, 693–697.
169. Fujisawa, S. *et al.* (2007) *Cancer Chemotherapy and Pharmacology*, **59**, 485–493.
170. de Botton, S. *et al.* (2006) *Leukemia*, **20**, 35–41.
171. Specchia, G., Lo Coco, F., Vignetti, M. *et al.* (2001) *Journal of Clinical Oncology*, **19**, 4023–4028.
172. Helwig, A., Klemm, M., Schüttig, R. *et al.* (2007) *Leukemia Research*, **31**, 703–705.
173. Meng, R., Zhou, J., Wang, D.S. *et al.* (2003) *Journal of Apoplexy and Nervous Diseases*, **20**, 350–352.

174. Chen, Z., Wang, Z.Y., and Chen, S.J. (1997) *Pharmacology & Therapeutics*, **76**, 141–149.
175. Zhou, J., Meng, R., Sui, X. *et al.* (2005) *Haematologica*, **90**, 1277–1279.
176. Wang, Z., Zhou, J., Lu, X. *et al.* (2004) *Chemical Research in Toxicology*, **17**, 95–103.
177. Benramdane, L., Accominotti, M., Fanton, L. *et al.* (1999) *Clinical Chemistry*, **45**, 301–306.
178. Lu, M., Wang, H., Li, X.F. *et al.* (2004) *Chemical Research in Toxicology*, **17**, 1733–1742.
179. Naranmandura, H. and Suzuki, K.T. (2008) *Toxicology and Applied Pharmacology*, **227**, 390–399.
180. Slejkovec, Z., Falnoga, I., Goessler, W. *et al.* (2008) *Analytica Chimica Acta*, **607**, 83–91.
181. Todorov, T.I., Ejnić, J.W., Mullick, F.G., and Centeno, J.A. (2005) *Microchimica Acta*, **151**, 263–268.
182. Cannon, J.R., Edmonds, J.S., Francesconi, K.A. *et al.* (1981) *Australian Journal of Chemistry*, **34**, 787–798.
183. Benramdane, L., Accominotti, M., Fanton, L., *et al.* (1999) *Clinical Chemistry*, **45**, 301–306.
184. Kaise, T., Watanabe, S., and Itoh, K. (1985) *Chemosphere*, **14**, 1327–1332.
185. Kaise, T. and Fukui, S. (1992) *Applied Organometallic Chemistry*, **6**, 155–160.
186. Camacho, L.H., Soignet, S.L., Chanel, S. *et al.* (2000) *Journal of Clinical Oncology*, **18**, 2620–2625.
187. Ohnishi, K., Yoshida, H., Shigeno, K. *et al.* (2002) *Leukemia*, **16**, 617–622.
188. Patel, S.P., Garcia-Manero, G., Ferrajoli, A. *et al.* (2006) *Leukemia Research*, **30**, 362–363.
189. Jones, R.L. and Ewer, M.S. (2006) *Expert Review of Anticancer Therapy*, **6**, 1249–1269.
190. Soignet, S.L. *et al.* (2001) *Journal of Clinical Oncology*, **19**, 3852–3860.
191. Shen, Z.X. *et al.* (2004) *Proceedings of the National Academy of Sciences of the United States of America*, **101**, 5328–5335.
192. Yoshida, T., Yamauchi, H., and Fan Sun, G. (2004) *Toxicology and Applied Pharmacology*, **198**, 243–252.
193. Wang, L.S. and Stoner, G.D. (2008) *Cancer Letters*, **269**, 281–290.
194. Feng, R., Ni, H.M., Wang, S.Y. *et al.* (2007) *The Journal of Biological Chemistry*, **282**, 13468–13476.
195. Kitagawa, S. (2006) *Biological & Pharmaceutical Bulletin*, **29**, 1–6.
196. Ko, C.H., Shen, S.C., and Chen, Y.C. (2004) *Free Radical Biology & Medicine*, **36**, 897–910.
197. Fimognari, C., Lenzi, M., and Hrelia, P. (2008) *Current Medicinal Chemistry*, **15**, 440–447.
198. Ramos, A.M. and Aller, P. (2008) *Biochemical Pharmacology*, **75**, 1912–1923.
199. Zava, D.T. and Duwe, G. (1997) *Nutrition and Cancer*, **27**, 31–40.
200. Markovits, J., Linossier, C., Fossé, P. *et al.* (1989) *Cancer Research*, **49**, 5111–5117.
201. Sarkar, F.H., Adsule, S., Padhye, S. *et al.* (2006) *Mini-Reviews in Medicinal Chemistry*, **6**, 401–407.
202. Chang, K.L., Kung, M.L., Chow, N.H., and Su, S.J. (2004) *Biochemical Pharmacology*, **67**, 717–726.
203. Ohyama, K., Akaike, T., Hirobe, C., and Yamakawa, T. (2003) *Biological & Pharmaceutical Bulletin*, **26**, 10–18.
204. Ohyama, K., Akaike, T., Imai, M. *et al.* (2005) *The International Journal of Biochemistry & Cell Biology*, **37**, 1496–1510.
205. Imai, M., Kikuchi, H., Denda, T. *et al.* (2009) *Cancer Letters*, **276**, 74–80.
206. Castro, A.F. and Altenberg, G.A. (1997) *Biochemical Pharmacology*, **53**, 89–93.
207. Fimognari, C., Nüsse, M., Berti, F. *et al.* (2003) *Annals of the New York Academy of Sciences*, **1010**, 393–398.
208. Jakubikova, J., Bao, Y., and Sedlak, J. (2005) *Anticancer Research*, **25**, 3375–3386.
209. Matsui, W., Smith, B.D., Vala, M. *et al.* (2005) *British Journal of Haematology*, **128**, 853–862.
210. Naito, K. and Ohnishi, K. (2005) *Gan To Kagaku Ryoho*, **32**, 292–296.
211. Chelbi-alix, M.K., Bobé, P., Benoit, G. *et al.* (2003) *Oncogene*, **22**, 9121–9130.
212. Bazarbachi, A., El-Sabban, M.E., Nasr, R. *et al.* (1999) *Blood*, **93**, 278–283.
213. El-Sabban, M.E., Nasr, R., Dbaiibo, G. *et al.* (2000) *Blood*, **96**, 2849–2855.
214. Yi, J., Yang, J., He, R. *et al.* (2004) *Cancer Research*, **64**, 108–116.

215. Brown, M., Bellon, M., and Nicot, C. (2007) *Blood*, **109**, 1653–1659.
216. Ushmorov, A., Ratter, F., Lehmann, V. *et al.* (1999) *Blood*, **93**, 2342–2352.
217. Yuan, B., Ohyama, K., Bessho, T., and Toyoda, H. (2006) *Biochemical and Biophysical Research Communications*, **341**, 822–827.
218. Yuan, B., Ohyama, K., Takeichi, M., and Toyoda, H. (2009) *The International Journal of Biochemistry & Cell Biology*, **41**, 1062–1069.
219. Ohyama, K., Yuan, B., Bessho, T., and Yamakawa, T. (2001) *European Journal of Biochemistry*, **268**, 6182–6189.
220. Vey, N., Bosly, A., Guerci, A. *et al.* (2006) *Journal of Clinical Oncology*, **24**, 2465–2471.
221. Kantarjian, H., O'Brien, S., Cortes, J. *et al.* (2008) *Cancer*, **113** (7 Suppl), 1933–1952.
222. Holtz, M., Forman, S.J., and Bhatia, R. (2007) *Cancer Research*, **67**, 1113–1120.
223. Ito, K., Bernardi, R., Morotti, A. *et al.* (2008) *Nature*, **453**, 1072–1078.
224. Bazarbachi, A., El-Sabban, M.E., Nasr, R. *et al.* (1999) *Blood*, **93**, 278–283.
225. El-Sabban, M.E., Nasr, R., Dbaibo, G. *et al.* (2000) *Blood*, **96**, 2849–2855.
226. Litzow, M.R., Lee, S., Bennett, J.M. *et al.* (2006) *Haematologica*, **91**, 1105–1108.
227. Bornhauser, B.C., Bonapace, L., Lindholm, D. *et al.* (2007) *Blood*, **110**, 2084–2091.
228. Lu, M., Levin, J., Sulpice, E. *et al.* (1999) *Experimental Hematology*, **27**, 845–852.
229. Lehmann, S., Bengtzen, S., Paul, A. *et al.* (2001) *European Journal of Haematology*, **66**, 357–364.

12

Anticancer Activity of Molecular Compounds of Arsenic, Antimony and Bismuth

Edward R.T. Tiekink

Department of Chemistry, University of Malaya, Kuala Lumpur 50603, Malaysia

12.1 Introduction

Metal based drugs continue to play a vital role in contemporary medicine. Accordingly, molecular complexes of platinum(II) for example, cisplatin (**I**) and carboplatin (**II**), find wide use as chemotherapeutic agents for the treatment of various forms of cancer; see Figure 12.1 for chemical structures of drugs discussed in this section. Gold(I) compounds, for example, monomeric auranofin (**III**) and polymeric myochrisine (**IV**), are still used in the amelioration of the inflammation and pain associated with the debilitating disease, rheumatoid arthritis. The silver(I) complex of sulfadiazine, (**V**), is used as an antimicrobial and antifungal agent. Age related macular degeneration disease may be remedied by the tin (IV) compound ethyl etiopurpurin, (**VI**), by exploiting the principles of photodynamic therapy. Owing to its ability to release NO to promote vascular muscle relaxation, sodium nitroprusside, containing iron(II), that is, $\text{Na}_2[\text{Fe}(\text{CN})_5(\text{NO})] \cdot 2\text{H}_2\text{O}$ (**VII**), is used clinically as a hypotensive agent. While not a coordination complex, lithium(I) carbonate, Li_2CO_3 (**VIII**), was introduced in the 1950s for the treatment of bipolar disorders and it still employed for that purpose. Another carbonate but associated with lanthanum(III), i.e. $\text{La}_2(\text{CO}_3)_3$ (**IX**), may be prescribed for chronic renal failure. It is evident from the

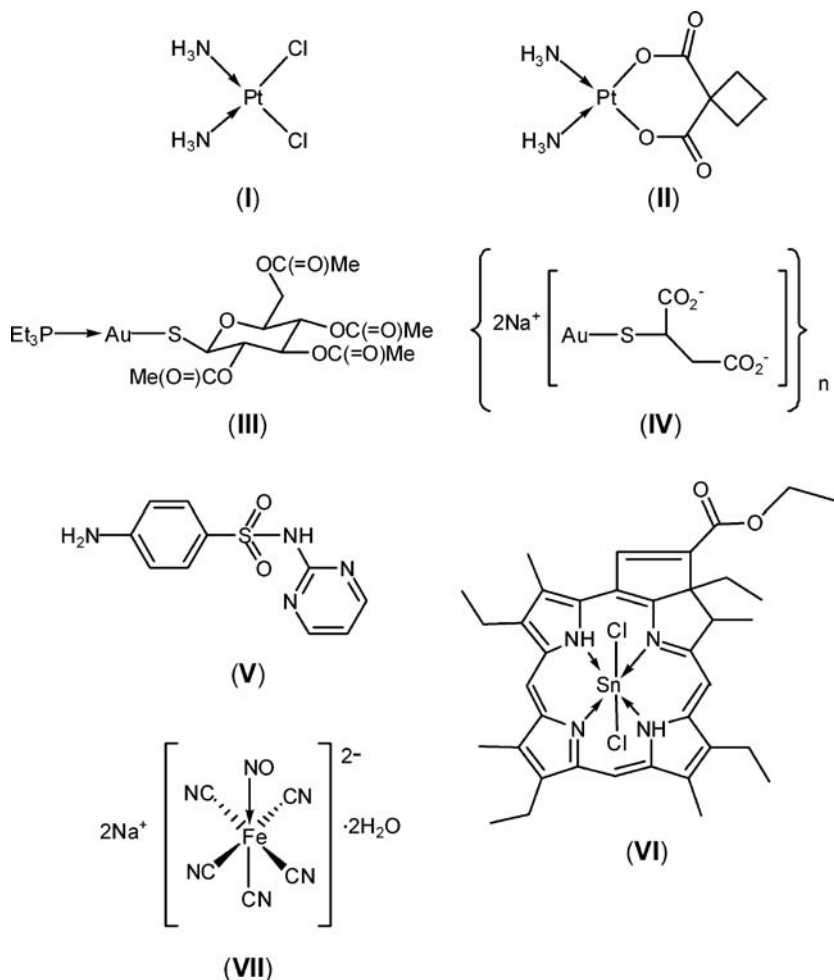


Figure 12.1 Chemical structures of molecules relevant in metal based drugs: cisplatin (I), carboplatin (II), auranofin (III), and polymeric sodium aurothiomate (IV), sulfadiazine, (V), tin ethyl etiopurpurin, (VI) and sodium nitroprusside (VII)

foregoing that there is a wide range of metal based chemotherapeutic agents: the important contribution metal complexes play in diagnostic medicine should also be acknowledged. In recognition of the special roles played by metal complexes in modern medicine, it is not surprising that there are books (e.g., [1–7]) and many reviews (e.g., [8–18]) addressing the general concept of metals in medicine.

While no mention has been yet made of the elements that form the focus of this Chapter, namely arsenic, antimony and bismuth, these too form an important part of modern medicine, as may be seen in other chapters collected in this book. Herein, the anticancer activity/potential of arsenic, antimony and bismuth compounds is summarized after a brief introduction of the history of each element in human medicine.

12.2 Arsenic Compounds

Arsenic holds a special place in medicinal inorganic chemistry. Paul Ehrlich's role in contemporary medicine partially revolved around the development of arsenic based therapeutic compounds for the treatment of syphilis and sleeping sickness, African trypanosomiasis. Indeed, it is the emergence of the arsenic containing compound Salvarsan, developed as a 'magic bullet' that probably marks the beginning of modern chemotherapy [19]. However, the use of arsenic in medicine predates Ehrlich by well over 2000 years [20–22]. Hippocrates recorded the use of the arsenic sulfur derivatives, realgar (red arsenic, As_2S_2) and orpiment (yellow arsenic, As_2S_3), for the treatment of ulcers. Arsenic trioxide (white arsenic, As_2O_3 ; **X**) was mentioned as a cure for tuberculosis. Arsenic as a medicine has figured prominently in Western society, being used as an important agent for the treatment of leukaemia from the 1700s, for about two centuries. A familiar reagent, Fowlers solution (arsenic trioxide in a potassium bicarbonate solution), was used for the treatment of a variety of human ailments, including leukaemia [23]. Inorganic arsenic compounds also feature in Traditional Chinese Medicine (TCM) and it is probably true to state that the resurgence of interest into their therapeutic use arose in that country. This came about after extensive clinical observations in the 1970s suggesting the efficacy of arsenic trioxide (contained within a TCM used for the treatment of leukaemia, incidentally also containing mercury) in the treatment of Acute Promyelocytic Leukaemia [24]. This is a cancer of the blood and bone marrow, and is a subtype of acute myeloid leukaemia. Subsequently, significant attention has been devoted to the development of arsenic trioxide (Trisenox) as a drug, determining its mechanisms of action and new modes of delivery.

A precise mechanism of action for Trisenox remains unknown and studies investigating the interaction of arsenic with biomolecules continue [25–28]. Patients suffering from acute promyelocytic leukaemia (AML) are characterized by an accumulation of immature granulocytes (i.e., promyelocytes: a category of white blood cells with granules in their cytoplasm) in their bone marrow. Further, patients test positive for a chromosome abnormality, that is, a chromosomal translocation involving the retinoic acid receptor α (*RAR α* or *RARA*) gene, which usually generates a leukemogenic fusion gene. This latter feature of AML makes this leukaemia susceptible to tretinoin therapy (tretinoin, the acid form of vitamin A, is often referred to as all-*trans* retinoic acid) [29, 30]. At high concentrations, the dominant effect of Trisenox is cell death by apoptosis while at low concentration, the effect appears due to its ability to disturb cell differentiation [23, 29]. A molecular mechanism for Trisenox is the degradation of the retinoic acid receptor of promyelocyte [30, 31].

The above notwithstanding, arsenic is widely, and correctly, regarded as a toxin and is implicated as a carcinogen, that is, it is a paradoxical species in human physiology [22, 32]. The emergence of Trisenox has prompted investigations into alternative and more effective means of delivery, for example exploiting principles of nanotechnology [33] and lipid encapsulation [34]. In addition, the quest for molecular forms of 'arsenic' as chemotherapeutic agents is ongoing.

It has already been mentioned that Salvarsan was the first compound to be developed specifically as a chemotherapeutic agent. Having spirochaeticidal activity, this and related compounds were used in the forefront of the eradication of *Treponema pallidum*, the bacterium implicated in syphilis; their use continued until the advent of penicillin [35]. It

was not until only recently that the chemical composition of Salvarsan was determined. It turns out that Salvarsan in fact comprises cyclic species, for example, tricyclic (**XI**) and pentacyclic (**XII**) [36], see Figure 12.2. Regardless of the true structure of Salvarsan, it functions as a prodrug, providing a slow release source of the therapeutically active species (3-amino-4-hydroxyphenyl)As(OH)₂.

Compared with the interest in molecular antimony and bismuth compounds as potential anticancer agents, investigations of molecular arsenic compounds are lagging, probably owing to perceived problems with toxicity. Amongst the first arsenic containing compounds examined for their potential as anticancer agents were those already used clinically. For example, the typanocide, melarsoprol (**XIII**), Figure 12.2, which is still used in the treatment of African typanosomiasis [37, 38], is effective against leukaemia cell lines, more so than arsenic trioxide and causes apoptosis but not cell differentiation [39]. *In vivo* studies in immune suppressed mice showed no advantage in terms of inhibiting myeloma growth [40]. More positive were investigations on human breast and prostate cancer cells inoculated in mice which indicated melarsoprol reduced the anticipated growth of the tumours [41]. While the previous study did not present any obvious side effects associated with administration of melarsoprol, further development as an anticancer agent is unlikely owing to (i) severe toxicity to the central nervous system resulting in encephalopathy, and (ii) lack of a clinical response [42–44]. The amoebicidal and bactericidal arsthinol (**XIV**),

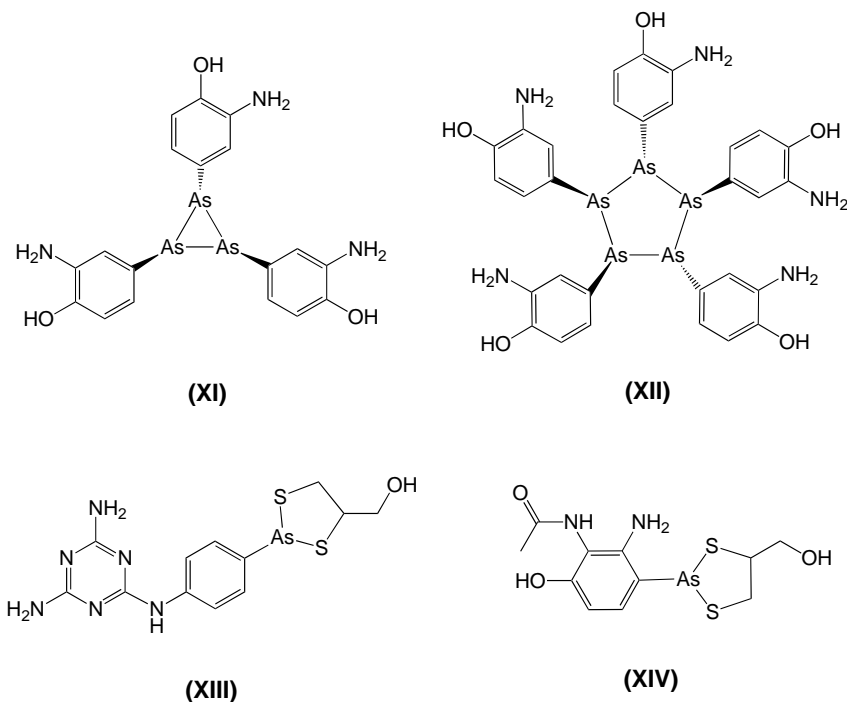


Figure 12.2 Chemical structures of molecules relevant to arsenic pharmacology: tricyclic component of Salvarsan (**XI**), pentacyclic component of Salvarsan (**XII**), melarsoprol (**XIII**), and arsthinol (**XIV**)

also known as Balarsen, displays significant cytotoxicity against the K562 erythroleukaemia and U937 myelomonocytic leukaemia cell lines [44]. Interestingly, the therapeutic index, calculated as LD_{50} in mice/ IC_{50} in cell line, was considerably better than either of arsenic trioxide and melarsoprol. With this background, synthetic arsenic analogues of arsenic based drugs have been investigated.

The simplest organoarsenic compound investigated for putative anticancer activity is dimethylarsenic acid (**XV**), Figure 12.3. An important, if not the, detoxification mechanism of 'inorganic' compounds is biomethylation. Here, methyl-metal bonds are formed to generate organometallic species that are more readily excreted from the body, for example, via respiration. Arsenic species are detoxified this way and dimethylarsenic acid is one of the metabolites. Compounds **XV** and As_2O_3 (**X**) were evaluated against a panel of eight leukaemia and multiple myeloma cell lines [45]. Concentrations of compound **XV**, on average, 1000 times more were required to achieve the same cytotoxic responses compared with (**X**). Compound **XV** induced apoptosis in the cancer cells but not in progenitor cells, and has little effect on the maturation of leukaemic cells [45].

The compound where organoarsenic is complexed to glutathione, 4-(*N*-(*S*-glutathionylacetyl)amino)phenylarsonous acid (**XVI**), inhibits the growth of a variety of cancer cells, including pancreatic, lung and prostate cancers, by a mechanism whereby the blood supply to the tumour is restricted, that is, halting angiogenesis by targeting mitochondria in endothelial cells [46, 47]. Compound **XVI** exhibits no obvious side effects and Phase I/IIA trials of the compound are ongoing [23]. A closely related compound **XVII**, a result of the

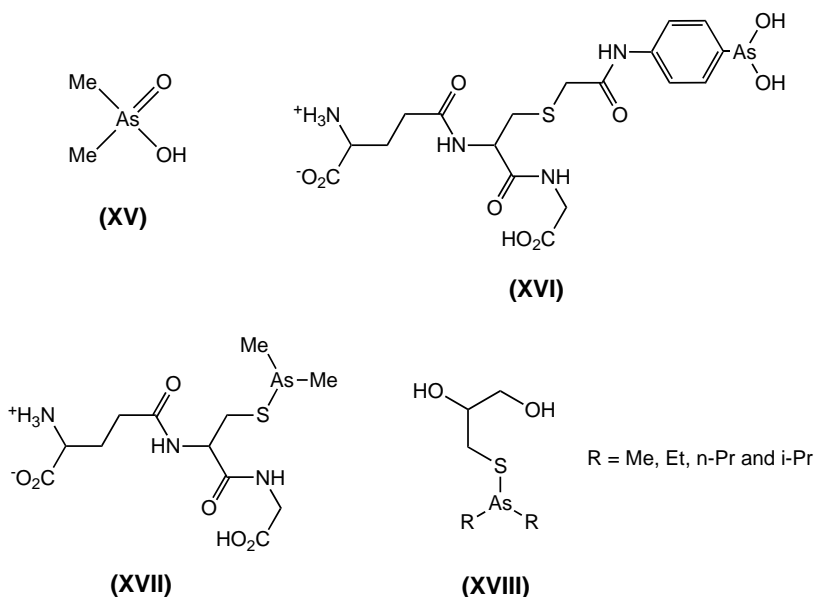


Figure 12.3 Chemical structures of synthetic arsenic containing molecules investigated for anticancer potential: dimethylarsinic acid (**XV**), 4-(*N*-(*S*-glutathionylacetyl)amino) phenylarsonous acid (**XVI**), *S*-dimethylarsino glutathione (**XVII**; Darinapsin) and generic structure of *S*-dialkylarsino-3-mercapto-1,2-propanediol (**XVIII**)

combination of the essential components found in compounds **XV** and **XVI**, *S*-dimethylarsino glutathione (Darinaparsin), also displays exciting potential as a metal based anticancer drug, having a similar profile of activity to **XVI**. For example, it has been reported that **XVII** was well tolerated by patients having advanced haematological malignancies in a Phase I trial [23]. In a complementary study based on the National Cancer Institute's panel of 60 cancer cell lines, that is *in vitro*, a series of compounds with the general formula shown in (**XVIII**) were evaluated [48]. Of the R = Me, Et, *n*-Pr and *i*-Pr compounds tested, the most cytotoxic was the R = *n*-Pr derivative clearly indicating that systematic studies of different organoarsenicals is warranted.

As a footnote to this section, it is of some interest that the principal author of the previous study [48] abandoned pioneering studies in this area in the mid 1970s, presumably owing to anxieties over toxicity issues, lack of funding and so on [49]. The foregoing summary of arsenic compounds and their cytotoxicity/antitumour activity quite plainly demonstrates that this is a field of endeavour well deserving of continued attention.

12.3 Antimony Compounds

Various antimony compounds find continued use in the treatment of tropical diseases, most notably leishmaniasis caused by *Leishmania* species, which are human protozoan parasites of the trypanosomatidae family [50–54]. The two most prominent antimony compounds used in the treatment of cutaneous and visceral leishmaniasis are sodium stibogluconate (**XIX**, Pentostam) and meglumine antimonate (**XX**, Glucantime): their molecular compositions let alone precise molecular structures remain uncertain [55]. While each of these drugs features an antimony(V) centre, it is likely that these are reduced to antimony(III) *in vivo* [51]. Besides these leishmaniacides, the other antimony compound relevant to contemporary medicine is potassium antimony tartrate (**XXI**, Tartar Emetic) which may also be used against leishmaniasis. This species has antimony present in the +III oxidation state and is also known to be highly toxic [51]. The biological targets of antimony containing therapeutics remain under investigation [50–54] and some progress has been made towards understanding their molecular mechanism (Chapters 3 and 8): this knowledge may have implications for the design of anticancer active antimony compounds. As indicated earlier, the antimony(V) drugs are prodrugs, being reduced *in vivo*, either enzymatically (e.g. by a thiol dependent reductase (designated TDR1) or the pentavalent antimony reductase, *Leishmania major*, LmACR2) or by some other bioreduction mechanism, yielding antimony(III). A key feature of the Trypanosomatidae family is their specific redox metabolism which gives a clue as to the mode of action of therapeutic antimonials. While other eukaryotes rely on glutathione/glutathione reductase system, trypanosomatidae utilize a trypanothione/trypanothione reductase system. Antimony(III) can inhibit trypanothione reductase and this disruption of the oxidative-stress defence mechanism is the likely cause of leishmanicidal activity exhibited by antimonials [51]. In support of this postulate, a recent crystal structure determination of the reduced form of trypanothione reductase, NADPH and antimony(III) shows coordination of antimony(III) by cysteine (x 2), threonine and histidine residues (Chapter 3, Figure 3.14) [52]. The aforementioned results suggest that enzymes or proteins may be biological targets for antimony anticancer agents as opposed to cellular DNA for cisplatin (**I**) and other transition metal complexes.

Some of the antimony compounds used for the treatment of leishmaniasis have also been investigated for potential antitumour activity [56–59]. Sodium stibogluconate has been evaluated for antileukaemic activity against the myeloid leukaemia cell lines (NB4, HL-60 and U937) and shown to induce differentiation of acute myeloid leukaemia. Further, the results suggest that sodium stibogluconate is functioning as a PTPase inhibitor in the leukaemia cells [57]. It appears that most attention in developing new antimony based anticancer agents has been directed to newly synthesized molecules [58, 59]. The following is an overview of recent studies in this area.

In probably the most sustained systematic study of antiproliferative activities of antimony compounds, their complexation with various heterocyclic thioamides was researched, with the latter being present in the neutral and/or deprotonated forms [60–63]. As a consequence, a full range of coordination geometries and aggregation patterns have been determined for these derivatives. Compounds formed with antimony trichloride and the heterocyclic thiones 2-mercapto-benzimidazole (MBZIM), 5-ethoxy-2-mercapto-benzimidazole (EtMBZIM) and 2-mercapto-thiazolidine (MTZD) thioamides are uniformly monomeric based on a distorted octahedron or a trigonal bipyramid whereby in each case the thioamide coordinates in the neutral mode via the sulfur atom only and a stereochemically active lone pair of electrons occupies a coordination site [62]. Representative compounds prepared in this study are $\text{Sb}(\text{MBZIM})_4\text{Cl}_2$ (**XXII**) and $\text{Sb}(\text{MTZD})_2\text{Cl}_3$ (**XXIII**), Figure 12.4. The antimony compounds were examined for cytotoxicity against the following cancer cell lines: L1210 (Murine Leukaemia Cells), FM3A (Murine Mammary Carcinoma Cells), Molt4/C8, CEM (Human T-lymphocyte Cells), and HeLa (Human Cervix Carcinoma Cells). The key result from this study was that the antimony compounds displayed selective antiproliferative activity against the HeLa cells, with up to and greater than 10-fold more potency against the other cell lines investigated. For example, compound **XXII** inhibited growth of the HeLa cells at $6.4 \pm 1.6 \mu\text{M}$ compared with 12 ± 7 , 36 ± 6 , 24 ± 16 , $90 \pm 19 \mu\text{M}$

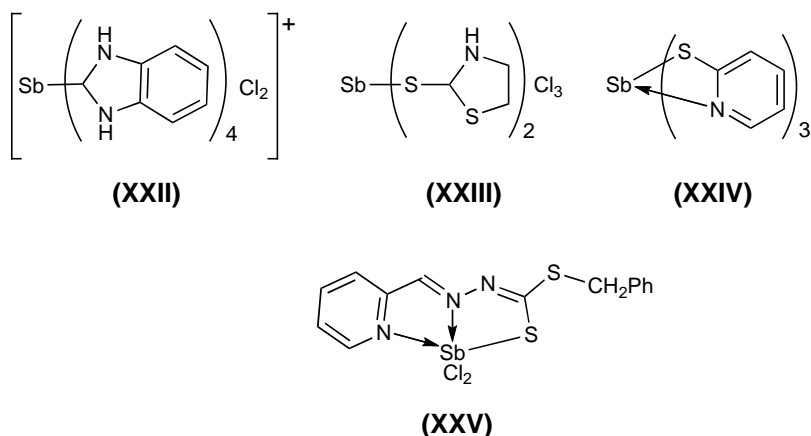


Figure 12.4 Chemical structures of synthetic antimony containing molecules investigated for anticancer potential: $\text{Sb}(\text{MBZIM})_4\text{Cl}_2$ (**XXII**), $\text{Sb}(\text{MTZD})_2\text{Cl}_3$ (**XXIII**), $\text{Sb}(\text{pmt})_3$ (**XXIV**) and $[\text{Sb}(\text{NNS})\text{Cl}_2]$ (**XXV**)

for the L1210, FM3A, Molt4/C8, and CEM cell lines, respectively. It was also reported that the antimony compounds were more potent than the standard drugs cisplatin (**I**) and carboplatin (**II**). In another study, comparable reactions with antimony bromides were conducted whereby distinctive structures as well as those resembling **XXII** and **XXIII** were isolated [60]. Dimerization and even polymerization was achieved in some of the antimony bromide derivatives owing to the presence of bridging bromide atoms. The antimony bromides were found to be less potent than the corresponding antimony chlorides [60], with only modest cytotoxicity found against almost the same panel of cancer cell lines. Interestingly, evidence was found for an enhanced antiproliferative activity against the HeLa cells.

The binary compound $\text{Sb}(\text{pmt})_3$ (**XXIV**), where pmtH is the heterocyclic thioamide 2-mercapto-pyrimidine, having a coordination geometry based on a pentagonal pyramid, proved ineffective in low doses against leiomyosarcoma cells. However, it inhibited cancer cell induced platelet aggregation [63].

The coordination of a Schiff base to antimony(III), leading to $[\text{Sb}(\text{NNS})\text{Cl}_2]$ (**XXV**), results in a compound that displays moderate activity against the CEM-SS (T-lymphoblastic leukaemia) human cell line [64].

The foregoing studies allow conclusions based on *in vitro* assays only, with no definitive indication of antitumour activity. However, antitumour activity is indicated by animal studies on antimony(III) compounds with aminopolycarboxylic acid ligands, that is in the sodium and ammonium salts of $[\text{Sb}(\text{nta})(\text{Hnta})]^{2-}$ ($\text{Na}^+ = \text{XXV_Na}$, $\text{K}^+ = \text{XXV_K}$), where H_3nta is nitrilotriacetic acid, $\text{N}(\text{CH}_2\text{COOH})_3$ [65]. The toxicities of **XXV_Na** and **XXV_K** were investigated in allogenic mice and found to be approximately 150 mg/kg (= LD_{50}). Next, mice were inoculated with Ehrlich Adenocarcinoma in the ascitic (fluid) form and survival rates were monitored. With doses of 25–50 mg/kg, survival rates increased significantly, up to 90%. The remaining studies to be described involve organoantimony species, with antimony in either the +III or +V oxidation states.

The majority of cytotoxicity trials with organoantimony have the antimony present as antimony(V), with only one study involving antimony(III). A series of diorganoantimony (III)-phthalimide and -succinimide derivatives, see representative structures, **XXV**, **XXVI** (and other organoantimony compounds) in Figure 12.5, were synthesized and their cytotoxicity against MCF-7 (breast adenocarcinoma) and EVSA-7 (mammary) cancer cell lines recorded [66]. Compounds **XXV** and **XXVI** and their derivatives with partially or fully fluorinated aryl groups displayed moderate to good activity with respect to the standard compound, β -oestradiol. It is also noted that these compounds also displayed antibacterial and antifungal activity [66].

The coupling of *N*-phenylglycine with tri-arylantimony(V) results in compounds of the general formula (**XXVII**), Figure 12.5 [67]. The amino acid derivatives displayed greater potency than Ph_3SBr_2 in KB (human epidermoid), Bel-7402 (hepatocellular carcinoma) and HCT-8 (colon) cancer cells. Interestingly, the screening of triarylantimony compounds showed evidence of systematic variations in that the triphenyl derivative was markedly most potent against the KB cell line compared with the other compounds tested, similarly the *p*-tolyl derivative exhibited the same trend against Bel-7402 and the *p*-chloro derivative against HCT-8, with the latter being the most potent compound of the series investigated [67]. Compound selectivity is of vital importance in developing new drug therapies and the foregoing results might provide pointers in this regard. This being stated,

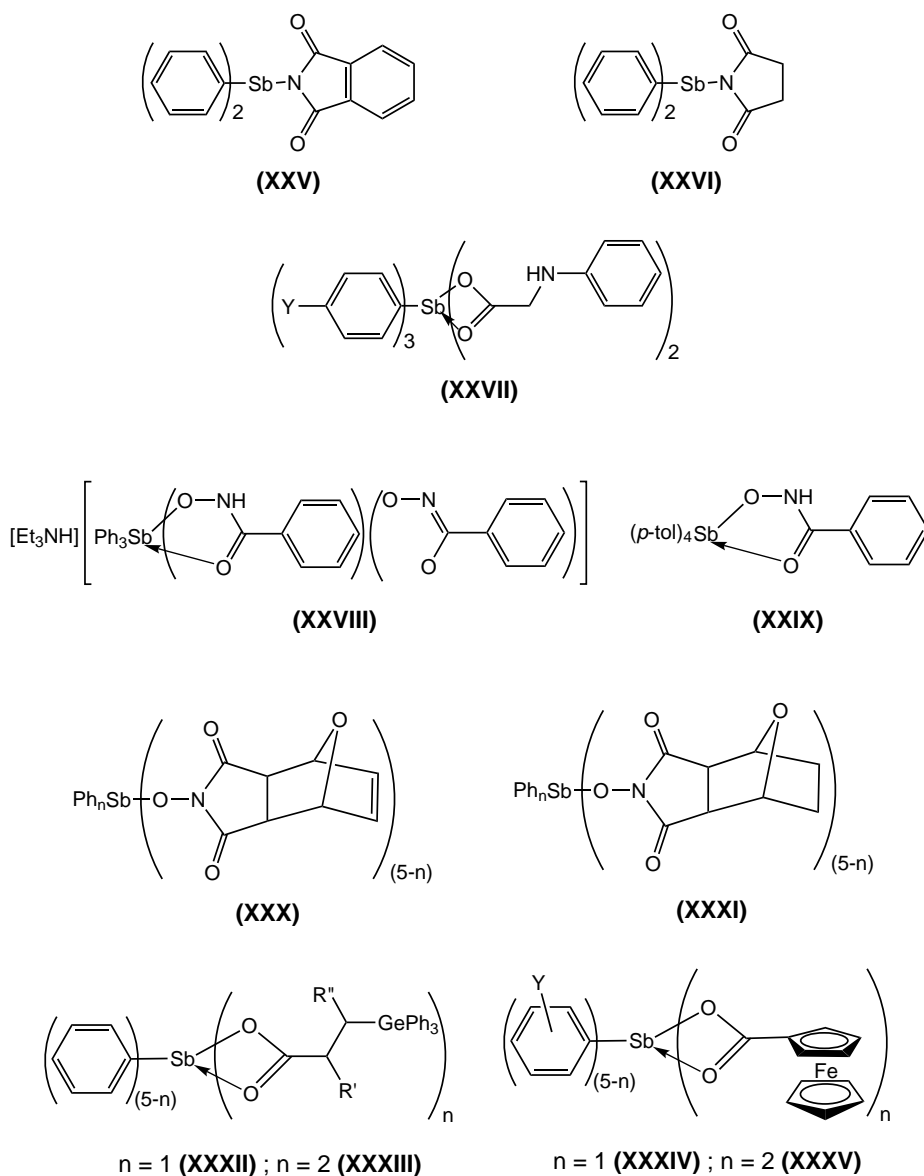


Figure 12.5 Chemical structures of synthetic organoantimony containing molecules investigated for anticancer potential: $\text{Ph}_2\text{Sb}(\text{phthalimide})$ (XXV), $\text{Ph}_2\text{Sb}(\text{succinimide})$ (XXVI), generic triarylantimony bis(*N*-phenylglycinate) (XXVII), triphenylantimony(*V*) bis(phenylhydroxamate) (XXVIII), tetra(*p*-tolyl)antimony phenylhydroxamate (XXIX), generic structure for phenylantimony (*N*-hydroxy-demethyldehydrogencantharimide) derivatives (XXX), generic structure for phenylantimony (*N*-hydroxy-demethyldehydrogencantharimide) derivatives (XXXI), $\text{Ph}_{(5-n)}\text{Sb}[\text{O}_2\text{CCH}(\text{R}')\text{CH}(\text{R}'')\text{GePh}_3]_n$; $n = 1$ (XXXII) and $n = 2$ (XXXIII), and $\text{Ph}_{(5-n)}\text{Sb}[\text{O}_2\text{C}(\text{C}_5\text{H}_4)\text{FeC}_5\text{H}_5]_n$; $n = 1$ (XXXIV) and $n = 2$ (XXXV)

the next studies to be described perhaps suggest that tetraarylantimony(V) compounds offer advantages over triarylantimony(V) derivatives.

A comprehensive series of tri- and tetra-arylantimony(V) arylhydroxamates, with examples **XXVIII** and **XXIX** shown in Figure 12.5, was synthesized and investigated for their cytotoxicity against the following panel of cancer cell lines: HL-60 (human immature granulocyte leukaemia), BGC-823 (human gastric carcinoma) and MDA-MB-435 (human mammary gland carcinoma) [68]. The neutral tetraorganoantimony(V) compound displayed significantly greater cytotoxicity than the charged (anionic) triorganoantimony(V) compounds. Of the latter series, with the additional substitution of $-\text{NH}_2$ in the 2-position of the arylhydroxamate ligands were more potent than those derivatives without this substitution pattern. The precursor compound was also included in this study, that is, $(4\text{-CH}_3\text{C}_6\text{H}_4)_3\text{SbBr}_2$, which had inhibition ratios compared to the $-\text{NH}_2$ substituted compounds. Against all three cell lines, cisplatin (**I**) was more potent than all of the triorganoantimony compounds. However, the $(4\text{-CH}_3\text{C}_6\text{H}_4)_4\text{Sb}[\text{ON}(\text{H})\text{C}(=\text{O})\text{Ph}]$ compound (**XXIX**) was more effective than cisplatin (**I**) against the HL-60 and MDA-MB-435 cell lines [68].

The influence of having three or four aryl substituents in organoantimony(V) compounds was further probed for two series of neutral compounds represented by compounds **XXX** and **XXXI** in Figure 12.5. Using a wider panel of human cancer cell lines, i.e. HL-60 (immature granulocyte leukaemia), PC-3MIE8 (prostatic carcinoma), BGC-823 (gastric carcinoma), MDAMB-435 (mammary gland carcinoma), Bel-7402 (hepatocellular carcinoma), and HeLa (carcinoma), it was again demonstrated that the tetraorganoantimony(V) compounds were markedly more potent than their triorganoantimony(V) analogues. For the tetraorganoantimony(V) series, the antimony-bound *p*-tolyl substituent generally gave rise to greater potency. No clear cut trends that could be related to the nature of saturation in the demethylcantharimide based ligands were discerned. Comparing the most active compounds with cisplatin (**I**) suggests that the organoantimony(V) compounds were more potent by up to a factor of two against the HL-60, MDA-MB-435 and Bel-7402 cell lines [69].

The remaining two studies to be summarized incorporate additional metal centres, that is, germanium and iron, with the aim to improve the efficacy of the organoantimony species. For the series of compounds with the generic formulae $\text{R}_4\text{Sb}[\text{O}_2\text{CCH}(\text{R}')\text{CH}(\text{R}'')\text{GePh}_3]$ (**XXXII**) and $\text{R}_3\text{Sb}[\text{O}_2\text{CCH}(\text{R}')\text{CH}(\text{R}'')\text{GePh}_3]_2$ (**XXXIII**), it was reported that the antimony compounds had greater potency than that exhibited by the carboxylic acid precursor compound, $\text{HO}_2\text{CCH}_2\text{CH}_2\text{GePh}_3$ [70]. No discernible trends in terms of the utility of tetra- versus tri-arylantimony derivatives were evident although the most potent compound against the cancer cell lines tested, that is HL-60 (leukaemia), EJ (bladder), SKOV-3 (ovarian), HeLa (cervical), BGC-823 (gastric) cancer cells, was the triaryl derivative, $(p\text{-ClC}_6\text{H}_4)_3\text{Sb}[\text{O}_2\text{CCH}_2\text{CH}(\text{Me})\text{GePh}_3]_2$ [70]. In a related study, arylantimony(V) ferrocenecarboxylate derivatives, $\text{Aryl}_{(5-n)}\text{Sb}[\text{O}_2\text{C}(\text{C}_5\text{H}_4)\text{FeC}_5\text{H}_5]_n$, where $n = 1$ and 2 for **XXXIV** and **XXXV** respectively, were investigated for their cytotoxicity against the HL-60, Bel-7402, KB and HeLa cancer cell lines [71]. Although, again, details are sparse, it is possible to conclude from the data included in the publication that (i) the presence of antimony increased potency and (ii) no discernible trends were found, *viz a viz*, whether tetra- versus tri-arylantimony compounds have greater potency. Within the tetraaryl series, the presence of a halide in the 4-position of the antimony bound aryl group clearly increased potency. Within the triaryl series, the *p*-tolyl derivative proved consistently more potent across the four cancer cell lines tested [71].

12.4 Bismuth Compounds

Along with arsenic and antimony, bismuth has a long history in medicine; its use was again motivated by the need to treat bacterial infections, such as caused by the pathogenic organism *Helicobacter pylori* [72, 73]. Gastric complaints began to be treated with bismuth formulations in the nineteenth century and this use continues today whereby De-Nol (colloidal bismuth subcitrate), Pepto-Bismol (bismuth subsalicylate) and Pylorid (ranitidine bismuth citrate), for example, are readily available, often over the counter [72–74]. Such availability attests to the relative nontoxic character of bismuth to humans. The utility of bismuth formulations has motivated many studies into their possible mechanism of action and to the discovery of their biological targets [51, 75]; as with antimony containing drugs, the precise molecular structures of bismuth drugs remain unknown. Studies show that bismuth can interact with enzymes generated by *Helicobacter pylori* such as the Jack Bean urease (responsible for the catalysis of the process whereby urea is hydrolysed to ammonia and carbon dioxide), ATPase (the class of enzymes that are responsible for catalysing the decomposition of adenosine triphosphate (ATP) into adenosine diphosphate (ADP) and free phosphate with the release of energy), and cytosolic alcohol dehydrogenase (ADH; the zinc containing enzyme responsible for the oxidation of alcohol to aldehyde). Bismuth is also known to interact with proteins such as transferrin, the glycoproteins responsible for the transportation of ferric ion [51, 73]. Thus, as for antimony, bismuth appears to target non-DNA sites, a feature which offers new opportunities for novel mechanisms of action in the treatment of cancer. Additional impetus to studying the medicinal chemistry of bismuth compounds was gained recently with the report of the ability of several bismuth compounds to inhibit the SARS coronavirus [76]. The antitumour potential of bismuth compounds has not attracted as much attention as have the lighter elements of this group. A bibliographic review summarising the screening of bismuth compounds appeared in 2002 [58] and herein, recent studies are summarized.

The first studies to be summarized are those on binary bismuth 1,1-dithiolates. Three xanthate structures, $\text{Bi}(\text{S}_2\text{COR})_3$ where R = Et (**XXXVI**), Figure 12.6, *i*-Pr, and cyclohexyl, displayed similar cytotoxicity against Calu-6 (lung adenocarcinoma), which is highly sensitive to cisplatin (**I**), indicating little influence exerted by the R group [77]. By contrast, the R = cyclohexyl derivative was significantly less cytotoxic against MCF 7 (mammary carcinoma), which is relatively non responsive to cisplatin (**I**), than the compounds with smaller R groups. Interestingly, when cytotoxicity was scored at pH = 6.8, mimicking the pH of a solid tumour, the potency was greater for the R = Et and *i*-Pr compounds [77]. It was determined that the comparable binary platinum(II) xanthates were significantly more cytotoxic than the bismuth compounds which have potency comparable to cisplatin (**I**). Changing the nature of the 1,1-dithiolate ligand to dithiocarbamate, S_2CNR_2 , a species renowned for its use/potential use in medicine [78], a very potent series of compounds is generated.

Compounds of general formula $\text{Bi}(\text{S}_2\text{CNR}_2)_3$, for example R = Et (**XXXVII**), Figure 12.6, were screened for potency against a panel of seven human cancer cell lines: A498 (renal), MCF-7 (breast), EVSA-T (breast), H226 (non-small cell lung), IGROV (ovarian), M19 MEL (melanoma), and WIDR (colon) [79]. Several compounds proved quite potent and a qualitative structure activity was established. Thus, for the compounds with straight chain R groups, potency varied in the following order:

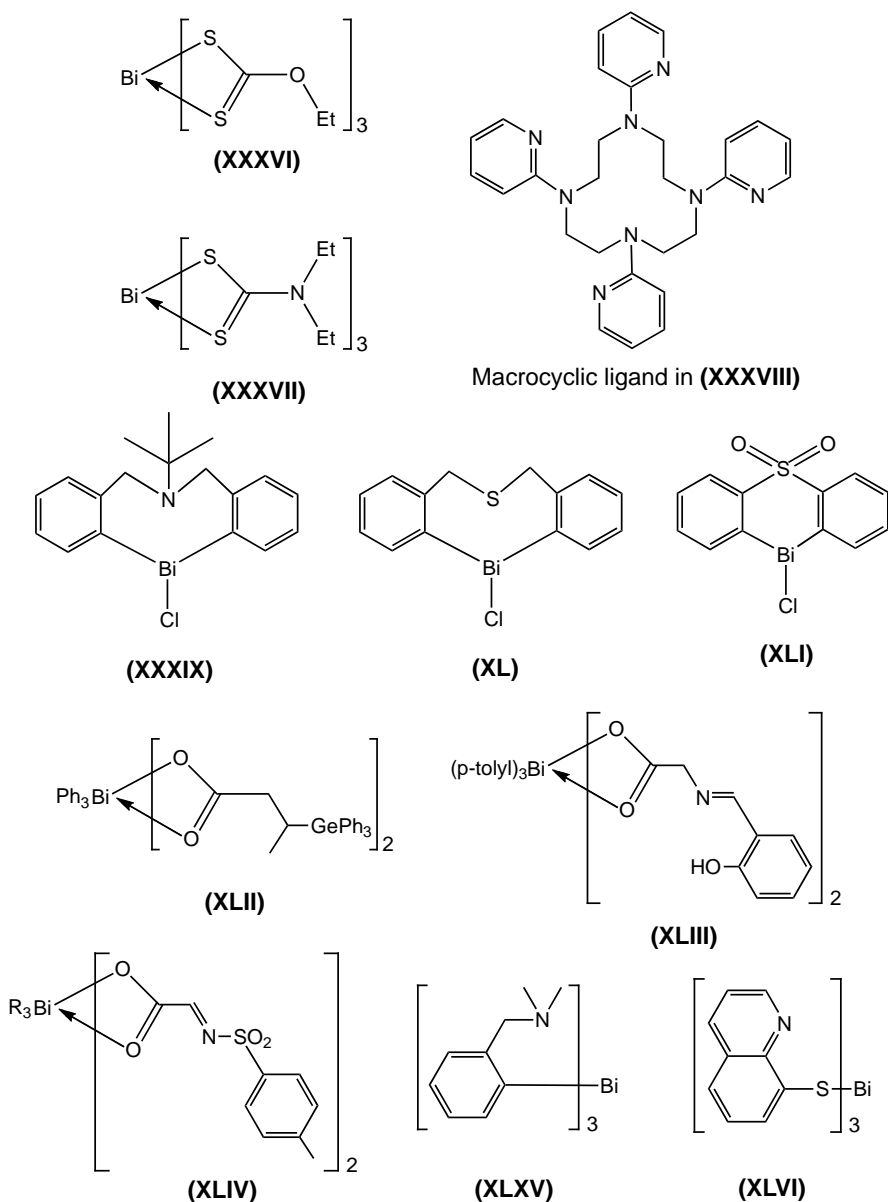


Figure 12.6 Chemical structures of synthetic bismuth containing molecules, including organobismuth molecules, with additional metal centres investigated for anticancer potential: $\text{Bi}(\text{S}_2\text{COEt})_3$ (XXXVI), $\text{Bi}(\text{S}_2\text{CN}(\text{Et})_2)_3$ (XXXVII), the 1,4,7,10-tetrakis(2-pyridylmethyl)-1,4,7,10-tetraazacyclododecane macrocyclic ligand in the structure of (XXXVIII), N-tert-butyl-bi-chlorodibenzo[c,f][1,5]azabismocine (XXXIX), bi-chlorodibenzo[c,f][1,5]thiabismocine (XL), bi-chlorophenothiabismocine-S,S-dioxide (XLI), $\text{Ph}_3\text{Bi}[\text{O}_2\text{CCH}(\text{Me})\text{CH}_2\text{GePh}_3]_2$ (XLII), $(p\text{-tolyl})_3\text{Bi}[\text{O}_2\text{CCH}_2\text{N}=\text{C}(\text{H})\text{C}_6\text{H}_4\text{OH}-2]_2$ (XLIII), generic structure for triaryl bismuth N-(p-toluenesulfonyl) aminoacetate XLIV, tris[2-(N,N-dimethylaminomethyl)phenyl]bismuth (XLV), and generic structure for bismuth tris(8-quinolinethiolate) (XLVI)

Me < Et > *n*-Pr > *n*-Bu. The introduction of branching decreased potency, for example *n*-Pr > *i*-Pr. For examples where NR₂ was a ring, smaller rings were more potent, such as, *n*=4 > *n*=6 for N(CH₂)_{*n*}. Finally, introducing aromatic rings decreased potency. Of the full series, compound **XXXVII** was chosen as the lead compound as it displayed uniformly high cytotoxicity and a broad range of potency in the cancer cell lines tested. Gross toxicity trials in a Balb/C murine model gave a maximum tolerated dose (LD₉₀) of 7 mg Bi/kg mouse; LD₅₀ = 3.6 mg Bi/kg mouse. While this value is low, the very low concentrations required to arrest the growth in the *in vitro* trial, for example IC₅₀ (μM): 0.009 [EVSA-T], 0.015 [H226], <0.005 [IGROV], and 0.006 [MCF-7] cf. <0.004 μM for Taxol in all cell lines, clearly justified *in vivo* trials for antitumour activity. The tumours inoculated in Nude Balb/C mice were OVCAR-3 (ovarian) and HT-29 (colon). Compound **XXXVII** returned an average tumour weight inhibition (TWI) score on Day 26 of 54%, indicating significant anti-tumour activity. Against the virulent HT-29 colon cancer, the tumour growth was curtailed compared to untreated animals. The foregoing results suggest that promising *in vitro* results obtained for the Bi(S₂CNR₂)₃ compounds are translated to antitumour activity and that further studies are clearly justified.

In a rare example of a study linking cytotoxicity assays with possible mechanisms of action, the cytotoxicity and DNA binding ability of a water soluble bismuth macrocyclic complex have been determined [80]. The precise structure of the compound **XXXVIII** is not known but is likely to be cationic. The structure of the macrocyclic ligand was shown in Figure 12.6. The complex of Bi³⁺ with the ligand (**XXXVIII**) is approximately 100 times more potent against B16-BL6 (melanoma) cells than cisplatin (**I**). Under physiologically relevant conditions, the compound was shown to form a non covalent interaction with calf thymus-DNA [80].

While studies on the antitumour potential of bismuth compounds currently used in medicine are lacking, some interesting indicators are forthcoming from studies of their putative mechanism of action. For example, very recent studies indicate that methylbismuth species, a biomethylated metabolite of bismuth drugs, are responsible for cytotoxic effects rather than the originally applied bismuth drugs [81]. Further, another recent report suggests that organobismuth compounds can induce apoptosis [82]. In this study, heterocyclic organobismuth compounds **XXXIX** – **XLI**, Figure 12.6, showed good activity against leukaemic cell lines and displayed lower cytotoxicity towards TIG cells (normal human fibroblasts). The IC₅₀ values in the ranges 0.059–4.7, 0.036–4.8 and 0.20–5.1 μM, respectively, indicate compound (**XLI**), with a six-membered heterocyclic ring, was less cytotoxic compared with the more flexible molecules with eight-membered rings. Studies on the possible mechanism of cell death were conducted and showed that at low concentrations of compound **XL**, that is 0.22–0.44 μM, the cell death was by apoptosis but at higher concentrations, that is, > 1.1 μM, the cell death was by acute necrosis [82].

Several more studies on the potential anticancer activity of organobismuth compounds have been reported. A range of triarylbismuth bis(carboxylates) related to the structure of Ph₃Bi[O₂CCH(Me)CH₂GePh₃]₂ (**XLII**), shown in Figure 12.6 and the antimony derivatives described above [70], have been synthesized and their cytotoxicity against the cancer cell lines KB (carcinoma of the nasopharynx), Bel-7402 (hepatocellular carcinoma) and HCT-8 (intestinal adenocarcinoma) cells explored [83]. As with the study of the antimony derivatives, the influence of varying the aryl group and the substituents in the carboxylate

ligand, $[\text{O}_2\text{CCH}(\text{R}')\text{CH}(\text{R}'')\text{GePh}_3]$, were investigated. First and foremost, many of the triarylbismuth bis(carboxylates) were significantly more potent than either of $\text{Ph}_3\text{GeCH}_2\text{CH}_2\text{COOH}$ and Ph_3BiCl_2 . In terms of the bismuth-bound aryl groups, phenyl and *p*-tolyl derivatives were more potent than their *p*-chlorophenyl and *p*-bromophenyl analogues. Interestingly, two of the three *p*-fluorophenyl derivatives synthesized in this study, namely $(p\text{-FC}_6\text{H}_4)_3\text{Bi}(\text{O}_2\text{CCH}(\text{Me})\text{CH}_2\text{GePh}_3)_2$ (all three cell lines) and $(p\text{-FC}_6\text{H}_4)_3\text{Bi}(\text{O}_2\text{CCH}_2\text{CH}(\text{Ph})\text{GePh}_3)_2$ (in the KB and Bel-7402 cell lines) gave indications of significant potency. The $\text{Ph}_3\text{Bi}(\text{O}_2\text{CCH}(\text{Me})\text{CH}_2\text{GePh}_3)_2$ compound was selected for a comparative assay with cisplatin (**I**) and proven to be more substantially more potent in the KB cell line when administered at concentrations of 0.5, 0.05 and 0.005 g mL^{-1} [83]. A related study of several carboxylate derivatives where the carboxylate is derived from *N*-salicylidene amino acids, e.g. (**LXIII**), again indicated significant cytotoxicity for the compounds investigated [84]. In this study, the advantage of combining bismuth with carboxylate was demonstrated as the bismuth compounds had significant better cytotoxicity profiles compared with the precursor compounds and cisplatin (**I**). The most potent compound in the trial was (**LXIII**), against the MDA-MB-435 (mammary carcinoma) but across the three human cell lines investigated, that is, MDA-MB-435, HL-60 (immature granulocyte leukaemia), and BGC-823 (gastric carcinoma), the triphenyl derivative with $\text{R} = \text{CH}_2\text{C}(\text{H})(\text{CH}_3)_2$ at the α -position of the carboxylic acid was the most potent [84]. Continuing the carboxylic acid theme, a series of triarylbismuth *N*-(*p*-toluenesulfonyl) aminoacetates were synthesized, see generic structure (**LXIV**) [85]. Similar observations were observed, that is, the compounds were more active than their precursor carboxylic acid and cisplatin (**I**) and the triphenylbismuth derivative was the most potent compared with the *p*-methyl, *p*-chloro and *p*-bromo derivatives. Particularly noteworthy was the potency of the triphenyl derivative against the PC-3MIE8 (prostatic carcinoma) cancer cells [85].

An obvious difficulty in gauging the potential of one series of compounds against another is that experimental protocols, let alone cell lines, vary from study to study. There are relatively few trials where both antimony and bismuth compounds have been studied concurrently. In a rare example, a study designed to discover a bismuth compound selective for vascular endothelial cells, a comprehensive series of organobismuth compounds and their antimony analogues were investigated [86]. The study revealed that a single derivative, namely tris[2-(*N,N*-dimethylaminomethyl)phenyl]bismuth (**LXV**), was cytotoxic to bovine aortic endothelial cells but not to bovine aortic smooth muscle cells and porcine kidney epithelial LLC-PK₁ cells. The antimony derivative did not exhibit cytotoxicity under the same conditions [86].

In a systematic study of compounds related to bismuth tris(8-quinolinethiolate) (**LXVI**), Lukevics *et al.* included both arsenic and antimony derivatives (along with many other metals). In a cytotoxicity trial of the selenolate derivatives, with methyl substituents in the ring with the heteroatom, against the HT-1080 (fibrosarcoma), MG-22A (mouse hepatoma), B16 (mouse melanoma), and Neuro 2A (mouse neuroblastoma) cell lines, arsenic compounds were generally more potent than the bismuth compounds which were in turn more potent than the antimony analogues [87]. It is noted that the tested compounds were also cytotoxic to non cancerous cells. No significant differences between bismuth (**LXVI**) and antimony 8-quinolinethiolates [88] and their methyl- and methoxy-substituted 8-quinolinethiolates [89] were noted in subsequent studies: again the compounds were highly toxic to non cancerous cells.

12.5 Conclusions

The foregoing summary of the development of arsenic, antimony and bismuth compounds as anticancer drugs clearly indicates the potential of these elements to augment their therapeutic roles. Perceived toxicity issues associated with these and other metal based drugs are clearly laid to rest by the arsenic containing drug used for the treatment of Acute Promyelocytic Leukaemia, i.e. Trisenox. Evidently, there are therapeutic windows in which these metal based drugs can provide significant clinical benefit. Systematic studies of arsenic, antimony and bismuth compounds in the context of anticancer potential are, regrettably, sparse. One can only wonder whether an easily synthesized, stable and effective molecule is awaiting discovery by the diligent chemist working in tandem with biomedical colleagues. The low toxicity and potent cytotoxicity exhibited by some of the reported compounds surely demand more attention. Fundamental questions such as (i) the relative efficacy of arsenic versus antimony versus bismuth compounds, (ii) 'inorganic' versus 'organometallic' species, and so on remain unanswered. The reliance on *in vitro* studies, the importance of which cannot be denied as an early indicator of potential antitumour activity, is also regrettable. For serious advances to be made, *in vivo* studies are essential. Further impetus to continued studies of arsenic, antimony and bismuth compounds as anticancer agents is warranted when it is considered that non DNA sites are the likely biological targets for these compounds offering differing mechanisms of action compared to the currently used anticancer platinum drugs. The prevalence of cancer diseases and the human suffering they cause is surely sufficient motivation for the necessary investment of resources, in all their guises, to investigate the potential utility of arsenic, antimony and bismuth compounds as anticancer agents.

References

1. Keppler, B.K.(ed.) (1993) *Metal Complexes in Cancer Therapy*, Wiley-VCH Verlag GmbH, Weinheim.
2. Fricker, S.P.(ed.) (1994) *Metal Compounds in Cancer Therapy*, Chapman & Hall, London.
3. Farrel, N.(ed.) (1999) *Uses of Inorganic Chemistry in Medicine*, RSC Publishing, Cambridge.
4. Williams, R.J.P. and Fraústo da Silva, J.J.R. (2001) *Biological Chemistry of the Elements*, Oxford University Press, Oxford.
5. Sigel, A. and Sigel, H.(eds) (2004) *Metal Ions and their Complexes in Medication. Metal Ions in Biological Systems*, vol. **41**, Marcel Dekker, New York.
6. Sigel, A. and Sigel, H.(eds) (2004) *Metal Complexes in Tumor Diagnosis and as Anticancer Agents. Metal Ions in Biological Systems*, vol. **42**, Marcel Dekker, New York.
7. Gielen, M. and Tiekink, E.R.T.(eds) (2005) *Metallotherapeutic Drugs and Metal-Based Diagnostic Agents: The use of Metals in Medicine*, John Wiley & Sons, Ltd, Chichester.
8. Gao, Z.J. and Sadler, P.J. (1999) *Angewandte Chemie-International Edition*, **38**, 1512–1531.
9. Desoize, B. (2004) *Anticancer Research*, **24**, 1529–1544.
10. Sánchez-Delgado, R.A. and Anzellotti, A. (2004) *Mini-Reviews in Medicinal Chemistry*, **4**, 23–30.
11. Fricker, S.P. (2006) *Chemical Society Reviews*, **35**, 524–533.
12. Thompson, K.H. and Orvig, C. (2006) *Dalton Transactions*, 761–764.
13. Dyson, P.J. and Sava, G. (2006) *Dalton Transactions*, 1929–1933.
14. Ronconi, L. and Sadler, P.J. (2007) *Coordination Chemistry Reviews*, **251**, 1633–1648.
15. Hambley, T.W. (2007) *Dalton Transactions*, 4929–4937.
16. Jakupec, M.A., Galanski, M., Arion, V.B. *et al.* (2008) *Dalton Transactions*, 183–194.

17. Bruijninx, P.C.A. and Sadler, P.J. (2008) New trends for metal complexes with anticancer activity. *Current Opinion in Chemical Biology*, **12**, 197–206.
18. Hartinger, C.G. and Dyson, P.J. (2009) *Chemical Society Reviews*, **38**, 391–401.
19. Bosch, F. and Rosich, L. (2008) *Pharmacology*, **82**, 171–179.
20. Jolliffe, D.M. (1993) *Journal of the Royal Society of Medicine*, **86**, 287–289.
21. Ho, P.C. (2005) ^{33}As Metallotherapeutic arsenic compounds, in *Metallotherapeutic Drugs and Metal-Based Diagnostic Agents: The use of Metals in Medicine* (eds M. Gielen and E.R.T. Tiekink), John Wiley & Sons, Ltd, Chichester.
22. Liu, J., Lu, Y., Wu, Q. *et al.* (2008) *The Journal of Pharmacology and Experimental Therapeutics*, **326**, 363–368.
23. Dilda, P.J. and Hogg, P.J. (2007) *Cancer Treatment Reviews*, **33**, 542–564.
24. Wang, Z.-Y. (2001) *Cancer Chemotherapy and Pharmacology*, **48** (Suppl 1), S72–S76.
25. Raab, A., Wright, S.H., Jaspars, M. *et al.* (2007) *Angewandte Chemie-International Edition*, **46**, 2594–2597.
26. Ngu, T.T. and Stillman, M.J. (2006) *Journal of the American Chemical Society*, **128**, 12473–12483.
27. Ramadan, D., Cline, D.J., Bai, S. *et al.* (2007) Effects of As(III) binding on β -hairpin structure. *Journal of the American Chemical Society*, **129**, 2981–2988.
28. Ben Zrirar, S., Gibaud, S., Camut, A. and Astier, A. (2007) *Journal of Organometallic Chemistry*, **692**, 1348–1352.
29. Sekeres, M.A. (2007) New data with arsenic trioxide in leukemias and myelodysplastic syndromes. *Clinical Lymphoma & Myeloma*, **8**, S7–S12.
30. Wang, L., Zhou, G.-B., Liu, P. *et al.* (2008) *Proceedings of the National Academy of Sciences of the United States of America*, **105**, 4826–4831.
31. Zhu, J., Chen, Z., Lallemand-Breitenbach, V. and de Thé, H. (2002) *Nature Reviews. Cancer*, **2**, 705–714.
32. Lau, A.T.Y. and Chiu, J.-F. (2003) *Recent Research Developments in Molecular & Cellular Biochemistry*, **1**, 1–19.
33. Wu, J.-Z. and Ho, P.C. (2006) *European Journal of Pharmaceutical Sciences*, **29**, 35–44.
34. Chen, H., MacDonald, R.C., Li, S. *et al.* (2006) *Journal of the American Chemical Society*, **128**, 13348–13349.
35. Sakurai, H., Yoshikawa, Y. and Yasui, H. (2008) *Chemical Society Reviews*, **37**, 2283–2392.
36. Lloyd, N.C., Morgan, H.W., Nicholson, B.K. and Ronimus, R.S. (2005) *Angewandte Chemie-International Edition*, **44**, 941–944.
37. Pépin, J., Milord, F., Khonde, A. *et al.* (1994) *Royal Society of Tropical Medicine and Hygiene*, **88**, 447–452.
38. Balasegaram, M., Young, H., Chappuis, F. *et al.* (2009) *Royal Society of Tropical Medicine and Hygiene*, **103**, 280–290.
39. Wang, Z.-G., Rivi, R., Delva, L. *et al.* (1998) *Blood*, **92**, 1497–1504.
40. Rousselot, P., Larghero, J., Labaume, S. *et al.* (2004) *European Journal of Haematology*, **72**, 166–171.
41. Koshiuka, K., Elstner, E., Williamson, E. *et al.* (2000) *British Journal of Cancer*, **82**, 452–458.
42. Soignet, S.L., Tong, W.P., Hirschfeld, S. and Warrell, R.P. (1999) *Cancer Chemotherapy and Pharmacology*, **44**, 417–421.
43. Rousselot, P., Larghero, J., Arnulf, B. *et al.* (2004) *Leukemia*, **18**, 1518–1521.
44. Gibaud, S., Alfonsi, R., Mutzenhardt, P. *et al.* (2006) *Journal of Organometallic Chemistry*, **691**, 1081–1084.
45. Duzkale, H., Jilani, I., Orsolich, N. *et al.* (2003). *Cancer Chemotherapy and Pharmacology*, **51**, 427–432.
46. Dilda, P.J., Don, A.S., Tanabe, K.M. *et al.* (2005) *Journal of the National Cancer Institute*, **97**, 1539–1547.
47. Dilda, P.J., Ramsay, E.E., Corti, A. *et al.* (2008). *The Journal of Biological Chemistry*, **283**, 35428–35434.

48. Gao, M., Tan, S., Chen, Y. and Zingaro, R.A. (2007) *Bioorganic and Medicinal Chemistry*, **15**, 2660–2666.
49. Quintas-Cardama, A., Verstovsek, S., Freireich, E. *et al.* (2008) *Anti-Cancer Agents in Medicinal Chemistry*, **8**, 904–909.
50. Yan, S., Jin, L. and Sun, H. (2005) $_{51}\text{Sb}$ Antimony in medicine, in *Metallotherapeutic Drugs and Metal-Based Diagnostic Agents: The use of Metals in Medicine* (eds M. Gielen and E.R.T. Tiekink) John Wiley & Sons, Ltd, Chichester.
51. Ge, R.G. and Sun, H. (2007) *Accounts of Chemical Research*, **40**, 267–274.
52. Baiocco, P., Colotti, G., Franceschini, S. and Ilari, A. (2009) *Journal of Medicinal Chemistry*, **52**, 2603–2612.
53. Mishra, J. (2007) *Current Medicinal Chemistry*, **14**, 1153–1169.
54. Sabbaga Amato, V., Tuon, F.F., Bacha, H.A. *et al.* (2008) *Acta Tropica*, **105**, 1–9.
55. Frézard, F., Martins, P.S., Barbosa, M.C.M. *et al.* (2008) *Journal of Inorganic Biochemistry*, **102**, 656–665.
56. Wyllie, S. and Fairlamb, A.H. (2006) *Biochemical Pharmacology*, **71**, 257–267.
57. Pathak, M.K., Hu, X. and Yi, T. (2002) *Leukemia*, **16**, 2285–2291.
58. Tiekink, E.R.T. (2002) *Critical Reviews in Oncology/Hematology*, **42**, 217–224.
59. Sharma, P., Perez, D., Cabrera, A. *et al.* (2008) *Acta Pharmaceutica Sinica*, **29**, 881–890.
60. Ozturk, I.I., Hadjikakou, S.K., Hadjiliadis, N. *et al.* (2009) *Inorganic Chemistry*, **48**, 2233–2245.
61. Hadjikakou, S.K., Ozturk, I.I., Xanthopoulou, M.N. *et al.* (2008) *Journal of Inorganic Biochemistry*, **102**, 1007–1015.
62. Ozturk, I.I., Hadjikakou, S.K., Hadjiliadis, N. *et al.* (2007) *Inorganic Chemistry*, **46**, 8652–8661.
63. Hadjikakou, S.K., Antoniadis, C.D., Hadjiliadis, N. *et al.* (2005) *Inorganica Chimica Acta*, **358**, 2861–2866.
64. Tarafder, M.T.H., Ali, M.A., Saravanan, N. *et al.* (2000) *Transition Metal Chemistry*, **25**, 295–298.
65. Popov, A.M., Davidovich, R.L., Li, I.A. *et al.* (2005) *Pharmaceutical Chemistry Journal*, **39**, 119–121.
66. Kant, R., Chandrashekar, A.K. and Kumar, A. (2008) *Phosphorus, Sulfur, Silicon*, **183**, 1410–1419.
67. Yu, L., Ma, Y.-Q., Wang, G.-C. and Li, J.-S. (2004) *Heteroatom Chemistry*, **15**, 32–36.
68. Wang, G.-C., Lu, Y.-N., Xiao, J. *et al.* (2005) *Journal of Organometallic Chemistry*, **690**, 151–156.
69. Wang, G.-C., Xiao, J., Lu, L. *et al.* (2004) *Journal of Organometallic Chemistry*, **689**, 1631–1638.
70. Ma, Y., Li, J., Xuan, Z. and Liu, R. (2001) *Journal of Organometallic Chemistry*, **620**, 235–242.
71. Liu, R.-C., Ma, Y.-Q., Yu, L. *et al.* (2003) *Applied Organometallic Chemistry*, **17**, 662–668.
72. Sun, H. and Zhang, L. (2004) Bismuth in medicine, in *Metal Ions and their Complexes in Medication. Metal Ions in Biological Systems*, **41** (eds A. Sigel and H. Sigel), Marcel Dekker, New York, pp. 333–378.
73. Burford, N. and Eelman, M.D. (2005) $_{83}\text{Bi}$ Bismuth-based pharmaceuticals, in *Metallotherapeutic Drugs and Metal-Based Diagnostic Agents: The use of Metals in Medicine* (eds M. Gielen and E.R.T. Tiekink), John Wiley & Sons, Ltd, Chichester.
74. Selgrad, M. and Malfetheriner, P. (2008) *Current Opinion in Pharmacology*, **8**, 593–597.
75. Yang, N. and Sun, H. (2007) *Coordination Chemistry Reviews*, **251**, 2354–2366.
76. Yang, N., Tanner, J.A., Zheng, B.J. *et al.* (2007) *Angewandte Chemie-International Edition*, **46**, 5464–5468.
77. Freibolin, W., Schilling, G., Zöller, M. and Amtmann, E. (2005) *Journal of Medicinal Chemistry*, **48**, 7925–7931.
78. Cvek, B. and Dvorak, Z. (2007) *Current Pharmaceutical Design*, **13**, 3155–3167.
79. Li, H., Lai, C.S., Wu, J. *et al.* (2007) *Journal of Inorganic Biochemistry*, **101**, 809–816.
80. Wang, X.Y., Zhang, X.M., Lin, J. *et al.* (2003) *Dalton Transactions*, 2379–2380.
81. von Recklinghausen, U., Hartmann, L.M., Rabieh, S. *et al.* (2008) *Chemical Research in Toxicology*, **21**, 1219–1228.
82. Iuchi, K., Hatano, Y. and Yagura, T. (2008) *Biochemical Pharmacology*, **76**, 974–986.

83. Yu, L., Ma, Y.-Q., Wang, G.-C. *et al.* (2003) *Journal of Organometallic Chemistry*, **679**, 173–180.
84. Wang, G.-C., Xiao, J., Lu, Y.-N. *et al.* (2005) *Applied Organometallic Chemistry*, **19**, 113–117.
85. Yu, L., Ma, Y.-Q., Wang, G.-C. *et al.* (2004) *Applied Organometallic Chemistry*, **18**, 187–190.
86. Fujiwara, Y., Mitani, M., Yasuike, S. *et al.* (2005) *Journal of Health Science*, **51**, 333–340.
87. Lukevics, E., Shestakova, I., Domaracheva, I. *et al.* (2006) *Chemistry of Heterocyclic Compounds*, **42**, 53–59.
88. Lukevics, E., Shestakova, I., Domaracheva, I. *et al.* (2006) *Chemistry of Heterocyclic Compounds*, **42**, 761–764.
89. Lukevics, E., Zaruma, D., Ashaks, J. *et al.* (2008) *Chemistry of Heterocyclic Compounds*, **44**, 559–564.

13

Radiobismuth for Therapy

Martin W. Brechbiel¹ and Ekaterina Dadachova²

¹*Radioimmune & Inorganic Chemistry Section, Radiation Oncology Branch,
National Cancer Institute, Building 10 Center Drive, Bethesda, Maryland, MD 20892, USA*

²*Albert Einstein College of Medicine of Yeshiva University, Bronx, New York, 10461, USA*

13.1 Introduction

Three main weapons in the arsenal for cancer treatment are surgery, external beam radiation therapy, and chemotherapy. Inoperable tumors, tumors situated close to radiation sensitive organs, metastatic disease, and diseases like leukaemia and lymphoma are frequently difficult to treat with traditional modalities. Use of targeted radiation therapy has been developed to address these obstacles. Targeted radiation therapy involves specific localization of a radionuclide emitting ionizing radiation to cancer cells to deliver a cytotoxic radiation dose to that cancerous tissue while sparing surrounding healthy tissue. Carrier molecules specifically targeting cancer cells are required to execute this strategy.

Monoclonal antibodies (mAbs), for example, are a viable strategy for delivery of therapeutic, particle emitting radionuclides specifically to tumor cells. Proper, rational selections of radionuclide and antibody combinations are a key to radioimmunotherapy (RIT) to be a standard therapeutic modality due to the fundamental, significant differences between α - and β^- -particles. Compared to β^- -particles, the α -particle has a shorter path length (50–80 μm) characterized by high linear energy transfer ($\sim 100 \text{ keV}/\mu\text{m}$). Actively targeted α -therapy offers a specific tumor cell killing action with less collateral damage to surrounding normal tissues than β^- -emitters. These properties make targeted α -therapy appropriate for the elimination of minimal residual or micrometastatic disease. The RIT

using α -emitters for example, ^{212}Bi , ^{213}Bi , ^{211}At , or ^{225}Ac has demonstrated significant activity in both *in vitro* and *in vivo* model systems (*vide infra*).

Limited clinical trials have demonstrated safety, feasibility, and therapeutic activity of targeted α -therapy, despite traversing complex obstacles [1]. One key aspect to this advancing modality is a need for additional sources of and more efficient production of these radionuclides. Refining conjugation and/or radiolabeling chemistry combined with rational applications for isotope delivery, targeting vectors, molecular targets, and identification of appropriate clinical applications continue to be active areas of research. At present, clinical evaluation has been limited to small Phase I/II trials, so it remains that randomized trials of targeted α -therapy combined with integration into existing standards of care treatment regimens will determine overall clinical utility.

Herein we present a review of those bismuth radionuclides, ‘Radiobismuth’, that are suitable for targeted radiation therapy applications. We take note of the fact that a very broad review of this field partially covered the therapy applications of bismuth radionuclides a number of years ago and we direct the reader to that additional reference [2]. As such, this chapter will cover those results and developments that have occurred within this field of study since that report.

13.2 Targeting Vectors

The seminal publication of Kohler and Milstein’s hybridoma/monoclonal antibody (mAb) technology provided a clear opening towards the development of antibody targeted radiation [3]. Murine mAbs against tumor associated antigens (TAA) generated multitudes of preclinical studies that initially provided proof-of-concept targeted radiation therapy results and then demonstrated disconnections in their predictability of efficacy in human trials. Issues such as production of human antimurine immunoglobulin antibodies (HAMA) by patients after one to three treatments, inadequate therapeutic dose delivery, insufficient activation of effector function(s), slow blood compartment clearance, low affinity and avidity, trafficking to or targeting of normal organs, antigen heterogeneity on tumor cells, and insufficient tumor penetration combined to compromise this therapeutic modality [4]. Many of these challenges have been addressed with genetic engineering eliminating HAMA by production of chimeric mAbs, complementarity-determining region (CDR) grafting, or complete humanization of the protein [5].

Investigators are now able to fully explore the real therapeutic potential of radiolabeled mAbs with the elimination of many obstacles and a better understanding of the inherent limitations of mAbs. As such, many radiolabeled mAbs have been, or currently are being evaluated in Phase III trials. The Food and Drug Administration (FDA) approved two radiolabeled mAbs for the treatment of non-Hodgkin’s lymphoma (NHL), Zevalin radiolabeled with the β^- -emitter, ^{90}Y ($t_{1/2} = 2.67$ d) and Bexxar radiolabeled with the β^- -emitter ^{131}I ($t_{1/2} = 8.07$ d), making the approval of additional targeted radiation therapy products probable [6].

Another option of delivery vector to complement the targeted delivery of radiobismuth is peptides that not only traffic to the targeted sites very rapidly but also clear from the body very rapidly. The former property promotes efficient delivery of the short half life radionuclide, however the latter property while generally sparing to normal tissue does

generally passage through the renal excretion pathway wherein considerable renal toxicity may be a limitation. Rapid internalization of the radiolabeled peptide with equally rapid re-expression of the cell surface target is a highly desirable property that enhances the total delivery of these radionuclides into malignant sites. Peptides such as octreotide, α -Msh, arginine-glycine-aspartic acid-containing peptides (RGD peptides), bombesin derivatives, and others may all be feasible for use with ^{213}Bi or ^{212}Bi [7].

13.3 α -Emitters versus β^- -Emitters

Radionuclides that decay by β^- -particle emission emit electrons with maximum kinetic energies of 0.3–2.3 MeV with corresponding ranges of ~ 0.5 –12 mm *in vivo*. This range decreases the requirement for cellular internalization while also providing for these β^- -particles to traverse several cells (10–1000). This effect has been termed ‘crossfire’ and improves tumor dose homogeneity and ensures delivery of the sufficient dose to each cell [8]. Single cell diseases such as leukaemia, micrometastases, postsurgical residual disease, and other disseminated types of cancer are not well addressed by targeted β^- -particle therapy. Humm *et al.* reported that in order to attain cell kill probability of 99.99% for single cells, several hundreds of thousands of β^- -decays at the cell membrane would be required [9]. In that specific scenario, a significant portion of the dose would then impact the surrounding normal tissue. Basic physics and radiobiology of β^- -particle radiation then defines a poor tumor-to-normal-tissue dose ratio for treating single cell disease. Selection of an α -particle emitter over a β^- -particle emitter promotes a viable strategy in which such diseases may be treated with targeted radiation therapy.

Due to the greater mass and charge of the α -particle with the average energy imparted per unit path length, termed linear energy transfer (LET), being 60–230 keV/ μm [10], the energy deposition per unit path length in tissue is far higher than that of β^- -particles. This confers the properties of a single α -particle traversal of the cell nucleus to have a 20–40% probability of killing that cell [11–13]. Typical α -particle kinetic energies of 5–9 MeV result in a 50–90 μm range *in vivo* translating to ~ 2 –10 cell diameters. Delivery of the α -emitting radionuclide at the cell membrane is sufficient to kill malignant cells and only a few hundred α -particle decays at the cell membrane, due to three dimensional emission geometry considerations, are required for a 99.99% level of cell kill with a correspondingly low normal tissue toxicity as opposed to 10^6 β^- -emissions [9]. Given a sufficiently precise targeting vector for an α -particle emitter, a highly localized and exquisitely cytotoxic radiation dose can be delivered to malignant cells with minimal damage to surrounding normal tissue since high LET radiation is well established as being far more lethal to cells than low LET radiation [14–18]. Toxicity originates from the increased frequency of clustered DNA double-strand breaks (DSBs) observed with high LET radiation [15, 19–21]. The cytotoxicity of α -particles has been shown as independent of both dose rate and oxygenation status of the cells [14].

13.4 Radionuclides

There are over 100 α -particle emitting radionuclides, however, the overwhelming majority of these radionuclides have half lives that are either too short or far too long to realistically

permit them to be of any meaningful therapeutic use, or there is no viable existing chemistry for this use, or there is no viable supply either by means or economics. Fortunately, ^{212}Bi and ^{213}Bi do meet the baseline parameters that define reasonable use within this context and as such both of them have also been investigated in animal models or humans.

Comprehensive reviews are available on the general medicinal chemistry of bismuth compounds [22, 23]. In brief, bismuth has an ionic radius of 103 pm with a normal oxidation state of $3+$ (Bi^{3+}) [24]; pentavalent species (Bi^{5+}) are well known as oxidative reagents [25]. Stable and non-radioactive bismuth has been used in antiulcer and antibacterial drugs. Beyond possessing a strong affinity for oxygen and nitrogen donors, bismuth is known to form very stable complexes with sulfur and halogens, especially iodide. Chelating agents with oxygen and nitrogen donors or compounds with thiolate donors can form very stable complexes with Bi(III) with the coordination number varying from 3 to 9. Bi(III) is known to bind to Zn(II) sites (e.g., metallothionein) and Fe(III) sites (e.g., transferrin) in proteins. Bi(III) has a high affinity for the kidneys and is excreted relatively quickly through the renal clearance system, with the kidneys also being a temporary deposition organ.

13.4.1 ^{212}Bi

^{212}Bi ($t_{1/2} = 60.6$ min) emits α -particles with a mean energy of 7.8 MeV to ultimately form stable ^{208}Pb (Figure 13.1). A generator that employs ion-exchange bound ^{224}Ra ($t_{1/2} = 3.4$ d) provides for on-site production of ^{212}Bi necessary for its use since the half-life limits the realistic transportation between sites [26]. ^{224}Ra is extracted from ^{228}Th , currently at Pacific Northwest Laboratories, with the ^{228}Th originating from ^{232}U [26]. A daughter radionuclide of ^{212}Bi , ^{208}Tl , emits a 2.6-MeV γ -ray that requires shielding to minimize the radiation exposure to personnel. This may limit the clinical utility of ^{212}Bi because of the uncertainty of what level of shielding is really necessary in a clinical setting due to the combination of both actual clinical dosing schedule and half life. ^{212}Bi may be eluted selectively from the ^{224}Ra generator in either the chloride form or as the tetra-iodide complex. After pH adjustment this material can be used to radiolabel mAbs, peptides, or other vectors that can conjugate with a suitable bifunctional chelating agent such as C-functionalized *trans*-cyclohexyldiethylenetriamine pentaacetic acid derivative, CHX-A' DTPA (Figure 13.2) [27–30].

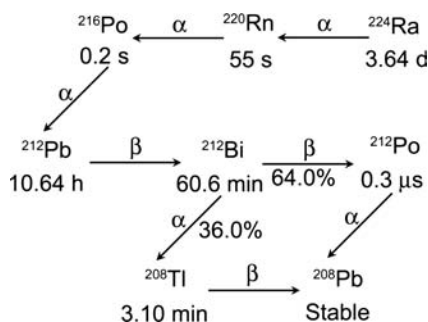


Figure 13.1 Decay scheme for ^{212}Bi from the parental radionuclide ^{224}Ra

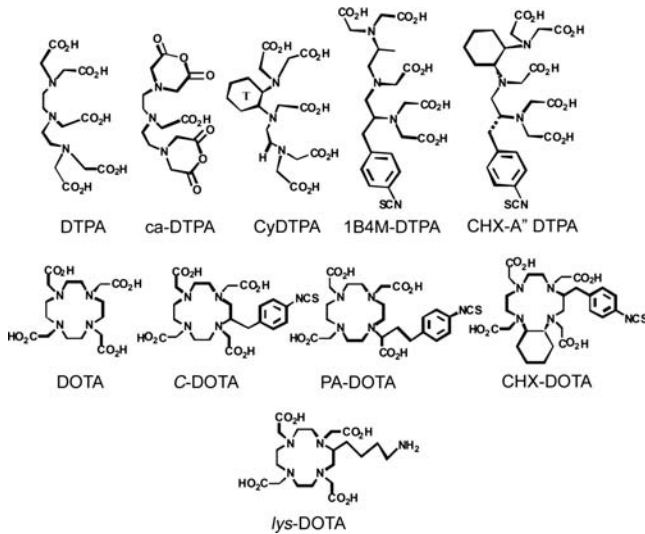


Figure 13.2 Structures of DTPA and bifunctional DTPAs such as the cyclic dianhydride of DTPA, CyDTPA, 1B4M-DTPA, and CHX-A'' DTPA, and structures of DOTA and bifunctional DOTAs, including C-DOTA, PA-DOTA, CHX-DOTA, and lys-DOTA

13.4.2 ^{213}Bi

^{213}Bi is similarly available via generator based technology from ^{225}Ac dispersed onto a cation exchange resin to prevent charring and decomposition of resin due to the confined radiation flux [31, 32]. The supply of ^{225}Ac in the United States is currently limited to Oak Ridge National Laboratories, although additional sources reside in both Germany and Russia. The ultimate source materials extend back through ^{225}Ra extracted from ^{229}Th that has its origin from ^{233}U [10, 33].

^{213}Bi decays to stable ^{209}Bi by emitting an α -particle and two β^- -particles (Figure 13.3). Fortunately, a 440-keV photon emission allows real time biodistribution, pharmacokinetic, and dosimetry studies to be performed within the context of the actual half life of the therapeutic. Again, ^{213}Bi can be selectively eluted from an ^{225}Ac generator, and can readily conjugate to mAbs, peptides, or other vectors that have been modified with a suitable bifunctional chelating agent, such as CHX-A'' DTPA [27–30].

13.5 Radiolabeling – Chemistry

The key fundamental requirement of targeted radiation therapy is the stable sequestration of the radionuclide *in vivo* to maximize the delivery of radiation to tumors while minimizing the toxicity [6]. All radionuclides have specific *in vivo* sites of deposition which when free pose as a source of toxicity concerns. Bismuth is very well established to have high affinity for localization in the kidney [34].

Radioconjugates are also susceptible to catabolism post-internalization into target cells or to radiolysis effects originating from radioactive decay. A large number of options have

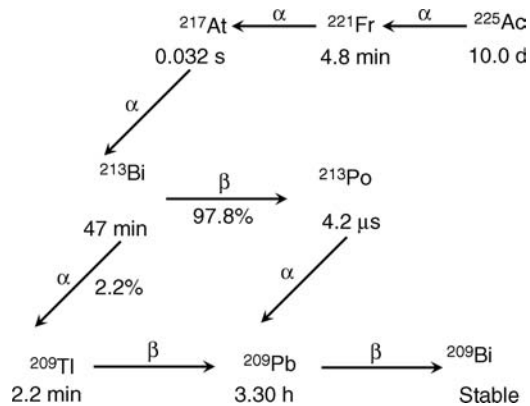


Figure 13.3 Decay scheme for ^{213}Bi from the parental radionuclide ^{225}Ac

been investigated for conjugating radioisotopes to antibodies, peptides, and so on, dependent on the chemical nature of the radionuclide [35].

^{213}Bi and ^{212}Bi , being metallic in nature, require chelation chemistry or bifunctional chelators for linkage to antibodies. Bifunctional chelating agents derived from DTPA include the cyclic dianhydride of DTPA [36], 1B4M-DTPA (MX-DTPA, tiuxetan) [37], and a family of *trans*-cyclohexyl derivatives that includes the specific stereoisomer, CHX-A'' DTPA (Figure 13.2) [28–30]. The CHX-A'' DTPA is the only reported DTPA derivative found to form suitably stable complexes with ^{213}Bi and ^{212}Bi conjugated to mAbs or peptides *in vivo* [28–30], resulting in radioimmunoconjugates used effectively in clinical trials [27]. While the fundamental studies of the physical characteristics and coordination chemistry have not been performed on the specific enantiomeric form, CHX-A'' DTPA, studies on the parental ligands CyDTPA and DTPA and their respective Bi(III) complexes are available [38]. While the adoption of eight-coordinate structures, that is, square antiprisms, for each complex was reported, the impact of inclusion of the *trans*-cyclohexyl ring is evident by shorter Bi-ligand bond distances, but more importantly by all eight donors of the coordination sphere originating from CyDTPA being bound to Bi(III). In contrast, one carboxylate donor in the simple parental DTPA complex originates from a neighboring molecule. This observation easily translates forward to the significant differences in *in vivo* complex stability found for the CHX-A'' DTPA versus DTPA [39].

Macrocyclic bifunctional analogs chelators for linkage to antibodies have been well represented by numerous analogs of 1,4,7,10-tetraazacyclododecanetetraacetic acid (DOTA) (Figure 13.2) which have been investigated for radiolabeling proteins and peptides with ^{111}In , ^{90}Y , ^{177}Lu , ^{212}Pb , and ^{212}Bi [8, 10, 40–43]. Structurally, DOTA complexes tend to be eight-coordinate square antiprisms that exist in an equilibrium between isomeric arrangements of the carboxylate arms and ring twists forms that also permit saturation of the coordination spheres about Bi(III). However, the complex formation mechanism associated with DOTA correlates with a time course that compromises the use of DOTA with ^{212}Bi (or ^{213}Bi) [44, 45]. There is no luxury of time when using short half life radionuclides except in select cases where the formation rate can be accelerated by significant heating, and this option is primarily limited to small molecules and peptides [46].

More recently, the efficient and short synthetic route to the structurally novel bimodal ligand NETA ($\{4-[2-(\text{Bis-carboxymethyl-amino})\text{-ethyl}]-7\text{-carboxymethyl}-[1,4,7]\text{triazolan-1-yl}\}$ -acetic acid) been reported which possesses both a macrocyclic cavity and a flexible acyclic moiety [47, 48]. Complexation kinetics, serum stability, and favorable *in vivo* biodistribution profile of its ^{205}Bi and ^{206}Bi complex make this ligand attractive for further evaluation as a chelator for ^{212}Bi and ^{213}Bi .

Several reactive functional groups for conjugating bifunctional chelating agents to proteins, peptides, or other vectors have been reported with an aryl isothiocyanate being one of the more prevalent [8]. Other groups such as reactive halogens, maleimide, and active esters have been relatively less studied. An important fact relevant to conjugation chemistry is that except in special cases, all conjugation strategies, when used with proteins do result in random distributions of products as a consequence of reacting with available functionalities. As a consequence, the optimal number of chelates possible per protein molecule has to be determined empirically to retain the biological activity of the targeting protein. That resulting number is not a discrete number but represents a distribution of products.

When conjugating with peptides, the chelating agent is generally at the *N*- or *C*-terminus in a 1 : 1 form arranged synthetically providing a discrete product. Generally, bifunctional chelating agents are conjugated to the targeting vector first and the conjugate then is radiolabeled after optimization of the reaction conditions. Pre-radiolabeling of the bifunctional chelating agent prior to conjugation, necessary in some selected cases, generally results in low conjugation yields potentially complicated by radiolysis issues and is not a feasible avenue for use with ^{212}Bi or ^{213}Bi due to the half life considerations.

13.6 Preclinical Studies

13.6.1 ^{212}Bi

The early reports on ^{212}Bi -containing radioimmunoconjugates were defined by Macklis *et al.* [36] and Simonson *et al.* [49], wherein tumor specific monoclonal antibodies were radiolabeled with ^{212}Bi using either the cyclic DTPA dianhydride or glycytyrosyl-lysyl-*N*- ϵ -DTPA, respectively. While prolonged survival of colon carcinoma bearing mice was reported, both of these studies also defined the result of inadequate chelation technology as indicated by significant renal deposition of ^{212}Bi .

To overcome this deficiency, the bifunctional chelating agent, CHX-A'' DTPA [28], was defined as suitable for sequestering ^{212}Bi *in vivo* after conjugation to anti-gp70 mAb 103A [50]. Therapy of murine Rauscher erythroleukaemia resulted in decreased splenic tumor growth and prolonged median survival. Additionally, the CHX-A'' DTPA was further validated by its use in forming ^{212}Bi -anti-Tac (anti-CD25) used to treat CD25+ tumor bearing mice that led to enhanced tumor free survival and prevented development of tumors in some animals [51].

13.6.2 ^{213}Bi

Similarly to the experience with the CHX-A'' DTPA studies with ^{212}Bi , Kennel *et al.* targeted blood vessels in lung tumors as a therapeutic approach with ^{213}Bi radiolabeled mAbs 201B and 34A in a murine model with lung tumors of EMT-6 mammary carcinoma

and IC-12 tracheal carcinoma [52]. Animals with tumor cross sections of 5–10 cell diameters (50–400 cells/tumor) achieved 100% cure at a dose of 5.6–7.4 MBq (150–200 μCi), but as expected for α -particle mediated therapy, the cure rate dropped markedly when attempting therapy studies with larger tumors.

In a relatively unique study, the engineered mAb, HuCC49 Δ CH2, radiolabeled with ^{213}Bi was evaluated for treating solid tumors which runs counter to accepted usage of α -particle mediated therapy [53]. Surprisingly, doses as high as 37 MBq (1.0 mCi) per animal were administered i.p. resulting in all animals exhibiting tumor growth arrest with $\sim 50\%$ being cured. Positive responses were also achieved using lower doses of (18.5–27.8 MBq (500–750 μCi)) with $\sim 33\%$ being cured, 33% responding with delayed tumor growth and $\sim 33\%$ not responding (Figure 13.4). These results were very encouraging and also challenge conventional belief that solid tumors cannot be successfully treated with α -emitters. The potential and limitations of ^{213}Bi may in fact more properly reside with the properties of the delivery vector.

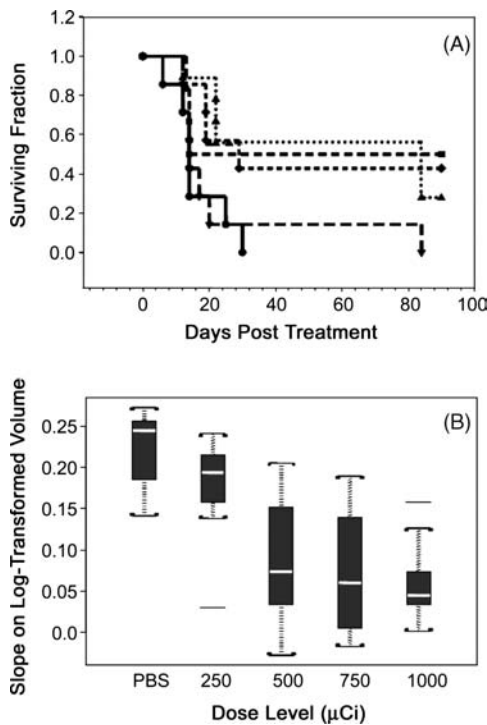


Figure 13.4 Kaplan-Meier survival curves for mice bearing 10–12 day s.c. LS-174T tumor following treatment with ^{213}Bi -HuCC49 Δ CH2 with increasing doses of ^{213}Bi -HuCC49 Δ CH2 in Panel A are: (●), PBS-treated; (▼) 250 μCi ; (■) 500 μCi ; (◆) 750 μCi ; and (▲) 1000 μCi . Panel B is the box plots of the estimated slopes for each dose level. The light line is the median, the upper region of the box represents the third quartile, the lower portion is the first quartile, the brackets delineate 1.5 times the interquartile range and the lines outside of the brackets represent outlying observations

The Allen group in Australia has performed a wide range of preclinical studies exploring the utility of ^{213}Bi [54–57]. Efficacy of ^{213}Bi labeled plasminogen activator inhibitor type 2 (PAI2) in regressing prostate cancer model has been reported. Tumor growth was inhibited with single doses of 947 or 1421 MBq kg⁻¹ (25.6–38.4 mCi kg⁻¹), while complete tumor growth inhibition was achieved at a total dose of 947 MBq kg⁻¹ (25.6 mCi kg⁻¹) given on five successive days [54]. A single local or i.p. injection of ^{213}Bi - PAI2 completely regressed tumor growth and lymph node metastases with no lymphatic spread of cancer resulting from administration of 222 MBq kg⁻¹ (6 mCi kg⁻¹) at two days and two weeks postcell inoculation [56]. Anticorectal cancer mAb c30.6 radiolabeled with ^{213}Bi demonstrated high tumor uptake and retention [56]. ^{213}Bi -PAI2 was also been evaluated for treating micro-metastatic breast cancer. A single local injection of ^{213}Bi -PAI2 completely inhibited tumor growth while a single systemic (i.p.) administration resulted in dose dependent tumor growth inhibition [57]. The same group evaluated ^{213}Bi labeling of bevacizumab, a humanized anti-VEGF monoclonal antibody has shown promise in various clinical trials, via both cDTPA and CHX-A'' chelators. They observed remarkable stability of radio-conjugates both *in vitro* and *in vivo* and concluded that RIT with ^{213}Bi -bevacizumab was superior to bevacizumab alone [58].

Locoregional therapy of disseminated gastric cancer was performed using single versus double i.p. injections of mAb d9MAB labeled with ^{213}Bi . Two administrations of 0.37 MBq (10 μCi) of ^{213}Bi -d9MAB at Days 1 and 8 after tumor inoculation significantly prolonged median survival vs. a single injection [59].

^{213}Bi -J591 has been assessed for efficacy in a murine model of prostate cancer using LNCaP tumors [60]. Significantly improved median tumor free survival (54 days) relative to controls (33 days), or no treatment (31 days) were observed. Reduction of PSA levels also correlated to tumor response.

Milenic *et al.* have evaluated ^{213}Bi -trastuzumab for treatment of disseminated peritoneal disease [61]. The maximum effective dose of 500 μCi was defined based on changes in animal weights treating three-day LS-174T i.p. xenografts. Median survival increased from 19 days to 43 days and 59 days with 18.5 and 27.8 MBq (500 and 750 μCi), respectively. Therapy with ^{213}Bi -trastuzumab treating five-day xenografts was also efficacious (Figure 13.5). RIT targeting HER2 was proposed to be potentially beneficial even for those patients currently ineligible for immunotherapy due to the low antigen expression. Myeloablative radiation preparative regimens cause significant toxicity despite being potentially curative for several malignancies when combined with allogeneic marrow transplantation. ^{213}Bi -labeled mAbs targeting CD45 and TCR $\alpha\beta$ were evaluated for immunosuppression prior to marrow transplantation in a canine model [62, 63]. Administration of either radiolabeled mAb combined with immunosuppressive agents resulted in engraftment of transplanted marrow and stable mixed chimerism. While transient myelosuppression and liver enzyme abnormalities were noted, actual clinical use of ^{213}Bi radiolabeled mAbs in this arena may be compromised by the estimated requirement of more than 74 MBq kg⁻¹ [2 mCi kg⁻¹] doses.

Wilbur *et al.* investigated the use of recombinant streptavidin (rSAv) as a carrier molecule for ^{213}Bi . rSAv was conjugated to CHX-A'' followed by further modification with succinic anhydride since succinylation of the protein lysine amines diminishes kidney localization. The *in vivo* data showed that ^{213}Bi -labeled succinylated rSAv has tissue concentrations similar to those of ^{125}I -labeled modified rSAv which points at its stability towards ^{213}Bi release [64].

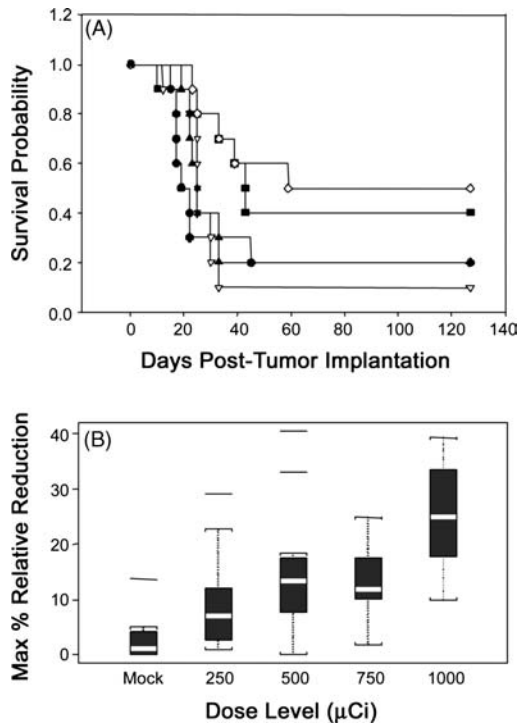


Figure 13.5 Kaplan-Meier survival curves for mice bearing 5 d LS-174T *i.p.* xenografts treated with increasing μCi doses of $^{213}\text{Bi-CHX-A}''\text{-Herceptin}$ were administered *i.p.* to mice bearing 5 d LS-174T *i.p.* xenografts. The injected doses were (●) mock-treated; (▽) 250 μCi ; (■) 500 μCi ; (◇) 750 μCi ; (▲) 1000 μCi ; and (○) 500 μCi $^{213}\text{Bi-HuIgG}$ was used as a non-specific control. Panel B shows the affects of $^{213}\text{Bi-CHX-A}''\text{-Herceptin}$ radioimmunotherapy on animal weights. The maximum relative weight reduction was calculated for each treatment group and presented as box plots. The light line is the median, the upper region of the box represents the third quartile, the lower portion is the first quartile, the brackets delineate 1.5 times the interquartile range, and the lines outside of the brackets represent outlying observations

Kelly and colleagues investigated the efficacy of RIT with ^{213}Bi -labeled humanized anti-Lewis Y (Le^{y}) monoclonal antibody humanized 3S193 (hu3S193) alone or in combination with a single dose of 300 μg of paclitaxel in mice bearing Le^{y} -positive MCF-7 breast carcinoma.

$^{213}\text{Bi-hu3S193}$ was efficacious in both mice with a minimal residual and with established tumors thus underscoring the utility of ^{213}Bi in treatment of palpable solid tumors. The efficacy was enhanced by paclitaxel to produce defined complete responses [65].

Synergy between RIT with ^{213}Bi -labeled antibodies and chemotherapy was also convincingly demonstrated *in vitro*. The response of B-Cell chronic lymphocytic leukaemia (B-CLL) cells to treatment with chemotherapy (cisplatin, fludarabine, doxorubicin, or vincristine) or other pharmaceuticals (colchicine, simvastatin, or cyclosporin A) in combination with ^{213}Bi -RIT induced a systematic, higher response, compared to treatment with drugs alone, even at the highest concentrations [66]. It is not inconceivable, that the samples of patients tumor cells could be screened *in vitro* for the response to the combination of

^{213}Bi -RIT and chemotherapy and that a variety of anticancer drugs and the most optimal therapy will subsequently be administered to create true personalized medicine.

Michel and colleagues studied ^{213}Bi -antibody to CD74 as a potential therapeutic agent for disseminated experimental Raji B-cell lymphoma. Their dosimetry calculations showed that as low as 30 decays of cell-bound ^{213}Bi was required for a 99% cell kill. An irrelevant control antibody, similarly radiolabeled, also produced toxicity, due to decays occurring in the medium, but was approximately threefold less potent than the reactive mAb. In SCID mice bearing Raji B-cell lymphoma, treatment with ^{213}Bi -antibody to CD74 resulted in suppression of tumor growth and cures in some mice [67].

Chemo-resistance and radio resistance which are quickly acquired by tumors during conventional therapies are considered to be some of the primary reasons for therapeutic failure in leukaemia and solid tumors. In a hallmark paper, Friesen *et al.* found that targeted radiotherapy using anti-CD45 antibody labeled with ^{213}Bi induced apoptosis, activated apoptosis pathways, and broke β^- -irradiation-, γ -irradiation-, doxorubicin-, and apoptosis-resistance in leukaemia cells. In regard to radiobiological mechanism of action, the ^{213}Bi -anti-CD45-induced DNA damage was not repaired, and apoptosis was not inhibited by the non homologous end joining DNA repair mechanism. In addition, ^{213}Bi -anti-CD45 reversed deficient activation of caspase-3, caspase-8, and caspase-9, deficient cleavage of poly(ADP-ribose) polymerase, and deficient activation of mitochondria in chemo-resistant and in radio resistant and apoptosis resistant leukaemia cells, thus showing the great promise of therapy in patients whose tumors have developed chemo- and/or radiation resistance [68].

13.7 Targeted α -Therapy versus Targeted β -Therapy

Several *in vitro* studies have compared the efficacy of α - versus β -labeled antibodies or peptides in killing cancer cells: the somatostatin analog [DOTA⁰-Tyr³]-octreotide (DOTATOC) was labeled with ^{213}Bi or ^{177}Lu and used against the somatostatin receptor (sstr)-positive cell line Capan-2 [69]; two antibodies against epithelial antigens Muc-1 and syndecan-1 were radiolabeled with ^{131}I or ^{213}Bi and used for evaluation of radiotoxicity against patient derived multiple myeloma cells lines [70]. In both studies, the ^{213}Bi -labeled molecules were superior in killing cancer cells when compared to ^{177}Lu or ^{131}I -labeled molecules, respectively (Table 13.1).

Despite the accepted paradigms that define the appropriate usage of α -emitters and β -emitters based in both physics and radiation biology, there are actually few studies in the

Table 13.1 Comparison of *in vitro* killing efficacy of alpha- versus beta-labeled antibodies and peptides

Cell line	Targeting molecule	Cell survival, %
Human pancreatic adeno-carcinoma Capan-2	^{177}Lu -DOTATOC peptide ^a	47.05
	^{213}Bi -DOTATOC peptide ^a	23.52
Human myeloma U266	^{131}I -B-B4 mAb ^b	90
	^{213}Bi -B-B4 mAb ^b	0.2

^aThe activities of ^{177}Lu -DOTATOC and ^{213}Bi -DOTATOC used in this experiment delivered the same 0.7 Gy dose to the nuclei of Capan-2 cells [69].

^b200 MBq/l of either ^{131}I -B-B4 mAb or ^{213}Bi -B-B4 mAb were used to produce the effect [70].

literature that directly compare the efficacy of α -emitters and β -emitters *in vivo*. Considerable enhanced efficacy in inhibiting tumor growth and improved survival rates have been demonstrated using α -emitters. For example, the ^{213}Bi -labeled Fab' fragment of mAb CO17-1A prevented growth of a human colon cancer xenograft while increasing survival as compared to the ^{90}Y -labeled Fab' [71].

Pre-targeted RIT technology (PRIT) was created to improve tumor-to-normal organ ratios concomitantly reducing radiation dose to normal organs. One PRIT strategy involves administering a mAb conjugated to streptavidin, followed by administration of a biotinylated *N*-acetylgalactosamine-containing 'clearing agent' to remove excess circulating antibody via the liver. Thereafter, radiolabeled biotin is infused to bind to the 'pre-targeted' streptavidin-antibody conjugate at the tumor while unbound radiolabeled biotin rapidly excrete by virtue of its small molecule nature [72]. PRIT was employed to directly compare ^{213}Bi to ^{90}Y in the treatment of disseminated CD25+ adult T-cell leukaemia [73]. While the α -particle therapy with ^{213}Bi reduced levels of surrogate tumor markers $\beta_2\mu\text{G}$ and soluble CD25, and improved survival, the treatment with ^{90}Y failed to improve survival and also resulted in significant toxicity. Extending this same PRIT strategy forward to evaluation of an anti-CD25 single-chain Fv-streptavidin fusion protein followed by ^{213}Bi -biotin resulted in a cure of seven out of 10 mice [74].

13.8 Clinical Studies

13.8.1 ^{213}Bi

The landmark clinical trial at the Memorial Sloan-Kettering Cancer Center introduced ^{213}Bi -labeled humanized anti-CD33 monoclonal antibody, HuM195, as an targeted α -particle mediated therapy [75]. Patients (18) with advanced myeloid leukaemia were treated in a Phase I dose-escalation trial using doses up to 37 MBq kg^{-1} (1 mCi kg^{-1}) resulting in myelosuppression and transient minor liver function abnormalities. Real time γ -camera imaging concurrent with therapy administration of ^{213}Bi -HuM195 demonstrated uptake in the bone marrow, liver, and spleen, without significant uptake in other organs, and most importantly, absence from the kidney. Dosimetry calculation provided estimated absorbed dose ratios between marrow, liver, and spleen and the whole body to be 1000 times greater than with HuM195 radiolabeled with β^- -emitters. While 14 of 18 patients benefited by a reduction of bone marrow blasts from this therapy, no complete remissions were achieved.

A Phase I/II ^{213}Bi -HuM195 study followed wherein patients were first treated with cytarabine ($200\text{ mg/m}^2/\text{d}$ for 5 d) to achieve partial cytorreduction of the leukaemic burden followed by ^{213}Bi -HuM195 at 4 dose levels ($18.5\text{--}46.25\text{ MBq kg}^{-1}$ [$0.5\text{--}1.25\text{ mCi kg}^{-1}$]) [76].

Prolonged myelosuppression was reached at the highest dose level while complete responses, complete responses with incomplete platelet recovery, and partial responses were achieved at the two highest dose levels. These clinical results indicate that sequential administration of cytarabine and ^{213}Bi -HuM195 can lead to complete remissions in patients with acute myeloid leukaemia.

Other groups have investigated locoregional administration of ^{213}Bi -labeled carrier molecules in solid cancers. Allen *et al.* reports the intralesional administration of ^{213}Bi -labeled antibody 9.2.27 to 16 patients with metastatic melanoma to the skin. The 9.2.27 antibody binds to the melanoma-associated chondroitin sulfate proteoglycan (MCSP). The

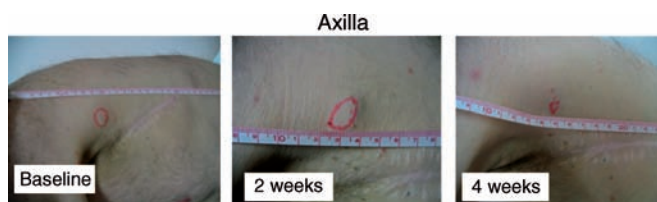


Figure 13.6 Tumor response from intralesional administration of 697 MBq (18.8 mCi) and in terms of body weight 8.3 MBq/kg of ^{213}Bi -labeled antibody 9.2.27. One can observe the tumor response and shrinkage achieved after four weeks. Courtesy of Drs. Barry Allen and Chand Raja, St. George Hospital, NSW, Australia

doses ranging from 150–1350 MBq were injected into the tumors of various dimensions and caused significant cell death which resulted in tumor inflammation and some shrinkage (Figure 13.6). No acute toxic effects such as changes in blood chemistry or HAMA reaction were observed in treated patients [77]. Kneifel and colleagues developed a new bifunctional peptidic vector (substance P) that targets the neurokinin type-1 receptor (NK1R) [78], which is consistently overexpressed in primary malignant gliomas, radiolabeled it with either ^{90}Y or ^{213}Bi , and administered the radiolabeled substance P via an implanted catheter system either into the tumor or into the resection cavity. Two patients with progressive glioblastoma and low grade oligodendroglioma were given an intracavitary injection of 375 and of 825 MBq of ^{213}Bi -labeled substance P, respectively, which was well tolerated. While response assessment was difficult in the glioblastoma patient due to bulky residual tumor, in the oligodendroglioma patient the resection of a mass lesion 33 months after therapy showed only radiation necrosis and absence of viable tumor cells [77]. Based on these encouraging preliminary results, a separate trial of ^{213}Bi -labeled substance P in patients with brain tumors is currently ongoing.

13.9 Alternate Delivery Methods and Uses

Peptides, as opposed to protein or mAb targeted α -therapy, have also been evaluated to take advantage of rapid targeting with cellular internalization combined with rapid clearance pharmacokinetics. The somatostatin analog [DOTA⁰-Tyr³]-octreotide (DOTATOC) labeled with ^{213}Bi , > 11 MBq (300 μCi), significantly decreased tumor growth rate in rats treated 10 days post-inoculation with tumor as compared with controls ($P < 0.025$). Higher doses, that is, > 20 MBq (540 μCi) resulting in greater tumor reduction [46].

RIT applications have been overwhelmingly oncological in nature. However, some alternative applications have recently emerged. Wesley and colleagues armed humanized anti-Tac (HAT) antibody with ^{212}Bi and evaluated the radioimmunoconjugate in a cynomolgus cardiac allograft model exploiting the fact that IL-2 receptors are expressed by T-cells responding to foreign antigens, but not by resting T-cells. Monkeys treated with ^{212}Bi -HAT survived significantly longer than controls which points to the possibility of using α -emitter labeled HAT in organ transplantation [79].

The field of infectious diseases is in crisis and novel approaches to treatment are urgently needed. Dadachova and coworkers have established a novel arena by demonstrating that RIT has also broad potential for the treatment of fungal and bacterial infections through

targeting microbial antigens with radiolabeled mAbs in experimental models [80, 81]. Thereafter, they extended their approach to treatment of fungal biofilms showing that with targeted α -therapy a reduction in biofilm metabolic activity by 50% was achieved versus no effect by controls which can be a novel option for the prevention or treatment of microbial biofilms on indwelling medical devices [82]. In addition, they found that HIV-1 infected cells were eliminated *in vitro* and *in vivo* by targeting gp120 and gp41 viral proteins expressed on the surface of infected cells with radiolabeled viral protein-specific antibodies (Figure 13.7) [83].

13.10 Prospects and Conclusions

The investigation and evaluation of radiolabeled mAbs for diagnosis and treatment of cancer remains a burgeoning enterprise with the vast overwhelming majority of RIT trials being performed with β^- -emitting isotopes. The shorter range and higher LET α -particles allow for more efficient and selective killing of individual tumor cells as opposed to β^- -emitters. Although some results from pre-clinical model experimentation have demonstrated that targeted α -therapy may have a significant impact on larger or solid tumor burdens, the majority of preclinical and clinical trials thereafter clearly remain within the accepted paradigm that α -emitters are best suited for the treatment of small volume disease. And, while both preclinical and early clinical studies continue to appear promising and generate valuable data supporting the exquisite potency of α -emitters, obstacles also continue to obstruct their pathways to widespread acceptance and use, primarily those associated with supply and economics. To traverse these obstacles, new sources and methods for production of these medically valuable radionuclides need to be resolved. Current supplies of both originating from the ^{225}Ac and ^{224}Ra decay pathways remain limited to those sources of naturally isolated by-products from weapons development within the United States. Additional sources of both reside within Russia and other locations and within recovery of nuclear fuel materials during reprocessing. However, ramping up production from any site seems unlikely at this time.

Beyond production of these radionuclides, the next phase of assembly and transport of generators of sufficient activity amounts to support clinical trials will also have to be addressed. Current clinical use of ^{213}Bi requires multiple generators linked together combined with multiple elutions and dose administrations to achieve the total patient dose. Lastly, simple economics provide a serious challenge to the continued development of these radionuclides. Their costs have more than tripled in the past decade for a variety of reasons while funding has seriously declined challenging the ability of many researchers from either remaining in or entering the field.

Opportunities remain within the area of conjugation chemistry. Despite having traversed issues pertaining to suitably stable chelation chemistry, more efficient conjugation and radiolabeling protocols will only promote further advances resulting in more consistent products with higher specific activities that will optimize therapeutic potentials. Better pharmacokinetic and dosimetry modeling techniques that actually address the cellular microdosimetry aspect of targeted α -emitters have only recently started to emerge with the most recent example being mathematical modeling and feasibility analysis of targeting cancer stem cell using ^{213}Bi [84, 85].

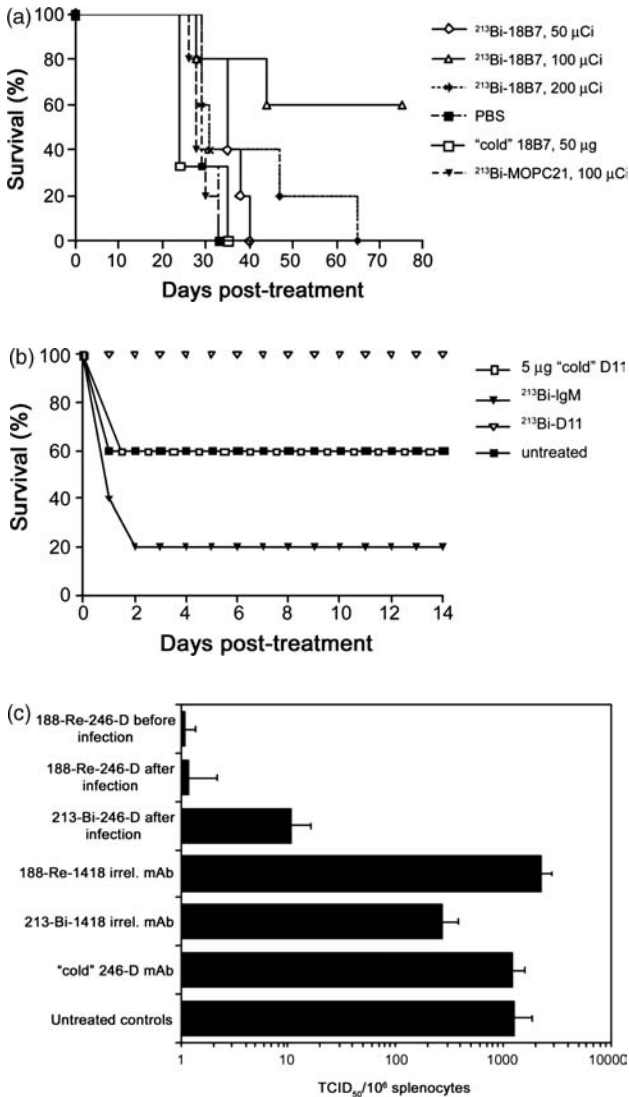


Figure 13.7 Radioimmunotherapy of experimental fungal, bacterial and viral infections with ^{213}Bi -labeled antibodies: (a) Kaplan-Meier survival curves for A/JCr mice infected with pathogenic fungus *C. neoformans*; (b) RIT of *S. pneumoniae* bacterial infection in C57BL/6 mice; (c) RIT of SCID mice infected intrasplenically with HIV1-infected human PBMCs with ^{188}Re - and ^{213}Bi -labeled antibodies to gp41 antigen

There remains room for development of novel efficient delivery methods which must be carefully studied. In part, this approach has been initiated (*vide infra*) although their adaptation to the burgeoning concept of molecular targets and personalized medicine remains in the distant future. Careful and truly comparable preclinical (and clinical investigations) will be required to define optimal dosing regimens and therapeutic strategies. This latter

aspect is rapidly growing in critical acceptance that while single dose administration protocols dominate clinical investigation, the clinical reality remains that RIT and thus targeted α -therapy will have to become integrated into clinical standards of care, to become combined with external beam radiation therapy, and/or with complex chemotherapy regimens to become a real, accepted therapeutic modality.

Abbreviations

CDR	complementarity-determining region
CHX-A'' DTPA	C-functionalized <i>trans</i> -cyclohexyldiethylene-triamine pentaacetic acid derivative
DOTA	1,4,7,10-tetraazacyclododecanetetraacetic acid
DSBs	double-strand breaks
FDA	Food and Drug Administration
HAMA	human anti-murine immunoglobulin antibodies
HAT	humanized anti-Tac
keV	kilo electron-Volt
LET	linear energy transfer
mAb	Monoclonal antibody
MeV	mega electron-Volt
NETA	{4-[2-(Bis-carboxymethyl-amino)-ethyl]-7-carboxymethyl-[1,4,7]triazonan-1-yl}-acetic acid
NHL	non-Hodgkin's lymphoma
PRIT	pre-targeted RIT technology
RIT	radioimmunotherapy
rSAv	recombinant streptavidin
TAA	tumor-associated antigens

Acknowledgements

This research was supported in part by the Intramural Research Program of the NIH, National Cancer Institute, Center for Cancer Research. E. Dadachova is a Sylvia and Robert S. Olnick Faculty Scholar in Cancer Research and is supported by the National Institute of Allergy and Infectious Disease (NIAID) grant AI60507. We also thank Diane Milenic for her assistance.

References

1. Mulford, D.A., Scheinberg, D.A., and Jurcic, J.G. (2005) *Journal of Nuclear Medicine*, **46**, 199S–204S.
2. Brechbiel, M.W. (2007) Targeted α -therapy: past, present, future? *Dalton Transactions*, 1–11.
3. Kohler, G. and Milstein, C. (1975) *Nature*, **256**, 495–497.
4. Schlom, J. (1990) *Molecular Foundations of Oncology* (ed. S. Broder) Williams and Wilkins, Baltimore, MD, pp. 95–134.

5. Milenic, D.E. (2000) *Seminars in Radiation Oncology*, **10**, 139–155.
6. Srivastava, S. and Dadachova, E. (2001) *Seminars in Nuclear Medicine*, **31**, 330–341.
7. Dijkgraaf, I., Boerman, O.C., Oyen, W.J. *et al.* (2007) *Journal of Medicinal Chemistry*, **7**, 543–551.
8. Milenic, D.E., Brady, E.D., and Brechbiel, M.W. (2004) *Nature Reviews. Drug Discovery*, **3**, 488–498.
9. Humm, J.L. and Cobb, L.M. (1990) *Journal of Nuclear Medicine*, **31**, 75–83.
10. Hassfjell, S. and Brechbiel, M.W. (2001) *Chemical Reviews*, **101**, 2019–2036.
11. Søyland, C. and Hassfjell, S.P. (2000) *International Journal of Radiation Biology*, **76**, 1315–1322.
12. Pugliese, M., Durante, M., Grossi, G.F. *et al.* (1997) *International Journal of Radiation Biology*, **72**, 397–407.
13. Hei, T.K., Wu, L., Liu, S. *et al.* (1997) *Proceedings of the National Academy of Sciences of the United States of America*, **94**, 3765–3770.
14. Hall, E.J. (1994) *Radiobiology for the Radiologist*, 4th edn, J. B. Lippincott Company, Philadelphia.
15. Blakely, E.A. and Kronenberg, A. (1998) *Radiation Research*, **150**, S126–S145.
16. Macklis, R.M., Lin, J.Y., Beresford, B. *et al.* (1992) *Radiation Research*, **130**, 220–226.
17. Walicka, M.A., Vaidyanathan, G., Zalutsky, M.R. *et al.* (1998) *Radiation Research*, **150**, 263–268.
18. Bishayee, A., Rao, D.V., Bouchet, L.G. *et al.* (2000) *Radiation Research*, **153**, 416–427.
19. Howell, R.W., Goddu, S.M., Narra, V.R. *et al.* (1997) *Radiation Research*, **147**, 342–348.
20. Azure, M.T., Archer, R.D., Sastry, K.S.R. *et al.* (1994) *Radiation Research*, **140**, 276–283.
21. Goodhead, D.T. (1994) *International Journal of Radiation Biology*, **65** (1), 7–17.
22. Sun, H., Li, H., and Sadler, P.J. (1997) *Chemische Berichte-Recueil*, **130**, 669.
23. Briand, G.G. and Burford, N. (1999) *Chemical Reviews*, **99**, 2601–2758.
24. Shannon, R.D. (1976) *Acta Crystallographica*, **A32**, 751–767.
25. Cotton, F.A. and Wilkinson, G. (1980) *Advanced Inorganic Chemistry: A Comprehensive Text*, John Wiley & Sons, Inc., New York.
26. Atcher, R.W., Friedman, A.M., and Hines, J.J. (1988) *International Journal of Radiation Applications and Instrumentation [A]*, **39**, 283–286.
27. Ma, D., McDevitt, M.R., Finn, R.D., and Scheinberg, D.A. (2001) *Applied Radiation and Isotopes*, **55**, 463–470.
28. Brechbiel, M.W. and Gansow, O.A. (1992) *Journal of the Chemical Society-Perkin Transactions 1*, 1173–1178.
29. Wu, C., Kobayashi, H., Sun, B. *et al.* (1997) *Bioorganic and Medicinal Chemistry*, **5**, 1925–1934.
30. Milenic, D.E., Garmestani, K., Chappell, L.L. *et al.* (2002) *Nuclear Medicine and Biology*, **29**, 431–442.
31. McDevitt, M.R., Finn, R.D., Sgouros, G. *et al.* (1999) *Applied Radiation and Isotopes*, **50**, 895–904.
32. Pippin, C.G., Gansow, O.A., Brechbiel, M.W. *et al.* (1995) *Chemists View of Imaging Centers* (ed. A.M. Emran) Plenum Press, New York, pp. 315–322.
33. Boll, R.A., Malkemus, D., and Mirzadeh, S. (2005) *Applied Radiation and Isotopes*, **62**, 667–679.
34. Larsen, A., Martiny, N., Stoltenberg, M. *et al.* (2003) *Pharmacology & Toxicology*, **93**, 82–90.
35. Wu, C., Gansow, O.A., and Brechbiel, M.W. (1999) *Nuclear Medicine and Biology*, **26**, 339–342.
36. Macklis, R.M., Kinsey, B.M., Kassis, A.I. *et al.* (1988) *Science*, **240**, 1024–1026.
37. Brechbiel, M.W. and Gansow, O.A. (1991) *Bioconjugate Chemistry*, **2**, 187–194.
38. Brechbiel, M.W., Gansow, O.A., Pippin, C.G. *et al.* (1996) *Inorganic Chemistry*, **35**, 6343–6348.
39. McMurry, T.J., Pippin, C.G., Wu, C. *et al.* (1998) *Journal of Medicinal Chemistry*, **27**, 3546–3549.
40. Parker, D. (1990) *Chemical Society Reviews*, **19**, 271–291.
41. Chappell, L.L., Rogers, B.E., Khazaeli, M.B. *et al.* (1999) *Bioorganic and Medicinal Chemistry*, **7**, 2313–2320.
42. Chappell, L.L., Ma, D., Milenic, D.E. *et al.* (2003) *Nuclear Medicine and Biology*, **30**, 581–595.
43. McMurry, T.J., Brechbiel, M.W., Kumar, K., and Gansow, O.A. (1992) *Bioconjugate Chemistry*, **3**, 108–117.

44. Moreau, J., Guillon, E., Pierrard, J.-C. *et al.* (2004) *Chemistry – A European Journal*, **10**, 5218–5232.
45. Ruegg, C.L., Anderson-Berg, W.T., Brechbiel, M.W. *et al.* (1990) *Cancer Research*, **50**, 4221–4226.
46. Norenberg, J.P., Krenning, B.J., Konings, I.R.H.M. *et al.* (2006) *Clinical Cancer Research*, **12**, 897–903.
47. Chong, H.S., Song, H.A., Birch, N. *et al.* (2008) *Bioorganic & Medicinal Chemistry Letters*, **18**, 3436–3439.
48. Chong, H.S., Ma, X., Le, T. *et al.* (2008) *Journal of Medicinal Chemistry*, **51**, 118–125.
49. Simonson, R.B., Ultee, M.E., Hauler, J.A., and Alvarez, V.L. (1990) *Cancer Research*, **50**, 985s–988s.
50. Huneke, R.B., Pippin, C.G., Squire, R.A. *et al.* (1992) *Cancer Research*, **52**, 5818–5820.
51. Hartmann, F., Horak, E.M., Garmestani, K. *et al.* (1994) *Cancer Research*, **54**, 4362–4370.
52. Kennel, S.J., Stabin, M., Roeske, J.C. *et al.* (1999) *Radiation Research*, **151**, 244–256.
53. Milenic, D.E., Garmestani, K., Dadachova, E. *et al.* (2004) *Cancer Biotherapy & Radiopharmaceuticals*, **19**, 135–148.
54. Rizvi, S.M.A., Li, Y., Song, E.Y.J. *et al.* (2006) *Cancer Biology & Therapy*, **5**, 386–393.
55. Li, Y., Rizvi, S.M.A., Ranson, M., and Allen, B.J. (2002) *British Journal of Cancer*, **86**, 1197–1203.
56. Rizvi, S.M.A., Allen, B.J., Tian, Z. *et al.* (2001) *Colorectal Disease*, **3**, 345–353.
57. Allen, B.J., Tian, Z., Rizvi, S.M.A. *et al.* (2003) *British Journal of Cancer*, **88**, 944–950.
58. Rizvi, S.M.A., Song, E.Y., Raja, C. *et al.* (2008) *Cancer Biology & Therapy*, **7**, 1548–1555.
59. Bloechl, S., Beck, R., Seidl, C. *et al.* (2005) *Clinical Cancer Research*, **11**, 7070s–7074s.
60. McDevitt, M.R., Barendsward, E., Ma, D. *et al.* (2000) *Cancer Research*, **60**, 6095–6100.
61. Milenic, D.E., Garmestani, K., Brady, E.D. *et al.* (2004) *Clinical Cancer Research*, **10**, 7834–7841.
62. Sandmaier, B.M., Bethge, W.A., Wilbur, D.S. *et al.* (2002) *Blood*, **100**, 318–326.
63. Bethge, W.A., Wilbur, D.S., Storb, R. *et al.* (2003) *Blood*, **101**, 5068–5075.
64. Wilbur, D.S., Hamlin, D.K., Chyan, M.K., and Brechbiel, M.W. (2008) *Bioconjugate Chemistry*, **19**, 158–170.
65. Kelly, M.P., Lee, F.T., Tahtis, K. *et al.* (2007) *Clinical Cancer Research*, **13**, 5604s–5612s.
66. Vandenbulcke, K., Thierens, H., De Vos, F. *et al.* (2006) *Cancer Biotherapy & Radiopharmaceuticals*, **21**, 364–372.
67. Michel, R.B., Rosario, A.V., Brechbiel, M.W. *et al.* (2003) *Nuclear Medicine and Biology*, **30**, 715–723.
68. Friesen, C., Glatting, G., Koop, B. *et al.* (2007) *Cancer Research*, **67**, 1950–1958.
69. Nayak, T., Norenberg, J., Anderson, T., and Atcher, R. (2005) *Cancer Biotherapy & Radiopharmaceuticals*, **20**, 52–57.
70. Supiot, S., Faivre-Chauvet, A., Couturier, O. *et al.* (2002) *Cancer*, **94**, 1202–1209.
71. Behr, T.M., Behe, M., Stabin, M.G. *et al.* (1999) *Cancer Research*, **59**, 2635–2643.
72. Axworthy, D.B., Reno, J.M., Hylarides, M.D. *et al.* (2000) *Proceedings of the National Academy of Sciences of the United States of America*, **97**, 1802–1807.
73. Zhang, M., Yao, Z., Garmestani, K. *et al.* (2002) *Blood*, **100**, 208–216.
74. Zhang, M., Zhang, Z., Garmestani, K. *et al.* (2003) *Proceedings of the National Academy of Sciences of the United States of America*, **100**, 1891–1895.
75. Jurcic, J.G., Larson, S.M., Sgouros, G. *et al.* (2002) *Blood*, **100**, 1233–1239.
76. Mulford, D.A., Pandit-Taskar, N., McDevitt, M.R. *et al.* (2004) *Blood*, **104**, 496a.
77. Allen, B.J., Raja, C., Rizvi, S. *et al.* (2005) *Cancer Biology & Therapy*, **4**, 1318–1324.
78. Kneifel, S., Cordier, D., Good, S. *et al.* (2006) *Clinical Cancer Research*, **12**, 3843–3850.
79. Wesley, J.N., McGee, E.C., Garmestani, K. *et al.* (2004) *Nuclear Medicine and Biology*, **31**, 357–364.
80. Dadachova, E., Bryan, R.A., Apostolidis, C. *et al.* (2006) *The Journal of Infectious Diseases*, **193**, 1427–1436.
81. Dadachova, E. and Casadevall, A. (2005) *Expert Opinion on Drug Delivery*, **2**, 1075–1084.

82. Martinez, L.R., Bryan, R.A., Apostolidis, C. *et al.* (2006) *Antimicrobial Agents and Chemotherapy*, **50**, 2132–2136.
83. Dadachova, E., Patel, M.C., Toussi, S. *et al.* (2006) *PLoS Medicine*, **3**, e427.
84. Akabani, G., Kennel, S.J., and Zalutsky, M.R. (2003) *Journal of Nuclear Medicine*, **44**, 792–805.
85. Sgouros, G. and Song, H. (2008) *Cancer Biotherapy & Radiopharmaceuticals*, **23**, 74–81.

14

Genetic Toxicology of Arsenic and Antimony

Toby G. Rossman and Catherine B. Klein

The Nelson Institute of Environmental Medicine, New York University Langone School of Medicine, Tuxedo, NY 10987, USA

14.1 Introduction

Interest in the genetic toxicology of arsenic (As) is motivated by the fact that it is considered as a human carcinogen [1]. The genetic toxicology of arsenicals mainly pertains to that of the trivalent arsenical arsenite (As^{III}) (Chapter 8) and its trivalent monomethylated and dimethylated metabolites (MMA^{III} and DMA^{III}) (Chapter 7). The corresponding pentavalent compounds are both less toxic and less genotoxic than the trivalent compounds. This is because the pentavalent compounds are less reactive than the trivalent compounds, which can enter cells more readily than the pentavalent compounds (Chapter 8). Once inside the cell, pentavalent compounds are immediately reduced to trivalent compounds, so the genetic toxicology is attributed to the trivalent species and their products. However, the thioarsenical metabolite dimethyldithioarsinic acid (DMDTA^{V}), which is pentavalent, shows cytotoxicity and genotoxicity that resembles DMA^{III} rather than DMA^{V} [2]. It must also be kept in mind that some cell lines are able to methylate arsenite. Although hepatocytes are not often used for assessing genotoxicity, rat hepatocytes have a higher rate of methylation than that of human hepatocytes [3]. Insignificant amounts or no methylation was seen in normal human keratinocytes [4], UROtsa cells (SV40-transformed human bladder epithelial line) [3], human lymphoblasts (M. Styblo, personal communication),

or various commonly used fibroblast lines such as mouse BALB/3T3 or Chinese hamster V79 [5, 6]. Thus, with the exception of hepatocytes, the effects of As^{III} appear to be caused by As^{III} itself, instead of the small amounts (if any) of the methylated metabolites made. A number of reviews on the genetic toxicology of As compounds have appeared recently [7–9].

14.2 DNA Damage in Cells Treated with Arsenicals

Arsenicals do not react with DNA to form DNA adducts (Chapter 2). Rather, the DNA damage and many of the cytotoxic effects are mediated by reactive oxygen species (ROS) or free radicals [10–14]. In some cells treated with As^{III}, increased ROS result from activation of membrane bound NAD(P)H oxidase [15, 16]. This produces superoxide that can be converted by superoxide dismutase (SOD) to hydroxyl radical, which can oxidize DNA and cause strand breaks [17]. The prooxidant enzyme cyclooxygenase 2 (COX-2), induced by As^{III} [18], could also contribute to oxidant stress.

The depletion of glutathione (GSH) in cells treated with high concentrations of As^{III} increases As^{III}'s toxic and clastogenic effects [19]. GSH is consumed in the reduction of As^V to As^{III}, and in the formation of As(SG)₃ and its efflux. Both GSH reductase and thioredoxin reductase are inhibited by trivalent arsenicals [20, 21], these effects could also increase oxidative stress.

In cell-free systems, high (toxic) concentrations of MMA^{III} and DMA^{III} (30 and 150 μM respectively) can break supercoiled phage øX174 DNA [22]. The strand breaks have been attributed to ROS, to other free radical species or by formation of dimethylarsine [12, 23–26]. Both dimethylarsine and trimethylarsine can nick DNA in cell-free systems and are much more potent than MMA^{III} and DMA^{III} [25]. Arsines are unstable and react with oxygen to form ROS. It is not known to what extent arsines are produced in humans, but they have been detected in animals given DMA^V [25]. DMA^V caused lung specific DNA damage in animals has been attributed to the DMA peroxy radical (CH₃)₂AsOO [27], which also induces DNA strand breaks and DNA-protein crosslinks in cultured cells [28]. TMA^{III}, produced in rat urine, is apparently more potent than DMA^{III} in terms of damaging purified DNA in *in vitro* systems [25].

Cells treated with low concentrations of trivalent arsenicals show increased oxidative DNA damage, which is often detected by measuring one of the most abundant oxidative lesions, 8-oxo-deoxyguanine (8-oxo-dG), in DNA or by using DNA repair enzymes that cleave oxidative lesion, inducing DNA strand breaks [24, 29]. The levels of 8-oxo-dG increased in the bladders of rats receiving 200 ppm DMA^V for two weeks, but the active species is thought to be DMA^{III} [30, 31]. 8-oxo-dG can be mutagenic by mispairing during DNA replication, causing G to T transversions [32]. Higher concentrations of arsenicals that induce cytotoxicity also cause DNA strand breaks and/or alkali-labile sites detectable in the Comet Assay without addition of DNA repair enzymes [22, 33, 34].

Oxidative DNA lesions can also affect DNA methylation patterns (*infra vide*). Using oligonucleotides containing 8-oxo-dG to replace dG, Cerda and Weitzman found that the enzymatic methylation of adjacent cytosines is profoundly altered [35]. This suggests that the effects of arsenicals on DNA methylation (*infra vide*) might be mediated by their ability to cause oxidative DNA damage.

Increased oxidative stress has been seen in As-exposed animals and humans in a number of different assays. Serum lipid peroxides and decreased levels of nonprotein sulfhydryls (indicating oxidant stress) were found in a Chinese population chronically exposed to As in drinking water [36]. Increased lipid peroxidation was also found in various tissues in rats exposed to arsenite [37]. Skin samples from individuals with As-related skin lesions have a higher amount of 8-oxo-dG (detected by immunohistochemistry) compared with non-As-related skin lesions [38]. Individuals drinking As-contaminated water in Taiwan had higher levels of reactive oxidants in plasma and lower levels of plasma antioxidant capacity [39].

NO levels are also increased in some cells after As^{III} exposure which may contribute to some of the toxic effects of arsenicals via reaction with superoxide to form peroxynitrite [14, 40, 41]. Because As^{III}-induced genotoxicity can be suppressed by both superoxide dismutase (SOD) and inhibitors of NO synthase in CHO cells, it has been suggested that NO and/or peroxynitrite mediate As^{III} genotoxicity [40, 42]. In addition to peroxynitrite formation, NO may also increase the formation of N-nitroso compounds, resulting in DNA alkylation, or react directly with DNA, causing deamination [40]. However, not all cells produce NO after As^{III} treatment. Cells that produce NO include CHO, C3H 10T^{1/2}, neonatal rat brain cells, bovine aorta endothelial cells, human fetal brain cells and human umbilical vein endothelial cells. Cells that do not produce NO, include rat aortic smooth muscle cells, rat hepatocytes, porcine endothelial cells, and human liver cells [40]. In human endothelial cells, > 5 μM of As^{III} is required to increase NO levels [15]. The iNOS activity also differs in different cell types treated with As^{III} [40].

Even at low concentrations, As^{III} induces proteins that are induced by, and protect against, oxidative stress [43–46]. The induction of these proteins can be blocked by antioxidants. Upregulation of metallothionein (MT) protects against arsenite toxicity even though MT doesn't have a high affinity for arsenite itself [47]. Most likely, MT reduces oxidative stress. Addition of various antioxidants to the culture medium protects cells against arsenite toxicity and genotoxicity [10, 48, 49]. Although the antioxidant α -tocopherol protects mice against As^{III}-induced cocarcinogenesis, the effect is partially on the solar UV component [50].

14.3 Mutagenesis in Cells Treated with Arsenicals

Trivalent arsenicals are not mutagenic in bacterial mutagenesis assays [7, 33], with the exception of dimethylarsine [51]. As^{III}, MMA^{III}, and DMA^{III} also failed to induce significant lambda prophage in *E. coli*, a process dependant on the *E. coli* SOS system that is responsive to DNA damage and is readily inducible after treatment with agents acting by oxidant mechanisms such as bleomycin, hydrogen peroxide, and iron compounds [33, 52]. Neither MMA^{III} nor DMA^{III} was mutagenic in the Ames Salmonella strain TA104, a strain developed primarily to aid in the detection of oxidative mutagens [33].

Trivalent arsenicals are not significant point mutagens in mammalian cells. A very common and useful genetic marker used in mammalian cell and *in vivo* mutagenesis assays, is the HPRT locus. As^{III} fails to induce significant HPRT mutations [48, 53]. Because of arsenite's clastogenicity (discussed below), it would be expected to yield deletion mutations. It was argued that a limitation of mutation assays at the HPRT locus is that the target

gene is on the X-chromosome, and large deletions may destroy essential neighboring genes, resulting in cell death and failure to recover mutants. However, molecular analysis of mutations in the HPRT gene shows that large deletions (up to ~3.5 Mb) can be recovered in the HPRT region of the human X chromosome [54, 55]. Also, other clastogens such as X-rays, are mutagenic at the HPRT locus in Chinese hamster V79 cells [56, 57].

Mouse lymphoma (L5178Y/TK^{+/−}) cells, which are heterozygous at the TK locus, can tolerate deletions of any size around the TK⁺ locus due to its autosomal location and the ability of the other autosome to complement missing genes. As^{III} was only slightly mutagenic at toxic doses in these cells [58]. The trivalent metabolites were also assayed in these cells. Concentrations of over IC₅₀ of MMA^{III} (0.38 μM) and DMA^{III} (1.29 μM) were required to give a positive response (doubling of the background mutant fraction) [33]. The authors conclude that the mutations caused by these compounds are unlikely to be important to arsenic carcinogenesis.

A number of transgenic cell lines has been developed in order to increase the efficiency of detecting deletion mutagens. G12 cells are Chinese hamster V79 cells containing a single copy of the *E. coli gpt* inserted into Chinese hamster chromosome 1 [59]. G12 cells can readily detect mutagenic clastogens such as X-rays and bleomycin [60]. Table 14.1 shows the gene mutations induced by As^{III}, MMA^{III} and DMA^{III} in G12 cells, compared with a classic clastogen, X-rays. Significant mutagenesis was never observed for As^{III} or MMA^{III} at concentrations yielding cell survival levels of >50%. Significant mutagenesis only occurs in cells treated with MMA^{III} at highly toxic concentrations (about fourfold over background at 11% survival) [57]. Most (79%) of the MMA^{III}-induced mutants were

Table 14.1 Mutagenesis at the transgenic *gpt* locus of G12 cells by trivalent arsenicals, compared with X-rays

Compound	Dose (μM)	Survival (% Control)	6TG ^R Mutant Frequency Per 10 ⁶ survivors ^a	Reference
As ^{III} (24 hr)	0	(100)	57	[88]
	5	89	74	
	10	68	86	
	15	37	94	
	0	(100)	48 (1.53)	
0.2	81	65 (12.00)		
0.4	58	74 (10.54)		
0.6	43	107 (17.56) ^b		
0.8	23	141 (19.70) ^b		
DMA ^{III} (72 hr)	1.0	11	227 (11.02) ^c	[57]
	0	(100)	47 (6.65)	
	0.1	82	72 (16.26)	
	0.2	23	104 (40.46)	
	0.3	7	238 (117.07)	
X-rays	0.4	5	577 (129.4)	[59]
	250 cGy	55	250	
	500 cGy	37	475	

^aData in parenthesis are standard errors of the mean for three experiments, except for DMA^{III} 0.4 μM which is a standard deviation for two experiments.

^b*p* < 0.05, two-tailed unpaired Student's *t*-test.

^c*p* < 0.01, two-tailed unpaired Student's *t*-test.

deletions. Such deletions may result from incomplete repair of oxidative DNA damage. DMA^{III}, which is more toxic than MMA^{III} in these cells, did not reach significant mutagenesis owing to the inconsistent responses elicited by DMA^{III}, similar to other reports [61]. On the other hand, X-rays induce significant mutagenesis (almost five times background) in these cells at an exposure dose yielding 55% survival, compared with MMA^{III} which only reaches a similar level of mutagenesis at a dose that is much more toxic (11% survival).

Similar results were seen at the transgenic *E. coli* gpt locus in AS52 Chinese hamster ovary cells treated with As^{III}. High concentrations increased mutagenesis only twice the background (spontaneous) level, and the proportion of deletions was higher than that in the spontaneous mutant group [62]. At toxic concentrations, As^{III} also increased large deletion mutations in human/hamster hybrid CHO-K1/A cells, which contain a single copy of human chromosome 11, through a mechanism involving ROS [48]. It should be noted that live cells exposed to the contents of dead necrotic cells may undergo genotoxic events similar to those seen in the ‘bystander effect’ after ionizing radiation [63].

It is paradoxical that trivalent arsenicals fail to induce significant point mutations despite the fact that low (nontoxic) concentrations of As^{III} cause oxidative DNA damage such as 8-oxo-dG, which is expected to cause G to T transversions. This may be due to efficient removal of oxidative DNA lesions. An analysis of the abilities of different DNA repair enzymes to induce single strand breaks in cells treated with trivalent arsenicals showed that As^{III}, MMA^{III} and DNA^{III} induce only oxidative DNA adducts and that the base excision repair (BER) enzymes 8-oxoguanine DNA glycosylase (OGG1) and MutY homolog (MYH) incise these oxidative DNA adducts in mammalian cells, whereas the nucleotide excision repair (NER) enzymes XPA, XPB, XPD, XPF, or XPG have no effect [64]. MYH appears to be a functional counterpart of the *E. coli* enzyme endonuclease III (MutY or EnIII) that cleaves the oxidized bases thymine glycol, 5,6-dihydrothymine, 5-hydroxydihydrothymine, 5-hydroxycytosine, 5-hydroxyuracil, and uracil glycol [65]. OGG1 is a functional counterpart of the *E. coli* Fpg that cleaves oxidative bases such as 8-oxo-7,8-dihydroguanine, 2,6-diamino-4-hydroxy-5-formamidopyrimidine, and 4,6-diamino-5-formamidopyrimidine [66]. After DNA glycosylases remove oxidized DNA bases, apurinic endonuclease (Ape1) processes the abasic site in BER. This enzyme is induced after 10T1/2 cells are treated with As^{III}, and suppression of Ape1 sensitized the cells to As^{III} and allowed mutagenesis at the TK and HPRT loci (at very high As^{III} concentrations) [67].

As mentioned above, high concentrations of DMA^V, administered orally to mice, caused oxidative DNA damage and DNA strand breaks in the lung, attributed to the DMA peroxy radical (CH₃)₂AsOO [27], and As^{III}-exposed mice showed increased oxidative stress [37]. However, treatment of MutaTM mouse IP with As^{III} or DMA^V (which would be converted to DMA^{III} in the liver) for five days caused no significant increase in *lacZ* mutations [68].

14.4 Other Genotoxic Events in Cells Treated with Arsenicals

The interpretation of the genotoxicity (other than mutagenicity) of arsenic compounds is problematic due to the very high cytotoxic concentrations used in many studies and the lack of statistical analysis in some. Unlike mutagenesis assays, which measure heritable changes in living cells (because the endpoint requires clonal survival), a number of other endpoints

do not require long term survival and thus cannot distinguish between living and dead cells. Traditional cytogenetic assays rely on short term cell survival to generate the mitotic figures necessary for analyses, but the long term viability of these treated cells cannot be determined. Since cytogenetic assays do not require cell survival for scoring, when clastogenic effects are seen in a population of cells with low survival, it is not possible to determine whether those cells with chromosome aberrations would be among the survivors, and thus capable of forming a clone. In many studies of clastogenesis, toxicity data are not given, but can be inferred from other mammalian cell studies.

The unrealistically high (cytotoxic) concentrations used are partly the fault of inappropriate assessments of cell survival following exposure to arsenic compounds [69]. The LD₅₀ (by clonal survival, after 24 h treatment) for As^{III} in most human cells is 1–2 μM [57], and the trivalent metabolites are even more toxic to most cells [3, 57, 70]. Human cells are generally more sensitive to arsenicals compared with Chinese hamster cells like CHO and V79. Low concentrations (1 μM) of arsenite have been shown to induce apoptosis in a fraction of human cells that is not evident until 48 h or more after a 24 h exposure, and cytotoxicity assays (other than clonal survival) are usually performed too soon after exposure to enable identification of these apoptotic cells. Short term survival assays, such as MTT, neutral red, and trypan blue, fail to detect these later dying cells unless the assays are delayed to allow time for apoptosis to develop [69, 71].

As^{III}, MMA^{III}, and DMA^{III} can induce chromosome aberrations and micronuclei (MN) in cultured cells [19, 33]. Statistically significant increases in chromosome aberrations occur only at toxic doses [57]. MN are defined as small, round, DNA-containing cytoplasmic bodies formed during cell division by loss of either acentric chromatin fragments (leading to clastogenesis) or whole chromosomes (leading to aneuploidy, i.e., change in the number of chromosomes per cell). The most reliable assay to identify whole chromosomes in MN is by fluorescent label of their kinetochores (with antibodies) or their centromeres (with DNA probes). An analysis of MN in normal human fibroblasts shows that low dose (relatively nontoxic), long term exposure to As^{III} acts as an aneugen by interfering with spindle function and inducing MN with centromeres (whole chromosomes), but high dose (toxic), short term exposure is clastogenic, inducing MN without centromeres (fragments) [72]. High concentrations of As^{III} may result in its sudden accumulation in cells and may have effects that differ from a slower accumulation, which would allow tolerance mechanisms to come into play. Treatment of mice with As^{III} resulted in MN in peripheral blood lymphocytes and in bone marrow [68, 73].

Aneuploidy is seen at concentrations of As^{III} lower than those that are clastogenic [61, 72, 74–76]. Aneuploidy can result from agents that interfere with normal spindle processes. Arsenical induced aneuploidy is seen in many cell types and has been associated with disruption of spindle tubulin [77–80]. Chinese hamster V79 cells treated with As^{III} showed disrupted mitotic spindles and persistent aneuploidy which was maintained even five days after removal of the As^{III} [74]. It is of interest that poly(ADP-ribose), whose synthesis can be blocked by trivalent arsenicals (discussed below), is required for bipolar spindle assembly and function [81].

The development of aneuploidy is a marker of genomic instability and is typical of many tumors. Humans exposed to arsenic show increased MN and sometimes chromosome aberrations in lymphocytes, exfoliated bladder epithelial cells, and buccal epithelial cells [82]. One study determined the types of MN in exfoliated bladder epithelial cells

from 18 individuals exposed to an average 1312 $\mu\text{g As/l}$ in drinking water and 18 matched controls exposed to an average 16 $\mu\text{g As/l}$ [83]. The exposed group had a 1.65-fold increase in MN with acentric fragments ($p=0.07$) and a 1.37-fold increase in MN with whole chromosomes ($p=0.15$). The combined difference (1.8-fold) was significant. Thus, exposure to high concentrations of As in drinking water induces MN of both types. Transformation induced by As^{III} and DMA^{III} is associated with aneuploidy [84, 85]. Bladder tumors of patients with exposure of high levels of As in drinking water showed higher levels of aneuploidy compared with those without As exposure [86].

14.5 Effects of Arsenicals on DNA Repair

A serious threat to genome stability is replication of DNA with unrepaired or badly repaired damage. Inhibition of a particular DNA repair pathway would enhance the mutagenicity of an agent that causes DNA damage that is normally repaired by that pathway. Nontoxic treatments of cells with As^{III} , while not being significantly mutagenic alone, enhance the mutagenicity of UVC in *E. coli* [87] and of N-methyl-N-nitrosourea (MNU) and UVA, UVB, and UVC in Chinese hamster V79 cells [88, 89]. As^{III} also enhances the mutagenicity and clastogenicity of many other agents in other mammalian cells [90–96] and in mouse skin [97]. The comutagenic effect of As and UVA, an important component of solar UV, in V79 cells is shown in Figure 14.1.

Further studies on the effects of As^{III} on repair of DNA damage induced by MNU were carried out. Since V79 cells lack 0^6 -methylguanine DNA methyltransferase, pre-mutagenic MNU adducts in those cells would be predominantly subject to base excision repair (BER). A nick-translation assay for DNA strand breaks showed that after V79 cells were treated with MNU and As^{III} , the breaks remained open three hours after MNU treatment, whereas in the absence of As^{III} , the breaks were closed by that time [88]. The data are consistent with

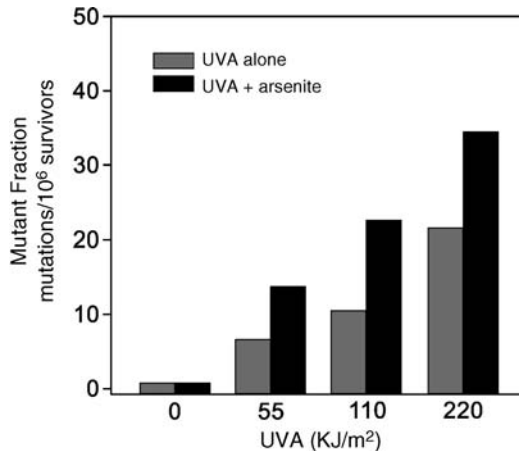


Figure 14.1 An example of comutagenesis by arsenite. Enhancement of mutagenesis by ultraviolet A (UVA) radiation at the *hprt* locus in Chinese hamster V79 cells. Cells were pretreated for 3 h with 10 μM sodium arsenite (a nontoxic treatment) prior to UVA radiation. Reprinted with permission from [89]. Copyright Springer Science + Business Media

inhibition of DNA polymerase β or DNA ligase in base excision repair by As^{III} . In cells treated with MNU, a robust activation of DNA ligase III activity was observed within three hours. Such activation was blocked by cotreatment of cells with As^{III} and, in fact, a 50% inhibition of ligase activity was seen even in cells treated with As^{III} alone. Nuclear extracts of cells treated with As^{III} were found to have reduced DNA ligase activity, and in particular the enzyme now called DNA ligase III (previously called DNA ligase II) [98]. However, inhibition was seen only at concentrations of arsenite 1000-fold higher than that seen after cellular exposure to As^{III} , indicating that As^{III} does not directly inhibit the DNA ligase enzyme [98]. More recently, similar results were obtained using purified DNA ligase III [99]. In CHO cells, As^{III} was found to inhibit DNA strand break rejoining, an effect attributed primarily to inhibition of DNA ligase III by using a ligase III-specific substrate [100].

Comutagenesis may occur by interference with nucleotide excision repair (NER) as well as BER, but the mechanism may involve an earlier step in the pathway [7, 45, 96, 101, 102]. The extent of inhibition of NER by trivalent arsenicals in human fibroblasts followed this order: $\text{MMA}^{\text{III}} > \text{DMA}^{\text{III}} > \text{As}^{\text{III}}$ [102]. Although the NER enzyme XPA appears somewhat sensitive to As^{III} [24], further evidence suggests that the inhibition of DNA repair by arsenicals is not via direct inhibition of repair enzymes, but rather via inhibition of activation and signaling that controls DNA repair.

An important signal pathway affected by trivalent As is that mediated by the tumor suppressor gene p53. In normal human fibroblasts treated with As^{III} and ionizing radiation, the p53-dependent increase in p21 expression, normally a block to cell cycle progression after DNA damage, is deficient [103]. These results were also confirmed in other systems [102, 104, 105]. The P53 protein appears to be inactivated by an ERK-dependent upregulation of MDM2 expression, resulting in its ubiquitin dependent proteolysis [106]. The inhibition of thioredoxin reductase by As^{III} , MMA^{III} and DMA^{III} [21] would cause the accumulation of oxidized thioredoxin, which may be partially responsible for P53 protein malfunction [107]. In cells with DNA damage, failure to transactivate p21 by P53 protein has the effect of overriding the growth arrest at G1 (normally an opportunity for DNA repair to take place prior to DNA replication), and might partially explain the comutagenic effect of As^{III} [103, 108, 109]. P53 is also required for proficient global NER [110]. Inhibition of P53 after DNA damage is expected to lead to faulty DNA repair, replication of damaged templates, increased mutagenesis and genomic instability. For example, gene amplification, which can occur in cells with compromised p53 and can lead to genomic instability, can be induced by As^{III} [111–113].

Another pathway controlling DNA repair which is affected by As^{III} is initiated by poly (ADP ribose) polymerase (PARP) [114–116]. Poly(ADP-ribose) polymerase 1 (PARP-1), the major PARP, is a nuclear protein that functions as a ‘nick sensor’.” It is constitutively expressed in most tissues, but its activity is stimulated several 100-fold by DNA strand breaks [81]. Upon DNA damage and PARP activation, there is an immediate transfer of ADP-ribosyl moieties from NAD^+ to PARP itself and to other nuclear proteins including P53, $\text{Nf}\kappa\text{B}$, histones and topoisomerases. Sequential attachments of ADP-ribosyl moieties create long chains up to 200 units with multiple branching points. Besides forming covalent adducts, poly(ADP-ribose) itself can also bind to proteins. A poly(ADP-ribose) binding motif of 20 amino acids was found in several proteins important for genomic stability, including DNA methyltransferase 1, P53, P21, XPA, MSH6, DNA ligase III, XRCC1, DNA

polymerase- β , DNA-PKcs, Ku70, NF κ B and telomerase [117]. Inhibition or depletion of PARP activity in cells results in genomic instability characterized by increased DNA strand breaks, recombination, gene amplification, and aneuploidy after exposure to genotoxins [118]. PARP-1-null mice exhibit chromosome instability, defects in DNA repair, immune deficiencies and increased susceptibility to nitrosamine carcinogenesis [119]. Studies on cells with abrogated PARP activity firmly establish a role for PARP-1 in cellular recovery from DNA damage, particularly damage repaired by BER [120]. During BER, PARP-1 binds to nicks in DNA along with other components of the BER complex (XRCC1, DNA polymerase β , and DNA ligase III). PARP-1 also induces decondensation of chromatin by poly(ADP-ribose)ating histones in nucleosomes and accelerates ongoing transcription while inhibiting *de novo* transcription, thus enabling DNA repair to take place. Extremely low concentrations of As^{III} inhibit synthesis of poly(ADP-ribose) (PAR) in HeLa cells after H₂O₂ treatment [115]. MMA^{III} and DMA^{III} are even more potent PARP inhibitors than As^{III} [121].

In addition to inhibiting particular proteins involved in DNA repair, As^{III} (at slightly toxic concentrations) can downregulate expression of some DNA repair genes [122–124]. However, very low, nontoxic concentrations, may have the opposite effect of upregulating some DNA repair proteins, along with antioxidant defenses [45, 124].

14.6 Indirect Mechanisms of Mutagenicity and Comutagenicity by Arsenicals

Beside damaging DNA or blocking DNA repair, there are a number of mechanisms by which arsenicals can indirectly cause genetic change. The effects of As^{III} on p53, which would prevent blockage of the cell cycle after genotoxic insult by a second agent, were mentioned above. Even in the absence of a second agent, low concentrations of As^{III} can stimulate cell proliferation both *in vivo* [125–127] and *in vitro* [69, 103, 128, 129] (Figure 14.2). In human keratinocytes, the order of stimulation of proliferation is: DMA^{III} > MMA^{III} > As^{III} [108]. As^{III} upregulates progrowth proteins such as cyclin D1, c-myc and E2F-1 [103, 129, 130]. The upregulation of cyclin D1 in mouse epidermal cells by As^{III} was mediated by the PI-3K/Akt/IKK β cascade [130]. The increased proliferation in mouse skin by arsenite alone (in drinking water) is not sufficient to induce skin cancer [125], but may contribute to its comutagenesis and cocarcinogenesis together with solar UV.

Another mechanism for As-related genotoxicity might be by acquired resistance to apoptosis. Long term growth of human skin (HaCaT) cells supplemented with low concentrations of As^{III} resulted in a generalized resistance to apoptosis and greatly increased stability of nuclear protein kinase B (NF κ B), an antiapoptotic molecule [131]. A weakened Nrf2-mediated antioxidant response coupled with acquired apoptosis resistance was found in long term, low dose (28 weeks, 100 nM) arsenite exposed HaCaT skin cells [132]. This might allow survival of cells with DNA damage, thus facilitating genotoxicity. Short term exposure to As^{III} can also block the apoptotic response to solar UV in a mouse keratinocyte cell line [101] or to UVB in normal human keratinocytes [133]. It is possible that the loss of P53 function partially mediates the reduction in the apoptotic response.

As^{III} has also been found to alter the metabolism of carcinogens, which can affect their mutagenicity. For example, As^{III} activated the tobacco specific nitrosamine NNK by

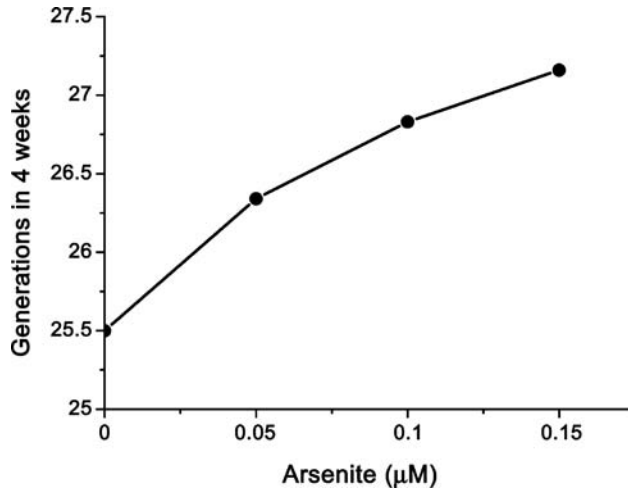


Figure 14.2 Very low concentrations of sodium arsenite enhance the growth of human keratinocytes (HaCat cells). Cells were continuously exposed to the arsenite

upregulating CYP2A [134]. On the other hand, As^{III} decreased induction of CYP1A1 and CYP1B1 by benzo(a)pyrene, probably via a post-translational mechanism [135].

14.7 Mutagenesis and Transformation as Secondary Effects of Genomic Instability

Arsenite induces transformation of various cells to a more malignant phenotype. Long term low dose treatment of cells with As^{III} (but not MMA^{III}) resulted in increased mutations and cell transformation as a secondary effect of genomic instability in human osteosarcoma (HOS) cells [113]. Although these cells are derived from a human tumor, they do not have a malignant phenotype, and are neither able to grow in soft agar (i.e., they are anchorage dependent) nor do they form tumors when injected into nude mice. Therefore transformation to anchorage independent growth signifies further progression toward a malignant phenotype. The dose relationships are similar to As^{III}-induced mutagenesis and transformation, with a maximum effect at 0.1 µM, supporting the idea that increased mutagenesis is necessary for the transformation. When HOS cells were grown in the presence or absence of 0.1 µM arsenite, the mutant fraction (*hprt* locus) remains the same in the two populations for almost 20 generations (six weeks). After that, the cells in As^{III} start mutating at a higher rate than the controls. This is more than 10 generations sooner than the transformation response, which took >30 generations (eight weeks). Gene amplification was seen to be induced earlier and with different dose-response relationships (Figure 14.3).

Delayed mutagenesis can be a secondary effect resulting from aneuploidy, gene amplification and/or changes in gene expression. As-induced aneuploidy was discussed above. Gene amplification [111–113] and DNA methylation changes that affect gene expression [57, 74, 136] are also seen after As^{III} exposure. Changes in gene expression by As^{III} can also be mediated by alterations of iRNA (or miRNA) patterns [137].

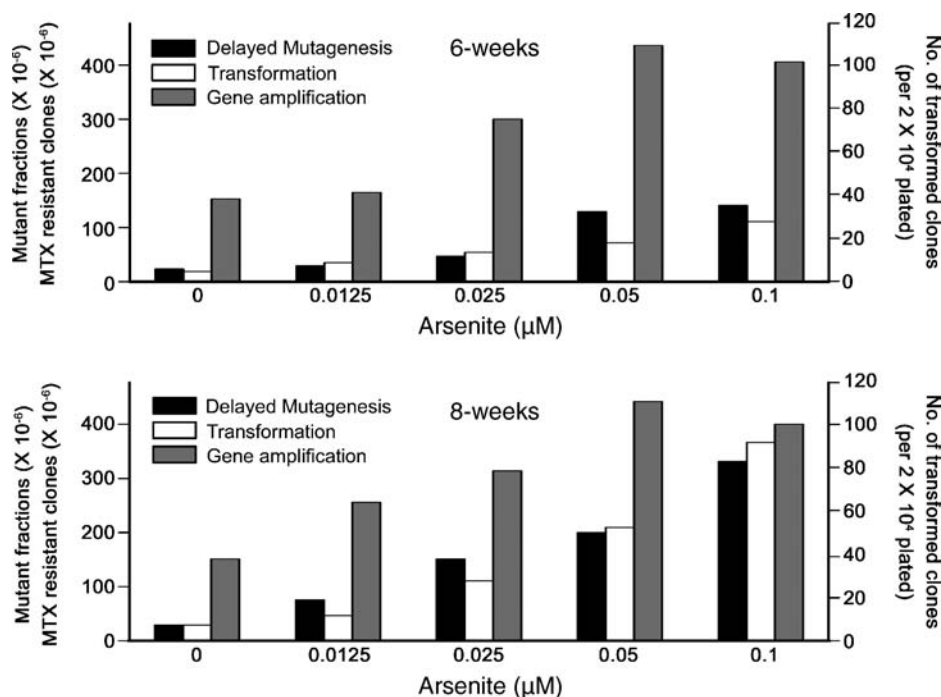


Figure 14.3 Delayed mutagenesis, transformation, and gene amplification in human osteosarcoma line HOS growing in low concentrations of sodium arsenite. Mutagenesis was measured at the *hprt* locus, transformation was measured by growth in soft agar (anchorage independence), and gene amplification was measured at the *dhfr* locus. Reprinted with permission from [113]. Copyright John Wiley & Sons, Ltd

It has become increasingly apparent that epigenetic influences, via gene promoter methylation at CpG sites [138] or by histone modifications [139], alter gene expression to confer selective advantage to cells undergoing neoplastic progression. Epigenetic effects can provide an additional layer of cell growth dysregulation, complimenting or adding to the effects of accumulating mutations. A variety of environmental exposures including cigarette smoke [140], cadmium [106] and folate deficiency [141, 142] have been reported to alter DNA methylation patterns. The first report of As^{III} induced DNA methylation was the increased cytosine methylation in the p53 promoter in human adenocarcinoma A549 cells [143]. Subsequently it was found that both hypo- and hypermethylation of different genes occurred after treatment with As^{III} [144], such effects have been associated with changes in gene expression [57, 74, 136, 145]. These findings are consistent with the usual DNA methylation changes observed in cancer, in which global DNA methylation is reduced but gene specific promoter methylation is increased [146]. Altered DNA methylation has also been observed in As-exposed humans [137, 147, 148].

Chinese hamster V79-13 cells grown in low concentrations of As^{III} for long periods of time also acquired genomic instability (increased chromosome aberrations) following changes in DNA methylation and aneuploidy [74, 75]. Chromosome instability has been linked to As^{III}-induced DNA hypomethylation [75], as well as to disruption of cytosine

DNA methyltransferase enzymes [149]. Oxidative damage to DNA has been shown to affect DNA methylation [35], suggesting one mechanism by which long term, low dose As^{III} might cause changes in DNA methylation. Changes in DNA methylation patterns could also result from altered S-adenosylmethionine (SAM) pools or downregulation of DNA methyltransferases [122, 136, 145]. Global DNA hypomethylation may result from competition for the methyl donor SAM which methylates arsenicals during metabolic transformation to form the mono- and dimethyl derivatives but also serves to maintain normal DNA methylation status. However, some cells, such as normal human prostate epithelial cell RWPE-1, poorly methylate As, yet still exhibit reduced methylation of DNA [150]. RWPE-1 cells subjected to 16 weeks exposure to 5 μ M As^{III} resulted in arsenic adaptation (indicated by increasing LC₅₀ over time), and also showed decreased SAM levels and increased DNA hypomethylation, the later being concurrent with increased S-adenosylhomocysteine hydrolase and homocysteine leading to a biochemical shift towards increased GSH production for As efflux at the expense of SAM remethylation [151]. Supplementation of SAM to cells treated with As^{III} was shown to reduce genomic instability, specifically by reducing the frequency of cells with micronuclei that contain whole chromosomes [152].

Long term exposure to low concentrations of As^{III} transforms mouse epidermal JB6 C141 cells to anchorage independence [153] and induces transformation (to tumorigenicity after injection into nude mice) of RWPE-1 cells, a line derived from normal human prostate epithelium immortalized with human papillomavirus [154]. In the prostate epithelium system, activation of K-ras was associated with malignant transformation [150]. Global DNA hypomethylation, along with hypermethylation of specific genes, was demonstrated in mouse hepatocellular carcinoma derived from transplacental As^{III}-exposure [145]. Transformation to anchorage independent growth by As^{III} in rat liver derived TRL 1215 cells was associated with global DNA hypomethylation, decreased DNA methyltransferase activity, and *c-myc* overexpression [155]. Hypomethylation is also important in As^{III}-induced transformation of Syrian hamster embryo (SHE) cells. Using long term culture after a 48 h treatment, hypomethylation of the 5'-CCGG sequences of *c-myc* and *c-Ha-ras* oncogenes was seen [156]. A model of cell transformation resulted from long term exposure to arsenicals is shown in Figure 14.4.

In addition to altered DNA methylation, gene expression can be modulated by altered histone modifications [139], as demonstrated for arsenic exposures with As^{III} and MMA^{III} [157–159]. The DNA associated histones, H3 and H4, are subject to modification of their lysine residues by methylation (mono-, di-, and trimethylation), acetylation, phosphorylation and other modifications to promote the activation or silencing of specific genes or genome regions. Some common gene silencing histone markers include, but are not limited to, histone H3 lysine 9 dimethylation (H3K9me₂), H3 lysine 27 trimethylation (H3K27me₃), and hypoacetylation of histones H3 and H4; whereas gene activating markers include H3 lysine 4 dimethylation (H3K4me₂) and acetylation of H3 lysines 9 and 14. Increased levels of the gene silencing marker H3K9me₂ but decreased levels of the silencing marker H3K27me₃, were detected in human lung carcinoma A549 cells upon exposure to very low dose (0.1 μ M) As^{III} [157]. Furthermore, the study identified increases in global levels of gene activating histone H3 lysine 4 trimethylation [157]. Using an epigenetic scanning approach to study the histone acetylation status of 13 000 genes in urothelial UROtsa cells or in As^{III} (1 μ M) or MMA^{III} (50 nM) transformed UROtsa derivative cells, loss of gene expression permissive histone H3 acetylation was observed for several dozen

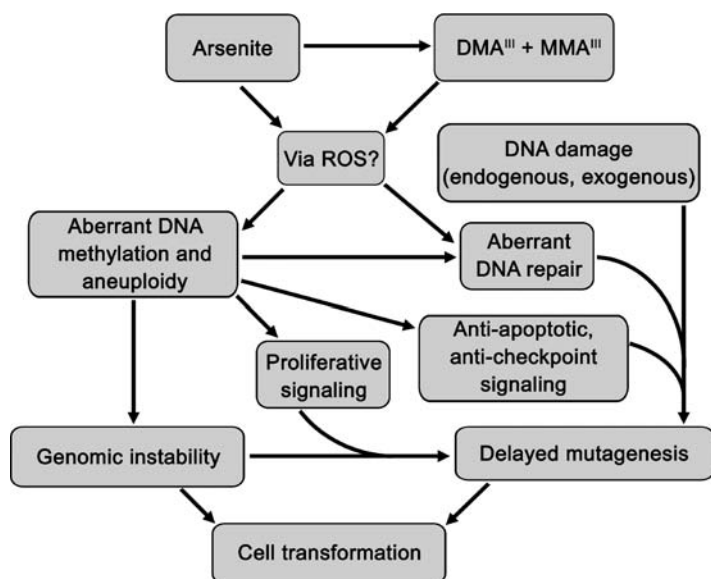


Figure 14.4 A model of cell transformation by trivalent arsenicals after chronic, low dose exposure

genes with coordinated increases in DNA methylation and reduced gene expression [158]. Of particular interest in this study was the As downregulated gene DBC1 ('Deleted in Bladder Cancer 1'), which is found to be transcriptionally silenced in some bladder tumor cell lines and is associated with bladder cell proliferation. Further studies with these As^{III} transformed UROtsa cells have identified the WNT family gene WNT5A as being over-expressed owing to increased H3K4Me2 and H3 lysine 9 and 14 acetylation with coordinated loss of the gene silencing markers H3K9Me2 and H3K27me3 [159].

Animals exposed to As in drinking water have also been examined for changes in gene or protein expression. Proteomic studies using differential in gel electrophoresis (DIGE) have been applied to examine global changes of protein patterns in male hamsters exposed to 173 mg As/l As^{III} in drinking water for six days [160]. The study identified 34 proteins that were overexpressed and 41 proteins that were underexpressed in the liver by 1.2-fold; in the urinary bladder, 36 proteins were overexpressed and 16 proteins were underexpressed. In contrast, animals exposed to chronic low dose As^{III} (1 mg As/l) for 10 days showed very few changes of protein expression levels.

Transgenerational epigenetics describes the study of altered gene expression occurring during gestational development that may have tumorigenic or other disease effects in later life, or even in subsequent generations [161]. As demonstrated by Jirtle and collaborators, exposures of female mice to a variety of dietary perturbations (e.g., folate, methyl donors, genistein) can alter gene expression yielding changes in the coat color (e.g., Agouti mice) of their offspring [162]. Inorganic As can cross both rodent and human placentas [163]. In humans exposed to As in drinking water during pregnancy there are emerging evidences of fetal growth effects, cancer and altered gene expression in the offspring. Reduced birth

weight and size, phenomena commonly noted as primary features of the Barker hypothesis of genotoxic exposures *in utero*, have been documented among offspring of Bangladeshi women exposed to As in drinking water [164, 165]. Lung cancer incidences are high among Chileans with documented As exposure *in utero* [166], and newborns in Thailand with known fetal exposure to As via the mother's drinking water show altered expression of 321 arsenic modulated gene products including but not limited to those related to stress response, inflammation, hypoxia and estrogen modulated genes, as well as genes associated with breast cancer [167].

Epigenetic imprinting of the genome is known to be erased and reset during embryogenesis [168] and epigenetic changes in gene expression have been demonstrated for transplacental As exposures, stem cells being a potential target. Gene expression profile in fetal mouse development after *in utero* As exposure (gestational days 8–18) has identified changes in fetal livers and lungs [169, 170] and in newborn livers [171]. Alterations were identified in genes related to As induced stress, As adaptation, steroid metabolism, estrogen signaling, insulin growth factor signaling and in α -fetoprotein (AFP), a tumor biomarker. DNA hypomethylation has been demonstrated in mouse hepatocellular carcinoma derived from transplacental As-exposure [145]. In Tg.AC mice, both squamous cell carcinomas and papillomas of the skin result from combined *in utero* exposure to As followed by topical TPA skin painting. However, in the As-exposed fetal mice the v-Ha-ras gene itself did not exhibit reduced levels of transgene promoter methylation compared to mice with TPA exposure alone [172]. Whether other genes exhibit methylation changes has not yet been reported.

Since exposure to iAs via drinking water to female mice induces liver tumors and aberrant gene expression in the offspring, the sensitivity of fetal cells to As has been analysed. Fetal liver cells were isolated from untreated CD1 mice at gestation day 13.5 and were cultured with 0–1.0 μM As^{III} for 72 h [173]. As^{III} yielded concentration dependent upregulation of stress response genes heme oxygenase-1 (~8 fold) and metallothionein-1 (up to five-fold). There was also evidence of altered expression of steroid metabolism genes, 17 β -hydroxysteroid dehydrogenase-7 (HSD17 β 7), Cyp2a4, estrogen receptor- α (ER- α) as well as several ER- α -linked genes. Exposure to As^{III} *in utero* followed by administration of estrogenic carcinogens such as diethylstilbestrol to newborn mice has been reported to have synergistic tumorigenic effects in adults [174]. Additional evidence for the endocrine disrupting ability of As is emerging, with evidence of perturbations of retinoic acid receptor- and thyroid hormone receptor-mediated regulation of genes [175, 176].

14.8 Antimony

Antimony (Sb) compounds are considered as possible human carcinogens, based on some positive experimental data in animals but inadequate human data [177]. The genotoxicity of Sb compounds reviewed by De Boeck *et al.* [178] is far more limited than the data for As, nevertheless resembles it to some extent. Because Sb and As belong to the same group in the periodic table and have the same oxidation states, it is reasonable to expect that the genotoxicity induced by Sb is similar to that for As. Like As, the trivalent compounds of Sb are more toxic and genotoxic than the pentavalent ones. However, Sb^{III} is about five times less toxic to V79 cells than As^{III} and about 100 times less potent in inducing MN or DNA

strand breaks in the Comet Assay [77, 179]. These results are not due to differences in cellular uptake or metabolism to the pentavalent species. Like As^{III}, Sb^{III} is more toxic and genotoxic to human cells compared with Chinese Hamster cells [178].

Similar to As, Sb compounds do not cause mutations in the Ames test or induce the SOS system in *E. coli* [178, 180]. Only Sb^{III}, but not Sb^V compounds cause chromosome aberrations at high concentrations in human lymphocytes [181], but high concentrations of Sb^V induced MN formation in human lymphocytes. These were mostly centromere negative, indicating clastogenesis [182]. Unlike As^{III}, the MN induced by Sb^{III} could not be suppressed by antioxidant enzymes. This is paradoxical, because Sb has been shown to induce ROS formation [183, 184]. Sb^{III} was equally effective as As^{III} in inducing heme oxygenase 1 (HO1) in human keratinocytes. HO1 is a marker for oxidative stress [185]. In spontaneously immortalized human skin cells, the effects of Sb^{III} are similar to those of As^{III} with regard to preventing degradation of EGFR and elevating of B-catenin via a mechanism that involves antagonism of insulin signaling [186].

In mammalian cells, Sb compounds give a negative response in almost every assay for mutagenicity [178], including the mouse lymphoma TK mutagenesis assay [181].

In one *in vivo* study, Sb^{III} failed to induce chromosome aberrations in mouse bone marrow after acute dosing, but did so after repeated dosing (14 days) at a dose that killed all the mice prior to the end of the experiment (21 days) [187]. However, Elliott *et al.* [181] did not find induction of MN in bone marrow after acute or chronic exposure of mice. To resolve this inconsistency [188], gave repeated doses (250, 500 and 1000 mg/kg) of antimony trioxide to rats by oral gavage for 14 or 21 days. Reduction in weight gain was seen in the high dose group. The internal dose after repeated exposure was higher than that obtained with single dosing, yet frequencies of chromosome aberrations and MN in bone marrow cells did not differ from control values. They conclude that Sb^{III} is not genotoxic to rodent bone marrow at doses close to the maximum tolerated dose.

Human textile workers exposed to Sb^{III} showed no increases in MN or sister chromatid exchange levels in blood cells, but the enzyme modified Comet Assay suggested an increase in oxidative DNA damage in the exposed group [189]. Treatment with meglumine antimoniate for leishmaniasis caused a later increase in MN levels in blood cells, but no increases in chromosome aberrations [190].

References

1. IARC (ed.) (2004) IARC monograph on the evaluation of carcinogenic risk to humans, in *Some Drinking Water Disinfectants and Contaminants, Including Arsenic*, vol. 84, International Agency for Research on Cancer, IARC Press, Lyon, France.
2. Ochi, T., Kita, K., Suzuki, T., Rumpler, A., Goessler, W., and Francesconi, K.A. (2008) *Toxicology and Applied Pharmacology*, 228, 59–67.
3. Styblo, M., Del Razo, L.M., Vega, L. *et al.* (2000) *Archives of Toxicology*, 74, 289–299.
4. Vega, L., Styblo, M., Patterson, R. *et al.* (2001) *Toxicology and Applied Pharmacology*, 172, 225–232.
5. Bertolero, F., Pozzi, G., Sabbioni, E., and Saffiotti, U. (1987) *Carcinogenesis*, 8, 803–808.
6. Wang, Z., Dey, S., Rosen, B.P., and Rossman, T.G. (1996) *Toxicology and Applied Pharmacology*, 137, 112–119.
7. Rossman, T.G. (2003) *Mutation Research*, 533, 37–66.
8. Tapio, S. and Grosche, B. (2006) *Mutation Research*, 612, 215–246.

9. IARC (ed.) (2002) IARC monographs on the evaluation of the carcinogenic risk of chemicals to humans, in *Some Drinking Water Disinfectants and Contaminants, Including Arsenic*, vol. **84**, International Agency for Research on Cancer, IARC Press, Lyon, France.
10. Lee, T.-C. and Ho, I.-C. (1995) *Archives of Toxicology*, **69**, 498–504.
11. Kessel, M., Liu, S.X., Xu, A. *et al.* (2002) *Molecular and Cellular Biochemistry*, **234/235**, 301–308.
12. Kitchin, K. and Ahmed, S. (2003) *Toxicology Letters*, **137**, 3–13.
13. Shi, H., Shi, X., and Liu, K.J. (2004) *Molecular and Cellular Biology*, **255**, 67–78.
14. Ding, W., Hudson, L.H., and Liu, K.J. (2005) *Molecular and Cellular Biology*, **279**, 104–112.
15. Barchowsky, A., Klei, L.R., Dudek, E.J. *et al.* (1999) *Free Radical Biology & Medicine*, **27**, 1405–1412.
16. Wang, J., Li, L., Cang, H. *et al.* (2008) *Leukemia Research*, **32**, 429–436.
17. Liu, S.X., Athar, M., Lippai, I. *et al.* (2001) *Proceedings of the National Academy of Sciences of the United States of America*, **98**, 1643–1648.
18. Trouba, K.J. and Germolec, D.R. (2004) *Toxicological Sciences*, **79**, 248–257.
19. Oya-Ohta, Y., Kaise, T., and Ochi, T. (1996) *Mutation Research*, **357**, 123–129.
20. Styblo, M., Serves, S.V., Cullen, W.R., and Thomas, D.J. (1997) *Chemical Research in Toxicology*, **10**, 27–33.
21. Lin, S., Cullen, W.R., and Thomas, D.J. (1999) *Chemical Research in Toxicology*, **12**, 924–930.
22. Mass, M.J., Tennant, A., Roop, B.C. *et al.* (2001) *Chemical Research in Toxicology*, **14**, 355–361.
23. Nesnow, S., Roop, B.C., Lambert, G. *et al.* (2002) *Chemical Research in Toxicology*, **15**, 1627–1634.
24. Schwerdtle, T., Walter, I., Mackiw, I., and Hartwig, A. (2003) *Carcinogenesis*, **24**, 967–974.
25. Andrewes, P., Kitchin, K.T., and Wallace, K. (2003) *Chemical Research in Toxicology*, **16**, 994–1003.
26. Yamanaka, K., Mizoi, M., Tachikawa, M. *et al.* (2003) *Toxicology Letters*, **143**, 145–153.
27. Yamanaka, K. and Okada, S. (1994) *Environmental Health Perspectives*, **102**, 37–40.
28. Tezuka, M., Hanioka, K.-I., Yamanaka, K., and Okada, S. (1993) *Biochemical and Biophysical Research Communications*, **191**, 1178–1183.
29. Wang, T.S., Chung, C.H., Wang, A.S. *et al.* (2002) *Chemical Research in Toxicology*, **15**, 1254–1258.
30. Wei, M., Wanibuchi, H., Yamamoto, S. *et al.* (1999) *Carcinogenesis*, **20**, 1873–1876.
31. Arnold, L.L., Eldan, M., van Gemert, M. *et al.* (2003) *Toxicology*, **190**, 197–219.
32. Klaunig, J.E. and Kamendulis, L.M. (2004) *Annual Review of Pharmacology and Toxicology*, **44**, 239–267.
33. Kligerman, A.D., Doerr, C.L., Tennant, A.H. *et al.* (2003) *Environmental and Molecular Mutagenesis*, **42**, 192–205.
34. Soto-Reyes, E., Del Razo, L.M., Valverde, M., and Rojas, E. (2005) *Biometals: An International Journal on the Role of Metal Ions in Biology, Biochemistry, and Medicine*, **18**, 493–506.
35. Cerda, S. and Weitzman, S.A. (1997) *Mutation Research*, **386**, 141–152.
36. Pi, J., Yamauchi, H., Kumagai, Y. *et al.* (2002) *Environmental Health Perspectives*, **110**, 331–336.
37. Ramos, O., Carrizales, L., Yanez, L. *et al.* (1995) *Environmental Health Perspectives*, **103**, 85–88.
38. Matsui, M., Nishigori, C., Toyokuni, S. *et al.* (1999) *The Journal of Investigative Dermatology*, **113**, 26–31.
39. Wu, M.M., Chiou, H.Y., Wang, T.W. *et al.* (2001) *Environmental Health Perspectives*, **109**, 1011–1017.
40. Gurr, J.-R., Yih, L.-H., Samikkannu, T. *et al.* (2003) *Mutation Research*, **533**, 173–182.
41. Wang, T.-C., Jan, K.-Y., Wang, A.S.S., and Gurr, J.-R. (2007) *Mutation Research*, **615**, 75–86.
42. Lynn, S., Shiung, N.-N., Gurr, J.-R., and Jan, K.Y. (1998) *Free Radical Biology & Medicine*, **24**, 442–449.

43. Del Razo, L.M., Quintanilla-Vega, B., Brambila-Colombres, E. *et al.* (2001) *Toxicology and Applied Pharmacology*, **177**, 132–148.
44. Andrew, A.S., Warren, A.J., Barchowsky, A. *et al.* (2003) *Environmental Health Perspectives*, **111**, 825–838.
45. Snow, E.T., Sykora, P., Durham, T.R., and Klein, C.B. (2005) *Toxicology and Applied Pharmacology*, **207**, S557–S564.
46. Kann, S., Estes, C., Reichard, J.F. *et al.* (2005) *Toxicological Sciences*, **87**, 365–384.
47. Goncharova, E.I. and Rossman, T.G. (1995) *Genetic Response to Metals* (ed. B. Sarkar) Marcel Dekker, Inc., New York, pp. pp.87–100.
48. Hei, T.K., Liu, S.X., and Waldren, C. (1998) *Proceedings of the National Academy of Sciences of the United States of America*, **95**, 8103–8107.
49. Nordenson, I. and Beckman, L. (1991) *Human Heredity*, **41**, 71–73.
50. Uddin, A.N., Burns, F.J., and Rossman, T.G. (2005) *Carcinogenesis*, **26**, 2179–2186.
51. Yamanaka, K., Ohba, H., Hasagawa, A. *et al.* (1989) *Chemical & Pharmaceutical Bulletin*, **37**, 2753–2756.
52. Rossman, T.G., Molina, M., Meyer, L. *et al.* (1991) *Mutation Research*, **260**, 349–367.
53. Rossman, T.G., Stone, D., Molina, M., and Troll, W. (1980) *Environmental Mutagenesis*, **2**, 371–379.
54. Nelson, S.L., Jones, I.M., Fuscoe, J.C. *et al.* (1995) *Radiation Research*, **141**, 2–10.
55. Lippert, M.J., Nicklas, J.A., Hunter, T.C., and Albertini, R.J. (1995) *Mutation Research*, **326**, 51–64.
56. Dahle, J. and Kvam, E. (2003) *Cancer Research*, **63**, 1464–1469.
57. Klein, C.B., Leszczynska, J., and Rossman, T.G. (2007) *Toxicology and Applied Pharmacology*, **222**, 289–297.
58. Moore, M., Harrington-Brock, K., and Doerr, C.L. (1997) *Mutation Research*, **386**, 279–290.
59. Klein, C.B., Su, L., Rossman, T.G., and Snow, E.T. (1994) *Mutation Research*, **304**, 217–228.
60. Klein, C.B., Su, L., Singh, J.T., and Snow, E.T. (1997) *Environmental and Molecular Mutagenesis*, **30**, 421–428.
61. Kligerman, A.D., Doerr, C.L., and Tennant, A.H. (2005) *Molecular and Cellular Biochemistry*, **279**, 113–121.
62. Meng, Z. and Hsie, A.W. (1996) *Mutation Research*, **356**, 255–259.
63. Huang, L., Kim, P.M., Nickoloff, J.A., and Morgan, W.F. (2007) *Cancer Research*, **67**, 1099–1104.
64. Pu, Y.-S., Jan, K.-Y., Wang, T.-C. *et al.* (2007) *Toxicological Sciences*, **95**, 376–382.
65. Sarker, A.H., Ikeda, S., Nakano, H. *et al.* (1998) *Journal of Molecular Biology*, **282**, 761–774.
66. Perlow-Poehnelt, R.A., Zharkov, D.O., Grollman, A.P., and Broyde, S. (2004) *Biochemistry*, **43**, 16092–16105.
67. Fung, H., Liu, P., and Demple, B. (2007) *Molecular and Cellular Biology*, **27**, 8834–8847.
68. Noda, Y., Suzuki, T., Kohara, A. *et al.* (2002) *Mutation Research*, **513**, 205–212.
69. Komissarova, E.T., Saha, S.K., and Rossman, T.G. (2005) *Toxicology and Applied Pharmacology*, **202**, 99–107.
70. Petrick, J.S., Ayala-Fierro, F., Cullen, W.R. *et al.* (2000) *Toxicology and Applied Pharmacology*, **163**, 203–207.
71. Brink, A., Schulz, B., Kobras, K. *et al.* (2006) *Mutation Research*, **603**, 121–128.
72. Yih, L.-H. and Lee, T.-C. (1999) *Mutation Research*, **440**, 75–82.
73. Tinwell, H., Stephens, S.C., and Ashby, J. (1991) *Environmental Health Perspectives*, **95**, 205–210.
74. Sciandrello, G., Barbaro, R., Caradonna, F., and Barbata, G. (2002) *Mutagenesis*, **17**, 99–103.
75. Sciandrello, G., Caradonna, F.M., Mauro, M., and Barbata, G. (2004) *Carcinogenesis*, **25**, 413–417.
76. Colognato, R., Coppede, F., Ponti, J. *et al.* (2007) *Mutagenesis*, **22**, 255–261.
77. Huang, S.-C. and Lee, T.-C. (1998) *Carcinogenesis*, **19**, 889–896.
78. Kligerman, A.D. and Tennant, A.H. (2007) *Toxicology and Applied Pharmacology*, **222**, 281–288.

79. Vega, L., Gonseblatt, M.E., and Ostrosky-Wegman, P. (1995) *Mutation Research*, **334**, 365–373.
80. Ramirez, P., Eastmond, D.A., Lacleite, J.P., and Ostrosky-Wegman, P. (1997) *Mutation Research*, **386**, 291–298.
81. Bürkle, A. (2005) *FEBS J*, **272**, 4576–4589.
82. Basu, A., Mahata, J., Gupta, S., and Giri, A.K. (2001) *Mutation Research*, **488**, 171–194.
83. Moore, L.E., Warner, M.J., Smith, A.H. *et al.* (1996) *Environmental and Molecular Mutagenesis*, **27**, 176–184.
84. Ochi, T., Suzuki, T., Barrett, J.C., and Tsutsui, T. (2004) *Toxicology*, **203**, 155–163.
85. Chien, C.-W., Chiang, M.-C., Ho, I.-C., and Lee, T.-C. (2004) *Environmental Health Perspectives*, **112**, 1704–1710.
86. Moore, L.E., Smith, A.H., Eng, C. *et al.* (2002) *Journal of the National Cancer Institute*, **94**, 1688–1696.
87. Rossman, T.G. (1981) *Mutation Research*, **91**, 207–211.
88. Li, J.-H. and Rossman, T.G. (1989) *Biological Trace Element Research*, **21**, 373–381.
89. Li, J.-H. and Rossman, T.G. (1991) *BioMetals*, **4**, 197–200.
90. Lee, T.-C., Huang, R.Y., and Jan, K.Y. (1985) *Mutation Research*, **148**, 83–89.
91. Lee, T.-C., Wang-Wuu, S., Huang, R.Y. *et al.* (1986) *Cancer Research*, **46**, 1854–1857.
92. Lee, T.-C., Lee, K.C., Tseng, Y.J. *et al.* (1986) *Environmental Mutagenesis*, **8**, 119–128.
93. Yang, J.L., Chen, M.F., Wu, C.W., and Lee, T.C. (1992) *Environmental and Molecular Mutagenesis*, **20**, 156–164.
94. Wiencke, J.K. and Yager, J.W. (1992) *Environmental and Molecular Mutagenesis*, **19**, 195–200.
95. Jha, A.N., Noditi, M., Nilsson, R., and Natarajan, A.T. (1992) *Mutation Research*, **284**, 215–221.
96. Danaee, H., Nelson, H.H., Liber, H. *et al.* (2004) *Mutagenesis*, **19**, 143–148.
97. Fischer, J.M., Robbins, S.B., Al-Zoughool, M. *et al.* (2005) *Mutation Research*, **588**, 35–46.
98. Li, J.-H. and Rossman, T.G. (1989) *Molecular Toxicology*, **2**, 1–9.
99. Hu, Y., Su, L., and Snow, E.T. (1998) *Mutation Research*, **408**, 203–218.
100. Lynn, S., Lai, H.T., Gurr, J.-R., and Jan, K.Y. (1997) *Mutagenesis*, **12**, 353–358.
101. Wu, F., Burns, F.J., Zhang, R. *et al.* (2005) *Environmental Health Perspectives*, **113**, 983–986.
102. Shen, S., Lee, J., Weinfeld, M., and Le, X.C. (2008) *Molecular Carcinogenesis*, **47**, 508–518.
103. Vogt, B. and Rossman, T.G. (2001) *Mutation Research*, **478**, 159–168.
104. Hernandez-Zavala, A., Cordova, E., Del Razo, L.M. *et al.* (2005) *Toxicology*, **207**, 49–57.
105. Tang, F., Liu, G., He, Z. *et al.* (2006) *Molecular Carcinogenesis*, **45**, 861–870.
106. Huang, D., Zhang, Y., Qi, Y. *et al.* (2008) *Toxicology Letters*, **179**, 43–47.
107. Merwin, J.R., Mustacich, D.J., Muller, E.G.D. *et al.* (2002) *Carcinogenesis*, **23**, 1609–1615.
108. Mudipalli, A., Owen, R.D., and Preston, R.J. (2005) *International Journal of Oncology*, **27**, 769–778.
109. Hartwig, A., Asmuss, M., Ehleben, I. *et al.* (2002) *Environmental Health Perspectives*, **110**, 797–799.
110. Ferguson, B.E. and Oh, D.H. (2005) *Cancer Research*, **65**, 8723–8729.
111. Lee, T.-C., Tanaka, N., Lamb, W.P. *et al.* (1989) *Science*, **241**, 79–81.
112. Rossman, T.G. and Wolosin, D. (1992) *Molecular Carcinogenesis*, **6**, 203–213.
113. Mure, K., Uddin, A.N., Lopez, L.C. *et al.* (2003) *Environmental and Molecular Mutagenesis*, **41**, 322–331.
114. Yager, J.W. and Wiencke, J.K. (1997) *Mutation Research*, **386**, 345–351.
115. Hartwig, A., Pelzer, A., Asmuss, M., and Bürkle, A. (2003) *International Journal of Cancer*, **104**, 1–6.
116. Qin, X.-J., Hudson, L.G., Liu, W. *et al.* (2008) *Toxicology and Applied Pharmacology*, **232**, 41–50.
117. Pleschke, J.M., Kleczkowska, H.E., Strohm, M., and Althaus, F.R. (2000) *The Journal of Biological Chemistry*, **275**, 40974–40980.

118. Simbulan-Rosenthal, C.M., Rosenthal, D.S., Luo, R. *et al.* (2001) *Nucleic Acids Research*, **29**, 841–849.
119. Tsutsumi, M., Masutani, M., Nozaki, T. *et al.* (2001) *Carcinogenesis*, **22**, 1–3.
120. Beneke, R., Geisen, C., Zevnik, B. *et al.* (2000) *Molecular and Cellular Biology*, **20**, 6695–6703.
121. Walter, I., Schwerdtle, T., Thuy, C. *et al.* (2007) *DNA Repair*, **6**, 61–70.
122. Hamadeh, H.K., Trouba, K.L., Amin, R.P. *et al.* (2002) *Toxicological Sciences*, **69**, 306–316.
123. Andrew, A.S., Bernardo, V., Warnke, L.A. *et al.* (2007) *Toxicol Sci*, **100**, 75–87.
124. Sykora, P. and Snow, E.T. (2008) *Toxicology and Applied Pharmacology*, **228**, 385–394.
125. Burns, F.J., Uddin, A.N., Wu, F. *et al.* (2004) *Environmental Health Perspectives*, **112**, 599–603.
126. Germolec, D.R., Spalding, J., Yu, H.-S. *et al.* (1998) *The American Journal of Pathology*, **153**, 1775–1785.
127. Luster, M.I. and Simeonova, P.P. (2004) *Toxicology and Applied Pharmacology*, **198**, 419–423.
128. Germolec, D.R., Spalding, J., Boorman, G.A. *et al.* (1997) *Mutation Research*, **386**, 209–218.
129. Trouba, K.J., Wauson, E.M., and Vorce, R.L. (2000) *Toxicology and Applied Pharmacology*, **164**, 161–170.
130. Ouyang, W., Li, J., Zhang, D. *et al.* (2007) *Journal of Cellular Biochemistry*, **101**, 969–978.
131. Pi, J., He, Y., Bortner, C. *et al.* (2005) *International Journal of Cancer*, **116**, 20–26.
132. Pi, J., Diwan, B.A., Sun, Y. *et al.* (2008) *Free Radical Biology & Medicine*, **45**, 651–658.
133. Chen, P.-H., Lan, C.-C.E., Chiou, M.-H. *et al.* (2005) *Chemical Research in Toxicology*, **18**, 139–144.
134. Lee, H.-L., Chang, L.W., Wu, J.-P. *et al.* (2008) *Toxicology and Applied Pharmacology*, **227**, 108–114.
135. Spink, D.C., Katz, B.H., Hussain, M.M. *et al.* (2002) *Drug Metabolism and Disposition*, **30**, 262–269.
136. Reichard, J.F., Schnekenburger, M., and Puga, A. (2007) *Biochemical and Biophysical Research Communications*, **352**, 188–192.
137. Marsit, C.J., Eddy, K., and Kelsey, K.T. (2006) *Cancer Research*, **66**, 10843–10848.
138. Jones, P.A. and Baylin, S.B. (2002) *Nature Reviews. Genetics*, **3**, 415–428.
139. Esteller, M. (2008) *New Engl J Med*, **358**, 1148–1159.
140. Russo, A.L., Thiagalingam, A., Pan, H.D. *et al.* (2005) *Clinical Cancer Research*, **11**, 2466–2470.
141. Davis, C.D. and Uthus, E.O. (2004) *Experimental Biology and Medicine*, **229**, 988–995.
142. Shelnutt, K.P., Kauwell, G.P., Gregory, J.F. III *et al.* (2004) *The Journal of Nutritional Biochemistry*, **15**, 554–560.
143. Mass, M.J. and Wang, L. (1997) *Mutation Research*, **386**, 263–277.
144. Zhong, C.X. and Mass, M.J. (2001) *Toxicology Letters*, **122**, 223–234.
145. Liu, J. and Waalkes, M.P. (2008) *Toxicological Sciences*, **105**, 24–32.
146. Baylin, S.B. and Herman, J.G. (2000) *Trends in Genetics*, **16**, 168–174.
147. Chandra, S., Dasgupta, U.B., GuhaMazumder, D. *et al.* (2006) *Toxicological Sciences*, **89**, 431–437.
148. Pilsner, J.R., Liu, X., Ahsan, H. *et al.* (2007) *The American Journal of Clinical Nutrition*, **86**, 1179–1186.
149. Karpf, A.R. and Matsui, S. (2005) *Cancer Research*, **65**, 8635–8639.
150. Benbrahim-Tallaa, L., Waterland, R.A., Styblo, M. *et al.* (2005) *Toxicology and Applied Pharmacology*, **206**, 288–298.
151. Coppin, J.-F., Qu, W., and Waalkes, M.P. (2008) *The Journal of Biological Chemistry*, **283**, 19342–19350.
152. Ramirez, T., Stopper, H., Hock, R., and Herrera, L.A. (2007) *Mutation Research*, **617**, 16–22.
153. Huang, C., Ma, W.-Y., Li, J. *et al.* (1999) *The Journal of Biological Chemistry*, **274**, 14595–14601.
154. Achanzar, W.E., Brambila, E.M., Diwan, B.A. *et al.* (2002) *Journal of the National Cancer Institute*, **94**, 1888–1891.

155. Zhao, C.Q., Young, M.R., Diwan, B.A. *et al.* (1997) *Proceedings of the National Academy of Sciences of the United States of America*, **94**, 10907–10912.
156. Takahashi, M., Barrett, J.C., and Tsutsui, T. (2002) *International Journal of Cancer*, **99**, 629–634.
157. Zhou, X., Sun, H., Ellen, T.P. *et al.* (2008) *Carcinogenesis*, **29**, 1831–1836.
158. Jensen, T.J., Novak, P., Eblin, K.E. *et al.* (2008) *Carcinogenesis*, **29**, 1500–1508.
159. Jensen, T.J., Wozniak, R.J., Eblin, K.E. *et al.* (2009) *Toxicology and Applied Pharmacology*, **235**, 39–46.
160. Chowdhury, U.K. and Aposhian, H.V. (2008) *Annals of the New York Academy of Sciences*, **1140**, 325–334.
161. Whitelaw, N.C. and Whitelaw, E. (2008) *Current Opinion in Genetics & Development*, **18**, 273–279.
162. Dolinoy, D.C., Weidman, J.R., and Jirtle, R.L. (2007) *Reproductive Toxicology (Elmsford, NY)*, **23**, 297–307.
163. Concha, G., Vogler, G., Lezcano, D., and Vahter, M. (1998) *Toxicological Sciences*, **44**, 185–190.
164. Huyck, K.L., Kile, M.L., Mahiuddin, G. *et al.* (2007) *Journal of Occupational and Environmental Medicine/American College of Occupational and Environmental Medicine*, **49**, 1097–1104.
165. Rahman, A., Vahter, M., Smith, A.H. *et al.* (2009) *American Journal of Epidemiology*, **169**, 304–312.
166. Smith, A.H., Marshall, G., Yuan, Y. *et al.* (2006) *Environmental Health Perspectives*, **114**, 1293–1296.
167. Fry, R.C., Navasumrit, P., Valiathan, C. *et al.* (2007) *PLoS Genetics*, **3** e207.
168. Edwards, T.M. and Myer, J.P. (2007) *Environmental Health Perspectives*, **115**, 1264–1270.
169. Liu, J., Xie, Y., Cooper, R. *et al.* (2007) *Toxicology and Applied Pharmacology*, **220**, 284–291.
170. Shen, J., Liu, J., Xie, Y. *et al.* (2007) *Toxicological Sciences*, **95**, 313–320.
171. Xie, Y., Liu, J., Benbrahim-Tallaa, L. *et al.* (2007) *Toxicology*, **236**, 7–15.
172. Waalkes, M.P., Liu, J., Germolec, D.R. *et al.* (2008) *Cancer Research*, **68**, 8278–8285.
173. Liu, J., Yu, L., Tokar, E.J. *et al.* (2008) *Annals of the New York Academy of Sciences*, **1140**, 368–375.
174. Waalkes, M.P., Liu, J., Ward, J.M., and Diwan, B.A. (2006) *Toxicology and Applied Pharmacology*, **215**, 295–305.
175. Davey, J.C., Nomikos, A.P., Wungjiranirun, M. *et al.* (2008) *Environmental Health Perspectives*, **116**, 165–172.
176. Watson, W.H. and Yager, J.D. (2007) *Toxicological Sciences*, **98**, 1–4.
177. IARC (ed.) (1989) IARC monographs on the evaluation of the carcinogenic risk of chemicals to humans, in *Some Organic Solvents, Resin Monomers and Related Compounds, Pigments and Occupational Exposures in Paint Manufacture and Painting*, vol. **47**, International Agency for Research on Cancer, IARC Press, Lyon, France.
178. De Boeck, M., Kirsch-Volders, M., and Lison, D. (2003) *Mutation Research*, **533**, 135–152.
179. Gebel, T., Berkenkamp, S., Luthin, S., and Dunkelberg, H. (1998) *Anticancer Research*, **18**, 4253–4258.
180. Lantzsch, H. and Gebel, T. (1997) *Mutation Research*, **389**, 191–197.
181. Elliott, B.M., Mackay, J.M., Clay, P., and Ashby, J. (1998) *Mutation Research*, **415**, 109–117.
182. Migliore, L., Cocchi, L., Nesti, C., and Sabbioni, E. (1999) *Environmental and Molecular Mutagenesis*, **34**, 279–284.
183. Timmerstein, M.A., Plews, P.I., Walker, C.V. *et al.* (1995) *Toxicology and Applied Pharmacology*, **130**, 41–47.
184. Lecreur, V., Lagodic-Gossmann, D., and Fardel, O. (2002) *International Journal of Oncology*, **20**, 1071–1076.
185. Patterson, T., Ngo, M., Aronov, P.A. *et al.* (2003) *Chemical Research in Toxicology*, **16**, 1624–1631.
186. Patterson, T.J. and Rice, R.H. (2007) *Toxicology and Applied Pharmacology*, **221**, 119–128.

187. Gurnami, N., Sharma, G., and Talukder, G. (1992) *Biometals: An International Journal on the Role of Metal Ions in Biology, Biochemistry, and Medicine*, **5**, 47–50.
188. Kirkland, D., Whitwell, J., Deyo, J., and Serex, T. (2007) *Mutation Research*, **627**, 119–128.
189. Cavello, D., Iavicoli, I., Setini, A. *et al.* (2002) *Environmental Health Perspectives*, **40**, 184–189.
190. Hantson, P., Leonard, E.D., Crutzen-Fayt, M.C. *et al.* (1996) *Pharmacotherapy*, **16**, 869–871.

15

Metalloproteomics of Arsenic, Antimony and Bismuth Based Drugs

Cheuk-Nam Tsang¹, Ruiguang Ge² and Hongzhe Sun¹

*¹Department of Chemistry and Open Laboratory of Chemical Biology,
The University of Hong Kong, Hong Kong SAR, P. R. China*

*²The Laboratory of Integrative Biology, College of Life Sciences,
Sun Yat-Sen University, Guangzhou 510006, P. R. China*

15.1 Introduction

Mineral elements, often at trace levels, play considerable roles in physiology and pathology. At least 25 elements are known to be essential or beneficial (e.g., Fe, Co, Cu, Zn, Mo and Se) for life. Whereas some elements, such as Cd, Hg, Pb, are generally toxic and their intracellular levels are thus precisely regulated [1]. Nearly $\frac{1}{3}$ of proteins are metalloproteins that are believed to require certain metal as cofactors, usually transition metal ions, to achieve specific catalytic, regulatory, and/or structural roles [2]. Some metalloproteins such as metallothionein, Hpn, and ferritin, are essential in metal homeostasis and detoxification processes [3–5] whereas others, for example, Fur, PerR, MtsR and NikR control the intracellular concentrations of metals [6, 7]. Metallochaperones try ensuring and delivering metals to target proteins; they protect and facilitate the maturation of metalloenzymes, which catalyse reactions including nucleotide synthesis, metabolism, antioxidation, and so on [8, 9]. To elucidate the biological significance and toxicity of the metal species on the molecular basis, various techniques have been developed for chemical speciation and localization in biological systems and applied in various scientific fields such as

biochemistry, biology, medicine, pharmacology, nutrition, agricultural and environmental science [10, 11].

Since the first sequencing of the entire genome in 1995 [12] and especially the completion of the human genome project in 2000 [13, 14], tremendous efforts have been made in the fields of systematic biology that ends in *-omics*. The best known are genomics and proteomics. The former uncovers complete genome sequences for living organisms, whereas the latter describes the localization, structure, function, modifications and interactions of the complete set of proteins expressed in a cell, tissue or an organism [15, 16]. The identification and characterization of proteins are benefited from the developments in high-throughput sample separation and detection methods, in particular liquid chromatography-electrospray ionization-mass spectrometry (LC-ESI-MS) and matrix assisted laser desorption ionization-mass spectrometry (MALDI-MS) [17–19].

The characterization of metallomes, which covers the entire metal and metalloid species present in a cell or tissue type, was coined as *metalloomics* to encompass the element distribution, equilibrium concentrations of free metal ions or as a free element content in a cellular compartment, cell or organism [20, 21], as well as the interactions with the genome, transcriptome, proteome and metabolome [22]. General studies include *in vivo* detection, localization, identification and quantification, *in vitro* functional analysis and *in silico* bioinformatics prediction. Metalloomics is thus a multidiscipline research area with an ultimate goal to provide a global and systematic understanding of the metal uptake, trafficking and function in biological systems, and is expected to be developed as an interdisciplinary science complementary to genomics and proteomics (Chapter 4).

Some areas of interest in metalloomics include:

- i. structure–function analysis of metalloproteins and their models;
- ii. coregulation of metals within a metallome including survey and identification of metalloproteins and metalloenzymes;
- iii. biological regulation of metals and their metabolisms;
- iv. physiological and pathological mechanisms related to metals in human health and diseases and;
- v. medical diagnosis of diseases in relation to trace elements as well as the (pre)clinical use of metallodrugs.

Arsenic, antimony and bismuth belong to the same group in the periodic table. Arsenic and antimony are metalloids that exhibit some of the features of both metals and nonmetals, whereas bismuth is a typical heavy metal. Arsenic is a well-documented carcinogen and its presence throughout nature causes global health problems, including cancers, cardiovascular diseases, peripheral neuropathies and diabetes mellitus [23]. Therefore, arsenic has been consistently ranked the first on the CERCLA Priority List of Hazardous Substances (<http://www.atsdr.cdc.gov/cercla/07list.html>) published by the Agency for Toxic Substances and Disease Registry (ATSDR) and the US Environmental Protection Agency (EPA). Paradoxically, high levels of arsenic have been used as therapeutic agents for the treatment of psoriasis, syphilis, rheumatosis for decades and a number of malignant tumors recently [24, 25]. Antimony-containing compounds have commonly been used to treat parasitic infections such as leishmaniasis, but drug resistance and side effects associated with the use of these antimony compounds have aroused concerns [26]. The chronic exposure to antimony will lead to respiratory problems, lung damage, cardiovascular

effects, gastrointestinal disorders and adverse reproductive outcome in humans. Bismuth has been used in medicine for treating gastric ulcers and *Helicobacter pylori* infections, and for the prevention and treatment of diarrhea [27–30] (Chapter 3). Besides, bismuth shows promise in radioimmunotherapy for treatment of cancer (α -particle emitting ^{212}Bi and ^{213}Bi) (Chapter 13) [31].

This chapter will introduce the fate of arsenic-, antimony- and bismuth-based drugs in biological system, focusing on the chemical speciation in biological matrices, proteomic approach on identification of protein targets of metallodrugs, and cellular regulation of metals especially the efflux transporters with close relevance to multidrug resistance. The related analytical techniques and strategies applied in metallomics and metalloproteomics are also summarized.

15.2 Chemical Speciation of Arsenic Based Drugs and their Metallometabolism

15.2.1 Metallometabolism in Biological Matrices

An essential assessment of the safety and effectiveness of new drug candidates may involve the investigation of their metabolism, including their biotransformations during the absorption, distribution, metabolism and excretion (ADME) processes in the body [32]. Such a study includes separation of the drug and its metabolites from *in vivo* complex biological matrices such as the whole blood or plasma, liver metabolism models (microsomes, hepatocytes and liver slices), excreta (urine, bile or feces), and/or cell extracts and supernatants from *in vitro* studies, and followed by quantification of each metabolite and identification of the major metabolites [32, 33]. Therefore, metabolite profiles are, in fact, equivalent to speciation analyses as they are traditionally named when the drug compounds are of inorganic origin.

The use of metal-based drugs (metalloodrugs) in medicine can be traced back to 5000 years ago, when Egyptians used copper in water sterilization [34]. Metallodrugs are attracting attention primarily due to their significant roles in therapeutic and diagnostic medicine, especially after the discovery of anticancer activity of *cis*-PtCl₂(NH₃)₂ (cisplatin) [35]. Biomolecules binding with drug substances are normally not referred to as drug metabolism. However, metallodrugs contain at least one metal ion in their active or structural centers, and do not normally follow the classical metabolic pathways. Our knowledge on their biotranslocation is still quite limited. Interaction of these drugs with proteins and other biomolecules is an important issue [36], which has significant effects on the distribution and biotransformation, and ultimately the mechanism of action of these metallodrugs.

15.2.2 Arsenic Metabolism

Inorganic arsenic is believed to be metabolized to the major urinary metabolite, a dimethylated arsenical, through consecutive reduction and oxidative methylation reactions [37] (Chapters 4 and 7). The postulated metabolic pathway follows: inorganic pentavalent arsenical (iAs^{V}) \rightarrow iAs^{III} \rightarrow monomethylarsonic acid (MMA^{V}) \rightarrow MMA^{III} \rightarrow dimethylarsinic acid (DMA^{V}) \rightarrow DMA^{III} [38, 39]. Arsenic trioxide (As_2O_3) was

already used clinically as an anticancer drug for the treatment of acute promyelocytic leukaemia [40, 41] (Chapter 11). Blood and urine samples from patients treated with As_2O_3 were analysed for arsenic species using HPLC-ICP-MS [42]. The main arsenic species found were iAs^{III} , MMA^{V} and DMA^{V} in urine and iAs^{V} , MMA^{V} and DMA^{V} in blood. The results agree well with the findings of other studies [43, 44], suggesting that methylated metabolites are the major metabolites *in vivo* and may contribute to the therapeutic effect of As_2O_3 in acute promyelocytic leukaemia patients [45, 46]. The pK_a of arsenite is 9.2, and is therefore expected to be protonated at physiological pH. However, EXAFS analysis demonstrated three oxygen ligands at 1.78 Å from the arsenic atom, showing that the major species in solution is $\text{As}(\text{OH})_3$ [47].

15.3 Metalloproteomics and its Applications to As-, Sb- and Bi-Based Metallo drugs

Since arsenic, antimony and bismuth exhibit anticancer [48], antiparasitic [26, 49] and antimicrobial properties [50, 51] respectively, they have long been used for treatment of various diseases (Table 15.1). Understanding the mechanisms of action and resistance at a molecular level will provide an insight into the development of new metallo drugs. This can be achieved by probing the interaction of drugs with their target proteins with the aid of traditional comparative proteomics, and metal selection, detection and characterization techniques developed in metalloproteomics [36, 52].

15.3.1 From Proteomics to Metalloproteomics

Conventional comparative proteomic study is based on the comparison of the protein expression profiles of drug treated and untreated samples visualized by two-dimensional gel

Table 15.1 Selective examples of As-, Sb-, and Bi-containing drugs for the treatment of various diseases

Elements	Metallo drugs	Medical treatment	Targeted cell
Arsenic (As) [48, 185]	Arsenic trioxide (Trisenox [®] and Arsenol [®])	Acute promyelocytic leukaemia (APL)	APL cells
Antimony (Sb) [26, 49]	Sodium stibogluconate (Pentosan [®]) Meglumin antimonite (Glucantime [®]) Potassium antimony tartrate	Cutaneous and visceral leishmaniasis	<i>Leishmania</i> spp. (parasite)
Bismuth (Bi) [30, 50, 51]	Bismuth subsalicylate (BSS) Colloidal bismuth subcitrate (CBS) Ranitidine bismuth citrate (RBC)	Gastrointestinal disorders, peptic ulcers and <i>H. pylori</i> infection	<i>Helicobacter pylori</i> (bacteria)

electrophoresis (2DE), in which up- or down-regulated proteins are probably associated with the cellular responses to the drug [36]. Interested protein spots are excised from the gel, digested with protease (e.g., trypsin) and identified by peptide sequencing and database searching [17, 53]. Extensive studies have shown the changes in proteome of different species (e.g., *Leishmania* spp. [54–58] and *Helicobacter pylori* [59–66], which are targets of antimony- and bismuth-based drugs respectively) in different stains, growing conditions and states of development (Table 15.2). The established techniques and acquired databases continually facilitate the further studies on the proteomic effects of metallodrugs.

The explicit subproteomic analysis on a set of metalloproteins and metal-binding proteins, and their metal-binding motifs in a given cell was referred to as *metalloproteomics* [53, 67]. Large scale metal-binding protein identification utilizes versatile metal (or element) specific selection and detection tools such as immobilized metal affinity chromatography (IMAC), X-ray fluorescence spectrometry (XRF) and inductively coupled plasma-mass spectrometry (ICP-MS) in combination with several key techniques in separation and protein identification such as two-dimensional gel electrophoresis (2DE), high-performance liquid chromatography (HPLC or FPLC) and mass spectrometry methods that employ soft desorption ionization methods (ESI-MS and MALDI-MS) used in proteomics.

Proposed metal-binding proteins including metallodrug targets can be structurally characterized by both X-ray crystallography and nuclear magnetic resonance (NMR) spectroscopy; and the ever increasing number of resolved metal-binding protein structures is the driving force for the development of bioinformatics focused on high-throughput and genome-wide *in silico* prediction of metalloproteins and functional annotation of hypothetical proteins from their protein sequences or apoprotein structures. An overview of general approaches and essential techniques utilized in metalloproteomics is shown in Figure 15.1.

15.3.2 Metal Specific Selection, Detection and Prediction Methods in Metalloproteomics

15.3.2.1 Immobilized Metal Affinity Chromatography (IMAC)

One of the metalloproteomic techniques for selective enrichment of proteins with metal-binding sites is immobilized metal affinity chromatography (IMAC) [67–69]. The interaction between proteins and the metal ions that are partially chelated on resin is mainly governed by the bio-coordination chemistry and the hard-soft acid-base (HSAB) character of metal ions (Figure 15.2). Numerous metal ions such as Ni^{II} , Cu^{II} , Zn^{II} and UO_2^{II} have been immobilized on IMAC columns for exploring the roles of metal-binding proteins in metal homeostasis, metal-associated diseases, metal-induced toxicity, protein phosphorylation and so forth (Table 15.3) [70–76]. Moreover, metal-binding motifs can be identified by on-column digestion of proteins retained on IMAC as the motifs are protected by the interaction with metal ions from enzymatic digestion (Figure 15.3) [73]. Such a methodology has been used for screening bismuth-based drug protein targets in *Helicobacter pylori* [77].

15.3.2.2 Laser Ablation-Inductively Coupled Plasma-Mass Spectrometry (LA-ICP-MS)

Inductively coupled plasma-mass spectrometry (ICP-MS) has been served as a highly sensitive, matrix independent and element specific tool for quantitative measurements. The

Table 15.2 Selective gel-based comparative proteome analysis on *Leishmania* species and *Helicobacter pylori*

	Specie(s) or stain(s)	Variant	Comparison	Ref.
<i>Leishmania</i> species (<i>L. spp.</i>)	<i>L. infantum</i> <i>L. donovani</i> and <i>L. panamensis</i>	Life stage	1. Amastigote and 2. Promastigote	[54, 56, 58]
	<i>L. mexicana</i>	Life stage	1. Procyclic promastigote; 2. Metacyclic promastigote; and 3. Amastigote	[57]
	<i>L. donovani</i>	Stain	1. Sb ^V sensitive stain and 2. Sb ^V resistance stain	[141]
	<i>L. infantum</i>	Nitric oxide (NO) exposure	1. Untreated and 2. Treated with NO donor	[55]
<i>Helicobacter pylori</i> (<i>H. pylori</i>)	/	Stain	1. 26695; 2. J99 and 3. SS1 (used in animal model)	[61]
	Clinical isolates	Patients suffered from different diseases	1. Duodenal ulcer; 2. Gastric cancer; and 3. Gastritis	[60]
	26695	pH of culturing media	1. pH 5.7 and 2. pH 7.5; or pH varied from 2.0 to 7.4	[64, 65]
	/	Stain	1. 26695 and 2. Metronidazole resistant stain	[63]
	26695 and its <i>fur</i> ⁻ mutant*	Fe content	1. Fe-rich and 2. Fe-depleted	[62]
	Clinical isolates	O ₂ content	1. Normal (5% O ₂) and 2. Oxidative stress (20% O ₂)	[59]
	26695	Culture media	1. Blood agar; 2. Brucella plate; 3. Brucella broth and 4. Brain heart infusion (BHI) broth	[66]
	26695	Bismuth drug	1. Untreated and 2. Treated with 20 ug/ml CBS	[77]

Metronidazole (MTZ): an antibiotic used in bismuth-based therapies against *H. pylori*.* *fur*: ferric uptake regulator protein.

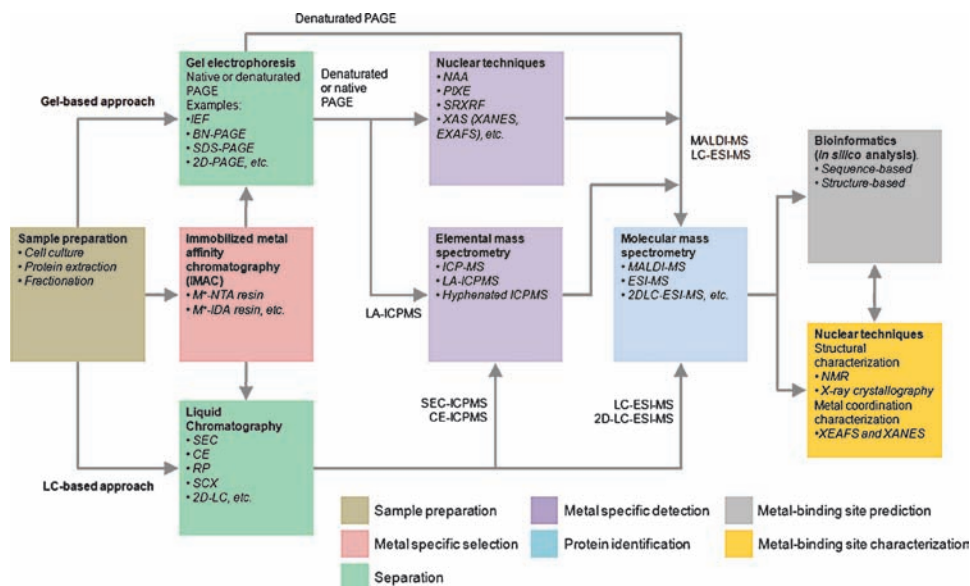


Figure 15.1 Flowchart of general approaches to metalloproteomics. High-throughput metal-binding protein identification from cellular system involves three essential steps including: (1) metal specific isolation or detection; (2) protein or peptide separation and (3) identification. Metal-binding sites and proteins are further characterized and frequently updated for searching new metalloproteins *in silico* across different species. Abbreviations: IEF, isoelectric focusing; BN-PAGE, blue native PAGE; SEC, size exclusion chromatography; CE, capillary electrophoresis; RP, reverse-phase chromatography; and SCX, strong cation exchange chromatography

hyphenation of the laser ablation system to ICP-MS further extends its application to gel-based proteomics in which metal-containing proteins [78, 79], selenoproteins [79], phosphorylated proteins [78, 80] and metallodrug target proteins [81] separated by gel electrophoresis or blotted on a membrane can be ablated by laser directly and the presence of heteroatoms is detected. For example, well separated spots in 2DE gel of human brain proteomes were analysed individually and various metal (e.g., Cu, Zn and Fe) and nonmetal (P and S) containing protein spots were detected [82, 83]. However, the denaturing condition in gel electrophoresis may lead to the loss (or partial loss) of metal ions from metal-protein complexes. Those undetected proteins can be recharged with isotope enriched tracer (i.e., minor isotopes such as ^{65}Cu and ^{67}Zn) doped into the gel and their signals are featured with a remarkable change in isotopic ratio with respect to their major isotopes (^{63}Cu and ^{64}Zn), whereas metal-binding proteins which can withstand in the denatured condition remained isotopic ratio in nature [84]. Such a strategy had also been applied for examining the metal exchange process in bovine serum albumin [85] and the metal-binding selectivity in different isoforms of human tau protein, a protein associated with Alzheimer's disease [86]. The detection of selenium, which is covalently incorporated in selenocysteine (Sec, the 21st amino acid) or selenomethionine, in selenoproteins opens a way to discover the members in this unusual class of protein family which are particularly essential in preventing human diseases by combating the damage in cells caused by reactive oxygen species [87, 88]. The

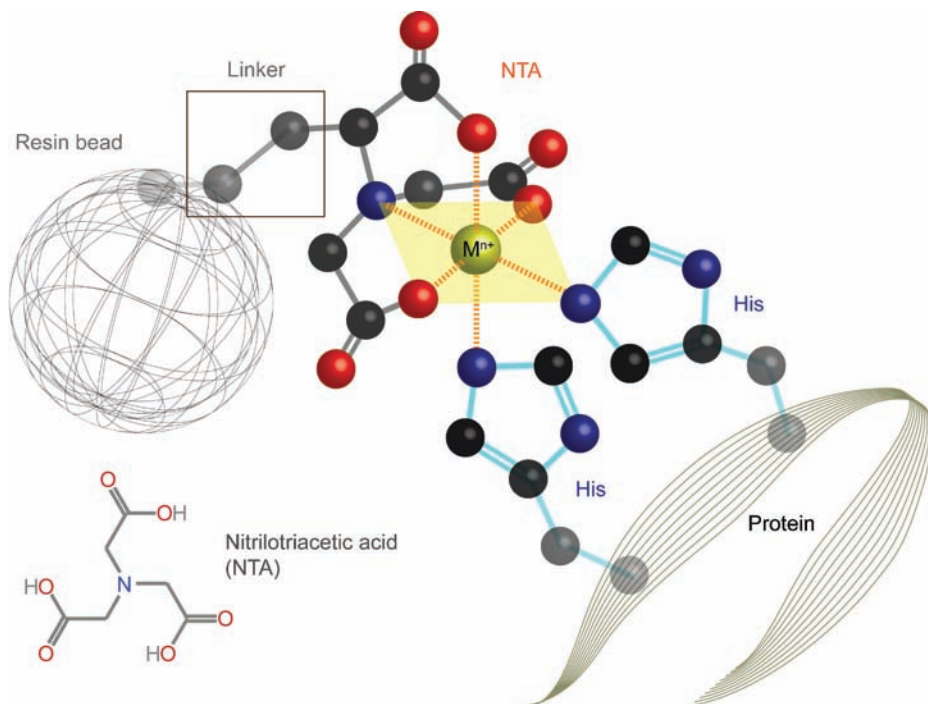


Figure 15.2 Illustration of immobilized-metal affinity chromatography (IMAC) and structure of nitrotriacetic acid (NTA). IMAC column consists of metal chelators (e.g., NTA) that are immobilized on resin beads. Metal ions are partially incorporated on the column and vacant coordination sites are available for retaining metal-binding proteins. Proteins bound on column can be eluted by reducing pH, high concentration of competitor (e.g., imidazole) or addition of EDTA (removal of metal ions from the column)

intensity of the major isotope ^{80}Se is severely interfered with the argon dimer ($^{40}\text{Ar}^{40}\text{Ar}$). Therefore, reduction of argon interference by dynamic reaction cell (DRC) or measurement of minor isotope ^{82}Se was necessary for detecting Se in 1D- or 2D-gel proteomes of Se-contaminated wildlife samples [89], Se-enriched yeast (a nutritional supplement) [90] and Se-fortified African catfish muscle tissue [91]. Se-containing peptides in tryptic digests of selenoproteins were further characterized by nanoHPLC with parallel ICP-MS identification and ESI-MS/MS peptide sequencing [90, 92]. The recent trend in LA-ICP-MS analysis or metal imaging on native-PAGE (e.g., BN-PAGE and native 2D-PAGE), in which metal protein interactions are presumably preserved, for investigating iron metalloproteins [93], cadmium uptake in Cd-exposed food plant spinach [94] and metal-binding proteins in rat tissues [95, 96] sheds light on the development of *in vivo* metalloproteomics.

15.3.2.3 Nuclear Analytical Techniques

Chemical speciation and characterization of trace elements based on atomic behavior is given by various nuclear techniques such as neutron activation analysis (NAA), proton

Table 15.3 Selective examples of IMAC-based approach for the identification of putative metal-binding proteins

Metal ion	Resin*	Sample	Research interest	No. of proteins indentified	Ref.
Cu ^{II} and Zn ^{II}	IDA	Three human hepatoma lines and one normal human liver specimen	Difference between metalloproteomes of Cu and Zn	19 (Cu-binding; Hep G2 cell) 19 (Zn-binding; Hep G2 cell)	[73]
Cu ^{II}	IDA	Human hepatoma line Hep G2 cell	Intracellular copper transport Cu toxicity (Wilson disease)	48 (cytosolic fraction) 19 (microsomal fraction)	[74]
Ni ^{II}	NTA	Human B cell	Ni-specific T cell activation	22	[71]
Cu ^{II}	IDA	<i>Arabidopsis</i> root tissues	Cu metalloproteome in plant	35	[72]
Bi ^{III}	NTA	<i>H. pylori</i> 11637	Bi proteome	7	[77]
Ni ^{II}	NTA	<i>H. pylori</i> 11637	Ni homeostasis	22	[75]
UO ₂ ^{II}	AP	Human serum	Examination of uranyl (UO ₂ ^{II}) toxicity	15 (gel-based approach)	[70]
UO ₂ ^{II}	AP	Human kidney-2 cell	Uranyl (UO ₂ ^{II}) toxicity	64 (MS-based approach)	[76]

*Abbreviations of the chelating groups on resin: IDA (iminodiacetic acid), NTA (nitrilotriacetic acid), AP (aminophosphonate, CH₂NHCH₂PO₃²⁻).

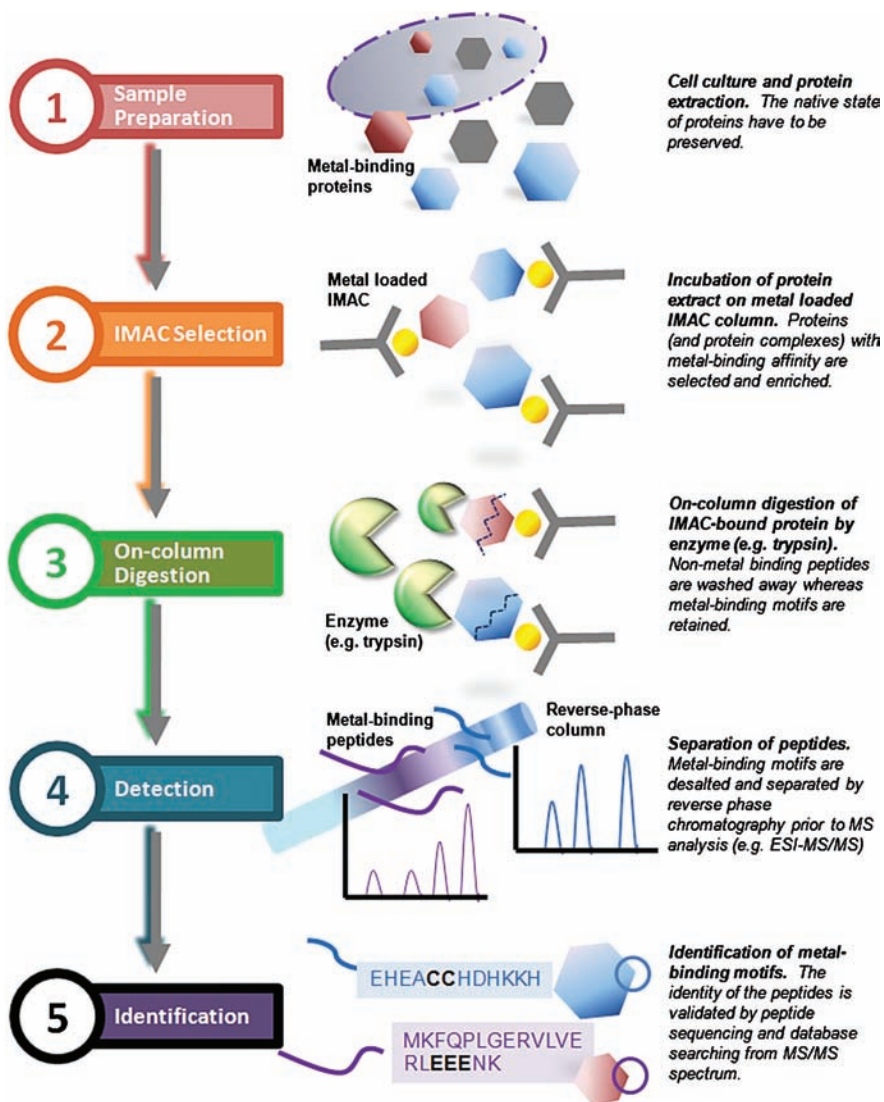


Figure 15.3 Mining metal-binding proteins by IMAC-based metalloproteomics

induced X-ray emission (PIXE), synchronous radiation X-ray fluorescence (SR-XRF) and X-ray absorption spectroscopy (XAS) which provide sensitive, multi-elementary and non destructive analysis [97, 98]. PIXE and SR-SRF have commonly been used for metal determination and quantification in metalloproteins embedded in electrophoresis gel because of their good spatial resolution (mm- μ m scale, which is higher than NAA) and detection limit (ppm level, which is more sensitive than XAS) [99, 100].

PIXE is particularly sensitive for Fe and its neighboring elements [101] and was introduced in 1987 for determination the amount of Fe in an iron-sulfur protein HiPIP [102]

and subsequently the Ni-Fe hydrogenase [103] and cytochrome C [104] separated by SDS-PAGE. Moreover, Ni and Fe signals were detected from different bands in denatured PAGE of hydrogenase, implying that Ni and Fe ions belong to different subunits [103, 105]. Besides, native PAGE and non-denaturing IEF in conjunction with PIXE further applied for the quantitative measurement of metals in separated bands of charged isomers or isoforms of metalloproteins such as zinc enzymes carbonic anhydrase and cytoplasmic pyrophosphatase (PPase) [106], and copper-zinc superoxide dismutase (Cu,Zn-SOD) [107].

The utilization of high energy synchrotron radiation (SR) as the exciting source for XRF contributed to the low absolute detection limit (10^{-12} to 10^{-15} g) and outstanding space resolution analysis for natural biological samples [97, 108]. For instance, metalloproteins that carry essential metals Fe, Cu and Zn in human liver cytosol were located in a SDS-PAGE gel [109] and a native IEF gel in which the sample was pre-fractionated by gel chromatography [110]. Moreover, native IEF gels analysed by SR-XRF constructed two distinguishable metalloprotein distributions in cytosol between hepatocellular carcinoma (HCC) and surrounding normal tissues; and featured in a lower Fe and Zn content in HCC [111]. Such an approach has also revealed the distribution on As-, Se- and Hg-containing proteins in the fish liver for exploring the roles of Se-proteins in As and Hg detoxification [112]. Furthermore, investigation of selenoproteins in rat testis homogenate isolated by SDS-PAGE detected four out of nine selenoproteins found in autoradiography [113, 114].

The high sensitivity and spatial resolution of microprobe SR-XRF allowed the elemental mapping in plants and animals to be explored, providing an integrative view of metal content, speciation and localization within a biological system. For example, iron was observed to be mainly localized at the provascular strands of the embryo in the wild type *Arabidopsis* seeds, whereas it is completely absent and located diffusely in the hypocotyls, radical and epidermal cells of the cotyledons in *vit1-1* (vacuolar iron transporter 1) mutant seeds. In both type of seeds, the distribution pattern of manganese is similar to that of iron in *vit1-1* mutant while zinc is distributed throughout the seed [115]. Microprobe SR-XRF elemental mapping of thin sectioned HepG2 cells showed that arsenic accumulates in the euchromatin region of the cell nucleus upon arsenite exposure, indicative of arsenic binding DNA and/or proteins relevant to DNA transcription [116].

X-ray absorption spectrometry (XAS) is mainly used for examining the local structural environment of metal sites and XAS spectrum can be roughly divided into two regions: X-ray absorption near edge structure (XANES) and extended X-ray absorption fine structure (EXAFS) [117, 118]. The former gives information about the oxidation state of metals, bonding covalence and molecular symmetry whereas the latter provides structural information about the metal-binding environment, such as the coordination number, type of donors bound, and the distance between metal and the ligand [97, 119]. Recently, an attempt was made for direct XANES chemical speciation of the three isoforms of Cu,Zn-SOD separated by native 2D-PAGE and partially reduced form of Cu,Zn-SOD, which contains both Cu^{I} and Cu^{II} , was observed [120].

15.3.2.4 Bioinformatics

Structural information of metal-binding protein models and domains with specified metals can be retrieved from databases (such as PDB, Pfam and SCOP) and the conserved

metal specific domains and their metal-binding patterns (MBPs) can be recognized by computational methods such as similarity-based sequence alignment and various learning machines (e.g., the Bayesian classifier [121], artificial neural network classifiers [122] and support vector machines [123]). Subsequently, putative metal-binding proteins are matched in database scale by a structural template comparison program or multiple sequence alignment tools based on the assembled MBP library [124, 125]. For example, predictions based on protein sequences estimated the population of zinc-binding proteins accounts for 10% in the human proteome whilst the majority of them are involved in the regulation of gene expression [126]; and more extensive surveys on zinc- [127], non-heme iron- [128] and copper-proteins [129] through a variety of archaeal, bacterial and eukaryotic proteomes highlighted the popularity and functional specificity of essential metals in different forms of life and in particular the essentiality of zinc-containing regulatory proteins in higher organisms [127]. Prediction on the basics of 3D metal-binding geometric features of apoprotein models provides an alternative way for discovering distinct metal structure motifs and especially important for those have low sequence homology to known MBPs [130–132]. Efforts have also been made to exploit the structural motifs corresponding to alkaline earth metals (Mg [133] and Ca [134]) and transition metals (e.g., Zn [121, 134] and non-heme Fe [135]) further elucidated their metal-oriented coordination.

15.3.3 Identification of Potential Targets of As-, Sb-, and Bi-Based Drugs by Metalloproteomics

15.3.3.1 Arsenic

The most profound and well-documented medical application of arsenic is the clinical use of arsenic trioxide (As_2O_3 , Trisenox[®]) in the treatment of acute promyelocytic leukaemia (APL) [136]. It was reported that arsenite at a high concentration induced apoptosis via c-Jun N-terminal kinase (JNK) signaling pathway, whereas at a low concentration is carcinogenic and stimulates the extracellular-signal-regulated kinase signaling pathway to enhance cell proliferation [137]. Several differentially regulated peptides in lung cancer cells treated with low concentrations of arsenite were identified when compared to untreated cells with SELDI-TOF analysis [138].

The biological responses to arsenite triggered apoptosis were revealed by a detailed comparative proteomic study on cultured rat lung epithelial cells (LECs) under a high level of sodium arsenite (NaAsO_2) [139]. Seven proteins were differentially expressed under oxidative stress induced by arsenite, in which four heat shock proteins (Hsp27, α B-crystallin, Hsp70 and heme oxygenase-1) and two antioxidative stress proteins (aldose reductase and ferritin light chain) were upregulated whereas one glycolytic enzyme (glyceraldehyde-3-phosphate dehydrogenase) was downregulated, Table 15.4 [139]. Moreover, the induction priority of certain proteins was discovered by subsequent time course experiments, indicative of the stepwise process of the cellular defense system [139]. Besides, the carcinogenic nature of arsenic was demonstrated by a similar proteome study that a low level exposure of arsenite for months initiates cell transformation, as demonstrated by the downregulation of three intermediate filaments [140].

Table 15.4 Proteins in cultured rat LECs associated with high concentrations of arsenite (AsO_2^-) [139]

Category	Protein	Fold difference ^a	Proposed drug action/ cellular defense
Heat shock proteins (Hsp)	HSP27	+11.3	Hsp activate pathways against apoptosis/ Maintain protein refolding process HO-1 generates free radical scavengers (associated with heme cleavage)
	α B-crystallin	+2.9	
	HSP70	NA ^b upregulated	
	Heme oxygenase-1 (HO-1; HSP32)	NA ^b upregulated	
Antioxidative stress proteins	Aldose reductase (AR)	+3.4	AR metabolize toxic aldehyde products induced by oxidative stress
	Ferritin light chain (FLC)	+7.9	Increase ferritin level and maintain Fe bioavailability perturbed by HO-1
Glycolytic enzyme	Glyceraldehyde-3-phosphate dehydrogenase (GAPDH)	-5.1	As-induced apoptosis represses glycolysis

^aFold difference: expression level of the particular protein of untreated cell versus that of treated cell.

^bNA: not applicable (No spot is detected in 2D gel of untreated cell).

15.3.3.2 Antimony

Pentavalent antimonials (Sb^{V} compounds) including Pentostam and Glucantime are the first-choice drugs for treatment of leishmaniasis, an endemic vector-borne disease in over 88 tropical and subtropical countries that is caused by protozoan parasites *Leishmania* [49]. Their pathologies are varied in different species. For instance, *L. major* associates with self-healing cutaneous lesions and *L. donovani* leads to life-threatening visceral leishmaniasis. The proteomes of Sb^{V} -sensitive and -resistant *L. donovani* isolated from patients were investigated by 2DE and differentially expressed proteins such as heat shock proteins (Hsp70 and Hsp83) and small kinetoplastid calpain-related protein SKCRP14.1 were highlighted in the regulation of antimony-mediated programmed cell death [141]. The process can be arrested by the repression of SKCRP14.1 or induction of heat shock proteins which might account for the treatment failure among Sb^{V} -unresponsive patients [141].

15.3.3.3 Bismuth

Bismuth-based triple and quadruple therapy is one of the first-line treatments for the eradication of *H. pylori*, a pathogen associated with human gastrointestinal disorders such as dyspepsia, gastritis and peptic ulcers (Chapter 3) [51, 142]. The global proteome alternation of *H. pylori* has been explored under treatment of colloidal bismuth subcitrate

(CBS) by a comparative proteomic approach, in which eight proteins were found to be significantly differentially expressed in 2DE gels, Table 15.5 [77]. Thioredoxin was upregulated in response to the oxidative stress induced by bismuth. Moreover, four regulated proteins involved in cellular processes including HspA, HspB, NapA and TsaA were also isolated by Bi^{III}-derived IMAC, implying that they were closely associated with bismuth drugs [77]. To validate the methodology, HspA, a form of chaperonin GroES, was overexpressed, purified and characterized. The protein binds two Bi^{III} ions with one at the C-terminus metal-binding domain and another one at the N-terminus redox-sensitive Zn^{II} site consisting of H45, C51 and C53. The zinc site may have evolved as a result of negative selection [143]. Importantly, binding of Bi^{III} disrupts the quaternary structure of HspA from its native heptamer to a dimer, implying that this ubiquitous chaperonin HspA may act as a potential target of bismuth-based drugs [144]. Other Bi-binding proteins selected by IMAC-2DE approach included urease subunit UreB, fumarase, and elongation factor Ef-Tu, suggesting that bismuth may interfere with nickel homeostasis, tricarboxylic acid metabolism and translational processes in *H. pylori* (Figure 15.4) [77].

15.4 Biological Regulation of Arsenic and Antimony

15.4.1 Arsenic and Antimony Uptake Systems

The two biological important states of arsenic are the pentavalent and trivalent forms. Trivalent arsenite is much more toxic than pentavalent arsenate, and is primarily responsible for the biological effects of this metalloid. Arsenite is toxic because of its propensity to form strong, almost covalent bonds with the thiolates of closely spaced cysteine residues, thereby inhibiting the function of proteins. In solution, the pentavalent form of arsenic, H₃AsO₄, exists as the oxyanion As^V, which is a substrate analog of phosphate (PO₄³⁻). *E. coli* has two phosphate transporters, Pit and Pst [145], both of them, especially the Pit system, facilitate arsenate uptake [146]. It is likely that arsenate is taken up similarly by the phosphate transporters in most organisms, such as the yeast *Saccharomyces cerevisiae* [147].

GlpF, a glycerol facilitator of *E. coli*, was found to uptake trivalent metalloids into cells during the screen for a random mutagenesis with resistance to arsenite or antimonite (Figure 8.1) [148]. The eukaryotic homologues of *E. coli* GlpF, such as Fps1p in the yeast *S. cerevisiae* [149, 150] and mammalian AQP7/9 [150, 151] were demonstrated to mediate the influx of both metalloids in yeast, human and rat. The discovery of an aquaglyceroporin as an arsenite and antimonite transporter is not much of a surprise, in view of the presence of As(OH)₃ and Sb(OH)₃ at physiological pH in aqueous solution [47, 152], both of which are inorganic molecular mimics of glycerol. An analysis of the predicated selectivity filters (Phe64 and Arg219) of AQP9 through single-site mutation based on the crystal structure of two aquaglyceroporin homologues, bovine AQP1 [153] and *E. coli* GlpF [154] supported the conclusion that As(OH)₃ and glycerol used the same translocation pathway in AQP9 [151].

AQP9 is highly expressed in the liver, where it plays an essential role in glycerol and urea transport [155]. In the liver, As(OH)₃ is methylated to a variety of species, of which the

Table 15.5 CBS-regulated and Bi-binding proteins in *H. pylori* identified by comparative proteomics and IMAC-2DE [77]

Category	Protein	Fold difference ^a	Affinity to IMAC		Proposed drug action or cellular defense
			Bi	Ni ^b	
Cellular processes	HspA	-3.0	✓	✓	Ni ^{II} delivery from HspA to urease may be perturbed by Bi ^{III}
	HspB	+4.2	✓	✓	HspB maintains urease activity
	Putative alkyl hydroperoxide reductase (TsaA)	+6.0	✓	✓	TsaA defense against oxidative stress induced by Bi ^{III}
	Neutrophil activating protein (NapA)	+2.2	✓	✓	NapA mediate neutrophil adhesion and sequester Bi ^{III}
Cofactors, prosthetic groups and carriers	Thioredoxin	+2.0	—	—	Thioredoxin cooperates with reductase (TsaA) to fight against oxidative stress
Hypothetical proteins	HP0367	+4.5	—	—	NA
Others	Hemoglobin	+3.7	—	—	NA (Absorbed via culturing medium)
Bi-binding proteins not regulated by CBS	Urease subunit B (UreB)	—	✓	✓	Urease activity is inhibited by Bi ^{III}
	Fumarase	—	✓	✓	Tricarboxylic acid metabolism is perturbed by Bi ^{III}
	Elongation factor Tu (Ef-Tu)	—	✓	—	Translation process is interfered by Bi ^{III}

^aFold difference: expression level of the particular protein of untreated cell versus that of treated cell.

^bFor details, see ref. [75].

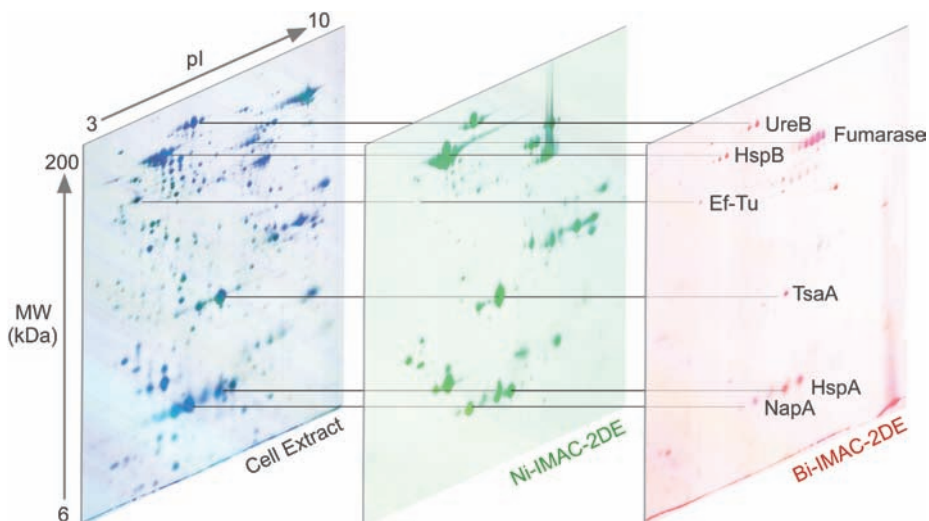


Figure 15.4 Identification of bismuth and nickel-binding proteins in *Helicobacter pylori* by IMAC-2DE approach. Proteins retained on Ni- and Bi-IMAC are isolated and enriched from cell lysate. Eluted proteins are denatured and separated according to their pIs and molecular weights by 2DE. Such an approach allows 22 and seven proteins to be identified in *H. pylori* strain 11637 respectively. Adapted with permission from [74] Copyright 2004 American Chemical Society., and [76] Copyright Elsevier (2009)

monomethylated $\text{CH}_3\text{As}(\text{OH})_2$ represents a significant fraction [156] and is structurally similar to, although less polar than, $\text{As}(\text{OH})_3$. Therefore, one model of the catalytic role of AQP9 in the uptake of $\text{As}(\text{OH})_3$ and efflux of $\text{CH}_3\text{As}(\text{OH})_2$ was proposed [157], that is, $\text{As}(\text{OH})_3$ flows down a concentration gradient from blood into hepatocytes through AQP9, and is either methylated and reduced to $\text{CH}_3\text{As}(\text{OH})_2$, or glutathionylated to $\text{As}(\text{GS})_3$ and methylars^{III} diglutathione ($\text{MAs}(\text{GS})_2$). $\text{As}(\text{GS})_3$ and $\text{MAs}(\text{GS})_2$ are pumped into bile by multidrug resistance-associated protein 2 (MRP2) or homologs [158, 159], and alternatively $\text{CH}_3\text{As}(\text{OH})_2$ flows down its concentration gradient via AQP9 into blood. On the other hand, the legume symbiont *Sinorhizobium meliloti* employs aquaglyceroporin as a novel route for arsenic detoxification [160]. Arsenate enters the cell through the phosphate transport system, is reduced to arsenite by the arsenate reductase, ArsC [161], and is extruded out of the cell by downhill movement through AqpS, an aquaglyceroporin homolog of GlpF (Figure 8.1) [160]. During an ArsC catalysis cycle, arsenate first binds to the anion site which is composed of three basic residues Arg60, Arg94 and Arg107 for *E. coli* ArsC, and is then followed by the formation of a covalent arsenate thioester intermediate with the active site Cys12 [162]. The intermediate is further reduced in two steps by glutaredoxin and glutathione, through a Cys12-S-As^{III} intermediate to the final product of arsenite. Therefore, it may represent a novel pathway of arsenate detoxification in *S. meliloti* and aquaglyceroporin can facilitate translocation of arsenite either in or out of cells depending on the concentration gradient [157].

15.4.2 Arsenic and Antimony Extrusion Systems

Many organisms, such as bacteria, fungi, algae and plants present in environments facing large amounts of arsenic, have developed mechanisms for arsenic resistance, which include arsenite oxidation (*aox* genes), respiratory arsenate reduction (*arr* genes) or arsenite efflux (*ars* genes). Bacteria have two basic mechanisms of arsenite extrusion, that is, a carrier mediated efflux via an arsenite carrier protein driven by the membrane potential, for example, AqpS and ArsC system in *S. meliloti*, [160] and the other one by an arsenite translocation ATPase [163]. The majority of bacteria use ArsB to extrude arsenite and antimonite. Some bacteria have three-gene *arsRBC* operons, whereas others, such as *E. coli*, have *ArsRDABC* systems encoded by the *ars* operon of plasmid R773 [161]. *ArsR* is a regulator to control the levels of *ars* operon expression [164], while *ArsD* is a metallochaperone to deliver arsenic to the *ArsAB* efflux pump [165]. Interaction with *ArsD* increases the affinity of *ArsA* for arsenite or antimonite by around 60-fold, and promotes its ATPase activity at lower concentrations of arsenite to enhance the rate of arsenite extrusion [165].

ArsB is a 429-residue integral membrane protein with 12 membrane-spanning segments [166]. It is responsible for the extrusion of As^{III} and Sb^{III} , and forms a complex with *ArsA* which provides the energy through the catalytic hydrolysis of ATP in the presence of As^{III} and Sb^{III} [167]. The 583-residue *ArsA* ATPase is composed of homologous N-terminal (A1) and C-terminal (A2) halves, both of which contain a consensus sequence of a nucleotide-binding domain (NBD) required for ATPase activity and metalloid transport. A1 and A2 are connected by a 25-residue linker [168]. The MBD contains one or more metalloid atoms, either Sb^{III} [169, 170] or As^{III} [170], coordinated to one residue from the A1 half and the other from the A2 half of the protein to bring the two NBD domains together for ATPase activation [171]. A trinuclear Sb^{III} -cluster was found to be located in the MBD of *E. coli* *ArsA* [169], and each of the three Sb^{III} atoms appears to be three-coordinate, with a non-protein ligand, chloride (Cl^-) and two ligands from A1 and A2 domains respectively (Figure 3.15). The first site involves Cys113 (A1) and Cys422 (A2), while the second site consists of Cys172 (A1) and the imidazole nitrogen of His453 (A2) and the third site contains His148 (A1) and the hydroxyl of Ser420 (A2). The first site was shown to be a high affinity metalloid-binding site [172]. It was found that Cys172 increased the affinity of the first site for Sb^{III} by around 10-fold and augmented metalloactivation of the *ArsA* ATPase activity. Conformational changes within the Cys172-localized loop between A1 helices H9 and H10 is proposed. It is disordered when ADP is bound to NBD1 and NBD2 and changes to well-folded upon the binding of ATP to NBD2 [170, 173]. This is a novel characteristic similar to the formation and breakage of the imidazolite bridge during the catalysis cycle of Cu,Zn-SOD [174, 175]. *ArsA* has two signature linkers that serve as signal transduction domains (STDs), $\text{D}_{142/447}\text{TAPTGH}_{148/453}$ in A1/A2, which corresponds to the switch II region of many other nucleotide binding proteins and have been proposed to be involved in transferring the energy of ATP hydrolysis to metalloid transport [176].

The human family of ATP-binding cassette (ABC) transporters includes at least 49 members within seven subfamilies designated A - G [177], among which MRP/ABCC transporters can collectively confer *in vitro* resistance to natural product anticancer drugs and their conjugated metabolites, platinum compounds, folate antimetabolites, nucleoside

and nucleotide analogs, arsenical and antimonial oxyanions, peptide-based agents, and in concert with alterations in phase II conjugating or biosynthetic enzymes, classical alkylating agents, alkylating agents [178]. Several MRP/ABCC members (MRP1/2/3) are associated with tumor resistance which is often caused by an increased efflux and decreased intracellular accumulation of natural product anticancer drugs and other anticancer agents [178, 179]. In humans, MRP1/ABCC1 is nearly present in all major tissues except in the adult liver where is usually not detectable and in all peripheral blood cell types, with highest levels found in the kidney, lung, testes, and placenta [180, 181]. MRP1/ABCC1 is able to cause arsenite resistance in the MRP1/ABCC1 gene transfected or arsenite/antimonite selected cells with the over expression of MRP1/ABCC1 [182], which has raised the question of whether MRP1/ABCC1 might be responsible for the arsenite resistance in patients with acute promyelocytic leukaemia. MRPA/ABCC1-deficient cells are hypersensitive to arsenite and antimony potassium tartrate, and conversely, overexpression of MRP1/ABCC1 [158, 183] and of the two subunits of γ -glutamylcysteine synthetase (γ -GCS) [183] result in higher intracellular GSH levels and greater resistance to arsenite, arsenate, and antimony potassium tartrate. Consistent with a role for multidrug resistance efflux pumps in arsenite and antimonite resistance, these arsenite resistant cells are cross-resistant to several anticancer drugs, such as vinblastine, doxorubicin, actinomycin D, and cisplatin, which are also substrates for MRP1/ABCC1 and P-glycoprotein (P-gp)/MDR1 [158]. Knockout of the MRP1/ABCC1 gene in mouse W9.5 embryonic stem cells resulted in increased sensitivity to arsenite [184].

15.5 Conclusions

Similar to metallomics, metalloproteomics is an emerging field dedicated to the understanding of the intrinsic mechanisms of biological functions of metals with genes, proteins, metabolites and other biomolecules in the biological systems [186, 187]. Metalloproteomics also complements functional genomics, structural genomics and is an important part of bioinorganic chemistry and bioanalytical chemistry. With the development of various (bio) analytical techniques, nuclear techniques such as neutron activation analysis, X-ray emission spectroscopy/fluorescence, isotope dilution and tracing techniques, in combination with the state-of-the-art separation techniques, metalloproteomics will definitely provide much more useful information at an integrated level on intracellular metal-biomolecule interactions which are closely related to metal relevant diseases (e.g., Wilson and Menkes diseases) and the mechanisms of actions of metallodrugs. IMAC-2DE approach together with MS allows us to find several key proteins for the bismuth antiulcer drug in *H. pylori* and it has been further validated by the biochemical characterization of the heat shock protein, HspA, also a form of GroES found in the pathogen. Disruption of the protein structure may lead to new therapeutics. We anticipate that more proteins will be mined in other microorganisms as well. Moreover, the putative metal-binding motifs and domains can be discovered by on-column tryptic digestion followed by biological MS analysis. Based on the metal-binding motif data bank, new information on the biocoordination chemistry of both bismuth and antimony (and other metals) will be obtained which may be important for medicinal chemistry of the metallodrugs and subsequently facilitate new metallodrug design.

Acknowledgements

This work was supported by the Research Grants Council of Hong Kong (HKU7043/06P, HKU2/06C HKU7042/07P, HKU1/07C, HKU7038/08P, HKU7049/09P and N_HKU752/09), the Area of Excellence Scheme of the University Grants Committee, Croucher Foundation, The University of Hong Kong, National Natural Science Foundation of China (No. 20801061) and Guangdong Natural Science Foundation (No. 8451027501001233).

References

1. Aitio, A., Aro, A., Jarvisalo, J., and Vainio, H. (1991) *Trace Elements in Health and Disease*, Royal Society of Chemistry, Cambridge.
2. Tainer, J.A., Roberts, V.A., and Getzoff, E.D. (1991) *Current Opinion in Biotechnology*, **2**, 582–591.
3. Ge, R. and Sun, H. (2007) *Accounts of Chemical Research*, **40**, 267–274.
4. Vašák, M. and Hasler, D.W. (2000) *Current Opinion in Chemical Biology*, **4**, 177–183.
5. Chasteen, N.D. (1998) *Metal Ions in Biological Systems*, **35**, 479–514.
6. Andrews, S.C., Robinson, A.K., and Rodriguez-Quinones, F. (2003) *FEMS Microbiology Reviews*, **27**, 215–237.
7. Dosanjh, N.S. and Michel, S.L. (2006) *Current Opinion in Chemical Biology*, **10**, 123–130.
8. Liberek, K., Lewandowska, A., and Ziętkiewicz, S. (2008) *The EMBO Journal*, **27**, 328–335.
9. Casalot, L. and Rousset, M. (2001) *Trends in Microbiology*, **9**, 228–237.
10. Szpunar, J. and Łobinński, R. (2002) *Analytical and Bioanalytical Chemistry*, **373**, 404–411.
11. Caruso, J.A. and Montes-Bayón, M. (2003) *Ecotoxicology and Environmental Safety*, **56**, 148–163.
12. Fleischmann, R.D., Adams, M.D., White, O. *et al.* (1995) *Science*, **269**, 496–512.
13. Lander, E.S., Linton, L.M., Birren, B. *et al.* (2001) *Nature*, **409**, 860–921.
14. Venter, J.C., Adams, M.D., Myers, E.W. *et al.* (2001) *Science*, **291**, 1304–1351.
15. Anderson, N.L. and Anderson, N.G. (1998) *Electrophoresis*, **19**, 1853–1861.
16. Tyers, M. and Mann, M. (2003) *Nature*, **422**, 193–197.
17. Aebersold, R. and Mann, M. (2003) *Nature*, **422**, 198–207.
18. Łobinński, R., Schaumlöffel, D., and Szpunar, J. (2006) *Mass Spectrometry Reviews*, **25**, 255–289.
19. Shah, M. and Caruso, J.A. (2005) *Journal of Separation Science*, **28**, 1969–1984.
20. Williams, R.J.P. (2001) *Coordination Chemistry Reviews*, **216–217**, 583–595.
21. Szpunar, J. (2004) *Analytical and Bioanalytical Chemistry*, **378**, 54–56.
22. Haraguchi, H. (2004) *Journal of Analytical Atomic Spectrometry*, **19**, 5–14.
23. Yoshida, T., Yamauchi, H., and Sun, G.F. (2004) *Toxicology and Applied Pharmacology*, **198**, 243–252.
24. Lau, A.T. and Chiu, J.F. (2003) *Recent Research Developments in Molecular & Cellular Biochemistry*, **1**, 1–19.
25. Zhu, J., Chen, Z., Lallemand-Breitenbach, V., and de Thé, H. (2002) *Nature Reviews. Cancer*, **2**, 705–714.
26. Yan, S., Jin, L., and Sun, H. (2005) *Metallotherapeutic Drugs and Metal-Based Diagnostic Agents: The use of Metals in Medicine*, vol. **1** (eds M. Gielen, and E.R.T. Tiekink), John Wiley & Sons, Ltd, Chichester, pp. 441–461.
27. Guo, Z. and Sadler, P.J. (1999) *Angewandte Chemie – International Edition in English*, **38**, 1513–1531.
28. Suerbaum, S. and Michetti, P. (2002) *The New England Journal of Medicine*, **347**, 1175–1186.
29. Sun, H., Zhang, L., and Szeto, K.Y. (2004) *Metal Ions in Biological Systems*, **41**, 333–378.
30. Yang, N. and Sun, H. (2007) *Coordination Chemistry Reviews*, **251**, 2354–2366.

31. McDevitt, M.R., Sgouros, G., Finn, R.D. *et al.* (1998) *European Journal of Nuclear Medicine*, **25**, 1341–1351.
32. Woolf, T.F. (1999) *Handbook of Drug Metabolism*, Marcel Dekker, New York.
33. Uetrecht, J.P. and Trager, W. (2007) *Drug Metabolism: Chemical and Enzymatic Aspects*, Informa Healthcare, New York.
34. Orvig, C. and Abrams, M.J. (1999) *Chemical Reviews*, **99**, 2201–2204.
35. Rosenberg, B., VanCamp, L., Trosko, J.E., and Mansour, V.H. (1969) *Nature*, **222**, 385–386.
36. Sun, X., Tsang, C.N., and Sun, H. (2009) *Metallomics*, **1**, 25–31.
37. Suzuki, K.T. (2005) *Analytica Chimica Acta*, **540**, 71–76.
38. Suzuki, K.T., Mandal, B.K., and Ogra, Y. (2002) *Talanta*, **58**, 111–119.
39. Aposhian, H.V., Zakharyan, R.A., Avram, M.D. *et al.* (2004) *Toxicology and Applied Pharmacology*, **198**, 327–335.
40. Zhang, T.D. (1984) *Zhong Xi Yi Jie He Za Zhi*, **4**, 19–20.
41. Shen, Z.X., Chen, G.Q., Ni, J.H. *et al.* (1997) *Blood*, **89**, 3354–3360.
42. Šlejkovec, Z., Falnoga, I., Goessler, W. *et al.* (2008) *Analytica Chimica Acta*, **607**, 83–91.
43. Yoshino, Y., Yuan, B., Miyashita, S.I. *et al.* (2009) *Analytical and Bioanalytical Chemistry*, **393**, 689–697.
44. Fukai, Y., Hirata, M., Ueno, M. *et al.* (2006) *Biological & Pharmaceutical Bulletin*, **29**, 1022–1027.
45. Chen, G.Q., Zhou, L., Styblo, M. *et al.* (2003) *Cancer Research*, **63**, 1853–1859.
46. Wang, Z., Zhou, J., Lu, X. *et al.* (2004) *Chemical Research in Toxicology*, **17**, 95–103.
47. Ramirez-Solis, A., Mukopadhyay, R., Rosen, B.P., and Stemmler, T.L. (2004) *Inorganic Chemistry*, **43**, 2954–2959.
48. Dilda, P.J. and Hogg, P.J. (2007) *Cancer Treatment Reviews*, **33**, 542–564.
49. Mishra, J., Saxena, A., and Singh, S. (2007) *Current Medicinal Chemistry*, **14**, 1153–1169.
50. Lambert, J.R. and Midolo, P. (1997) *Alimentary Pharmacology & Therapeutics*, **11** (Suppl. 1), 27–33.
51. Sadler, P.J., Li, H., and Sun, H. (1999) *Coordination Chemistry Reviews*, **185–186**, 689–709.
52. Garcia, J.S., de Magalhães, C.S., and Arruda, M.A.Z. (2006) *Talanta*, **69**, 1–15.
53. Shi, W. and Chance, M.R. (2008) *Cellular and Molecular Life Sciences*, **65**, 3040–3048.
54. Bente, M., Harder, S., Wiesgigl, M. *et al.* (2003) *Proteomics*, **3**, 1811–1829.
55. Dea-Ayuela, M.A., Ordonez-Gutierrez, L., and Bolas-Fernandez, F. (2009) *International Journal of Medical Microbiology*, **299**, 221–232.
56. Fakhry, Y.E., Ouellette, M., and Papadopoulou, B. (2002) *Proteomics*, **2**, 1007–1017.
57. Nugent, P.G., Karsani, S.A., Wait, R. *et al.* (2004) *Molecular and Biochemical Parasitology*, **136**, 51–62.
58. Walker, J., Vasquez, J.J., Gomez, M.A. *et al.* (2006) *Molecular and Biochemical Parasitology*, **147**, 64–73.
59. Chuang, M.H., Wu, M.S., Lin, J.T., and Chiou, S.H. (2005) *Proteomics*, **5**, 3895–3901.
60. Enroth, H., Akerlund, T., Sillen, A., and Engstrand, L. (2000) *Clinical and Diagnostic Laboratory Immunology*, **7**, 301–306.
61. Jungblut, P.R., Bumann, D., Haas, G. *et al.* (2000) *Molecular Microbiology*, **36**, 710–725.
62. Lee, H.W., Choe, Y.H., Kim, D.K. *et al.* (2004) *Proteomics*, **4**, 2014–2027.
63. McAttee, C.P., Hoffman, P.S., and Berg, D.E. (2001) *Proteomics*, **1**, 516–521.
64. Shao, C., Zhang, Q., Tang, W. *et al.* (2008) *Journal of Microbiology (Seoul, Korea)*, **46**, 331–337.
65. Slonczewski, J.L., McGee, D.J., Phillips, J. *et al.* (2000) *Helicobacter*, **5**, 240–247.
66. Uwins, C., Deitrich, C., Argo, E. *et al.* (2006) *Electrophoresis*, **27**, 1136–1146.
67. Mounicou, S., Szpunar, J., and Lobinski, R. (2009) *Chemical Society Reviews*, **38**, 1119–1138.
68. Gaberc-Porekar, V. and Menart, V. (2001) *Journal of Biochemical and Biophysical Methods*, **49**, 335–360.
69. Sun, X., Chiu, J.F., and He, Q.Y. (2005) *Expert Review of Proteomics*, **2**, 649–657.
70. Basset, C., Dedieu, A., Guerin, P. *et al.* (2008) *Journal of Chromatography. A*, **1185**, 233–240.
71. Heiss, K., Junkes, C., Guerreiro, N. *et al.* (2005) *Proteomics*, **5**, 3614–3622.
72. Kung, C.C.S., Huang, W.N., Huang, Y.C., and Yeh, K.C. (2006) *Proteomics*, **6**, 2746–2758.

73. She, Y.M., Narindrasorasak, S., Yang, S. *et al.* (2003) *Molecular & Cellular Proteomics*, **2**, 1306–1318.
74. Smith, S.D., She, Y.M., Roberts, E.A., and Sarkar, B. (2004) *Journal of Proteome Research*, **3**, 834–840.
75. Sun, X., Ge, R., Chiu, J.F. *et al.* (2008) *Metal-Based Drugs*, **2008**, 289490. (10.1155/2008/289490).
76. Dedieu, A., Bérenguer, F., Basset, C. *et al.* (2009) *Journal of Chromatography. A*, **1216**, 5365–5376.
77. Ge, R., Sun, X., Gu, Q. *et al.* (2007) *Journal of Biological Inorganic Chemistry: JBIC: a Publication of the Society of Biological Inorganic Chemistry*, **12**, 831–842.
78. Becker, J.S., Zoriy, M., Becker, J.S. *et al.* (2003) *Journal of Analytical Atomic Spectrometry*, **19**, 149–152.
79. Chéry, C.C., Günther, D., Cornelis, R. *et al.* (2003) *Electrophoresis*, **24**, 3305–3313.
80. Becker, J.S., Boulyga, S.F., Becker, J.S. *et al.* (2003) *International Journal of Mass Spectrometry*, **228**, 985–997.
81. Allardyce, C.S., Dyson, P.J., Abou-Shakra, F.R. *et al.* (2001) *Chemical Communications*, 2708–2709.
82. Becker, J.S., Zoriy, M., Przybylski, M., and Becker, J.S. (2007) *International Journal of Mass Spectrometry*, **261**, 68–73.
83. Becker, J.S., Zoriy, M., Becker, J.S. *et al.* (2005) *Analytical Chemistry*, **77**, 5851–5860.
84. Becker, J.S., Zoriy, M., Pickhardt, C. *et al.* (2005) *International Journal of Mass Spectrometry*, **242**, 135–144.
85. Becker, J.S., Pozebon, D., Dressler, V.L. *et al.* (2008) *Journal of Analytical Atomic Spectrometry*, **23**, 1076–1082.
86. Becker, J.S., Zoriy, M., Przybylski, M., and Becker, J.S. (2006) *Journal of Analytical Atomic Spectrometry*, **22**, 63–68.
87. Bellinger, F.P., Raman, A.V., Reeves, M.A., and Berry, M.J. (2009) *The Biochemical Journal*, **422**, 11–22.
88. Steinbrenner, H. and Sies, H. (2009) *Biochimica Biophys Acta*, **1790**, 1478–1485.
89. Fan, T.W.M., Pruszkowski, E., and Shuttleworth, S. (2002) *Journal of Analytical Atomic Spectrometry*, **17**, 1621–1623.
90. Tastet, L., Schaumlöffel, D., Bouyssiere, B., and Lobinski, R. (2008) *Talanta*, **75**, 1140–1145.
91. Pedrero, Z., Madrid, Y., Cámara, C. *et al.* (2009) *Journal of Analytical Atomic Spectrometry*, **24**, 775–784.
92. Ballihaut, G., Pécheyran, C., Mounicou, S. *et al.* (2007) *Trends in Analytical Chemistry*, **26**, 183–190.
93. Añorbe, M.G., Messerschmidt, J., Feldmann, I., and Jakubowski, N. (2007) *Journal of Analytical Atomic Spectrometry*, **22**, 917–924.
94. Polatajko, A., Azzolini, M., Feldmann, I. *et al.* (2007) *Journal of Analytical Atomic Spectrometry*, **22**, 878–887.
95. Becker, J.S., Mounicou, S., Zoriy, M.V. *et al.* (2008) *Talanta*, **76**, 1183–1188.
96. Becker, J.S., Lobinski, R., and Becker, J.S. (2009) *Metallomics*, **1**, 312–316.
97. Gao, Y., Chen, C., and Chai, Z. (2007) *Journal of Analytical Atomic Spectrometry*, **22**, 856–866.
98. Chai, Z.F., Zhang, Z.Y., Feng, W.Y. *et al.* (2004) *Journal of Analytical Atomic Spectrometry*, **19**, 26–33.
99. Chai, Z., Mao, X., Hu, Z. *et al.* (2002) *Analytical and Bioanalytical Chemistry*, **372**, 407–411.
100. Ma, R., McLeod, C.W., Tomlinson, K., and Poole, R.K. (2004) *Electrophoresis*, **25**, 2469–2477.
101. Bertrand, M., Weber, G., and Schoefs, B. (2003) *Trends in Analytical Chemistry*, **22**, 254–262.
102. Szökefalvi-Nagy, Z., Demeter, I., Bagyinka, C., and Kovács, K.L. (1987) *Nuclear Instruments & Methods in Physics Research Section B-BEAM Interactions with Materials and Atoms*, **22**, 156–158.

103. Szökefalvi-Nagy, Z., Bagyinka, C., Demeter, I. *et al.* (1990) *Biological Trace Element Research*, **26**, 93–101.
104. Strivay, D., Schoefs, B., and Weber, G. (1998) *Nuclear Instruments & Methods in Physics Research Section B-BEAM Interactions with Materials and Atoms*, **136–138**, 932–935.
105. Szökefalvi-Nagy, Z., Bagyinka, C., Demeter, I. *et al.* (1999) *Fresenius Journal of Analytical Chemistry*, **363**, 469–473.
106. Solš, C., Oliver, A., Andrade, E. *et al.* (1999) *Nuclear Instruments & Methods in Physics Research Section B-BEAM Interactions with Materials and Atoms*, **150**, 222–225.
107. Chevreux, S., Roudeau, S., Fraysse, A. *et al.* (2009) *Biochimie*, **91**, 1324–1327.
108. Ortega, R. (2009) *Metallomics*, **1**, 137–141.
109. Gao, Y., Chen, C., Zhang, P. *et al.* (2003) *Analytica Chimica Acta*, **485**, 131–137.
110. Gao, Y., Chen, C., Chai, Z. *et al.* (2002) *Analyst*, **127**, 1700–1704.
111. Gao, Y., Liu, Y., Chen, C. *et al.* (2005) *Journal of Analytical Atomic Spectrometry*, **20**, 473–475.
112. Li, L., Wu, G., Sun, J. *et al.* (2008) *Journal of Toxicology and Environmental Health, Part A*, **71**, 1266–1269.
113. Kühbacher, M., Weseloh, G., Thomzig, A. *et al.* (2005) *X-Ray Spectrom*, **34**, 112–117.
114. Weseloh, G., Kühbacher, M., Bertelsmann, H. *et al.* (2004) *Journal of Radioanalytical and Nuclear Chemistry*, **259**, 473–477.
115. Kim, S.A., Punshon, T., Lanzirrotti, A. *et al.* (2006) *Science*, **314**, 1295–1298.
116. Munro, K.L., Mariana, A., Klavins, A.I. *et al.* (2008) *Chemical Research in Toxicology*, **21**, 1760–1769.
117. Ascone, I. and Strange, R. (2009) *Journal of Synchrotron Radiation*, **16**, 413–421.
118. Penner-Hahn, J.E. (2009) *Coordination Chemistry Reviews*, **249**, 161–177.
119. Koningsberger, D.C. and Prins, R. (1988) *X-ray Absorption: Principles, Applications, Techniques of EXAFS, SEXAFS, and XANES*, John Wiley & Sons, Inc., New York.
120. Chevreux, S., Roudeau, S., Fraysse, A. *et al.* (2008) *Journal of Analytical Atomic Spectrometry*, **23**, 1117–1120.
121. Ebert, J.C. and Altman, R.B. (2008) *Protein Science: A Publication of the Protein Society*, **17**, 54–65.
122. Passerini, A., Punta, M., Ceroni, A. *et al.* (2006) *Proteins*, **65**, 305–316.
123. Shu, N., Zhou, T., and hovmöller, S. (2008) *Bioinformatics (Oxford, England)*, **24**, 775–782.
124. Andreini, C., Bertini, I., and Rosato, A. (2009) *Accounts of Chemical Research*, **42**, 1471–1479.
125. Bertini, I. and Cavallaro, G. (2010) *Metallomics*, **2**, 39–51.
126. Andreini, C., Banci, L., Bertini, I., and Rosato, A. (2006) *Journal of Proteome Research*, **5**, 196–201.
127. Andreini, C., Banci, L., Bertini, I., and Rosato, A. (2006) *Journal of Proteome Research*, **5**, 3173–3178.
128. Andreini, C., Banci, L., Bertini, I. *et al.* (2007) *Proteins*, **67**, 317–324.
129. Andreini, C., Banci, L., Bertini, I., and Rosato, A. (2008) *Journal of Proteome Research*, **7**, 209–216.
130. Sodhi, J.S., Bryson, K., McGuffin, L.J. *et al.* (2004) *Journal of Molecular Biology*, **342**, 307–320.
131. Babor, M., Gerzon, S., Raveh, B. *et al.* (2008) *Proteins*, **70**, 208–217.
132. Levy, R., Edelman, M., and Sobolev, V. (2009) *Proteins*, **76**, 365–374.
133. Dudev, M. and Lim, C. (2007) *BMC Bioinformatics*, **8**, 106. (10.1186/1471-2105-8-106)
134. Torrance, J.W., MacArthur, M.W., and Thornton, J.M. (2008) *Proteins*, **71**, 813–830.
135. Andreini, C., Bertini, I., Cavallaro, G. *et al.* (2009) *Journal of Molecular Biology*, **388**, 356–380.
136. Wang, Z.Y. and Chen, Z. (2008) *Blood*, **111**, 2505–2515.
137. Lau, A.T., Li, M., Xie, R. *et al.* (2004) *Carcinogenesis*, **25**, 21–28.
138. He, Q.Y., Yip, T.T., Li, M., and Chiu, J.F. (2003) *Journal of Cellular Biochemistry*, **88**, 1–8.
139. Lau, A.T., He, Q.Y., and Chiu, J.F. (2004) *The Biochemical Journal*, **382**, 641–650.
140. Lau, A.T.Y. and Chiu, J.F. (2006) *Proteomics*, **6**, 1619–1630.
141. Vergnes, B., Gourbal, B., Girard, I. *et al.* (2007) *Molecular & Cellular Proteomics*, **6**, 88–101.
142. Selgrad, M. and Malfertheiner, P. (2008) *Current Opinion in Pharmacology*, **8**, 593–597.

143. Cun, S. and Sun, H. (2010) *Proceedings of the National Academy of Sciences of the United States of America*, **107**, 4943–4948.
144. Cun, S., Li, H., Ge, R. *et al.* (2008) *The Journal of Biological Chemistry*, **283**, 15142–15151.
145. Rosenberg, H., Gerdes, R.G., and Chegwidden, K. (1977) *Journal of Bacteriology*, **131**, 505–511.
146. Willsky, G.R. and Malmay, M.H. (1980) *Journal of Bacteriology*, **144**, 356–365.
147. Bun-ya, M., Shikata, K., Nakade, S. *et al.* (1996) *Current Genetics*, **29**, 344–351.
148. Sanders, O.I., Rensing, C., Kuroda, M. *et al.* (1997) *Journal of Bacteriology*, **179**, 3365–3367.
149. Wysocki, R., Chery, C.C., Wawrzycka, D. *et al.* (2001) *Molecular Microbiology*, **40**, 1391–1401.
150. Liu, Z., Shen, J., Carbrey, J.M. *et al.* (2002) *Proceedings of the National Academy of Sciences of the United States of America*, **99**, 6053–6058.
151. Liu, Z., Carbrey, J.M., Agre, P., and Rosen, B.P. (2004) *Biochemical and Biophysical Research Communications*, **316**, 1178–1185.
152. Porquet, A. and Filella, M. (2007) *Chemical Research in Toxicology*, **20**, 1269–1276.
153. Sui, H., Han, B.G., Lee, J.K. *et al.* (2001) *Nature*, **414**, 872–878.
154. Fu, D., Libson, A., Miercke, L.J. *et al.* (2000) *Science*, **290**, 481–486.
155. Carbrey, J.M., Gorelick-Feldman, D.A., Kozono, D. *et al.* (2003) *Proceedings of the National Academy of Sciences of the United States of America*, **100**, 2945–2950.
156. Hughes, M.F., Kenyon, E.M., Edwards, B.C. *et al.* (2003) *Toxicology and Applied Pharmacology*, **191**, 202–210.
157. Bhattacharjee, H., Rosen, B.P., and Mukhopadhyay, R. (2009) *Handbook of Experimental Pharmacology*, **190**, 309–325.
158. Liu, J., Chen, H., Miller, D.S. *et al.* (2001) *Molecular Pharmacology*, **60**, 302–309.
159. Kala, S.V., Neely, M.W., Kala, G. *et al.* (2000) *The Journal of Biological Chemistry*, **275**, 33404–33408.
160. Yang, H.C., Cheng, J., Finan, T.M. *et al.* (2005) *Journal of Bacteriology*, **187**, 6991–6997.
161. Rosen, B.P. (1999) *Trends in Microbiology*, **7**, 207–212.
162. Martin, P., DeMel, S., Shi, J. *et al.* (2001) *Structure (London, England: 1993)*, **9**, 1071–1081.
163. Rosen, B.P. (2002) *FEBS Letters*, **529**, 86–92.
164. Wu, J. and Rosen, B.P. (1991) *Molecular Microbiology*, **5**, 1331–1336.
165. Lin, Y.F., Walmsley, A.R., and Rosen, B.P. (2006) *Proceedings of the National Academy of Sciences of the United States of America*, **103**, 15617–15622.
166. Wu, J., Tisa, L.S., and Rosen, B.P. (1992) *The Journal of Biological Chemistry*, **267**, 12570–12576.
167. Dey, S. and Rosen, B.P. (1995) *Journal of Bacteriology*, **177**, 385–389.
168. Li, J. and Rosen, B.P. (2000) *Molecular Microbiology*, **35**, 361–367.
169. Zhou, T., Radaev, S., Rosen, B.P., and Gatti, D.L. (2000) *The EMBO Journal*, **19**, 4838–4845.
170. Zhou, T., Radaev, S., Rosen, B.P., and Gatti, D.L. (2001) *The Journal of Biological Chemistry*, **276**, 30414–30422.
171. Rosen, B.P., Bhattacharjee, H., Zhou, T., and Walmsley, A.R. (1999) *Biochimica et Biophysica Acta*, **1461**, 207–215.
172. Ruan, X., Bhattacharjee, H., and Rosen, B.P. (2006) *The Journal of Biological Chemistry*, **281**, 9925–9934.
173. Ruan, X., Bhattacharjee, H., and Rosen, B.P. (2008) *Molecular Microbiology*, **67**, 392–402.
174. Ascone, I., Castañer, R., Tarricone, C. *et al.* (1997) *Biochemical and Biophysical Research Communications*, **241**, 119–121.
175. Murphy, L.M., Strange, R.W., and Hasnain, S.S. (1997) *Structure (London, England: 1993)*, **5**, 371–379.
176. Zhou, T. and Rosen, B.P. (1997) *The Journal of Biological Chemistry*, **272**, 19731–19737.
177. Borst, P. and Elferink, R.O. (2002) *Annual Review of Biochemistry*, **71**, 537–592.
178. Zhou, S.F., Wang, L.L., Di, Y.M. *et al.* (2008) *Current Medicinal Chemistry*, **15**, 1981–2039.
179. Cole, S.P., Sparks, K.E., Fraser, K. *et al.* (1994) *Cancer Research*, **54**, 5902–5910.
180. Zaman, G.J., Versantvoort, C.H., Smit, J.J. *et al.* (1993) *Cancer Research*, **53**, 1747–1750.

181. Burger, H., Nooter, K., Zaman, G.J. *et al.* (1994) *Leukemia*, **8**, 990–997.
182. Leslie, E.M., Haimeur, A., and Waalkes, M.P. (2004) *The Journal of Biological Chemistry*, **279**, 32700–32708.
183. Lorico, A., Bertola, A., Baum, C. *et al.* (2002) *Biochemical and Biophysical Research Communications*, **291**, 617–622.
184. Lorico, A., Rappa, G., Flavell, R.A., and Sartorelli, A.C. (1996) *Cancer Research*, **56**, 5351–5355.
185. Au, W.Y., Kumana, C.R., Kou, M. *et al.* (2003) *Blood*, **102**, 407–408.
186. Sun, H. and Chai, Z.F. (2010) *Annual Reports on the Progress of Chemistry, Section A: Inorganic Chemistry*, **106**, 20–38.
187. Da Silva, M.A., Sussulini, A., and Arruda, M.A. (2010) *Expert Review of Proteomics*, **7**, 387–400.

Index

Page numbers in *italics* refer to figures and schemes. Page numbers in **bold** refer to tables.

- Acr3, 196, 200–1, 201
- acute promyelocytic leukemia (APL), 263–4
- As treatment, 40, 113–14
 - combination therapies, potential, 281–4
 - modes of action *see* arsenic trioxide (ATO):
 - modes of action
 - pharmacokinetics, 276–81
- adenocarcinoma, 245
- S-adenosylmethionine (SAM), 28, 33, 148, 149, 150, 168, 342
- alcohol dehydrogenase (ADH), 75–6, 258
- all-*trans* retinoic acid (ATRA), 123, 263, 272–4, 282
- allotropes, 3, 3, **4**
- amino acids, 61–2
- As interaction, 20, 22, 23, 125–6, 342–3
 - Bi interaction, 61–2, 74
 - Sb interaction, 58–9, 60, 66, 298
 - in synthetic peptides, **22**
- aneuploidy, 336–7
- anion exchanger 2 (AE2), 273, 274
- antibodies
- use in RIT, 311, 312
 - clinical studies, 322–3
 - infections, targeting, 323–4, 325
 - preclinical studies, 317–18, 318, 319, 320–1
 - targeted therapy, **321**, 321–2
 - use with RBC, 55
- antimony (Sb)
- allotropes, 3, 3, **4**
 - aqueous chemistry, 14
 - biological activity, 2, **3**
 - bond energies, **4**, 4
 - geological data, **13**, 14
 - methylated species, 159, **160**, 161
 - oxidation states, 4–5, 5, 53–4, 182
 - properties, 1–2, **2**
 - structures, 9–10, 10, 165
 - toxicity, 2, **3**, 54, 366
 - see also* pnictogens
- APL *see* acute promyelocytic leukemia (APL)
- apoptosis, 267
- ATO-induced, 117, 123, 124–5, 125
 - Bcl-2, role of, 267, 269
 - pathways, 267–70, 272–3
 - reactive oxygen species, 270–2
- Bi radionuclide-induced, 321
- organobismuth-induced, 305
- realgar-induced, 117, 125, 126–7
- resistance to, 339
- aquaglyceroporins (AQPs), 185
- As uptake, 119–20, 184–90, 265, 366, 368
 - Sb uptake, 63, 63–4, 64, 184–90, 366
- aqueous environments, 14, 135–6, 136, 139–41, 158, 265
- arginine, 20, 22
- ars* operons, 136–7, 150, 182, 196, 196–200, 369
- ArsAB pump, 66–8, 68
- arsenic (As), 181–2
- allotropes, 3, 3, **4**
 - aqueous chemistry, 14
 - biological activity, 2, **3**
 - bond energies, 4, **4**
 - compounds, **90**
 - geological data, **13**, 14
 - hepatic circulation, 187
 - information sources, 40, **41–6**
 - in marine organisms, 14, 14
 - oxidation states, 4–5, 5, 21, 182
 - properties, 1–2, **2**
 - structures, 9, 9, 264
 - toxicity *see* toxicity:of As
 - see also* pnictogens

- arsenic methyltransferase, 28, 151
 arsenic trioxide (ATO), 113–14, 182, 263–4, 264, 295
 APL, treatment of *see* acute promyelocytic leukemia (APL):As treatment
 combination therapies, potential, 281–4
 metabolism, 119–21
 modes of action, 65, 122–5, 125, 187, 269
 angiogenesis inhibition, 275–6
 apoptosis induction, 117, 123, 124–5, 125, 126–7, 267–73
 differentiation induction, 123–4, 125–6, 273–4
 growth arrest, 126–7, 275
 PML-RAR α , degradation of, 274–5
 pharmacokinetics in APL patients, 276–81
 therapies, potential, 284–5
 arsenious acid, 115, 116, 119
 arsenobetaine, 14, 14, 136, 156–9, 157, 280
 arsenocholine, 14, 14
 arsenolite, 14, 113, 114, 115, 115
 medical applications, 116
 asthma prevention, 127–8
 processing for, 117–18
 metabolism of, 119–21
 arsenosugars, 156–9, 157
 arsenous acid *see* arsenic trioxide (ATO)
 arsines, 21, 21
 ascorbic acid, 123, 283
 asthma, 116, 127–8
 ATO *see* arsenic trioxide (ATO)
 ATRA (all-*trans* retinoic acid), 123, 263, 272–4, 282
- bacteria *see Helicobacter pylori*; microorganism interactions
 Bcl-2, 267, 268–9
 bioinformatics, 357, 363–4
 biomethylation, 145, 146
 analysis methods, 145–6
 of As, 268, 277, 297
 environmental compounds, 156, 156–9, 157
 mammalian, 150–3, 152, 153, 154
 and toxicity, 154–6
 microbial, 147–50, 148, 149
 research history, 146–7
 of Bi, 169, 171
 environmental compounds, 171, **171**
 microbial, 171–4, **172**, 174
 research history, 147
- Challenger mechanism, 147, 148
 of Sb, 165
 abiotic reactions, 169, 170
 environmental compounds, 159, **160**, 161
 mammalian, 161–2
 mechanisms, 168
 microbial, 162, **163–4**, 165–8
 research history, 147
- bismuth (Bi)
 allotropes, 3, 3, **4**
 aqueous chemistry, 14
 biological activity, 2, **3**
 bond energies, 4, **4**
 geological data, **13**, 14
 isotopes, 209
 orbital contraction, 6
 oxidation states, 4–5, 5, 54
 properties, 1–2, **2**
 structures, 9–11, 10
 toxicity, 2, **3**, 68–9, 253, 258–9
see also pnictogens
 bismuth citrate, 55, 56, 250–2, 255
 bismuth oxyhalides, 9
 bismuth subsalicylate (BSS), 55, 242, **242**, 246–9, 250
H. pylori susceptibility to, 253–4
 pH, effect of, 254–5
 toxicity, 253
 boron (B), 189, 191–3, 202, 236, 237
 brain protection, 128
 BSS *see* bismuth subsalicylate (BSS)
 buthionine sulfoxide, 283
- calcium chloride, 76, 76
 carcinogenesis, As-induced
 animal studies, 38–40, 39
 human-animal differences, 40
 human carcinogenicity, 34–8, **37**, **38**
 modes of action
 DNA methylation, 33–4, **34**, 35, 36
 oxidative stress, **31**, 31–3, **32**, 33
 RSH groups, binding to, 30–1
 CBS *see* colloidal bismuth subcitrate (CBS)
 cell microcosm, 86–7, 87
 cellular efflux
 of As, 151, 183, 195–201, 196, 201, 266–7, 268
 red blood cells, 104–5, 108
 of B, 202
 of Sb, 195–201, 369–70
 of Si, 196

- cellular uptake
 of As, 119–21, 183, 183–91, 265–6, 268, 366, 368
 AQPs, role of, 63
 p*K_a* values, 182
 red blood cells, 104, 104–5, 108, 109
 of B, 191–3, 202
 of Bi, 62, 71
 of Fe, 71, 71
 of Ge, 195
 of Sb, 63, 64, 184–90, 366
 of Si, 193–5, 201–2
- chemical speciation
 of As, 88–9, 94
 analysis methods, 85–9, 86, 88, 89
 in hamsters and rats, 98–103, 100, 101, 102
 in human blood serum, 96–8, 98, 99
 in human urine, 93–6, 95, 96
 after seaweed ingestion, 105–9, 107, 108
 in salmon egg cells, 89–93, 91, 92
 in seaweeds, 105–6, 106
 separation graph, 90
 uptake by red blood cells, 103–5, 104, 105
 of As-based drugs, 355–6
 of trace elements, 87–9
see also metalloproteomics
- chemotherapy *see* medical applications
- chromatography
 IMAC, 357, 360, 361, 362
 SEC, 88, 88
- chromosome aberrations, 336, 345
- cimetidine, 249–50, 251, 254
- colloidal bismuth pectin, 56, 246, 255
- colloidal bismuth subcitrate (CBS), 242, 243, 250–2
H. pylori, action against, 55–6, 76, 76, 249–50
- cot death (SIDS), 161–2
- cysteine
 As interaction, 20, 22, 23, 24, 24–5, 26, 29
 in zinc finger proteins, 26, 27
 Bi interaction, 61, 62, 72, 74–5
 conservation of, 28
 Sb interaction, 58–60, 60, 61, 64, 66, 67
- Cyt19 methyltransferase, 150, 151–3, 153
- cytokines, 123–4, 127, 282–3
- cytotoxicity
 of As, 22, 30, 127, 155, 271, 335–6
 of Bi, 58, 303, 305–6
 of Sb, 55, 299–300, 302
- diarrhea, 246–8
- diethylene triamine pentaacetic acid (DTPA), 314, 315, 316, 317
- dissociation constants (p*K_a*), 20, 54, 182, 191, 195, 356
- DNA interactions
 As, 20–6, 363
 DNA damage, 270, 332–3
 DNA methylation, 33–4, 34, 35, 36, 332, 341–2
 DNA repair, 124, 337, 337–9
 and zinc finger proteins, 26–30
 Bi, 59, 72, 73, 305, 313
 Sb, 66
- DOTA (1,4,7,10-tetraazacyclododecane tetraacetic acid), 315, 316
- drug resistance, 62, 195–6
- drugs *see* medical applications
- DTPA (diethylene triamine pentaacetic acid), 314, 315, 316, 317
- Ef-Tu, translational factor, 257, 366
- emodin, 283
- enzyme interactions
 As, 28, 137, 138, 139, 190–1, 266, 338–9
see also apoptosis:ATO-induced;
 bi-methylation:of As
 Bi, 75, 75–6, 76, 252, 256–8, 303
 Sb, 64, 65, 66–8, 67, 68
- excretion
 of As, 21, 28, 40, 121, 151, 278–9
see also chemical speciation:of As
 of Bi, 251, 314
- Extended all-present theory of the elements* (Haraguchi), 86–7
- flavonoids, 281–2
- fumarase, 257, 366
- genetic toxicology
 of As, 331–2
 aneuploidy, 336–7
 chromosome aberrations, 336
 cytotoxicity, 335–6
 DNA damage, 332–3
 DNA repair, effects on, 337, 337–9
 indirect effects, 339–40, 340
 micronuclei (MN), 336–7
 mutagenesis, 333–5, 334
 secondary effects, 340–4, 341, 343

- genetic toxicology (*Continued*)
transgenerational epigenetics, 343–4
of Sb, 344–5
- genomics, 84, 84, 354, 370
- geological data, **13**, 14
- germanium (Ge), 194–5
- glucose permeases, 190–1, 266
- glutathione (GSH), 59, 64, 271
As interaction, 25, 108, 120–1, *121*, 266, 283, 332
Bi interaction, 61
Sb interaction, 59, **60**, 60–1, **61**
- glutathione peroxidase (GPx), 271
- glutathione S-transferase (GST), 266, 271–2
- glycine, 60, **60**, 61
- P-glycoprotein (P-gp), 266, 268
- GSH *see* glutathione (GSH)
- heat shock proteins, 74, 128, 256–7, 364, 370
- Helicobacter pylori*, 243–5, *244*, *248*
associated diseases, 245–6
Bi treatments for, 55–6, 73–6, 74, 246–50, *247*, 255
bismuth citrate, 55, 56, 250–2, 255
BSS, 55, **242**, 242, 246–9, 250, 253–5
CBS, 55–6, 76, 76, 249–52
modes of action, 61–2, 250–2, 256–8
RBC, 55–6, 72–3, 73, 74, 246, 255, 303
metalloproteomic studies, 74–6, 76, **358**, 365–6, **367**, 368, 370
- hijiki seaweed, 105–9, *106*, *107*, *108*
- histidine, 20, 22, 59, 73–4, 74
- histones, 20, 342–3
- human glucose transporters (GLUT), 266
- human telomerase, 272–3
- hybridization, 11–12
- 8-hydroxydeoxyguanosine (8-OHdG), 20, 27, 32–3, 33, 270
- immobilized-metal affinity chromatography (IMAC), 357, *360*, **361**, 362
- inductively coupled plasma atomic emission spectrometry (ICP-AES), 85–7, 86, 87
- inductively coupled plasma-mass spectrometry (ICP-MS), 85–7, 86, 87, 88, 88, 357, 359–60
- inversion, *11*, 11–12, **12**
- iron (Fe), 69, 69–70, 70, 140, 257
- JNK (c-Jun N-terminal kinase) pathway, 126, 272, 364
- JWA molecule, 273
- laser ablation-inductively coupled plasma-mass spectrometry (LA-ICP-MS), 357, 359–60
- lead (Pb) porphyrin complexes, 225, 229, *231*
compared to Bi complexes, 227–30, 228, 232, *233*, *234*, 235
electron deformation, 235–6, 236
- Leishmania* spp.
metalloproteomic studies, **358**
Sb treatment, 54, *54*, 60–1, 298, 365
drug resistance, 62, 354
modes of action, 62–4, *63*, *64*, *65*, 66
- leukemia, 40, 284–5, 321, 322
see also acute promyelocytic leukemia (APL)
- Lewis acceptor properties, 9–10
- Lewis acid behavior, 12
- LmACR2, 64, 65, 66
- lymphoma, 246, 279, 285, 312
- lysine, 20, 22
- major intrinsic proteins (MIPs), 184, 188, 193
- medical applications, 293–4, *294*, 307, 353, **356**
anticancer studies, comparative, 306
As, 40, 127–8, 264–5, 295–7, 296, 355
anticancer studies, 297, 297–8
modes of action, 122–7, *125*
in TCM *see* Traditional Chinese Medicine,
As use in
toxicity issues, 114–15, 295
- Bi, 55–6, 56, 57, 73, 242–3
anticancer studies, 303, *304*, 305–6
bacterial infections, 246–9, 253–5
biochemical targets, 256–8
compound preparations, 255
compounds in use, **242**, 242–3
delivery systems, 255–6
Helicobacter pylori control *see*
Helicobacter pylori:Bi treatments for
history of use, 303
infections, 323–4, 325
 α -radioimmunotherapy (RIT) *see*
 α -radioimmunotherapy (RIT)
SARS, treatment of, 72–3, 209
transferrin binding, 258
- Sb, *54*, 54–5, 62–4, 66, 298
anticancer studies, 298–300, 299, *301*, 302

- metabolism, As, 119–22, 120, 121, 151, 277, 355–6
 animal species differences, 103–4, 105
 genes involved, 155–6
 in hamsters and rats, 98–103, 100, 101, 102
- metallomics, 83–5, 87, 354
 ICP-AES and ICP-MS, 85–7, 86, 87
 relationship to other -omics sciences, 84
 research subjects, **85**
 trace elements, 87–9
- metalloproteomics, 357, 359, 370
 As and Sb extrusion systems, 369–70
 As and Sb uptake systems, 366, 368
 methods
 bioinformatics, 363–4
 IMAC, 357, **358**, 359, 360, **361**, 362
 LA-ICP-MS, 357, 359–60
 nuclear analytical techniques, 360, 362–3
 target identification, 364–6, **365**, **367**, 368
- metallothionein (MT), 72, 72, 333
- methionine, 22
- N-methyl-N-nitrosourea (MNU), 337
- methylation, As, 28, 93–4, 103, 120, 120–1, 121
 animal species differences, 103–4
see also biomethylation:of As
- methylcobalamin, 149, 149
- micronuclei (MN), 21–2, 336–7, 345
- microorganism interactions
 As, 135–6, 136
 As-resistance, 137
 biomethylation, 147–50, 148, 149
 identification of organisms, 140–1
 mobilization of As, 139–41
 oxidation of As, 138–9
 reduction of As, 137–8
 research priorities, 141–2
 sediment analysis techniques, 140–1
- Bi
 biomethylation, 171–4, **172**, 174
see also Helicobacter pylori
- Sb
 biomethylation, **163–4**
 aerobic conditions, 162, 165–6
 anaerobic conditions, 166–8
see also Leishmania spp.
- MIPs (major intrinsic proteins), 184, 188, 193
- mitochondria, 267, 269, 270
- MNU (N-methyl-N-nitrosourea), 337
- multidrug resistance associated proteins, 186, 195–6, 266–8
- mutagenesis, As-induced, 333–5, **334**, 340–4, 341, 343
- NADPH oxidase, 271
- nickel porphyrin complexes, 225, 226, 226–30
- nitric oxide, 284, 333
- nitrogen (N), 1, 11, 11–12
- nodulin 26-like intrinsic proteins (NIPs), 188–90
- nuclear factor kappa B (NF- κ B), 272
- nucleoside interactions, 56–8, 58, 151
- nucleotide interactions, 56–8, 57
- nutrition, 186–7
- orbital contraction, 5–6
- orpiment, 14, 113, 115, 116, 118–19, 264, 295
 metabolism of, 121–2
 modes of action, 125, 129
- oxidation states, 4–5, 5
- oxidative stress, As-induced, **31**, 31–3, **32**, 33, 333
- 8-oxo-deoxyguanine (8-oxo-dG), 332–3
- oxygen-pnictogen compounds, 7, 9, 9
- p38 MAPK pathway, 27, 126, 272, 281, 284
- P53 protein, 338
- pararealgar, 115
- PARP (poly (ADP ribose) polymerase), 284, 338–9
- pepsin, 257
- peptides
 As interaction, 20–6, 24, 28
 Bi interaction, 61–2, 62
 RIT, use in, 312–13, 317
 Sb interaction, 58–61, 59, **60**, 60, **61**
 synthetic, **22**
- pharmacokinetics, As, 119–22, 276–81
- phorbol myristate acetate, 271, 283
- phosphatidylcholine, 97, 97
- phospholipases, 76, 76, 257
- phosphorus (P), 1
- phytosphingosine, 284
- pKa values, 20, 54, 182, 191, 195, 356
- plants
 boron uptake, 191–2
 metalloid distribution, 188–90, 189
 silicon uptake, 193–5
- PML-RAR α , degradation of, 274–5

- pnictogens, 1
 analysis methods, 15
 coordination chemistry, 12
 hybridization, *11*, 11–12
 inversion, *11*, 11–12, **12**
 orbital contraction, 5–6
 oxidation states, 4–5, 5
 pnictogen-oxygen compounds, 7, 9, 9
 relativistic effects, 5–6
 structure and bonding, 6–7, 7, **8**
 structures, 8, 9, 9–11, *10*
- poly (ADP ribose) polymerase (PARP), 268, 284, 338–9
- porphyrin complexes, 209–11
 with Bi, functionalized porphyrins, 212–13, 237
 bis-strapped porphyrins, 223, 225–6, 230–2, 235–6
 compared to other complexes, 226–30, 228, 232, 233, 234, 235–6
 synthesis, 225, 231
 picket porphyrins, 213–16, 215, 217, 218–23, 221, 222
 synthesis, 214, 219, 224
 single-strapped porphyrins, 236–7, 238
 with Bi, unfunctionalized porphyrins, 211–12, 212, 213
 medical applications, 209, 216, 217, 218, 227
 with Ni, 225, 226, 226–30
 with Pb, 225, 229, 231
 compared to Bi, 227–30, 228, 232, 233, 234, 235
 electron deformation, 235–6, 236
 with pnictogens, 210–11
 with Zn, 225, 226, 226–30
- potassium antimony tartrate, 54, 54, 55, 165, 298
- proteins
 As interaction, 20–6, 333, 343
 zinc finger proteins, 26–7
 Bi interaction, 67–75, 71, 73, 74, 256–7, 258–9, 303
 RIT, use in, 317
 Sb interaction, 62–4, 63, 64, 66–8, 68
- proteomics, 84, 84, 354, 356–7, **358**
see also metalloproteomics
- proton-induced X-ray emission (PIXE), 362–3
- α -radioimmunotherapy (RIT), 209, 210, 216, 217, 227, 311–12, 323
 chelating agents, 315, 315–17
 clinical studies, 322–3, 323
 non-cancer uses, 323–4, 325
 obstacles, 324
 peptides as delivery agents, 323
 preclinical studies, 317–21, 318, 320
 radionuclides, 313–14
²¹²Bi, 314, 314
²¹³Bi, 315, 316
 radiolabeling, 315–16
 research priorities, 325–6
 solid tumors, use against, 318, 318
 v. β -radioimmunotherapy, 311–12, 313, **321**, 321–2
 vectors, targeting, 312–13
- radionuclides, 312, 313–14, 314, 316
- ranitidine, 250
- ranitidine bismuth citrate (RBC), 55–6, 72–3, 73, 74, 246, 255, 303
- reactive oxygen species (ROS), 109, 124, 270–2, 332
- realgar, 14, 113, 114, 115, 128, 264, 264
 medical applications, 116–17
 metabolism of, 121–2
 modes of action, 125–7
 processing, 118–19
- relativistic effects, 5–6
- retinoic acid, 272
 all-*trans* retinoic acid (ATRA), 263, 295
 RIT *see* α -radioimmunotherapy (RIT)
- ROS (reactive oxygen species), 109, 124, 270–2, 332
- salmon egg cells, 87, 87
- SAM (S-adenosylmethionine), 28, 33, 148, 149, 150, 168, 342
- seaweed, 105–9, 106, 107, 108
- sediment analysis techniques, 140–1
- Severe Acute Respiratory Syndrome (SARS)
 coronavirus, 72, 72–3, 73, 303
- silicic acid, 188, 189, 193
- silicon transport systems, 193–5, 201–2, 295
- size exclusion chromatography (SEC), 88, 88
- SOD (superoxide dismutase), 271, 272, 332, 333
- sodium stibogluconate, 54, 54, 55, 298, 299
- spectrometry
 ICP-AES, 85–7, 86, 87
 ICP-MS, 85–7, 86, 87, 88, 88, 357, 359–60
 LA-ICP-MS, 357, 359–60
- stable isotope probing (SIP), 140–1
- sudden infant death syndrome (SIDS), 161–2

- sulfhydryl groups, 22, 184, 272, 273, 276
- sulfur-As complexes, 22, 24, 25, 29–30
- superoxide dismutase (SOD), 271, 272, 332, 333
- synchronous radiation X-ray fluorescence (SRXRF), 362, 363
- 1,4,7,10-tetraazacyclododecane tetra acetic acid (DOTA), 315, 316
- thioarsenicals, 29, 102, 120–1, 156, 156–9
- thiol dependent reductase TDR1, 64
- thiols
- As interaction, 22–5, 137, 184, 266
 - Bi interaction, 220
 - Sb interaction, 59, **60**, 60, **61**
- thioredoxin reductase (TrxR), 150, 271, 332
- toxicity
- of As, 2, **3**, 14, 113, 366
 - and biomethylation, 154–6, 277
 - medical applications, 114–15, 277
 - of Bi, 2, **3**, 68–9, 253, 258–9
 - of Sb, 2, **3**, 54, 366
 - see also* cytotoxicity; genetic toxicology
- Traditional Chinese Medicine, As use in, 113–15, **114**, 128–30
- arsenic trioxide (ATO), 119–21, 120, 121, 122–5, 125
 - arsenolite, 115, 115–16, 117–18, 119–21, 120, 121, 127–8
 - composites, importance of, 114, 122
 - orpiment, 115, 116–17, 118–19, 121–2
 - realgar, 115, 116–17, 118–19, 121–2, 125–7, 128
 - see also* medical applications:As
 - transferrins, 69, 69–75, 70, 71, 258–9
 - trimethylantimony chloride, 169
 - trypanothione, 59, 59, 60, **61**, 66
 - trypanothione reductase, 66, 67, 298
 - tubulin, 273
 - tyrosine, 20
 - ulcers, 245, 249
 - As treatment, 295
 - Bi treatment, 55–6, 246, 249, 251–2, 254, 255
 - urease, 75, 75, 245, 256–7, 258
 - UV visible spectroscopy, 210, 215
 - X-ray absorption spectroscopy (XAS), 363
 - zinc finger proteins, 26–7, 59–60, 60
 - zinc porphyrin complexes, 225, 226, 226–30